

Advances in
INORGANIC CHEMISTRY
AND
RADIOCHEMISTRY

Volume 29

CONTRIBUTORS TO THIS VOLUME

Kim Carneiro
Tsai-lih Hwang
Chao-shiuan Liu
S.-W. Ng
John F. Nixon
Paul R. Raithby
Maria J. Rosales
Motoharu Tanaka
Jack M. Williams
Hiromichi Yamada
J. J. Zuckerman

Advances in
INORGANIC CHEMISTRY
AND
RADIOCHEMISTRY

EDITORS

H. J. EMELÉUS

A. G. SHARPE

*University Chemical Laboratory
Cambridge, England*

VOLUME 29

1985



ACADEMIC PRESS, INC.

Harcourt Brace Jovanovich, Publishers

Orlando San Diego New York Austin
London Montreal Sydney Tokyo Toronto

COPYRIGHT © 1985 BY ACADEMIC PRESS, INC.
ALL RIGHTS RESERVED.
NO PART OF THIS PUBLICATION MAY BE REPRODUCED OR
TRANSMITTED IN ANY FORM OR BY ANY MEANS, ELECTRONIC
OR MECHANICAL, INCLUDING PHOTOCOPY, RECORDING, OR
ANY INFORMATION STORAGE AND RETRIEVAL SYSTEM, WITHOUT
PERMISSION IN WRITING FROM THE PUBLISHER.

ACADEMIC PRESS, INC.
Orlando, Florida 32887

United Kingdom Edition published by
ACADEMIC PRESS INC. (LONDON) LTD.
24-28 Oval Road, London NW1 7DX

LIBRARY OF CONGRESS CATALOG CARD NUMBER: 59-7692

ISBN 0-12-023629-X

PRINTED IN THE UNITED STATES OF AMERICA

85 86 87 88 9 8 7 6 5 4 3 2 1

CONTENTS

CONTRIBUTORS	ix
------------------------	----

Inorganic Silylenes. Chemistry of Silylene, Dichlorosilylene, and Difluorosilylene

CHAO-SHIUAN LIU AND TSAI-LIH HWANG

I. Introduction	1
II. Chemistry of Silylene	2
III. Chemistry of Dichlorosilylene	6
IV. Chemistry of Difluorosilylene	15
References	36

Trifluorophosphine Complexes of Transition Metals

JOHN F. NIXON

I. Introduction	42
II. Binary Compounds	43
III. Hydrides	45
IV. Structures	52
V. Bonding	59
VI. Dinuclear Complexes Containing Bridging PF_2 Ligands	68
VII. Polynuclear Complexes	69
VIII. Halogeno-Metal Complexes	73
IX. Transition Metal-Alkene Complexes	77
X. Transition Metal-Alkyne Complexes	88
XI. Transition Metal-Arene Complexes.	89
XII. Transition Metal η^3 -Allyl Complexes	93
XIII. Transition Metal η^5 -Cyclopentadienyl and Related Complexes	97
XIV. Transition Metal Carbonyl Complexes	104
XV. Transition Metal Nitrosyl Complexes	109
XVI. Transition Metal Complexes Containing Other Ligands with Nitrogen, Phosphorus, or Arsenic Donor Atoms	111
XVII. Transition Metal Alkyl and Alkenyl Complexes	122
XVIII. Transition Metal Complexes Containing σ -Bonded Group IV Elements Other than Carbon	126
XIX. Transition Metal Complexes Containing Anionic or Cationic Ligands	128
References	131

Solvent Extraction of Metal Carboxylates

HIROMICHI YAMADA AND MOTOHARU TANAKA

I. Introduction	143
II. Partition of a Carboxylic Acid between the Aqueous and Organic Phases	145
III. Solvent Extraction of Metal Ions with Carboxylic Acids	147
IV. Concluding Remarks	164
References	164

Alkyne-Substituted Transition Metal Clusters

PAUL R. RAITHBY AND MARIA J. ROSALES

I. Introduction	170
II. Reactions of Clusters with Unsaturated Ligands	171
III. Methods of Characterization of Alkyne-Substituted Clusters	182
IV. Types of Bonding of Alkynes in Cluster Complexes	194
V. Fluxionality in Solution	225
VI. The Reactivity of Alkyne-Substituted Clusters	226
References	231

Organic Superconductors: Synthesis, Structure, Conductivity, and Magnetic Properties

JACK M. WILLIAMS AND KIM CARNEIRO

I. Introduction	249
II. The Synthesis of TMTSF and BEDT-TTF (ET), and Crystal Growth of Conducting Salts	253
III. Crystal Structure of (TMTSF) ₂ X and (ET) ₂ X Conductors	258
IV. Electrical Conduction	278
V. Magnetic Properties	286
Concluding Remarks	291
References	292

Where Are the Lone-Pair Electrons in Subvalent Fourth-Group Compounds?

S.-W. NG AND J. J. ZUCKERMAN

I. Introduction	297
II. Divalent Fourth-Group Structures	299

CONTENTS

vii

III. History	302
IV. Symmetrical Subvalent Systems	304
V. Conclusions	319
References	321
 INDEX	 327

This Page Intentionally Left Blank

CONTRIBUTORS

Numbers in parentheses indicate the pages on which the authors' contributions begin.

- KIM CARNEIRO (247), *Physics Laboratory I, University of Copenhagen, H. C. Ørsted Institute, DK 2100, Copenhagen 0, Denmark*
- TSAI-LIH HWANG (1), *Department of Chemistry, Chung Shan Institute of Science and Technology, Lung-tan, Taiwan, Republic of China*
- CHAO-SHIUAN LIU (1), *Department of Chemistry, National Tsing Hua University, Hsinchu, Taiwan, Republic of China*
- S.-W. NG¹ (297), *Department of Chemistry, University of Oklahoma, Norman, Oklahoma 73019*
- JOHN F. NIXON (41), *School of Chemistry and Molecular Sciences, University of Sussex, Brighton BN1 9QJ, Sussex, England*
- PAUL R. RAITHBY (169), *Department of Chemistry, University of Cambridge, Cambridge CB2 1EW, England*
- MARIA J. ROSALES (169), *Instituto de Química, Universidad Nacional Autónoma de México, Circuito Exterior, Ciudad Universitaria, Coyoacán 04510, México D.F., México*
- MOTOHARU TANAKA (143), *Faculty of Science, Nagoya University, Nagoya 464, Japan*
- JACK M. WILLIAMS (247), *Chemistry and Materials Science and Technology Divisions, Argonne National Laboratory, Argonne, Illinois 60439*
- HIROMICHI YAMADA (143), *Faculty of Engineering, Gifu University, Yanagido, Gifu 501-11, Japan*
- J. J. ZUCKERMAN (297), *Department of Chemistry, University of Oklahoma, Norman, Oklahoma 73019*

¹ Present address: Institute of Advanced Studies, University of Malaya, Pantai Valley, Kuala Lumpur, Malaysia.

This Page Intentionally Left Blank

INORGANIC SILYLENES. CHEMISTRY OF SILYLENE, DICHLOROSILYLENE, AND DIFLUOROSILYLENE

CHAO-SHIUAN LIU* and TSAI-LIH HWANG**

*Department of Chemistry, National Tsing Hua University,
Hsinchu, Taiwan, Republic of China, and

**Department of Chemistry, Chung Shan Institute of Science and
Technology, Lung-tan, Taiwan, Republic of China

I. Introduction	1
II. Chemistry of Silylene	2
III. Chemistry of Dichlorosilylene	6
IV. Chemistry of Difluorosilylene	15
References	36

I. Introduction

To a certain extent, silicon chemistry developed in the shadow of organic chemistry. The development may be divided into three stages: (1) period of mimicking, when investigators of silicon chemistry relied on tenuous analogies to organic chemistry and on speculation that a framework reminiscent of organic chemistry could be developed; (2) period of realization of the close similarities and gross differences between the two chemistries; and (3) period of utilization of these differences in various applications. The latter is evidenced by the rapid growth in studies using organosilicon compounds for special organic syntheses. As a result, it is perhaps reasonable to state that silicon chemistry will soon become divided into two areas of almost equal importance: conventional organosilicon chemistry and silaorganic chemistry. Similarly, silylene chemistry seems to have developed in the shadow of carbene chemistry. This is particularly obvious, as one often finds the silylenes referred to in the literature as "carbene analogues."

During the past 10 years, because of discoveries of better reaction conditions and better means to generate silylenes, the chemistry of various silylenes has been studied thoroughly and has reached the stage

where general and unique behaviors of each silylene can be described systematically.

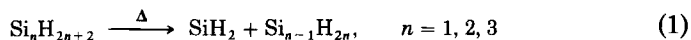
Partly because of the direct impact on organosilicon chemistry and partly because of the interests in searching for other related reactive intermediates such as silenes and disilenes, the development of the chemistry of organic silylenes has received much more attention than that of inorganic silylenes. The rapid and exciting development in organic silylene chemistry is apparent from the number of excellent review articles that have appeared (5, 19, 36, 37, 39, 48, 57, 60, 75). However, as far as the fundamental reaction mechanism is concerned, studies on inorganic silylenes should perhaps provide more basic information because of the simplicity in both structures and reaction pathways of the inorganic silylenes. In addition, systematic studies on the reaction mechanisms of silylene, dichlorosilylene, and difluorosilylene (most significantly, sometimes quantitative data are becoming available) have clarified a number of basic points that had long confused investigators. For example, the reaction mechanism of difluorosilylene has so far been described in a very confused manner in the review literature (113). We will therefore reexamine these results and present an updated summary for these basic silylene species.

No attempt is made to include every known reaction of the three silylenes; rather, we hope to describe in this chapter, in a systematic and critical manner, our understanding of how inorganic silylenes participate in reactions of fundamental interest.

II. Chemistry of Silylene

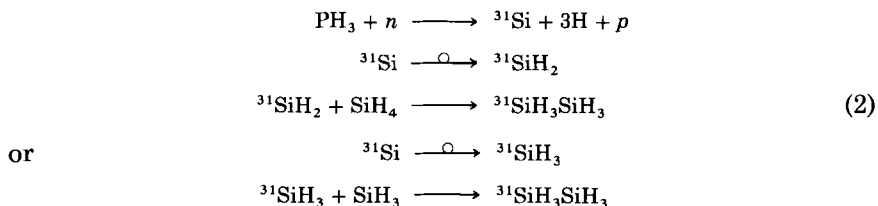
In view of the fact that silylene, SiH_2 , is the simplest divalent silicon species, the variety of reactions that have been studied is surprisingly small. Effort has so far been concentrated on the study of its reaction mechanisms.

Although the existence of SiH_2 was first postulated in pyrolysis studies on silane and higher silanes long ago (50), the evidence for the formation of silylene has been controversial (50, 81, 84). A balanced view on this matter is that while the possibility of a primary process leading to the formation of silyl radicals cannot be ruled out (84), the involvement of SiH_2 in these pyrolysis reactions is generally accepted (50, 81).



The controversy of silylene vs. silyl radical exists in almost every experimental preparation of silylene. For example, in the fast-neutron

bombardment experiment, $^{31}\text{P}(n,p)^{31}\text{Si}$ in phosphine-silane mixtures, another useful method for studying silylene chemistry, the formation of disilane has been explained by mechanisms involving either silylene or silyl radicals (43, 74, 76, 85, 115, 116):



The most studied reaction of silylene is the insertion reaction into silicon-hydrogen bonds. It was first postulated on the basis that higher silanes were generally formed in pyrolysis of silane, disilane, and trisilane (74, 81, 98). If silylene is the major intermediate, the higher silanes are formed by insertion reactions of the type



When alkylsilanes are copyrolyzed together with Si_2H_6 , the reactions are best interpreted by SiH_2 insertion (14). For example,

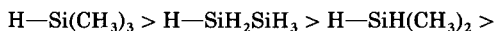


When Si_2D_6 was used in the same reaction, the fact that $\text{CH}_3\text{SiH}_2\text{SiHD}_2$ and SiD_4 were obtained instead of $\text{CH}_3\text{SiH}_2\text{SiD}_3$ and SiD_3H was considered evidence of silylene intermediacy over silyl radicals.

In recoil-atom experiments, disilane has been found to be five times more reactive than silane (42). Statistically, a reactivity ratio of 3:2 would be expected. Also, trisilane has been found to produce *n*-tetrasilane and *i*-tetrasilane in the ratio 4.4-5.2:1, much higher than the value expected on the basis of statistical considerations (14). These results seem to suggest the competing insertion of silylene into the Si-Si bonds in these reactions. However, the fact that Si-H bond strengths in different silanes vary would also result in a statistically unexpected ratio (51).

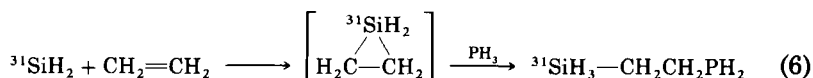
Measurements of the relative rates of insertion of SiH_2 into M-H bonds (M = Si, Ge, P) have shown the reactivity to decrease in the

following order (89):

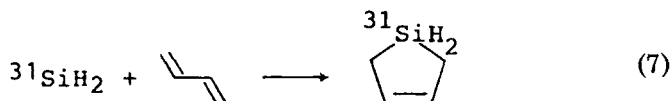


The sequence can be rationalized in terms of the partial negative charge on the target hydrogen atom. In view of this, it is not surprising that SiH_2 does not insert into $\text{P}-\text{H}$ bonds (89, 90). The reluctance of SiH_2 to insert into $\text{C}-\text{H}$ bonds is probably a related matter (46, 47).

The recoil-atom reaction with phosphine-ethylene mixture (38) produced a product identified as $^{31}\text{SiH}_3\text{CH}_2\text{CH}_2\text{PH}_2$. This finding was rationalized by a mechanism involving addition of silylene to the π -bond of ethylene:

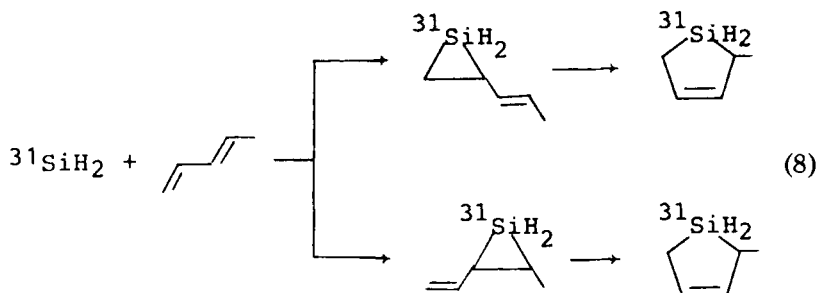


The best studied addition reactions of silylene have been those with conjugated dienes. Earlier studies using the nuclear recoil system have shown that $^{31}\text{SiH}_2$ added to 1,3-butadiene to give silacyclopent-3-ene (44, 99, 100).

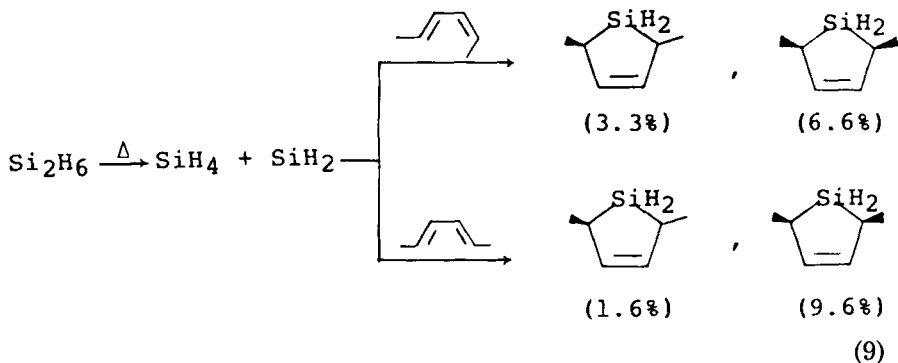


Studies using NO as scavenger suggested that the reacting silylene was present as 80% triplet and 20% singlet (118). In the reactions with conjugated pentadienes the evaluated singlet to triplet ratio was 1:6 (95). This result contrasts very much with the result of the reaction of thermally generated silylene, which has a singlet spin state (35, 79).

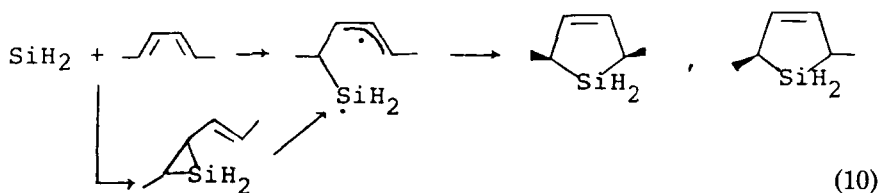
The singlet silylene was proposed to add to the diene system via 1,2-addition, followed by rearrangement involving cleavage of a $\text{C}-\text{Si}$ bond, by either a concerted or a diradical mechanism (40).



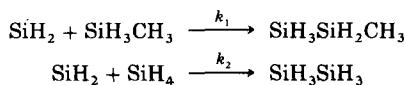
The reactions of SiH_2 with *cis,trans*- and *trans,trans*-2,4-hexadiene were studied in order to differentiate the mechanisms (37, 40).



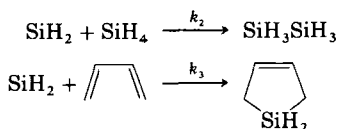
The nonstereospecific addition was explained by a diradical process, for example, the reaction with *trans,trans*-2,4-hexadiene:



More recently, competition experiments have been undertaken with substrate mixture (79). Two systems have been chosen for studies of relative reactivities:



and



Both thermally generated and hot-atom generated silylene were employed in these studies. The results showed that within the temperature range 385–460°C, thermally generated SiH_2 gave a more or less constant k_1/k_2 ratio (~ 1.35 – 1.40), in good agreement with the reactivity

ratio of 1.32 found in the recoil experiment (41). The value of k_2/k_3 for thermally generated SiH_2 was found to be 13 ± 4 at room temperature, which was also similar to the reactivity ratio 9 ± 1 obtained in the recoil experiment (41).

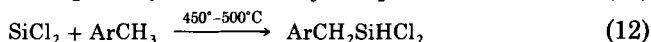
Thus quantitative agreement has been found between the relative reactivity of the intermediate from the high-energy silicon atoms in mixtures containing labile hydrogen and ground state singlet silylene. The earlier suggestion based on studies using radical scavengers that silylene reacts principally in a triplet electronic state must be considered a misinterpretation (118). The effect of scavengers could be on a species, initiated by silicon atoms, that appeared earlier in the reaction sequence, rather than on the formation of silylene intermediates.

III. Chemistry of Dichlorosilylene

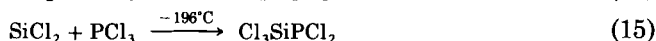
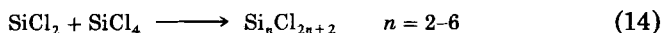
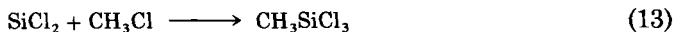
The chemistry of dichlorosilylene can be studied by either gas-phase or cocondensation reactions (17, 62, 103, 104). In most cases, dichlorosilylene generated by pyrolysis of perchloropolysilanes was used in the gas-phase reactions whereas thermal reduction was used for cocondensation experiments.

As in the case of SiH_2 chemistry, dichlorosilylene has been found to undergo mainly two types of reactions, namely, insertions and additions according to the types of reaction products formed.

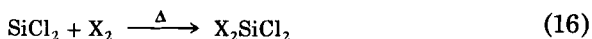
Dichlorosilylene inserts into a great number of compounds involving $\text{B}-\text{X}$ (101, 102), $\text{C}-\text{H}$ (9, 10, 16, 18, 21, 22, 24, 32), $\text{C}-\text{X}$ (10, 24, 26-28, 33, 34, 87), $\text{Si}-\text{H}$ (119), $\text{Si}-\text{X}$ (88), and $\text{P}-\text{X}$ (101, 102) and $\text{O}-\text{H}$ (10, 25) bonds ($\text{X} = \text{halogen}$). For example,



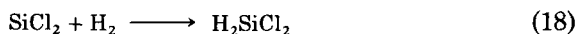
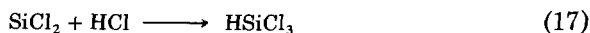
where $\text{Ar} = \text{phenyl}$, *o*- and *p*-tolyl, *p*-biphenyl, α - and β -naphthyl, 2- and 3-thienyl, etc.



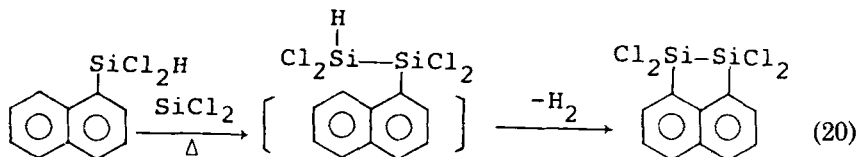
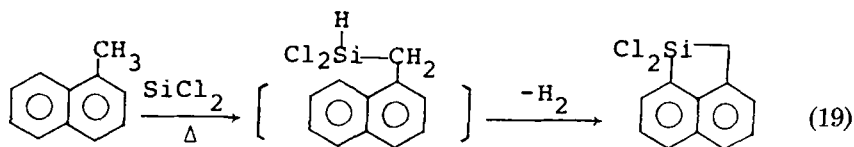
Dichlorosilylene also inserts into halogens, hydrogen chloride, and the hydrogen molecule:



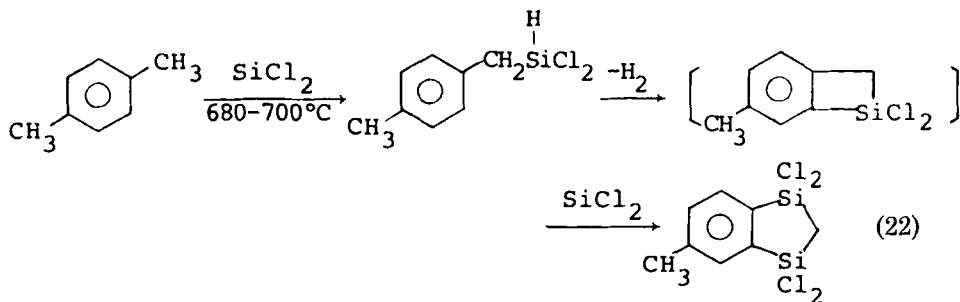
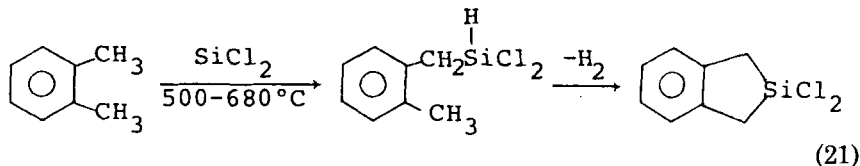
where X = Cl (111), Br, and I (87).



It is particularly interesting to note that at elevated temperatures some of the products from SiCl_2 insertion into C—H and Si—H bonds would undergo hydrogen elimination on cyclization (10, 24, 119), for example, Eqs. (19) and (20).

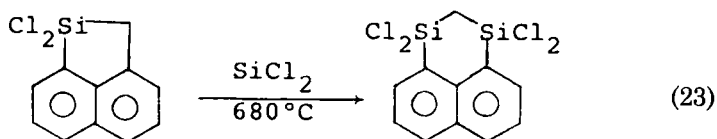


In cases where the cyclization process mentioned above produced strained rings, further SiCl_2 insertion into the rings was observed. This is best illustrated by comparing the two reactions shown [Eq. (21) vs. Eq. (22)] (9, 18, 21, 22):

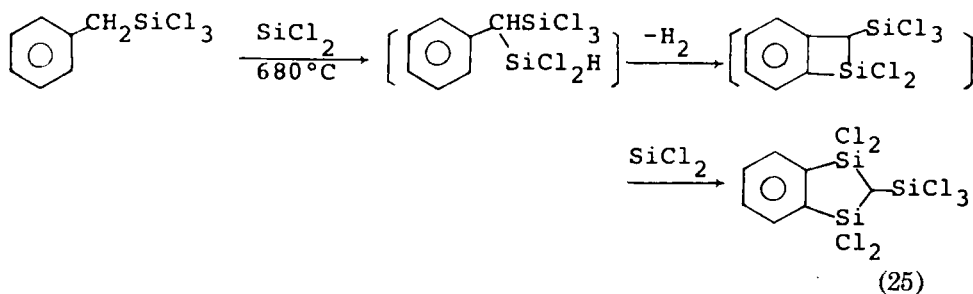
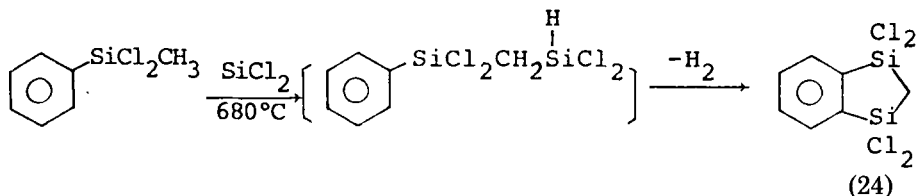


Further SiCl_2 insertion occurred in Eq. (22), but not in Eq. (21), presumably because the silacyclobutene intermediate is much more strained than silacyclopentene.

This is confirmed experimentally by the reaction in Eq. (23) (9, 32).

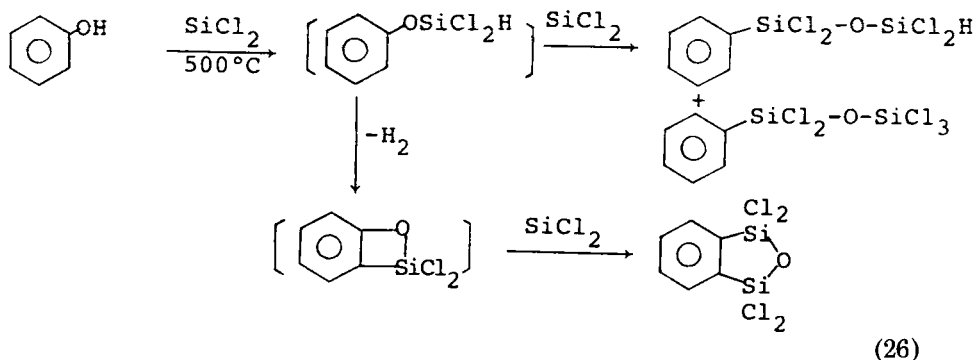


Gas-phase reactions have also shown that the $\alpha\text{-C-H}$ bond involving the α -carbon atom attached to the silicon atom is prone to SiCl_2 insertion reactions (9, 22) [e.g., Eqs. (24) and (25)].

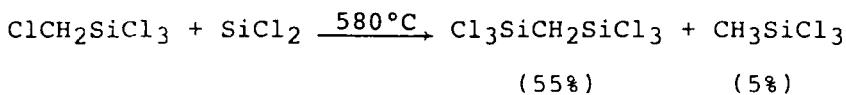
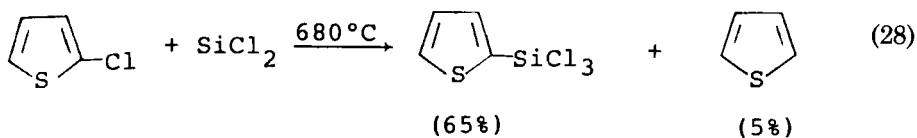
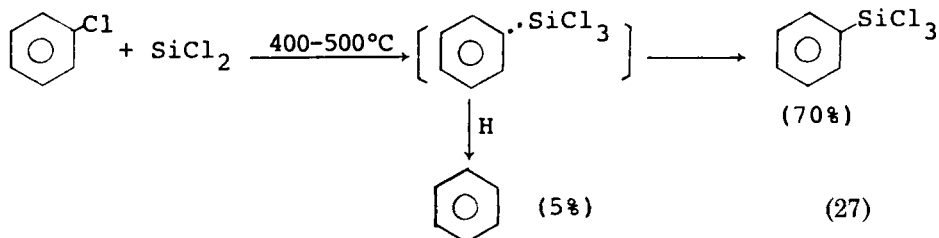


In the reaction with phenol [Eq. (26)], SiCl_2 insertions into both O-H and O-C bonds were observed. This is probably due to the unusually strong affinity of silylenes to the oxygen atom (10, 25).

Since data for the mechanistic details, such as the spin states and initial attacking site of the insertion of dichlorosilylene is lacking, inferences about the nature of the insertion reactions are at best a straightforward assumption based on the molecular structure of the final products. However, the insertion reactions of SiCl_2 into C-X bonds, which proceed through elimination-recombination steps, do resemble the chemistry of singlet carbenes (59). It seems reasonably safe



to state that SiCl_2 first extracts the halogen atom from the reactant to form a radical pair, which may either recombine to form the "insertion" product or separate to cause halogen elimination (10, 24, 26-28) [Eqs. (27)-(29)].

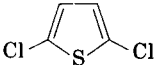
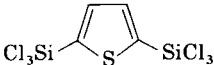
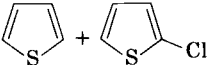
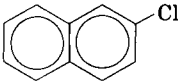
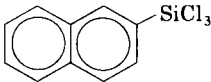
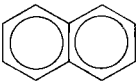
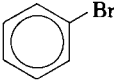
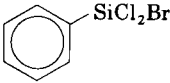
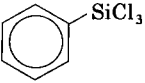
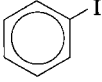
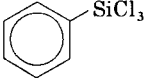
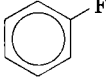
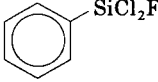
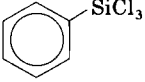
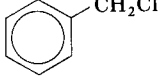
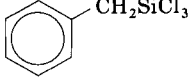
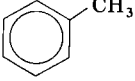
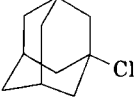
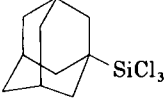


(29)

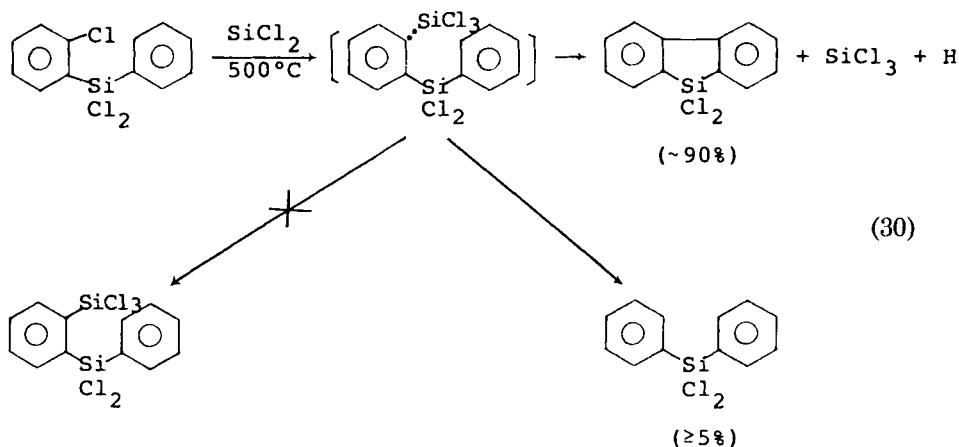
Other reactions with apparently similar mechanisms are summarized in Table I. In almost all cases, the observation of about 5% product from X-elimination/H-abstraction, though small in quantity, is a mechanistically important support to the proposal of radical pair intermediacy.

TABLE I

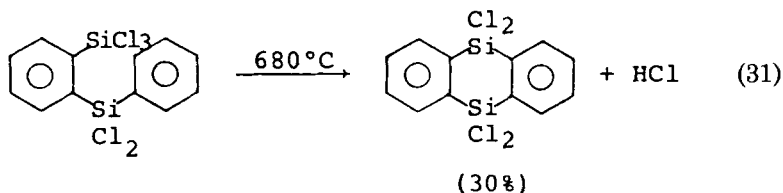
SOME INSERTION REACTIONS OF DICHLOROSILYLENE INTO C—X BONDS

Reactant	Product	
		 (5%)
	 (55%)	 (5%)
	 (22%)	 (44%)
	 (40%)	
	 (15%)	 (20%)
	 (35%)	 (5%)
	 (60%)	

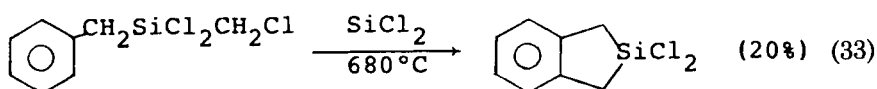
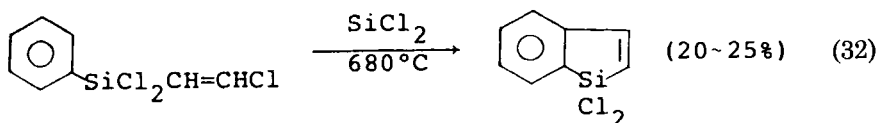
When the chlorine elimination pathway prevails, one observes mainly products from intramolecular cyclization (10, 33, 34). Although no inserted SiCl_2 group is involved in the products, the reaction mechanism [Eq. (30)] is related to the "insertion reactions" described above.

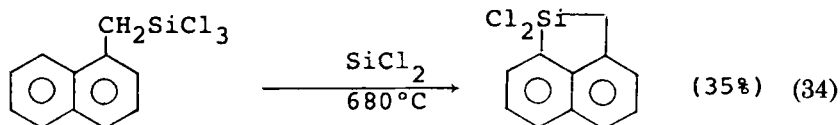


That the phenyldichlorosilylphenyl radical did not recombine with trichlorosilyl radical to form the insertion product was confirmed by the thermal decomposition reaction of *o*-trichlorosilylphenylphenyldichlorosilane, obtained by means of another preparation, which yielded a product via a different cyclization route [Eq. (31)].



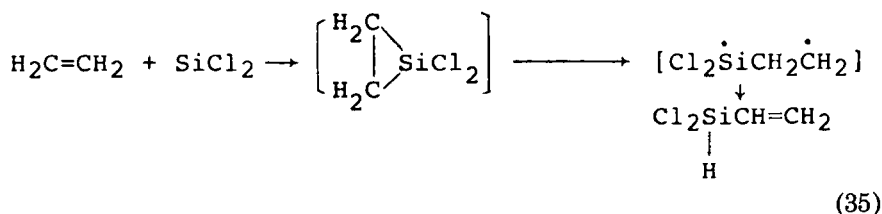
Other reactions of this type were observed with compounds involving $C_{\text{aryl}}-\text{Cl}$, $C_{\text{alkenyl}}-\text{Cl}$, $C_{\text{alk}}-\text{Cl}$, and $\text{Si}-\text{Cl}$ bonds (10, 24, 26-28, 33, 34, 87):





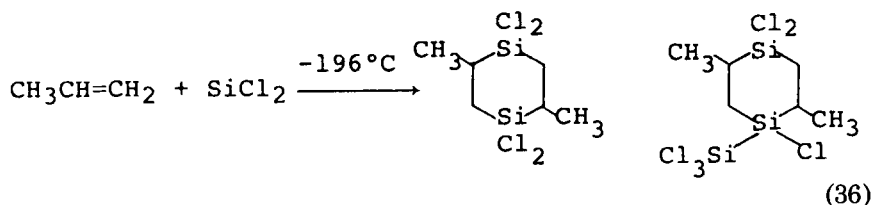
The addition reaction with an unsaturated compound is one of the most characteristic reactions of all silylenes. Alkenes and alkynes are the most popular trapping agents. As in the case of SiH_2 , it has been generally believed that the primary step is the addition of dichlorosilylene to the double bond of the alkene or to the triple bond of the alkyne to form the silirane or silirene, respectively. The success in synthesizing derivatives of dimethylsilirane and dimethylsilirene has not only confirmed the initial step but made it possible to investigate the subsequent mechanistic details by studying the chemistry of such strained silacycles (112).

No stable dichlorosilirane has been prepared. The gas-phase reaction of SiCl_2 with ethylene is best explained by formation of dichlorosilirane, which opens up and rearranges to dichlorovinylsilane (9, 30).

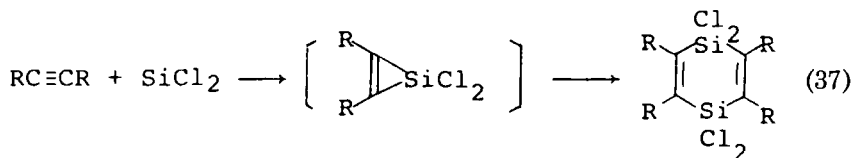


Other products of the reaction [including $\text{Cl}_3\text{SiCH}=\text{CH}_2$, $\text{Cl}_3\text{SiC}_2\text{H}_5$, $(\text{H}_2\text{C}=\text{CH})\text{Cl}_2\text{SiC}_2\text{H}_5$, and $(\text{C}_2\text{H}_5)_2\text{SiCl}_2$] are believed to be the results of secondary reactions of the intermediates.

Under cocondensation conditions, propene was reported to react with dichlorosilylene to form tetrachloro-1,4-disilacyclohexane derivatives (96, 103).



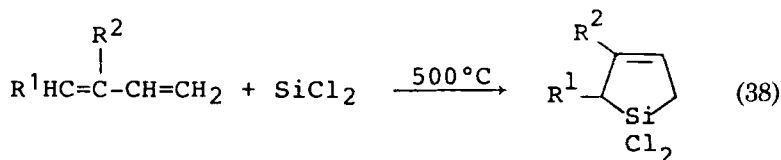
The gas-phase reactions of SiCl_2 with alkynes resulted in the formation of 1,4-disilacyclohex-2,5-dienes (9, 16, 18, 23) [Eq. (37)].



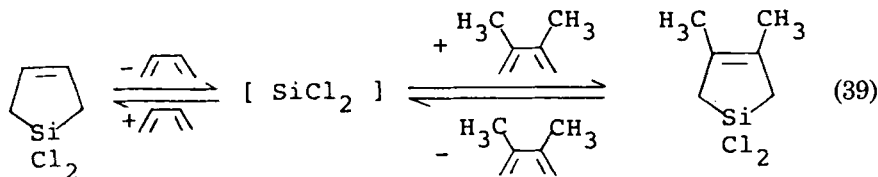
The reaction mechanism for dimerization of the silirene intermediate has been a controversial subject for many years (3, 4, 7, 45, 49, 58, 86). It is now generally accepted that in the case of dialkylsilylene, σ -dimerization is probably the true mechanism. Dichlorosilylene is expected to behave similarly.

The reaction of dichlorosilylene with acetylene carried out by a co-condensation experiment also yielded 1,4-disilacyclohexa-2,5-diene, but the result was regarded as unreliable (103, 104).

Studies on the gas-phase reactions of dichlorosilylene with conjugated dienes provided more systematic information about the addition reactions of dichlorosilylene (1, 10, 15, 16, 20, 30, 91):



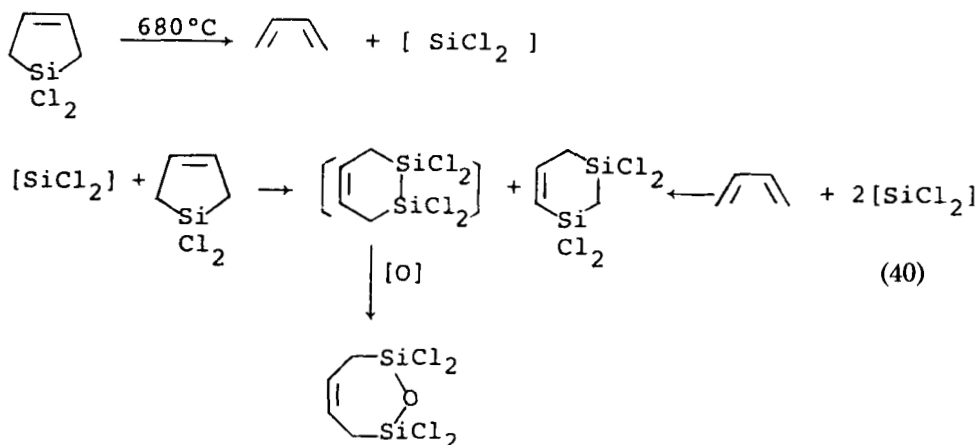
where $\text{R}^1=\text{H}, \text{CH}_3$; $\text{R}^2=\text{H}, \text{CH}_3, \text{Cl}, \text{C}_6\text{H}_5$. The reaction was found to be reversible, as the following reactions [Eq. (39)] were established experimentally:



The decomposition of dichlorosilacyclopent-3-ene has been proved to be unimolecular by the study of inert dilution. The mass spectral study suggested that the decomposition was concerted, and, in the opinion of the investigators, it corresponded formally to the retro Diels-Alder reaction (13, 29). Thus the reaction in Eq. (38) was believed to proceed via a concerted 1,4-cycloaddition.

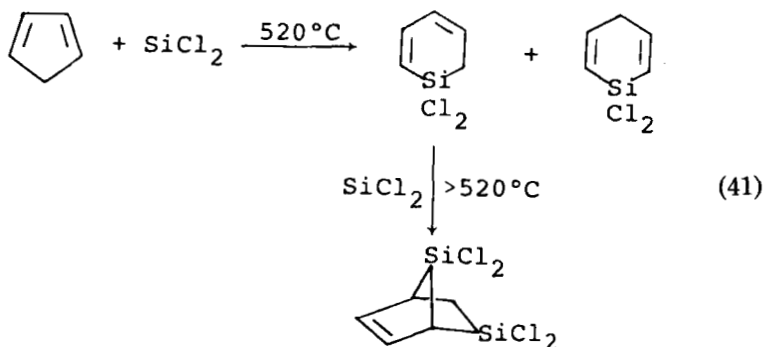
Above 500°C dichlorosilacyclopent-3-ene can be converted to disilacycles in the absence of trapping agent. The dichlorosilylene, formed

by the retro-diene decomposition, was presumed to react with either the initial silacyclopentene or the intermediate diene (29) [Eq. (40)].



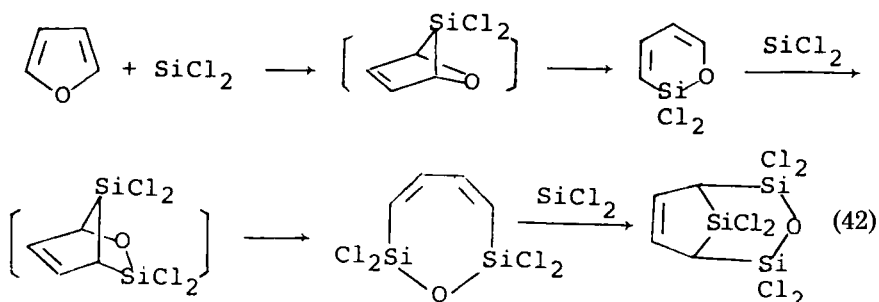
In view of the well-established silirane diradical mechanism in reactions of silylene [Eq. (10)] and dimethylsilylene (40, 62), and the involvement of difluorosilane in the gas-phase reaction of difluorosilylene [Eq. (61), Section IV], it is somewhat surprising to find that dichlorosilylene alone should take a concerted 1,4-addition route toward butadiene. Further studies are needed to settle this argument.

The gas-phase reaction of dichlorosilylene with cyclopentadiene yielded silacyclohexadienes as the major products, one of which underwent further SiCl_2 insertion to form a bicyclic product (31).

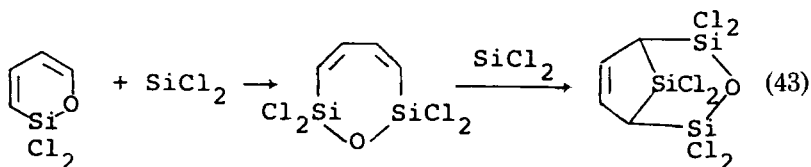


The reaction with furane apparently proceeded via a similar route (9, 16, 20). Here, because of the strong affinity of silicon for oxygen,

consecutive 1,4-cycloaddition was proposed which was subjected to a subsequent ring expansion process:

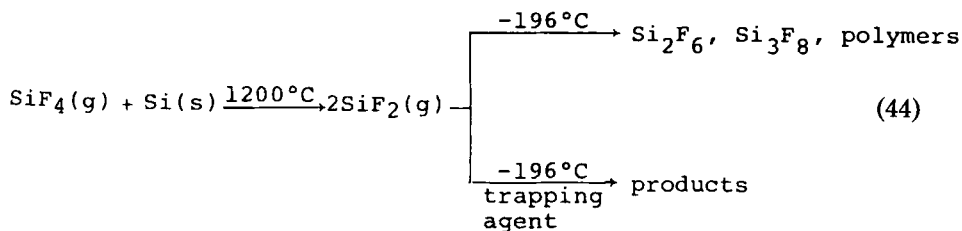


The instability of the two bicyclic intermediates involving oxaheterocycle can be rationalized by the energetic advantage of Si—O—(Si) bond formation. The reaction mechanism is supported by the observation of the following reactions:

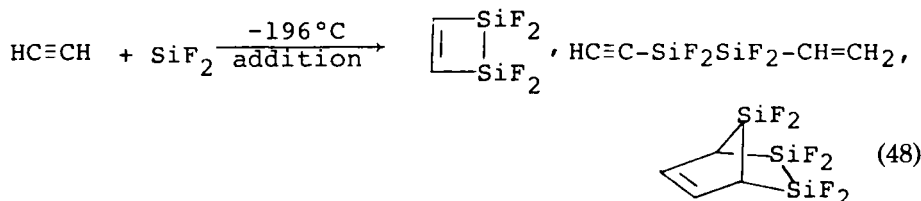
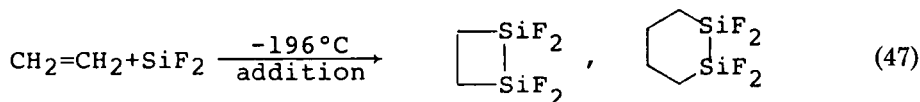
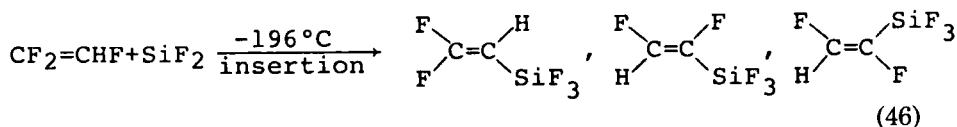
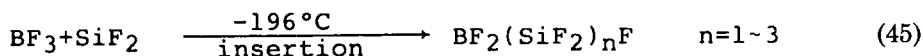


IV. Chemistry of Difluorosilylene

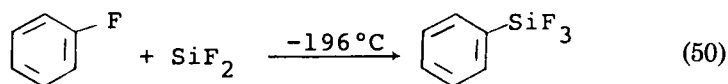
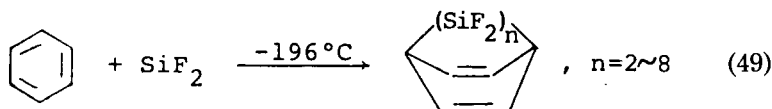
Difluorosilylene has always been considered the exceptional case of the silylene family. Unlike other silylenes, difluorosilylene had been believed to be quite inactive chemically in the gas phase (73). As a result, most studies of its chemistry were carried out under cocondensation conditions (73, 103, 104, 106, 108). At -196°C , difluorosilylene forms a pale yellowish condensate, which polymerizes and forms small quantities of volatile perfluoropolysilanes (10% of the total yield) when the reaction trap is warmed to room temperature.



Earlier studies on the chemistry of difluorosilylene were focused on the reactions with nonmetal halides (8, 72, 77, 105, 106, 109) and unsaturated organic compounds (65-69, 77). [e.g., Eqs. (45)-(48)].



The reactions of difluorosilylene with olefins and fluoroolefins [e.g., Eqs. (46) and (47)] appear to proceed by quite different pathways. Similarly, the reaction with benzene resulted in addition products (71, 107) [Eq. (49)], whereas reaction with fluorobenzene led to insertion products (107) [Eq. (50)].

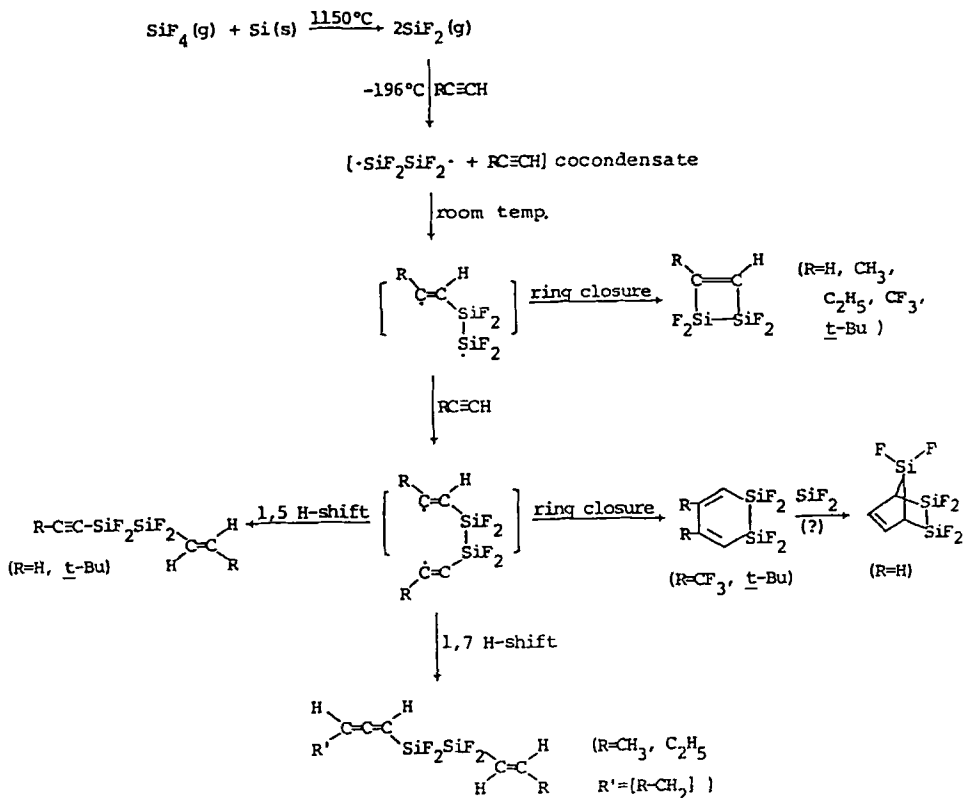


According to these earlier studies, a reaction mechanism involving diradical intermediates of the type $(\text{SiF}_2)_n$ (where $n = 1, 2, 3$, etc.) was established (70, 73, 80). This idea is particularly attractive if one considers the facts that in co-condensation reactions polymers are the major products obtained, and that volatile products of co-condensation reactions often contain $(\text{SiF}_2)_n$ units with $n > 1$. The earlier ESR study also supported this idea (52).

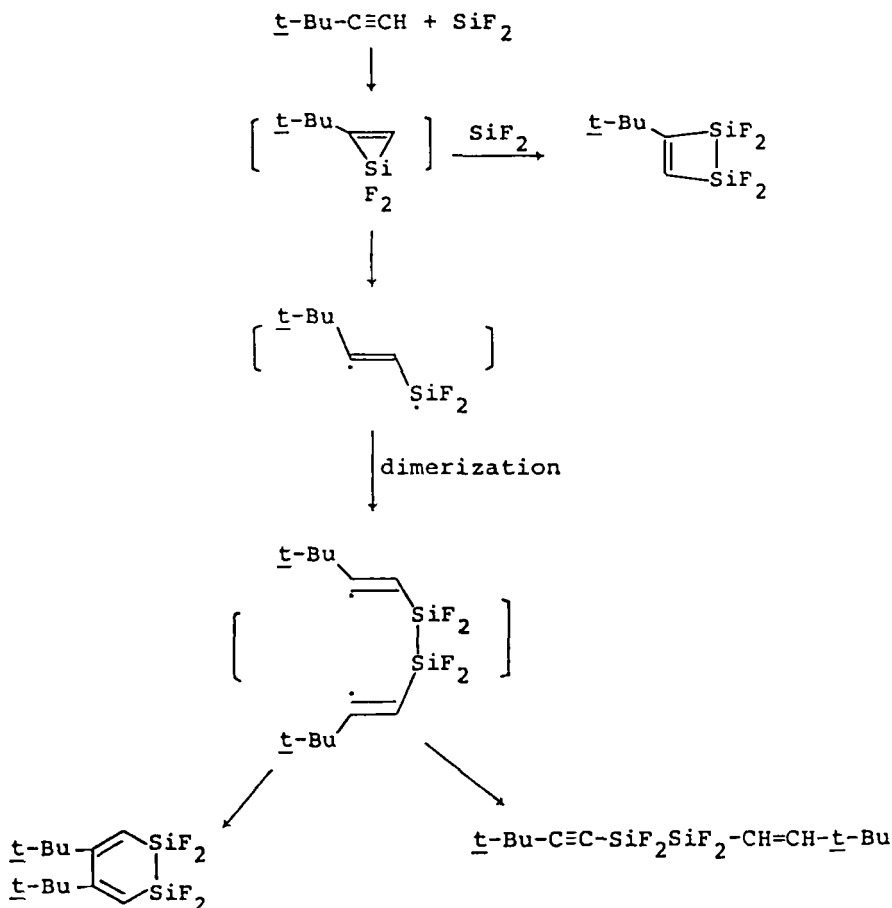
For addition reactions with unsaturated organic compounds, all the reaction products contained the $-\text{SiF}_2\text{SiF}_2-$ moiety, which led to the conclusion that the most reactive species in these co-condensation reactions must be the $\cdot\text{SiF}_2\text{SiF}_2\cdot$ diradical (65, 66). The reaction mechanism for alkyne system is illustrated in Scheme 1.

When such an $(\text{SiF}_2)_n$ polymer (or oligomer) mechanism was cited in the literature, one could not but wonder whether difluorosilylene behaved as a "carbene analogue" at all. With considerable foresight, Gaspar and Herold stated more than a decade ago (39), "in view of the poor Si—Si π interaction and the relative weakness of Si—Si single bond, it is very likely that characteristic reactions of difluorosilylene other than polymerization will be found in the near future."

More recently, the synthesis and chemistry of 2,2,3,3-tetramethyl-1,1-difluoro-1-silirane, a long sought possible intermediate species of monomeric SiF_2 chemistry, suggested an alternative reaction mechanism for the addition reactions of SiF_2 with both alkenes and alkynes



SCHEME 1



SCHEME 2

(91).¹ For example, the reaction with *t*-Bu—C≡CH is illustrated in Scheme 2.

It has been reported that the ²⁹Si NMR spectrum of the soluble part of the polymer, which accounted for 70% of the total products in the cocondensation reaction of SiF₂ and propene, was consistent with the structure [$\text{>C}(\text{CH}_3)\text{—CH}_2\text{SiF}_2\text{—}]_n$. This is strong evidence supporting the silirane mechanism (110).

Both schemes explain the results of the "addition" reactions of SiF₂ with alkynes and alkenes well. However, neither of these two mecha-

¹ Tetramethyl-1,1-difluoro-1-silirane is the only difluorosilirane ever prepared. Statements about the reactions of nonsubstituted difluorosilirane appear in refs. 48 and 113.

nisms satisfactorily accounts for the details of the "insertion" reactions between SiF_2 and fluoroalkenes.

Three questions closely related to the reaction mechanism must be answered before any conclusion can be reached:

1. Why does SiF_2 "add" to alkenes but "insert" into the C—F bond of fluoroalkenes?

2. In the insertion reactions does SiF_2 attack the C—F bond directly, or does it attack the C=C double bond and then rearrange to the insertion products?

3. For both addition and insertion reactions, which one, the monomeric difluorosilylene or the diradicals $\cdot(\text{SiF}_2)_n\cdot$, is the true reaction intermediate?

Questions (1) and (2) above are actually the problem of addition vs. insertion. When the reactions of SiF_2 with *trans*- and *cis*- $\text{CHF}=\text{CHF}$ were carried out under co-condensation conditions (64), all products were found to be insertion products, with no silacyclopropanes or disilacyclobutanes being observed [Eqs. (51) and (52)]. The most interesting result is the fact that both reactions appear to be nonstereospecific. The relative abundances of the various isomers of the insertion products are shown in Table II.

TABLE II

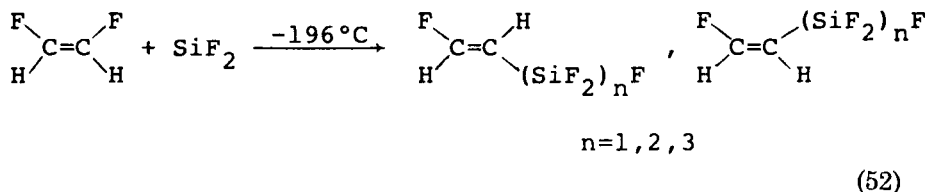
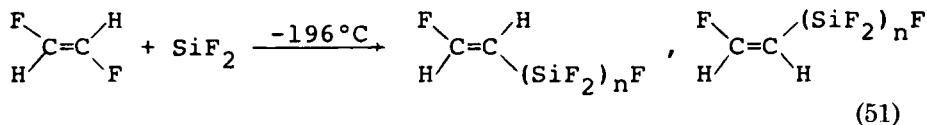
RELATIVE YIELDS OF THE VOLATILE PRODUCTS OF THE REACTIONS WITH
trans- AND *cis*- $\text{CHF}=\text{CHF}$ IN VARIOUS CONDITIONS

Reaction product	Relative yield ^a (%)					
	Cocondensation		Alternate layer		Gas phase	
	<i>cis</i> ^b	<i>trans</i> ^c	<i>cis</i> ^b	<i>trans</i> ^c	<i>cis</i> ^b	<i>trans</i> ^c
<i>trans</i> - $\text{CHF}=\text{CHSiF}_3$	5 (77)	16 (62)	6 (78)	18 (64)	64	64
<i>cis</i> - $\text{CHF}=\text{CHSiF}_3$	17	10	21	10	36	36
<i>trans</i> - $\text{CHF}=\text{CHSiF}_2\text{SiF}_3$	6 (88)	57 (85)	8 (86)	43 (77)		
<i>cis</i> - $\text{CHF}=\text{CHSiF}_2\text{SiF}_3$	44	10	51	13		
<i>trans</i> - $\text{CHF}=\text{CHSiF}_2\text{SiF}_2\text{SiF}_3$	2 (93)	6 (86)	2 (86)	13 (81)		
<i>cis</i> - $\text{CHF}=\text{CHSiF}_2\text{SiF}_2\text{SiF}_3$	26	1	12	3		

^a Numbers in parentheses are the percentage of configuration retention.

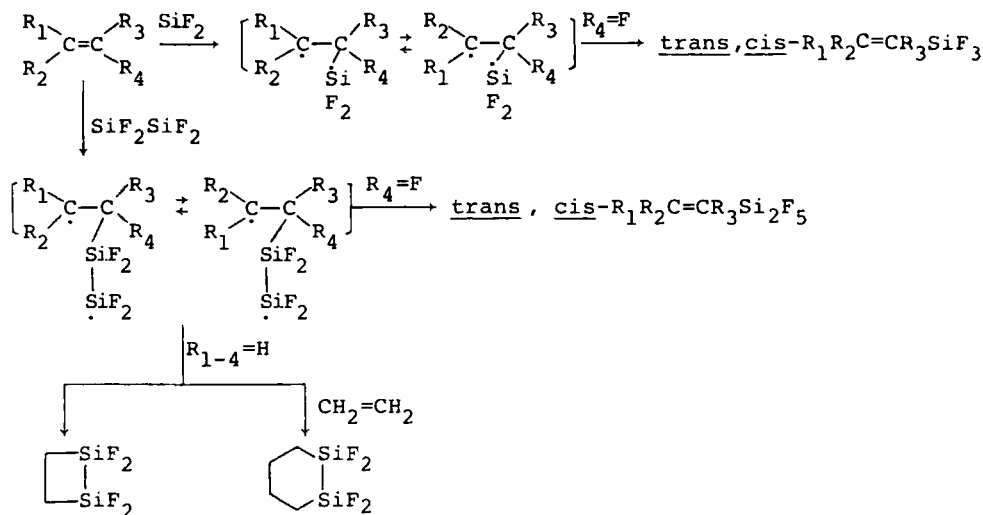
^b *cis*, Reaction with *cis*- $\text{CHF}=\text{CHF}$.

^c *trans*, Reaction with *trans*- $\text{CHF}=\text{CHF}$.



Since no trans-cis isomerization of the starting materials was observed, the only reasonable reaction path which leads to both trans and cis isomers of the product of each reaction is an initial attack of $(\text{SiF}_2)_n$ on the carbon-carbon double bond, followed by rearrangement. The higher ratio of configuration retention for the reaction of *cis*-difluoroethylene agrees with the known fact that *cis*-CHF=CHF is more stable than its trans isomer (12).

This type of reaction pattern can be extended to $(\text{SiF}_2)_3$ or even higher units. In fact, both addition and insertion products involving trimeric SiF_2 units are known (77, 105, 107, 109). In this reaction scheme (Scheme 3) both insertion and addition reactions can be rationalized



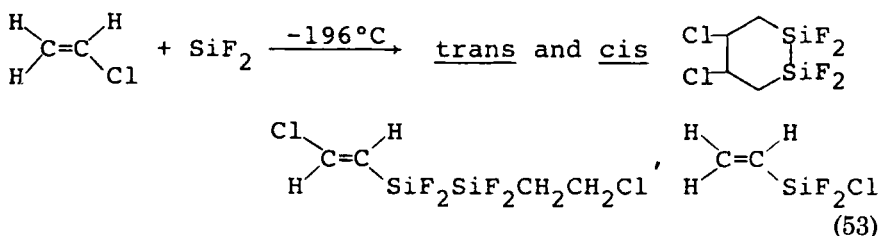
SCHEME 3

with the same initial attack of $(\text{SiF}_2)_n$ on the double bond, monomeric SiF_2 being no exception. Fluorine atoms cause the different preferences in reaction paths after the initial attack.

The bond energies decrease in the order $\text{Si}-\text{F} > \text{C}-\text{F} > \text{C}-\text{H} > \text{Si}-\text{H}$ (Table III). The formation of an exceedingly strong $\text{Si}-\text{F}$ bond in the insertion reactions must have contributed to the driving force of insertion whenever a fluorine is attached to an olefinic carbon.

Since the difference in bond energies between $\text{Si}-\text{X}$ and $\text{C}-\text{X}$ decreases with increasing halogen atomic weight (Table III), somewhere along the line one should expect to observe both insertion and addition products from the same reaction, which would reflect the competitive preference of insertion vs. addition after the initial attack of the oligomeric difluorosilylene.

The co-condensation reaction of SiF_2 with vinyl chloride produced, in addition to the addition products, a small quantity of insertion product. However, here the results mainly reflect the very large difference in the preference of initial radical attack on the two sides of the double bond (63).



The true competitive preference of insertion vs. addition is shown in the cocondensation reactions of SiF_2 with *cis*- and *trans*- $\text{CHCl}=\text{CHCl}$.

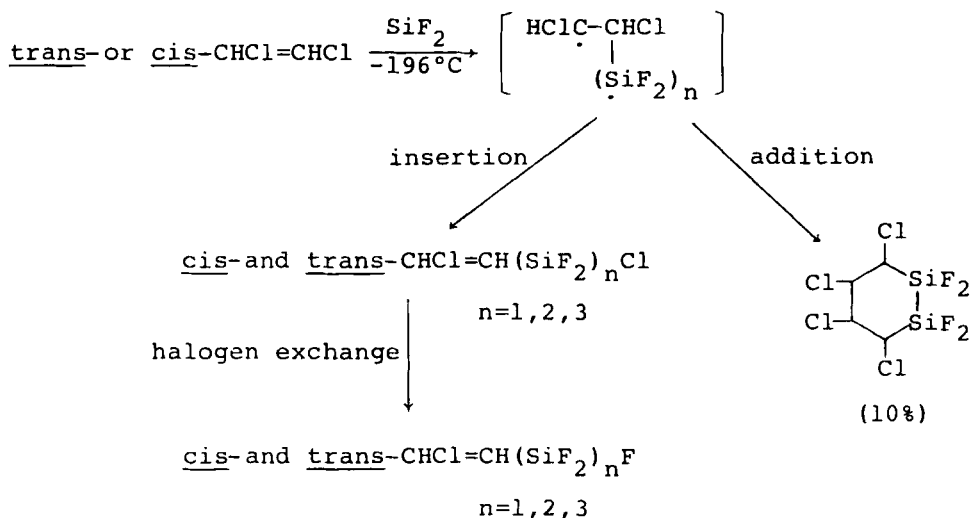
TABLE III

BOND ENERGIES^a OF $\text{Si}-\text{X}$ AND $\text{C}-\text{X}$

X	$\text{Si}-\text{X}(\text{kcal/mol})$	$\text{C}-\text{X}(\text{kcal/mol})$	$\Delta(\text{kcal/mol})^b$
F	135	116	19
Cl	91	78.2	12.8
Br	74	68	6
I	56	51	5
H	76	98.3	-22.3

^a Data taken from ref. 54.

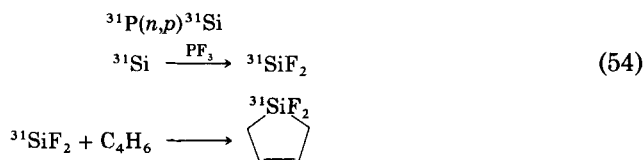
^b $\Delta = (\text{Bond energy})_{\text{Si}-\text{X}} - (\text{bond energy})_{\text{C}-\text{X}}$



SCHEME 4

Indeed both insertion and addition products were obtained (56b). The reactions are best interpreted by the mechanism shown in Scheme 4.

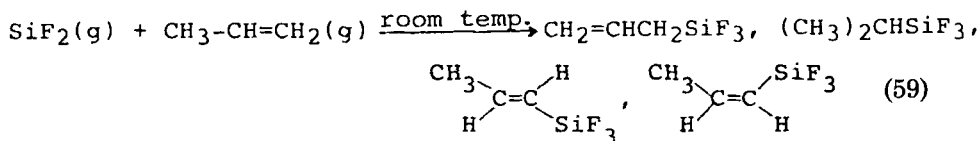
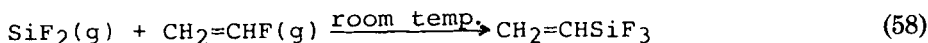
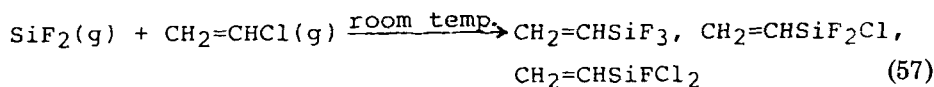
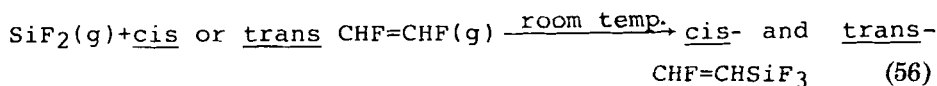
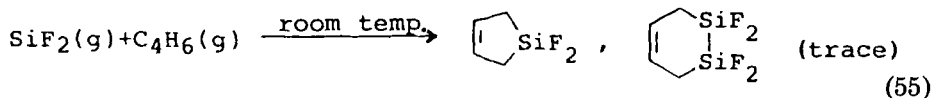
Although a number of cocondensation reactions ($\text{SiF}_2/\text{H}_2\text{O}$, $\text{SiF}_2/\text{H}_2\text{S}$, $\text{SiF}_2/\text{C}_6\text{F}_6$, etc.) (73, 103) yielded products containing only one SiF_2 unit, monomeric SiF_2 in the gas phase has for many years been considered not reactive. One exception is the study of the reaction of ethylene and conjugated dienes with $^{31}\text{SiF}_2$ formed in nuclear recoil systems (95, 117). The $^{31}\text{SiF}_2$ molecules generated in such system may possess different properties from those generated thermally, and the reaction conditions are very different; nevertheless, the work does show that monomeric $^{31}\text{SiF}_2$ in the gas phase is reactive toward unsaturated organic compounds.



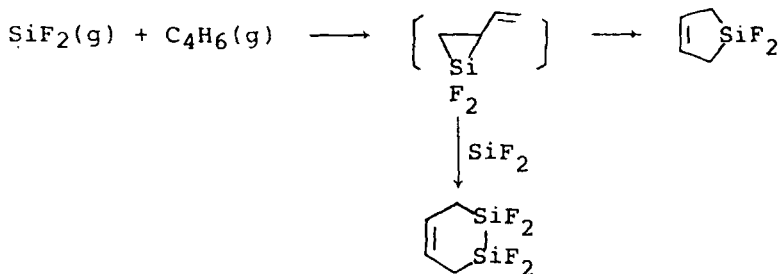
The singlet to triplet $^{31}\text{SiF}_2$ ratios evaluated from these diene systems are all around 1:3. It was proposed that triplet $^{31}\text{SiF}_2$ formed $^{31}\text{SiF}_2\cdot$ donor complexes with paramagnetic molecules such as NO, NO_2 , or O_2 before reacting with dienes.

Since a study on the competitive reactions of $^{31}\text{SiH}_2$ with silane, methylsilane, and butadiene has rejected the possibility of triplet involvement (41), the role of triplet $^{31}\text{SiF}_2$ in the present case will have to be subjected to further confirmation.

More recently, it has been found that under proper conditions thermally generated SiF_2 also reacted in reasonably good yield with 1,3-butadiene, *cis*- and *trans*-difluoroethylenes, vinyl chloride, vinyl fluoride, and propene in the gas phase [Eqs. (55)–(59)].



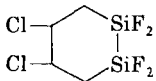
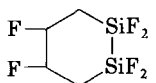
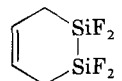
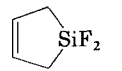

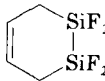
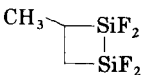
Except the trace amount of 1,2-disilacyclohex-4-ene obtained in the reaction of butadiene, all products in the gas phase consist of only one SiF_2 unit. The formation of 1,2-disilacyclohex-4-ene could be the result of further reaction of the silirane intermediate with SiF_2 (55) (Scheme 5).

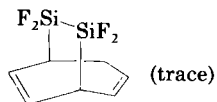
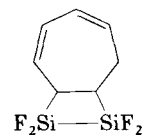
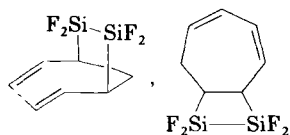
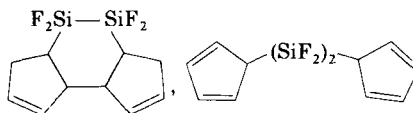
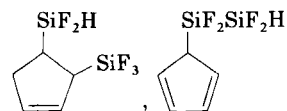
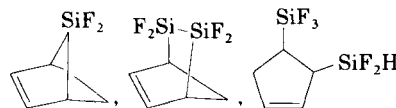
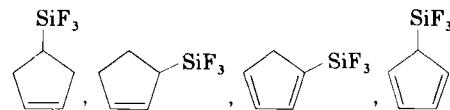
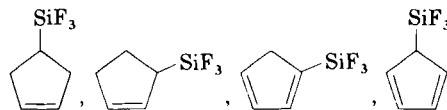
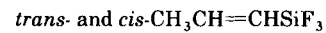
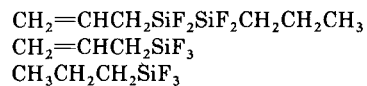
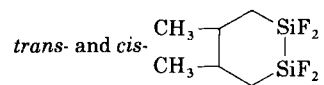


SCHEME 5

TABLE IV

PRODUCTS FROM THE DIFLUOROSILYLENE REACTIONS UNDER VARIOUS EXPERIMENTAL CONDITIONS

Reaction	Experimental conditions	
	Cocondensation	Gas phase
<i>trans</i> -CHF=CHF	<i>trans</i> - and <i>cis</i> -CHF=CHSiF ₃ <i>trans</i> - and <i>cis</i> -CHF=CHSiF ₂ SiF ₃ <i>trans</i> - and <i>cis</i> -CHF=CHSiF ₂ SiF ₂ SiF ₃	<i>trans</i> - and <i>cis</i> -CHF=CHSiF ₃
CH ₂ =CHCl	CH ₂ =CHSiClF ₂ (trace) CHCl=CHSiF ₂ SiF ₂ CH ₂ CH ₂ Cl <i>trans</i> - and <i>cis</i> - 	CH ₂ =CHSiClF ₂ CH ₂ =CHSiCl ₂ F CH ₂ =CHSiF ₃
CH ₂ =CHF	CH ₂ =CHSiF ₃ CH ₂ =CHSiF ₂ SiF ₃ <i>trans</i> - and <i>cis</i> -  (CH ₂ =CH) ₂ SiF ₂	CH ₂ =CHSiF ₃
CH ₂ =CH-CH=CH ₂	 CH ₂ =CHCH=CHSiF ₂ SiF ₂ CH ₂ CH ₂ CH=CH ₂  (trace)	  (trace)
CH ₃ CH=CH ₂		(CH ₃) ₂ CHSiF ₃ CH ₂ =CHCH ₂ SiF ₃



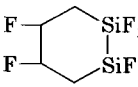
A comparison of the products from cocondensation and gas-phase experiments of each reaction is shown in Table IV. It is interesting to note that the ratio of relative yield of *trans*-CHF=CHSiF₃ to *cis*-CHF=CHSiF₃ is constant (64:36) in both reactions of *trans*- and *cis*-CHF=CHF carried out in the gas phase, which is in sharp contrast to the results of co-condensation reactions (Table II). This is rationalized by the fact that under the experimental conditions of the gas-phase reactions the reaction product CHF=CHSiF₃, when initially formed in the gas phase, would carry approximately 95 kcal/mol of energy, which is much more than the activation energy of *cis*/*trans* isomerization of various substituted ethylenes (50–60 kcal/mol) (11); therefore the constant ratio of *trans*/*cis* products actually reflects the thermodynamic distribution according to the energies of the products, namely *trans*- and *cis*-CHF=CHSiF₃.

When the cocondensation reactions are carried out at –196°C, the kinetic competition of the radical species among various reaction pathways becomes a controlling factor. It is therefore quite reasonable to observe the various relative yields of *trans* and *cis* products in these cocondensation reactions (Table II).

The reaction of difluorosilylene with vinyl fluoride in the gas phase gives apparently only one product in good yield, CH₂=CHSiF₃ (56a). The reaction under cocondensation conditions produced CH₂=CHSiF₃, CH₂=CHSiF₂SiF₃, 4,5-difluoro-1,1,2,2-tetrafluoro-1,2-disilacyclohexane (1) and divinylldifluorosilane (2). The relative yields of CH₂=CHSiF₃, CH₂=CHSiF₂SiF₃, (2), and (1) are 18:23:35:24 (Table V).

TABLE V

RELATIVE YIELDS OF VOLATILE PRODUCTS OF THE REACTION OF DIFLUOROSILYLENE WITH VINYL FLUORIDE IN VARIOUS CONDITIONS

Reaction product	Reactive yield (%)				Gas phase
	Cocondensation		Alternate layer		
	<i>a</i>	<i>b</i>	<i>a</i>	<i>b</i>	
CH ₂ =CHSiF ₃	18	57	20	55	100
CH ₂ =CHSiF ₂ SiF ₃	23	5	25	6	
(CH ₂ =CH) ₂ SiF ₂	35	28	36	30	
	24	10	19	9	

^a Volatile products from reactions under various conditions.

^b Products from pyrolysis (at 100°C) of the polymers obtained under various reaction conditions.

One may suspect that vinyltrifluorosilane, which was the major product in the gas-phase reaction (Table IV), might have come from the gas-phase reaction prior to condensation. To clarify this point, the co-condensation experiment was carried out in an "alternate layer" manner so that no gas mixing was allowed. The results are summarized in Table II and Table V.

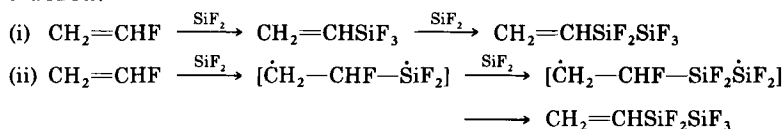
The products of the alternate layer reactions between SiF_2 and *trans*- $\text{CHF}=\text{CHF}$, $\text{CH}_2=\text{CHCl}$, $\text{CH}_2=\text{CHF}$, and C_4H_6 are found to be the same as those in the corresponding cocondensation experiments; only the absolute yields are substantially reduced due to poor mixing of the reagents in such alternate layer experiments. The most important observation is that the relative yields of the products do not differ significantly from those of the cocondensation experiments. For example, a carefully controlled "alternate layer" reaction was studied quantitatively for the reaction of $\text{CH}_2=\text{CHF}$. The relative yields of $\text{CH}_2=\text{CHSiF}_3$, $\text{CH}_2=\text{CHSiF}_2\text{SiF}_3$, (2), and (1) were found to be 20:25:36:19, very close to those in the co-condensation experiment. These results indicate that the formation of $\text{CH}_2=\text{CHSiF}_3$ in the gas phase prior to condensation contributes negligibly to the yield of $\text{CH}_2=\text{CHSiF}_3$ in the co-condensation experiment, and the reaction taking place at -196°C did involve monomeric SiF_2 .

The polymer formed in the reaction of $\text{CH}_2=\text{CHF}$ decomposes under mild conditions. When the yellowish polymer was pyrolyzed, the products include SiF_4 , Si_2F_6 , Si_3F_8 , $\text{CH}_2=\text{CHSiF}_3$, $\text{CH}_2=\text{CHSiF}_2\text{SiF}_3$, $(\text{CH}_2=\text{CH})_2\text{SiF}_2$, and (1). The relative yield of the last four compounds was found to be 57:5:28:10 (Table V).

For comparison, the polymer obtained in the alternate layer condensation experiment was also subjected to pyrolysis. The same products were obtained in much poorer total yield, but the ratio of relative yield of $\text{CH}_2=\text{CHSiF}_3$, $\text{CH}_2=\text{CHSiF}_2\text{SiF}_3$, $(\text{CH}_2=\text{CH})_2\text{SiF}_2$, and (1) was found to be 55:6:30:9, almost the same as that of the co-condensation experiment (Table V).

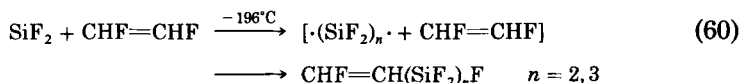
The observation of $\text{CH}_2=\text{CHSiF}_2\text{SiF}_3$ from pyrolysis of the polymer, though in relatively small quantity, strongly suggests that $(-\text{CH}_2-\text{CHF}-\text{SiF}_2\text{SiF}_2-)$ units are involved in the polymer.

There remains an ambiguity about the formation of $\text{CH}_2=\text{CHSiF}_2\text{SiF}_3$ [and also $\text{CHF}=\text{CH}(\text{SiF}_2)_n\text{F}$, $n = 2, 3$, in the reactions of *trans*- and *cis*- $\text{CHF}=\text{CHF}$]. Two possible reaction pathways could be considered:



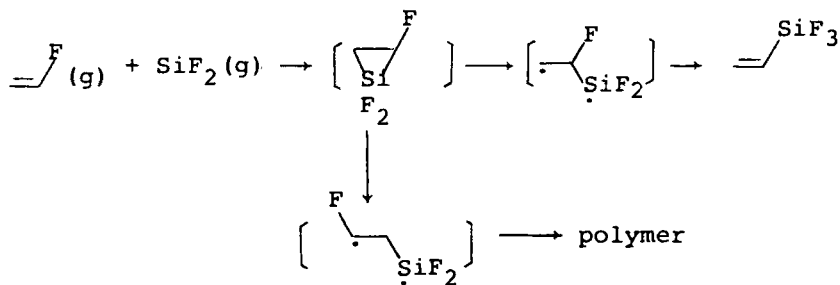
Path (i) is ruled out because in both gas-phase and co-condensation experiments no further insertion of SiF_2 was observed when pure $\text{CH}_2=\text{CHSiF}_3$ and SiF_2 were mixed. Path (ii) was not favored because the ratio of configurational retention of the products $\text{CHF}=\text{CH}(\text{SiF}_2)_n\text{F}$ in the reactions of *trans*- and *cis*- $\text{CHF}=\text{CHF}$ increases with n , the number of SiF_2 units involved in the products; for example, in the reaction of *trans*- $\text{CHF}=\text{CHF}$, 62% for $n = 1$, 85% for $n = 2$, and 86% for $n = 3$ (Table II). If reactions occurred according to (ii), one would expect the order of the retention ratio to be reversed.

On the other hand, if the products $\text{CHF}=\text{CH}(\text{SiF}_2)_n\text{F}$ are formed through direct attack at the carbon-carbon double bond by $\cdot(\text{SiF}_2)_n\cdot$ diradicals, the intermediates $\dot{\text{C}}\text{HF}-\text{CH}(\text{SiF}_2)_n\text{F}$ find a facile path for F migration via either a four-centered (for $n = 2$) or five-centered (for $n = 3$) transition state.



Having clarified the points mentioned above, it seems possible now to draw some conclusions about the reaction mechanism. The reactions of SiF_2 in the gas phase seem rather simple. Difluorosilylene behaves quite similarly to the chemistry of other silylenes. The initial attack of SiF_2 at the carbon-carbon double bond is followed by rearrangement whenever possible. Otherwise it may lead to polymerization. For example, $\text{CH}_2=\text{CHF}$ reacts according to the mechanisms in Scheme 6.

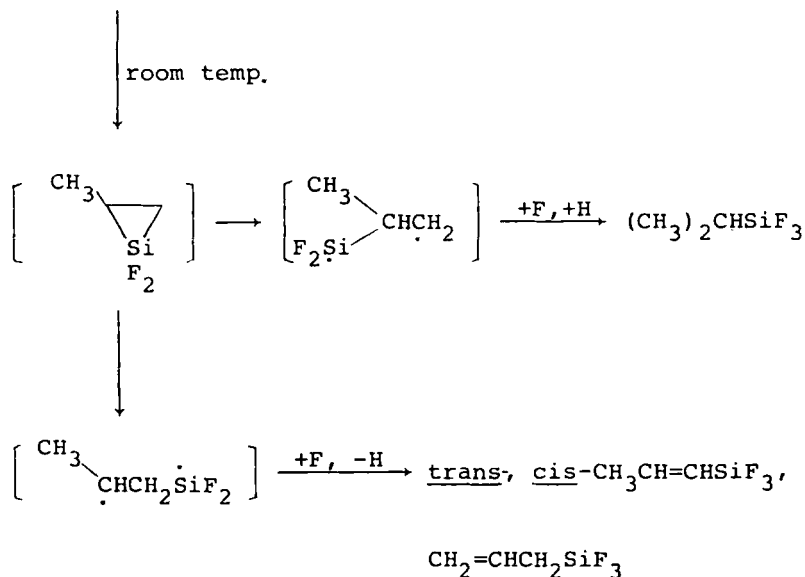
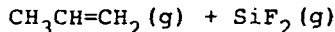
The reactions in cocondensation conditions are much more complicated. If silirane does exist as an intermediate, for example, in the case of $\text{CH}_2=\text{CHF}$, the pathway shown in Scheme 7 can be proposed. Paths a and b (Scheme 7) are the two ways of cleavage of the silirane. Path a_3 results in the product $\text{CH}_2=\text{CHSiF}_3$. Paths a_1 , a_2 and b_1 , b_2 lead to all possible dimerizations of the diradicals from ring opening,



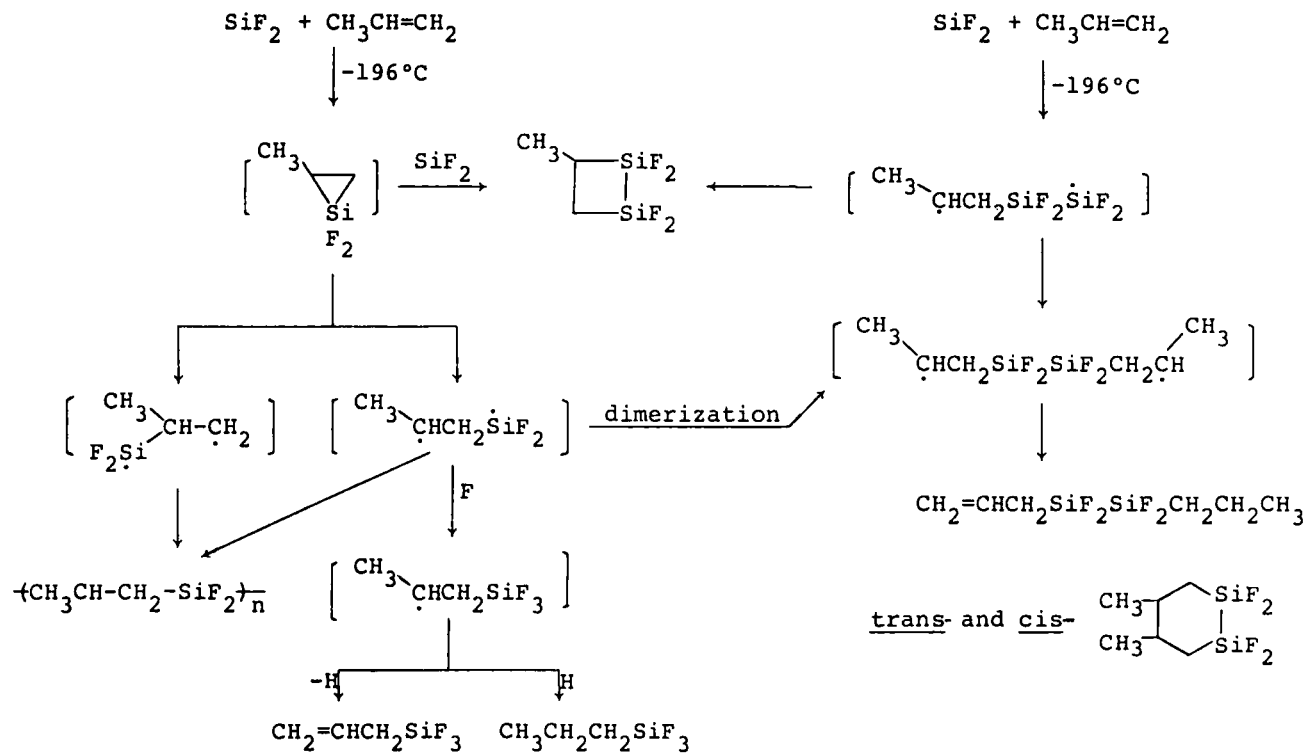
SCHEME 6

respectively, which are in turn involved in polymerization. In the case of b_2 , ring closure may lead to the product disilacyclohexane. All other products from pyrolysis of the polymers are verified experimentally. Path c represents the other possible pathway, the link of the two different radicals from ring opening of the silirane. This path leads to the formation of $(CH_2=CH)_2SiF_2$. Although it seems conceivable to obtain $CH_2=CHSiF_2SiF_3$ from the polymer pyrolysis, the observation of this compound in the cocondensation reaction cannot be explained without raising more skeptical assumptions in this reaction scheme based solely on the silirane intermediate. On the other hand, if the $\cdot SiF_2SiF_2 \cdot$ diradical is involved, the formation of $CH_2=CHSiF_2SiF_3$ becomes straightforward. While the extent each mechanism contributes may vary from reaction to reaction, one tends to conclude that both are generally involved in the cocondensation experiments.

This is true not only for halogen-substituted ethylenes. The reactions of alkyl-substituted ethylenes (82, 83, 93) seem to follow the same reaction mechanisms. The products from the reaction of propene under various reaction conditions are summarized in Table IV. The overall picture of the reaction is illustrated in Schemes 8 and 9 (93). These reaction mechanisms seem to be generally applicable. Studies on the reactions with cyclic olefins could serve as a further evidence (61, 78).



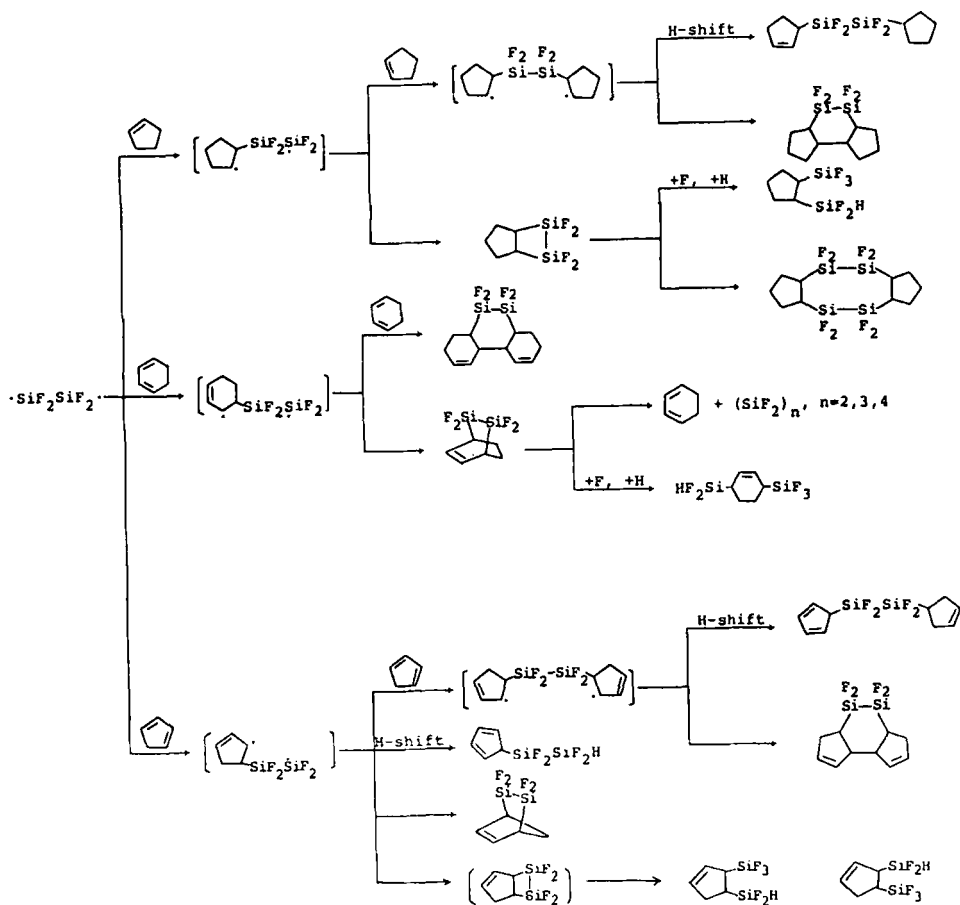
SCHEME 8



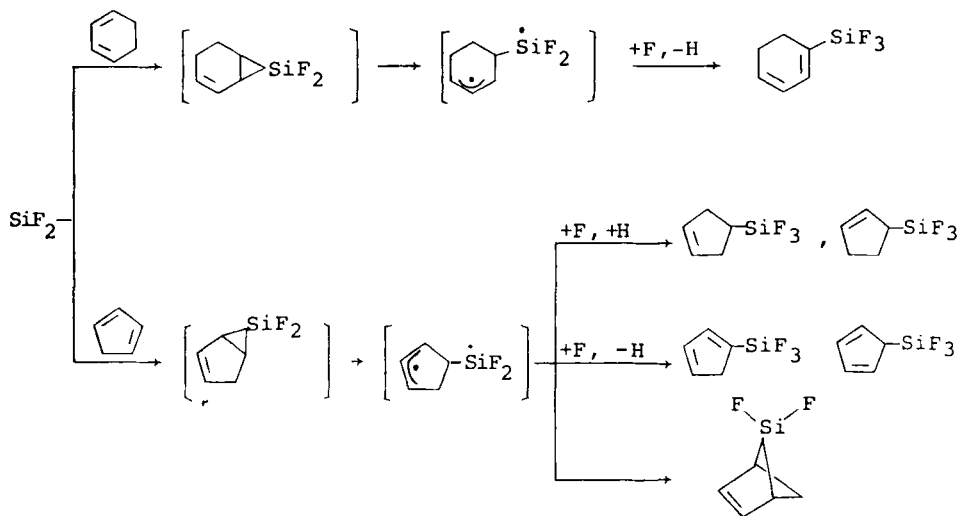
SCHEME 9

The cocondensation reactions with cyclopentene, cyclohexa-1,3-diene, and cyclopentadiene give structurally interesting products which are shown in Schemes 10 and 11 (61, 78). Since products involving both SiF_2 and $-\text{SiF}_2\text{SiF}_2-$ are obtained, it is quite possible that both silirane and $\cdot\text{SiF}_2\text{SiF}_2\cdot$ mechanisms are involved. For the latter mechanism, Scheme 10 summarizes the three reactions involved. Scheme 11 illustrates the reactions involving monomeric SiF_2 .

The gas-phase reaction of cyclopentadiene gives the same products involving monomeric SiF_2 units (Table IV). These are the products from genuine difluorosilylene reactions, quite parallel to the chemistry of other silylenes.



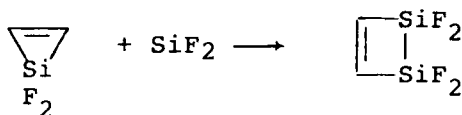
SCHEME 10



SCHEME 11

Reasonable as the mechanisms seem to be, a closer examination of the reaction scheme immediately reveals that all products involving two SiF_2 units can be explained equally well by the mechanism involving silirane intermediates, which dimerize either directly or followed by hydrogen-shift to form the observed products. The strategy used to differentiate these two mechanisms for insertion products in the reaction of vinyl fluoride was simple: choosing a product, $\text{CH}_2=\text{CHSiF}_2\text{SiF}_3$, which could not possibly be formed via dimerization of the silirane intermediate, only to prove that it could not be formed by sequential insertion of SiF_2 either.

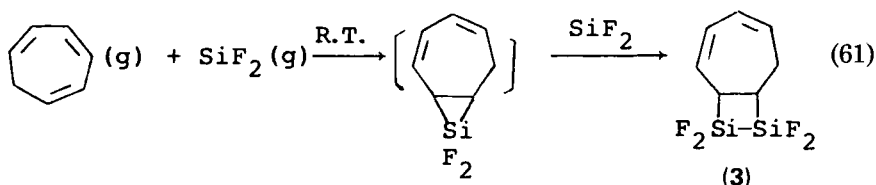
A similar strategy faces difficulty in the case of addition products. The only products that could not be formed by dimerization of the corresponding silirane intermediates are the four-membered ring compounds (disilacyclobutanes in the reactions of alkenes and disilacyclobutenes in the case of alkynes). But these four-membered ring compounds may well be formed by further insertion of difluorosilylene into intermediate three-membered silacycles, for example:



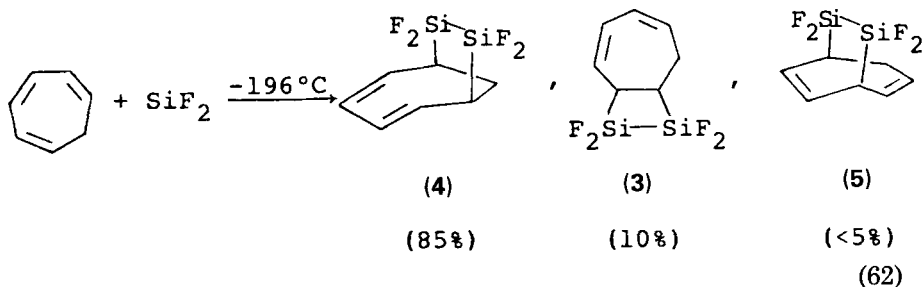
Although this type of reaction has not been observed experimentally

with difluorosilylene, it is a well accepted reaction pathway in the chemistry of dimethylsilylene (2, 6, 92).

In the gas-phase reaction of difluorosilylene with cycloheptatriene (94), in addition to a small amount of unidentified products, compound (3) was obtained as the major product. Since only monomeric SiF_2 is involved in the gas phase, the formation of (3) is best viewed as the result of further insertion of SiF_2 into the initially formed silirane. This is the first experimental evidence for such insertion as far as difluorosilylene is concerned.

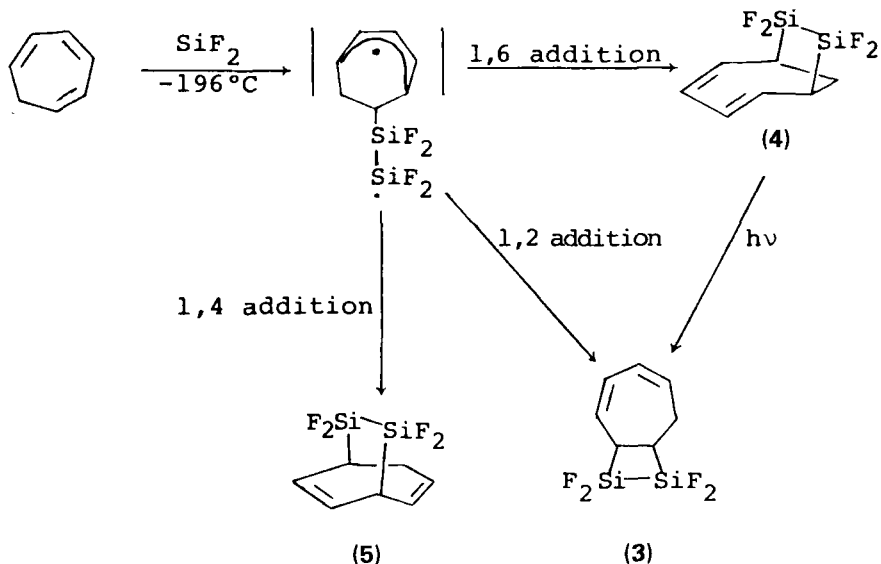


When the reaction was carried out under cocondensation conditions (94), three products, (3), (4), and (5), were obtained [Eq. (62)]. The major product was compound (4), and compound (5) was found only in trace abundance.



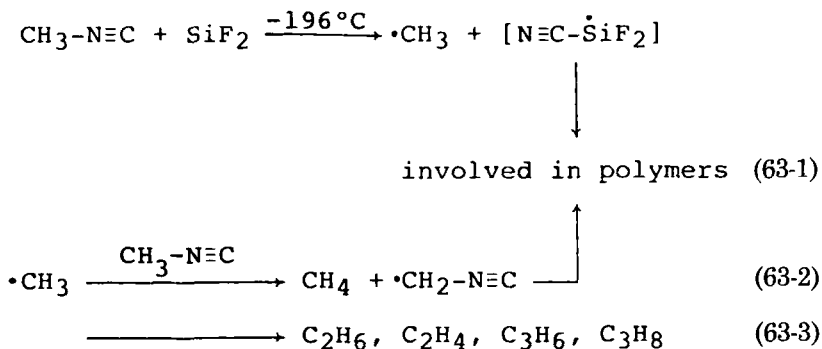
While compound (3) obtained in the cocondensation reaction may still be formed through the contribution from the silirane mechanism, just as it is formed in the gas phase, the formation of (4) and (5) cannot be rationalized with the same reaction mechanism. The fact that compound (4) was found to be the major product in the cocondensation reaction strongly indicates that the reaction proceeds via the diradical mechanism shown in Scheme 12. Compounds (3) and (4) are both thermally stable. It is interesting to note that compound (4) can be converted into compound (3) in *n*-hexane solution by UV irradiation.

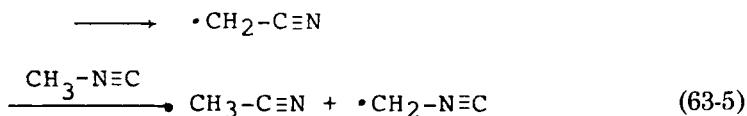
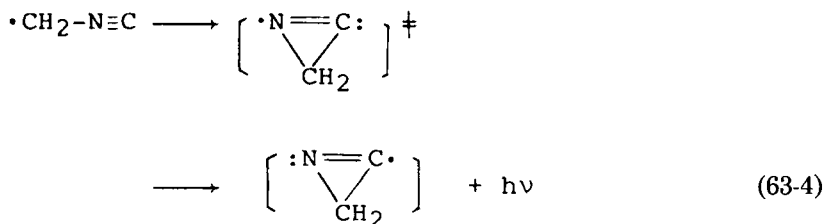
One more type of reaction worth mentioning is that with isonitriles (53). This can be best illustrated by the reaction with methyl isocyanide.



SCHEME 12

The reaction did not produce any volatile product involving the SiF_2 group (except the polymeric products which contained SiF_2 units); instead, CH_4 , C_2H_4 , C_3H_6 , C_3H_8 , and CH_3CN were obtained in a total yield of 46%. Most interestingly, the isomerization of the starting material to methyl cyanide and a flash of chemiluminescence were observed at low temperatures during the reaction. Both phenomena appeared to accompany the evolution of a large quantity of methane gas as the cocondensate started to warm above -196°C . The reaction has been proposed to proceed by the mechanism of Eqs. (63-1)–(63-5).





The key steps in this mechanism are the initial attack of SiF_2 [Eq. (63-1)] and the hydrogen abstraction of CH_3NC by methyl radicals at low temperature [Eq. (63-2)]. The former resembles the reaction pattern of triplet carbenes; the latter had been demonstrated experimentally to be an extremely facile process at low temperatures (97).

At this point, we feel that the "difference" between the silirane mechanism and the diradical mechanism has been overemphasized in the past. In fact, the silirane intermediate may be considered as a special case in the $(\text{SiF}_2)_n$ homologue with $n = 1$.

If so, one most important question yet to be answered in the chemistry of difluorosilylene is the spin states of the reacting monomeric SiF_2 generated by various methods. The formation of silirane as an initial step in addition reactions is consistent with the chemistry of singlet SiF_2 , which is in agreement with the spectroscopic studies in Margrave's earlier work (73, 80). An *ab initio* calculation also showed that SiF_2 has a singlet ground state (114). On the other hand, a number of chemical observations have suggested the participation of triplet SiF_2 in some reactions (53, 95, 117). It is obvious that more work along this line, preferably quantitative, is required to clarify the basic confusion in the chemistry of difluorosilylene.

REFERENCES

1. Atwell, W. H., F. R. G. Pat. 1,921,833 (1969); *Chem. Abstr.* **72**, 31611 (1970).
2. Atwell, W. H., and Uhlmann, J. G., *J. Organomet. Chem.* **52**, C21 (1973).
3. Atwell, W. H., and Weyenberg, D. R., *J. Am. Chem. Soc.* **90**, 3438 (1968).
4. Atwell, W. H., and Weyenberg, D. R., *Angew. Chem., Int. Ed. Engl.* **8**, 469 (1969).
5. Atwell, W. H., and Weyenberg, D. R., *Angew. Chem.* **81**, 485 (1969).

6. Barton, T. J., and Kilgour, J. A., *J. Am. Chem. Soc.* **98**, 7746 (1976).
7. Barton, T. J., and Kilgour, J. A., *J. Am. Chem. Soc.* **96**, 7150 (1974).
8. Bassler, J. M., Timms, P. L., and Margrave, J. L., *Inorg. Chem.* **5**, 729 (1966).
9. Bashkistrova, S. A., Ph.D. Thesis, M. Kh. P. Moscow (1974).
10. Bashkistrova, S. A., Komalenkova, N. G., and Chernyshev, E. A., in "Gas Phase High Temperature Methods of Organosilicon Monomer Synthesis," pp. 51, 59. NIITEKhim, Moscow, 1979.
11. Benson, S. W., and O'Neal, H. E., *Data Ser. (U.S. Natl. Bur. Stand.)* **15** (1970).
12. Binkley, J. S., and Pople, J. A., *Chem. Phys. Lett.* **45**, 197 (1977).
13. Bochkarev, V. N., Polivanov, A. N., Chernyshev, E. A., Komalenkova, N. G., and Bashkistrova, S. A., *Zh. Obshch. Khim.* **43**, 785 (1973).
14. Bowrey, M., and Purnell, J. H., *J. Am. Chem. Soc.* **92**, 2594 (1970).
15. Chernyshev, E. A., in "Chemistry and Engineering of Organoelement Compounds," p. 49. Proc. NIITEKhim, Ser. I., Moscow, 1972.
16. Chernyshev, E. A., Komalenkova, N. G., and Bashkistrova, S. A., *Dokl. Akad. Nauk S.S.S.R.* **205**, 868 (1972).
17. Chernyshev, E. A., Komalenkova, N. G., and Bashkistrova, S. A., *J. Organomet. Chem.* **271**, 129 (1984).
18. Chernyshev, E. A., Komalenkova, N. G., and Bashkistrova, S. A., *Proc. All-Union Conf. Chem. Carbenes Their Analog.* 1973, p. 243.
19. Chernyshev, E. A., Komalenkova, N. G., and Bashkistrova, S. A., *Russ. Chem. Rev.* **45**, 913 (1976).
20. Chernyshev, E. A., Komalenkova, N. G., and Bashkistrova, S. A., *Usp. Khim.* **45**, 1782 (1976).
21. Chernyshev, E. A., Komalenkova, N. G., and Bashkistrova, S. A., U.S.S.R. Pat. 432,154 (1974).
22. Chernyshev, E. A., Komalenkova, N. G., and Bashkistrova, S. A., U.S.S.R. Pat. 437,769 (1974).
23. Chernyshev, E. A., Komalenkova, N. G., and Bashkistrova, S. A., *Zh. Obshch. Khim.* **41**, 1175 (1971).
24. Chernyshev, E. A., Komalenkova, N. G., and Bashkistrova, S. A., *Zh. Obshch. Khim.* **46**, 1286 (1976).
25. Chernyshev, E. A., Komalenkova, N. G., Bashkistrova, S. A., Botygina, N. A., and Kisin, A. V., *Zh. Obshch. Khim.* **47**, 1196 (1977).
26. Chernyshev, E. A., Komalenkova, N. G., Bashkistrova, S. A., Fedotov, N. S., Evert, G. E., and Mironov, V. F., *Zh. Obshch. Khim.* **48**, 649 (1978).
27. Chernyshev, E. A., Komalenkova, N. G., Bashkistrova, S. A., Kuz'mina, T. M., Fedotov, N. S., and Mironov, V. F., U.S.S.R. SU 518498, *Byull. Izobret.*, No. 23 (1976).
28. Chernyshev, E. A., Komalenkova, N. G., Bashkistrova, S. A., and Pazdersky, Y. A., U.S.S.R. SU 739073, *Byull. Izobret.*, No. 21 (1980).
29. Chernyshev, E. A., Komalenkova, N. G., Bashkistrova, S. A., Sokolova, T. M., and Fouks, M. Y., *Zh. Obshch. Khim.* **52**, 2135 (1981).
30. Chernyshev, E. A., Komalenkova, N. G., Bashkistrova, S. A., and Sokolova, V. V., *Zh. Obshch. Khim.* **48**, 830 (1978).
31. Chernyshev, E. A., Komalenkova, N. G., Bashkistrova, S. A., Turkel'taub, G. N., and Kisin, A. V., *Zh. Obshch. Khim.* **50**, 697 (1980).
32. Chernyshev, E. A., Komalenkova, N. G., Klochkova, T. A., Shchepinov, S. A., and Mosin, A. M., *Zh. Obshch. Khim.* **41**, 122 (1971).
33. Chernyshev, E. A., Komalenkova, N. G., and Shamshin, L. N., U.S.S.R. SU 514818, *Byull. Izobret.*, No. 19 (1976).

34. Chernyshev, E. A., Komalenkova, N. G., and Shamshin, L. N., U.S.S.R. SU 514840, *Byull. Izobret.*, No. 19 (1976).
35. Dzarnoski, J., Rickborn, S. F., O'Neal, H. E., and Ring, M. A., *Organometallics* **1**, 1217 (1982).
36. Gaspar, P. P., *React. Intermed.* **2**, 335 (1981).
37. Gaspar, P. P., *React. Intermed.* **1**, 229 (1978).
38. Gaspar, P. P., Bock, S. A., and Eckelman, W. C., *J. Am. Chem. Soc.* **90**, 6914 (1968).
39. Gaspar, P. P., and Herold, B. J., in "Carbene Chemistry" (W. Kirmse, ed.). Academic Press, New York, 1971.
40. Gaspar, P. P., and Hwang, R. J., *J. Am. Chem. Soc.* **96**, 6198 (1974).
41. Gaspar, P. P., Konieczny, S., and Mo, S. H., *J. Am. Chem. Soc.* **106**, 424 (1984).
42. Gaspar, P. P., and Markusch, P., *J. Chem. Soc., Chem. Commun.*, p. 1331 (1970).
43. Gaspar, P. P., Pate, B. D., and Eckelman, W. C., *J. Am. Chem. Soc.* **88**, 3878 (1966).
44. Gennaro, G. P., Su, Y. Y., Zeck, O. F., Daniel, S. H., and Tang, Y. N., *J. Chem. Soc., Chem. Commun.*, p. 637 (1973).
45. Gilman, H., Cottis, S. G., and Atwell, W. H., *J. Am. Chem. Soc.* **86**, 1596 (1969).
46. Gordon, M. S., *J. Chem. Soc., Chem. Commun.*, p. 890 (1981).
47. Grev, R. S., and Schaefer, H. F. III., *J. Chem. Soc., Chem. Commun.*, p. 785 (1983).
48. Gusel'nikov, L. E., and Nametkin, N. S., *Chem. Rev.* **79**, 529 (1979).
49. Halevi, E. A., and West, R., *J. Organomet. Chem.* **240**, 129 (1982).
50. Hogness, T. R., Wilson, T. L., and Johnson, W. C., *J. Am. Chem. Soc.* **58**, 108 (1936).
51. Hollandsworth, R. P., and Ring M. A., *Inorg. Chem.* **8**, 1635 (1969).
52. Hopkins, H. P., Thompson, J. C., and Margrave, J. L., *J. Am. Chem. Soc.* **90**, 901 (1968).
53. Hsu, M. T., Lee, C. Y., and Liu, C. S., *Proc. Natl. Sci. Council, Repub. China, Pt. B* **5**, 344 (1981).
54. Huheey, J. E., "Inorganic Chemistry," p. 699. Harper, New York, 1974.
55. Hwang, T. L., and Liu, C. S., *J. Am. Chem. Soc.* **102**, 385 (1980).
- 56a. Hwang, T. L., Pai, Y. M., and Liu, C. S., *J. Am. Chem. Soc.* **102**, 7519 (1980).
- 56b. Hwangs T. L., Ph.D. Thesis, National Tsing Hua University, Hsinchu, Taiwan (1980).
57. Imoto, M., *Setchaku* **21**, 162 (1977).
58. Ishikawa, M., Fuchikami, T., and Kumada, M., *J. Organomet. Chem.* **142**, C45 (1977).
59. Kirmse, W., ed., "Carbene Chemistry," 2nd Ed., p. 442. Academic Press, New York, 1971.
60. Kumada, M., *Kem. Kozl.* **52**, 347 (1979).
61. Lee, W. L., M. S. Thesis, National Tsing Hua University, Hsinchu, Taiwan (1983).
62. Lei, D., Hwang, R.-J., and Gaspar, P. P., *J. Organomet. Chem.* **271**, 1 (1984).
63. Liu, C. S., and Hwang, T. L., *J. Am. Chem. Soc.* **101**, 2996 (1979).
64. Liu, C. S., and Hwang, T. L., *J. Am. Chem. Soc.* **100**, 2577 (1978); *J. Chin. Chem. Soc. (Taipei)* **25**, 203 (1978).
65. Liu, C. S., Margrave, J. L., Thompson, J. C., and Timms, P. L., *Can. J. Chem.* **50**, 459 (1972).
66. Liu, C. S., Margrave, J. L., and Thompson, J. C., *Can. J. Chem.* **50**, 465 (1972).
67. Liu, C. S., Nyburg, S. C., Szmanski, J. T., and Thompson, J. C., *J. Chem. Soc., Dalton Trans.*, p. 1129 (1972).
68. Liu, C. S., and Thompson, J. C., *Inorg. Chem.* **10**, 1100 (1971).
69. Liu, C. S., and Thompson, J. C., *J. Organomet. Chem.* **38**, 249 (1972).
70. Margrave, J. L., and Perry, D. L., *Inorg. Chem.* **16**, 1820 (1977).
71. Margrave, J. L., and Timms, P. L., *U.S. Pat.* 3,485,862 (1969).
72. Margrave, J. L., Timms, P. L., and Ehlert, T. C., *U.S. Pat.* 3,379,512 (1968).

73. Margrave, J. L., and Wilson, P. W., *Acc. Chem. Res.* **4**, 145 (1971), and references therein.
74. Nay, M. A., Woodall, G. N. C., Strausz, O. P., and Gunning, H. E., *J. Am. Chem. Soc.* **87**, 179 (1965).
75. Nefedov, O. M., and Manakov, M. N., *Angew. Chem.* **78**, 1039 (1966).
76. Niki, H., and Mains, G. J., *J. Phys. Chem.* **68**, 304 (1964).
77. Orlando, A., Liu, C. S., and Thompson, J. C., *J. Fluorine Chem.* **2**, 103 (1972).
78. Pai, Y. M., Chen, C. K., and Liu, C. S., *J. Organomet. Chem.* **226**, 21 (1982).
79. Paquin, D. P., and Ring, M. A., *J. Am. Chem. Soc.* **99**, 1793 (1977).
80. Perry, D. L., and Margrave, J. L., *J. Chem. Educ.* **53**, 696 (1976).
81. Purnell, J. H., and Walsh, R., *Proc. R. Soc. London, Ser. A* **293**, 543 (1966).
82. Reynolds, W. F., Thompson, J. C., and Wright, A. P. G., *Can. J. Chem.* **58**, 419 (1980).
83. Reynolds, W. F., Thompson, J. C., and Wright, A. P. G., *Can. J. Chem.* **58**, 425 (1980).
84. Ring, M. A., Puentes, H. J., and O'Neal, H. E., *J. Am. Chem. Soc.* **92**, 4845 (1970).
85. Ring, M. A., Beverly, G. D., Koester, F. H., and Hollandsworth, R. P., *Inorg. Chem.* **8**, 2033 (1969).
86. Sakurai, H., Kobayashi, T., and Nakadaira, Y., *J. Organomet. Chem.* **162**, C43 (1978).
87. Schenk, P. W., and Bloching, H., *Z. Anorg. Allg. Chem.* **334**, 57 (1964).
88. Schmeisser, M., and Voss, P., *Z. Anorg. Allg. Chem.* **334**, 50 (1964).
89. Sefcik, M. D., and Ring, M. A., *J. Am. Chem. Soc.* **95**, 5168 (1973).
90. Sefcik, M. D., and Ring, M. A., *J. Organomet. Chem.* **59**, 167 (1973).
91. Seyferth, D., and Duncan, D. P., *J. Am. Chem. Soc.* **100**, 7734 (1978).
92. Seyferth, D., and Vick, S. C., *J. Organomet. Chem.* **125**, C11 (1977).
93. Shiau, C. C., Hwang, T. L., and Liu, C. S., *J. Organomet. Chem.* **214**, 31 (1981).
94. Shieh, C. F., M. S. Thesis, National Tsing Hua University, Hsinchu, Taiwan, (1984).
95. Siefert, E. E., Ferrieri, R. A., Zeck, O. F., and Tang, Y. N., *Inorg. Chem.* **17**, 2802 (1978).
96. Smith, D. L., Kirk, R., and Timms, P. L., *J. Chem. Soc., Chem. Commun.*, p. 295 (1972).
97. Sprague, E. D., Takeda, K., Wang, J. T., and Williams, F., *Can. J. Chem.* **52**, 2840 (1974).
98. Stokland, K., *Skr., K. Nor. Vidensk. Selsk.* [N. S.] No. 3, p. 1 (1950).
99. Tang, Y. N., *React. Intermed. (Plenum)* **2**, 297 (1982).
100. Tang, Y. N., Gennaro, G. P., and Su, Y. Y., *J. Am. Chem. Soc.* **94**, 4355 (1972).
101. Timms, P. L., *Chem. Eng. News* **47**, 57 (1967).
102. Timms, P. L., *Inorg. Chem.* **7**, 387 (1968).
103. Timms, P. L., *Acc. Chem. Res.* **6**, 118 (1973).
104. Timms, P. L., *Adv. Inorg. Chem. Radiochem.* **14**, 121 (1972).
105. Timms, P. L., Ehlert, T. C., Binckman, F., Farrar, T. C., Coyle, T. P., and Margrave, J. L., *J. Am. Chem. Soc.* **87**, 3819 (1965).
106. Timms, P. L., Kent, R. A., Ehlert, T. C., and Margrave, J. L., *Nature (London)* **207**, 186 (1965).
107. Timms, P. L., Stump, D. D., Kent, R. A., and Margrave, J. L., *J. Am. Chem. Soc.* **88**, 940 (1966).
108. Thompson, J. C., and Margrave, J. L., *Science* **155**, 669 (1967).
109. Thompson, J. C., and Margrave, J. L., *J. Chem. Soc., Chem. Commun.*, p. 566 (1966).
110. Thompson, J. C., Wright, A. P. G., and Reynolds, W. F., *J. Am. Chem. Soc.* **101**, 2236 (1979).
111. Wieland, K., and Heise, M., *Angew. Chem.* **63**, 438 (1951).
112. Wilkinson, G., Stone, F. G. A., and Abel, E. W., eds., "Comprehensive Organometallic Chemistry," Chapt. 9.2, and references therein. Pergamon, Oxford, 1982.
113. Wilkinson, G., Stone, F. G. A., and Abel, E. W., eds., "Comprehensive Organometallic

- Chemistry," Chapt. 9.1. Pergamon, Oxford, 1982.
114. Wirsam, B., *Chem. Phys. Lett.* **22**, 360 (1973).
115. Wolf, A. P., *Adv. Phys. Org. Chem.* **2**, 202 (1964).
116. Wolfgang, R., *Prog. React. Kinet.* **3**, 97 (1965).
117. Zeck, O. F., Su, Y. Y., Gennaro, G. P., and Tang, Y. N., *J. Am. Chem. Soc.* **98**, 3474 (1976).
118. Zeck, O. F., Su, Y. Y., and Tang, Y. N., *J. Am. Chem. Soc.* **96**, 5967 (1974).
119. Zubkov, V. I., Tikhomirov, M. V., Andrianov, K. A., and Golubstov, S. A., *Dokl. Akad. Nauk SSSR* **188**, 594 (1969).

TRIFLUOROPHOSPHINE COMPLEXES OF TRANSITION METALS

JOHN F. NIXON

School of Chemistry and Molecular Sciences,
University of Sussex, Brighton, Sussex, England

I. Introduction	41
II. Binary Compounds	43
III. Hydrides	45
IV. Structures	52
A. Mononuclear Complexes	52
B. Dinuclear Complexes	58
V. Bonding	59
A. Trifluorophosphine	59
B. Transition Metal-PF ₃ Complexes	62
C. PF ₃ Adsorbed on Metal Surfaces	65
D. Comparison of CO and PF ₃ as Ligands	67
VI. Dinuclear Complexes Containing Bridging PF ₂ Ligands	68
VII. Polynuclear Complexes	69
VIII. Halogeno-Metal Complexes	73
IX. Transition Metal-Alkene Complexes	77
X. Transition Metal-Alkyne Complexes	88
XI. Transition Metal-Arene Complexes	89
XII. Transition Metal η^3 -Allyl Complexes	93
XIII. Transition Metal η^5 -Cyclopentadienyl and Related Complexes	97
XIV. Transition Metal Carbonyl Complexes	104
XV. Transition Metal Nitrosyl Complexes	109
XVI. Transition Metal Complexes Containing Other Ligands with Nitrogen, Phosphorus, or Arsenic Donor Atoms	111
XVII. Transition Metal Alkyl and Alkenyl Complexes	122
XVIII. Transition Metal Complexes Containing σ -Bonded Group IV Elements Other Than Carbon	126
XIX. Transition Metal PF ₃ Complexes Containing Other Anionic or Cationic Ligands	128
References	131

I. Introduction

Transition metal carbonyl chemistry originated with the discovery of [Ni(CO)₄] in 1890. Although the first trifluorophosphine coordination complex was prepared the following year by Moissan (263) by treating

phosphorus pentafluoride with platinum black, its identity was not recognized at the time, and almost 60 years passed before interest in PF_3 as a ligand arose.

In 1949, Chatt (62) suggested that the trans influence of ligands like ethylene, carbon monoxide, and, to a lesser extent, trialkylphosphines in square-planar platinum(II) complexes was related to back donation of d -electron density from the transition metal to suitable empty orbitals of the ligands. It was proposed that such back bonding should be enhanced in PF_3 complexes because of the presence of the highly electronegative fluorine atoms.

Soon afterwards, Chatt and Williams (63) tested this idea by bubbling PF_3 over heated platinum(II) chloride and isolated the crystalline complexes $[\text{PtCl}_2(\text{PF}_3)_2]$ and $[\text{PtCl}_2(\text{PF}_3)]_2$. Carbon monoxide was also readily displaced from $[\text{Ni}(\text{CO})_4]$ by PF_3 and later work showed that all possible $[\text{Ni}(\text{CO})_x(\text{PF}_3)_{4-x}]$ complexes can be formed. In the same year Wilkinson (361) achieved the first synthesis of the volatile liquid complex $[\text{Ni}(\text{PF}_3)_4]$ which exhibited considerably greater thermal stability than $[\text{Ni}(\text{CO})_4]$.

The close similarity between transition metal PF_3 complexes and their CO analogues is indicated by a variety of studies (72, 174, 272), and has been rationalized in terms of a bonding scheme for PF_3 involving (1) a σ -donor component from donation of the phosphorus lone pair electrons to the metal, and (2) a symmetry-allowed π bond involving back donation of metal d electrons into empty $3d$ orbitals on phosphorus.

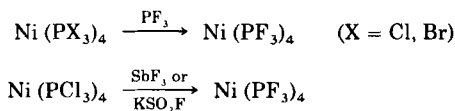
Experimental methods to study the nature of the metal-phosphorus bond in transition metal-phosphine complexes usually reveal only its overall nature, and the degree of $d_\pi-d_\pi$ participation can only be inferred after assumptions have been made about the σ component. This area has been controversial (248) and a review by Pidcock (299) gives an excellent account of all the factors involved. Clearly the degree of any π bonding will be affected by the nature of the metal and its oxidation state, its attendant ligands, and the type of phosphines involved. The formation of $[\text{BH}_3 \cdot \text{PF}_3]$ and $[\text{AlCl}_3 \cdot \text{PF}_3]$ indicates that back donation is not a prerequisite for the existence of trifluorophosphine complexes; however, these compounds are extremely unstable compared to their transition metal- PF_3 counterparts and σ bonding alone is unlikely to account for the extensive range of PF_3 transition metal complexes now known (*vide infra*). Likewise, in metallate salts of the type $[\text{M}(\text{PF}_3)_x]^{n-}$ some mechanism is almost certainly necessary for removal of the negative charge. Further insight into the nature of PF_3 bonded to transition metals has come both from theoretical calculations and gas-phase photo-

electron spectroscopic measurements on the volatile complexes (see Section V).

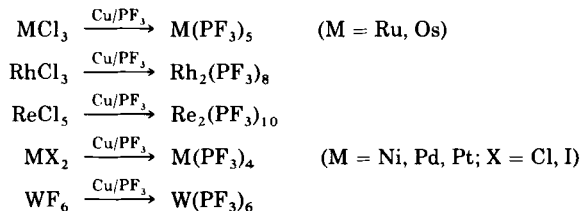
This article is concerned with synthetic, structural, and spectroscopic aspects of an extensive range of transition metal PF₃ complexes including a wide variety of organometallic derivatives. Often, PF₃ can stabilize novel systems which have no precedent with other phosphine ligands. Likewise, the presence of ³¹P and ¹⁹F nuclei (both $I = \frac{1}{2}$, 100% abundant) offers NMR spectroscopic advantages in structural assignments and in the study of inter- and intramolecular ligand-exchange processes. This review covers publications up to early 1984 and complements previous articles (72, 174, 272, 273, 292, 323) covering the period up to 1975.

II. Binary Compounds

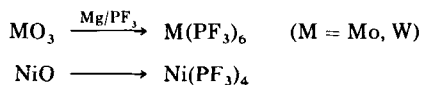
The first zero-valent binary transition metal-trifluorophosphine complex to be reported was [Ni(PF₃)₄] made by Wilkinson in 1951 (361) by the interaction of [Ni(PX₃)₄] (X = Cl, Br) with PF₃ (50–100 atm, 100°C) (method A). This is not a generally useful route, however, and although it was shown by using ³²PCl₃ that the mechanism of the reaction involves ligand exchange rather than halogen exchange, the latter can be readily achieved (method B) using SbF₃ or KSO₂F as fluorinating agents.



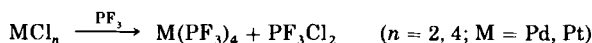
By far the most extensively used synthetic route involves the technique of “reductive fluorophosphination” developed by T. Kruck and co-workers (174), who have made many important contributions to the development of the field of transition metal–PF₃ chemistry. In this method the appropriate metal halide is heated in an autoclave (usually copper-lined) with reducing agents, e.g., copper or zinc, in the presence of PF₃ (50–500 atm) (method C). For example,



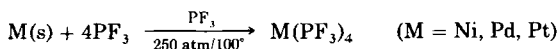
A few complexes have been made by reduction of their oxides in the presence of PF_3 under extremely forcing conditions (method D) (e.g., 300°C , 4000 atm).



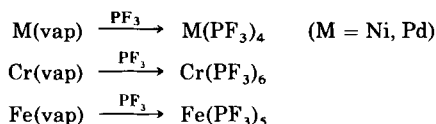
In some cases the presence of a metal reducing agent is superfluous since PF_3 can act as both a reducing agent and as a ligand (method E).



Likewise, the direct synthesis of $[\text{M}(\text{PF}_3)_4]$ ($\text{M} = \text{Ni}, \text{Pd}, \text{Pt}$) complexes has been achieved from the appropriate metal powder (method F), or alternatively under very mild conditions from highly reactive forms of the metal (e.g., Ni) generated either from the decomposition of nickel oxalate or nickel tetracarbonyl or activated by sulfide (method G).



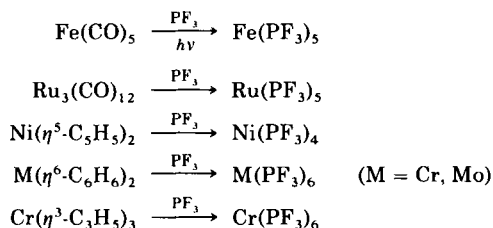
Not surprisingly, in recent years the technique of metal vapor synthesis, in which the metal vapor and PF_3 are cocondensed at liquid nitrogen temperatures, has found general application since PF_3 is readily condensable (in contrast to CO) and the high volatility of the resulting metal- PF_3 complexes facilitates their isolation (method H).



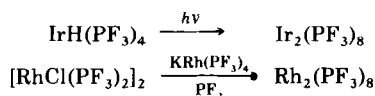
Interestingly, no PF_3 complex has been obtained so far using Mn vapor and there is a very recent report of the formation of the uranium complex $[\text{U}(\text{PF}_3)_6]$ using this technique, although the formulation is based solely on its mass spectrum (302).

Other synthetic routes involving mild conditions and not requiring specialized apparatus involve displacement of carbon monoxide from metal carbonyls (method I) or coordinated organic ligands (arenes,

η^5 -cyclopentadienyl, η^3 -allyl, etc.) (method J), e.g.,



Dinuclear complexes have been made by photolysis of the related hydrido complex (*vide infra*) (method K) or by interaction of halogeno PF₃-metal derivatives with the trifluorophosphine metallate salt (method L).



Binary complexes are listed in Table I, together with references to physical and spectroscopic measurements made on them.

III. Hydrides

An interesting feature of hydrido transition metal-PF₃ complexes is that apart from a few dinuclear systems (Section VI) only mononuclear systems are so far known and there is as yet no corresponding chemistry analogous to that of polynuclear carbonyl hydrido compounds. The trifluorophosphine metal hydrido compounds are usually highly acidic and can readily form metallate ions such as [M(PF₃)_n]^{x-} and [MH(PF₃)_n]^{y-}.

The reductive fluorophosphination of metal halides in the presence of copper and hydrogen gas at high temperature and pressure offers a useful synthetic route for a number of hydrido trifluorophosphine metal complexes (method A).

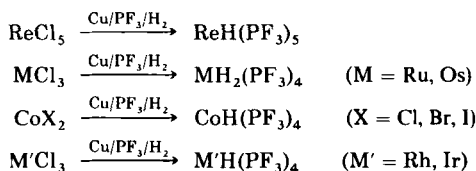


TABLE I

BINARY TRANSITION METAL TRIFLUOROPHOSPHINE COMPLEXES

Complex	Method of preparation	Color	M.P. (°C), B.P. (°C/mmHg)	δ_P^a	ϕ_F^b	$^1J_{PF}^c$	Remarks	Reference
$Cr(PF_3)_6^d$	(H) (I) (J)	Colorless	193 subl., 30/10 ⁻³ , dec. > 300	—	-8.4	1271	IR (175, 176, 183, 215, 228) NMR (183) MS (228) Raman (228)	125, 174-176, 183 215, 228, 340, 341
$Fe(PF_3)_5^e$	(C) (H) (I) (J)	Yellow	44, 45, subl. 30/10 ⁻³ , (dec. > 270	-163.5	-1.9 + 11.0	1275 1218 ^f	IR (70, 191, 218, 219) NMR (191, 218) Raman (218) MS (105, 218) Var. temp. ¹⁹ F NMR (251)	70, 118, 174, 191 218, 219, 251, 325, 340, 341
$Ni(PF_3)_4^{g,h}$	(A) (B) (C) (D) (F) (G) (I) (H) (J)	Colorless	-55, dec. > 155, (0/33.8) (14/69.3) (25/120.5) (67.8/730) (70.5/760) v.p. 0/32.5 0/34	+137.7	+16.8	1347	NMR (11, 61, 71, 191, 233, 235, 249, 254, 274, 275, 258, 305, 312, 334-336) IR (92-95, 108, 178, 191, 215, 230-233, 275, 324, 331, 360, 363, 364) Raman (93, 108, 231, 233, 363, 364) MS (181, 267, 268, 335)	68, 71, 75, 108, 128, 174, 178, 180, 191, 233, 264, 274, 275, 286, 287, 312, 324, 325, 334, 340, 341, 361, 364
$Mo(PF_3)_6^{i,j}$	(C) (D) (I) (J)	Colorless	196, dec. < 250, subl. 20/10 ⁻³ , v.p. 1.5 torr at 295 K	—	-2.6	1246	IR (73, 176, 183, 215, 228) NMR (10, 183) MS (228) Raman (228)	73, 128, 174, 176, 183, 215, 228

$\text{Ru}(\text{PF}_3)_5^k$	(C) (I)	Colorless	30, subl. $25/10^{-3}$, dec. > 155	-148.5	-2.4 $+ 11.2$	1320 1209 ^f	NMR (218) IR (218, 350) Raman (218) Var. temp. ^{19}F NMR (251)	174, 218, 350
$\text{Rh}_2(\text{PF}_3)_8^l$	(C) (K)	Orange-red	92.5, dec. > 100 , subl. $20/10^{-3}$	-114 ± 2	$+ 2.98$	1342	NMR (17) IR (17) Variable temp. ^{19}F NMR (19)	17, 174, 182
$\text{Pd}(\text{PF}_3)_4^m$	(C) (D) (E) (H) (I) (J)	Colorless liquid	-41 , dec. > -20	-95.5	$+ 14.92$	1350	NMR (177, 336) IR (108, 177, 179, 331, 336, 360) Raman (108)	108, 174, 177, 179, 180, 331, 336, 341
$\text{W}(\text{PF}_3)_6^n$	(C) (D) (I)	Colorless	214, subl. $40/10^{-3}$, dec. > 320 , v.p. 1.5 torr at 295 K	—	0.5	1241	IR (183, 210, 228) NMR (183) Raman (228)	174, 183, 210, 228 128
$\text{Re}_2(\text{PF}_3)_{10}$	(C)	Colorless	182, subl. $70/10^{-3}$, dec. > 228	—	—	—	—	174, 186
$\text{Os}(\text{PF}_3)_5$	(C)	Colorless		—	-8.0	1250 ^f	IR (218) Var. temp. ^{19}F NMR (251) Raman (218)	174, 218, 251
$\text{Ir}_2(\text{PF}_3)_8^o$	(K) (L)	Yellow	105, 113–116, subl. $20/10^{-3}$	—	$+ 5.2$ $+ 5.8$	1230 1238	NMR (17, 221) IR (17, 221) MS (220, 221) Variable temp. ^{19}F NMR (19)	17, 221

(continued)

TABLE I (continued)

Complex	Method of preparation	Color	M.P. (°C), B.P. (°C/mmHg)	δ_p^a	ϕ_F^b	$^1J_{PF}^c$	Remarks	Reference
Pt(PF ₃) ₄ ^p	(C) (E) (F)	Colorless liquid	−15, dec. >90, (38/100) (85.5/730) (86/730)	−97.8	+11.5	1320	NMR (177, 318) IR(108, 177, 179, 360) Raman (108)	108, 166, 177, 174, 179, 180, 287 287
U(PF ₃) ₆	(H)	—	—	—	—	—	MS (302)	302

^a In ppm relative to 85% H₃PO₄.

^b In ppm relative to FCCl₃.

^c In Hz.

^d Magnetic susceptibility (175), He(I) PES (139).

^e Dipole moment, optical density (218); ionization potential (267); magnetic susceptibility (219); He(I) PES (139); Mössbauer spectrum (199).

^f ($^1J_{PF} + 4J_{PF}$).

^g Ionization potential (267); magneto optical properties, Faraday effect (255, 317, 318, 319); electron diffraction (5, 246); He(I) PES (14, 122, 145, 267).

^h ⁶¹Ni NMR, see text (129).

ⁱ He(I) PES (139).

^j $^1J_{MOP} = 279$ Hz (10).

^k He(I) PES (139).

^l Magnetic susceptibility (182); stereochemical nonrigidity by NMR (19); X-ray structure determination (19, 326) a red complex of uncertain composition, Rh₃(PF₃)₉ or Rh₃(PF₃)₈(PF₂), was obtained by heating either Rh₂(PF₃)₈ or HRh(PF₃)₄ (17, 182).

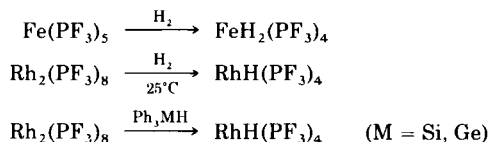
^m He(I) PES (14).

ⁿ He(I) PES (139).

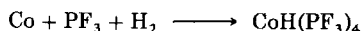
^o Stereochemical nonrigidity (19).

^p $d_x^{20} 2.4069$, $d_D^{20} 1.3613$ (318), magneto optical properties (318); He(I) PES (14, 122, 145); electron diffraction (246, 310, 311).

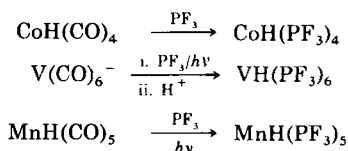
In some cases H₂ can interact directly with binary metal-trifluorophosphine complexes under mild conditions with or without addition of PF₃ or UV irradiation (method B), and group IV hydrides have also been utilized (method C).



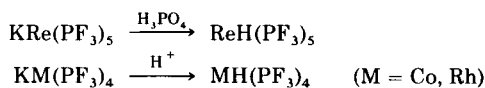
There is a single report of the direct reaction between a metal, PF₃, and hydrogen at elevated temperature and pressure (method D) to give a 97% yield of the desired hydrido complex (180).



Transition metal carbonyl complexes can be suitable precursors, for example, treatment of hydrido complexes or their alkali salts with PF₃ under UV irradiation followed if necessary by acidification of the reaction mixture (method E). Interestingly, vanadium forms the hydrido trifluorophosphine complex [VH(PF₃)₆], whereas with CO, the paramagnetic [V(CO)₆] is formed.



A related synthetic method involves hydrolysis of the metallate salt made by another route (method F).



There is one report (method G) of the ready hydrogenation of an η^3 -allyl metal PF₃ system under very mild conditions in the presence of PF₃.

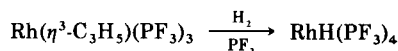


TABLE II

HYDRIDO-TRANSITION METAL TRIFLUOROPHOSPHINE COMPLEXES

Complex	Method of preparation	Color	M.P. (°C), B.P. (°C/mm Hg)	δ_P^a	ϕ_F^b	J_{PF}^c	Remarks	Reference
VH(PF ₃) ₆	(E)	—	Subl. 60/10 ⁻² , dec. 135	—	—	—	IR { (216) ^d NMR ^e MS { (259)	216
MnH(PF ₃) ₅ ^f	(E)	Colorless	18.5	—	—	—	¹⁹ F NMR (217)	185, 259
FeH ₂ (PF ₃) ₄ ^g	(A) (B)	Colorless	-71, (87/760) dec. 220	-148	trans + 2.9 cis + 3.2	1235 (trans) 1270 (cis)	³¹ P NMR (217) IR (217) MS (198) Variable temp. ¹ H, ¹⁹ F, and ³¹ P NMR (199, 253)	118, 174 198, 217
CoH(PF ₃) ₄ ^h	(A) (D) (E) (F)	Very pale yellow	-51, (80/730), dec. 250	-147.7	2.6 (ax), 0.7 (eq)	1230 ⁱ	IR (15, 210) Variable temp. ¹ H and ¹⁹ F NMR (251, 252) Raman (15) MS (313)	68, 180, 202, 209, 210, 351
RuH ₂ (PF ₃) ₄ ^j	(A) (B)	Colorless	-76, dec. 290	-101	trans + 5.05 cis + 3.57	1320 (trans) 1240 (cis)	¹⁹ F NMR (217) ³¹ P NMR (217) IR (217) Variable temp. ¹ H, ¹⁹ F, and ³¹ P NMR (199, 253)	217
RhH(PF ₃) ₄ ^k	(A) (B) (C) (F) (G)	Colorless	-40, (89/725)	-133.4	0.7 (ax) 4.8 (eq)	1293 ⁱ	IR (208) Variable ¹ H and ¹⁹ F NMR (19, 251)(252)	17, 182, 208, 209 293

ReH(PF ₃) ₅	(A) (E)	Colorless —	42 Subl. 20/10, dec. > 160	—	—	—	IR (185) ¹ H NMR (185)	185
OsH ₂ (PF ₃) ₄ ⁱ	(A)	Colorless	−72, dec. 340	—	trans 6.55 cis 7.8	1275 (trans) 1225 (cis)	¹ H and ¹⁹ F NMR (217) IR (217) Variable temp. ¹ H and ¹⁹ F NMR (251, 252)	217
IrH(PF ₃) ₄ ^m	(A)	Colorless	−39, (95/730), dec. 245	−93.5	20.3 (ax), 15.6 (eq)	1244 ⁱ	IR (203), Variable temp. ¹ H and ¹⁹ F NMR (251, 252)	174, 203, 209

^a In ppm against 85% H₃PO₄ as external reference.

^b In ppm against FCCl₃ as internal reference.

^c In Hz.

^d Magnetic susceptibility, ¹H NMR (216).

^e Detailed NMR on [V(PF₃)₆][−] and Nb analogue (see text) (114, 307, 308, 309, 321).

^f ⁵⁵Mn NMR (201), He(I) PES (139, 141).

^g He(I) PES (141), Mössbauer spectrum (198), variable temp. ¹H and ¹⁹F NMR of the anion [FeH(PF₃)₄][−] (251, 252).

^h Density (15), molecular conductance (209), Δ*H* (313), ¹H NMR (21, 203), ⁵⁹Co NMR of [Co(PF₃)₄][−] (234) He(I) PES (139, 141), negative ion MS (313), neutron scattering spectrum (359), X-ray structure (115).

ⁱ *J*_{PF} + 3*J*_{PF′}.

^j Free energy of activation for exchange (253), variable temp. ¹H and ¹⁹F NMR of the anion [RuH(PF₃)₅][−] (251, 252), molecular conductance in aqueous solution (217).

^k Molecular conductance in aqueous solution (209), ¹H NMR (251), activation energy of ¹⁹F exchange (19), He(I) PES (139), Molecular structure (46).

^l Molecular conductance in aqueous solution (217), ¹H and ¹⁹F NMR of the anion [OsH(PF₃)₄][−] (251, 252).

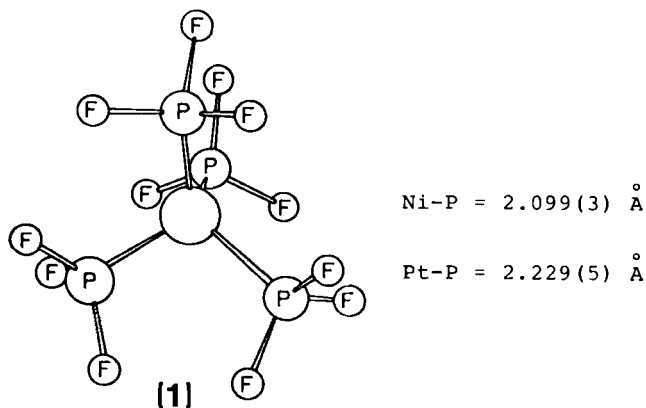
^m Molecular conductance in aqueous solution (209), He(I) PES (139).

Hydrido trifluorophosphine complexes are listed in Table II together with their methods of preparation.

IV. Structures

A. MONONUCLEAR COMPLEXES

A variety of spectroscopic techniques (e.g., ^{19}F and ^{31}P NMR, IR, Raman) have been applied to $[\text{M}(\text{PF}_3)_4]$ ($\text{M} = \text{Ni}, \text{Pd}, \text{Pt}$) and $[\text{M}(\text{PF}_3)_4]^-$ complexes ($\text{M} = \text{Co}, \text{Rh}, \text{Ir}$) and have been interpreted in terms of a regular tetrahedral arrangement of PF_3 ligands around the central metal atom. These conclusions have been confirmed by electron diffraction studies on $[\text{Ni}(\text{PF}_3)_4]$ and $[\text{Pt}(\text{PF}_3)_4]$ (1) (5, 246, 310, 311), in which the PF_3 groups undergo free rotation about the metal-phosphorus bond. Although the $\text{Ni}-\text{P}$ bond length in $[\text{Ni}(\text{PF}_3)_4]$ is exceptionally short, this is not the case for the platinum complex, in which the $\text{Pt}-\text{PF}_3$ bond length is not significantly shorter than in other platinum phosphorus complexes.



The tetrahedral environment around nickel in $[\text{Ni}(\text{PF}_3)_4]$ makes the electrical field gradient tensor zero and its ^{61}Ni NMR spectrum shown in Fig. 1 exhibits minimum quadrupole line broadening. Both the directly bounded $^{61}\text{Ni}-^{31}\text{P}$ coupling ($^1J_{\text{NiP}} = 482 \text{ Hz}$) and the two-bond $^{61}\text{Ni}-^{19}\text{F}$ coupling ($^2J_{\text{NiF}} = 28 \text{ Hz}$) have been recorded (129).

The ^{59}Co NMR spectrum of the isoelectronic tetrahedral $[\text{Co}(\text{PF}_3)_4]^-$ anion has also been recorded.

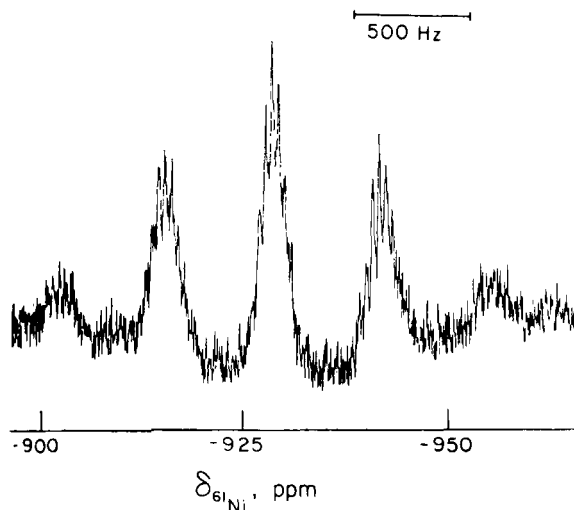


FIG. 1. Natural-abundance ^{61}Ni NMR spectrum of $\text{Ni}(\text{PF}_3)_6$ recorded at 35.727 MHz. [Reproduced from reference (129) by permission.]

The almost certainly regular octahedron proposed for $[\text{M}(\text{PF}_3)_6]$, ($\text{M} = \text{Cr}, \text{Mo}, \text{and W}$) and $[\text{VH}(\text{PF}_3)_6]$, based on spectroscopic data, has not yet been substantiated by X-ray or electron diffraction methods; however, the well-resolved ^{51}V and ^{93}Nb NMR spectra of the anions $[\text{M}'(\text{PF}_3)_6]^-$ ($\text{M}' = \text{V}, \text{Nb}$), and the ^{95}Mo NMR spectrum of $[\text{Mo}(\text{PF}_3)_6]$ indicate that the metal atoms are certainly in a high symmetrical environment.

The beautiful ^{93}Nb NMR spectrum shown in Fig. 2 for the niobium complex $[\text{Nb}(\text{PF}_3)_6]^-$ exhibits a binomial septet arising from the one-bond metal-phosphorus coupling ($^1J_{\text{NbP}} = 1050 \text{ Hz}$) and further fine splitting arising from the two-bond metal-fluorine coupling ($^2J_{\text{NbF}} = 55 \text{ Hz}$). Chemical shift data have been compared to $[\text{Nb}(\text{CO})_6]^-$ and interpreted as indicating that PF_3 is a slightly weaker π acceptor than CO (*vide infra*) (307).

No structural data are available for the pentakis(trifluorophosphine) complexes $[\text{M}(\text{PF}_3)_5]$ ($\text{M} = \text{Fe}, \text{Ru}, \text{Os}$), which almost certainly have trigonal-bipyramidal structures. Detailed ^{19}F and ^{31}P NMR studies indicate clearly that these molecules are fluxional even at temperatures as low as -160°C and the barrier to intramolecular ligand exchange between equatorial and axial positions of the trigonal bipyramid is less than $\sim 20 \text{ kJ/mol}$ (251). Figure 3 shows the temperature-dependent ^{19}F NMR spectrum of $[\text{Ru}(\text{PF}_3)_5]$, which is typical for all the MP_5

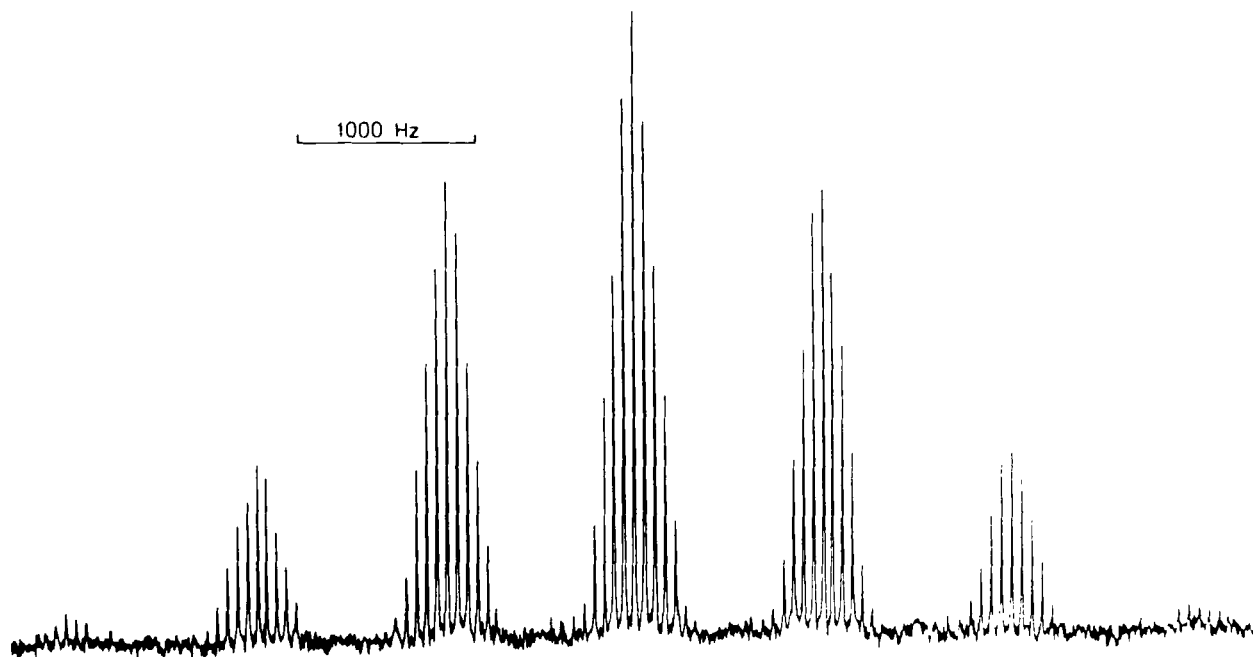


FIG. 2. The 22.00-MHz ^{93}Nb spectrum of $[\text{Et}_4\text{N}][\text{Nb}(\text{PF}_3)_6]$. [Reproduced from reference (307) by permission.]

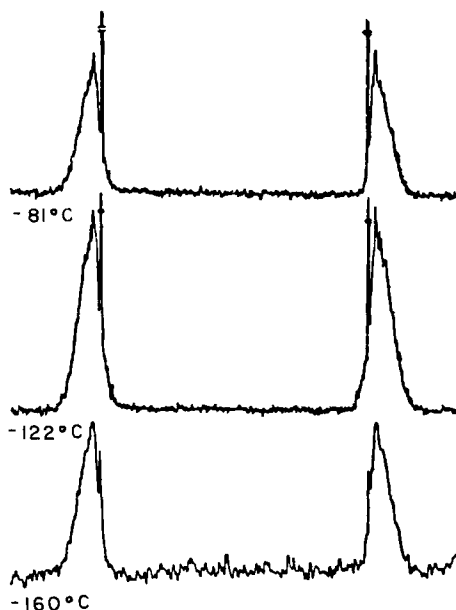


FIG. 3. ^{19}F (84.66 MHz) NMR spectra for $\text{Ru}(\text{PF}_3)_5$ in CHClF_2 taken at three temperatures. [Reproduced from reference (251) by permission.]

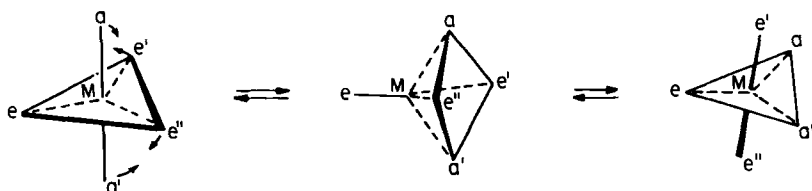


FIG. 4. Possible intramolecular ligand-exchange mechanism in $\text{M}(\text{PF}_3)_5$ complexes.

complexes. The possible mechanism for the PF_3 ligand interchange first proposed by Berry for other five-coordinate systems is depicted in Fig. 4.

The crystal structure of $[\text{CoH}(\text{PF}_3)_4]$ (Fig. 5) has been determined from X-ray data collected at -125°C . It can be described either as a distorted trigonal bipyramid with the hydrogen atom occupying an axial position, or alternatively as a tetrahedral array of PF_3 groups with hydrogen on one of the faces of the tetrahedron. The $\text{Co}-\text{P}$ [2.052(5) Å average] bond distance is exceptionally short. The analogous $[\text{RhH}(\text{PF}_3)_4]$ (Fig. 6) has a similar structure which has been determined in the gas phase by electron diffraction (46).

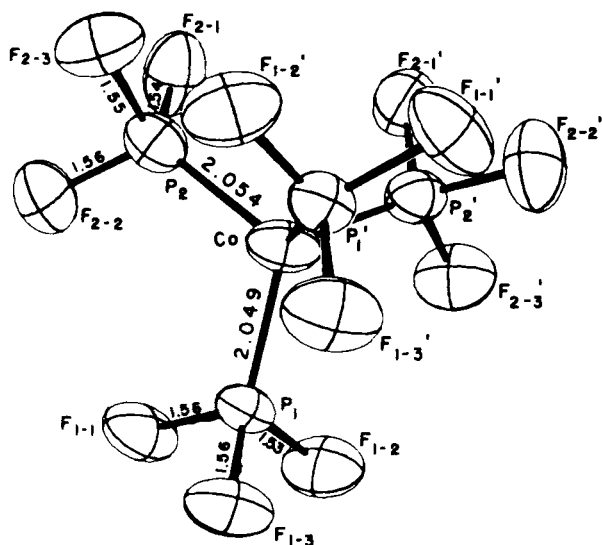


FIG. 5. A drawing of the $\text{CoH}(\text{PF}_3)_4$ molecule, with the H atom omitted. The 50% probability ellipsoids are shown. [Reproduced from reference (115) with permission.]

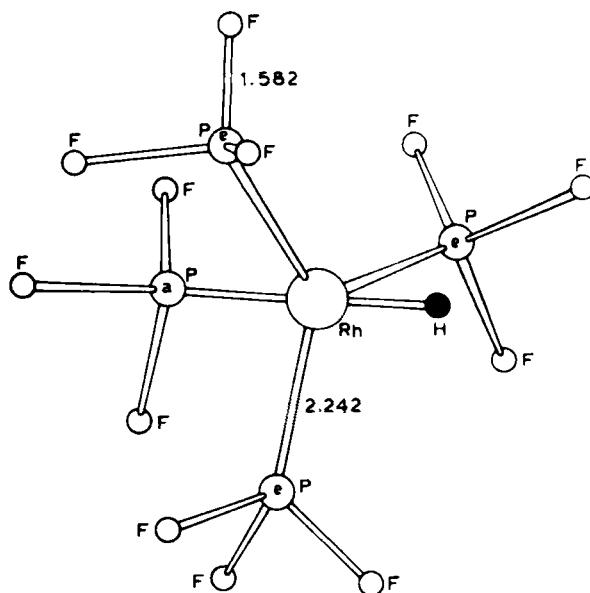


FIG. 6. The structure of $\text{RhH}(\text{PF}_3)_4$ as determined in the gas phase by electron diffraction. [Reproduced from references (46, 292) with permission.]

The $[\text{MH}(\text{PF}_3)_4]$ complexes ($\text{M} = \text{Co}, \text{Rh}, \text{Ir}$) and the isoelectronic species $[\text{M}'\text{H}(\text{PF}_3)_4]^-$ ($\text{M}' = \text{Fe}, \text{Ru}, \text{Os}$) are all stereochemically non-rigid, and detailed multinuclear NMR spectroscopic studies have been carried out and activation parameters determined. It has been proposed that the phosphorus environments are interchanged by a "tetrahedral tunnelling" rearrangement mechanism. Some typical temperature-dependent ^1H and ^{19}F NMR spectra are shown in Fig. 7.

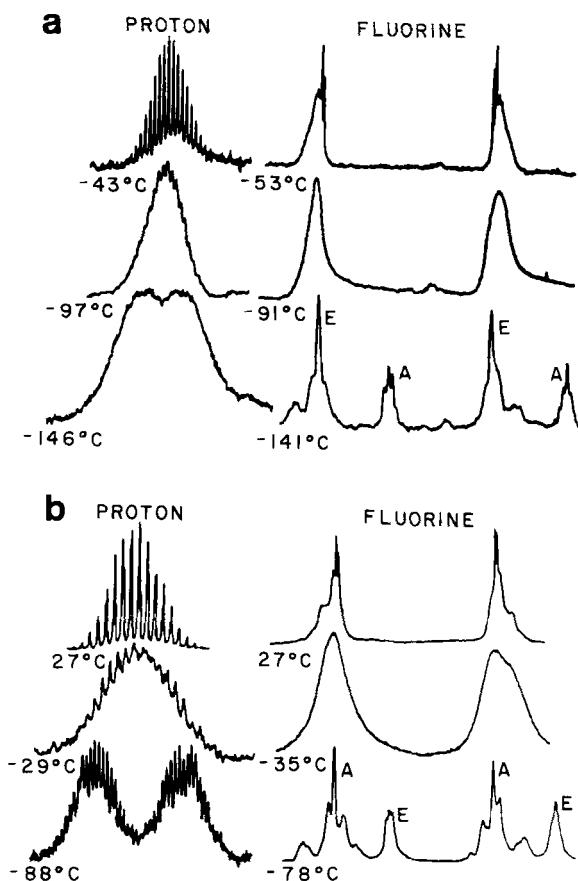
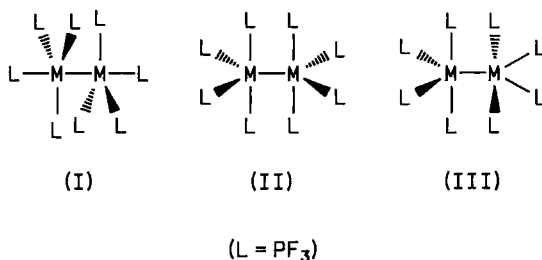


FIG. 7. (a) Temperature dependence of the ^1H (90 MHz) and ^{19}F (84.66 MHz) NMR spectra for $\text{RuH}(\text{PF}_3)_4$ in CHClF_2 . A and E indicate axial and equatorial fluorine resonances. (b) Temperature dependence of the ^1H (90 MHz) and ^{19}F (84.66 MHz) NMR spectra for $\text{IrH}(\text{PF}_3)_4$. The ^{19}F spectra were taken in CH_2Cl_2 , the 27°C ^1H spectrum in toluene- d_8 , and the two low-temperature ^1H spectra in acetone- d_6 . A and E indicate axial and equatorial fluorine resonances. [Reproduced from reference (251) with permission.]

Complexes of the type $[\text{MH}_2(\text{PF}_3)_4]$ ($\text{M} = \text{Fe}, \text{Ru}, \text{Os}$) have been assigned a cis structure on the basis of NMR spectroscopic data.

B. DINUCLEAR COMPLEXES

The structures of $[\text{M}_2(\text{PF}_3)_8]$ ($\text{M} = \text{Rh}, \text{Ir}$) consist of $\text{M}(\text{PF}_3)_4$ units joined together by a metal-metal bond, and could adopt any of the arrangements (I)–(III) involving axial-axial linkage (I) or equatorial-equatorial linkage (II and III). The ^{19}F NMR spectra of



these complexes are temperature dependent and the problem has been simplified by ^{31}P decoupling experiments (see Fig. 8), which show that

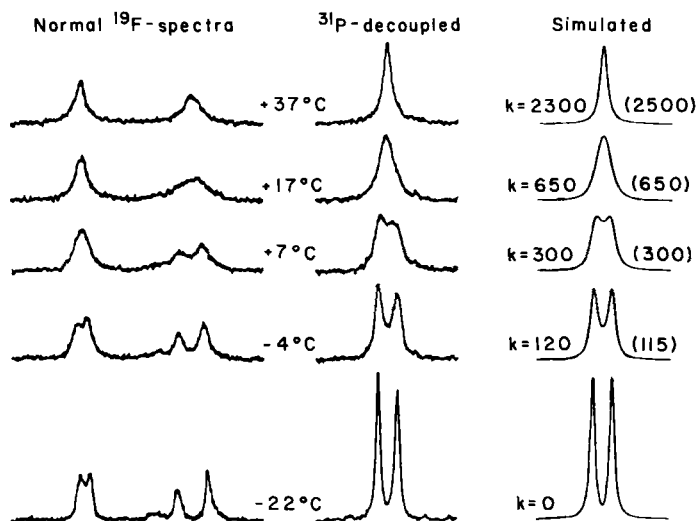


Fig. 8. Normal and ^{31}P -noise decoupled ^{19}F NMR spectra at 56.45 MHz of $\text{Rh}_2(\text{PF}_3)_8$ in $\text{C}_3\text{F}_5\text{Br}$ at various temperatures with calculated NMR line shapes at rates (K) indicated. [Reproduced from reference (19) with permission.]

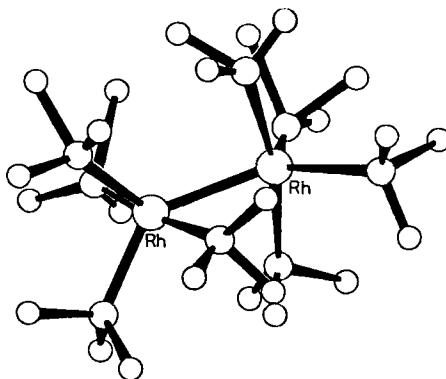


FIG. 9. Molecular structure of $[\text{Rh}_2(\text{PF}_3)_8]$ (326).

in the slow exchange limit two equally intense singlet signals are obtained, indicative of (II) or (III) rather than the 3:1 ratio expected for structure (I).

The $(\text{PF}_3)_4$ units can be either eclipsed (II) (D_{2h} microsymmetry) or staggered (III) (D_{2d} microsymmetry). The latter alternative, which is favored on steric grounds, has been confirmed by an unpublished X-ray study of a poor quality crystal of $[\text{Rh}_2(\text{PF}_3)_8]$ (Fig. 9) (19, 326). The accuracy of the molecular structure as shown above is limited by thermal motions and disorder of the fluorine atoms. The Rh—Rh distance [2.88(2) Å] is longer than in $[\text{Rh}_2(\text{PF}_3)_4(\text{PPh}_3)_2(\mu\text{-PhC}_2\text{Ph})]$ (*vide infra*) and may be related to the ready cleavage of the metal—metal bond by H_2 or group IV hydrides.

V. Bonding

A. TRIFLUOROPHOSPHINE

Before discussing the nature of the bonding in PF_3 and its transition metal complexes it is interesting to note that quantitative data on the gas-phase basicity of PF_3 have recently become available using the technique of ion cyclotron resonance spectroscopy. The proton affinity of PF_3 was originally determined as 160 ± 5 kcal/mol (84) and later improved to 158 ± 1 kcal/mol (104). The corresponding value for CO is 143 kcal/mol. Surprisingly, the order of gas-phase basicities of the group V trifluorides is found to be $\text{NF}_3 < \text{AsF}_3 < \text{PF}_3$ and this anomalous order has been attributed to the greater p_π – d_π overlap in PF_3 and PF_3H^+ .

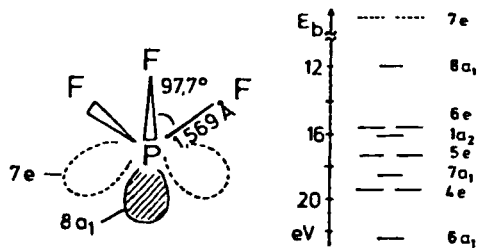


FIG. 10. Structure and ionization potentials of free PF_3 .

COMPARISON OF EXPERIMENTAL AND THEORETICAL IONIZATION
POTENTIALS FOR PH_3 , $\text{P}(\text{CH}_3)_3$, AND PF_3

Molecule	Orbital	Ionization potentials (eV)			
		Expt.	SCM-X α -DV	SCF-MO	SCF-X α -SW
PH_3	$5a_1$	10.58	10.39	10.02 ^a	10.61
	$2e$	13.50	13.09	13.70	13.42
	$4a_1$	21.2	20.43		20.55
$\text{P}(\text{CH}_3)_3$	$8a_1$	8.58	8.41	8.49	
	$6e$	11.31	10.67	12.04	
	$1a_2$		12.01	13.87	
	$5e$	12.7	12.11	14.63	
	$7a_1$		13.13	15.88	
	$4e$	15.8	13.07	15.89	
	$6a_1$		15.75	na	
	$3e$	19.6	19.53	na	
PF_3	$8a_1$	12.27	12.19	12.68	
	$6e$	15.88	15.00	18.32	
	$1a_2$	16.30	14.68	17.93	
	$5e$	17.46	16.00	19.67	
	$7a_1$	18.60	17.17	21.11	
	$4e$	19.50	17.83	21.45	

Early self-consistent field molecular orbital (SCF-MO) studies on PH₃, PF₃, and PMe₃ by Hillier and co-workers (123, 144) predicted ionization potential data which were in good agreement with the experimental values determined by UV photoelectron spectroscopy (241). More recently, the electronic structures of these phosphines have been reexamined (67, 366). Self-consistent multipolar X α calculations (SCM-X α -DV) by Xiao *et al.* (366) give excellent agreement between the theoretical and experimental ionization energies. When the transition-state procedure is used, the first ionization potentials of 10.39, 8.41, and 12.19 eV for PH₃, PMe₃, and PF₃ are calculated compared with the experimental values of 10.58, 8.58, and 12.27 eV (Fig. 10).

The nature of the frontier orbitals is also of interest and a Mulliken population analysis of the constituent orbitals establishes that the highest occupied molecular orbital (HOMO) of each phosphine consists primarily of a lone pair *sp* hybrid on phosphorus. The orbital energy ordering PMe₃ < PH₃ < PF₃ also parallels the percentage phosphorus *s*-character of the HOMO of PMe₃ (11% *s* and 60% *p*), PH₃ (14% *s*, 67% *p*) and PF₃ (29% *s*, 32% *p*). In each case the back lobe of the *sp* hybrid interacts with the substituent attached to phosphorus in a σ -bonding fashion.

Especially interesting is the π -symmetry *pd* hybrid that comprises the lowest unoccupied molecular orbital (LUMO) and the SCM-X α -DV results show that there are several important quantitative differences in the PX₃ systems. The energy of the 7*e* (LUMO) in PF₃ is lower than that in either PH₃ or PMe₃, and this should enhance back bonding to PF₃ when complexed to a transition metal compared to PH₃ or PMe₃. Furthermore, the nature of the lowest unoccupied *e* orbital changes so that whereas in PH₃ 3*e* is a hybrid of 36% *p* and 23% 3*d* on phosphorus, the corresponding percentages for PMe₃ are 14% and 10% (7*e*) and 44% and 23% for PF₃ (7*e*).

Thus contrary to the normally accepted view (86, 124) which ascribes π -acceptor properties of PF₃ to empty 3*d* orbitals, the π -acceptor orbital on phosphorus is mainly 3*p* in character. Mixing in 3*p* orbital character has the effect of directing the empty π orbital in the direction of the lone pair where the metal would bind. It is also worth noting that the 7*e* orbital for PF₃ has antibonding P—F character.

The most recent view on the π -accepting abilities of phosphines in transition metal-phosphine complexes is by Marynick (247) who has used approximate and *ab initio* MO theory to demonstrate that π accepting into σ^* orbitals is important for PF₃. Calculations on the model complex [Cr(NH₃)₅(PF₃)] compared to [Cr(NH₃)₅(PH₃)] showed

greater π -accepting ability for PF_3 even without d orbitals on phosphorus. The reasons for the enhanced π -accepting ability via σ^* orbitals of PF_3 are related to the highly polar P—F bonds which characteristically have low-lying σ^* orbitals. These σ^* orbitals are composed of $3s$ and $3p$ orbitals which overlap more effectively with metal $3d$ orbitals than do the $2s$ and $2p$ orbitals of amines.

B. TRANSITION METAL- PF_3 COMPLEXES

Molecular orbital (CNDO/2) theoretical calculations have been carried out on $[\text{Cr}(\text{PF}_3)_6]$, $[\text{Ni}(\text{PF}_3)_4]$, and $[\text{Fe}(\text{PF}_3)_5]$ (320), and the results compared with experimental ionization energies determined by UV photoelectron spectroscopic measurements of these complexes in the gas phase. The metal-phosphorus bonds show large $\sigma(\text{P} \rightarrow \text{M})$ and $\pi(\text{M} \rightarrow \text{P})$ charge transfers but small *total* charge transfers ($\text{M} \rightarrow \text{P}$) which induce on the metal a small positive charge.

The high volatility of binary metal- PF_3 complexes and hydrides has enabled photoelectron data to be measured on the following complexes: $[\text{M}(\text{PF}_3)_6]$ ($\text{M} = \text{Cr}, \text{Mo}, \text{W}$) (139, 276); $[\text{M}(\text{PF}_3)_5]$ ($\text{M} = \text{Fe}, \text{Ru}$) (139, 267, 276); $[\text{M}(\text{PF}_3)_4]$ ($\text{M} = \text{Ni}, \text{Pd}, \text{Pt}$) (122, 146, 267); $[\text{MH}(\text{PF}_3)_4]$ ($\text{M} = \text{Co}, \text{Rh}, \text{Ir}$) (139, 276); $[\text{MnH}(\text{PF}_3)_5]$ (139); and $[\text{FeH}_2(\text{PF}_3)_4]$ (141).

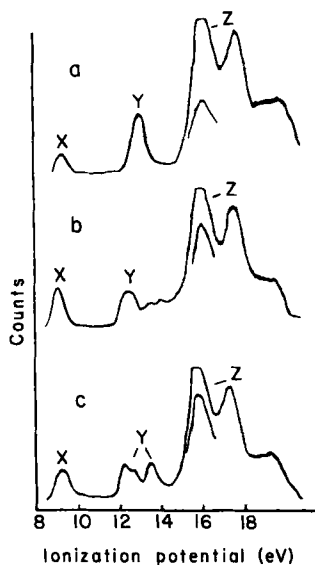


Fig. 11. He(I) photoelectron spectra of $[\text{M}(\text{PF}_3)_6]$ [$\text{M} = \text{Cr}$ (a), Mo (b), and W (c)]. [Reproduced from reference (139) with permission.]

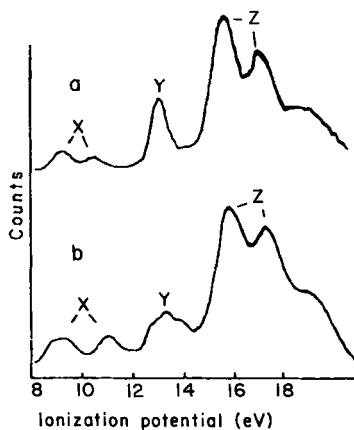


FIG. 12. He(I) spectra of $[M(PF_3)_5]$ [$M = Fe$ (a) and Ru (b)]. [Reproduced from reference (139) with permission.]

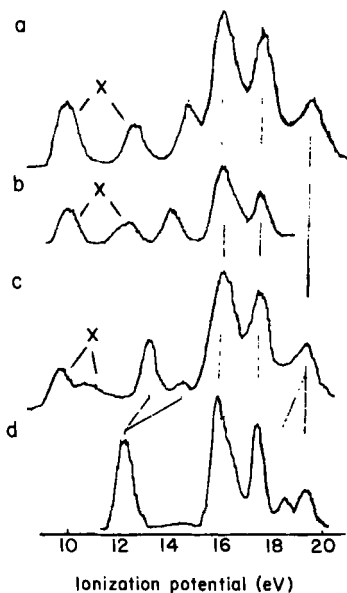


FIG. 13. He(I) Photoelectron spectra of (a) $[Pt(PF_3)_4]$, (b) $[Pd(PF_3)_4]$, (c) $[Ni(PF_3)_4]$, and (d) PF_3 . [Reproduced from reference (146) with permission.]

Some typical He(I) photoelectron spectra are shown in Figs. 11–13, and the ionization energy data are summarized in Table III, together with relevant values for the corresponding carbonyl complexes.

The photoelectron spectra are usually easily assigned in view of the

TABLE III

IONIZATION POTENTIALS (eV) OF TRANSITION METAL TRIFLUOROPHOSPHINE AND HYDRIDOTRIFLUOROPHOSPHINE COMPLEXES. DATA FOR ANALOGOUS CARBONYL COMPLEXES ARE GIVEN IN PARENTHESES WHERE APPLICABLE

Orbital	[M(PF ₃) ₆](O _h)				[M(PF ₃) ₅](D _{3h})		[MH(PF ₃) ₄](C _{3v})			[M(PF ₃) ₄](T _d)				
	Cr	Mo	W	[MnH(PF ₃) ₅](C _{4v})	Fe	Ru	Co	Rh	Ir	Ni	Pd	Pt		
Metal <i>d</i>	<i>e_g</i>			<i>a</i> ₁	<i>a</i> ₁ '	<i>a</i> ₁			<i>t</i> ₂	9.69 (8.93)	9.9	9.83		
	<i>t</i> _{2g}	9.29 (8.40)	9.17 (8.50)	9.30 (8.56)	<i>b</i> ₁	<i>e</i> '	9.15 (8.60)	9.17 <i>e</i>	9.58 (8.90)	9.70	9.82 <i>e</i>	10.74 (9.76)	12.2	12.45
				<i>e</i> } <i>b</i> ₂ } <i>a</i> ₁ }	(8.85) <i>e</i> '' 9.47 (9.14) 11.30 (10.55)	10.43 (9.86)	11.07 <i>e</i>	10.56 (9.90)	11.79	11.95				
M—H							<i>a</i> ₁	12.12 (11.5)						
M—P	<i>t</i> _{1μ} } <i>a</i> _{1g} } <i>e</i> _g }	12.84	12.94 13.48 13.93	<i>a</i> ₁ } <i>e</i> } <i>e</i> }	12.93	<i>a</i> ₁ } <i>a</i> ₁ } <i>e</i> ' } <i>a</i> ₂ ' }	13.08	12.8 <i>a</i> ₁ } 13.25 <i>e</i> }	13.25	13.83	14.18 <i>a</i> ₁	13.17 14.65	13.7	14.54
Fluorine lone pair		15.80 17.36 19.3	15.80 17.36 19.1	15.85 17.44 18.7	15.85 17.43 19.4	15.83 17.24 19.1	15.75 17.18 18.9	16.00 17.46 19.4	15.90 17.42 19.3	16.01 17.42 19.4	15.97 17.48	15.8 17.4	15.87 17.53	

widely separated bands. Thus the bands labeled X in the spectra of the octahedral d^6 [M(PF₃)₆] complexes (Fig. 11) (M = Cr, Mo, W) can be clearly assigned to ionization of the filled t_{2g} orbital. Likewise, in the d^8 trigonal-bipyramidal [M(PF₃)₅] complexes (M = Fe, Ru) (Fig. 12) the X bands arise from the e' ($d_{x^2-y^2}$, d_{xy}) and e'' (d_{xz} , d_{yz}) orbitals. Bands labeled Y and Z arise from the M—P σ orbitals and orbitals principally involving P—F and F lone pair electrons, respectively.

Figure 13 shows the photoelectron spectra of tetrahedral d^{10} [M(PF₃)₄] complexes (M = Ni, Pd, Pt) where the X bands arise from filled metal t_2 and e orbitals. The figure shows how the orbital energies change relative to PF₃ itself. The photoelectron studies suggest that (1) in the [M(PF₃)₄] series σ and π bonding are both strongest for Pt and weakest for Pd, (2) d -orbital ionization energies generally increase along a series and down a group, and (3) metal–phosphorus σ bonding increases across a series and down a group.

C. PF₃ ADSORBED ON METAL SURFACES

An important link between the chemistry of transition metal complexes and that of metal surfaces has been established recently by studies of the chemisorption of PF₃ on a series of transition metals by Ertl and co-workers (112, 227, 271). Although strictly the chemisorption of PF₃ is beyond the scope of this article, a brief summary of the results is given below.

The electronic properties of PF₃ bonded to surfaces of Cr, Fe, Ni, Cu, Ru, Pd, Ir, and Pt have been investigated mainly by UV photoelectron spectroscopy, low-energy electron diffraction (LEED), and electron energy loss spectroscopy (271). Bond formation may be described as involving the coupling of the highest occupied PF₃ orbital (σ donor $8a_1$) to metallic s states and "back donation" of metallic d electrons into the empty π acceptor ($7e$) orbital. Of special importance is the observation that the observed lowering of the ionization energy of the $8a_1$ level shows behavior very similar to the properties of the corresponding zero-valent mononuclear PF₃ complex [M(PF₃)_n], suggesting that the chemisorption bond should be considered as an essentially local phenomenon. Agreement is especially good with the face-centered cubic metals (Ni, Pd, Pt, and Ir), whereas large variations were found for body-centered cubic metals Cr and Fe. Figure 14 shows He(I) and He(II) data for PF₃/Fe (110) and [Fe(PF₃)₅], and the data in Table IV list the relative ionization energies of chemisorbed PF₃ (in eV) (271).

Interactions of single transition metal atoms (e.g., Cr, Fe, Co, and Ni) with PF₃ (and CO) have been studied by an *ab initio* MO theory and the

TABLE IV

RELATIVE IONIZATION POTENTIALS OF CHEMISORBED PF_3 (IN eV) WITH RESPECT TO AN INTERNAL REFERENCE ($6a + 1a_1 = 16.1$ eV)^a

Level	$\text{PF}_3(\text{free})$	$\text{Cr}(\text{poly})$	$\text{Fe}(111)$	$\text{Fe}(110)$	$\text{Ni}(111)$	$\text{Cu}(110)$	$\text{Ru}(0001)$	$\text{Pd}(110)^b$	$\text{Pd}(100)$	$\text{Ir}(100)$ (-5×1)	$\text{Ir}(100)$ (-1×1)	$\text{Pt}(111)$	Peak
$8a_1$	12.27	12.75	13.1*	13.90	13.75	13.45	13.75	13.85	13.90	14.20	—	14.60	<i>a</i>
$6e$	15.88	16.1	16.1	16.1	16.1	16.1	16.1	16.1	16.1	16.1	16.1	16.1	<i>b</i>
$1a_2$	16.30												
$5e$	17.46	17.60	17.30	17.40	17.40	17.30	17.35	17.40	17.30	17.45	17.50	17.40	<i>c</i>
$7a_1$	18.60												
$4e$	19.50	19.30	19.50	19.45	19.45	19.40	19.40	19.35	19.35	19.55	19.55	19.55	<i>d</i>
$6a_1$	22.55	22.50	22.60	22.65	22.60	22.55	22.60	22.60	22.60	22.70	22.75	22.75	<i>e</i>
Complex		$\text{Cr}(\text{PF}_3)_6$	$\text{Fe}(\text{PF}_3)_5$		$\text{Ni}(\text{PF}_3)_4$		$\text{Ru}(\text{PF}_3)_3$		$\text{Pd}(\text{PF}_3)_4$		$\text{Hf}(\text{PF}_3)_4$		$\text{Pt}(\text{PF}_3)_4$
$8a_1$		12.84	13.08		13.17(t_2)		12.8		13.7		14.18		14.54
					14.65(a_1)		13.25						
					-13.54(av)		13.65						
							-13.25(av)						

^a The ionization potentials of the $8a_1$ levels of the corresponding mononuclear complexes are included for comparison.^b HeI data.

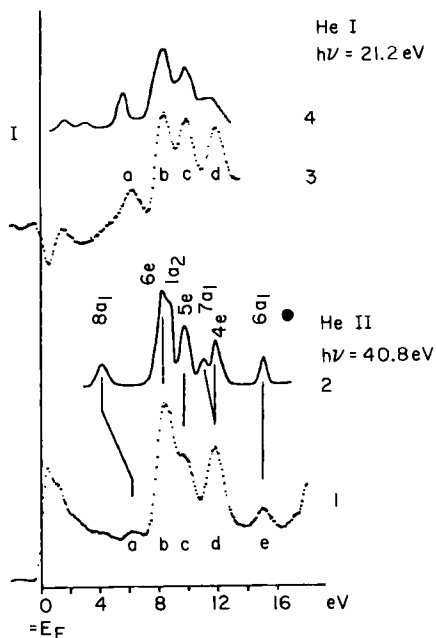


FIG. 14. Comparison of UPS data. (1) He(II) spectrum of PF₃/Fe(110); (2) He(II) spectrum of free PF₃; (3) He(I) difference spectrum (PF₃ covered clean surface) of PF₃/Fe(110); (4) He(I) spectrum Fe(PF₃)₅. The energy scales were adjusted in order to line up peak *b* with the (*6e* + *1a*₂) maximum. [Reproduced from references (112, 227, 271) with permission.]

HOMO levels of both ligands (*8a*₁ for PF₃; *5σ* for CO) move toward lower energies due to interaction with the metal *4s* and *3dz*² orbitals (163). Calculations for Ni(*3d*¹⁰) reveal that there is a more pronounced electron transfer to PF₃ than to CO (162). More recently a surface molecule approach to the adsorbate derived ionization energies for both PF₃ and CO on transition metal surfaces has been developed (106).

D. COMPARISON OF CO AND PF₃ AS LIGANDS

As mentioned in Section I, various physical evidence suggests that PF₃ and CO are very similar in their behavior toward transition metals (72, 174, 272). Mass spectroscopic data (313) on mixed CO/PF₃ metal complexes show that within experimental error the M—CO and M—PF₃ bond energies are the same. IR and Raman studies also indicate that the CO stretching force constants change less on PF₃ substitution

than with any other neutral $2e$ donor. The very small cone angle (344) of PF_3 compared with other phosphines (except for PH_3 and cage phosphines) is also likely to contribute significantly to its coordinating properties.

Jolly and co-workers (7) showed that the carbon $1s$ and oxygen $1s$ binding energies of a CO ligand in transition metal carbonyls are a good measure of the $d_\pi-\pi^*$ back bonding involved. The Mo $3d_{5/2}$, C $1s$, and O $1s$ binding energies measured by X-ray photoelectron spectroscopy (XPES) on complexes of the type $[\text{M}(\text{CO})_5\text{L}]$ ($\text{L} = \text{CO}, \text{PX}_3$) are linearly related to each other and to the phosphorus lone pair ionization energy of the free PX_3 . The XPES results indicate that both σ donor and π acceptor properties of PX_3 are important and that PF_3 seems to be a slightly better π acceptor than CO.

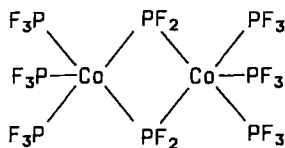
He(I) photoelectron spectroscopic data on mixed CO/ PF_3 complexes of Fe(0) and Cr(0) (142, 267) show a steady increase in the metal $3d$ -orbital energies as PF_3 replaces CO, thus suggesting that there is a greater *overall* electron-withdrawing ability for PF_3 . Similarly, where data are available for complexes of the type $[\text{ML}_n]$ ($\text{L} = \text{CO}$ or PF_3 ; $n = 4, 5, 6$), $[\text{MHL}_n]$ ($n = 4$ or 5), and $[\text{MH}_2\text{L}_4]$, the metal nd ionization energies are always larger for the PF_3 derivative.

Detailed UV photoelectron spectra have been published on $[\text{ML}(\text{CO})_5]$ [$\text{M} = \text{Cr}, \text{Mo}, \text{W}$; $\text{L} = \text{PX}_3$; $\text{X} = \text{F}, \text{Cl}, \text{Br}$ (96) and $\text{M} = \text{Cr}, \text{Mo}, \text{W}$; $\text{L} = \text{PET}_3, \text{PMe}_3, \text{P}(\text{NMe}_2)_3, \text{P}(\text{OR})_3, \text{PF}_3$ (367)]. It was concluded that (i) the electron density on the metal increases along the series $\text{PF}_3 < \text{CO} < \text{PCl}_3 < \text{PBr}_3$ and in the order $\text{W} < \text{Mo} < \text{Cr}$, and (ii) PF_3 is similar but a somewhat poorer π acceptor than CO. A theoretical study of a series of complexes $[\text{Ni}(\text{CO})_3\text{L}']$ using the nonempirical Hartree-Fock Slater transition state method suggested an order of σ donation as $\text{CO} > \text{PF}_3$ and for back bonding $\text{CO} > \text{PF}_3$ (368).

VI. Dinuclear Complexes Containing Bridging PF_2 Ligands

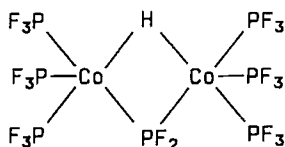
The first complex of this type was reported by Kruck and Lang (205) who obtained the red liquid compound $[\text{Co}_2(\text{PF}_3)_6(\mu\text{-PF}_2)_2]$ (2) by heating CoI_2 and copper at 170°C with high-pressure (400 atm) PF_3 (method A). The structure (2) was elucidated by ^{19}F NMR spectroscopy.

The structurally related bright-red crystalline iron compound $[\text{Fe}_2(\text{PF}_3)_6(\mu\text{-PF}_2)_2]$ has been obtained by Timms by metal vapor synthesis (method B) in which iron atoms and PF_3 are cocondensed at liquid nitrogen temperature (340, 341). A similar reaction using cobalt

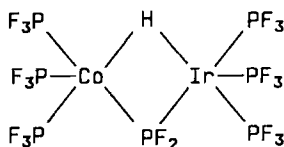


(2)

was originally thought to afford [Co₂(PF₃)₈] (341) but the product is more likely to be [Co₂(PF₃)₆(μ-PF₂)H] (3) (342). The latter has also been obtained by UV irradiation of the hydrido complex [CoH(PF₃)₄] (method C) and when a mixture of [CoH(PF₃)₄] and [IrH(PF₃)₄] is used the mixed metal complex [CoIr(PF₃)₆(μ-PF₂)H] (4) results.



(3)



(4)

Dinuclear iron complexes containing bridging PF₂ ligands have been made by UV irradiation of [FeH₂(PF₃)₄] in the presence of iodine or ethylmercaptan (method D) (198). There is a very interesting report of the interaction of PF₃ with a uranium cathode at 77 K (method E) which affords a PF₃ complex of uranium formulated tentatively as containing a triple-bridging PF₂ system, viz [U₂F₂(PF₃)₄(μ-PF₂)₃], but no confirmatory structural or spectroscopic data are available (9). Complexes made by the above methods are listed in Table V.

VII. Polynuclear Complexes

In marked contrast to the large number of polynuclear metal carbonyl complexes known there are as yet relatively few reports of analogous polynuclear (i.e., containing more than two metal atoms) transition metal-PF₃ complexes. Trifluorophosphine can displace up to half the coordinated CO ligands in [Ru₃(CO)₁₂] (method A) before the metal cluster is broken and mononuclear complexes are formed.

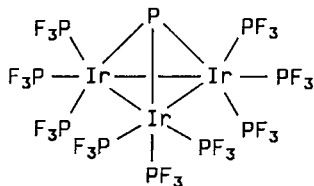
TABLE V

DINUCLEAR TRANSITION METAL TRIFLUOROPHOSPHINE COMPLEXES CONTAINING PF_2 -BRIDGING LIGANDS

Complex ^a	Method of preparation	Color	M.P. (°C), B.P. (°C/mmHg)	ϕ_{F} ^b	$^1J_{\text{PF}}$ ^{c,d}	Reference
$\text{Fe}_2(\text{PF}_3)_6(\text{PF}_2)_2$	(B) (C)	Bright-red	34	-0.7^e	—	198, 340, 341
$\text{Fe}_2(\text{PF}_3)_6(\text{PF}_2)(\text{SC}_2\text{H}_5)$	(D)	Red	Oil	—	—	198
$\text{Fe}_2(\text{PF}_3)_6(\text{PF}_2)(\text{I})$	(D)	Red	Oil	—	—	198
$\text{Co}_2(\text{PF}_3)_6(\text{PF}_2)_2$	(A)	Red	$25, 50/10^{-3}$	13.2^f	1330	205, 341, 342
$\text{Co}_2(\text{PF}_3)_6(\text{PF}_2)(\text{H})$	(C)	Red-violet	$64, \text{subl. } 40/10^{-3}$	7.0^g	1290	220
$\text{CoIr}(\text{PF}_3)_6(\text{PF}_2)(\text{H})$	(C)	Red oil	$40/10^{-3}$	—	—	220
$\text{U}_2\text{F}_2(\text{PF}_3)_4(\text{PF}_2)_3$	(E)	—	—	—	—	9

^a The complexes $\text{Cr}_2(\text{PF}_3)_8(\text{PF}_2)_2$ and $\text{CrFe}(\text{PF}_3)_7(\text{PF}_2)_2$ have also been described briefly (341) as has $\text{Fe}_3(\text{PF}_3)_9(\text{PF}_2)_2$ (256).^b In ppm (relative to CCl_3F).^c In Hz.^d $^1J_{\text{PF}}$ quoted is only approximate.^e $(\text{PF}_2) \phi_{\text{F}} = -30.6; +36.7$ ppm.^f $(\text{PF}_2) \phi_{\text{F}} = 33.8$ ppm, $^1J_{\text{PF}} = 1230$ Hz.^g $(\text{PF}_2) \phi_{\text{F}} = 14.4$ ppm, $^1J_{\text{PF}} = 1160$ Hz.

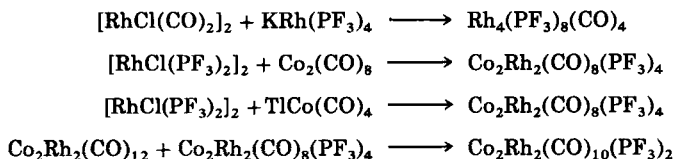
Reductive fluorophosphination of IrCl₃ with copper at 80–200 atm PF₃ (method B) leads to the formation of the interesting orange-red crystalline μ -phosphidononakis(trifluorophosphine)triiridium compound [Ir₃(PF₃)₉(μ -P)] (5), containing the stable Ir₃P cluster.



(5)

Pyrolysis of [Rh₂(PF₃)₈] at 170° (method C) evolves two molecules of PF₃ per dimer and gives a dark red volatile crystalline solid which has been formulated as [Rh₃(PF₃)₈(μ -PF₂)] or [Rh₃(PF₃)₉] mainly on the basis of mass spectroscopic results. However, the possibility that this complex is in fact [Rh₄(PF₃)₁₂] cannot be ruled out in view of the synthesis of the complex [Rh₄(PF₃)₈(CO)₄] from the reaction between [Rh(CO)₂Cl]₂ and [KRh(PF₃)₄] (method D).

Several other tetranuclear complexes containing different metals have been obtained from the reaction between metal carbonyl and metal trifluorophosphine complexes (method E) or by intermolecular ligand-exchange reactions (method F) between tetranuclear complexes. The following structures have been proposed on the basis of ¹⁹F NMR and mass spectroscopic studies.



The trimetallic complex [Fe₃(CO)₈(μ -PPh)₂(PF₃)] has been obtained from the corresponding [Fe₃(CO)₈(μ -PPh)₂(MeCN)] compound by displacement of MeCN (method G). The structure, which is based on a square-pyramidal array of three iron and two phosphorus atoms, consists of isomers whose interconversion has been studied by variable-temperature ¹⁹F and ³¹P NMR spectroscopy. A trimetallic PF₃ complex containing mercury bonded to two metals results from the reactions

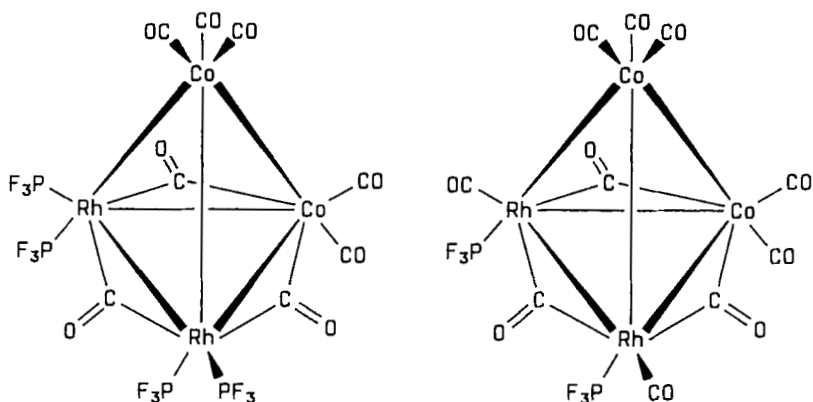
TABLE VI

POLYNUCLEAR TRANSITION METAL TRIFLUOROPHOSPHINE COMPLEXES

Complex	Method of preparation	Colour	M.P. (°C), B.P. (°C/mmHg)	ϕ_F^a	$^1J_{PF}^{b,c}$	Reference
$Fe_3(CO)_8(\mu-PPh)_2(PF_3)$	(G)	Red	—	-174; -166 ^d	1289, 1306	173
$Co_2Rh_2(PF_3)_4(CO)_8$	(E)	Deep-brown	—	10.3, 13.8 ^e	1410, 1465	155, 156
$Co_2Rh_2(PF_3)_2(CO)_{10}$	(E) (F)	Deep-brown	—	11.9 ^f	1459	155, 156
$Co_2Ir_2(PF_3)_4(CO)_8$	(E)	Dark-brown	—	—	—	155, 156
$Ru_3(PF_3)_x(CO)_{12-x} (x = 1-6)$	(A)	Red	—	—	—	350
$Rh_3(PF_3)_9^g$	(C)	Red	—	—	—	17
$Rh_2Hg(PF_3)_8$	(H)	White	105-106	—	—	17
$Rh_4(PF_3)_8(CO)_4$	(E)	Dark-red	subl. 60/10 ⁻³	—	—	155, 156
$Os_3(PF_3)(CO)_8(Ph_2C_2)$	(A)	Violet	—	—	—	113
$Ir_2Hg(PF_3)_8$	(G)	Yellow	113-116	—	—	17
$Ir_3P(PF_3)_9$	(B)	Orange-red	subl. 80/10 ⁻³	—	—	220

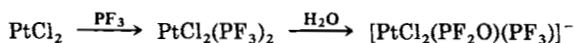
^a In ppm relative to CCl₃F.^b In Hz.^c Spectra complex and temperature dependent.^d Standard not given. (Mixture of isomers).^e ϕ_P [relative to P(OMe)₃] = 18.2 ppm.^f ϕ_P [relative to P(OMe)₃] = 26.9 ppm.^g See text for discussion of this formulation.

(method H) between potassium amalgam and [RhCl(PF₃)₂]₂ (in the presence of PF₃) or [IrCl(PF₃)₄]. Polynuclear complexes containing PF₃ are listed in Table VI.



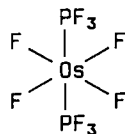
VIII. Halogeno-Metal Complexes

Probably the first metal-PF₃ complex to be synthesized was [PtF₂(PF₃)₂], made by Moissan as early as 1891 (263) from the reaction of PF₅ with platinum black (method A); however, its identity was not recognized at that time. Much later, in 1951, Chatt and Williams (63) passed PF₃ over heated PtCl₂ (method B) to give both [PtCl₂(PF₃)₂] and [PtCl₂(PF₃)₂]. This method is not generally applicable for halogeno-trifluorophosphine complexes, however, recently it has been extended to the bromo complex. Hydrolysis of the coordinated PF₃ in these complexes is rapid (174).



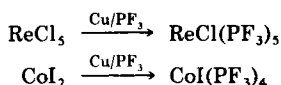
There is a very recent report (51) of the exothermic reaction between [OsF₆] and PF₃ to give [OsF₄(PF₃)₂] which is a monomeric nonelectrolyte and has been assigned the trans structure (6). This seems to be the first well-authenticated fluorometal to contain PF₃. It is also noteworthy in involving the high oxidation state Os(IV). No evidence has been found for the analogous Ir(IV) complex but a polymeric [RuF₄(PF₃)] has been described (50).

Kruck and co-workers (174) have shown that reductive fluorophosphination of transition metal halides with high pressures of PF₃ in the

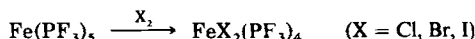


(6)

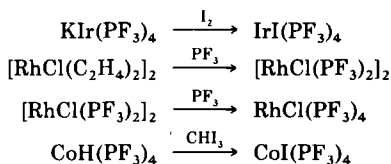
presence of copper metal at elevated temperatures is a general route to zero-valent metal- PF_3 complexes (see earlier sections), but this route can be used (method C) in certain circumstances to afford halogeno complexes.



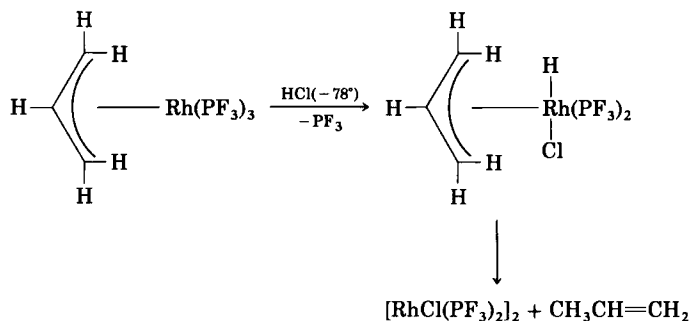
The dihalogenotetrakis(trifluorophosphine)iron complexes can readily be obtained by direct oxidation of $[\text{Fe(PF}_3)_5]$ with the appropriate halogen under mild conditions (method D). NMR studies establish that the halogens lie in *cis*-positions of the octahedron.



Other synthetic routes reported involve the interactions of trifluorophosphine metallates and iodine (method E), displacement of carbon monoxide, alkenes, etc. by PF_3 from the corresponding halide complexes (method F), addition of PF_3 to dinuclear halogeno-bridged PF_3 complexes at low temperatures (method G), and treatment of a metal hydrido- PF_3 complex with iodoform (method H).



A particularly interesting synthetic route to complexes of the type $[\text{RhX(PF}_3)_2]$ ($\text{X} = \text{Cl, Br}$) is via the oxidative addition of HCl (or $t\text{-BuBr}$) to the η^3 -allylic rhodium(I) complex $[\text{Rh(C}_3\text{H}_5)(\text{PF}_3)_3]$ (method I) (Scheme 1), followed by alkene elimination.



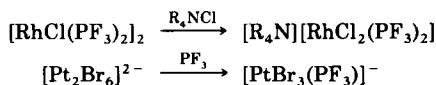
SCHEME 1

At low temperatures the intermediate η^3 -allylrhodium(III) hydride PF₃ complex was detected by ¹H and ¹⁹F NMR spectroscopy and provided supportive evidence for the isomerisation of alkenes via an allyl-metal-hydride mechanism (285, 293).

The dinuclear complexes [MX(PF₃)₂]₂ (M = Rh, Ir; X = Cl, Br, I) are sufficiently volatile for their He(I) and He(II) photoelectron spectra to be recorded (288, 289) and the data have assisted in the assignments of bands in the photoelectron spectra of the corresponding carbonyl complexes for which transition state SCF-X α -SW calculations of ionization energies have been made.

Another interesting feature of the dinuclear iridium complex [IrCl(PF₃)₂]₂ is its very dark color and metallic luster in the solid state, indicative of intermetallic bonding. A recent single-crystal structure determination (149) reveals that the structure consists of infinite zig-zag chains of iridium atoms with short inter- and intramolecular Ir...Ir contacts (see Figs. 15 and 16).

Anionic halogeno complexes listed in Table VII are usually obtained by addition of either tetraalkylammonium or tetraphenylarsonium halides to a dinuclear halogeno-bridged metal-PF₃ complex (method J) or, alternatively, by simple addition of PF₃ to dinuclear halogeno-bridged anions, e.g., of the type [M₂X₆]²⁻ (M = Pt) (method K).



These synthetic routes are of interest since it is possible to oxidize these anionic species further with halogen to give rather rare examples

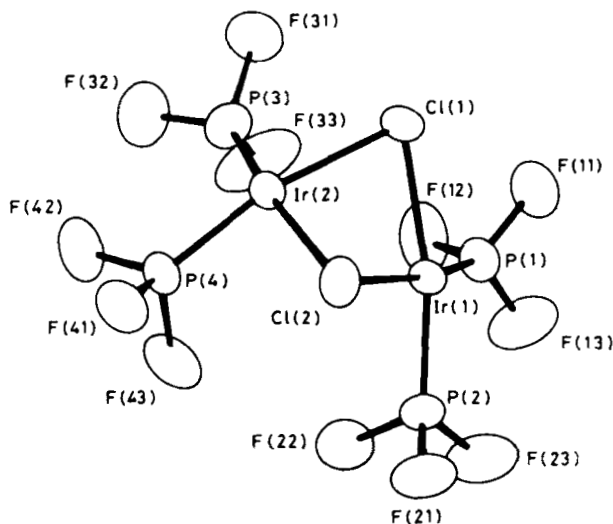


FIG. 15. The molecular structure of $[\text{IrCl}(\text{PF}_3)_2]_2$. Ir-P (av.), 2.134(5); Ir-Cl (av.), 2.413(5); P-F (av.), 1.517 Å. [Reproduced from reference (149) with permission.]

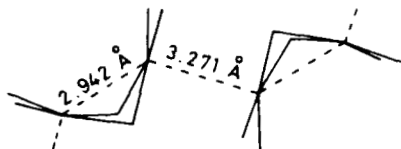
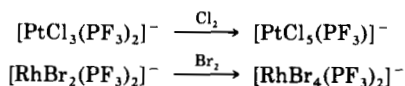


FIG. 16. The chain structure of $[\text{IrCl}(\text{PF}_3)_2]_2$.

of PF_3 complexes of metals in a high oxidation state (method L) (87-90).



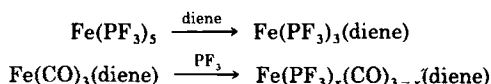
The measurement of $^1J_{\text{PtP}}$ for these anionic PF_3 complexes of metals in two oxidation states has been utilized to ascertain the importance of π bonding in these systems. Thus the ratio of $^1J_{\text{PtP}}$ in Pt(II) complexes of the type $[\text{PtX}_3(\text{PF}_3)]^-$ and Pt(IV) complexes $[\text{PtX}_5(\text{PF}_3)]^-$ ($\text{X} = \text{Cl}, \text{Br}$) is about 1:0.6, which is similar to related data for the corresponding trialkylphosphine and -phosphite complexes.

There is a single report (168) (method M) of the reaction between a metal fluoride- BrF_3 adduct and PF_3 , in which the PF_3 acts as both a

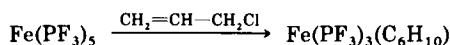
reducing agent and a ligand. Halogeno-transition metal complexes containing PF₃ are summarized in Table VII.

IX. Transition Metal-Alkene Complexes

A variety of synthetic routes to monoene and polyene tri-fluorophosphine-transition metal complexes have been devised. Direct photochemically induced reaction of a metal-PF₃ complex with an activated alkene or diene (method A) has proved useful only for iron, the products being either [Fe(PF₃)₄(alkene)] or [Fe(PF₃)₃(diene)] (194). Mixed carbonyl-trifluorophosphine complexes of the type [Fe(PF₃)_x(CO)_{3-x}(diene)] result from either thermal or photochemical reactions of dieneiron carbonyl complexes and PF₃ (52, 53) (method B). The compounds are fluxional.



There is one report (193) of the formation of a hexa-1,3-dienemetal complex formed by a coupling reaction of the allyl ligands (method C) in the reaction of [Fe(PF₃)₅] with allyl chloride.



The most generally applicable route to diene or triene metal PF₃ complexes is via metal vapor synthesis (method D), in which the metal vapors are cocondensed with PF₃ and the polyene at liquid nitrogen temperatures.

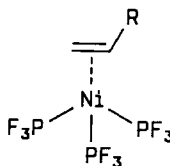
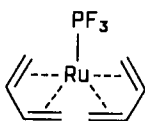
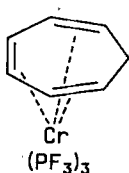
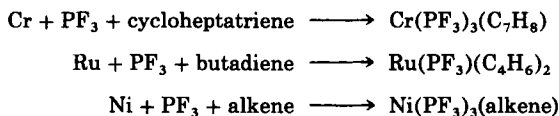


TABLE VII

HALOGENO-TRANSITION METAL-TRIFLUOROPHOSPHINE COMPLEXES

Complex	Method of preparation	Color	M.P. (°C), B.P. (°C/mmHg)	ϕ_F^a	$^1J_{PF}^{b,c}$	Reference
$FeCl_2(PF_3)_4$	(D)	Yellow-orange	subl. $20/10^{-3}$ (dec. 45)	4.2, 12	1330	200
$FeBr_2(PF_3)_4$	(D)	Orange-red	subl. $20/10^{-3}$ (dec. 65)	4.4, 230	1355	200
$FeI_2(PF_3)_4$	(D)	Purple	subl. $30/10^{-3}$ (dec. 95)	1.6, 264	1310	199, 200 ^d
$CoI(PF_3)_4$	(C) (H)	Red-brown	dec. 77	—	—	174, 202
$RhCl(PF_3)_4$	(G)	Yellow	stable at -78	—	—	17, 18, 87, 291
$RhBr(PF_3)_4$	(G)	Yellow	stable at -78	—	—	17, 18, 87, 291
$RhI(PF_3)_4$	(G)	Yellow	stable at -78	—	—	17, 18, 87, 291
$[RhCl(PF_3)_2]_2^e$	(C) (F) (I)	Red	69–70	17.0	1328	17, 18, 80, 87–89, 182, 282, 288, 291, 293
$[RhBr(PF_3)_2]_2^e$	(F) (I)	Red	61.5–62	15.9	1309	17, 18, 87–89, 285, 289, 291
$[RhI(PF_3)_2]_2$	(F)	Red	62.5	14.2	1316	17, 18, 87, 289, 291
$[RhCl_2(PF_3)_2][(CH_3)_4N]$	(J)	Pale-yellow	—	—	—	17, 18, 87–89
$[RhCl_2(PF_3)_2][(C_6H_5)_4As]$	(J)	Pale-yellow	—	—	—	17, 18, 87–89
$[RhCl_2(PF_3)_2][Bu_4N]$	(J)	Lemon	88–92	20.6	1298	17, 18, 87–89
$[RhBr_2(PF_3)_2][Bu_4N]$	(J)	Lemon	107–108	19.9	1392	17, 18
$[RhCl_4(PF_3)_2][Bu_4N]^e$	(L)	Deep-yellow	130–132	34.5	1367	87, 89
$[RhBr_4(PF_3)_2][Bu_4N]^e$	(L)	Deep-orange	169–172	29.5	1355	87, 89
$ReCl(PF_3)_5$	(C)	Colorless	153(dec.)(subl. $20/10^{-3}$)	—	—	174, 186
$[RuF_4(PF_3)]_n$	(B)	Rust-brown	—	—	—	50
$OsF_4(PF_3)_2$	(B)	Yellow	—	—	—	51

$\text{PdCl}_2(\text{PF}_3)_2^e$	(B) (F)	—	—	34.5	1383	87, 89
$[\text{PdCl}_3(\text{PF}_3)] [\text{Bu}_4\text{N}]^f$	(K)	Golden-yellow	86–96	34.7	1408	87
$\text{IrCl}(\text{PF}_3)_4$	(F)	Pale-yellow	32.5	19.5	1252	17
$\text{IrI}(\text{PF}_3)_4$	(E)	Yellow	dec. > 25	—	—	174, 186
$[\text{IrCl}(\text{PF}_3)_2]_2^i$	(F)	Dark-blue	76–78	24.1	1270	17, 149, 289
$[\text{PtF}_2(\text{PF}_3)]_2$	(A)	—	—	—	—	263
$\text{PtCl}_2(\text{PF}_3)_2^e$	(B)	Colorless	102	29.0 ^g	1316	63, 88, 89, 143, 312
$[\text{PtCl}_2(\text{PF}_3)]_2$	(B)	Orange-yellow	155–156	—	—	63, 88
$\text{PtBr}_2(\text{PF}_3)_2^e$	(B) (F) (M)	Colorless	97–100	33.9	1323	87–89, 168
$[\text{PtCl}_3(\text{PF}_3)] [\text{Bu}_4\text{N}]$	(K)	Yellow	131–134	40.4 ^{h,i}	1311	91, 119
$[\text{PtBr}_3(\text{PF}_3)] [\text{Bu}_4\text{N}]$	(K)	Yellow	114–118	37.7 ^{i,j}	1313	91
$[\text{PtI}_3(\text{PF}_3)] [\text{Bu}_4\text{N}]$	(K)	Orange	130–131	33.1 ^{i,k}	1320	91
$[\text{PtI}_3(\text{PF}_3)] [\text{C}_5\text{H}_{11}]_4\text{N}$	(K)	Orange	73–75	—	—	91
$[\text{PtCl}_5(\text{PF}_3)] [\text{Bu}_4\text{N}]$	(L)	—	—	—	—	90
$[\text{PtBr}_5(\text{PF}_3)] [\text{Bu}_4\text{N}]$	(L)	—	—	—	—	90

^a In ppm relative to CCl_3F .

^b In Hz.

^c $^1J_{\text{PF}}$ listed is equal to $^1J_{\text{PF}} + n^3J_{\text{PF}}$ for $(\text{PF}_3)_{n+1}$ complexes.

^d Mössbauer spectrum (199), $\delta = 0.44$ (mm/sec), ε (mm/sec) = 0.26.

^e Full NMR analysis (89).

^f Relative signs determined.

^g δ_{P} [relative to $\text{P}(\text{OMe})_3$] = –68.0 ppm.

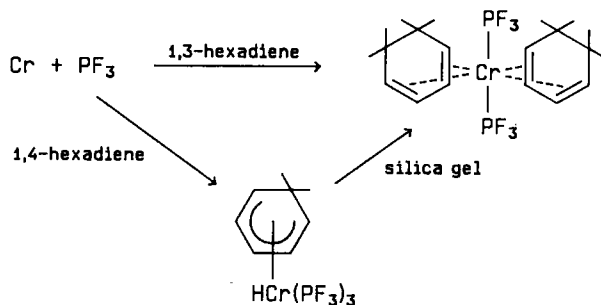
^h δ_{P} = –50.2 ppm, $^1J_{\text{PtP}}$ = 7464 Hz.

ⁱ Pt chemical shift data available.

^j δ_{P} = –52.1 ppm, $^1J_{\text{PtP}}$ = 7257 Hz.

^k δ_{P} = –60.3 ppm, $^1J_{\text{PtP}}$ = 6959 Hz.

^l X-Ray structure (149).

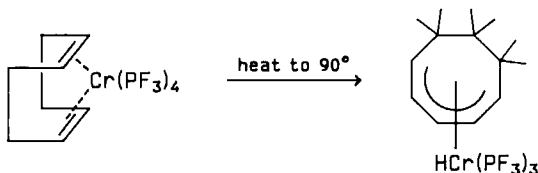


SCHEME 2

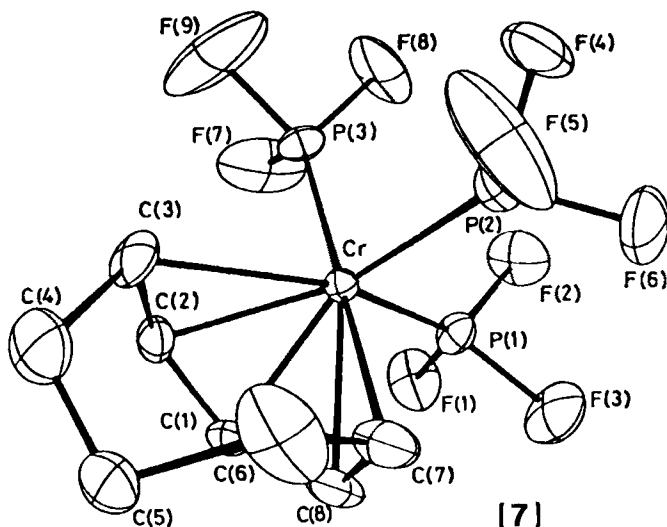
Interestingly, although the reaction of 1,3-cyclohexadiene, chromium atoms, and PF_3 yields bis(η^4 -cyclohexadiene)bis(trifluorophosphine)chromium, the corresponding reaction with 1,4-cyclohexadiene yields the η^5 -cyclohexadienyl hydrido tris(trifluorophosphine)chromium complex, which rearranges in the presence of silica gel to form $[\text{Cr}(\eta^4\text{-C}_6\text{H}_8)_2(\text{PF}_3)_2]$ rather than (η^4 -cyclohexadiene)tetrakis(trifluorophosphine)chromium (40) (Scheme 2).

Similar reactions using 1,3-cyclooctadiene, chromium atoms, and PF_3 led only to the η^5 -(cycloocta-1,3-dienyl) hydrido tris(trifluorophosphine)chromium complex $[\text{Cr}(\text{C}_8\text{H}_{11})(\text{PF}_3)_3\text{H}]$ (7), whose structure has been established by X-ray crystallography (125). (See also Section VIII). The chromium-phosphorus bond lengths [ave. 2.146(3) Å] are, as expected, particularly short.

Reaction of chromium atoms, 1,5-cyclooctadiene(1,5-cod), and PF_3 on the other hand yielded a separable mixture of $[\text{Cr}(\text{C}_8\text{H}_{11})(\text{PF}_3)_3\text{H}]$ and (η^4 -cycloocta-1,5-diene)tetrakis(trifluorophosphine)chromium. The latter is readily converted to the former by warming a solution of it to 90°C (Scheme 3). This rearrangement is impaired under an atmosphere of PF_3 and the 1,5-cod is preferentially displaced to give $[\text{Cr}(\text{PF}_3)_6]$.

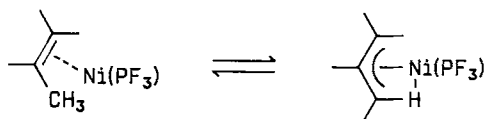


SCHEME 3



The [Ni(alkene)(PF₃)₃] complexes (alkene = ClCH=CH₂, CH₃CH=CH₂, CF₃CH=CH₂, and FCH=CH₂) made by metal vapor synthesis are much less thermally stable than the polyene complexes (28) and decompose readily to give [Ni(PF₃)₄], alkene, and nickel metal.

The propene complex is the most stable and of special interest is the failure to observe any evidence for metal hydride formation prior to thermal decomposition. This contrasts markedly with the temperature-dependent equilibrium between metal-propene and metal-allyl-hydride first observed by Bönnemann (42) for the related complex [Ni(C₃H₆)(PF₃)] and studied by variable-temperature NMR spectroscopy.



The η^4 -cyclohexadiene complex [Ru(η^4 -C₆H₈)(PF₃)₃], which is readily obtained by displacement of benzene (method E) from [Ru(η^4 -C₆H₈)(η^6 -C₆H₆)], is a fluxional molecule (1). The ³¹P{¹H} NMR spectrum at room temperature (Fig. 17) exhibits a basic 1-3-3-1 quartet pattern (coupling to F) and shows the further complicated fine structure expected for an [AX₃]₃ spin system (X = F, A = P) indicative of

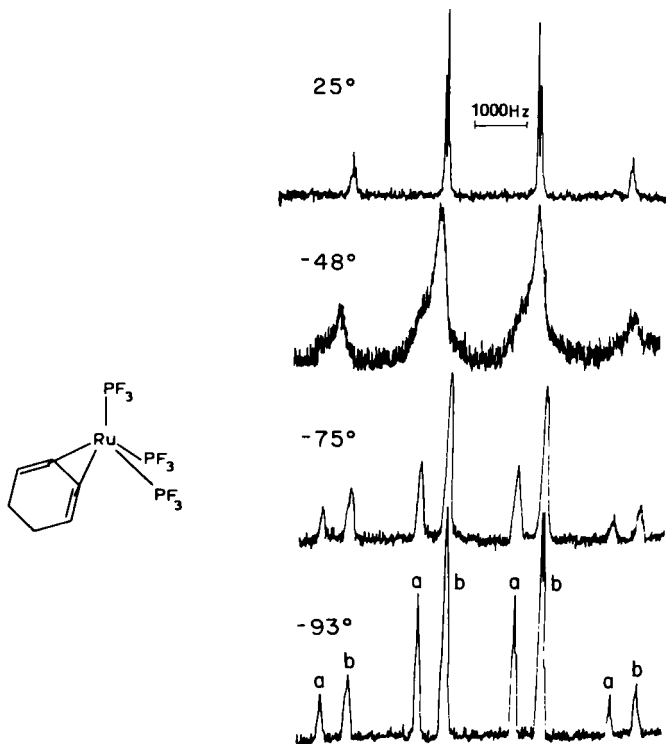
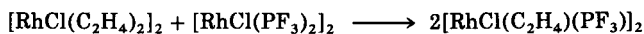


FIG. 17. Variable-temperature ^{31}P NMR spectra of $\text{Ru}(\eta^4\text{-C}_6\text{H}_8)(\text{PF}_3)_3$. [Reproduced from reference (1) with permission.]

equivalence of the three PF_3 ligands. The limiting NMR spectrum obtained at -93°C shows two overlapping quartet patterns in the ratio 1:2 with much further fine structure evident (1).

Other synthetic routes to alkene-metal complexes reported in the literature involve bridge cleavage reactions of halogeno complexes (method F), facile intermolecular scrambling reactions involving metal-alkene and metal- PF_3 complexes (18, 81) (method G) (Scheme 4), and the coupling together of two alkyne units to afford a metallocyclopentadiene derivative (method H).

Complexes obtained by all of the above routes are listed in Table VIII.



SCHEME 4

TABLE VIII

ALKENE TRANSITION METAL COMPLEXES CONTAINING TRIFLUOROPHOSPHINE

Complex	Method of preparation	Color	M.P. (°C), B.P. (°C/mmHg)	ϕ_F^a	$^1J_{PF}^{b,c}$	References
Cr(PF ₃) ₄ (buta-1,3-diene)	(D)	Yellow-brown	205–210	—	—	330
Cr(PF ₃) ₄ (cycloocta-1,5-diene) ^d	(D)	Yellow	—	3.3 } 16.7 }	1280 ± 25	37
Cr(PF ₃) ₃ (cycloheptatriene) ^e	(D)	Orange-yellow	223 (subl. 150/760)	—7.3 } —12.5 }	1264	38, 343
Cr(PF ₃) ₂ (cyclohexa-1,3-diene) ₂	(D)	Orange-red	—	0.7	1250	40
Fe(PF ₃) ₄ (acrylonitrile)	(A)	Yellow	45–46 (~30/10 ⁻³)	—	—	194
Fe(PF ₃) ₄ (crotonitrile)	(A)	Yellow	73–74 (~40/10 ⁻³)	—	—	194
Fe(PF ₃) ₄ (styrene)	(A)	Yellow	28–29 (~40/10 ⁻³)	—	—	194
Fe(PF ₃) ₄ (methylacrylate)	(A)	Orange	ca. –5 (~25/10 ⁻³)	—	—	194
Fe(PF ₃) ₃ (methylmethacrylate)	(A)	Red	ca. 0 (~25/10 ⁻³)	—	—	194
Fe(PF ₃) ₃ (crotonaldehyde)	(A)	Orange	ca. –15 (~25/10 ⁻³)	—	—	194
Fe(PF ₃) ₃ (methyl vinyl ketone)	(A)	Yellow	ca. –20 (~25/10 ⁻³)	—	—	194
Fe(PF ₃) ₃ (buta-1,3-diene)	(A) (B)	Yellow	118–119	4.8	1290	52, 53, 197, 357
Fe(PF ₃) ₃ (isoprene)	(A)	Yellow	84–86; 65	5.8	1290	52, 53, 197, 293
Fe(PF ₃) ₃ (<i>cis</i> -penta-1,3-diene)	(A) (B)	Yellow	55–58	5.8	1293	52, 53, 197
Fe(PF ₃) ₃ (cyclopentadiene)	(A)	Yellow	112–114	—	—	195
Fe(PF ₃) ₃ (<i>trans</i> -penta-1,3-diene)	(A) (B)	Yellow	97–98	3.8	1291	52, 53, 197
Fe(PF ₃) ₃ (2,3-dimethylbutadiene)	(A) (B)	Yellow	88–89	6.5	1289	52, 53, 197
Fe(PF ₃) ₃ (hexa-1,3-diene)	(C)	Yellow	85	—	—	193
Fe(PF ₃) ₃ (<i>trans,trans</i> -hexa-2,4-diene)	(A) (B)	Yellow	34–35	—	—	52, 53, 197
Fe(PF ₃) ₃ (<i>cis,trans</i> -hexa-2,4-diene)	(A)	Yellow	106	—	—	197
Fe(PF ₃) ₃ (2,4-dimethyl-1,3-pentadiene)	(A) (B)	Yellow	116–119	5.4	1300	52, 53, 197
Fe(PF ₃) ₃ (methylsorbate)	(A)	Yellow	42–44	—	—	197
Fe(PF ₃) ₃ (1,3-cyclohexadiene)	(A) (B)	Yellow	102	—	1290	197, 355
Fe(PF ₃) ₃ (1,3-cycloheptadiene)	(A)	Yellow	34–35	—	—	197
Fe(PF ₃) ₃ (1,3-cyclooctadiene)	(A)	Yellow	31	—	—	197

(continued)

TABLE VIII (continued)

Complex	Method of preparation	Color	M.P. (°C), B.P. (°C/mmHg)	ϕ_F^a	$^1J_{PF}^{b,c}$	References
$Fe(PF_3)_3(1,5\text{-cyclooctadiene})^f$	(D)	Yellow	—	—	—	54, 237
$Fe(PF_3)_3(\text{norbornadiene})$	(A)	Yellow	52–53	—	—	197
$Fe(PF_3)(\text{buta-1,3-diene})_2^g$	(D)	Orange-yellow	185–192	—	—	126, 224, 343, 362
$Fe(PF_3)_2(CO)(\text{buta-1,3-diene})$	(B)	Yellow	—	6.6	1310	52, 53, 357
$Fe(PF_3)_2(CO)(\text{isoprene})$	(B)	Yellow	—	—	—	52, 53
$Fe(PF_3)_2(CO)(2,3\text{-dimethylbuta-1,3-diene})$	(B)	Yellow	—	8.3	1303	52, 53
$Fe(PF_3)_2(CO)(\text{trans,trans-2,4-hexadiene})$	(B)	Yellow	—	6.9	1304	52, 53
$Fe(PF_3)_2(CO)(\text{trans-1,3-pentadiene})$	(B)	Yellow	—	—	—	52, 53
$Fe(PF_3)_2(CO)(\text{cis-1,3-pentadiene})$	(B)	Yellow	—	—	—	52, 53
$Fe(PF_3)_2(CO)(1,3\text{-cyclohexadiene})$	(B)	Light-yellow	—	—	1302	358
$Fe(PF_3)_2(CO)(2,4\text{-dimethyl-1,3-pentadiene})$	(B)	Yellow	—	—	—	52, 53
$Fe(PF_3)(CO)_2(\text{buta-1,3-diene})$	(B)	Yellow	—	—	1300	52, 53, 357
$Fe(PF_3)(CO)_2(\text{isoprene})$	(B)	Yellow	—	7.4	1307	52, 53
$Fe(PF_3)(CO)_2(2,3\text{-dimethylbutadiene})$	(B)	Yellow	—	8.0	1308	52, 53
$Fe(PF_3)(CO)_2(\text{trans,trans-2,4-hexadiene})$	(B)	Yellow	—	10.4	1304	52, 53
$Fe(PF_3)(CO)_2(\text{trans-1,3-pentadiene})$	(B)	Yellow	—	8.7	1305	52, 53
$Fe(PF_3)_x(CO)_{4-x}(\text{pentene})$	(B)	—	—	—	1300	78
$Fe(PF_3)(CO)_2(\text{cis-1,3-pentadiene})$	(B)	Yellow	—	8.2	1311	52, 53
$Fe(PF_3)(CO)_2(1,3\text{-cyclohexadiene})$	(B)	Light-yellow	—	—	1316	358
$Fe(PF_3)(CO)_2(2,4\text{-dimethyl-1,3-pentadiene})$	(B)	Yellow	—	10.4	1309	52, 53
$Fe(PF_3)_x(CO)_{3-x}(\text{trimethylenemethane})$	(B)	Light-yellow	Liquid	6.4	1310	74
$Ni(PF_3)_x(\text{propene})$	—	—	—	—	—	42
$Ni(PF_3)_3(\text{propene})$	(D)	Yellow	liquid, (dec. -45°)	20.3	1270	28
$Ni(PF_3)_3(CF_3CH=CH_2)$	(D)	Yellow	liquid, (dec. -30°)	20.8	1305	28
$Ni(PF_3)_3(FCH=CH_2)$	(D)	Yellow	liquid, (dec. -96 to -45)	21.3	1284	28

Σ	Ni(PF ₃) ₃ (ClCH=CH ₂)	D	Yellow	liquid, (dec. -96 to -45)	—	—	28
	Ru(PF ₃) ₃ (buta-1,3-diene) ₂ ^a	(D)	Red-yellow	—	-2.91	1334	262
	Ru(PF ₃) ₃ (cyclohexadiene)	(E)	Pale-yellow	Liquid	3.5	1309	1
	Ru(PF ₃) ₂ (PPh ₃)(buta-1,3-diene)	(B)	Pale-yellow	Oil	3.2	1307	1
	[RhCl(PF ₃) ₃](ethylene) ₂	(G)	Yellow	50 (dec.)	24.6	1332	28, 81
	RhCl(PF ₃) ₂ (buta-1,3-diene)	(F)	Yellow	60	—	—	294
	RhCl(PF ₃) ₂ (1,3-pentadiene)	(F)	Yellow	60	—	—	294
	RhCl(PF ₃) ₂ (2-methylbuta-1,3-diene)	(F)	Yellow	Oil	—	—	294
	RhCl(PF ₃) ₂ (acrylonitrile)	(F)	Yellow	100 (dec.)	—	—	294
	Rh ₂ (PF ₃) ₅ (CH ₃ O ₂ CC ₂ CO ₂ CH ₃) ₂	(H)	Red	162	13.0, 15.6 ⁱ	1337, 1376	22
	Rh ₂ (PF ₃) ₅ (CH ₃ O ₂ CC ₂ H) ₂	(H)	Red	—	10.0, 13.9 ⁱ	1337, 1360	22
	Rh ₂ (PF ₃) ₃ (PPh ₃)(CH ₃ CO ₂ C ₂ CO ₂ CH ₃) ₂	(H)	Red	167	14.0, 17.2,	1353, 1391,	22
					13.7	1345	
	RhCl(PF ₃)(SbPh ₃) ₂ (C ₈ H ₁₂)	(H)	Lemon-yellow	—	—	—	238
	[Rh(PF ₃) ₃](spp) ₂ [(BF ₄) ^j]	(F)	—	—	—	—	24
	[Rh(PF ₃) ₃](spas) ₂ [(BF ₄) ^k]	(F)	—	—	—	—	24
	[Ir(PF ₃) ₃](spp) ₂ [(BF ₄) ^j]	(F)	—	—	—	—	24
	[Ir(PF ₃) ₃](spas) ₂ [(BF ₄) ^k]	(F)	—	—	—	—	24
	IrCl(PF ₃) ₃ (cyclooctene) ₂	(F)	Yellow	106-109	—	—	17
	Ir(acac)(PF ₃) ₃ (cyclooctene)	(F)	Yellow	—	—	—	17

^a In ppm relative to CCl₃F.

^b In Hz.

^c ¹J_{PF} quoted = ¹J_{PF} + n³J_{PF} for (PF₃)_{n+1} complexes.

^d Cr(PF₃)₃(η⁵-cyclooctadienyl)hydridotris(trifluorophosphine) also formed (see Section XIII).

^e δ_P [in ppm relative P(OMe)₃] = 178.6, 206.7 (343).

^f The analogous cyclooctatetraene complex is also known (343).

^g X-Ray crystallographic structure done (224); Fe-PF₃ = 2.024 Å.

^h δ_P = 172.5 ppm.

ⁱ Temperature-dependent spectra.

^j spp = *o*-Styryldiphenylphosphine.

^k spas = *o*-Styryldiphenylarsine.

TABLE IX

TRANSITION METAL ALKYNE COMPLEXES CONTAINING TRIFLUOROPHOSPHINE

	Complex	Method of preparation	Color	M.P. (°C), B.P. (°C/mmHg)		ϕ_F^a	$^1J_{PF}^b$	Temperature (°C)	References
8	$Rh_2(PF_3)_6(HC_2H)$	(B)	Yellow	60–61		7.1	1400	24	20, 26
	$Rh_2(PF_3)_6(C_6H_5C_2H)$	(B)	Dark-brown	Oil		6.1	1385	–145	20, 26
	$Rh_2(PF_3)_6(n-C_4H_9C_2H)$	(B)	Brown	Oil		6.5	1400	24	20, 26
	$Rh_2(PF_3)_6(t-C_4H_9C_2H)$	(B)	Orange-brown	18		6.1	1400	–40	20, 26
	$Rh_2(PF_3)_6(CH_3C_2CH_3)$	(B)	Yellow	118		7.5	1380	–70	20, 26
	$Rh_2(PF_3)_6(n-C_3H_7C_2CH_3)$	(B)	Yellow	—		8.9	1405	24	20
	$Rh_2(PF_3)_6(C_6H_5C_2CH_3)$	(A)	Orange	68		8.6	1405	24	20, 26
	$Rh_2(PF_3)_6(C_6H_5C_2C_2H_5)$	(A)	Red	Oil		7.3	1385	–55	20
	$Rh_2(PF_3)_6(C_6H_5C_2C_6H_5)$	(A)	Red	143–145		8.4	1415	–9	20
	$Rh_2(PF_3)_6(C_6H_5C_2CO_2CH_3)$	(A)	Orange	Oil		9.0	1400	24	20
	$Rh_2(PF_3)_6(p-NO_2C_6H_4C_2CO_2C_2H_5)$	(A)	Yellow	58		8.7	1405	24	20, 26
	$Rh_2(PF_3)_6(CF_3C_2CF_3)$	(B)	Yellow	159		6.3 } 7.7 }	1395 } 1355 }	–104	20
	$Rh_2(PF_3)_6(CH_3C_2CO_2CH_3)$	(B)	Yellow	—		8.6	1400	24	20, 26
	$Rh_2(PF_3)_6(t-C_4H_9C_2-t-C_4H_9)$	(C)	Red	—		5.3	1402	24	23
	$Rh_2(PF_3)_5(t-C_4H_9C_2-t-C_4H_9)$	(A)	Yellow	145–148		–1.5 } 12.1 } 8.1 } 14.1 }	1381 } 1353 } 1375 } 1324 }	24 24 24 24	23

$\text{Rh}_2(\text{PF}_3)_4(\text{PPh}_3)_2(\text{C}_6\text{H}_5\text{C}_2\text{C}_2\text{H}_5)$	(D)	Burgundy	164–165 (dec.)	5.6	1390	24	21
$\text{Rh}_2(\text{PF}_3)_4(\text{PPh}_3)_2(\text{C}_6\text{H}_5\text{C}_2\text{C}_6\text{H}_5)(\text{Et}_2\text{O})^c$	(D)	Burgundy	110–113 (dec.)	—	—	—	21, 26
$\text{Rh}_2(\text{PF}_3)_4(\text{AsPh}_3)_2(\text{C}_6\text{H}_5\text{C}_2\text{C}_6\text{H}_5)$	(D)	Red	189 (dec.)	5.7	1385	24	21
$\text{Rh}_2(\text{PF}_3)_4(\text{PMePh}_2)_2(\text{C}_6\text{H}_5\text{C}_2\text{C}_6\text{H}_5)$	(D)	Red	146–148	5.8	1385	24	21
$\text{Rh}_2(\text{PF}_3)_4(\text{PPh}_3)_2(\text{C}_6\text{H}_5\text{C}_2\text{CH}_3)$	(D)	Red	147–151 (dec.)	4.4, 5.7	1360, 1380	24	21
$\text{Rh}_2(\text{PF}_3)_4(\text{AsPh}_3)_2(\text{C}_6\text{H}_5\text{C}_2\text{CH}_3)$	(D)	Red	176–180	5.5	1385	24	21
				4.0, 5.2	1360, 1390	—30	
$\text{Rh}_2(\text{PF}_3)_4(\text{PMePh}_2)_6(\text{C}_6\text{H}_5\text{C}_2\text{CH}_3)$	(D)	Red	105	4.6, 5.8	1360, 1385	24	21
				3.2	1410	110	
$\text{Rh}_2(\text{PF}_3)_4(\text{AsMePh}_2)_2(\text{C}_6\text{H}_5\text{C}_2\text{CH}_3)$	(D)	Red	136–138	5.4	1385	55	21
				4.8, 5.8	1365, 1385	24	
$\text{Rh}_2(\text{PF}_3)_4(\text{AsPh}_3)_2(p\text{-NO}_2\text{C}_6\text{H}_4\text{C}_2\text{CO}_2\text{C}_2\text{H}_5)$	(D)	Red	174 (dec.)	4.4, 6.1	1385, 1405	24	21
				5.8	1415	85	
$\text{Rh}_2(\text{PF}_3)_2(\text{diars})_2(\text{C}_6\text{H}_5\text{C}_2\text{C}_6\text{H}_5)^d$	(D)	Red	196 (dec.)	—0.2	1375	24	21
$\text{Rh}_2(\text{PF}_3)_2(\text{diars})_2(\text{C}_6\text{H}_5\text{C}_2\text{CH}_3)^d$	(D)	Red	180–183	0.2	1360	24	21
$\text{Rh}_2(\eta^5\text{-C}_5\text{H}_5)_2(\text{CO})(\text{PF}_3)(\text{CF}_3\text{C}_2\text{CF}_3)^e$	(E)	Orange	155 (dec.)	8.2	1340	—	103
$\text{Os}_3(\text{CO})_8(\text{PF}_3)(\text{C}_6\text{H}_5\text{C}_2\text{C}_6\text{H}_5)_2$	(E)	Violet	—	—	—	—	113

^a In ppm relative to CCl_3F .

^b $^1J_{\text{PF}}$ in Hz, all J_{PF} values are approximate and spectra are temperature dependent.

^c X-Ray structure done (21).

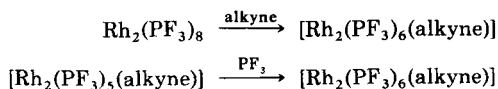
^d diars = $o\text{-C}_6\text{H}_4(\text{AsMe}_2)_2$.

^e $\delta_{\text{P}} = 124.9$ ppm, $^1J_{\text{Prh}} = 360$ Hz (103).

X. Transition Metal-Alkyne Complexes

No mononuclear alkyne complexes containing PF_3 have been reported to date but a number of complexes of the type $[\text{Rh}_2(\text{PF}_3)_6(\text{alkyne})]$ listed in Table IX have been obtained by heating a solution of $[\text{Rh}_2(\text{PF}_3)_8]$ in *n*-hexane under reflux in an inert atmosphere with an equimolar amount of the alkyne (method A). Care must be taken in the case of $\text{MeCO}_2\text{C}\equiv\text{CCO}_2\text{Me}$ and $\text{HC}\equiv\text{CCO}_2\text{Me}$ since reactions occur below room temperature to give the red complexes $[\text{Rh}_2(\text{PF}_3)_5(\text{alkyne})_2]$ (see Section IX), while explosive polymerization of the alkyne occurs above room temperature. The $[\text{Rh}_2(\text{PF}_3)_5(\text{alkyne})_2]$ compounds have been assigned a metallocyclopentadiene structure.

In a number of cases an excess of the alkyne can be condensed onto solid $[\text{Rh}_2(\text{PF}_3)_8]$ using a conventional high vacuum system (method B), and in one case addition of PF_3 to an $[\text{Rh}_2(\text{PF}_3)_5(\text{alkyne})]$ complex has been reported (method C) (23).

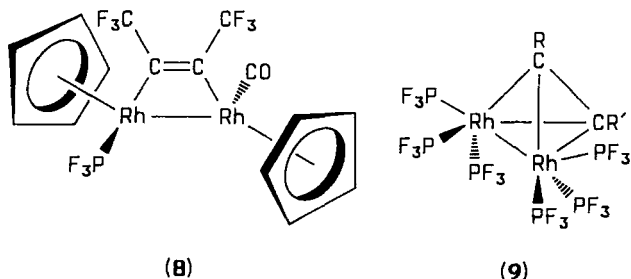


Complexes containing coordinated tertiary phosphines or arsines of the type $[\text{Rh}_2(\text{PF}_3)_4\text{L}_2(\text{alkyne})]$ and $[\text{Rh}_2(\text{PF}_3)_2\text{L}'_2(\text{alkyne})]$ (L = monodentate, L' = bidentate ligand) are readily obtained by displacement of PF_3 from $[\text{Rh}_2(\text{PF}_3)_6(\text{alkyne})]$ under mild conditions (method D). There are also reports of displacement of CO by PF_3 from an alkyne metal carbonyl complex (method E) e.g., (113).



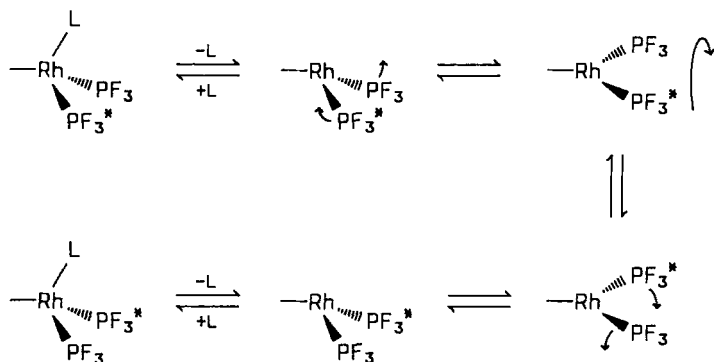
More recently, decarbonylation of the bridging η^1 -alkyne complex $[\text{Rh}_2(\eta^5\text{-C}_5\text{H}_5)_2(\text{CO})_2(\text{CF}_3\text{CCCF}_3)]$ with Me_3NO gave the η^2 -complex, which, when treated with PF_3 , afforded high yields of the η^1 -alkyne mixed carbonyl-trifluorophosphine derivative (8), in which the ligands are mutually trans (103).

By contrast, the structures of the $[\text{Rh}_2(\text{PF}_3)_6(\text{alkyne})]$ (9) complexes contain a bridging alkyne ligand lying over and perpendicular to the metal-metal bond, similar to that in $[\text{Co}_2(\text{CO})_6(\text{RCCR})]$. Variable-temperature ^{19}F NMR studies show that the PF_3 groups undergo intramolecular exchange leading to NMR equivalence at room temperature, and possible mechanisms for exchange have been discussed.



A single-crystal X-ray analysis of the complex $[\text{Rh}_2(\text{PF}_3)_4(\text{PPh}_3)_2(\text{PhCCPh})]$ (21) confirmed that it has a similar structure and that the PPh_3 ligands are on the same side of the molecule as the bridging alkyne.

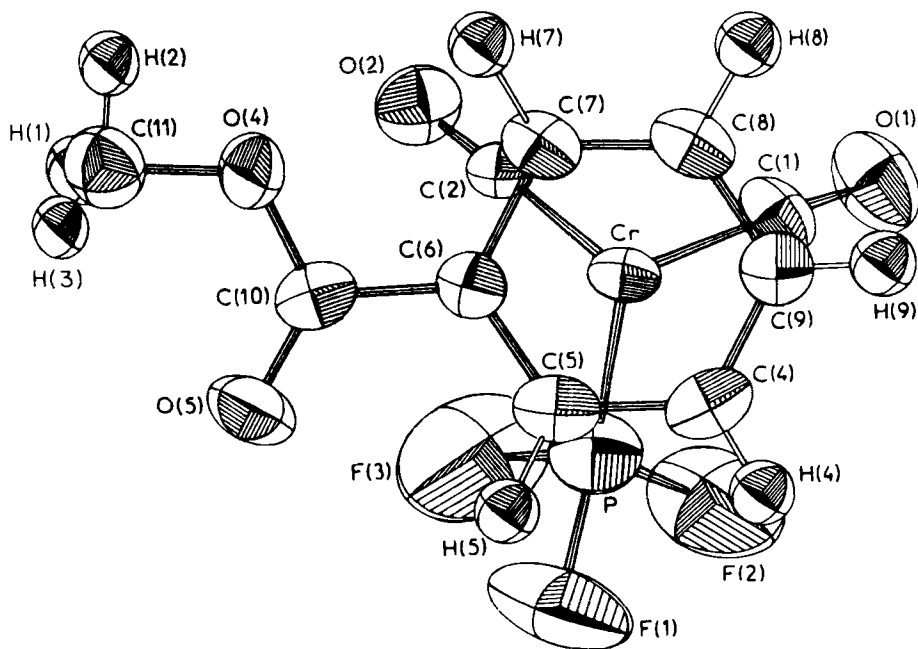
Interestingly this type of complex is stereochemically rigid at around room temperature but undergoes an intramolecular exchange of PF_3 on warming. Such a process suggested the formation of a coordinatively unsaturated intermediate by phosphine dissociation (Scheme 5). Support for this comes from the synthesis of $[\text{Rh}_2(\text{PF}_3)_5(\text{BuCC}^t\text{Bu})]$, which reacts reversibly with PF_3 at room temperature to form $[\text{Rh}_2(\text{PF}_3)_6(\text{BuCC}^t\text{Bu})]$.



SCHEME 5. Proposed mechanism for fluxional behaviour of $[\text{Rh}_2(\text{PF}_3)_4\text{L}_2(\text{alkyne})]$ (21).

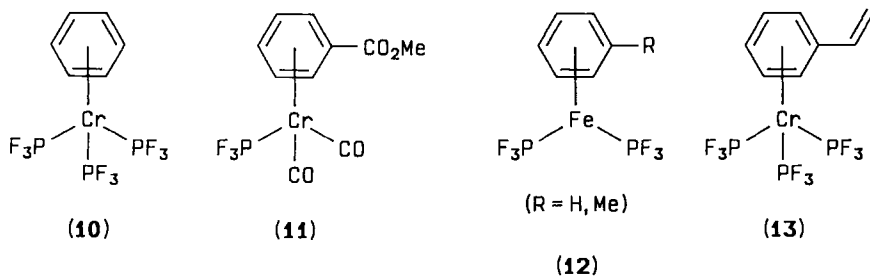
XI. Transition Metal-Arene Complexes

The first reported arene-transition metal trifluorophosphine complex $[\text{Cr}(\eta^6\text{-C}_6\text{H}_6)(\text{PF}_3)_3]$ was obtained by UV irradiation of $[\text{Cr}(\eta^6\text{-C}_6\text{H}_6)(\text{CO})_3]$ with PF_3 (method A), whereas the corresponding thermal reaction afforded instead the mixed carbonyl trifluorophos-



[11]

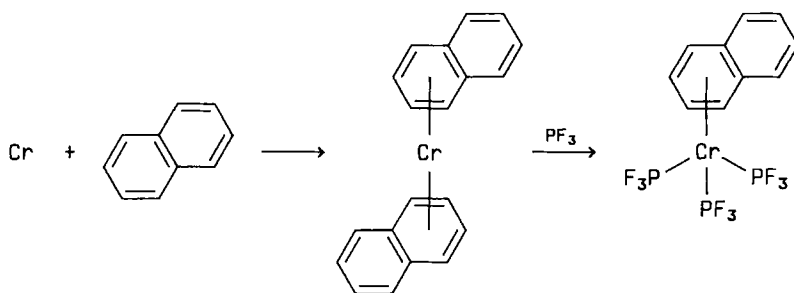
phine complex (174). The ^{19}F NMR spectrum of $[\text{Cr}(\eta^6\text{-C}_6\text{H}_6)(\text{PF}_3)_3]$ (10) has been fully analyzed (277) and is consistent with the complex having C_{3v} symmetry. The crystal and molecular structure of the related complex $[\text{Cr}(\eta^6\text{-C}_6\text{H}_5\text{CO}_2\text{Me})(\text{CO})_2(\text{PF}_3)]$ (11), made by a similar synthetic route (97, 315, 316), has been determined by a single crystal X-ray study. The Cr—P distance of 2.123(3) Å is very much shorter than other known chromium(0)–trivalent phosphorus distances [e.g., 2.252(1) Å in $\{\text{Cr}(\text{CO})_4[\text{P}(\text{OMe})_3]_2\}$, 2.346(3) Å in $[\text{Cr}(\text{CO})_5(\text{PH}_3)]$, and 2.422(1) Å in $[\text{Cr}(\text{CO})_5(\text{PPh}_3)]$] and this has been attributed to



the π -acceptor properties of PF₃. The Cr—P bond length in [Cr(C₈H₁₁)(PF₃)₃H] is also very short [ave. 2.146(3) Å] (see Section IX).

More recently, the technique of metal vapor synthesis has been generally used (method B) to synthesize a variety of arene-metal-PF₃ complexes, and the method has been extended to include pyridine acting as an η^6 -bonded ligand. The report from Skell's group (362) of [Fe(η^6 -toluene)(PF₃)₃] using this route was followed shortly thereafter by Timms's preparation of [Fe(η^6 -C₆H₆)(PF₃)₂] (12), and styrene has also been successfully utilized in the preparation of [Cr(η^6 -styrene)(PF₃)₃] (13) (39). This synthetic method is attractive because the metal can often be sublimed from a spiral of tungsten or molybdenum wire heated electrically and the vapor deflected into the bottom half of a liquid nitrogen cooled vacuum vessel. PF₃ and the arene are then condensed at -196°C and subsequently unreacted ligands are pumped off on warming to room temperature. The arene-metal-PF₃ complexes are invariably volatile and can be sublimed from the reaction vessel. Electron beam and laser techniques are also useful in these metal vapor syntheses (16, 125).

The metal vapor synthesis can also be used to obtain bisarenemetal complexes, which then readily react with PF₃ to displace one arene ring (method C). This route has been used effectively in the synthesis of [Cr(η^6 -naphthalene)(PF₃)₃] (225, 226) (Scheme 6).



SCHEME 6

Interestingly, the presence of the acceptor PF₃ ligands in [Cr(η^6 -naphthalene)(PF₃)₃] makes the coordinated naphthalene become activated toward attack by nucleophiles. Thus treatment with stabilized carbanions and either I₂ or Ce(IV) salts affords high yields of the α -substituted naphthalenes (102) (Scheme 7).

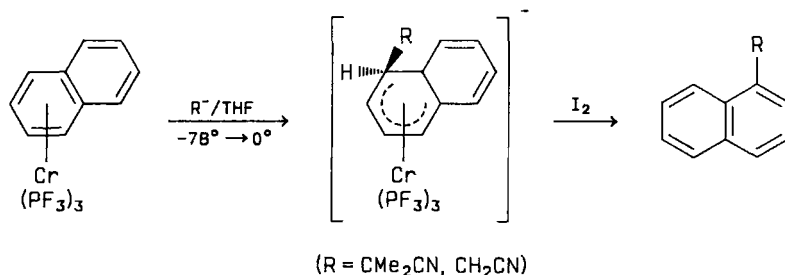
A rather unusual synthetic route to an η^6 -arene-metal-trifluorophosphine complex has been described in which displacement

TABLE X

 η^6 -ARENE TRANSITION METAL COMPLEXES CONTAINING TRIFLUOROPHOSPHINE

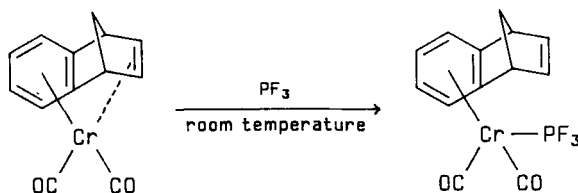
Complex	Method of preparation	Color	M.P. (°C), B.P. (°C/mmHg)	ϕ_F^a	$^1J_{PF}^{b,c}$	Reference
Cr(PF ₃) ₃ (C ₆ H ₆) ^c	(A)(B)	Pale-yellow	dec. > 220	-12.4	1295	174, 257, 277, 338, 339
Cr(PF ₃) ₃ (C ₆ F ₆)	(B)	Pale-yellow	—	—	—	257
Cr(PF ₃) ₃ (mesitylene)	(B)	Cream	dec. > 130	-11.1	1250	257
Cr(PF ₃) ₃ (cumene)	(B)	Pale-green	47-48	-12.7	1284	257
Cr(PF ₃) ₃ (styrene)	(B)	—	Oil	—	—	39
Cr(PF ₃) ₃ (styrene) _n	(B)	Red	—	—	—	39
Cr(PF ₃) ₃ (pyridine)	(B)	—	—	—	—	338
Cr(PF ₃) ₃ (naphthalene)	(C)	Yellow-orange	153 ± 1	—	—	102, 225, 226
Cr(PF ₃)(CO) ₂ (benzonorbornadiene)	(D)	Yellow	—	—	—	161
Cr(PF ₃)(CO) ₂ (C ₆ H ₅ CO ₂ Me) ^d	(A)	Yellow-orange	—	—	—	97, 315, 316
Cr(PF ₃)(CO) ₂ [C ₆ H ₄ (CO ₂ Me) ₂]	(A)	Yellow-orange	88	—	—	97, 315, 316
Fe(PF ₃) ₂ (C ₆ H ₆)	(B)	Red	dec. > 50	-0.4	1305	257
Fe(PF ₃) ₂ (toluene)	(B)	Red	Liquid	—	—	362
Mo(PF ₃) ₃ (mesitylene) ^e	(A)	Colorless	dec. 160 (subl. 100/10 ⁻³)	—	—	174

^a In ppm relative to CCl₃F.^b In Hz.^c Except for Cr(PF₃)₃(C₆H₆), $^1J_{PF}$ as listed is actually $^1J_{PF} + 2^3J_{PF}$ for the (PF₃)₃ complexes and $^1J_{PF} + ^3J_{PF}$ for the (PF₃)₂ complexes. A full NMR spectroscopic analysis has been carried out (277).^d Single-crystal X-ray structure done; Cr—PF₃ = 2.123(3) Å.^e This complex is also formed when Mo(PF₃)₆ and mesitylene are irradiated with UV light (174).



SCHEME 7

of the complexed exocyclic carbon-carbon double bond of η^8 -benzonorbornadiene(dicarbonyl)chromium occurs only in the presence of good π -acceptor ligands (Scheme 8) (method D). The known transition metal-arene complexes containing trifluorophosphine are summarized in Table X.

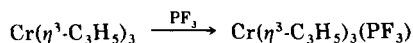


SCHEME 8

XII. Transition Metal η^3 -Allyl Complexes

A variety of different preparative routes to this class of compounds have been utilized and the known complexes are listed in Table XI.

There is only one report to date of the simple addition of PF₃ to an η^3 -allyl-metal complex containing no other ligands (method A), namely,



However, the complex slowly converts to [Cr(PF₃)₆]. A related route (method B) involves the displacement of one or more coordinated η^3 -allyl ligands, viz.,

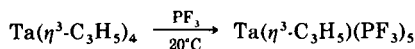


TABLE XI

TRANSITION METAL η^3 -ALLYL COMPLEXES CONTAINING TRIFLUOROPHOSPHINE

Complex	Method of preparation	Color	M.P. ($^{\circ}\text{C}$), B.P. ($^{\circ}\text{C}/\text{mmHg}$)	ϕ_{F}^a	$^1J_{\text{PF}}^{b,c}$	Reference
$\text{Cr}(\eta^3\text{-C}_3\text{H}_5)_3(\text{PF}_3)$	(A)	Dark-green	—	—	—	183
$\text{Fe}(\eta^3\text{-C}_3\text{H}_5)(\text{PF}_3)_3$	(G)	Purple	Unstable	—	—	338
$\text{Fe}(\eta^3\text{-C}_3\text{H}_5)(\text{PF}_3)_3\text{Br}$	(D)	Red-brown	Subl. $25/10^{-1}$	—	—	193
$\text{Fe}(\eta^3\text{-C}_3\text{H}_5)(\text{PF}_3)_3\text{I}$	(D)	Red-brown	110 (dec.), subl. $45/10^{-3}$	—	—	193
$\text{Co}(\eta^3\text{-C}_3\text{H}_5)(\text{PF}_3)_3$	(B) (E) (F) (G)	Yellow	22 (55/760)	10.7	1268	56, 220, 338
$\text{Co}(\eta^3\text{-1-methylallyl})(\text{PF}_3)_3(\text{anti})$	(C) (F)	Yellow	45	11.3	1268	56, 220
$\text{Co}(\eta^3\text{-1-methylallyl})(\text{PF}_3)_3(\text{syn})$	(C) (F)	Yellow	0	10.6	1265	56, 220
$\text{Co}(\eta^3\text{-1-methyl-2-chloroallyl})(\text{PF}_3)_3$	(C)	Yellow	65 (subl. 60/1)	—	—	220
$\text{Co}(\eta^3\text{-1,1-dimethylallyl})(\text{PF}_3)_3$	(F)	Orange	56	12.5	1265	56
$\text{Co}(\eta^3\text{-1,2-dimethylallyl})(\text{PF}_3)_3(\text{anti})$	(F) (G)	Orange	98	11.8	1268	56
$\text{Co}(\eta^3\text{-1,3-dimethylallyl})(\text{PF}_3)_3(\text{syn,syn})$	(C) (F)	Orange	−12	11.4	1290	56, 220
$\text{Co}(\eta^3\text{-2-ethylallyl})(\text{PF}_3)_3$	(F)	—	—	11.3	1268	56
$\text{Co}(\eta^3\text{-cycloheptatrienyl})(\text{PF}_3)_3$	(C) (J)	Yellow	80/1	−13.6	1316	56, 338, 343
$\text{Co}(\eta^3\text{-1-methyl-2-ethylallyl})(\text{PF}_3)_3$	(C)	Red	35	—	—	220
$\text{Co}(\eta^3\text{-1,1,2-trimethylallyl})(\text{PF}_3)_3$	(C)	Yellow	Subl. $25/10^{-3}$	—	—	220
$\text{Co}(\eta^3\text{-cycloheptadienyl})(\text{PF}_3)_3$	(F) (I)	Orange	−15	14.3	1273	56
$\text{Co}(\eta^3\text{-cyclooctenyl})(\text{PF}_3)_3$	(C) (F)	Orange	35	11.6	1265	56, 220
$\text{Co}(\eta^3\text{-cyclohexenyl})(\text{PF}_3)_3$	(C)	Red oil	Subl. $/10^{-3}$	—	—	55, 220
$\text{Co}(\eta^3\text{-C}_3\text{H}_5)(\text{PF}_3)_2(\text{PPh}_3)$	(F)	Orange	145–147	12.9	1278	55
$\text{Co}(\eta^3\text{-1-methylallyl})(\text{PF}_3)_2(\text{PPh}_3)(\text{anti})$	(F)	Orange	114–115	13.4 11.6	1288 1265	55
$\text{Co}(\eta^3\text{-1-methylallyl})(\text{PF}_3)_2(\text{PPh}_3)(\text{syn})$	(F)	Red-orange	125–126	13.5 11.0	1287 1268	
$\text{Co}(\eta^3\text{-1,1-dimethylallyl})(\text{PF}_3)_2(\text{PPh}_3)$	(F)	Red-brown	153–157	13.9 11.8	1323 1304	
$\text{Co}(\eta^3\text{-1,2-dimethylallyl})(\text{PF}_3)_2(\text{PPh}_3)(\text{anti})$	(F) (G)	Orange	150–152	13.3 12.0	1290 1274	
$\text{Co}(\eta^3\text{-1,3-dimethylallyl})(\text{PF}_3)_2(\text{PPh}_3)(\text{syn,syn})$	(F)	Red	114–115	11.6	1277	55

Co(η^3 -2-ethylallyl)(PF ₃) ₂ (PPh ₃)	(F)	Orange	96–98	11.6	1282	55
Co(η^3 -2-ethylallyl)(PF ₃)(PPh ₃) ₂	(F)	Red	145–152	7.4	1308	55
Co(η^3 -cyclooctenyl)(PF ₃) ₂ (PPh ₃)	(F)	Red	137–139	12.9	1281	55
Co(η^3 -cycloheptadienyl)(PF ₃) ₂ (PPh ₃)	(I)	Red	116–118	16.3	1297	55
				14.7	1287	
Co(η^3 -1-methylallyl)(C ₄ H ₆)(PF ₃)(<i>anti</i>)	(C)	Yellow	85–87	13.2	1308 (RT)	58
				13.0	1313	} (–20°C)
				12.4	1316	
Co(η^3 -1,1,3-trimethylallyl)(PF ₃) ₃	(C)	Orange	—	12.8	1269	157
(Ni(η^3 -C ₃ H ₅)(PF ₃)H) ^d	—	—	—	—	—	42
RuCl ₂ (PF ₃)(η^3 -C ₁₀ H ₁₆) ^{e,f}	(H)	Orange	130–131 (dec.)	22.0	1374	140, 148
Rh(η^3 -C ₃ H ₅)(PF ₃) ₃ ^g	(B) (C) (E)	Yellow	Liquid	8.1	1342 ^h	82, 277, 295
Rh(η^3 -1-methylallyl)(PF ₃) ₃	(C) (E)	Yellow	–20	8.2 (<i>syn</i>)	1340,	82, 295
				8.2 (<i>anti</i>)	1341 ^h	
Rh(η^3 -2-methylallyl)(PF ₃) ₃	(E)	Yellow	–20	8.3	1340 ^h	82, 295
Rh(η^3 -cyclohexenyl)(PF ₃) ₃	(C)	Yellow	0	8.4	1346 ^h	82, 295
Rh(η^3 -1,1-dimethylallyl)(PF ₃) ₃	(E)	Yellow	0	9.6	1340 ^h	59, 82, 295
Rh(η^3 -1,2-dimethylallyl)(PF ₃) ₃	(E) (G)	Yellow	35	8.7 (<i>syn</i>)	1347,	59, 82, 295
				8.7 (<i>anti</i>)	1342 ^h	
Rh(η^3 -1,3-dimethylallyl)(PF ₃) ₃	(C)	Yellow	–15	9.3 (<i>syn,syn</i>)	1342 ^h	82, 295
				9.3 (<i>anti,syn</i>)	1340	
Rh(η^3 -1-ethyl-3-methylallyl)(PF ₃) ₃	(C)	Yellow	0	9.2 (<i>syn,syn</i>)	1333 ^h	82, 295
Rh(η^3 -allyl)(PF ₃)(PPh ₃) ₂	(H)	Yellow	140–150	8.3	1381	280
Rh(η^3 -2-methylallyl)(PF ₃)(PPh ₃) ₂	(H)	Yellow	116–120	—	—	280
Rh(η^3 -1-methylallyl)(PF ₃)(PPh ₃) ₂	(H)	Orange	145–155	10.5	1373	280
Ta(η^3 -allyl)(PF ₃) ₅	(B)	Ruby-red	20 (dec.)	—	—	187

^a In ppm relative to CCl₃F.

^b In Hz.

^c Except where stated, ¹J_{PF} listed is equal to ¹J_{PF} + n³J_{PF} for (PF₃)_{n+1} complexes.

^d Low-temperature species in equilibrium with the propene-Ni-PF₃ complex (42).

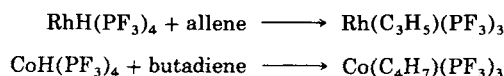
^e An X-ray crystallographic study has been made (148); Ru–PF₃ = 2.237 Å.

^f η^3 -C₁₀H₁₆ = 2,7-dimethylocta-2,6-diene-1,8-diyl.

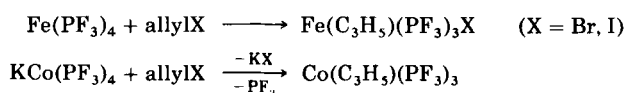
^g A full NMR spectroscopic analysis has been made (277); ¹J_{PF} = –1422 Hz; ³J_{PF} = +40 Hz.

^h All spectra are temperature dependent.

A useful general synthetic approach involves the insertion of allene or dienes into the metal-hydrogen bond of transition metal hydrido-trifluorophosphine complexes (method C).

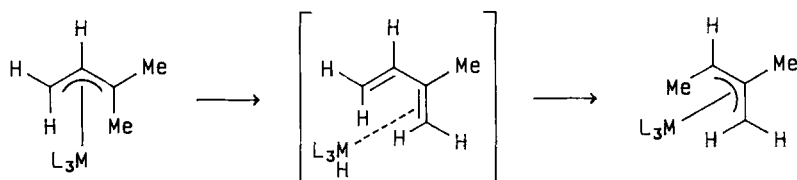


Oxidative addition of an allyl halide to a zero-valent complex (method D) or treatment of a trifluorophosphine metallate complex with an allylic halide followed by loss of PF_3 (method E) have also been briefly reported.

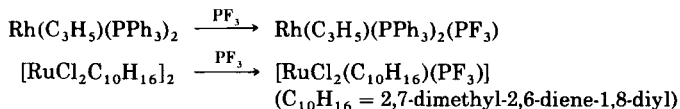


A fairly general synthetic route involves the PF_3 -induced displacement of ligands such as dienes and phosphines coordinated to metal allyl complexes (method F), and it has also been possible in certain complexes to interconvert η^3 -allyl-metal- PF_3 complexes by an intramolecular thermal rearrangement (method G).

Thus when the η^3 -1,1-dimethylallyltris(trifluorophosphine) complexes of cobalt or rhodium are gently warmed a rearrangement to the η^3 -1,2-isomer occurs (56, 295). The postulated mechanism involves a diene-metal hydride intermediate (Scheme 9). The small PF_3 ligand can also be added directly to coordinatively unsaturated η^3 -allylic systems or to chloro-bridged structures (method H).



SCHEME 9. ($\text{M} = \text{Co, Rh}$; $\text{L} = \text{PF}_3$)



The molecular structure of the latter compound has been determined

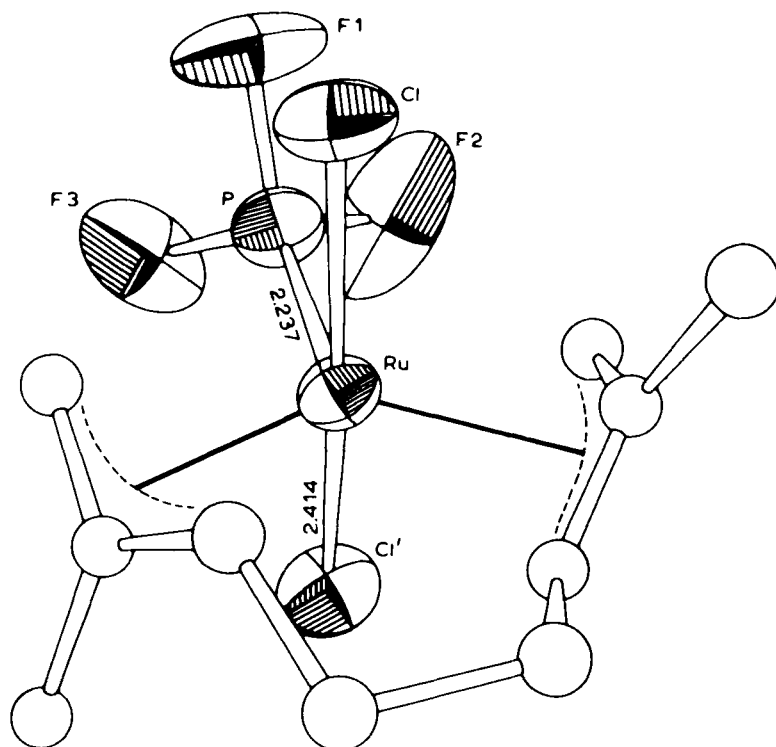


FIG. 18. Molecular structure of the complex $\text{RuCl}_2(\text{PF}_3)(\text{C}_{10}\text{H}_{16})$. [Reproduced from reference (148) with permission.]

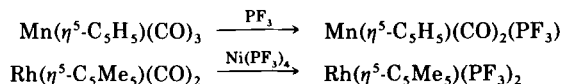
(Fig. 18) and is a rare example of a PF_3 complex of a metal formally in oxidation state IV.

Addition of PF_3 to an η^5 -heptadienyl metal PF_3 complex can lead to the corresponding η^3 -allylic complex (method I). Finally, the method of metal vapor synthesis (see Sections IX and X) has not found general application for allylic systems (method J), but in one case, cocondensation of Fe, PF_3 , and $[\text{Sn}(\text{allyl})_4]$ gave the unstable paramagnetic complex $[\text{Fe}(\text{PF}_3)_3(\eta^3\text{-allyl})]$.

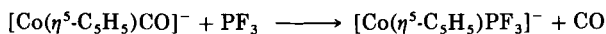
XIII. Transition Metal η^5 -Cyclopentadienyl and Related Complexes

A common synthetic approach to this class of compounds involves thermally or UV induced substitution of coordinated CO or N_2 from a

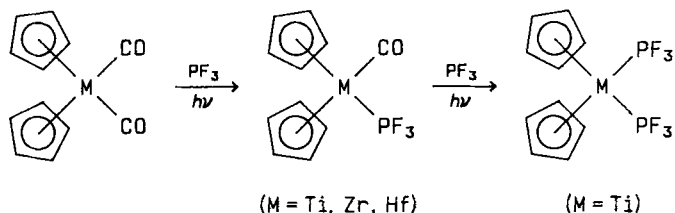
cyclopentadienyl metal complex by PF_3 , or, alternatively, by $[\text{Ni}(\text{PF}_3)_4]$ as a source of PF_3 (method A).



The gas-phase negative ion chemistry of $[\text{Co}(\eta^5\text{-C}_5\text{H}_5)(\text{CO})_2]^-$ has been studied by ion cyclotron resonance spectroscopy and the first observed example of a ligand displacement of an anionic transition metal complex involves the use of PF_3 in the formation of $[\text{Co}(\eta^5\text{-C}_5\text{H}_5)(\text{PF}_3)]^-$ and $[\text{Co}(\eta^5\text{-C}_5\text{H}_5)(\text{PF}_3)_2]^-$ (84). These results indicate that PF_3 is a stronger π acceptor than CO.



A particularly interesting example of CO displacement involves the photochemical reaction of the early transition metal complexes $[\text{M}(\eta^5\text{-C}_5\text{H}_5)_2(\text{CO})_2]$ ($\text{M} = \text{Ti}, \text{Zr}, \text{Hf}$) with PF_3 (Scheme 10). In the case of ($\text{M} = \text{Hf}$) this complex represented the first hafnocene-phosphine complex to be reported. A slightly better synthetic route to the mono(trifluorophosphine)titanium(II) complex involves displacement of PET_3 from $[\text{Ti}(\eta^5\text{-C}_5\text{H}_5)_2(\text{CO})(\text{PET}_3)]$.



SCHEME 10

A single-crystal X-ray diffraction study on $[\text{Ti}(\eta^5\text{-C}_5\text{H}_5)_2(\text{PF}_3)_2]$ was the first structural determination of a PF_3 complex of an early transition metal. The structure (Fig. 19) reveals a number of features of interest. There are two crystallographically independent molecules in the unit cell, one residing on a mirror plane, but no apparent conformational differences between them. The Ti—P bond lengths range from 2.340(6) to 2.349(6) Å, which are considerably shorter than the value of 2.585(1) Å found in the related complex $[\text{Ti}(\eta^5\text{-C}_5\text{H}_5)_2(\text{CO})(\text{PET}_3)]$. Two independent methods of estimating a normal Ti—P bond distance give values of 2.48 and 2.53 Å, indicating that the

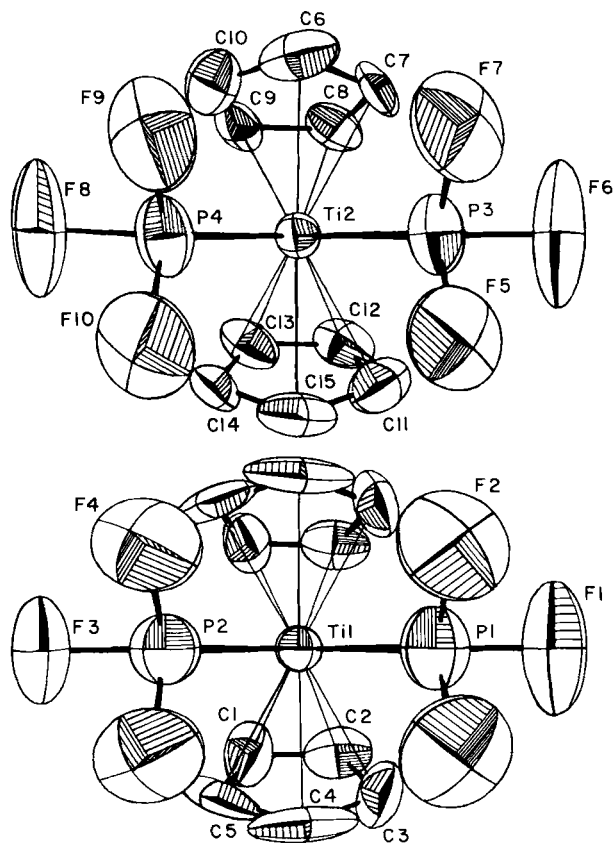
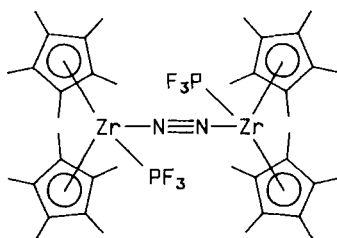


FIG. 19. Views of the two crystallographically independent molecules of $\text{Cp}_2\text{Ti}(\text{PF}_3)_2$. [Reproduced from references (109, 329) with permission.]

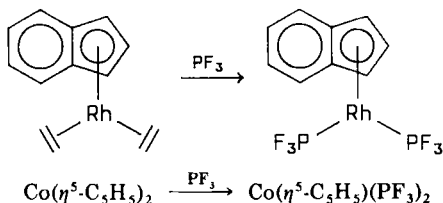
Ti—PF₃ bond distance in $[\text{Ti}(\text{C}_5\text{H}_5)_2(\text{PF}_3)_2]$ is perhaps 0.15 Å less than expected (109, 329). Similarly, the novel green dinuclear complex $[\{(\eta^5\text{-C}_5\text{Me}_5)_2\text{Zr}(\text{PF}_3)\}_2\text{N}_2]$ (14) has been obtained by displacement of the



(14)

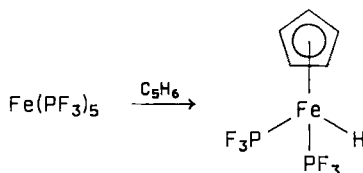
terminally coordinated N_2 molecules in $[(\eta^5-C_5Me_5)_2Zr(N_2)]_2N_2$ (method A), although it exhibits low stability in solution, decomposing within minutes at room temperature (245).

Ethylene can be displaced by PF_3 from $[Rh(\eta^5-C_5H_5)(C_2H_4)_2]$ (284) and from $[Rh(\eta^5-C_9H_7)(C_2H_4)_2]$ (158) (method B), and there is one report of displacement of one $\eta^5-C_5H_5$ ring from a bis($\eta^5-C_5H_5$) metal complex (method C).



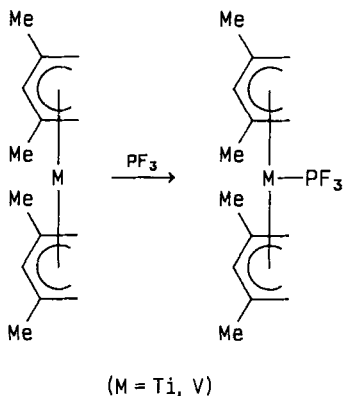
Other routes involve treatment of a metal-trifluorophosphine halide with either sodium or lithium cyclopentadienide (method D), or direct reaction between a metal- PF_3 complex and cyclopentadiene (method E).

This latter reaction is exemplified by the reaction of $[\text{Fe}(\text{PF}_3)_5]$ with cyclopentadiene, which, in contrast with the analogous iron carbonyl system, gives the stable hydrido complex $[\text{Fe}(\eta^5-C_5H_5)(\text{PF}_3)_2H]$.



More recent developments have utilized metal vapor synthesis (method F) involving cocondensation at low temperature of the metal, cyclopentadiene (or other dienes), and PF_3 . The hydrido-cyclooctadienyl complex $[\text{Cr}(\eta^5-C_8H_{11})(\text{PF}_3)_3H]$ (125) (see Section IX) made in this fashion exhibits variable-temperature NMR spectra which establish the existence of an exchange between the hydrido atom and a methylenic hydrogen bound to an sp^3 carbon adjacent to the diene unit.

Direct addition of PF_3 to η^5 -pentadienyl metal complexes offers an alternative synthetic route (method G) and this has been reported in the case of the formation of bis(2,4-dimethylpentadienyl)trifluorophosphine complexes of titanium and vanadium $[\text{M}(\text{C}_7\text{H}_{11})_2\text{PF}_3]$ ($\text{M} = \text{Ti}, \text{V}$) (Scheme 11) (111).



SCHEME 11

The formation of the 17-electron paramagnetic vanadium complex is not surprising in view of the known corresponding carbonyl complex, however the 16-electron titanium derivative is unexpected in view of the ready formation of the 18-electron biscarbonyl and bistrifluorophosphine metal complexes containing the η^5 -cyclopentadienyl ligand. The solid-state structure of the PF₃ adduct of bis[2,4-dimethyl-(pentadienyl)]titanium has recently been determined (111) and is shown in Fig. 20. The corresponding vanadium complex is isomorphous. The metal-PF₃ distances are 2.326(Ti) and 2.275(V) Å.

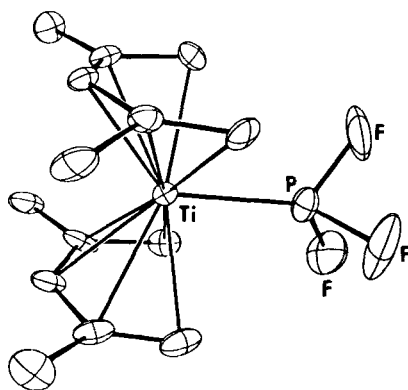


FIG. 20. The solid-state structure of the trifluorophosphine adduct of bis(2,4-dimethylpentadienyl)titanium. The corresponding vanadium compound is isomorphous. [Reproduced from reference (111) with permission.]

TABLE XII

TRANSITION METAL η^5 -CYCLOPENTADIENYL AND RELATED COMPLEXES CONTAINING TRIFLUOROPHOSPHINE

Complex	Method of preparation	Color	M.P. (°C), B.P. (°C/mmHg)	ϕ_F^a	$^1J_{PF}^{b,c}$	Reference
Ti(η^5 -C ₅ H ₅) ₂ (CO)(PF ₃)	(A)	Orange	—	—	—	109, 329
Ti(η^5 -C ₅ H ₅) ₂ (PF ₃) ₂ ^d	(A)	Yellow-orange	Sublimes	—	—	109, 329
Ti(η^5 -C ₇ H ₁₁) ₂ (PF ₃) ^e	(G)	Lime-green	Sublimes	21.8	1340	111
V(η^5 -C ₇ H ₁₁) ₂ (PF ₃) ^f	(G)	Blue-green	Sublimes	—	—	111
V(η^5 -C ₅ H ₅)(NO) ₂ (PF ₃)	(A)	—	—	—	—	270
V(η^5 -C ₅ H ₅)(CO) _x (PF ₃) _{4-x} ^g	(A)	Yellow	—	—	—	306, 308, 309, 321
CrH(PF ₃) ₃ (η^5 -cyclohexadienyl)	(F)	Orange	—	—	—	40
CrH(PF ₃) ₃ (η^5 -cyclooctadienyl) ^h	(F)	Orange ⁱ	—	7.7, 3.9	1280 ± 25	125
Mn(PF ₃) ₃ (η^5 -C ₅ H ₅)	(A)	Yellow	165–167 (subl. 40/10 ⁻³)	14.4, -0.4	—	201
Mn(PF ₃) ₂ (CO)(η^5 -C ₅ H ₅)	(A)	Yellow	Subl. 40/10 ⁻³	13.2, -1.2	—	201, 127
Mn(PF ₃) ₂ (CO) ₂ (η^5 -C ₅ H ₅)	(A)	Yellow	—	3.7	1279	127, 201, 266, 333
FeH(PF ₃) ₂ (η^5 -C ₅ H ₅)	(E)	Orange	40/10 ⁻³	—	—	196
Fe(PF ₃) ₂ (η^5 -C ₅ H ₅)(C ₄ H ₄ N)	(G)	—	—	—	—	110
Fe(PF ₃) ₂ (η^5 -C ₅ H ₅)K	—	White	—	—	—	196
Fe(PF ₃) ₂ (η^5 -C ₅ H ₅)(Et ₃ NH)	—	Colorless	—	—	—	196
Fe(PF ₃) ₂ (CO)(η^5 -C ₅ H ₅)(I)	(A)	Brown	102–103	—	—	170
Co(PF ₃) ₂ (η^5 -C ₅ H ₅)	(C) (F)	Deep-red	-8, 51/13	—	—	132, 188
ZrH ₂ (PF ₃)[η^5 -C ₅ (CH ₃) ₅] ₂	(G)	Red-brown	Unstable	—	—	243
{Zr(η^5 -C ₅ Me ₅) ₂ PF ₃ } ₂ N ₂	(A)	Metallic-green	—	—	—	245

Hf(η^5 -C ₅ H ₅) ₂ (CO)(PF ₃)	(A)	—	—	—	—	328
Nb(η^5 -C ₅ H ₅)(PF ₃) ₄	(A)	Red-brown	—	—	1330	308
Mo(PF ₃)(CO) ₂ (η^5 -C ₅ H ₅)CH ₃	(A)	Yellow	—	—	—	170
Mo ₂ (PF ₃) ₂ (CO) ₄ (η^5 -C ₅ H ₅) ₂	(A)	Dark-red	175 dec.	—	—	170
Mo ₂ (PF ₃)(CO) ₅ (η^5 -C ₅ H ₅) ₂	(A)	Dark-red	159–160	—	—	170
Rh(PF ₃) ₂ (η^5 -C ₅ H ₅)	(E) (D)	Orange	–8	1.1	1308	17, 159, 278, 284
Rh(PF ₃) ₂ (η^5 -C ₉ H ₇)	(B)	Orange	Oil	4.8	1332	158
Rh(PF ₃) ₂ [η^5 -C ₅ (CH ₃) ₅]	(A)	Orange	88–89	10.8	1334	170
Ir(PF ₃) ₂ [η^5 -C ₅ (CH ₃) ₅]	(A)	Yellow	90–92	16.6	1250	170
Ir(PF ₃)(PF ₂)(F)[η^5 -C ₅ (CH ₃) ₅]	(A)	Pale-yellow	~104	4.4	1177	170

^a Relative to CCl₃F.

^b In Hz.

^c ¹J_{PF} for the (PF₃)₂ complexes is equal to ¹J_{PF} + ³J_{PF}, and equals ¹J_{PF} + 2³J_{PF} for the (PF₃)₃ complex.

^d Single-crystal structure done.

^e δ_P = 209.6.

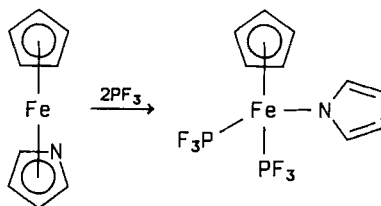
^f μ_{eff} = 1.6 BM; EPR data available.

^g V chemical shift and J_{VP} coupling data reported.

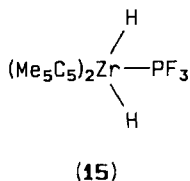
^h A 1% yield of Cr(PF₃)₄(1,5-cyclooctadiene) is also reported (125).

ⁱ A single-crystal X-ray study has been carried out (see Section IX for details).

Another interesting example of addition of PF_3 to an η^5 -cyclopentadienyl metal system involves an $\eta^5 \rightarrow \eta^1$ rearrangement of the coordinated pyrrolyl ring in azaferrocene (110). The rearrangement only occurs for π -acid ligands.



The unstable 18-electron complex $[(\eta^5\text{-C}_5\text{Me}_5)_2\text{ZrH}_2(\text{PF}_3)]$ is also readily formed by direct addition (method G) of PF_3 to the formally 16-electron complex $[(\eta^5\text{-C}_5\text{Me}_5)_2\text{ZrH}_2]$. On the basis of its ^1H NMR spectrum the structure of the PF_3 adduct (15) appears to be analogous to $[(\eta^5\text{-C}_5\text{H}_5)_2\text{TaH}_3]$ with PF_3 occupying the central equatorial position mutually cis to both hydride ligands (27, 243, 244). Complexes synthesized by all the above routes are listed in Table XII.



XIV. Transition Metal Carbonyl Complexes

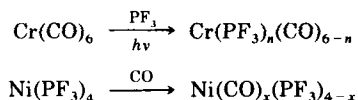
Trifluorophosphine and carbon monoxide readily undergo ligand-exchange reactions in their transition metal complexes. The close similarity in bonding characteristics of the two ligands toward transition metals has been discussed extensively in several review articles (72, 174, 272) and the evidence will not be repeated here. Extensive vibrational spectroscopic studies have been made on mixed carbonyl- PF_3 metal complexes (72, 174) and force constant calculations have been carried out in some cases.

More recently, the volatility of metal- PF_3 complexes, metal carbonyls, and mixed PF_3 -CO compounds has enabled UV photoelectron spectroscopic studies to be carried out (see Section V), and the data

suggest that PF₃ has a slightly greater overall electron-withdrawing effect than CO when attached to a transition metal.

Several ¹⁹F and ³¹P NMR studies of mixed PF₃-CO transition metal complexes have appeared and the fluxional nature of five-coordinated complexes such as [Fe(PF₃)_{5-n}(CO)_n] and [CoR_f(PF₃)_{4-n}(CO)_n] were among the first examples of this structural type to be studied in detail. So far, structural data are available only for [Mo(PF₃)(CO)₅] from an electron diffraction study in the gas phase (47).

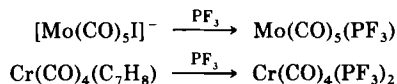
Synthetic routes to these complexes are summarized in Table XIII, which also lists the spectroscopic studies that have been made on this class of complexes. The action of PF₃ or CO usually under pressure with simultaneous UV irradiation on metal carbonyls or metal trifluorophosphine complexes, respectively, is of general applicability (method A). More recently, photolysis using a KrF laser has also been utilised, e.g.,



Often because of the close similarity in volatility and solubility of the mixed carbon-trifluorophosphine metal complexes the best separative method involves gas chromatography. Vapor pressures and enthalpy of sublimation data for the complexes [M(PF₃)(CO)₅] (M = Cr, W) are comparable with the values for the corresponding hexacarbonyl complexes.

Intermolecular ligand-exchange reactions often occur extremely easily between metal-PF₃ complexes and the corresponding metal carbonyls (method B), for example, all possible [Ni(CO)_x(PF₃)_{4-x}] complexes result on gently heating a mixture of [Ni(PF₃)₄] and [Ni(CO)₄].

A useful synthetic route to specific carbonyl-PF₃ transition metal complexes (method C) involves displacement of relatively weakly bound ligands such as ammonia, iodide ion, or unsaturated organic ligands (e.g., dienes, arenes) from suitable metal carbonyl complexes.



The direct interaction between the metal, hydrogen, and mixtures of CO and PF₃ under pressure has been used successfully in the

TABLE XIII. TRANSITION METAL CARBONYL

Complex	Method of preparation	Color	M.P. (°C), B.P. (°C/mmHg)	δ_P^a
$\text{Cr}(\text{PF}_3)_3(\text{CO})_3$	(A) (B) (C)	White	34	—
$\text{Cr}(\text{PF}_3)_2(\text{CO})_4$ (<i>cis</i>)	(A) (B) (C)	White	Liquid	-173.2
$\text{Cr}(\text{PF}_3)_2(\text{CO})_4$ (<i>trans</i>)	(A) (B) (C)	White	Liquid	-179.8
$\text{Cr}(\text{PF}_3)(\text{CO})_5^f$	(A) (B) (C)	White	—	—
$\text{MnH}(\text{PF}_3)_4(\text{CO})^g$	(A)	Colorless	-56 to -52	—
$\text{MnH}(\text{PF}_3)_3(\text{CO})_2^g$	(A)	Colorless	-73 to -51	—
$\text{MnH}(\text{PF}_3)_2(\text{CO})_3^g$	(A)	Colorless	< -108	—
$\text{MnH}(\text{PF}_3)(\text{CO})_4^g$	(A)	Colorless	-56 to -24	—
$\text{Mn}_2(\text{PF}_3)_3(\text{CO})_7$	(A) (F)	Yellow	38	—
$\text{Mn}_2(\text{PF}_3)_2(\text{CO})_8$	(A) (F)	Yellow	45	—
$\text{Mn}_2(\text{PF}_3)_2(\text{CO})_8^h$	(A) (F)	Yellow	81	—
$\text{Mn}_2(\text{PF}_3)(\text{CO})_9$	(A) (F)	Yellow	90	—
$\text{Mn}(\text{PF}_3)_3(\text{CO})_2\text{K}$	(A)	—	—	—
$\text{Mn}(\text{PF}_3)_3(\text{CO})_2\text{I}$	(A)	—	—	—
$\text{Fe}(\text{PF}_3)_4(\text{CO})^i$	(A) (B)	Yellow	—	—
$\text{Fe}(\text{PF}_3)_3(\text{CO})_2^i$	(A) (B)	Yellow	—	—
$\text{Fe}(\text{PF}_3)_2(\text{CO})_3^i$	(A) (B)	Yellow	—	—
$\text{Fe}(\text{PF}_3)(\text{CO})_4^i$	(A) (B)	Yellow	—	—
$\text{CoH}(\text{PF}_3)_3(\text{CO})$	(A) (D)	Yellow	-67 (80.5/715)	—
$\text{CoH}(\text{PF}_3)_x(\text{CO})_{4-x}$	(A) (E)	—	—	—
$\text{Co}(\text{PF}_3)_3(\text{CO})\text{K}$	(A)	Colorless	205 dec.	—
$\text{Ni}(\text{PF}_3)_3(\text{CO})$	(A) (B)	Colorless	-93 (0/88)	-137.2
$\text{Ni}(\text{PF}_3)_2(\text{CO})_2$	(A) (B)	Colorless	-93 (0/56)	-136.8
$\text{Ni}(\text{PF}_3)(\text{CO})_3$	(A) (B)	Colorless	(0/41)	-136.5
$\text{Mo}(\text{PF}_3)_5(\text{CO})^l$	(A) (B)	White	45	—
$\text{Mo}(\text{PF}_3)_4(\text{CO})_2$ (<i>cis</i>) ^l	(A) (B) (C)	White	117	—
$\text{Mo}(\text{PF}_3)_4(\text{CO})_2$ (<i>trans</i>) ^l	(A) (B)	White	94	—
$\text{Mo}(\text{PF}_3)_3(\text{CO})_3$ (<i>cis</i>) ^l	(A) (B) (C)	White	64	—
$\text{Mo}(\text{PF}_3)_3(\text{CO})_3$ (<i>trans</i>) ^l	(A) (B) (C) (G)	White	42	-150.6
$\text{Mo}(\text{PF}_3)_2(\text{CO})_4$ (<i>cis</i>) ^l	(A) (B) (C)	White	27-28; 32	-148.0
$\text{Mo}(\text{PF}_3)_2(\text{CO})_4$ (<i>trans</i>) ^l	(A) (B) (C)	White	10	—

COMPLEXES CONTAINING TRIFLUOROPHOSPHINE

ϕ_F^b	$^1J_{PF}^{c,d}$	Remarks	Reference
—	—	MS (267), IR (175, 176), magnetic susceptibility (175)	175, 176, 272, 349
-0.2	1312 ^e	MS (267)	98, 228, 296
1.1	1318	MS (267)	165, 236, 267
2.1	1315	MS (267), PES (96, 367), ESCA (8)	8
—	—	IR (259)	
—	—	IR (259)	
0.4, 3.5	1298, 1292	IR (259)	259-261
3.7, 2.6	1302, 1302		
5.2, 1.6	1310, 1307	IR (259), ¹ H NMR (260)	
—	—	IR (76, 127)	
—	—	IR (76, 127, 167, 297)	
—	—	IR (76, 127)	76, 127
—	—	IR (76, 127)	167, 170
—	—	—	185, 297
—	—	—	
—	— ^{j,k}	MS (267, 354), IR (70, 127, 239, 347, 354), Raman (36), PES (142, 267), ¹³ C NMR (239)	70, 176, 215
—	— ^{j,k}	MS (267, 354), IR (70, 127, 239, 347, 354), PES (142, 267), ¹³ C NMR (239)	34, 35, 269, 296
5.6	1322 ^{j,k}	MS (267, 354), IR (70, 127, 239, 347, 354), PES (142, 267), ¹³ C NMR (239)	30, 127, 239, 240, 269, 327, 347, 354
6.2	1329 ^{j,k}	MS (354), IR (70, 127, 239, 347, 354), PES (142), ¹³ C NMR (239)	36, 142, 267, 269
—	—	IR (204, 351), magnetic susceptibility (204)	180, 204, 351
—	—	IR (204, 351)	120, 180, 204, 351
—	—	IR (204), magnetic susceptibility (204)	204
—	—	IR (32, (33), 35, 44, 49, 85, 127, 233), Raman (35, 233)	30, 31, 32, 75
18.9	1357	Force constants (30, 34, 43, 230) IR (32, (33), 35, 44, 48, 49, 71, 85, 127), Raman (35), Force Constants (30, 34, 43, 230)	11, 43, 44, 48, 49 63, 71, 85,
—	—	IR ((32, (33), 35, 44, 71, 85, 127), Raman (35), Force Constants (30, 34, 43, 230)	73, 230, 233, 249, 250, 296
—	—	IR (73, 121, 127)	
—	—	IR (73, 127)	35, 117, 215
—	— ^m	IR (73, 127)	34, 73, 117, 127
1.2	1296 ^{e,m}	IR (12, 73, 85, 127, 176, 215, 332), magnetic susceptibility (11)	12, 85, 121
3.0	1300 ^m	IR (12, 73, 127)	47, 98, 228, 332
2.9	1305 ^{e,m}	IR (12, 73, 127)	11, 13, 130, 236, 258
4.0	1320 ^m	IR (73, 127)	305, 322

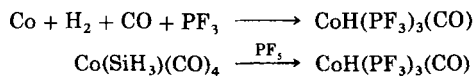
(continued)

TABLE XIII

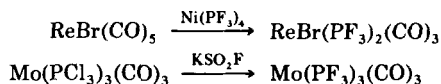
Complex	Method of preparation	Color	M.P. (°C), B.P. (°C/mmHg)	δ_p^a
$\text{Mo}(\text{PF}_3)(\text{CO})_5^{1,n}$	(A) (B) (C)	White	5°	—
$\text{Ru}(\text{PF}_3)_x(\text{CO})_{5-x}$	(A)	Yellow	—	—
$[\text{RhCl}(\text{PF}_3)(\text{CO})]_2$	(A) (B)	Red	40.5–41.5	—
$\text{Rh}_2\text{Cl}_2(\text{PF}_3)_3(\text{CO})$	(A) (B)	Red	—	—
$[\text{RhBr}(\text{PF}_3)(\text{CO})]_2$	(A) (B)	Red	—	—
$[\text{RhI}(\text{PF}_3)(\text{CO})]_2$	(A) (B)	Red	—	—
$\text{W}(\text{PF}_3)_2(\text{CO})_4$ (<i>cis</i>)	(A) (B) (C)	White	—	–122.0
$\text{W}(\text{PF}_3)_2(\text{CO})_4$ (<i>trans</i>)	(A) (B)	White	—	—
$\text{W}(\text{PF}_3)(\text{CO})_5^{p,q}$	(A)	White	—	—
$\text{ReH}(\text{PF}_3)_n(\text{CO})_{5-n}$	(A)	—	—	—
$\text{ReBr}(\text{PF}_3)_2(\text{CO})_3$	(F)	White	40–41	—

^a In ppm relative to $\text{P}(\text{OMe})_3$.^b In ppm and CCl_3F .^c In Hz.^d In general, $^1J_{\text{PF}}$ listed = $^1J_{\text{PF}} + n^3J_{\text{PF}}$ for $(\text{PF}_3)_{n+1}$ complexes.^e Accurate $^1J_{\text{PF}}$ values from full spectral analysis.^f $\Delta H_{\text{subl.}} = 85.5 \pm 2.9$ kJ/mol (45).^g ^{55}Mn shifts (ppm relative to LiMnO_4) are 2888, complex (CO); 2813 (complex (CO)₂); 2742, complex (CO)₃; and 2673, complex (CO)₄ (261).^h Diaxial isomer.ⁱ Alkene isomerization catalysts (337).

preparation of $[\text{CoH}(\text{PF}_3)_3(\text{CO})]$ (method D), while certain σ -bonded silyl metal carbonyls react with phosphorus pentafluoride to afford the desired complexes (method E).



$\text{Ni}(\text{PF}_3)_4$ can act as a source of PF_3 in reactions with metal carbonyl complexes (method F), and fluorination of preformed carbonyl metal- PCl_3 complexes using potassium fluorosulfate has also been described (method G).



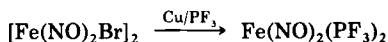
(continued)

ϕ_F^b	$^1J_{PF}^{c,d}$	Remarks	Reference
4.7	1310 ^m	IR (73, 127, 332), PES (96, 367), electron diffraction(47), ESCA(8)	8, 117
—	~1300	MS, IR (350)	350
17.0	1328	MS, IR (18, 291)	18, 291
—	—	MS, IR (18, 291)	18, 291
17.9	1343	—	18, 291
16.3	1358	—	18, 291
6.0	1281	} — }	169, 228, 236, 332
7.0	1286		
7.9	1245		
11.0, 5.5	1282, 1293 ^r	IR (169), PES (96, 367)	260
—	—	MS, IR, ¹ H NMR (260)	260
—	—	IR (170)	170

^j ¹³C NMR data available (239).^k Temperature-dependent spectra (240).^l Hot atom chemistry reported (117).^m ¹J_{MoP} data (10, 258).ⁿ Mo-P (2.369 Å).^o Corrected later (117) to 175°C.^p ¹J_{WP} = 485 Hz (169).^q ΔH_{subl} = 77.4 ± 1.5 kJ/mol (45).^r Data for ReH(PF₃)(CO)₄.

XV. Transition Metal Nitrosyl Complexes

PF₃-containing transition metal nitrosyl complexes such as [Co(NO)(PF₃)₃] and [Fe(NO)₂(PF₃)₂] were first prepared by Kruck and Lang (206, 207) by reduction of dimeric nitrosyl halide complexes with copper in the presence of PF₃ (method A).



More recently these volatile complexes have also been made by metal vapor syntheses (method B) in which vapors of the metals were cocondensed with NO, PF₃, and boron trifluoride at liquid nitrogen temperature. The method also afforded [Mn(NO)₃(PF₃)], however, it is important to point out that in the absence of BF₃ the condensate exploded violently on warming a little above -196°C (257).

Other useful methods involve displacement of CO by PF₃ from mixed-metal carbonyl nitrosyl complexes (method C), passing CO₂ through a

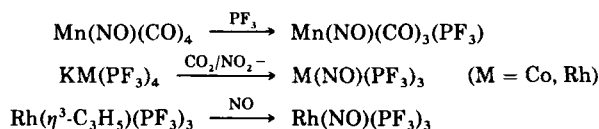
TABLE XIV

TRANSITION METAL NITROSYL COMPLEXES CONTAINING TRIFLUOROPHOSPHINE

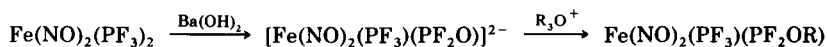
Complex	Method of preparation	Color	M.P. (°C), B.P. (°C/mmHg)	ϕ_F^a	$^1J_{PF}^{b,c}$	Reference
$Mn(PF_3)(NO)_3$	(B)	Green	-120 ± 2	—	—	206, 257
$Mn(PF_3)(NO)(CO)_3$	(C)	—	—	6.5	1337	353
$Mn(PF_3)_2(NO)(CO)_2$	(C)	—	—	—	1319	353
$Mn(PF_3)_3(NO)(CO)$	(C)	—	—	—	—	353
$Fe(PF_3)_2(NO)_2$	(A) (B)	Red	-72 (dec. 118), 97/227	9.4	1360	69, 174, 206, 207
$Fe(PF_3)_3(NO)H$	(G)	Orange	-86 , 80/720	—	—	207
$Fe(PF_3)_3(NO)K$	(G)	Yellow	—	—	—	207
$Fe(PF_3)(PF_2OC_2H_5)(NO)_2$	(F)	Red	-78 , 80/10 ⁻³	—	—	223
$[Fe(PF_3)(PF_2O)(NO)_2]Ba$	(F)	—	—	—	—	233
$Co(PF_3)_3(NO)$	(A) (B) (D)	Orange-red	-92 , 81/732	9.9	1375	69, 174, 206, 207, 257
$Co(PF_3)_2(CO)_{3-x}(NO)$	(C)	Red	—	—	—	69, 77
$Co(PF_3)_2(PF_2OC_2H_5)(NO)$	—	—	—	—	—	—
$[Co(PF_3)_2(PF_2O)NO][Pr^i_2NH]$	(F)	Red	-78 , 70/10 ⁻³	—	—	223
$[Co(PF_3)_2(PF_2O)(NO)]_2Ba$	(F)	Ochre	—	—	—	223
$Rh(PF_3)_3(NO)^{d,e}$	(C) (D) (E)	Orange	-87	3.8	1416	46, 80, 174, 277, 293

^a In ppm relative to CCl₃F.^b In Hz.^c $^1J_{PF} + J_{PF'}$ in $(PF_3)_2$ complexes and $^1J_{PF}$ in (PF_3) complexes.^d Rh—P bond length = 2.245 Å (46).^e A full NMR analysis has been carried out (277).

trifluorophosphine metallate salt in the presence of nitrite (method D), and displacement of η^3 -allylic ligands (which are 3e donors) coordinated to metals via treatment with NO or NOCl (method E).

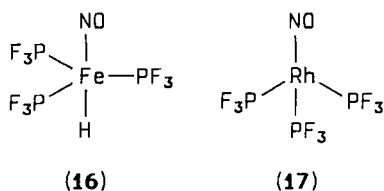


Since the P—F bonds are labile in these complexes some mixed trifluorophosphine–fluorophosphite nitrosyl complexes have been prepared by reactions with either diisopropyl–water mixtures or barium hydroxide (method F) to give the $(\text{PF}_2\text{O})^-$ compounds which can be alkylated.



Treatment of $[\text{Fe(NO)}_2(\text{PF}_3)_2]$ with potassium amalgam and PF₃ (method G) gives the salt $\text{K}[\text{Fe(NO)(PF}_3)_3]$, which on acidification gives the hydride complex $[\text{FeH(NO)(PF}_3)_3]$.

The molecular structure of $[\text{FeH(NO)(PF}_3)_3]$ (16) has been proposed to be based on a trigonal bipyramid with the H and NO ligands occupying axial positions and the PF₃ groups likely to be distorted toward the small hydride. The molecular structure of $[\text{Rh(NO)(PF}_3)_3]$ (17) has been determined in the gas phase by an electron diffraction study (46) and has the expected C_{3v} symmetry with an Rh–P distance of 2.245(5) Å. Nitrosyl complexes containing PF₃ are listed in Table XIV.



XVI. Transition Metal Complexes Containing Other Ligands with Nitrogen, Phosphorus, or Arsenic Donor Atoms

A very large number of trifluorophosphine–metal complexes of this type are known, as evidenced by the number of entries in Table XV. The most widely used synthetic methods are displacement of PF₃ from a

TABLE XV

METAL TRIFLUOROPHOSPHINE COMPLEXES CONTAINING OTHER LIGANDS HAVING N, P, OR AS DONOR LIGANDS

Complex	Method of preparation	Color	M.P. (°C), B.P. (°C/mmHg)	ϕ_F^a	$^1J_{PF}^{b,c}$	Reference
Ti(CO) ₂ (PF ₃)(dmpe) ₂ ^d	(B)	Red	—	—	—	365
Fe(PF ₃) ₄ (PF ₂ OEt)	(D)	Bright-yellow	−45 (121/760)	1.0	1260	191
[Fe(PF ₃) ₄ PF ₂ O] ₂ Ba	(D)	Bright-yellow	—	1.5	1265	191
Fe(PF ₃) ₂ (PMe ₃) ₃	(A)	Yellow	—	—	—	265, 303
Fe(PF ₃) ₂ [P(OMe) ₃] ₃	(A) (B)	Colorless	—	—	1213	131, 265
Fe(PF ₃)(dppe) ₂	(B)	Orange	225–230	—	—	164
Fe(PF ₃)(dppe) ₂	(B) (I)	—	—	—	—	6, 345
Fe(PF ₃)(dmpe) ₂	(B) (I)	—	—	12.6	—	164
CoH(PF ₃) ₃ (PH ₃)	(A) (B)	Pale-yellow	25	9.8	1117	60
CoH(PF ₃) ₃ (PPh ₃)	(A) (B)	Yellow	175–176 subl.	8.0	1231	57, 58, 209
CoH(PF ₃) ₃ (AsPh ₃)	(A)	Yellow	83 (dec. 120)	—	—	209
CoH(PF ₃) ₃ (SbPh ₃)	(A)	Yellow	62 (dec. 100)	—	—	209
CoH(PF ₃) ₂ (PPh ₃) ₂	(B)	Yellow	200 dec.	6.2	1265	58
Co(PF ₃) ₂ (PPh ₃) ₂ K	(A)	—	—	—	—	202
CoI(PF ₃) ₂ (PPh ₃) ₂	(A)	Dark-brown	144 dec.	—	—	202
CoH(PF ₃) ₃ (PPh ₃) ₃	(B)	Yellow	147–149 dec.	0.8	1239	58
CoH(PF ₃) ₃ P(CF ₃) ₂ OCH ₂ -CH ₂ Cl	(A)	Colorless	—	—	—	79
Ni(PF ₃) ₃ (PH ₃)	(A) (C)	Colorless	−22	19.8	—	341, 346
Ni(PF ₃) ₂ (PH ₃) ₂	(C)	Colorless	Liquid	—	—	341
Ni(PF ₃) ₃ (C ₆ H ₁₁ NC)	(A)	Pale-yellow	—	—	—	166
Ni(PF ₃) ₃ (pyridine) ^e	(A)	Yellow	—	—	—	181
Ni(PF ₃) ₃ (PPh ₃)	(A)	Colorless	123–125	—	—	181
Ni(PF ₃) ₃ (AsPh ₃)	(A)	Colorless	111	—	—	177
Ni(PF ₃) ₃ (SbPh ₃)	(A)	Colorless	96–97	—	—	177
Ni(PF ₃) ₃ (PF ₂ OEt)	(D)	Colorless	−67 (110/760)	17.5	1340	191

Ni(PF ₃) ₃ (PF ₂ NEt ₂)	(D)	Colorless	(67.2–68.2/12)	17.5	1266	190, 192
Ni(PF ₃) ₃ (PF ₂ NH ₂)	(D)	Colorless	Liquid	—	—	213
Ni(PF ₃) ₃ (PF ₂ NHPr ⁿ)	(D)	Colorless	(56.5/12)	18.5	1295	190, 192
Ni(PF ₃) ₃ (PF ₂ NHBu ⁿ)	(D)	Colorless	(68.5/12)	17.0	—	212
Ni(PF ₃) ₃ (PF ₂ NHMe)	(D)	Colorless	(48/12)	—	—	212
Ni(PF ₃) ₃ [PFNH(CH ₂) ₂ NH]	(D)	Colorless	—	18.0	1287	190, 192
Ni(PF ₃) ₂ [PF ₂ NH(CH ₂) ₂]	(D)	Colorless solid	(92–93/10 ⁻²)	17.6	1254	190, 192
Ni(PF ₃) ₃ [PF ₂ N(SiMe ₃) ₂]	(D)	Colorless	(49/10 ⁻³)	—	—	213
Ni(PF ₃) ₃ (PF ₂ NHSiMe ₃)	(D)	Colorless	(60–70/10 ⁻³)	—	—	213
Ni(PF ₃) ₃ (PF ₂ NMeSiMe ₃)	(D)	Colorless	(36/10 ⁻¹)	—	—	212
Ni(PF ₃) ₃ (PF ₂ NEtSiMe ₃)	(D)	Colorless	(27/10 ⁻¹)	—	—	212
Ni(PF ₃) ₃ (PF ₂ NBuSiMe ₃)	(D)	Colorless	(40/10 ⁻¹)	16.5	—	212
Ni(PF ₃) ₃ (PF ₂ NPhSiMe ₃)	(D)	Colorless	(63.5/10 ⁻³)	—	—	212
Ni(PF ₃) ₃ (PF ₂ N ₂ H ₃)	(D)	Colorless	31	—	—	130
[Ni(PF ₃) ₃ PF ₂ O] ⁻	(D)	Colorless	—	—	—	190
Ni(PF ₃) ₂ (PPh ₃) ₂	(A)	Yellow	213	—	—	177, 178, 181
Ni(PF ₃) ₂ (AsPh ₃) ₂	(A)	Colorless	157 dec.	—	—	181
Ni(PF ₃) ₂ (SbPh ₃) ₂	(A)	Colorless	177	—	—	181
Ni(PF ₃) ₂ (o-phen)	(A)	Red	225 dec.	—	—	181
Ni(PF ₃) ₂ (dipyridyl)	(A)	Orange-red	120 dec.	—	—	181
Ni(PF ₃) ₂ [(PPh ₂) ₂ C ₂ H ₄]	(A)	Yellow	203–205	—	—	175
Ni(PF ₃) ₂ (PF ₂ NEt ₂) ₂	(D)	Colorless	(76–77/0.5)	17.4	1295	189, 190, 192
Ni(PF ₃) ₂ (PF ₂ NH ₂) ₂	(D)	Colorless	(46.5/0.8)	9.1	1259	190, 192
Ni(PF ₃) ₂ (PF ₂ NPr ⁿ) ₂	(D)	Colorless	—	18.4	1298	189, 190, 192
Ni(PF ₃) ₂ (PF ₂ NBu ⁿ) ₂	(D)	Colorless	—	17.4	1292	190, 192
Ni(PF ₃) ₂ (PF ₂ NHMe) ₂	(D)	Colorless	(28/10 ⁻³)	—	—	212
Ni(PF ₂) ₂ [PF ₂ N(SiMe ₃) ₂] ₂	(D)	Pale-yellow	60 dec.	—	—	213
Ni(PF ₃) ₂ (PClPh ₂)[PF ₂ N(PPh ₂) ₂]	(A) (D)	Yellow	(108–110 dec.)	—	—	213
Ni(PF ₃) ₃ [P(OPh) ₃] ₃	(A)	Colorless	89	—	—	178
Ni(PF ₃) ₃ (PPh ₂ Cl) ₃	(A)	Colorless	114 dec.	—	—	181
Ni(PF ₃) ₃ (PF ₂ NEt ₂) ₃	(D)	Colorless	Oil	17.9	1349	190, 192
Ni(PF ₃) ₃ (PF ₂ NC ₆ H ₁₀) ₃	(D)	Colorless	45	17.1	1292	189, 190, 192
Ni(PF ₃) ₃ (PF ₂ NHBu ⁿ) ₃	(D)	Colorless	—	—	—	190

(continued)

TABLE XV (continued)

Complex	Method of preparation	Color	M.P. (°C), B.P. (°C/mmHg)	ϕ_F^a	$^1J_{PF}^{b,c}$	Reference
$Ni(PF_3)(PF_2NMeSiMe_3)_3$	(D)	Colorless	-10	—	—	212
$Ni(PF_3)(PF_2NHMe)_3$	(D)	Colorless	(68/10 ⁻³)	—	—	212
$Ni(PF_3)_3(PF_2Ph)$	(D)	Colorless	38/10 ⁻¹	15.9	1330	211
$Ni(PF_3)_3(PFPh_2)$	(D)	Colorless	—	—	—	211
$Ni(PF_3)_2(PF_2Et)_2$	(D)	Colorless	35/10 ⁻³	16.7	1330	211
$Ni(PF_3)_3(PFEt_2)$	(D)	Colorless	—	—	—	211
$Ni(PF_3)_2(PF_2Et)(PFEt_2)$	(D)	Colorless	—	—	—	211
$Ni(PF_3)(PF_2Et)_3$	(D)	Colorless	—	15.6	1320	211
$Ni(PF_3)_3(PF_2Bu)$	(D)	Colorless	26/10 ⁻¹	—	—	211
$Ni(PF_3)_2(PF_2Bu)_2$	(D)	Colorless	42/10 ⁻³	—	—	211
$Ni(PF_3)_2(PF_2Me)_2$	(D)	Colorless	14/10 ⁻¹	—	—	211
$Ni(PF_3)_3(PFMe_2)$	(D)	Colorless	—	—	—	211
$Ni(PF_3)(PF_2Bu)_3$	(D)	Colorless	—	—	—	211
$Ni(PF_3)_2(PFBu_2)(PF_2Bu)$	(D)	Colorless	90/10 ⁻³	—	—	211
$Ni(PF_3)_3(PBu_3)$	(D)	Colorless	—	—	—	211
$Ni(PF_3)(PF_2Me)_3$	(D)	Colorless	—	—	—	211
$Ni(PF_3)_2(PFMe_2)(PF_2Me)$	(D)	Colorless	26/10 ⁻¹	—	—	211
$Ni(PF_3)_3(PMe_3)$	(D)	Colorless	—	—	—	211
$Ni(PF_3)_3(PF_2C_6H_{11})$	(D)	Colorless	34/10 ⁻¹	—	—	211
$Ni(PF_3)_3[P(C_3H_5)_3]$	(D)	Colorless	—	—	—	211
$Ni(PF_3)_2(PF_2C_3H_5)[PF(C_3H_5)_2]$	(D)	Colorless	—	—	—	211
$Ni(PF_3)(PF_2C_3H_5)_3$	(D)	Colorless	—	—	—	211
$Ni(PF_3)_3(PEt_3)$	(D)	Colorless	—	—	—	211
$Ni(PF_3)_2(PF_2Et)(PFEt_2)$	(D)	Colorless	46/10 ⁻³	—	—	211
$Ni(PF_3)(PF_2Et)_3$	(D)	Colorless	—	—	—	211
$Ni(PF_3)_3(PCl_3)$	(A)	—	—	-19.4	—	312
$Ni(PF_3)_2(PCl_3)_2$	(A)	—	—	-22.1	—	312
$Ni(PF_3)(PCl_3)_3$	(A)	—	—	-24.3	1359	312

$\text{Ni}(\text{PF}_3)_3(\text{PBr}_3)$	(A)	—	—	—20.8	1286	312
$\text{Ni}(\text{PF}_3)_2(\text{PBr}_3)_2$	(A)	—	—	—23.8	1292	312
$\text{Mo}(\text{PF}_3)_2(\text{bipy})_2$	(B)	Red-black	—	—	965 ^f	83
$\text{Mo}(\text{CO})_2(\text{PF}_3)_2\text{PhP}(\text{Me}_2\text{pz})_2$	(G)	—	—	—	~1300	298
$\text{ReCl}(\text{PF}_3)_3(\text{N}_2)(\text{PPh}_3)_2$	(B)	Orange	—	—	—	64
$\text{Ru}(\text{PF}_3)_4(\text{PPh}_3)$	(I)	Colorless	Oil	—1.1	1234	2, 4, 279
$\text{Ru}(\text{PF}_3)_3(\text{PPh}_3)_2$	(I)	Colorless	170 (dec.)	4.3	1288	2, 4
$\text{RuClIL}^R(\text{PF}_3)(\text{PEt}_3)_2^g$	(G)	Colorless	180–190 (dec.)	—	1301	152
$\text{RuClIL}^R(\text{PF}_3)(\text{PPh}_3)_2$	(G)	Colorless	140–150	—	1304	151, 152
$[\text{RuClIL}^R(\text{PF}_3)]\text{BF}_4$	(B)	Pink	214	—	—	151, 152
$\text{RuCl}_2(\text{PF}_3)(\text{L}^R)_4$	(B)	White-pink	130	—	—	150
$\text{Ru}_2\text{Cl}_4(\text{PF}_3)(\text{PPh}_3)_4$	(B)	Deep-red	166	—	—	134, 137
$\text{Ru}_2\text{Cl}_4(\text{PF}_3)_2(\text{PPh}_3)_3$	(B)	Orange-yellow	191–192	—	1290 ^h	134, 136, 137
$\text{Ru}_2\text{Cl}_4(\text{PF}_3)(\text{CO})(\text{PPh}_3)_3$	(B)	Yellow	184	—	—	134
$\text{RuCl}_2(\text{PF}_3)(\text{DMA})(\text{PPh}_3)_2$	(B)	Yellow	—	—	—	134
$\text{RuCl}_2(\text{PF}_3)_2(\text{PPh}_3)_2^i$	(B) (E) (H)	Pale-yellow	191–193 (dec.)	12.4	1285	3, 134, 136, 140, 148
$\text{RuBr}_2(\text{PF}_3)_2(\text{PPh}_3)_2$	(B)	Orange	141 (dec.)	12.4	1291	134
$\text{RuCl}_2(\text{CO})(\text{PF}_3)(\text{PPh}_3)_2$	(B)	Colorless	225	12.6	1305	137
$\text{RuCl}_2(\text{DMF})(\text{PF}_3)(\text{PPh}_3)_2$	(B)	Yellow	170	4.7	1257	136
$\text{Ru}(\text{O}_2\text{CCF}_3)_2(\text{PF}_3)(\text{PPh}_3)_2$	(D)	—	203–205	8.6	1283	3
$\text{Ru}(\text{O}_2\text{CCF}_3)[\text{PF}_2(\text{OCCF}_3)](\text{PF}_3)(\text{PPh}_3)_2$	(D)	—	200	5.9	1276	3
$\text{Ru}_2\text{Cl}_3(\text{CF}_3\text{COCHOCF}_3)(\text{PF}_3)(\text{PPh}_3)_4$	(A)	Pink	184 (dec.)	—	—	137
$\text{RuH}_2(\text{PF}_3)_2(\text{PPh}_3)_2$	(B)	Colorless	169–170	6.8	1291	135
$\text{RuH}_2(\text{PF}_3)(\text{PPh}_3)_3$	(B)	Colorless	171	4.8	1285	135
$\text{RuHCl}(\text{PF}_3)_2(\text{PPh}_3)_2$	(B)	Colorless	164	13.2, 4.2	1350, 1244	3
$\text{RuH}(\text{O}_2\text{CCF}_3)(\text{PF}_3)_2(\text{PPh}_3)_2$	(H)	—	170	13.4, 1.8	1351, 1254	3
$\text{RuH}_2(\text{PF}_3)(\text{PF}_2\text{NMe}_2)(\text{PPh}_3)_3$	(B)	Colorless	175.6	6.2	1300	135
$[\text{RuH}(\text{PF}_3)(\text{CH}_3\text{CN})(\text{ttp})]\text{BF}_4^j$	(B)	White	130 (dec.)	—	1323	229
$\text{OsH}_2(\text{PF}_3)(\text{PPh}_3)_3$	(B)	Colorless	198	7.4	1300	135
$\text{OsH}_2(\text{PF}_3)_2(\text{PPh}_3)_2$	(B)	Colorless	185–187	8.3	1296	135

(continued)

TABLE XV (continued)

	Complex	Method of preparation	Color	M.P. (°C), B.P. (°C/mmHg)	ϕ_F^a	$^1J_{PF}^{b,c}$	Reference
911	OsHCl(PF ₃) ₂ (PPh ₃) ₂	(H)	Colorless	207–209	7.4, 10.3	1346, 1254	3
	OsCl ₂ (PF ₃) ₂ (PMe ₂ Ph) ₃	(H)	Colorless	228	13.1	1208	3
	OsCl ₂ (PF ₃) ₂ (PMe ₂ Ph) ₂ ^k	(B)	Colorless	—	18.8	1230	3
	OsCl ₂ (PF ₃) ₂ (PMe ₂ Ph) ₂ ^l	(B)	Yellow	149	32.9	1453	3
	OsCl ₂ (PF ₃) ₂ (PMe ₂ Ph) ₃	(B)	Yellow	171	25.4	1267	3
	OsCl ₂ (PF ₃) ₂ (PPh ₃) ₂	(H)	Colorless	> 230	18.4	1234	136
	Pd(PF ₃) ₂ (PPh ₃) ₂	(A)	Colorless	156–158 (dec.)	—	—	177
	Pd(PF ₃)(CO)(PPh ₃) ₂	(A)	Colorless	—	—	—	177
	[IrH(PF ₃)(dppe) ₂](BF ₄) ₂	(G)	White	174 (dec.)	14.8	1338	154
	IrCl(PF ₃)(PPh ₃) ₂	(B) (I)	Yellow	134	—	—	25, 348
	IrCl(PF ₃)(diphos)	(B)	White	270 (dec.)	—	—	356
	Pt(PF ₃) ₃ (PPh ₃)	(A)	Colorless	121	—	—	177
	Pt(PF ₃) ₃ (C ₆ H ₁₁ NC)	(A)	Off-white	—	—	—	166
	Pt(PF ₃) ₂ (PPh ₃) ₂	(A)	Colorless	202 (dec.)	—	—	177
	Pt(PF ₃)[MeC(CH ₂ PPh ₂) ₃]	(B)	—	—	—	1321	65
	PtCl ₂ (PF ₃)(PEt ₃) ^m	(B)	White	—	—	—	143, 153, 242
	PtCl ₂ (PF ₃)(PCl ₃)	(A)	—	—	—	—	312
	RhH(PF ₃)(PPh ₃) ₃ ⁿ	(B)	Yellow	—	—	1333°	147, 160, 290
	RhH(PF ₃) ₂ (PPh ₃) ₂	(B)	White	—	—	—	290
	RhCl(PF ₃)(PPh ₃) ₂	(B) (E)	Yellow	144–148	15.2	1286	18, 80, 81, 182
	RhCl(PF ₃)(AsPh ₃) ₂	(B) (E)	Yellow	165–170	15.2	1271	18
	RhCl(PF ₃)(PPh ₃)(AsPh ₃)	(B)	Yellow	130–136 (dec.)	13.9	1281	18
	RhCl(PF ₃)[P(NMe ₂) ₃] ₂	(B)	Yellow	—	15.6	1279	18
	RhBr(PF ₃)(PPh ₃) ₂	(E)	Yellow	70 (dec.)	17.7	1248	18
	RhCl(PF ₃)[{C ₆ H ₅ (PPh ₂)(NMe ₂) ₂ }]	(B)	Yellow	200	—	—	304

$[\text{RhCl}(\text{PF}_3)(\text{Azb})]_2^p$	(B) (E)	Dark-red	—	19.3	1333	281
$\text{Rh}_2\text{Cl}_2(\text{PF}_3)(\text{CO})(\text{Azb})_2^p$	(B)	Red	—	20.3	1346	281
$\text{RhCl}_3(\text{PF}_3)(\text{PPh}_3)_2$	(B) (F)	Yellow	152–154	30.9	1349	18, 133, 138
$\text{RhCl}_3(\text{PF}_3)(\text{AsPh}_3)_2$	(B)	Yellow	—	—	—	18
$\text{RhHCl}_2(\text{PF}_3)(\text{PPh}_3)_2$	(B)	Yellow	—	—	—	18
$\text{RhHBrCl}(\text{PF}_3)(\text{PPh}_3)_2$	(B)	Yellow	—	—	—	18
$\text{RhCl}(\text{SO}_2)(\text{PF}_3)(\text{PPh}_3)$	(B)	Yellow	—	—	—	18
$\text{RhCl}(\text{SO}_2)(\text{PF}_3)(\text{AsPh}_3)$	(B)	Yellow	—	—	—	18
$[\text{RhCl}(\text{PF}_3)(\text{PPh}_3)]_2$	(E)	Yellow	180–183 (dec.)	—	—	18
$\text{RhCl}(\text{PF}_3)_2(\text{benzo-[c]-cinnoline})$	(E)	Yellow	140–145	19.2, 20.2	1304, 1324	283
$\text{RhCl}(\text{PF}_3)_2(\text{R-dim})^g$	(E)	—	—	Several	1300	300

^a In ppm relative to CCl_3F .

^b In Hz.

^c Some spectra are second order and in general $^1J_{\text{PF}}$ quoted equals $^1J_{\text{PF}} + n^3J_{\text{PF}}$ for $(\text{PF}_3)_{n+1}$ complexes.

^d X-Ray structure.

^e The related $\text{Cr}(\text{PF}_3)_5(\text{pyridine})$ complex has been briefly reported (338).

^f Value likely to be in error.

^g L^{R} = carbene ligand $\begin{array}{c} \text{R} \\ | \\ \text{N} \\ | \\ \text{N} \\ | \\ \text{R} \end{array} \text{C}(\text{R} = \text{Me})$.

^h Spectra complex, isomers present.

ⁱ X-Ray crystal structure (148) ($\text{Ru}-\text{PF}_3 = 2.180, 2.160 \text{ \AA}$; $\text{Ru}-\text{PPh}_3 = 2.471, 2.456 \text{ \AA}$).

^j $\text{tpp} = \text{PhP}(\text{CH}_2\text{CH}_2\text{CH}_2\text{PPh}_2)_2$.

^k *cis*-Isomer.

^l *trans*-Isomer.

^m X-Ray crystal structure (153) ($\text{Pt}-\text{PF}_3 = 2.141 \text{ \AA}$; $\text{Pt}-\text{PEt}_3 = 2.272 \text{ \AA}$).

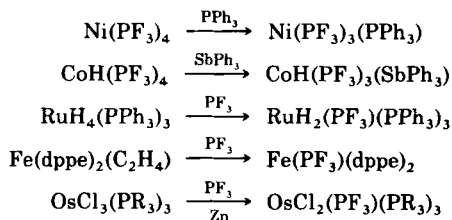
ⁿ X-Ray crystal structure (147) ($\text{Rh}-\text{PF}_3 = 2.155 \text{ \AA}$; $\text{Rh}-\text{PPh}_3 = 2.34 \text{ \AA}$).

^o $^2J_{\text{PRh}} = 254 \text{ Hz}$ (PF_3). ^{19}F NMR spectrum temperature dependent.

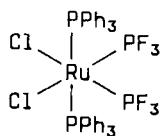
^p AzbH = azobenzene.

^q R-dim = RNCHCHNR ($\text{R} = \text{'Bu}$)

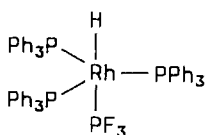
metal trifluorophosphine complex under the influence of the added ligand (method A); alternatively, the reverse reaction can be utilized (method B), since PF_3 invariably displaces most other coordinated ligands. A reducing agent may also be added. Some typical examples are listed below ($\text{dppe} = \text{Ph}_2\text{PCH}_2\text{CH}_2\text{PPh}_2$).



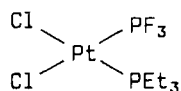
Single-crystal X-ray crystallographic studies have been carried out to establish the molecular structures of complexes **18**–**20**. However, in these and many other such complexes, the characteristic patterns of lines in the ^{31}P NMR spectrum resulting from spin–spin coupling between the various types of phosphorus and/or metal nuclei can often be diagnostic for a particular structure.



(18)



(19)



(20)

As expected in these mixed phosphine–trifluorophosphine complexes, the metal–phosphorus bond lengths to PF_3 are usually significantly shorter than to the PR_3 ligands (e.g., in **18**, $\text{Ru}-\text{PF}_3 = 2.180 \text{ \AA}$, 2.160 \AA ; $\text{Ru}-\text{PPh}_3 = 2.471 \text{ \AA}$, 2.456 \AA ; in **19**, $\text{Rh}-\text{PF}_3 = 2.155 \text{ \AA}$, $\text{Rh}-\text{PPh}_3 = 2.34 \text{ \AA}$; and in **20**, $\text{Pt}-\text{PF}_3 = 2.141 \text{ \AA}$; $\text{Pt}-\text{PEt}_3 = 2.272 \text{ \AA}$).

Of special interest is the recently described red zero-valent titanium complex $[\text{Ti}(\text{CO})_2(\text{PF}_3)(\text{dmpe})_2]$ ($\text{dmpe} = \text{Me}_2\text{PCH}_2\text{CH}_2\text{PMe}_2$) which is a PF_3 derivative of the nonexistent titanium carbonyl complex $[\text{Ti}(\text{CO})_7]$ (365). A single-crystal X-ray crystallographic study has established the structure shown in Fig. 21 in which the geometry around the metal is approximately a capped trigonal prism.

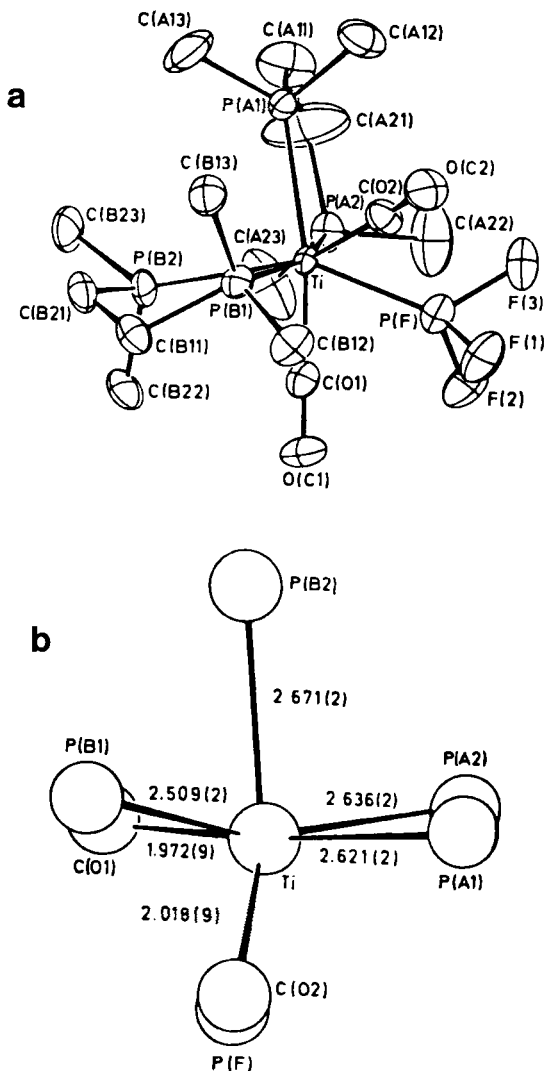
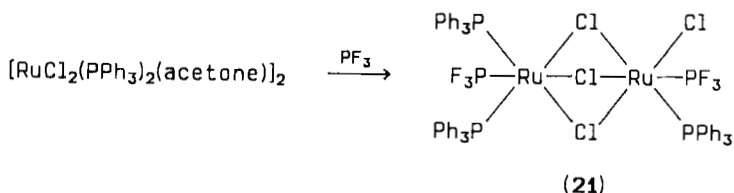
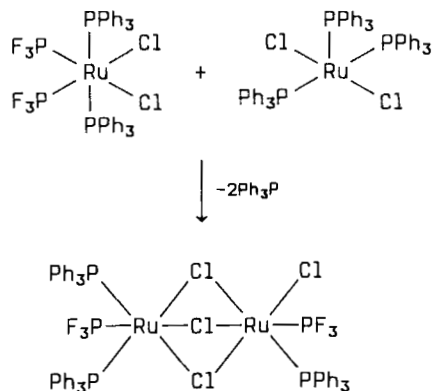


FIG. 21. (a) Structure of $\text{Ti}(\text{CO})_2(\text{PF}_3)(\text{dmpe})_2$. (b) Inner coordination sphere. [Reproduced from reference (365) with permission.]

In certain cases treatment of monomeric complexes with PF_3 can lead to more complicated products, for example, displacement of acetone and PPh_3 from $[\text{RuCl}_2(\text{PPh}_3)_2(\text{acetone})]_2$ leads to the triply chloro-bridged diruthenium complex **21** (134, 136, 137).

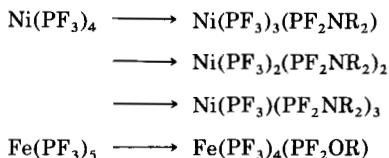


Similar behavior is observed in controlled reactions of PF_3 with $[\text{RuCl}_2(\text{PPh}_3)_3]$ and $[\text{RuCl}_2(\text{PF}_3)(\text{PPh}_3)_2(\text{DMA})]$ ($\text{DMA} = \text{CH}_3\text{CONMe}_2$). The dimeric product is also obtained when $[\text{RuCl}_2(\text{PPh}_3)_3]$ and $[\text{cis-RuCl}_2(\text{PF}_3)_2(\text{PPh}_3)_2]$ are refluxed together in an unusual ligand-exchange reaction.

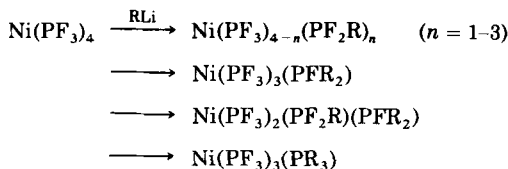


The technique of metal vapor synthesis (method C) is obviously restricted to volatile ligands and has only been utilized so far in the synthesis of $[\text{Ni}(\text{PF}_3)_2(\text{PH}_3)_2]$ and $[\text{Ni}(\text{PF}_3)_3(\text{PH}_3)]$.

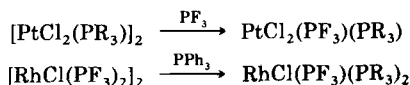
Kruck and co-workers have used cleavage reactions of the phosphorus-fluorine bonds of coordinated PF_3 ligands to synthesize a wide variety of complexes of the type $[\text{M}(\text{PF}_3)_n(\text{PF}_2\text{X})_m]$ ($\text{X} = \text{NHR}$, NR_2 , OR , etc.) (method D), e.g., (190, 192),



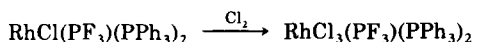
More recently, the fluorine atoms in $[\text{Ni}(\text{PF}_3)_4]$ have been partially substituted by organic groups using RLi or RMgCl (211).



Metal-halogeno bridge cleavage reactions by PF₃ or other phosphines have also been useful in certain cases (method E), e.g.,



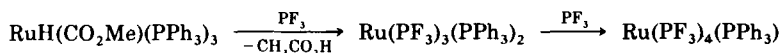
Although normally PF₃ stabilizes low oxidation states of transition metals it has been possible in some cases to directly oxidize a low-valent complex with chlorine (method F).



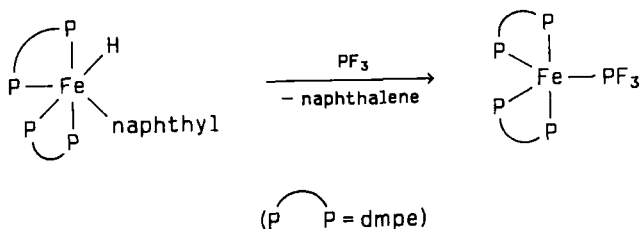
The structure of the Rh(III) product has been established by a detailed study of its ³¹P NMR spectrum.

Addition of PF₃ to a coordinatively unsaturated complex has been used (method G), and mixed PF₃-ligand hydrides can be converted to the corresponding hydrochloride or dichloride systems by treatment with HX (usually HCl or HBF₄) and Et₄NCl (method H).

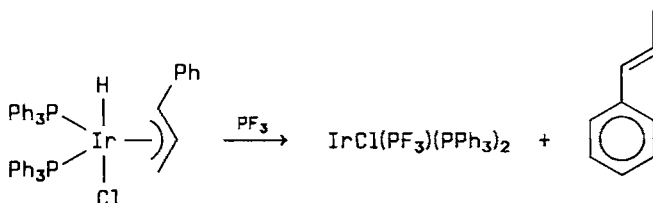
An interesting synthesis of zero-valent ruthenium phosphine-trifluorophosphine complexes has been reported (2, 4) (method I) via reductive elimination of acetic acid from the ruthenium(II) hydrido acetato complex [RuH(CO₂Me)(PPh₃)₃].



A related reaction is that of the naphthyl hydrido derivative of iron(II), which forms the corresponding zero-valent PF₃ iron complex (164):



Also noteworthy is the interaction of PF_3 with the stable iridium(III) allyl hydride $[\text{IrClH}(\eta^3\text{-C}_3\text{H}_4\text{Ph})(\text{PPh}_3)_2]$ to eliminate β -Me-styrene and generate $[\text{IrCl}(\text{PF}_3)(\text{PPh}_3)_2]$ (348).

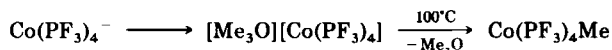


These reactions underline the tendency for PF_3 to stabilize low oxidation states of metals.

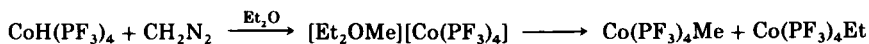
XVII. Transition Metal Alkyl and Alkenyl Complexes

Relatively few examples of σ -bonded η^1 -alkyl or alkenyl metal trifluorophosphine complexes of formula $[\text{MR}_x(\text{PF}_3)_y]$ are known (see Table XVI).

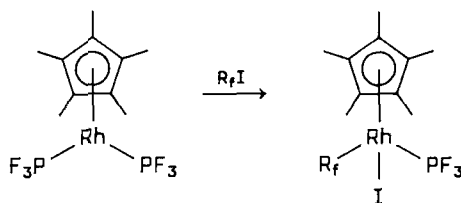
Alkyltetraakis(trifluorophosphine)cobalt complexes can be prepared from the anion $[\text{Co}(\text{PF}_3)_4]^-$ only with strong alkylating agents because of the low nucleophilicity of the anion (method A). Thus, treatment of $[\text{Co}(\text{PF}_3)_4]^-$ with an oxonium salt yields $[\text{Me}_3\text{O}][\text{Co}(\text{PF}_3)_4]$, which on heating gives the desired product.



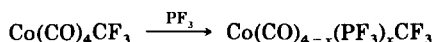
An alternative route utilizes the reaction between the appropriate hydrido-metal PF_3 complex with diazomethane at low temperatures, followed by pyrolysis of the resulting salt (method B).



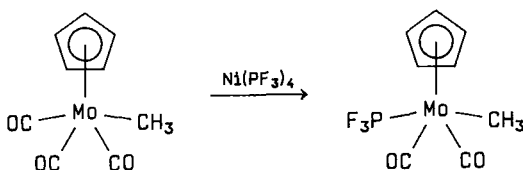
Good yields of certain rhodium(III) perfluoroalkyl derivatives have been obtained in oxidative addition reactions of perfluoroalkyl iodides (R_fI) with rhodium(I) trifluorophosphine complexes (method C).



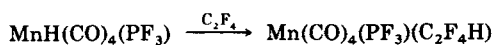
Substitution of CO in the perfluoroalkyl metal carbonyl derivative provides a synthetic route to perfluoroalkyl mixed-carbonyl trifluorophosphine metal complexes (method D).



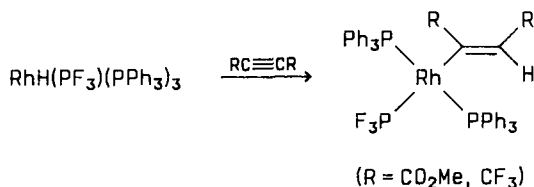
Alternatively, [Ni(PF₃)₄] has proved effective as the source of PF₃ in some reactions (method E).



Fluoroolefins have been inserted into the metal-hydrogen bond of a metal hydride (method F).



Likewise, alkynes undergo similar reactions to produce alkenyl complexes, however, both single- and double-insertion reactions can occur (Scheme 12). A surprising feature of the double-insertion



SCHEME 12

reaction is that the same product is obtained by insertion into either an Rh—C or a C—H bond (see Scheme 13) (160). Finally, a synthetic route

TABLE XVI

TRANSITION METAL ALKYL DERIVATIVES CONTAINING TRIFLUOROPHOSPHINE

	Complex	Method of preparation	Color	M.P. (°C), B.P. (°C/mmHg)		ϕ_F^a	$J_{PF}^{b,c}$	Reference
124	Mn(PF ₃)(CO) ₄ CF ₃	(D)	—	—	—	—	—	259
	Mn(PF ₃)(CO) ₄ COCF ₃	(D)	—	—	—	—	—	259
	Mn(PF ₃)(CO) ₄ C ₂ F ₄ H	(D) (F)	—	—	—	—	—	259
	Co(PF ₃) ₄ CH ₃	(A) (B)	Yellow	104.4/760	—	—	—	222
	Co(PF ₃) ₄ C ₂ H ₅	(A) (B)	Yellow	25/0.5 (dec. > 40)	—	—	—	222
	Co(PF ₃) ₄ C ₇ H ₇	(A)	Yellow	dec. 130	—	—	—	222
	Co(PF ₃)(CO) ₃ CF ₃	(D)	—	Liquid	47.8 ^d	1371	—	351, 352, 355
	Co(PF ₃) ₂ (CO) ₂ CF ₃	(D)	—	Liquid	47.1 ^d	1337	—	351, 352, 355
	Co(PF ₃) ₃ (CO)CF ₃	(D)	—	Liquid	47.3 ^d	1395	—	351, 352, 355
	Co(PF ₃) ₄ CF ₃	(D)	—	Liquid	50.1 ^d	1319	—	351, 352, 355
	Co(PF ₃)(CO) ₃ C ₂ F ₅	(D)	—	Liquid	49.7 ^d	1371	—	351, 352, 355
	Co(PF ₃) ₂ (CO) ₂ C ₂ F ₅	(D)	—	Liquid	49.0 ^d	1348	—	351, 352, 355
	Co(PF ₃) ₃ (CO)C ₂ F ₅	(D)	—	Liquid	49.7 ^d	1342	—	351, 352, 355
	Co(PF ₃) ₄ C ₂ F ₅	(D)	—	Liquid	51.4 ^d	1329	—	351, 352, 355
	Co(PF ₃)(CO) ₃ C ₃ F ₇	(D)	—	Liquid	49.6 ^d	1373	—	351, 352, 355
	Co(PF ₃) ₂ (CO) ₂ C ₃ F ₇	(D)	—	Liquid	49.0 ^d	1348	—	351, 352, 355
	Rh(PF ₃) ₃ { η^5 -C ₅ (CH ₃) ₅ }CF ₃ I	(C)	Orange-brown	dec. > 200	24.7	1392	—	170, 171

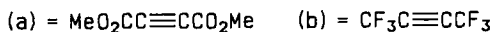
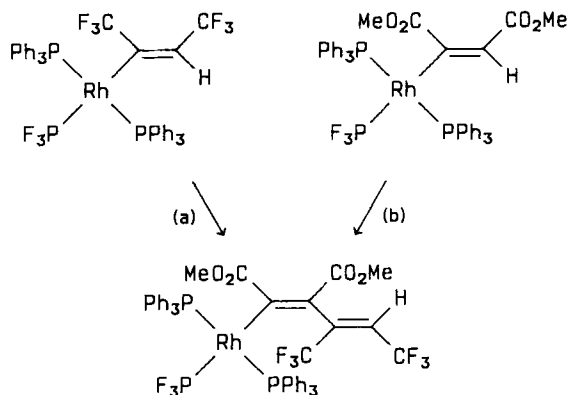
$\text{Rh}(\text{PF}_3)\{\eta^5\text{-C}_5(\text{CH}_3)_5\}\text{C}_2\text{F}_5\text{I}$	(C)	Red-brown	230–231	22.5	1383	170, 171
$\text{Rh}(\text{PF}_3)\{\eta^5\text{-C}_5(\text{CH}_3)_5\}\text{C}_3\text{F}_7\text{I}$	(C)	Deep-red	147–149	21.2	1389	170, 171
$\text{Rh}(\text{PF}_3)\{\eta^5\text{-C}_5(\text{CH}_3)_5\}\text{C}_7\text{F}_{15}\text{I}$	(C)	Orange	86–88	22.2	1379	170
$\text{Rh}(\text{PF}_3)(\text{PPh}_3)_2(\text{CF}_3\text{C}=\text{CHCF}_3)$	(F)	Yellow	137–142	18.3	1308	160
$\text{Rh}(\text{PF}_3)(\text{PPh}_3)_2(\text{CO}_2\text{MeC}=\text{CH}-\text{CO}_2\text{Me})$	(F)	Yellow	—	19.6	1307	160
$\text{Rh}(\text{PF}_3)(\text{PPh}_3)_2[(\text{CO}_2\text{MeC}=\text{C}-\text{CO}_2\text{Me})\text{CF}_3\text{C}=\text{CHCF}_3]$	(F)	Yellow	90 (dec.)	18.8	1310	160
$\text{Mo}(\text{PF}_3)(\eta\text{-C}_5\text{H}_5)(\text{CO})_2\text{CH}_3$	(E)	Yellow	—	—	—	170
$\text{W}(\text{PF}_3)(\eta\text{-C}_5\text{H}_5)(\text{CO})_2\text{CH}_3$	(E)	Yellow	119–121	—	—	170
$\text{W}(\eta^5\text{-C}_5\text{H}_5)(\text{CO})(\text{PF}_3)(\text{PMe}_3)\text{CH}(\text{CO}_2\text{H})\text{C}_6\text{H}_4\text{Me}$	(G)	Orange	—	—	—	107

^a In ppm relative to CCl_3F .

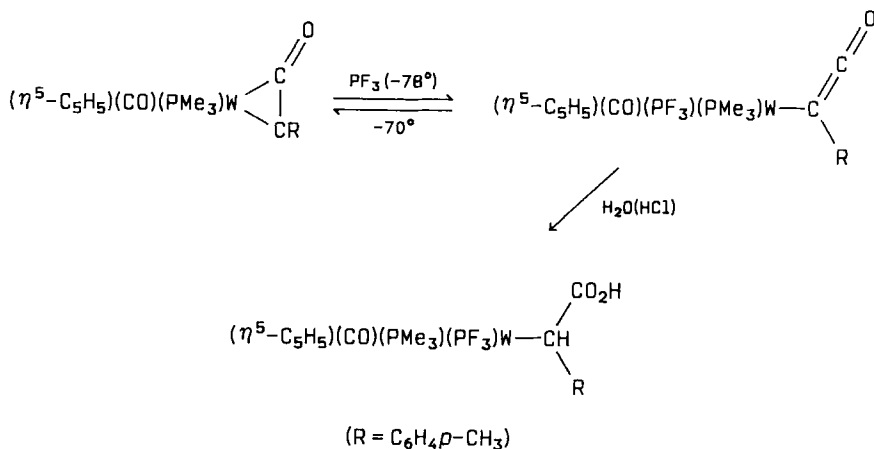
^b In Hz.

^c $^1J_{\text{PF}}$ is correct for *mono* PF_3 complexes, equals $^1J_{\text{PF}} + n^3J_{\text{PF}}$, for $(\text{PF}_3)_{n+1}$ complexes.

^d In ppm relative to PhCF_3 (355).



SCHEME 13. (a) = $\text{MeO}_2\text{CC}\equiv\text{CCO}_2\text{Me}$; (b) = $\text{CF}_3\text{C}\equiv\text{CCF}_3$.



SCHEME 14

to a σ -alkyl complex involving a PF_3 -containing thermolabile η^1 -ketene complex (method G) has been reported (Scheme 14) (107).

XVIII. Transition Metal Complexes Containing σ -Bonded Group IV Elements Other Than Carbon

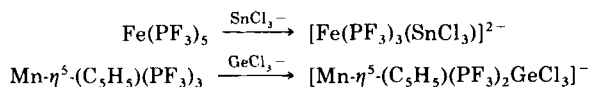
Synthetic routes to the class of compounds listed in Table XVII include UV photochemical displacement of PF_3 from a metal PF_3 complex with MCl_3 anions (M = group IV element) (method A).

TABLE XVII

TRANSITION METAL TRIFLUOROPHOSPHINE COMPLEXES CONTAINING σ -BONDED GROUP IV ELEMENTS

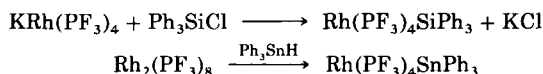
Complex	Method of preparation	Color	M.P. (°C), B.P. (°C/mmHg)	ϕ_F^a	$^1J_{PF}^{b,c}$	Reference
$Mn(PF_3)_x(CO)_{5-x}SiMe_3$	(D)	Pale-yellow	-52.4 to -51.8	16.2	1316	29, 314
$[Mn(PF_3)_2(\eta^5-C_5H_5)GeCl_3]^{-d}$	(A)	Gold	144	9.2	1250	184
$[Mn(PF_3)_2(\eta^5-C_5H_5)SnCl_3]^{-e}$	(A)	Gold-yellow	210	11.9	1230	184
$[Fe(PF_3)_3SnCl_3]^{2-e}$	(A)	Orange	75	-1.5	1235	184
$[Fe(PF_3)(NO)_2GeCl_3]^{-d}$	(A)	Red-brown	dec. > 78	—	—	184
$[Co(PF_3)_2(NO)SnCl_3]^{-d}$	(A)	Red	45	—	—	214
$Co(PF_3)_x(CO)_{4-x}SiH_2CH_3$	(E)	—	—	—	—	29, 120, 314
$Co(PF_3)_x(CO)_{4-x}SiCl_3$	(E)	—	—	—	—	29, 120, 314
$[Ni(PF_3)_3SnCl_3]^{-d}$	(A)	Colorless	115-117	15.8	1295	184
$Ru(CO)_3(PF_3)(SiCl_3)_2$	(D)	White	—	—	—	301
$Ru(CO)_2(PF_3)_2(SiCl_3)_2$	(D)	White	—	—	—	301
$Rh(PF_3)_4Si(OEt)_3$	(C)	White	-20	—	—	17
$Rh(PF_3)_4SiCl_3$	(C)	Yellow	20-22.5	—	—	17
$Rh(PF_3)_4SiPh_3$	(C)	White	105 dec.	5.6	1355	17
$Rh(PF_3)_4GePh_3$	(C)	White	105-108 dec.	—	—	17
$Rh(PF_3)_4SnPh_3$	(B)(C)	White	100 dec.	—	—	17
$Ir(PF_3)_4SiPh_3$	(C)	White	98-101	—	—	17
$Ir(PF_3)_4SnPh_3$	(B)(C)	White	113-114	—	—	17
$Ir(PF_3)_4PbPh_3$	(C)	White	117-118	—	—	17
$IrHCl(Si(OEt)_3)(PF_3)(PPh_3)_2$	(F)	White	—	—	—	41
$[Mo(PF_3)_5SnCl_3]^{-e}$	(A)	Pink	173	-5.7	1230	184

^a In ppm relative to CCl₃F.^b In Hz.^c $^1J_{PF}$ quoted in $^1J_{PF} + n^3J_{PF}$ for $(PF_3)_{n+1}$ complexes.^d $[AsPh_4]^+$ salt.^e $[Et_4N]^+$ salt.

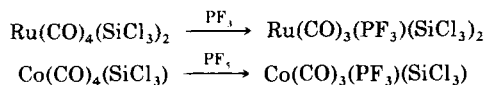


The products are usually isolated as their $[\text{Ph}_4\text{As}]^+$ or $[\text{Et}_4\text{N}]^+$ salts.

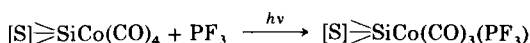
Alternatively, treatment of trifluorophosphine metallates with R_3MCl (method B) or via metal-metal bond cleavage reactions of dinuclear PF_3 metal complexes with a group IV metal hydride R_3MH (method C) have been useful synthetic methods, e.g.,



Carbonyl precursors of the type $[\text{R}_3\text{MM}'(\text{CO})_5]$ (M = group IV metal; M' = transition metal) react readily with PF_3 either thermally or under the influence of UV irradiation (method D), and PF_5 has also been utilized in the case of silyl-substituted metal carbonyl complexes (method E).



An interesting extension of this type of reaction involves the photosubstitution of the surface-confined cobalt tetracarbonyl system $[\text{S}]\text{SiCo}(\text{CO})_4$ (where $[\text{S}]$ represents a high surface-area silica) and the technique of Fourier transform infrared photoacoustic spectroscopy (FTIR/PAS) has been applied for the first time (172) to study photoreactions of a species on the surface.



Small ligands like PF_3 can be added to the five-coordinate iridium(III) complex $[\text{IrHX}(\text{SiR}_3)\text{L}_2]$ (method F) to give six-coordinate complexes in which the PF_3 group has predominantly entered trans to the silyl group.

XIX. Transition Metal PF_3 Complexes Containing Other Anionic or Cationic Ligands

The small number of complexes of this type (listed in Table XVIII) have been obtained via the reaction of a trifluorophosphine metallate

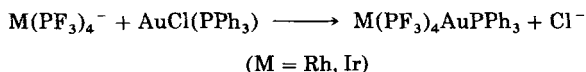
TABLE XVIII

TRANSITION METAL TRIFLUOROPHOSPHINE COMPLEXES CONTAINING OTHER ANIONIC OR CATIONIC LIGANDS

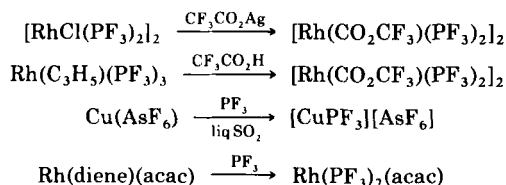
Complex	Method of preparation	Color	M.P. (°C), B.P. (°C/mmHg)	ϕ_F^a	$^1J_{PF}^{b,c}$	Reference
Mn(CO) ₃ (PF ₃)(B ₃ H ₈)	(F)	Yellow-orange	—	—	—	116
[Cu(PF ₃)] [AsF ₆]	(D)	Colorless	—	—	—	101
[Ag(PF ₃)] [HF ₂]	(D)	—	—	—	—	101
Rh ₂ (PF ₃) ₂ (CH ₃ CO ₂) ₄ ^d	(G)	—	—	—	—	66
[Rh(PF ₃) ₂ (CH ₃ CO ₂)] ₂	(B)	Red-brown	126–128	17.2	1308	285
[Rh(PF ₃) ₂ (CF ₃ CO ₂)] ₂	(B) (C)	Magenta	123–125	18.1	1306	285
Rh(PF ₃) ₂ (acac) ^e	(B) (E)	Orange	75–77	20.5	1322 ^g	17, 278
Rh(PF ₃) ₂ (facac) ^f	(B)	Red	—	—	—	278
Rh(PF ₃) ₄ (AuPPh ₃)	(A)	White	158–159	—	—	17
Ir(PF ₃) ₂ (acac)	(E)	Orange	—	26.4	1205	17
Ir(PF ₃)(C ₈ H ₁₄)(acac)	(E)	Yellow	—	—	—	17
Ir(PF ₃) ₄ (AuPPh ₃)	(A)	White	161–162	—	—	17
Hg ₂ (PF ₃)(AsF ₆) ₂	(D)	White	—	47.7	1555	99, 100
Hg ₂ (PF ₃) ₂ (AsF ₆) ₂	(D)	—	—	—	—	99, 100

^a In ppm relative to CCl₃F.^b In Hz.^c $^1J_{PF}$ listed = $^1J_{PF} + nJ_{PF'}$, for (PF₃)_{n+1} complexes.^d Rh—PF₃ = 2.42(1) Å (X-ray).^e acac = CH₃COCHCOCH₃.^f facac = CF₃COCHCOCF₃.^g Accurate value for $^1J_{PF}$; $^3J_{PF'}$ = 4 Hz.

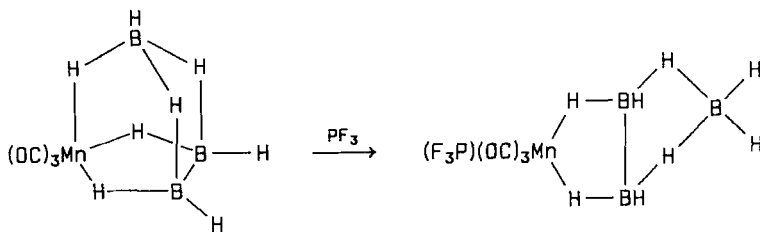
with an appropriate halide (method A), e.g.,



by treatment of halogeno-trifluorophosphine complexes with thallium or silver salts of other anions (e.g., acac, facac, trifluoroacetate) (method B), from η^3 -allyl trifluorophosphine complexes by treatment with acids (method C), via direct interaction between PF_3 and transition metal salts containing complex ions in liquid SO_2 or liquid HF (method D), and by ligand displacement by PF_3 from suitable salts (method E).

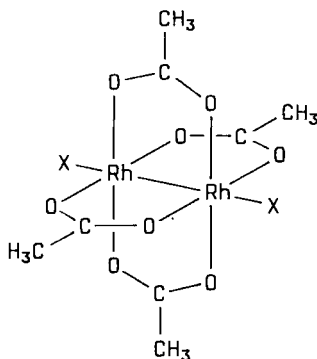


A rather interesting synthetic method for a PF_3 manganese complex containing the unusual octahydrotriborate anion (B_3H_8^-) involves a change in the denticity of the coordinated anion on addition of PF_3 (Scheme 15) (method F).

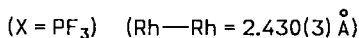


SCHEME 15

An important paper describes the formation of the metal-metal bonded dirhodium tetracarboxylate trifluorophosphine complex $[\text{Rh}_2(\text{OCOCH}_3)_4(\text{PF}_3)_2]$ made directly from the dirhodium tetraacetate complex by direct addition of PF_3 to the formally metal-metal triple bond. The structure was determined by a single-crystal X-ray study, and has been compared with other $[\text{Rh}_2(\text{OAc})_4\text{X}_2]$ systems (X = py, Et_2NH , CO, and $\text{P}(\text{OR})_3$).



(22)



The Rh—Rh distance is much shorter than the 2.7 Å expected for a single Rh—Rh bond, thus suggesting that an Rh—Rh triple bond exists. However, this is inconsistent with spectroscopic data. The situation is best considered as involving extensive mixing of metal and bridging ligand orbitals, but could also be due in part to interactions arising from mixing of higher energy empty orbitals into the ground state MOs for the complex. As a consequence of these interactions, the formal bond order is not a useful indication of the metal-metal interactions in these systems.

ACKNOWLEDGMENT

I would like to thank Professor Ionel Haiduc, Chemistry Department, Babes-Bolyai University, Cluj-Napoca, Romania, for help in compiling data for the binary and hydride sections of this review article.

REFERENCES

1. Al-Ohaly, A. R., and Nixon, J. F., *J. Organomet. Chem.* **202**, 297 (1980).
2. Al-Ohaly, A. R., Head, R. A., and Nixon, J. F., *J. Organomet. Chem.* **156**, C43 (1978).
3. Al-Ohaly, A. R., Head, R. A., and Nixon, J. F., *J. Chem. Soc., (Dalton) Trans.*, p. 889 (1978).
4. Al-Ohaly, A. R., Head, R. A., and Nixon, J. F., *J. Organomet. Chem.* **205**, 99 (1981).
5. Almenningen, A., Anderson, B., and Astrup, E. E., *Acta Chem. Scand.* **24**, 1579 (1970).
6. Antle, P. E., and Tolman, C. A., *J. Organomet. Chem.* **159**, 5 (1978).

7. Avanzio, S. C., Chen, H. W., Donahue, C. J., and Jolly, W. L., *Inorg. Chem.* **19**, 2201 (1980).
8. Avancino, S. C., Bakke, A. A., Chen, H. W., Donahue, C. J., Jolly, W. L., Lee, T. H., and Ricco, A. J., *Inorg. Chem.* **19**, 1931 (1980).
9. Babichev, A. P., Klimov, V. D., Kushlyanikii, O. A., Legasov, V. A., Lebedev, A. V., Nastyukha, A. I., and Khorashev, S. S., *Dokl. Acad. Nauk. SSSR* **259**, 109 (1981).
10. Bailey, T. J., Clark, R. J., and Levy, G. C., *Inorg. Chem.* **21**, 2085 (1982).
11. Barlow, C. G., and Nixon, J. F., *Inorg. Nucl. Chem. Lett.* **2**, 323 (1966).
12. Barlow, C. G., Nixon, J. F., and Webster, M., *J. Chem. Soc. A*, p. 2216 (1968).
13. Barlow, C. G., Nixon, J. F., and Swain, J. R., *J. Chem. Soc. A*, p. 1082 (1969).
14. Bassett, P. J., Higginson, B. R., Lloyd, D. R., Lynaugh, N., and Roberts, P. J., *J. Chem. Soc., Dalton Trans.*, p. 2316 (1974).
15. Benazeth, S., Loutellier, A., and Bigorgne, M., *J. Organomet. Chem.* **24**, 479 (1970).
16. Benfield, F. W. S., Green, M. L. H., Ogden, J. S., and Young, D., *J. Chem. Soc., Chem. Commun.*, p. 866 (1973).
17. Bennett, M. A., and Patmore, D. J., *Inorg. Chem.* **10**, 2387 (1971).
18. Bennett, M. A., and Turney, T. W., *Aust. J. Chem.* **26**, 2321 (1973).
19. Bennett, M. A., Johnson, R. N., and Turney, T. W., *Inorg. Chem.* **15**, 2938 (1976).
20. Bennett, M. A., Johnson, R. N., and Turney, T. W., *Inorg. Chem.* **15**, 90 (1976).
21. Bennett, M. A., Johnson, R. N., Robertson, G. B., Turney, T. W., and Whimp, P. O., *Inorg. Chem.* **15**, 97 (1976).
22. Bennett, M. A., Johnson, R. N., and Turney, T. W., *Inorg. Chem.* **15**, 107 (1976).
23. Bennett, M. A., Johnson, R. N., and Turney, T. W., *Inorg. Chem.* **15**, 111 (1976).
24. Bennett, M. A., Hann, E. J., and Johnson, R. N., *J. Organomet. Chem.* **124**, 189 (1977).
25. Bennett, M. A., and Milner, D. L., *J. Am. Chem. Soc.* **91**, 6983 (1969).
26. Bennett, M. A., Johnson, R. N., Robertson, G. B., Turney, T. W., and Whimp, P. O., *J. Am. Chem. Soc.* **94**, 6540 (1972).
27. Bercaw, J. E., *Adv. Chem. Ser.* **167**, 136 (1978).
28. Berry, A. D., *Organometallics* **2**, 895 (1983).
29. Berry, A. D., and MacDiarmid, A. G., *Inorg. Nucl. Chem. Lett.* **5**, 601 (1969).
30. Besnainov, S., and Labarbe, P., *J. Chim. Phys.* **67**, 512 (1970).
31. Bigorgne, M., *Bull. Soc. Chim. Fr.*, p. 1986 (1960).
32. Bigorgne, M., *J. Inorg. Nucl. Chem.* **26**, 107 (1964).
33. Bigorgne, M., *J. Organomet. Chem.* **2**, 68 (1964).
34. Bigorgne, M., and Bernard, J., *Rev. Chim. Miner.* **3**, 831 (1966).
35. Bigorgne, M., and Bouquet, G., *C.R. Hebd. Seances Acad. Sci., Ser. C* **264**, 1485 (1967).
36. Bigorgne, M., and Tripathi, J. B. P., *J. Mol. Struct.* **10**, 449 (1971).
37. Blackborow, R. J., Eady, C. R., Grevels, F. W., Koerner Von Gustorf, E. A., Scrivanti, A., Wolfbeis, O. S., Benn, R., Brauer, D. J., Kruger, C., Roberts, P. J., and Tsay, Y. H., *J. Chem. Soc., Dalton Trans.*, p. 661 (1981).
38. Blackborow, J. R., Eady, C. R., Koerner Von Gustorf, E. A., Scrivanti, A., and Wolfbeis, O., *J. Organomet. Chem.* **108**, C32 (1976).
39. Blackborow, J. R., Grubbs, R., Miyashita, A., and Scrivanti, A., *J. Organomet. Chem.* **120**, C49 (1976).
40. Blackborow, J. R., Grubbs, R. H., Miyashita, A., Scrivanti, A., and Koerner Von Gustorf, E. A., *J. Organomet. Chem.* **122**, C6 (1976).
41. Blackburn, S. N., Haszeldine, R. N., Parish, R. V., and Setchfield, J. H., *J. Chem. Res. (S)*, p. 170 (1980); *J. Chem. Res. (M)*, p. 2442 (1980).
42. Bönemann, H., *Angew. Chem., Int. Ed. English* **9**, 736 (1970).
43. Bouquet, G., and Bigorgne, M., *Spectrochim. Acta, Part A* **27**, 139 (1971).

44. Bouquet, G., Loutellier, A., and Bigorgne, M., *J. Mol. Struct.* **1**, 211 (1968).
45. Boxhoorn, G., Jesse, A. C., Ernstring, J. M., and Oskam, A., *Thermochim. Acta* **27**, 261 (1978).
46. Bridges, D. M., Rankin, D. W. H., Clement, D. A., and Nixon, J. F., *Acta Crystallogr., Sect. B* **28**, 1130 (1972).
47. Bridges, D. M., Holywell, G. C., Rankin, D. W. H., and Freeman, J. M., *J. Organomet. Chem.* **32**, 87 (1971).
48. Burg, A. B., and Street, G. B., *Inorg. Chem.* **5**, 1532 (1966).
49. Burg, A. B., and Street, G. B., *J. Am. Chem. Soc.* **85**, 3522 (1963).
50. Burns, R. C., and O'Donnell, T. A., *J. Inorg. Nucl. Chem.* **42**, 1613 (1980).
51. Burns, R. C., and O'Donnell, T. A., *J. Inorg. Nucl. Chem.* **42**, 1285 (1980).
52. Busch, M. A., and Clark, R. J., *Inorg. Chem.* **14**, 219 (1975).
53. Busch, M. A., and Clark, R. J., *Inorg. Chem.* **14**, 226 (1975).
54. Cable, R. A., Green, M., Mackenzie, R. E., Timms, P. L., and Turney, T. W., *J. Chem. Soc., Chem. Commun.*, p. 270 (1976).
55. Cairns, M. A., and Nixon, J. F., *J. Organomet. Chem.* **87**, 109 (1975).
56. Cairns, M. A., and Nixon, J. F., *J. Organomet. Chem.* **51**, C27 (1973); *J. Chem. Soc., Dalton Trans.*, p. 2001 (1974).
57. Cairns, M. A., and Nixon, J. F., *J. Organomet. Chem.* **64**, C19 (1974).
58. Cairns, M. A., and Nixon, J. F., *J. Organomet. Chem.* **74**, 263 (1974).
59. Cairns, M. A., Nixon, J. F., and Wilkins, B., *J. Chem. Soc., Chem. Commun.*, p. 86 (1973).
60. Campbell, J. M., and Stone, F. G. A., *Angew. Chem., Int. Ed. English* **8**, 140 (1967).
61. Cassoux, P., Savariault, J.-M., Laurent, J. P., and Commenges, G., *J. Chim. Phys.* **67**, 258 (1970).
62. Chatt, J., *J. Chem. Soc.*, p. 3340 (1949).
63. Chatt, J., and Williams, A. A., *J. Chem. Soc.*, p. 3061 (1951).
64. Chatt, J., Dilworth, J. R., and Leigh, G. J., *J. Chem. Soc., Dalton Trans.*, p. 612 (1973).
65. Chatt, J., Mason, R., and Meek, D. W., *J. Am. Chem. Soc.* **97**, 3826 (1979).
66. Christoph, G. G., and Koh, Y. B., *J. Am. Chem. Soc.* **101**, 1422 (1979).
67. Ciullo, G., Sgmellotti, A., Tarantelli, F., De Alti, G., and Decleva, P., *Gazz. Chim. Ital.* **110**, 305 (1980).
68. Clark, R. J., *New Aspects Chem. Met. Carbonyls Deriv. Int. Symp. Proc. 1st, 1968*, A5 (1968).
69. Clark, R. J., *Inorg. Chem.* **6**, 299 (1967).
70. Clark, R. J., *Inorg. Chem.* **3**, 1395 (1964).
71. Clark, R. J., and Brimm, E. O., *Inorg. Chem.* **4**, 651 (1965).
72. Clark, R. J., and Busch, M. A., *Acc. Chem. Res.* **6**, 246 (1973), and references therein.
73. Clark, R. J., and Hoberman, P. I., *Inorg. Chem.* **4**, 1771 (1965).
74. Clark, R. J., Abraham, M., and Busch, M. A., *J. Organomet. Chem.* **35**, C33 (1972).
75. Clark, R. J., Hoberman, P. I., and Brimm, E. O., *J. Inorg. Nucl. Chem.* **27**, 2109 (1965).
76. Clark, R. J., Hargaden, J. P., Haas, H., and Sheline, R. K., *Inorg. Chem.* **7**, 673 (1968).
77. Clark, R. J., and Morgan, K. A., *Inorg. Chim. Acta* **2**, 93 (1968).
78. Clark, R. J., Swartz, G. L., and George, H. A., *Fundam. Res. Homogeneous Catal.* **3**, 835 (1979).
79. Clegg, W., and Morton, S., *J. Chem. Soc., Dalton Trans.*, p. 1452 (1978).
80. Clement, D. A., Nixon, J. F., and Sexton, M. D., *J. Chem. Soc., Chem. Commun.*, p. 1509 (1969).
81. Clement, D. A., and Nixon, J. F., *J. Chem. Soc., Dalton Trans.*, p. 2553 (1972).
82. Clement, D. A., Nixon, J. F., and Wilkins, B., *J. Organomet. Chem.* **37**, C43 (1972).

83. Connor, J. A., and Overton, C., *J. Chem. Soc., Dalton Trans.*, p. 2397 (1982).
84. Corderman, R. R., and Beauchamp, J. L., *Inorg. Chem.* **17**, 1585 (1978); *ibid* **16**, 3159 (1977).
85. Cotton, F. A., *Inorg. Chem.* **3**, 702 (1964).
86. Cotton, F. A., and Wilkinson, G., "Advanced Inorganic Chemistry." Wiley, New York, 1980.
87. Crocker, C., and Goggin, P. L., *J. Chem. Res. (S)*, p. 36 (1981); *J. Chem. Res. (M)*, p. 701 (1981).
88. Crocker, C., Goggin, P. L., and Goodfellow, R. J., *J. Chem. Res. (S)*, p. 37 (1981); *J. Chem. Res. (M)*, p. 720 (1981).
89. Crocker, C., and Goodfellow, R. J., *J. Chem. Res. (S)*, p. 38 (1981); *J. Chem. Res. (M)*, p. 742 (1981).
90. Crocker, C., Goggin, P. L., and Goodfellow, R. J., *J. Chem. Soc., Chem. Commun.*, p. 1056 (1978).
91. Crocker, C., Goggin, P. L., and Goodfellow, R. J., *J. Chem. Soc., Dalton Trans.*, p. 2494 (1976).
92. Cyvin, S. J., *J. Mol. Struct.* **30**, 311 (1971).
93. Cyvin, S. J., *Z. Anorg. Allg. Chem.* **403**, 193 (1974).
94. Cyvin, S. J., and Lyham, L., *J. Mol. Struct.* **25**, 151 (1975).
95. Cyvin, S. J., and Müller, A., *Acta Chem. Scand.* **25**, 1149 (1971).
96. Daamen, H., Boxhoorn, G., and Oskam, A., *Inorg. Chim. Acta* **28**, 2631 (1978).
97. Dabard, R., Jaouen, G., Simonneaux, G., Cais, M., Kohn, D. H., Lapid, A., and Tartarsky, D., *J. Organomet. Chem.* **184**, 91 (1980).
98. Dalton, J., Paul, I., Smith, J. G., and Stone, F. G. A., *J. Chem. Soc. (A)*, p. 1195 (1968).
99. Dean, P. A. W., and Ibbott, D. G., *Inorg. Nucl. Chem. Lett.* **11**, 119 (1975).
100. Dean, P. A. W., and Ibbott, D. G., *Can. J. Chem.* **54**, 177 (1976).
101. Desjardins, C. D., Edwards, D. B., and Passmore, J., *Can. J. Chem.* **57**, 2714 (1979).
102. Desobry, V., and Kundig, E. P., *Helv. Chim. Acta* **64**, 1288 (1981).
103. Dickson, R. S., Oppenheim, A. P., and Pain, G. N., *J. Organomet. Chem.* **224**, 377 (1982).
104. Doiran, C. E., and McMahon, T. B., *Inorg. Chem.* **19**, 3037 (1980).
105. Dougherty, R. C., Krevalis, M. A., and Clark, R. J., *J. Am. Chem. Soc.* **101**, 2642 (1979).
106. Doyen, G., *Surf. Sci.* **122**, 505 (1982).
107. Eberl, K., Wolfgruber, M., Sieber, W., and Kreissl, F. R., *J. Organomet. Chem.* **236**, 171 (1982).
108. Edwards, H. G. M., and Woodward, L. A., *Spectrochim. Acta Part A* **26**, 897 (1970).
109. Edwards, B. H., Rogers, R. D., Sikora, D. J., Atwood, J. L., and Rausch, M. D., *J. Am. Chem. Soc.* **105**, 416 (1983).
110. Efraty, A., and Jubran, N., *Inorg. Chim. Acta* **44**, L191 (1980).
111. Ernst, R. D., Liu, J.-Z., and Wilson, D. R., *J. Organomet. Chem.* **250**, 257 (1983).
112. Ertl, G., Küppers, J., Nitschké, F., and Weiss, M., *Chem. Phys. Lett.* **52**, 309 (1977).
113. Ferrari, R. P., Vaglio, G. A., Gambino, O., Valle, M., and Cetini, G., *J. Chem. Soc., Dalton Trans.*, p. 1998 (1972).
114. Fjare, K. L., and Ellis, J. E., *Organometallics* **1**, 1373 (1982).
115. Frenz, B. A., and Ibers, J. A., *Inorg. Chem.* **9**, 2403 (1970).
116. Gaines, D. F., and Hildebrandt, S. J., *Inorg. Chem.* **17**, 794 (1978).
117. Gedris, T. E., Clark, R. J., and Catral-Navarreté, J., *J. Inorg. Nucl. Chem.* **43**, 431 (1981).
118. Gerlach, D. H., Peet, W. G., and Muettterties, E. L., *J. Am. Chem. Soc.* **94**, 4545 (1972).

119. Goggin, P. L., Goodfellow, R. J., Haddock, S. R., Taylor, B. F., and Marshall, I. R. H., *J. Chem. Soc., Dalton Trans.*, p. 459 (1976).
120. Gondal, S. K., MacDiarmid, A. G., Saalfeld, F. E., and McDowell, M. V., *Inorg. Nucl. Chem. Lett.* **5**, 351 (1969).
121. Graham, W. A. G., *Inorg. Chem.* **7**, 315 (1968).
122. Green, J. C., King, D. I., and Eland, J. H. D., *J. Chem. Soc., Chem. Commun.*, p. 1121 (1970).
123. Guest, M. F., Hillier, I. H., and Saunders, V. R., *J. Chem. Soc., Faraday Trans. 2*, p. 867 (1972).
124. Huheey, J. E., "Inorganic Chemistry." Harper, New York, 1983.
125. Koerner Von Gustorf, E. A., Jaenicke, O., Wolfbeis, G., and Eady, C. R., *Angew. Chem., Int. Ed. Engl.* **14**, 278 (1975).
126. Koerner Von Gustorf, E. A., Jaenicke, O., and Polansky, O. C., *Angew. Chem., Int. Ed. Engl.* **11**, 532 (1972).
127. Haas, H., and Sheline, R. K., *J. Chem. Phys.* **47**, 2996 (1967).
128. Hagen, A. P., and Elphinstone, E. A., *J. Inorg. Nucl. Chem.* **35**, 3719 (1973).
129. Hao, N., McGlinchey, M. J., Sayer, B. G., and Schrobilgen, G. J., *J. Magn. Reson.* **46**, 158 (1982).
130. Harris, R. K., Woplin, J. R., and Schmutzler, R., *Ber. Bunsenges. Phys. Chem.* **75**, 134 (1971).
131. Harris, T. V., Rathke, J. W., and Muetterties, E. L., *J. Am. Chem. Soc.* **100**, 6966 (1978).
132. Havel, J. J., Ph.D. Thesis, Pennsylvania State University, University Park (1972).
133. Head, R. A., and Nixon, J. F., *J. Chem. Soc., Chem. Commun.*, p. 62 (1976).
134. Head, R. A., and Nixon, J. F., *J. Chem. Soc., Chem. Commun.*, p. 135 (1975).
135. Head, R. A., and Nixon, J. F., *J. Chem. Soc., Dalton Trans.*, p. 885 (1978).
136. Head, R. A., and Nixon, J. F., *J. Chem. Soc., Dalton Trans.*, p. 895 (1978).
137. Head, R. A., and Nixon, J. F., *J. Chem. Soc., Dalton Trans.*, p. 901 (1978).
138. Head, R. A., and Nixon, J. F., *J. Chem. Soc., Dalton Trans.*, p. 909 (1978).
139. Head, R. A., Nixon, J. F., Sharp, G. J., and Clark, R. J., *J. Chem. Soc., Dalton Trans.*, p. 2054 (1975).
140. Head, R. A., Nixon, J. F., Swain, J. R., and Woodard, C. M., *J. Organomet. Chem.* **76**, 393 (1974).
141. Head, R. A., Nixon, J. F., and Clark, R. J., *J. Organomet. Chem.* **135**, 209 (1977).
142. Head, R. A., Nixon, J. F., Westwood, N. P. C., and Clark, R. J., *J. Organomet. Chem.* **145**, 75 (1978).
143. Heaton, B. T., D. Phil. Thesis, University of Sussex (1967).
144. Hillier, I. H., and Saunders, V. R., *Trans. Faraday Soc.* **66**, 2401 (1970).
145. Hillier, I. H., Saunders, V. R., Ware, M. J., Bassett, P. J., Lloyd, D. R., and Lynaugh, N., *J. Chem. Soc., Chem. Commun.*, p. 1316 (1970).
146. Hillier, I. H., Higginson, B. R., Lloyd, D. R., Lynaugh, N., and Roberts, P. J., *J. Chem. Soc., Dalton Trans.*, p. 2316 (1974).
147. Hitchcock, P. B., Nixon, J. F., and Swain, J. A., *Acta Crystallogr., Sect. B* **29**, 154 (1973).
148. Hitchcock, P. B., Nixon, J. F., and Sinclair, J., *J. Organomet. Chem.* **86**, C34 (1975).
149. Hitchcock, P. B., Morton, S., and Nixon, J. F., *J. Chem. Soc., Chem. Commun.*, p. 603 (1984). *J. Chem. Soc., Dalton Trans.*, p. 1295 (1985).
150. Hitchcock, P. B., Lappert, M. F., and Pye, P. L., *J. Chem. Soc., Chem. Commun.*, p. 644 (1976).
151. Hitchcock, P. B., Lappert, M. F., and Pye, P. L., *J. Chem. Soc., Dalton Trans.*, p. 826 (1978).

152. Hitchcock, P. B., Lappert, M. F., Pye, P. L., and Thomas, S., *J. Chem. Soc., Dalton Trans.*, p. 1929 (1979).
153. Hitchcock, P. B., Jacobson, B., and Pidcock, A., *J. Chem. Soc., Dalton Trans.*, p. 2043 (1977).
154. Hopkinson, M. J., and Nixon, J. F., *J. Organomet. Chem.* **148**, 201 (1978).
155. Hosseini, H. E., and Nixon, J. F., *J. Organomet. Chem.* **97**, C24 (1975).
156. Hosseini, H. E., and Nixon, J. F., *J. Organomet. Chem.* **150**, 129 (1978).
157. Hosseini, H. E., and Nixon, J. F., *J. Organomet. Chem.* **192**, C9 (1980).
158. Hosseini, H. E., and Nixon, J. F., *J. Less-Common Met.* **61**, 107 (1978).
159. Hosseini, H. E., Nixon, J. F., and Pinkerton, A. A., unpublished results.
160. Hosseini, H. E., Nixon, J. F., and Poland, J. S., *J. Organomet. Chem.* **164**, 107 (1979).
161. Howell, B. A., and Trahanovsky, W. S., *J. Am. Chem. Soc.* **97**, 2136 (1975).
162. Itoh, H., and Ertl, G., *Z. Naturforsch. A* **37**, 346 (1982).
163. Itoh, H., and Kunz, B. A., *Chem. Phys. Lett.* **64**, 576 (1979).
164. Ittel, S. D., Tolman, C. A., Krusic, P. J., English, A. D., and Jesson, J. P., *Inorg. Chem.* **17**, 3432 (1978).
165. Johnson, T. R., Lynden-Bell, R. M., and Nixon, J. F., *J. Organomet. Chem.* **21**, P15 (1970).
166. Johnston, R. D., Basolo, F., and Pearson, R. G., *Inorg. Chem.* **10**, 247 (1971).
167. Kasenally, A. S., Nyholm, R. S., Parker, D. J., Stiddard, M. H. B., Hodder, D. R. J., and Powell, H. M., *Chem. Ind. (London)*, p. 2097 (1965).
168. Kemmitt, R. D. W., Peacock, R. D., and Wilson, P. L., *J. Chem. Soc., Chem. Commun.*, p. 772 (1968).
169. Keiter, R. L., and Verkade, J. G., *Inorg. Chem.* **8**, 2115 (1969).
170. King, R. B., and Efraty, A., *J. Am. Chem. Soc.* **94**, 3768 (1972).
171. King, R. B., and Efraty, A., *J. Organomet. Chem.* **36**, 371 (1972).
172. Kinney, J. B., Staley, R. H., Reichel, C. L., and Wrighton, M. S., *J. Am. Chem. Soc.* **103**, 4273 (1981).
173. Kouba, J. K., Muetterties, E. L., Thompson, M. R., and Day, V. W., *Organometallics* **2**, 1065 (1983).
174. Kruck, T., *Angew. Chem., Int. Ed. Engl.* **6**, 53 (1967), and references therein.
175. Kruck, T., *Chem. Ber.* **97**, 2018 (1964).
176. Kruck, T., *Z. Naturforsch. B: Anorg. Chem. Org. Chem.* **19**, 165 (1964).
177. Kruck, T., and Baur, K., *Z. Anorg. Allg. Chem.* **364**, 192 (1969).
178. Kruck, T., and Baur, K., *Chem. Ber.* **98**, 3070 (1965).
179. Kruck, T., and Baur, K., *Angew. Chem., Int. Ed. Engl.* **4**, 521 (1965).
180. Kruck, T., Baur, K., and Lang, W., *Chem. Ber.* **101**, 138 (1968).
181. Kruck, T., Baur, K., Glinka, K., and Stadler, M., *Z. Naturforsch. B: Anorg. Chem. Org. Chem.* **23**, 1147 (1968).
182. Kruck, T., Derner, N., and Lang, W., *Z. Naturforsch. B: Anorg. Chem. Org. Chem.* **21**, 1020 (1966).
183. Kruck, T., Diederhagen, H., and Engelmann, A., *Z. Anorg. Allg. Chem.* **397**, 31 (1973).
184. Kruck, T., Ehlert, K., and Molls, W., *Z. Anorg. Allg. Chem.* **422**, 59 (1976).
185. Kruck, T., and Engelmann, A., *Angew. Chem., Int. Ed. Engl.* **5**, 836 (1966).
186. Kruck, T., Engelmann, A., and Lang, W., *Chem. Ber.* **99**, 2473 (1966).
187. Kruck, T., and Hempel, H. U., *Angew. Chem., Int. Ed. Engl.* **10**, 408 (1971).
188. Kruck, T., Hieber, W., and Lang, W., *Angew. Chem., Int. Ed. Engl.* **5**, 247 (1966).
189. Kruck, T., Höfler, M., Jung, H., and Blume, H., *Angew. Chem., Int. Ed. Engl.* **8**, 522 (1969).
190. Kruck, T., Höfler, M., and Blume, H., *Chem. Ber.* **107**, 2145 (1974).

191. Kruck, T., Hofler, M., Baur, K., Junkes, P., and Glinka, K., *Chem. Ber.* **101**, 3827 (1968).
192. Kruck, T., Jung, H., Höfler, M., and Blume, H., *Chem. Ber.* **107**, 2156 (1974).
193. Kruck, T., and Knoll, L., *Z. Naturforsch. B: Anorg. Chem. Org. Chem.* **28**, 34 (1973).
194. Kruck, T., and Knoll, L., *Chem. Ber.* **106**, 3578 (1973).
195. Kruck, T., and Knoll, L., *Chem. Ber.* **105**, 3765 (1972).
196. Kruck, T., and Knoll, L., *Chem. Ber.* **105**, 3783 (1972).
197. Kruck, T., Knoll, L., and Laufenberg, J., *Chem. Ber.* **106**, 697 (1973).
198. Kruck, T., and Kobelt, R., *Chem. Ber.* **105**, 3765 (1972).
199. Kruck, T., and Kobelt, R., *Chem. Ber.* **105**, 3772 (1972).
200. Kruck, T., Kobelt, R., and Prasch, A., *Z. Naturforsch. B: Anorg. Chem. Org. Chem.* **27**, 344 (1972).
201. Kruck, T., and Krause, V., *Z. Naturforsch. B: Anorg. Chem. Org. Chem.* **27**, 302 (1972).
202. Kruck, T., and Lang, W., *Z. Anorg. Allg. Chem.* **343**, 181 (1966).
203. Kruck, T., and Lang, W., *Angew. Chem., Int. Ed. Engl.* **4**, 870 (1965).
204. Kruck, T., and Lang, W., *Chem. Ber.* **98**, 3060 (1965).
205. Kruck, T., and Lang, W., *Angew. Chem., Int. Ed. Engl.* **6**, 454 (1967).
206. Kruck, T., and Lang, W., *Angew. Chem., Int. Ed. Engl.* **3**, 700 (1964).
207. Kruck, T., and Lang, W., *Chem. Ber.* **99**, 3794 (1968).
208. Kruck, T., Lang, W., and Derner, N., *Z. Naturforsch. B: Anorg. Chem. Org. Chem.* **20**, 705 (1965).
209. Kruck, T., Lang, N., Derner, N., and Stadler, M., *Chem. Ber.* **101**, 3816 (1968).
210. Kruck, T., Lang, W., and Engelmann, A., *Angew. Chem., Int. Ed. Engl.* **4**, 148 (1965).
211. Kruck, T., and Mäueler, G., *Z. Anorg. Allg. Chem.* **475**, 156 (1981).
212. Kruck, T., Mäueler, G., and Schmidgen, G., *Z. Anorg. Allg. Chem.* **412**, 239 (1975).
213. Kruck, T., Mäueler, G., and Schmidgen, G., *Chem. Ber.* **107**, 2421 (1974).
214. Kruck, T., and Molls, W., *Z. Anorg. Allg. Chem.* **411**, 54 (1975).
215. Kruck, T., and Prasch, A., *Z. Naturforsch. B: Anorg. Chem. Org. Chem.* **19**, 669 (1964).
216. Kruck, T., and Hempel, H. U., *Angew. Chem., Int. Ed. Engl.* **13**, 201 (1974).
217. Kruck, T., and Prasch, A., *Z. Anorg. Allg. Chem.* **371**, 1 (1969).
218. Kruck, T., and Prasch, A., *Z. Anorg. Allg. Chem.* **356**, 118 (1968).
219. Kruck, T., and Prasch, A., *Angew. Chem., Int. Ed. Engl.* **3**, 754 (1964).
220. Kruck, T., Sylvester, G., and Kunau, I. P., *Z. Naturforsch. B: Anorg. Chem., Org. Chem.* **28**, 38 (1973).
221. Kruck, T., Sylvester, G., and Kunau, I. P., *Angew. Chem., Int. Ed. Engl.* **10**, 725 (1971).
222. Kruck, T., Sylvester, G., and Kunau, I. P., *Z. Anorg. Allg. Chem.* **396**, 165 (1973).
223. Kruck, T., Waldmann, J., Hofler, M., Birkenhager, G., and Odenbrett, C., *Z. Anorg. Allg. Chem.* **402**, 16 (1973).
224. Kruger, C., and Tsay, Y.-H., *Abstr. A6, 1st Eur. Crystallogr. Meet., Bordeaux* (1973).
225. Kundig, E. P., and Timms, P. L., *J. Chem. Soc., Chem. Commun.*, p. 912 (1973).
226. Kundig, E. P., and Timms, P. L., *J. Chem. Soc., Dalton Trans.*, p. 991 (1980).
227. Küppers, J., Nitschké, F., Wandelt, K., and Ertl, G., *Ned. Tijdschr. Vacuumtech.* **16**, 131 (1978).
228. Lee, K. M., and Hester, R. E., *J. Organomet. Chem.* **57**, 169 (1973).
229. Letts, J. B., Mazanec, T. J., and Meek, D. W., *Organometallics* **2**, 695 (1983).
230. Loutellier, A., and Bigorgne, M., *J. Chim. Phys. Phys.-Chim. Biol.* **67**, 79 (1970).
231. Loutellier, A., and Bigorgne, M., *J. Chim. Phys. Phys.-Chim. Biol.* **67**, 99 (1970).
232. Loutellier, A., and Bigorgne, M., *J. Chim. Phys. Phys.-Chim. Biol.* **67**, 107 (1970).
233. Loutellier, A., and Bigorgne, M., *Bull. Soc. Chim. Fr.*, p. 3186 (1965).
234. Lucken, E. A. C., Noack, K., and Williams, D. F., *J. Chem. Soc. A*, p. 148 (1967).

235. Lynden-Bell, R. M., Nixon, J. F., and Schmutzler, R., *J. Chem. Soc. A*, p. 565 (1970).
236. Lynden-Bell, R. M., Nixon, J. F., Roberts, J., Swain, J. R., and McFarlane, W., *Inorg. Nucl. Chem. Lett.* **7**, 1187 (1971).
237. MacKenzie, R. E., and Timms, P. L., *J. Chem. Soc. Chem. Commun.*, p. 650 (1974).
238. Mague, J. T., and Wilkinson, G., *Inorg. Chem.* **7**, 542 (1968).
239. Mahnke, H., Clark, R. J., Rosanske, R., and Sheline, R. K., *J. Chem. Phys.* **60**, 2997 (1974).
240. Mahnke, H., Clark, R. J., and Sheline, R. K., *J. Chem. Phys.* **66**, 4822 (1977).
241. Maier, J. P., and Turner, D. W., *J. Chem. Soc., Faraday Trans. 2*, p. 711 (1972).
242. Manojlovic-Muir, L., Muir, K. W., and Solomon, T., *J. Organomet. Chem.* **142**, 265 (1977).
243. Manriquez, J. M., McAllister, D. R., Sanner, R. D., and Bercaw, J. E., *J. Am. Chem. Soc.* **98**, 6733 (1976).
244. Manriquez, J. M., McAllister, D. R., Sanner, R. D., and Bercaw, J. E., *J. Am. Chem. Soc.* **100**, 2716 (1978).
245. Manriquez, J. M., McAllister, D. R., Rosenberg, E., Skillner, A. M., Williamson, K. L., Chan, S. I., and Bercaw, J. E., *J. Am. Chem. Soc.* **100**, 3078 (1978).
246. Marriott, J. C., Salthouse, J. A., Ware, M. J., and Freeman, J. M., *J. Chem. Soc., Chem. Commun.*, p. 595 (1970).
247. Marynick, D. S., *J. Am. Chem. Soc.* **106**, 4064 (1984).
248. Mason, R., and Meek, D. W., *Angew. Chem., Int. Ed. Engl.* **17**, 183 (1978).
249. Mathieu, R., Lenzi, M., and Poilblanc, R., *C.R. Hebd. Seances Acad. Sci. Ser. C* **266**, 806 (1968).
250. Mathieu, R., Lenzi, M., and Poilblanc, R., *Inorg. Chem.* **9**, 2030 (1970).
251. Meakin, P., Muettterties, E. L., and Jesson, J. P., *J. Am. Chem. Soc.* **94**, 5271 (1972).
252. Meakin, P., Jesson, J. P., Tebbe, F. N., and Muettterties, E. L., *J. Am. Chem. Soc.* **93**, 1797 (1971).
253. Meakin, P., Muettterties, E. L., and Jesson, J. P., *J. Am. Chem. Soc.* **95**, 75 (1973).
254. Meriwether, L. S., and Leto, J. R., *J. Am. Chem. Soc.* **83**, 3192 (1961).
255. Micoud, M. H., Savariault, J. M., and Cassoux, P., *Bull. Soc. Chim. Fr.*, p. 3774 (1972).
256. Middleton, W., Ph.D. Thesis, University of Bristol, Bristol, England (1974).
257. Middleton, R., Hull, J. R., Simpson, J. R., Tomlinson, C. H., and Timms, P. L., *J. Chem. Soc., Dalton Trans.*, p. 120 (1973).
258. Milbrath, D. S., Verkade, J. G., and Clark, R. J., *Inorg. Nucl. Chem. Lett.* **12**, 921 (1976).
259. Miles, W. J., Jr., and Clark, R. J., *Inorg. Chem.* **7**, 1801 (1968).
260. Miles, W. J., Jr., and Clark, R. J., *J. Organomet. Chem.* **131**, 93 (1977).
261. Miles, W. J., Jr., Garrett, B. B., and Clark, R. J., *Inorg. Chem.* **8**, 2817 (1969).
262. Minniti, D., and Timms, P. L., *J. Organomet. Chem.* **258**, C12 (1983).
263. Moissan, H., *Bull. Soc. Chim. Fr.*, p. 454 (1891).
264. Montmayor, R. G., and Parry, R. W., *Inorg. Chem.* **18**, 1470 (1979).
265. Muettterties, E. L., and Rathke, J. W., *J. Chem. Soc., Chem. Commun.*, p. 850 (1974).
266. Müller, J., and Fenderl, K., *Chem. Ber.* **104**, 2207 (1971).
267. Müller, J., Fenderl, K., and Mertschenk, B., *Chem. Ber.* **104**, 700 (1971).
268. Müller, J., and Goll, W., *J. Organomet. Chem.* **69**, C23 (1974).
269. Nathanson, G., Gitlin, B., Rosan, A. M., and Yardley, J. T., *J. Chem. Phys.* **74**, 361 (1981).
270. Naumann, F., and Rehder, D., *J. Organomet. Chem.* **204**, 411 (1981).
271. Nitschké, F., Ertl, G., and Küppers, J., *J. Chem. Phys.* **74**, 5911 (1981).

272. Nixon, J. F., *Adv. Inorg. Chem. Radiochem.* **13**, 364 (1970), and references therein.
273. Nixon, J. F., *Endeavour* **32**, 19 (1973), and references therein.
274. Nixon, J. F., *J. Chem. Soc., Chem. Commun.*, p. 34 (1966).
275. Nixon, J. F., *J. Chem. Soc. A*, p. 1136 (1967).
276. Nixon, J. F., *J. Chem. Soc., Dalton Trans.*, p. 2226 (1973).
277. Nixon, J. F., *J. Fluorine Chem.* **3**, 179 (1973).
278. Nixon, J. F., "Nmr Spectra of Nuclei Other Than Protons" (T. Axenrod and G. A. Webb, eds.), Wiley, New York, 1974. Ch. 25.
279. Nixon, J. F., unpublished results.
280. Nixon, J. F., Clement, D. A., and Poland, J. S., *J. Organomet. Chem.* **76**, 117 (1974).
281. Nixon, J. F., and Kooti, M., *J. Organomet. Chem.* **63**, 415 (1973).
282. Nixon, J. F., and Kooti, M., *J. Organomet. Chem.* **104**, 231 (1976).
283. Nixon, J. F., and Kooti, M., *J. Organomet. Chem.* **149**, 71 (1978).
284. Nixon, J. F., and Pinkerton, A. A., *J. Organomet. Chem.* **37**, C47 (1972).
285. Nixon, J. F., Poland, J. S., and Wilkins, B., *J. Organomet. Chem.* **92**, 393 (1975).
286. Nixon, J. F., and Sexton, M. D., *J. Chem. Soc. A*, p. 1089 (1969).
287. Nixon, J. F., and Sexton, M. D., *Inorg. Nucl. Chem. Lett.* **4**, 275 (1968).
288. Nixon, J. F., Suffolk, R. J., Taylor, M. J., Norman, J. G., Jr., Hoskins, D. E., and Gmur, F. J., *Inorg. Chem.* **19**, 810 (1980).
289. Nixon, J. F., Suffolk, R. J., Taylor, M. J., Green, J. C., and Seddon, E. A., *Inorg. Chim. Acta* **47**, 147 (1981).
290. Nixon, J. F., and Swain, J. R., *J. Organomet. Chem.* **72**, C15 (1974).
291. Nixon, J. F., and Swain, J. R., *J. Chem. Soc., Dalton Trans.*, p. 1044 (1972).
292. Nixon, J. F., and Swain, J. R., *Platinum Met. Rev.* **19**, 22 (1975).
293. Nixon, J. F., and Wilkins, B., *J. Organomet. Chem.* **80**, 129 (1974).
294. Nixon, J. F., and Wilkins, B., *J. Organomet. Chem.* **87**, 341 (1975).
295. Nixon, J. F., Wilkins, B., and Clement, D. A., *J. Chem. Soc., Dalton Trans.*, p. 1993 (1974).
296. Ogilvie, F., Clark, R. J., and Verkade, J. G., *Inorg. Chem.* **8**, 1904 (1969).
297. Parker, D. J., and Stiddard, M. H. B., *J. Chem. Soc. A*, p. 695 (1966).
298. Peterson, L. K., Davis, H. B., Leung, F. Y., and Hoyano, J. K., *Inorg. Chim. Acta* **48**, 259 (1981).
299. Pidcock, A., "Transition Metal Complexes of Phosphorus, Arsenic, and Antimony Ligands" (C. A. McAuliffe, ed.), MacMillan, New York, 1973.
300. der Poel, H. V., Van Koten, G., and Vrieze, K., *Inorg. Chim. Acta* **51**, 241 (1981).
301. Pomeroy, R. K., and Wijesekera, K. S., *Inorg. Chem.* **19**, 3729 (1980).
302. Prusakov, V. N., Petrov, Y. V., Terent'ev, A. A., and Simonev, N. F., *Radiokhimiya* **23**, 319 (1981).
303. Rathke, J. W., and Muetterties, E. L., *J. Am. Chem. Soc.* **97**, 3272 (1975).
304. Rauchfuss, T. B., and Roundhill, D. M., *J. Am. Chem. Soc.* **96**, 3098 (1974).
305. Reddy, G. S., and Schmutzler, R., *Inorg. Chem.* **6**, 823 (1967).
306. Rehder, D., *J. Magn. Reson.* **38**, 419 (1980).
307. Rehder, D., Bechtold, H. C., and Paulsen, K., *J. Magn. Reson.* **40**, 305 (1980).
308. Rehder, D., Bechtold, H. C., Kececi, A., Schmidt, H., and Siewing, M., *Z. Naturforsch. B: Anorg. Chem., Org. Chem.* **37**, 631 (1982).
309. Rehder, D., Dorn, W. L., and Schmidt, J., *Transition Met. Chem. (Weinheim Ger.)* **1**, 233 (1976).
310. Ritz, C. L., and Bartell, L. S., *J. Mol. Struct.* **31**, 73 (1976).
311. Ritz, C. L., Ph.D. Dissertation, University of Michigan, Ann Arbor (1974), *Diss. Abstr. B* **35**, 3271 (1975).

312. Rycroft, D. S., Sharp, D. W. A., and Wright, J. G., *Inorg. Nucl. Chem. Lett.* **14**, 451 (1978).
313. Saalfeld, F. E., McDowell, M. V., Gondal, S. K., and MacDiarmid, A. G., *J. Am. Chem. Soc.* **90**, 3684 (1968).
314. Saalfeld, F. E., McDowell, M. V., De Coreo, J. J., Berry, A. D., and MacDiarmid, A. G., *Inorg. Chem.* **12**, 48 (1973).
315. Saillard, J. Y., Lissilous, R., and Grandjean, D., *J. Organomet. Chem.* **210**, 365 (1981).
316. Saillard, J. Y., Grandjean, D., Le Beuze, A., and Simonneaux, G., *J. Organomet. Chem.* **204**, 197 (1981).
317. Savariault, J. M., Cassoux, P., and Gallais, F., *C.R. Hebd. Seances Acad. Sci. Ser. C* **271**, 477 (1970).
318. Savariault, J. M., Cassoux, P., and Gallais, F., *C. R. Hebd. Seances Acad. Sci. Ser. C* **277**, 759 (1973).
319. Savariault, J. M., and Labarre, J. F., *Theor. Chim. Acta* **42**, 207 (1976).
320. Savariault, J. M., Serafini, A., Pelissier, M., and Cassoux, P., *Theor. Chim. Acta* **42**, 155 (1976).
321. Schmidt, H., and Rehder, D., *Transition Met. Chem.* **5**, 214 (1980).
322. Schmutzler, R., *Adv. Chem. Ser.* **37**, 150 (1963).
323. Schmutzler, R., *Adv. Fluorine Chem.* **5**, 31 (1965).
324. Seel, F., Ballreich, K., and Schmutzler, R., *Chem. Ber.* **94**, 1173 (1961).
325. Severson, S. J., Cymbaluk, T. H., Ernst, R. D., Higaski, J. M., and Parry, R. W., *Inorg. Chem.* **22**, 3833 (1983).
326. Sheldrick, W. S., personal communication.
327. Sheline, R. K., and Mahnke, H., *New Synth. Methods* **3**, 219 (1975).
328. Sikora, D. J., Rausch, M. D., Rogers, R. D., and Atwood, J. L., *J. Am. Chem. Soc.* **101**, 5079 (1979).
329. Sikora, D. J., Rausch, M. D., Rogers, R. D., and Atwood, J. L., *J. Am. Chem. Soc.* **103**, 982 (1981).
330. Skell, P. S., Williams-Smith, D. L., and McGlinckey, M. J., *J. Am. Chem. Soc.* **95**, 3337 (1973).
331. Staplin, D. C., and Parry, R. W., *Inorg. Chem.* **18**, 1473 (1979).
332. Stelzer, O., and Unger, E., *Chem. Ber.* **108**, 1246 (1975).
333. Stroheimer, W., and Müller, F. J., *Z. Naturforsch. B: Anorg. Chem. Org. Chem.* **22**, 451 (1967).
334. Street, G. B., and Burg, A., *Inorg. Nucl. Chem. Lett.* **1**, 47 (1965).
335. Sullivan, R. E., and Kiser, R. W., *J. Chem. Soc., Chem. Commun.*, p. 1425 (1968).
336. Svatos, G. F., and Flagg, E. E., *Inorg. Chem.* **4**, 422 (1965).
337. Swartz, G. L., and Clark, R. J., *Inorg. Chem.* **19**, 3191 (1980).
338. Timms, P. L., *Angew. Chem. Int. Edn.* **14**, 273 (1975).
339. Timms, P. L., *Adv. Inorg. Chem. Radiochem.* **14**, 121 (1972).
340. Timms, P. L., *J. Chem. Soc., Chem. Commun.*, p. 1033 (1969).
341. Timms, P. L., *J. Chem. Soc. A*, p. 2526 (1970).
342. Timms, P. L., personal communication (1978).
343. Timms, P. L., and Turney, T. W., *J. Chem. Soc., Dalton Trans.*, p. 2021 (1976).
344. Tolman, C. A., *J. Am. Chem. Soc.* **92**, 2956 (1970).
345. Tolman, C. A., Ittel, S. D., English, A. D., and Jesson, J. P., *J. Am. Chem. Soc.* **100**, 4080 (1978).
346. Trabelsi, M., Loutellier, A., and Bigorgne, M., *J. Organomet. Chem.* **56**, 369 (1973).
347. Tripathi, J. B. P., and Bigorgne, M., *J. Organomet. Chem.* **9**, 307 (1967).
348. Tulip, T. H., and Ibers, J. A., *J. Am. Chem. Soc.* **101**, 4201 (1979).

349. Tumas, W., Gitlin, B., Rosan, A. M., and Yardley, J. T., *J. Am. Chem. Soc.* **104**, 55 (1982).
350. Udovich, C. A., and Clark, R. J., *J. Organomet. Chem.* **36**, 355 (1972).
351. Udovich, C. A., and Clark, R. J., *Inorg. Chem.* **8**, 938 (1969).
352. Udovich, C. A., and Clark, R. J., *J. Am. Chem. Soc.* **91**, 526 (1969).
353. Udovich, C. A., and Clark, R. J., *J. Organomet. Chem.* **25**, 199 (1970).
354. Udovich, C. A., Clark, R. J., and Haas, H., *Inorg. Chem.* **8**, 1066 (1969).
355. Udovich, C. A., Krevalis, M. A., and Clark, R. J., *Inorg. Chem.* **15**, 900 (1976).
356. Vaska, L., and Catone, D. L., *J. Am. Chem. Soc.* **88**, 5324 (1966).
357. Warren, J. D., and Clark, R. J., *Inorg. Chem.* **9**, 373 (1970).
358. Warren, J. D., Busch, M. A., and Clark, R. J., *Inorg. Chem.* **11**, 452 (1972).
359. White, J. W., and Wright, C. J., *J. Chem. Soc., Faraday Trans. 2* **68**, 1423 (1972).
360. Whitmer, J. C., and Cyvin, S. J., *J. Mol. Struct.* **38**, 277 (1977).
361. Wilkinson, G., *J. Am. Chem. Soc.* **73**, 5501 (1951).
362. Williams-Smith, D. L., Wolf, L. R., and Skell, P. S., *J. Am. Chem. Soc.* **94**, 4042 (1972).
363. Woodward, L. A., and Hall, J. R., *Nature (London)* **181**, 831 (1958).
364. Woodward, L. A., and Hall, J. R., *Spectrochim. Acta* **16**, 654 (1960).
365. Wreford, S. S., Fischer, M. B., Lee, S., James, E. J., and Nyburg, S. C., *J. Chem. Soc., Chem. Commun.*, p. 458 (1981).
366. Xiao, S. X., Trogler, W. C., Ellis, D. E., and Berkovitch-Yellin, Z., *J. Am. Chem. Soc.* **105**, 7033 (1983).
367. Yarbrough, L. W., and Hall, M. B., *Inorg. Chem.* **17**, 2269 (1978).
368. Ziegler, T., and Rauk, A., *Inorg. Chem.* **18**, 1755 (1979).

This Page Intentionally Left Blank

SOLVENT EXTRACTION OF METAL CARBOXYLATES

HIROMICHI YAMADA* and MOTOHARU TANAKA**

*Faculty of Engineering, Gifu University, Yanagido, Gifu, Japan, and

**Faculty of Science, Nagoya University, Nagoya, Japan

I. Introduction	143
II. Partition of a Carboxylic Acid between the Aqueous and Organic Phases	145
III. Solvent Extraction of Metal Ions with Carboxylic Acids	147
A. Equilibrium Treatment	147
B. Extraction of Metal Ions	151
C. Coextraction	160
D. Synergistic Extraction of Metal Carboxylates	160
E. Solvent Effect on the Extraction of Metal Carboxylates	162
IV. Concluding Remarks	164
References	164

I. Introduction

Carboxylic acids are conveniently utilized in the extraction of a number of metal ions. The dissolution of metal soaps in trichlorobenzene was first noticed by Biffen and Snell (12). The first example of the liquid-liquid extraction involving a metal carboxylate appears to be the extraction of scandium with benzoic acid prior to the colorimetric determination (54).

In the early 1950s there were proposed several procedures involving carboxylic acids for separation of metals such as copper and beryllium (9, 87, 140, 149). After these analytical applications of the carboxylate extraction system, Hök-Bernström published a series of papers dealing with the quantitative analysis of the extraction equilibria involving metal carboxylates (48-50). Since then the extraction of metal carboxylates has been extensively studied and the subject has been reviewed from time to time by the following authors: Fletcher and Flett (23), Flett and Jaycock (26), Ashbrook (8), Miller (85), Rice (118), and Brzózka and Rózycki (14). Martinov has elaborated a data compilation

of the extraction of metals with organic acids including carboxylic acids (78*b*).

The carboxylate extraction system has been recognized as more advantageous than the chelate extraction system, since one can deal with more concentrated metal solutions in the former than in the latter. Thus the application of the carboxylate extraction to hydrometallurgy has been attempted, and in this connection extensive studies have been carried out in the Soviet Union and the United Kingdom.

There have been a number of physicochemical studies on the organic solutions of metal soaps and the critical solution temperature has been determined for a metal soap-organic solvent pair: below this temperature we observe no appreciable dissolution of the metal soap, while above this particular temperature, dissolution becomes appreciable. According to these studies, metal soaps are in the form of micelles composed of several formula units of metal carboxylate, and the composition of the solute species was said to be indefinite (78*a*, 94).

With nonchelating agents such as carboxylates, the coordination-saturation is not expected to occur at the same time as the charge neutralization, which would be the case with some chelating agents. Thus, in order to satisfy the coordination number of a metal ion in a carboxylate, it is necessary either to add neutral ligands such as carboxylic acids or to form polymerized species, in which metal ions share apices or edges with each other. The polymerization of metal carboxylates is characterized either by the liberation of free carboxylic acid or by the formation of hydroxo or oxo bridges.

Though the extraction of metals with carboxylic acids is sometimes very complicated, we have in effect extracted species of definite composition when we study the system as a function of the concentration of free carboxylic acid.

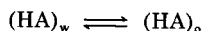
The formation of a dimerized extracted species was first reported for the extraction of copper(II) with propanoic acid (40, 41). Later, nickel and cobalt were found to be extracted as dimers (22), and a mixed copper(II) carboxylate dimer involving acetate and decanoate was reported (147). More recently, attention has been drawn to the extraction of heteropolynuclear metal carboxylates (90, 91).

In these complicated extraction systems containing the polymeric and/or hydroxo species, one would expect the solvent used as a diluent to exert a considerable effect on the extraction equilibrium. In the extraction of gallium(III) with decanoic acid it has been found that the less polar the solvent, the more polymerized the extracted species (150). More recently, the solvent effect on the extraction (156) and dimerization (151, 153) of copper(II) decanoate has been interpreted according to regular solution theory (141, 142).

II. Partition of a Carboxylic Acid between the Aqueous and Organic Phases

In the solvent extraction of metal ions with carboxylic acids, it is indispensable to have information about the partition of the carboxylic acid between the aqueous and organic phases. The carboxylic acid is known to dimerize in nonsolvating solvents.

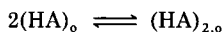
The partition of a carboxylic acid HA into an organic solvent is written as



where the subscripts refer to the water (w) or organic (o) phase. The partition constant is defined as

$$K_{D,HA} = [HA]_o/[HA]_w^{-1}. \quad (1)$$

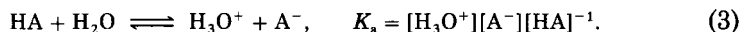
The dimerization of HA in the organic phase is given by the following:



with $(HA)_{2,o}$ denoting the dimeric acid in the organic phase, and the dimerization constant defined as

$$K_2 = [(HA)_2]_o/[HA]_o^{-2}. \quad (2)$$

In the solvent extraction of metal ions with carboxylic acids, these equilibria should be considered along with the dissociation of HA in the aqueous phase:



In Table I, the partition and dimerization constants of some carboxylic acids are given.

Values of K_D are higher for polar solvents such as 4-methyl-2-pentanone and octanol than for nonpolar solvents such as benzene and hexane. On the contrary, K_2 values are higher in nonpolar solvents than in polar solvents. These facts result from the extensive solvation of carboxylic acids in polar or coordinating solvents. Thus for a carboxylic acid (18, 19, 67)

$$\log K_2 = -2 \log K_D + \text{constant}. \quad (4)$$

TABLE I

PARTITION AND DIMERIZATION CONSTANTS OF CARBOXYLIC ACIDS AT 25°C^a

Acid	Solvent					
	Toluene	Benzene	Chloroform	1,2-DCE ^b	NB ^c	IPE ^d
Propanoic: $\log K_D$	-1.47	-1.36	-0.96	-0.99	-0.86	-0.09
$\log K_2$	2.39	2.21	1.94	1.53	0.97	-0.30
Butanoic: $\log K_D$	0.68 ^e	-0.79	-0.27 ^f	-0.39	-0.34	0.48
$\log K_2$	1.98 ^e	2.28	1.69 ^f	1.45	0.95	-0.37
Pentanoic: $\log K_D$	-0.20 ^f	-0.16	0.19 ^f	0.23	0.23	1.05
$\log K_2$	2.30 ^f	2.36	1.82 ^f	1.35	1.01	-0.20
Hexanoic: $\log K_D$	0.56 ^f	0.31	1.05 ^f	0.82	0.77	1.48
$\log K_2$	2.13 ^f	2.45	1.40 ^f	1.19	0.96	-0.19
Octanoic: $\log K_D$		1.67 ^g	2.17 ^g			
$\log K_2$		2.51 ^g	2.46 ^g			
Decanoic: $\log K_D$		2.41 ^h				
$\log K_2$		2.80 ^h				
Benzoic: $\log K_D$	0.06 ⁱ	0.14 ⁱ		0.59 ⁱ		
$\log K_2$	2.48 ⁱ	2.46 ⁱ		1.56 ⁱ		

^a Data from reference 67.^b 1,2-Dichloroethane.^c Nitrobenzene.^d Isopropyl ether.^e Ref. 65.^f Ref. 134.^g Ref. 128.^h Ref. 144.ⁱ Ref. 29.

The more extensive the solvation of monomeric acid, the less extensive the dimerization. The extensive solvation favors the partition of an acid and a higher partition constant results.

Values of $\log K_D$ increase with increasing carbon number in carboxylic acids. The increment of $\log K_D$ for an added methylene group is mainly due to the volume contribution of the methylene group to the partition, and thus it varies little from solvent to solvent, i.e., $\Delta \log K_D / \text{CH}_2 = 0.56 - 0.64$ (21, 31, 141). The different $\Delta \log K_D / \text{CH}_2$ values for different solvents are ascribable to the different solute-solvent interactions, and have been discussed elsewhere in more detail (31).

In the partition of an acid between the aqueous and organic phases, hydration of the acid inevitably occurs. In addition to the monohydrates of monomer and dimer, the dimer dihydrate (29) and trihydrate (30) have been found in some organic solvents. Högfeldt has also

proposed the trihydrate of dimeric trichloroacetic acid and the monohydrate of tetrameric acetic acid in some solvents (47, 71).

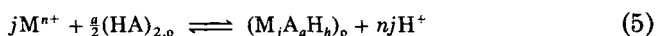
The dimerization constants of carboxylic acids determined by the partition method are usually lower than the values obtained by IR spectroscopy, cryoscopy, or dielectric measurements (100). The correction for hydration gives dimerization constants expected from values in dry solvents by spectroscopic or dielectric measurements (29, 30).

III. Solvent Extraction of Metal Ions with Carboxylic Acids

A. EQUILIBRIUM TREATMENT

As stated earlier the polymeric species are often involved in the extraction of metal carboxylates. Therefore, the extraction equilibrium is sometimes more complicated than in the chelate extraction system. As is evident from the following treatment, it is advantageous and often indispensable to study the total metal concentration in the organic phase [Eq. (8)] instead of the conventionally utilized distribution ratio of the metal [Eq. (7)].

When a j -merized metal carboxylate of the composition $M_jA_aH_h$ ($nj = a - h$) is responsible for the extraction of a metal ion M^{n+} with a carboxylic acid HA, the extraction equilibrium is written as:



with

$$K_{ex(jah)} = \frac{[M_jA_aH_h]_o [H^+]^{nj}}{[M^{n+}]^j [(HA)_2]_o^{a/2}} \quad (6)$$

The distribution ratio (D) of the metal between the organic and aqueous phases is given by

$$\begin{aligned} D &= \frac{C_{M,o}}{C_{M,w}} = \sum_j \sum_a j [M_jA_aH_h]_o / [M^{n+}] \alpha_M \\ &= \sum_j \sum_a (j K_{ex(jah)} [M^{n+}]^{(j-1)} \alpha_M^{-1} [(HA)_2]_o^{a/2} [H^+]^{-nj}), \end{aligned} \quad (7)$$

where $C_{M,o}$, $C_{M,w}$, and α_M are the total concentrations of the metal in the organic and aqueous phases, and the side-reaction coefficient taking into account the complexation of the metal in the aqueous phase (119), respectively. On the other hand, the total concentration of the metal in

the organic phase is written as

$$C_{M,o} = \sum_j \sum_a j [M_j A_a H_h]_o = \sum_j \sum_a (j K_{ex(jah)} [M^{n+}]^j [(HA)_2]_o^{a/2} [H^+]^{-nj}). \quad (8)$$

When only $M_j A_a H_h$ is responsible for the extraction, Eqs. (9) and (10) are derived from Eqs. (7) and (8), respectively:

$$\begin{aligned} \log D = (j-1) \log [M^{n+}] + \frac{a}{2} \log [(HA)_2]_o - nj \log [H^+] - \log \alpha_M \\ + \log j + \log K_{ex(jah)}, \end{aligned} \quad (9)$$

and

$$\log C_{M,o} = j(\log [M^{n+}] - n \log [H^+]) + \frac{a}{2} \log [(HA)_2]_o + \log j + \log K_{ex(jah)}. \quad (10)$$

According to Eq. (9), the conventional plot of $\log D$ against $-\log[H^+]$ at a constant $[(HA)_2]_o$ should yield a straight line with a slope of n only when j and α_M are equal to unity. For the polymeric extracted species, the distribution ratio, D , depends not only on $[H^+]$ and $[(HA)_2]_o$ but also on the metal ion concentration. Therefore, the plot according to Eq. (9) yields a curve (Fig. 1). As shown in Fig. 1, the plot falls on the straight

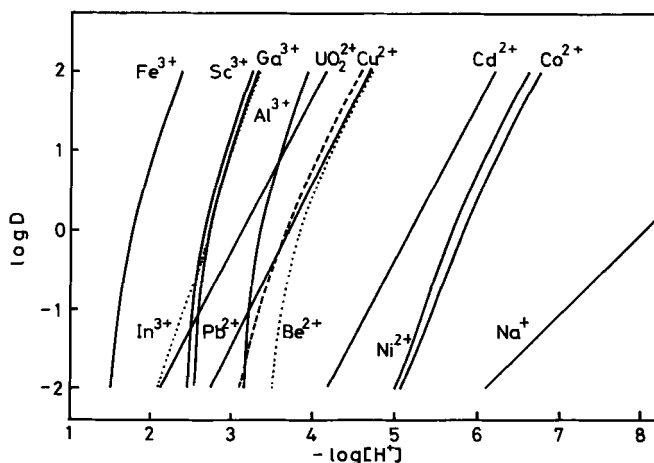


FIG. 1. Plot of $\log D$ vs. $-\log[H^+]$ for the extraction of metal ions with decanoic acid in benzene. Solid lines are calculated by Eq. (9) with the results taken from refs. 63, 89, 91, 92, 143–146, 154–156, at the total metal concentration $C_M = 5 \times 10^{-3} \text{ mol dm}^{-3}$, and the total concentration of decanoic acid $C_{HA} = 1.0 \text{ mol dm}^{-3}$.

line with a slope of n for relatively high values of D ($D > 10$). In such cases, we may conclude quite erroneously a monomeric species like MA_n , even for a polymeric extracted species $(MA_n)_j$.

According to Eq. (10), on the other hand, the plot of $\log C_{M,o}$ against $(\log[M^{n+}] - n\log[H^+])$ at a constant carboxylic acid concentration should yield a straight line with a slope of j , the degree of polymerization. If two or more species with different degrees of polymerization are responsible for the extraction, as in the case of indium, cobalt, and nickel (145, 143, 144), this plot gives rise to a curve (Fig. 2). By analysis of this curve we see the variation in the degree of polymerization of the extracted species (143–145). It may be noted that in most cases free carboxylic acid is liberated in the polymerization of the metal carboxylate. Thus the higher the carboxylic acid concentration and the lower the metal concentration in the organic phase, the lower will be the degree of polymerization of the extracted carboxylate.

The plot according to Eq. (10) is of general use in studies not only on the carboxylate extraction system but also on the chelate extraction system. For instance, vanadium (V) 8-quinolinolate was found to be extracted as an oxo-bridged dimeric form (158), whose structure was later established by X-ray crystallography (157).

Equation (10) yields directly the following relation:

$$\log C_{M,o} - j(\log[M^{n+}] - n\log[H^+]) = \frac{a}{2}\log[(HA)_2]_o + \log j + \log K_{ex(jah)} \quad (11)$$

The left-hand side of Eq. (11) can be plotted against $\log[(HA)_2]_o$ under conditions where only one j -merized carboxylate is responsible for the

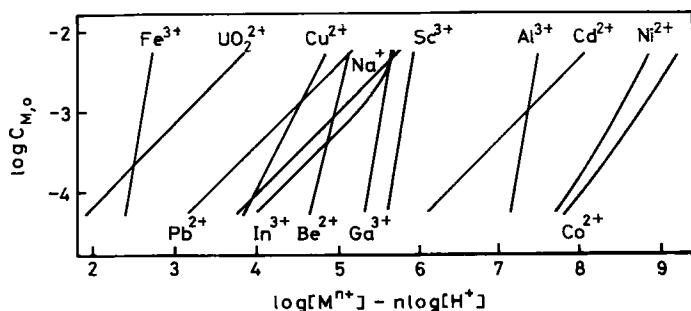


FIG. 2. Plot of $\log C_{M,o}$ vs. $(\log[M^{n+}] - n\log[H^+])$ for the extraction of metal ions with decanoic acid in benzene. Solid lines are calculated by Eq. (10) with the results taken from the same references as in Fig. 1 under the same conditions as in Fig. 1.

extraction. The plot gives rise to a straight line with a slope of $a/2$, thus permitting the determination of the number of carboxylate residues involved in the extracted species. From the intercept of the plot, we find the extraction constant $\log K_{\text{ex}(jah)}$. When two or more species involving a different number of carboxylate residue are responsible for the extraction, the plot of the left-hand side of Eq. (11) vs. $\log[(\text{HA})_2]_0$ gives rise to a curve. In this case, according to the curve-fitting method, in which the plot is compared with a family of normalized curves, the total number of carboxylate residues involved in the extracted species and the corresponding extraction constants can be determined (89, 92, 155).

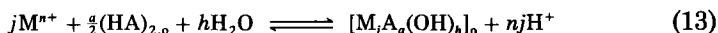
When the coordination number of the metal ion in the extracted species is not satisfied with carboxylate and carboxylic acid, the water determination should be made on the extracted species. If a hydrated extracted species is involved in the extraction, the following equilibrium is relevant to the extraction:



with

$$K_{\text{ex}(jahw)} = [\text{M}_j\text{A}_a\text{H}_h(\text{H}_2\text{O})_w]_0 [\text{H}^+]^{nj} [\text{M}^{n+}]^{-j} [(\text{HA})_2]_0^{-a/2}.$$

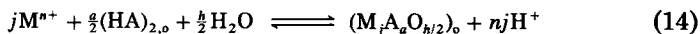
When the charge on the metal ion is completely neutralized with carboxylate, h is zero or positive and $a \geq nj$. However in some cases we find a negative h . In these cases, the water determination is indispensable in finding the correct composition of the extracted species. If we find h water molecules for $\text{M}_j\text{A}_a\text{H}_{-h}$, the extracted species should be written as $\text{M}_j\text{A}_a(\text{OH})_h$ with the following extraction equilibrium:



with

$$K_{\text{ex}(ja-h)} = [\text{M}_j\text{A}_a(\text{OH})_h]_0 [\text{H}^+]^{nj} [\text{M}^{n+}]^{-j} [(\text{HA})_2]_0^{-a/2}.$$

If, on the other hand, the number of water molecules found for $\text{M}_j\text{A}_a\text{H}_{-h}$ is $h/2$, then $h/2$ oxo group(s) should be involved in the extracted species instead of h hydroxo group(s). In that case, following equilibrium becomes relevant to the extraction:



with

$$K_{\text{ex}(ja-h/2)} = [\text{M}_j\text{A}_a\text{O}_{h/2}]_0 [\text{H}^+]^{nj} [\text{M}^{n+}]^{-j} [(\text{HA})_2]_0^{-a/2}.$$

B. EXTRACTION OF METAL IONS

The composition and extraction constant of various metal carboxylates are tabulated in Table II.

1. Alkali Metals

Alkali metal salts are generally used in order to keep constant the ionic strength of the aqueous phase. Therefore, even in the extraction of a metal ion other than alkali metal ions with carboxylic acids, we should also consider the extraction of alkali metal ions either as a simple carboxylate or a mixed-metal carboxylate.

In the extraction of alkali metal ions with C₇–C₉ aliphatic carboxylic acids, Mikhailichenko and Rozen found the following order of extractability: K⁺ > Cs⁺ > Na⁺ > Li⁺ (83, 120).

For the extraction of sodium ions with decanoic acid in benzene, Nakasuka *et al.* (91) proposed the following extraction equilibria:

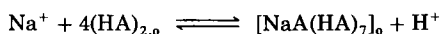
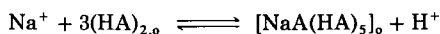
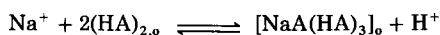


TABLE II

EXTRACTION OF METAL IONS WITH CARBOXYLIC ACIDS

Organic Phase ^a	Extracted Species, log K _{ex}	Reference
Alkali metals		
Nona/decane	NaA(HA) ₄ (H ₂ O) _w	55, 56
Nona/isooctanol	NaA(H ₂ O) _w , -9.69	59
Deca/benzene	NaA(HA) ₃ , -8.28; NaA(HA) ₅ , -7.22; NaA(HA) ₇ , -7.64	91
Vers/ <i>n</i> -octane	NaA(HA) ₂ ; NaA(HA) ₃	79
Alkaline earth metals		
Deca/benzene	Be ₄ A ₆ O, -22.6	63
Naph/kerosene	BeA ₂ , -8.37	5
Naph/kerosene	MgA ₂ , -13.90	5
C ₇ –C ₉ mix/octane	MgA ₂ (HA) ₄ , -12.16	81
Naph/kerosene	CaA ₂ , -12.63	5
C ₇ –C ₉ mix/octane	CaA ₂ (HA) ₄ , -11.13	81
(Penta, Hexa, Octa, Deca)/octane	SrA ₂ (HA) ₄ (H ₂ O) ₄ , -10.68, -10.57, -10.46, -10.38	82
Vers/ <i>n</i> -octane	SrA ₂ (HA) ₂ ; SrA ₂ (HA) ₃	79
Naph/kerosene	SrA ₂ , -11.28	5
C ₇ –C ₉ mix/octane	SrA ₂ (HA) ₄ , -10.42	81

(continued)

TABLE II (continued)

Organic Phase ^a	Extracted Species, log K_{ex}	Reference
Naph/kerosene	BaA ₂ , -9.77	5
C ₇ -C ₉ mix/octane	BaA ₂ (HA) ₄ , -9.64	81
Al, Ga, In, and Tl		
Deca/benzene	Al ₆ A ₁₂ (OH) ₆ , -46.1	146, 155
Deca/benzene	Ga ₆ A ₁₈ (H ₂ O) ₆ , -34.3; Ga ₆ A ₁₂ (OH) ₆ , -35.8; Ga _j A _a H _h ($j < 6$)	155
Deca/toluene	Ga ₆ A ₁₈ (H ₂ O) _w ($w > 6$), -33.21; Ga _j A _a H _h ($j < 6$)	150
Deca/CB	Ga ₃ A ₉ , -19.14	150
Deca/1,2-DCE	GaA ₃ , -9.42; Ga ₃ A ₉ , -18.9	150
Deca/1-octanol	GaA ₂ (OH), -9.54; Ga ₂ A ₄ (OH) ₂ , -14.92; Ga ₂ A ₆ , -15.26	150
Hexa/CHCl ₃	InA ₃ (HA) ₃	125
Deca/benzene	InA ₃ (HA) ₃ , -7.34; In ₃ A ₉ (HA) ₃ , -18.6; In ₆ A ₁₂ (OH) ₆ , -36.1	145
Hexa/MIBK	TlA(HA) ₂	130
Hexa/benzene, CHCl ₃	TlA(HA) ₃	130
Hexa/NB	TlA(HA) ₄	130
Pb		
Deca/benzene	PbA ₂ (HA) ₂ , -7.12; PbA ₂ (HA) ₄ , -6.80	92
Vers 9/benzene	PbA ₂ (HA) ₂	115
Sc, Y, and Lanthanides		
Buta/ <i>i</i> -butanol	ScA ₃ , -8.53	36
Hexa, α -BrHexa/CHCl ₃	ScA ₃ (HA) ₃	138
Deca/benzene	Sc ₆ A ₁₈ , -32.8	154
α, α' -DAC/heptane	LnA ₃ (HA) ₃ ; La, -13.90; Ce, -13.61; Pr, -13.16; Nd, -12.85; Sm, -12.17; Eu, -12.28; Gd, -12.96; Dy, -12.81; Ho, -12.66; Tm, -13.26; Yb, -13.16; Lu, -13.13	20
Hexa/heptane	LnA ₃ (HA) ₃	20
Hexa, α -BrHexa/CHCl ₃	LaA ₃ (HA) ₃	138
Vers/benzene	CeA ₄	117
Me ₂ (OH)Hexa/CHCl ₃	NdA ₃ (HA) ₅ ; Nd ₂ A ₆ (HA) _h ; Nd ₂ A ₆ ; (NdA ₃) _j ($j > 2$)	86
Naph/ <i>n</i> -octane	Nd ₂ A ₆ (HA) ₆ (H ₂ O) _w ($w = 5-6$)	84
St/kerosene	EuA ₃ , -7.58	75
Hexa/MIBK	TmA ₃ HA	129
Hexa/CHCl ₃	TmA ₃ (HA) ₅	129
Actinides		
Deca/benzene	ThA ₄ (HA) ₄	64
Salicylic/MIBK	Th(HA) ₄ ·H ₂ A(H ₂ A, salicylic acid)	49
Methoxybenzoic/MIBK	ThA ₄	49
Hexa/CHCl ₃	UO ₂ A ₂ (HA) ₂	135
Deca/benzene	UO ₂ A ₂ (HA) ₂ (H ₂ O) ₂ , -5.66; UO ₂ A ₂ (HA) ₄ (H ₂ O) ₂ , -5.83	89

TABLE II (continued)

Organic Phase ^a	Extracted Species, log K_{ex}	Reference
Deca/benzene	$UO_2A_2(HA)_2$	64
Vers 9/benzene	UO_2A_2HA	116
Salicylic/MIBK	$UO_2(HA)_2$; $UO_2(HA)_2 \cdot H_2A$	48
Methoxybenzoic/MIBK	UO_2A_2	48
Deca/benzene	$AmA_3(HA)_5$	64
Mn, V, and Fe		
Deca/benzene	$Mn_2A_4(HA)_4$	11
Naph/decane	$MnA_2(HA)_2$, -10.94	39
Deca/benzene	$(VO)_2A_4$, -13.7	93
Octa/(decane, benzene, NB + CCl_4 , CCl_4 , TCB, <i>i</i> -amOAc, (<i>i</i> -Pr) $_2$ CO, <i>i</i> -amOH ^b)	$Fe_3A_9(H_2O)_3$, -14.54, -14.63, -14.77, -15.00, -15.47, -18.74, -19.17,	58, 61
Deca/benzene	Fe_3A_9 , -9.9	143
Co and Ni		
(Hexa, Octa, Deca)/heptane	$CoA_2(HA)_2$, -11.88, -11.44, -11.26; $CoA(OH)(HA)_2 \cdot H_2O$	70
Octa/heptane	$CoA_2(HA)_4$, -12.04; $Co_2A_4(HA)_4$, -20.32	53
Octa/decane	$Co_2A_4(HA)_4(H_2O)_w$	37
Octa/octanol	CoA_2	127
Deca/benzene	$CoA_2(HA)_4$, -11.2, -11.21 ^c ; $Co_2A_4(HA)_4$, -19.7, -19.28 ^c	143
Naph/benzene	$Co_2A_4(HA)_4$	22
Octa/heptane	$Ni_2A_4(HA)_4$, -19.13	53
Octa/decane	$Ni_2A_4(HA)_4(H_2O)_w$	37
Deca/benzene	$NiA_2(HA)_4$, -11.34, -11.27 ^c ; $Ni_2A_4(HA)_4$, -19.15, -19.17 ^c	144
Naph/benzene	$Ni_2A_4(HA)_4$	22
Cu		
Propa/ $CHCl_3$	Cu_2A_4	40
Propa/ $CHCl_3$	$Cu_2A_4(HA)_2$	41
(Buta, Penta, Hexa, Hepta, Octa, Nona, Deca)/benzene	$Cu_2A_4(HA)_2$, -11.50, -11.56, -11.48, -11.58, -11.65, -11.56, -11.58	66
Octa/heptane	$Cu_2A_4(HA)_2$, -12.57	53
Deca/ CCl_4	$Cu_2A_4(HA)_2$, -10.97	10
Deca/benzene	$Cu_2A_4(HA)_2$	147
Deca/(<i>n</i> -Hexn, cy-Hexn, CCl_4 , toluene, benzene, CB, 1,2-DCE)	$Cu_2A_4(HA)_2$, -11.88, -11.67, -11.61, -11.57, -11.36, -11.30, -11.10	156

(continued)

TABLE II (continued)

Organic Phase ^a	Extracted Species, log K_{ex}				Reference
	Cu				
	CuA ₂	CuA ₂ HA	Cu ₂ A ₄	Cu ₂ A ₄ (HA) ₂	
Deca/alcohols					
1-Octanol	-8.41	-8.65	-13.36	-13.77	152
1-Heptanol	-8.26		-13.48	-13.72	151
1-Hexanol	-8.25		-13.73	-13.77	151
1-Pentanol	-8.13		-14.00	-14.03	151
Cyclohexanol	-8.34		-14.45	-14.19	151
Deca/ketones	CuA ₂	CuA ₂ HA	Cu ₂ A ₄	Cu ₂ A ₄ (HA) ₂	153
2-Octanone	-9.74	-9.33	-13.88	-14.22	
5-Methyl-2-Hexanone	-9.70	-9.50	-14.18	-14.44	
MIBK	-9.65	-9.47	-14.34	-14.58	
2-Hexanone	-9.54	-9.40	-14.35	-14.43	
2-Pentanone	-9.36	-9.39	-14.74	-14.74	
3-Pentanone	-9.29	-9.37	-14.70	-14.50	
Pal/benzene	Cu ₂ A ₄ (HA) ₂ , -12.0				42
St/benzene	Cu ₂ A ₄ (HA) ₂				13
α-BrSt/benzene	CuA ₂ (HA) ₂				13
Piva/toluene	Cu ₂ A ₄ (HA) ₂ , -13.2; monomer				43
Vers 10/ <i>n</i> -hexn	Cu ₂ A ₄ (HA) ₂ , -12.96				52
cy-PA/benzene	CuA ₂ (HA) ₂				121
cy-Hexa/benzene	CuA ₂ (HA) ₄ ; Cu ₂ A ₄ (HA) ₄				15
Naph/benzene	Cu ₂ A ₄ (HA) ₂				22
	Zn, Cd, and Hg				
Hexa/CCl ₄	ZnA ₂ ; ZnA ₂ (HA) ₄				88
Vers 9/benzene	ZnA ₂ (HA) ₂				114
Vers 10/benzene	ZnA ₂ (HA) ₄ , -10.82; Zn ₂ A ₄ , -19.29				124
Naph/PE	ZnA ₂ HA·H ₂ O, -10.72				132
Naph/PE	CdA ₂ (HA) ₂ , -9.29				132
Hexa/CHCl ₃	HgA ₂ (HA) ₂				133
Naph/PE	Hg ₂ A ₄ (HA) ₄ , 0.76				132

^a Propa, Propanoic acid; Buta, butanoic acid; Penta, pentanoic acid; Hexa, hexanoic acid; Hepta, heptanoic acid; Octa, octanoic acid; Nona, nonanoic acid; Deca, decanoic acid; Pal, palmitic acid; St, stearic acid; Piva, trimethylacetic acid; Vers, Versatic acid; α -BrHexa, α -bromohexanoic acid; α -BrSt, α -bromostearic acid; Me₂(OH)Hexa, 2,5-dimethyl-2-hydroxyhexanoic acid; α,α' -DAC, α,α' -dialkylcarboxylic acid; Naph, naphth- enic acid; cy-PA, cyclopentylacetic acid; cy-Hexa, cyclohexanecarboxylic acid; C₇-C₉ mix, C₇-C₉ mixture; CB, chlorobenzene; cy-Hexn, cyclohexane; 1,2-DCE, 1,2-dichloro- ethane; (*i*-Pr)₂CO, diisopropyl ketone; *i*-amOAc, isoamyl acetate; *i*-amOH, isoamyl alcohol; MIBK, 4-methyl-2-pentanone; NB, nitrobenzene; *n*-Hexn, *n*-hexane; PE, petro- leum ether; TCB, 1,2,4-trichlorobenzene.

^b Depolymerized.

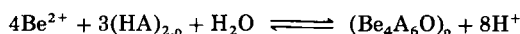
^c Values from ref. 90.

2. Alkaline Earth Metals

According to Mikhailichenko and co-workers (81), the extraction constant decreases with increasing hydration of the extracted species: $\text{Ba}^{2+} > \text{Sr}^{2+} > \text{Ca}^{2+} > \text{Mg}^{2+}$. They (82) have also found the extracted species $\text{SrA}_2(\text{HA})_4(\text{H}_2\text{O})_4$ in octane. The coordination number of 10 for strontium is quite unlikely. The increase in the length of the carbon chain causes only a slight increase of the extraction constant.

Alekperov *et al.* (5) suggested the polymerization of Sr(II) naphthenate in kerosene from the fact that the extraction curve ($\log D$ vs. pH) was shifted to the lower pH region with increasing initial concentration of strontium.

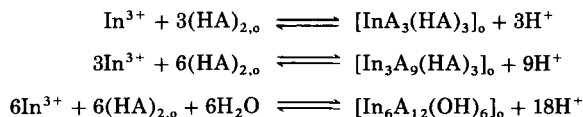
Kodama *et al.* (63) found that Eq. (14) was relevant to the extraction of beryllium(II) with decanoic acid in benzene. The Karl-Fischer titration revealed one water per four Be, and these authors proposed the following extraction equilibrium:



Beryllium is unique among the metal ions so far studied in that it is extracted as a tetrameric carboxylate, whose structure was thought to be similar to the tetrameric beryllium acetate. In the latter, four beryllium atoms are bridged by one oxo and six acetates (148).

3. Aluminum, Gallium, Indium, and Thallium

These metal ions are known to form up to hexameric decanoate in noncoordinating solvents such as toluene and benzene (145, 146, 150, 155). In the indium extraction, the three species, i.e., monomer, trimer, and hexamer, all having a definite composition, are in equilibrium with each other in the organic phase (145):



Schweitzer and Anderson (125), working at a very low metal concentration, found the monomeric indium species $\text{InA}_3(\text{HA})_3$ in the extraction with hexanoic acid in chloroform. This composition is in accord with that found in the decanoate extraction (145).

Because of its strong hydrolytic tendency, the extraction behavior of Tl(III) has not been studied, while Tl(I) was reported to be extracted as monomers of different composition in different organic solvents (130).

4. Germanium, Tin, and Lead

Andrianov and Poladyan (7) extracted germanium with octanoic acid in the presence of iron(III).

Mikami and Takei (80) extracted tripropyltin(IV) with acetic, monochloroacetic, dichloroacetic, and formic acids in carbon tetrachloride. The partition constant of the extracted species, Pr_3SnA (Pr = propyl; $\text{A} = \text{CH}_3\text{COO}^-$, $\text{CH}_2\text{ClCOO}^-$, and $\text{CHCl}_2\text{COO}^-$), increased with increasing chlorine substitution of acetic acid.

Two extracted species, $\text{PbA}_2(\text{HA})_2$ and $\text{PbA}_2(\text{HA})_4$, have been found in the extraction of lead with decanoic acid in benzene (92).

5. Scandium, Yttrium, and Lanthanides

A series of investigations (32–35, 101) on the extraction of these elements with carboxylic acids has been carried out by workers in the Soviet Union. Miller and associates (86) extracted lanthanides with 2,5-dimethyl-2-hydroxyhexanoic acid in chloroform. The heavy lanthanides after samarium were not extracted. In the extraction of neodymium the extracted species such as $\text{NdA}_3(\text{HA})_5$ and $\text{Nd}_2\text{A}_6(\text{HA})_8$ were found together with small amounts of Nd_2A_6 and still smaller amounts of further aggregates (NdA_3)_{*j*} (86).

Danilov and co-workers (20) studied the extraction of lanthanides with α, α' -dialkylcarboxylic and hexanoic acids in *n*-heptane. The extracted species is invariably $\text{LnA}_3(\text{HA})_3$. As is obvious from Table II, the "gadolinium break" is observed in the extraction constants.

The hexameric scandium decanoate extracted in benzene is different from the hexameric Al(III) , Ga(III) , and In(III) decanoates in that the former is neither hydrated nor hydrolyzed (154). Galkina and Strel'tsova (36), in the butanoic acid/*iso*-butanol system, attempted to separate Sc from rare earths and the other metals. They proposed the monomeric Sc(III) butanoate, ScA_3 , as the extracted species. In this extraction system, the polymerization of scandium butanoate in the organic phase seems to be prevented by solvation with *iso*-butanol. In the study of the synergistic effect of various amines on the extraction of lanthanum and scandium with hexanoic and α -bromohexanoic acids in chloroform, Sukhan *et al.* (138) proposed $\text{LaA}_3(\text{HA})_3$ and $\text{ScA}_3(\text{HA})_3$ as the extracted species.

6. Actinides

The extractability of 20 different metal ions with a series of aliphatic carboxylic acids (from pentanoic to decanoic acids) in chloroform was

examined by Pietsch and Sinic (99). In this work, the maximum extractability of thorium was obtained with hexanoic acid and that of uranium with nonanoic acid. Pietsch (97) also described the extraction of thorium with hexanoic acid in chloroform together with lead and iron. The extraction of thorium butanoate by chloroform is useful for the separation of thorium from the following metals: Ca, Mg, Ba, Pb, Zn, Cd, Be, Ni, and Co (98).

Hök-Bernström carried out the extraction of UO_2^{2+} with salicylic(H_2A) and methoxybenzoic(HA) acids in 4-methyl-2-pentanone. She proposed the extracted species $\text{UO}_2(\text{HA})_2$ and $\text{UO}_2(\text{HA})_2 \cdot \text{H}_2\text{A}$ for salicylic acid and UO_2A_2 for methoxybenzoic acid (48). In a subsequent study (49) on the extraction of thorium (IV) with salicylic, methoxybenzoic, and cinnamic acids in 4-methyl-2-pentanone, thorium was extracted as $\text{Th}(\text{HA})_4 \cdot \text{H}_2\text{A}$ by salicylic acid and ThA_4 by methoxybenzoic acid. Koehly *et al.* (64) found that, in decanoic acid-benzene systems, americium(III), thorium(IV), and uranium(VI) were extracted as $\text{AmA}_3(\text{HA})_5$, $\text{ThA}_4(\text{HA})_4$, and $\text{UO}_2\text{A}_2(\text{HA})_2$, respectively. According to a study on the extraction of uranium(VI) with decanoic acid in benzene, uranium was extracted as $\text{UO}_2\text{A}_2(\text{HA})_2(\text{H}_2\text{O})_2$ and $\text{UO}_2\text{A}_2(\text{HA})_4(\text{H}_2\text{O})_2$ (89). Later, Sukhan and co-workers (135) showed that $\text{UO}_2\text{A}_2(\text{HA})_2$ was responsible for the extraction of uranium (VI) with hexanoic acid in chloroform.

7. Transition Metals

Kyrš tried to separate Zr from Nb by the extraction with aliphatic carboxylic acids (from C_7 to C_9) in benzene (72), and proposed $\text{Zr}(\text{OH})_3\text{A}$ (73), which does not appear to be extractable.

Nakasuka *et al.* (93) found the dimeric species $(\text{VO})_2\text{A}_4$ in the extraction of vanadium(IV) with decanoic acid in benzene.

In the extraction of Mn(II) from ammonium chloride solution with decanoic acid benzene, Bartecki *et al.* (11) reported that the prevailing species in the organic phase was a dimeric complex, $\text{Mn}_2\text{A}_4(\text{HA})_4$, in addition to a small amount of tri- and tetramers. The monomeric extracted species $\text{MnA}_2(\text{HA})_2$, found in decane (39), seems unlikely.

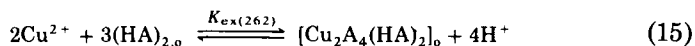
a. Iron. Trimeric iron(III) decanoate Fe_3A_9 was found in the extraction of iron with decanoic acid in benzene (143). A composition such as $\text{Fe}_3(\text{OH})_h\text{A}_{9-h}$ or $\text{Fe}_3\text{A}_9\text{O}$ cannot be excluded. In the extraction of iron (III) by octanoic acid in decane, Khol'kin *et al.* (57) described a hydrated trimer, $\text{Fe}_3\text{A}_9(\text{H}_2\text{O})_3$, as an extracted species.

Monomeric(17, 24) and dimeric(159) iron(III) carboxylates are not realistic in nonpolar solvents.

b. Cobalt and Nickel. These two metal ions behave very similarly in the extraction with carboxylic acids. A monomer $MA_2(HA)_4$ and a dimer $M_2A_4(HA)_4$ are in equilibrium in nonpolar solvents, while in coordinating solvents such as octanol, a monomer, MA_2 , prevails (see Table II). The monomeric extracted species $CoA_2(HA)_2$ and $CoA(OH)(HA)_2 \cdot H_2O$ (70) seem unlikely.

c. Copper. Copper(II) is extracted as a dimer $Cu_2A_4(HA)_2$ in nonpolar solvents (10, 22, 41–43, 51–53, 66, 147, 156). The stability of the dimer is so high that no appreciable amount of monomer can be detected in most nonpolar solvents. However, with some sterically crowded carboxylic acids such as trimethylacetic acid (43), α -bromostearic acid (13), cyclohexanecarboxylic acid (15), and cyclopentylacetic acid (121), a monomeric species is found together with the dimer. Because of the extensive solvation by alcohols and ketones, monomeric and dimeric species are in equilibrium in these solvents (151, 153).

The extraction of copper(II) by various aliphatic carboxylic acids (from butanoic to decanoic acids) in benzene is written as



The extraction constant is formulated as

$$\log K_{ex(262)} = \beta_{26} K_{D,Cu_2A_4(HA)_2} K_{D,(HA)_2}^{-3}, \quad (16)$$

where β_{26} denotes the overall formation constant of $Cu_2A_4(HA)_2$ in the aqueous phase, i.e.,

$$\beta_{26} = [Cu_2A_4(HA)_2][H^+]^4[Cu^{2+}]^{-2}[(HA)_2]^{-3},$$

and $K_{D,Cu_2A_4(HA)_2}$ and $K_{D,(HA)_2}$ denote the partition constants of the dimeric copper decanoate and the dimeric carboxylic acid. Kojima *et al.* (66) found that the extraction constants for $Cu_2A_4(HA)_2$ fell in the region from -11.5 to -11.6 , irrespective of the number of carbon atoms in the carboxylic acid (see Table II).

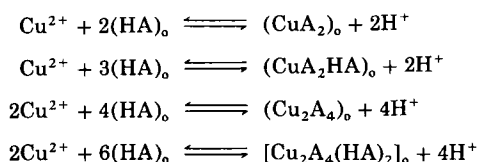
From the additive nature of the molar cohesive energy and molar volume of the ligand in a complex, it has been shown that the \log (partition constant) of a complex MA_n is approximately n times that of the ligand HA (141) [cf. Eqs. (17) and (18)]. Then from Eq. (16) we see that $K_{ex(262)} \simeq \beta_{26}$. Since pK_a is almost the same for these aliphatic carboxylic acids, one may realize that β_{26} and hence $\log K_{ex(262)}$ should

not differ much for aliphatic carboxylic acids with different numbers of carbon atoms. A finer picture of the subject will be drawn below in Eq. (21).

The extraction constant was found to remain constant also for the extraction of cobalt (70) and strontium (82) by different carboxylic acids.

Inoue *et al.* (51) studied the extraction kinetics of copper(II) versatate and the interfacial adsorption equilibrium of Versatic 10.

In the extraction of copper(II) with decanoic acid in 1-octanol, Yamada *et al.* (152) noted that the monomeric and dimeric Cu(II) decanoates were responsible for the extraction:



Further in the extraction of copper(II) decanoates by various alcohols (151) and ketones (153), Yamada *et al.* revealed that the monomeric Cu(II) decanoate was extracted together with the dimeric ones. We will come back to this subject later.

Bold and Bălușescu (13) found the monomeric copper(II) α -bromostearate $\text{CuA}_2(\text{HA})_2$ in the extraction of Cu(II) with α -bromostearic acid in benzene. The bromine in the α -position was said to prevent sterically the formation of dimeric copper(II) species. α -Bromocarboxylic acid, being stronger than the nonsubstituted homologues, is anticipated to form a less stable copper carboxylate dimer.

The selective extraction of copper(II) with phenylacetic acid and its derivatives has been described by Adam and co-workers (2-4).

d. Zinc, Cadmium, and Mercury. Zinc(II) is extracted as monomers involving different numbers of free carboxylic acid units $[\text{ZnA}_2(\text{HA})_h]$, with $h = 0, 1, 2, 4$] in different nonpolar solvents (88, 114, 124, 132). In the presence of sodium, a mixed-metal complex $\text{ZnNaA}_3(\text{HA})_5$ is extracted with decanoic acid in benzene (91). Also, in the extraction of cadmium, $\text{CdNaA}_3(\text{HA})_5$ and $\text{CdNaA}_3(\text{HA})_7$ were found in addition to $\text{CdA}_2(\text{HA})_4$.

In the naphthenic acid (mixture of cyclopentylalkylcarboxylic acids)-petroleum ether systems, Singh *et al.* (132) found the extracted species of Zn(II), Cd(II), and Hg(II) to be $\text{ZnA}_2\text{HA} \cdot \text{H}_2\text{O}$, $\text{CdA}_2(\text{HA})_2$, and $\text{Hg}_2\text{A}_4(\text{HA})_4$, respectively, and the extraction constant to decrease in the order $\text{Hg} > \text{Cd} > \text{Zn}$. They also extracted $\text{HgA}_2(\text{HA})_2$ with hexanoic acid in chloroform (133).

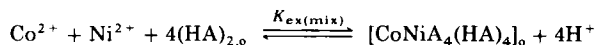
C. COEXTRACTION

Ruthenium(III) butanoate and naphthenate are well extracted when copper (149) or iron (76) is present but not at all in their absence. For Cr(III), Nb(V), Sr(II), Ce(III), and Y(III) naphthenates, the higher extractability was observed in the presence of iron (60, 76). Alekperov and Makov (6) noted that the coextraction of Ru with Fe(III), Co(II), and Cu(II) naphthenates increased in the order $\text{Cu} < \text{Co} < \text{Fe}$.

In the decanoic acid–benzene system, Nakasuka *et al.* (91) found the coextraction of sodium ion with zinc(II) and cadmium(II) as the following mixed-metal decanoates: $\text{ZnNaA}_3(\text{HA})_5$ and $\text{CdNaA}_3(\text{HA})_a$ ($a = 5, 7$). Lead was also reported to be extracted with sodium ion [as $\text{Na}_2\text{PbA}_4(\text{HA})_8$] (95), as was cobalt (131).

Pyatnitskii and associates (104) found the coextraction of iron(III) in the extraction of copper(II) from tartaric acid solutions with hexanoic acid in chloroform containing pyridine. The coextraction was claimed to be due to the formation of an ion associate $\text{Cu}(\text{Py})_x\text{AFeT}$ (Py, pyridine; T, tartarate; and A, hexanoate).

Nakasuka *et al.* (90) found the following extraction equilibrium for the extraction of cobalt by decanoic acid in benzene in the presence of nickel:



with $\log K_{\text{ex(mix)}} = -19.1$.

Since the coextraction is not unusual, particularly in the extraction of polymerized metal carboxylates, much attention should be paid to the formation of mixed-metal carboxylates in the separation of metal ions.

D. SYNERGISTIC EXTRACTION OF METAL CARBOXYLATES

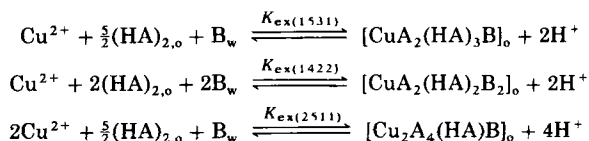
A number of investigations on the synergistic effect of a second extractant, such as amines and oximes, on the extraction of metal carboxylates have been carried out. The utilized synergists include 8-hydroxyquinoline-2-aldoxime for Zr(IV) and Hf(IV) (122, 123), various amines (25), Lix 63 (27) and nonylphenol (28) for Cu(II), dialkylphosphoric acids for Hf(IV) (44), rhodamine B for Be(II) (102), trioctylphosphine oxide for U(VI) (69, 77), *p*-alkylphenol for Cs(I) (1), collidine for Zr(IV) and Sc(III) (62), and nonchelating oximes for Ni(II) and Co(II) (103). Mareva *et al.* (77) have successfully utilized a salicylic acid–trioctylphosphine oxide mixture for the separation of uranium from rare earths, thorium, zirconium, and iron.

Studies on the stoichiometry of mixed-ligand carboxylate complexes involved in synergistic extraction systems include $\text{Sn}(\text{Ox})_2\text{A}_2$ (HA, trichloroacetic acid; HOx, 8-quinolinol) by Petrukhin *et al.* (96); ZnA_2Q and ZnA_2Q_2 (HA, butanoic, pentanoic, and hexanoic acids; Q, quinoline) in carbon tetrachloride by Moriya and Sekine (88); $\text{CoX}_2\text{A}_2\text{H}_2$ (HA, Versatic 911; HX, Kelex 100) in kerosene by Lakshmanan and Lawson (74); VOA_2B_3 (HA, trichloroacetic acid; B, neutral oxygen and nitrogen donors) by Rao and Sarma (113); $\text{UO}_2\text{ClO}_4(\text{TOPO})_2$ (HA, benzoic acid; TOPO, trioctylphosphine oxide) in carbon tetrachloride by Konstantinova (68); and $\text{UO}_2\text{A}_2\text{B}_2$ (HA, hexanoic acid; B, pyridine, 2-aminopyridine, benzylamine or 1,10-phenanthroline) in chloroform by Sukhan and co-workers (135).

Pyatnitskii and associates have extensively studied the synergistic extraction of metal ions with various carboxylic acids (HA) and amines (B) in chloroform. According to their results, iron(II) is extracted as FeA_2B_2 (112); iron(III) as FeA_3B_b ($b = 1, 2, 3$) (109, 110, 139); cobalt(II) and nickel(II) as MA_2B_b ($b = 2, 3$) (106, 107, 109, 136, 137); copper(II) as CuA_2B_b ($b = 1, 2$) (105, 107, 108, 111, 136).

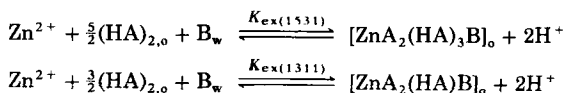
Hirose and co-workers extracted copper(II) (45) and zinc(II) (46) with decanoic acid in benzene in the presence of pyridine (B). They found the following equilibria.

For copper:



with the extraction constants $\log K_{\text{ex}(1531)} = -4.31$, $\log K_{\text{ex}(1422)} = -0.61$, and $\log K_{\text{ex}(2511)} = -7.88$.

For zinc:



with the extraction constants $\log K_{\text{ex}(1531)} = -6.09$ and $\log K_{\text{ex}(1311)} = -7.02$.

The synergistic effect of pyridine is larger for zinc than for copper. This will stem from the high stability of dimeric copper carboxylate in the organic phase.

E. SOLVENT EFFECT ON THE EXTRACTION OF METAL CARBOXYLATES

Plaksin *et al.* (101) found that $\text{pH}_{1/2}$ values for the extraction of lanthanides with aliphatic carboxylic acids ($\text{C}_7\text{--C}_9$) decreased in the order heptanol > decanol > isoamyl acetate > *m*-xylene > dichlorodiethyl ether > carbon tetrachloride > kerosene.

Schweitzer and associates investigated the extraction of metal hexanoates and found $\text{TIA}(\text{HA})_3$ in benzene and chloroform, $\text{TIA}(\text{HA})_2$ in 4-methyl-2-pentanone, and $\text{TIA}(\text{HA})_4$ in nitrobenzene (130); $\text{TmA}_3(\text{HA})_5$ in chloroform and TmA_3HA in 4-methyl-2-pentanone (129); and ZnA_2HA in all studied solvents (126). This latter composition seems unlikely since the normal coordination number of zinc is 4 or 6.

In the extraction systems with octanoic acid, Gindin *et al.* (38) revealed that the formation of dimeric cobalt(II) and nickel(II) octanoates tended to decrease with increasing dielectric constant of the organic solvent: decane > benzene > α -chloronaphthalene > chloroform > nitrobenzene > 3-methyl-1-butanol. Because 3-methyl-1-butanol is a solvating solvent, no dimerization of Co(II) and Ni(II) octanoates was observed in this solvent.

Brzózka and Rózycki (16) stated that $\text{pH}_{1/2}$ for copper(II) cyclohexanecarboxylate and the concentration of the monomeric copper(II) species in the organic phase increased in the order carbon tetrachloride < benzene < 3-methyl-1-butanol. Yamada *et al.* found that the less polar the solvent, the more polymerized is the extracted species of gallium(III) decanoate (150) (see Table II).

In most inert solvents the extraction equilibrium of copper(II) is given by Eq. (15), with the extraction constant formulated as Eq. (16).

The molar volume and the solubility parameter of the dimeric copper decanoate are given (141) as

$$V_{\text{Cu}_2\text{A}_4(\text{HA})_2} = 3 \times 0.9 V_{(\text{HA})_2}, \quad (17)$$

$$\delta_{\text{Cu}_2\text{A}_4(\text{HA})_2} = 1/0.9^{1/2} \delta_{(\text{HA})_2}. \quad (18)$$

The partition constant of a solute B in terms of molar concentration is given by

$$\log K_{\text{D,B}} = 0.43 V_{\text{B}} (\delta_{\text{w}} - \delta_{\text{o}}) (\delta_{\text{w}} + \delta_{\text{o}}' - 2\delta_{\text{B}}) / RT, \quad (19)$$

where

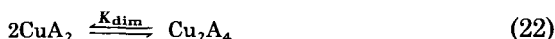
$$\delta_{\text{o}}' = \delta_{\text{o}} + \frac{RT}{\delta_{\text{w}} - \delta_{\text{o}}} \left(\frac{1}{V_{\text{o}}} - \frac{1}{V_{\text{w}}} \right), \quad (20)$$

and V_B , V_o , V_w , δ_B , δ_o , and δ_w denote the molar volumes and the solubility parameters for the solute B, the organic solvent, and water, respectively. Combining Eqs. (16)–(20), we obtain

$$\log K_{\text{ex}(262)} = \frac{-0.13 V_{(\text{HA})_2}(\delta_w - \delta_o)(\delta_w + \delta'_o - 1.03\delta_{(\text{HA})_2})}{RT} + \log \beta_{26} \quad (21)$$

As predicted from Eq. (21), $\log K_{\text{ex}(262)}$ is indeed linearly related with $(\delta_w - \delta_o)(\delta_w + \delta'_o - 1.03\delta_{(\text{HA})_2})$ with the theoretical slope of $-0.13 V_{(\text{HA})_2}/RT$. Equation (21) describes the solvent effect on the copper decanoate extraction very nicely (156).

The influence of solvent on the extraction of copper(II) with decanoic acid in some alcohols (151) and ketones (153) was studied by Yamada and associates who found that in these solvents both the monomeric and dimeric Cu(II) decanoates were responsible for the extraction. In this case the dimerization of copper carboxylate was formulated as in Eq. (22):



This is an important factor in the solvent extraction. Yamada *et al.* attempted to understand the solvent effect on the above reaction in the following manner.

According to the regular solution theory, the dimerization constant of copper(II) decanoate, K_{dim} , described above can be written as follows (142, 151):

$$\log K_{\text{dim}} - \log V_o = 0.43n V_o(\delta_o - \delta')^2/RT + \log K_{\text{dim}}^\circ - 3.$$

Here δ' refers to the solubility parameter of copper(II) decanoate; K_{dim}° denotes the dimerization constant of Cu(II) decanoate in an ideal solution; and n represents the number of solvent molecules set free in the dimerization of Cu(II) decanoate, that is, $n V_o = 2V_{\text{CuA}_2} - V_{\text{Cu}_2\text{A}_4}$, where V_{CuA_2} and $V_{\text{Cu}_2\text{A}_4}$ indicate the molar volume of the solvated monomeric and dimeric Cu(II) decanoates. CuA_2 and Cu_2A_4 are assumed to have the same solubility parameter (141), and δ' was found to be $24.1 \text{ (J}^{1/2} \text{ cm}^{-3/2})$ (151). The plot of $(\log K_{\text{dim}} - \log V_o)$ against $0.43 V_o(\delta_o - \delta')^2/RT$ was remarkably linear (151, 153). From this plot the values of n and $\log K_{\text{dim}}^\circ$ were found to be 4.5 and 3.14 for alcohols, and 2.8 and 3.19 for ketones by the least-squares method. From these results they concluded that, because of extensive solvation, the monomeric copper(II) decanoate is more stabilized in alcohols than in ketones.

IV. Concluding Remarks

Despite a considerable effort during the last two decades, relatively slow progress has been made in physicochemical aspects of the metal carboxylate extraction. The stoichiometry proposed for the extracted species still appears quite unlikely in some cases.

In the extraction of metal ions with carboxylic acids, it is not unusual to find polymerized species with carboxylates, hydroxo, and/or oxo groups acting as bridging ligands. In this connection, one is strongly recommended to utilize, instead of the conventional $\log D$ plot, the plot of logarithmic total metal concentration in the organic phase against $(\log[M^{n+}] - n \log[H^+])$ in order to find the correct composition of the extracted species.

The formation of heteropolynuclear carboxylates is a common phenomenon, which must be taken into account particularly in the separation of metal ions.

It is encouraging to see that regular solution theory has been utilized with success in understanding the effect of solvent and extractant on the metal carboxylate extraction.

To conclude, it may be said at present that problems of fundamental importance still await careful study from different points of view.

REFERENCES

1. Abisheva, Z. S., Plyushchev, V. E., and Reznik, A. M., *Zh. Neorg. Khim.* **19**, 2843 (1974).
2. Adam, J., and Přibil, R., *Talanta* **19**, 1105 (1972).
3. Adam, J., and Přibil, R., *Talanta* **21**, 113 (1974).
4. Adam, J., Přibil, R., and Veselý, V., *Talanta* **19**, 825 (1972).
5. Alekperov, R. A., Geibatova, S. S., and Makov, N. N., *Zh. Neorg. Khim.* **14**, 542 (1969).
6. Alekperov, R. A., and Makov, N. N., *Zh. Anal. Khim.* **23**, 460 (1968).
7. Andrianov, A. M., and Poladyan, V. E., *Zh. Anal. Khim.* **31**, 2391 (1976).
8. Ashbrook, A. W., *Miner. Sci. Eng.* **3**, 169 (1973).
9. Banerjee, S., Sundaram, A. K., and Sharma, H. D., *Anal. Chim. Acta* **10**, 256 (1954).
10. Bartecki, A., and Apostoluk, W., *J. Inorg. Nucl. Chem.* **40**, 109 (1978).
11. Bartecki, A., Apostoluk, W., and Mager, J., *J. Inorg. Nucl. Chem.* **41**, 1461 (1979).
12. Biffen, F. M., and Snell, F. D., *Ind. Eng. Chem. Anal. Ed.* **6**, 169 (1934).
13. Bold, A., and Bălușescu, L., *Rev. Roum. Chim.* **23**, 1631 (1978).
14. Brzózka, Z., and Rózycki, C., *Chem. Anal. (Warsaw)* **25**, 3 (1980).
15. Brzózka, Z., and Rózycki, C., *Chem. Anal. (Warsaw)* **28**, 585 (1983).
16. Brzózka, Z., and Rózycki, C., *Chem. Anal. (Warsaw)* **28**, 757 (1983).
17. Cattrall, R. W., and Walsh, M. J., *J. Inorg. Nucl. Chem.* **36**, 1643 (1974).
18. Christian, S. D., Johnson, J. R., Affsprung, H. E., and Kilpatrick, P. J., *J. Phys. Chem.* **70**, 3376 (1966).

19. Christian, S. D., Johnson, J. R., Affsprung, H. E., and Kilpatrick, P. J., *J. Phys. Chem.* **72**, 3223 (1968).
20. Danilov, N. A., Korpusov, G. V., Kr'lov, Yu. S., Puzitskii, K. V., and Eidus, Ya. T., *Zh. Neorg. Khim.* **19**, 194 (1974).
21. Davis, S. S., *Sep. Sci.* **10**, 1 (1975).
22. Fletcher, A. W., and Flett, D. S., *J. Appl. Chem.* **14**, 250 (1964).
23. Fletcher, A. W., and Flett, D. S., "Solvent Extraction Chemistry of Metals" (H. A. C. McKay *et al.*, eds.), p. 359. MacMillan, New York, 1966.
24. Fletcher, A. W., Flett, D. S., and Wilson, J. C., *Bull. Inst. Min. Metall.* **73**, 765 (1964).
25. Flett, D. S., *Trans. Natl. Res. Inst. Met. Jpn.* **9**, 215 (1967).
26. Flett, D. S., and Jaycock, M. J., in "Ion Exchange and Solvent Extraction" (J. Marinsky and Y. Marcus, eds.), Vol. 3, p. 1. Dekker, New York, 1973.
27. Flett, D. S., and Titmuss, S., *J. Inorg. Nucl. Chem.* **31**, 2612 (1969).
28. Flett, D. S., and West, D. W., *J. Inorg. Nucl. Chem.* **29**, 1365 (1967).
29. Fujii, Y., Sobue, K., and Tanaka, M., *J. Chem. Soc., Faraday Trans. 1* **74**, 1467 (1978).
30. Fujii, Y., and Tanaka, M., *J. Chem. Soc., Faraday Trans. 1* **73**, 788 (1977).
31. Fujii, Y., and Tanaka, M., *Bull. Chem. Soc. Jpn.* **54**, 3696 (1981).
32. Galkina, L. L., *Radiokhimiya* **8**, 358 (1966).
33. Galkina, L. L., *Radiokhimiya* **9**, 116 (1967).
34. Galkina, L. L., and Glazunova, L. A., *Zh. Anal. Khim.* **21**, 1058 (1966).
35. Galkina, L. L., and Sosnovskaya, E. Yu., *Zh. Anal. Khim.* **24**, 938 (1969).
36. Galkina, L. L., and Strel'tsova, S. A., *Zh. Anal. Khim.* **25**, 889 (1970).
37. Gindin, L. M., and Khol'kin, A. I., *Izv. Sib. Otd. Akad. Nauk SSSR, Ser. Khim. Nauk* **1966**, 23 (1966).
38. Gindin, L. M., Savkina, L. Ya., Khol'kin, A. I., and Grankina, Z. A., *Izv. Sib. Otd. Akad. Nauk SSSR Ser. Khim. Nauk* **1971**, 73 (1971).
39. Gorbanev, A. I., Tsvetkova, Z. N., Sobol', N. L., and Kalm'kova, R. V., *Izv. Akad. Nauk SSSR, Met.*, **1975**, 47 (1975).
40. Graddon, D. P., *J. Inorg. Nucl. Chem.* **11**, 337 (1959).
41. Graddon, D. P., *Nature (London)* **186**, 715 (1960).
42. Grzegorzka, E., Chodowska, Z., and Maciejko, G., *Chem. Anal. (Warsaw)* **24**, 1019 (1979).
43. Haffenden, W. J., and Lawson, G. J., *J. Inorg. Nucl. Chem.* **29**, 1133 (1967).
44. Håla, J., and Sotulářová, L., *J. Inorg. Nucl. Chem.* **31**, 2247 (1969).
45. Hirose, K., Matsumoto, N., and Tanaka, M., *J. Inorg. Nucl. Chem.* **39**, 2261 (1977).
46. Hirose, K., and Tanaka, M., *J. Inorg. Nucl. Chem.* **40**, 1153 (1978).
47. Högfeldt, E., *Abstr. Semin. Meet. Int. Soc. Study Solute/Solute/Solvent Interact. Sept. 1972 Marseille*.
48. Hök-Bernström, B., *Acta Chem. Scand.* **10**, 163 (1956).
49. Hök-Bernström, B., *Acta Chem. Scand.* **10**, 174 (1956).
50. Hök-Bernström, B., *Sven. Kem. Tidskr.* **68**, 34 (1956).
51. Inoue, K., Amano, H., and Nakamori, I., *Hydrometallurgy* **8**, 309 (1982).
52. Inoue, K., Amano, H., Yayama, Y., and Nakamori, I., *J. Chem. Eng. Jpn.* **13**, 281 (1980).
53. Jaycock, M. J., Jones, A. D., and Robinson, C., *J. Inorg. Nucl. Chem.* **36**, 887 (1974).
54. Johnson, S. E. J., Unpublished work (1942), cited by E. B. Sandell, in "Colorimetric Determination of Traces of Metals," p. 801. Wiley (Interscience), New York, 1959.
55. Khol'kin, A. I., and Gindin, L. M., *Izv. Sib. Otd. Akad. Nauk SSSR, Ser. Khim. Nauk* **1969**, 63 (1969).
56. Khol'kin, A. I., and Gindin, L. M., *Izv. Sib. Otd. Akad. Nauk SSSR, Ser. Khim. Nauk* **1969**, 70 (1969).

57. Khol'kin, A. I., Gindin, L. M., Luboshnikova, K. S., Mühl, P., and Gloe, K., *Izv. Sib. Otd. Akad. Nauk SSSR, Ser. Khim. Nauk* **1976**, 82 (1976).
58. Khol'kin, A. I., Gindin, L. M., Luboshnikova, K. S., Mühl, P., and Gloe, K., *J. Radioanal. Chem.* **30**, 383 (1976).
59. Khol'kin, A. I., Gindin, L. M., Savkina, L. Ya., and Fleitlikh, I. Yu., *Izv. Sib. Otd. Akad. Nauk SSSR, Ser. Khim. Nauk* **1972**, 76 (1972).
60. Khol'kin, A. I., Gloe, K., Luboshnikova, K. S., Mühl, P., Gindin, L. M., and Fedyuk, N. V., *Izv. Sib. Otd. Akad. Nauk SSSR, Ser. Khim. Nauk* **1984**, 75 (1984).
61. Khol'kin, A. I., Gloe, K., Mühl, P., Luboshnikova, K. S., and Gindin, L. M., *Izv. Sib. Otd. Akad. Nauk SSSR, Ser. Khim. Nauk* **1980**, 67 (1980).
62. Kochetkova, S. K., Fadeeva, V. I., and Kalistratova, V. P., *Zh. Anal. Khim.* **31**, 44 (1976).
63. Kodama, N., Yamada, H., and Tanaka, M., *J. Inorg. Nucl. Chem.* **38**, 2063 (1976).
64. Koehly, G., Madic, C., and Berger, R., *Solvent Extr. Proc. Int. Solvent Extr. Conf.*, **1971**, p. 768 (1971).
65. Kojima, I., Kako, M., and Tanaka, M., *J. Inorg. Nucl. Chem.* **32**, 1651 (1970).
66. Kojima, I., Uchida, M., and Tanaka, M., *J. Inorg. Nucl. Chem.* **32**, 1333 (1970).
67. Kojima, I., Yoshida, M., and Tanaka, M., *J. Inorg. Nucl. Chem.* **32**, 987 (1970).
68. Konstantinova, M., *Anal. Chim. Acta* **90**, 185 (1977).
69. Konstantinova, M., Mareva, St., and Jordanov, N., *Anal. Chim. Acta* **68**, 237 (1974).
70. Kopach, S., Shantulya, Ya., Kalem'kevich, Ya., and Pardelya, T., *Zh. Neorg. Khim.* **26**, 1625 (1981).
71. Kuča, L., and Högfeltdt, E., *Acta Chem. Scand.* **21**, 1017 (1967).
72. Kyrš, M., *Radiochim. Acta* **2**, 202 (1964).
73. Kyrš, M., Jedináková, V., and Caletka, R., *Collect. Czech. Chem. Commun.* **30**, 2179 (1965).
74. Lakshmanan, V. I., and Lawson, G. J., *J. Inorg. Nucl. Chem.* **35**, 4285 (1973).
75. Lobanov, F. I., Glad'shev, V. N., Nurtaeva, A. K., and Andreeva, N. N., *Zh. Neorg. Khim.* **26**, 209 (1981).
76. Makov, N. N., Alekperov, R. A., and Efendiev, G. Kh., *Dokl. Akad. Nauk Az. SSR* **21**, 22 (1965).
77. Mareva, St., Jordanov, N., and Konstantinova, M., *Anal. Chim. Acta* **59**, 319 (1972).
- 78a. Martin, E. P., and Pink, R. C., *J. Chem. Soc.*, p. 1750 (1948).
- 78b. Martinov, "Extraction of Organic Acids and Their Salts" (in Russ.). Atomizdat, Moscow, 1978.
79. McDowell, W. J., and Harmon, H. D., *J. Inorg. Nucl. Chem.* **31**, 1473 (1969).
80. Mikami, T., and Takei, S., *J. Inorg. Nucl. Chem.* **33**, 4283 (1971).
81. Mikhailichenko, A. I., Klimenko, M. A., and Bulgakova, V. B., *Zh. Neorg. Khim.* **17**, 765 (1972).
82. Mikhailichenko, A. I., Klimenko, M. A., and Fedulova, T. V., *Zh. Neorg. Khim.* **19**, 3344 (1974).
83. Mikhailichenko, A. I., and Rozen, A. M., *Zh. Neorg. Khim.* **12**, 1628 (1967).
84. Mikhlin, E. B., Mikhailichenko, A. I., Berengard, I. B., and Klimenko, M. A., *Zh. Neorg. Khim.* **17**, 492 (1972).
85. Miller, F., *Talanta* **21**, 685 (1974).
86. Miller, J. H., Powell, J. E., and Burkholder, H. R., *J. Inorg. Nucl. Chem.* **40**, 1575 (1978).
87. Mills, G. F., and Whetsel, H. B., *J. Am. Chem. Soc.* **77**, 4690 (1955).
88. Moriya, H., and Sekine, T., *Bull. Chem. Soc. Jpn.* **46**, 1178 (1973).
89. Nakasuka, N., Hirose, K., and Tanaka, M., *J. Inorg. Nucl. Chem.* **35**, 265 (1973).

90. Nakasuka, N., Ito, T., and Tanaka, M., *Chem. Lett.*, p. 553 (1973).
91. Nakasuka, N., Mitsuoka, Y., and Tanaka, M., *J. Inorg. Nucl. Chem.* **36**, 431 (1974).
92. Nakasuka, N., Nakai, M., and Tanaka, M., *J. Inorg. Nucl. Chem.* **32**, 3667 (1970).
93. Nakasuka, N., Onishi, A., and Tanaka, M., *J. Inorg. Nucl. Chem.* **40**, 1598 (1978).
94. Nelson, S. M., and Pink, R. C., *J. Chem. Soc.*, p. 1744 (1952).
95. Osipov, N. N., Char'kov, A. K., and Panichev, N. A., *Izv. Vyssh. Uchebn. Zaved., Khim. Khim. Tekhnol.* **25**, 830 (1982).
96. Petrukhin, O. M., Zolotov, Yu. A., and Izosenkova, L. A., *Radiokhimiya* **11**, 139 (1969).
97. Pietsch, R., *Anal. Chim. Acta* **53**, 287 (1971).
98. Pietsch, R., and Sinic, H., *Mikrochim. Acta* **1968**, 1287 (1968).
99. Pietsch, R., and Sinic, H., *Anal. Chim. Acta* **49**, 51 (1970).
100. Pimentel, G. C., and McClellan, A. L., "The Hydrogen Bond." Freeman, San Francisco, 1960.
101. Plaksin, I. N., Strizhko, V. S., and Fedotov, Yu. S., *Dokl. Akad. Nauk SSSR* **171**, 1348 (1966).
102. Poluektov, N. S., Meshkova, S. B., Beltyukova, S. V., and Tselik, E. I., *Zh. Anal. Khim.* **27**, 1721 (1972).
103. Preston, J. S., *Hydrometallurgy* **11**, 105 (1983).
104. Pyatnitskii, I. V., Boryak, A. K., and Mikhel'son, P. B., *Zh. Anal. Khim.* **30**, 900 (1975).
105. Pyatnitskii, I. V., Omode, A., and Sukhan, V. V., *Zh. Anal. Khim.* **28**, 2317 (1973).
106. Pyatnitskii, I. V., Sidorenko, V. M., and Sukhan, V. V., *Zh. Anal. Khim.* **26**, 683 (1971).
107. Pyatnitskii, I. V., Sidorenko, V. M., and Sukhan, V. V., *Zh. Anal. Khim.* **28**, 42 (1973).
108. Pyatnitskii, I. V., and Slobodenyuk, T. A., *Zh. Anal. Khim.* **29**, 1697 (1974).
109. Pyatnitskii, I. V., and Slobodenyuk, T. A., *Ukr. Khim. Zh. (Russ. Ed.)* **42**, 188 (1976).
110. Pyatnitskii, I. V., Sukhan, V. V., and Frankovskii, V. A., *Zh. Anal. Khim.* **28**, 1696 (1973).
111. Pyatnitskii, I. V., Sukhan, V. V., and Frankovskii, V. A., *Zh. Anal. Khim.* **28**, 1991 (1973).
112. Pyatnitskii, I. V., Sukhan, V. V., and Glitsenko, E. N., *Zh. Anal. Khim.* **25**, 1949 (1970).
113. Rao, V. P. R., and Sarma, V. V., *J. Inorg. Nucl. Chem.* **38**, 1179 (1976).
114. Ray, U. S., *Indian J. Chem. Sect. A* **21**, 330 (1982).
115. Ray, U. S., *Indian J. Chem. Sect. A* **21**, 444 (1982).
116. Ray, U. S., and Modak, S. C., *Indian J. Chem., Sect. A* **20**, 933 (1981).
117. Ray, U. S., and Modak, S. C., *Indian J. Chem., Sect. A* **20**, 935 (1981).
118. Rice, N. M., *Hydrometallurgy* **3**, 111 (1978).
119. Ringbom, A., "Complexation in Analytical Chemistry," p. 38. Wiley (Interscience), New York, 1963.
120. Rozen, A. M., and Mikhailichenko, A. I., *Dokl. Akad. Nauk SSSR* **168**, 828 (1966).
121. Rozycki, C., *Chem. Anal. (Warsaw)* **26**, 37 (1981).
122. Rudenko, N. P., Avilina, V. N., and Kremenskaya, I. N., *Zh. Neorg. Khim.* **11**, 947 (1966).
123. Rudenko, N. P., Dziomko, V. M., and Kremenskaya, I. N., *Radiokhimiya* **7**, 492 (1965).
124. Sanuki, S., Izaki, T., and Majima, H., *Nippon Kinzoku Gakkaishi* **46**, 591 (1982).
125. Schweitzer, G. K., and Anderson, M. M., *Anal. Chim. Acta* **41**, 23 (1968).
126. Schweitzer, G. K., and Clifford, F. C., *Anal. Chim. Acta* **45**, 57 (1969).
127. Schweitzer, G. K., and Howe, L. H., *J. Inorg. Nucl. Chem.* **29**, 2027 (1967).
128. Schweitzer, G. K., and Morris, D. K., *Anal. Chim. Acta* **45**, 65 (1969).
129. Schweitzer, G. K., and Sanghvi, S. M., *Anal. Chim. Acta* **47**, 19 (1969).
130. Schweitzer, G. K., and Stevens, R. H., *Anal. Chim. Acta* **45**, 192 (1969).

131. Shikheeva, L. V., *Zh. Neorg. Khim.* **10**, 1486 (1965).
132. Singh, J. M., Gogia, S. K., and Tandon, S. N., *Indian J. Chem., Sect. A* **21**, 333 (1982).
133. Singh, J. M., Singh, O. V., and Tandon, S. N., *Indian J. Chem., Sect. A* **16**, 1001 (1978).
134. Smith, H. W., and White, T. A., *J. Phys. Chem.* **33**, 1953 (1929).
135. Sukhan, V. V., Gorlach, V. F., and Yakimenko, L. N., *Ukr. Khim. Zh. (Russ. Ed.)* **50**, 270 (1984).
136. Sukhan, V. V., Pyatnitskii, I. V., and Frankovskii, V. A., *Zh. Anal. Khim.* **29**, 1278 (1974).
137. Sukhan, V. V., Pyatnitskii, I. V., and Frankovskii, V. A., *Zh. Anal. Khim.* **29**, 1690 (1974).
138. Sukhan, V. V., Pyatnitskii, I. V., and Frankovskii, V. A., and Lipkovskaya, N. A., *Ukr. Khim. Zh. (Russ. Ed.)* **45**, 883 (1979).
139. Sukhan, V. V., Pyatnitskii, I. V., and Sakhno, A. G., *Zh. Anal. Khim.* **28**, 541 (1973).
140. Sundaram, A. K., and Banerjee, S., *Anal. Chim. Acta* **8**, 526 (1953).
141. Tanaka, M., *Solvent Extr., Proc. Int. Solvent Extr. Conf.*, 1971, p. 16 (1971).
142. Tanaka, M., *Z. Phys. Chem. (Wiesbaden)* **96**, 239 (1975).
143. Tanaka, M., Nakasuka, N., and Goto, S., in "Solvent Extraction Chemistry" (D. Dyrssen *et al.*, eds.), p. 154. North-Holland Publ., Amsterdam, 1967.
144. Tanaka, M., Nakasuka, N., and Sasane, S., *J. Inorg. Nucl. Chem.* **31**, 2591 (1969).
145. Tanaka, M., Nakasuka, N., and Yamada, H., *J. Inorg. Nucl. Chem.* **32**, 2759 (1970).
146. Tanaka, M., Nakasuka, N., and Yamada, H., *J. Inorg. Nucl. Chem.* **32**, 2791 (1970).
147. Tanaka, M., and Niinomi, T., *J. Inorg. Nucl. Chem.* **27**, 431 (1965).
148. Tulinsky, A., and Worthington, C. R., *Acta Crystallogr.* **12**, 626 (1959).
149. West, P. W., Lyons, T. G., and Carlton, J. K., *Anal. Chim. Acta* **6**, 400 (1952).
150. Yamada, H., Imai, S., and Takeuchi, E., *Bull. Chem. Soc. Jpn.* **56**, 1401 (1983).
151. Yamada, H., Kitazaki, R., and Kakimi, I., *Bull. Chem. Soc. Jpn.* **56**, 3302 (1983).
152. Yamada, H., Suzuki, S., and Tanaka, M., *J. Inorg. Nucl. Chem.* **43**, 1873 (1981).
153. Yamada, H., Takahashi, K., Fujii, Y., and Mizuta, M., *Bull. Chem. Soc. Jpn.* **57**, 2847 (1984).
154. Yamada, H., Tanaka, K., and Tanaka, M., *J. Inorg. Nucl. Chem.* **37**, 2016 (1975).
155. Yamada, H., and Tanaka, M., *J. Inorg. Nucl. Chem.* **35**, 3307 (1973).
156. Yamada, H., and Tanaka, M., *J. Inorg. Nucl. Chem.* **38**, 1501 (1976).
157. Yamada, S., Katayama, C., Tanaka, J., and Tanaka, M., *Inorg. Chem.* **23**, 253 (1984).
158. Yuchi, A., Yamada, S., and Tanaka, M., *Anal. Chim. Acta* **115**, 301 (1980).
159. Zeeuw, A. J. V. D., *Hydrometallurgy* **4**, 21 (1979).

ALKYNE-SUBSTITUTED TRANSITION METAL CLUSTERS

PAUL R. RAITHBY* and MARIA J. ROSALES**

*Department of Chemistry, University of Cambridge, Cambridge, England, and

**Instituto de Química, Universidad Nacional Autónoma de México, Circuito Exterior,
Ciudad Universitaria, Coyoacán 04510, México D.F., México

I. Introduction	170
II. Reactions of Clusters with Unsaturated Ligands	171
A. Trinuclear Clusters	171
B. Tetranuclear Clusters	178
C. Higher Clusters	179
D. Reactions That Involve Cluster Build-up	181
E. Alkylidyne Clusters	181
III. Methods of Characterization of Alkyne-Substituted Clusters	182
A. Introduction	182
B. Infrared Spectroscopy	182
C. ¹ H NMR Spectroscopy	184
D. ¹³ C NMR Spectroscopy	187
E. Mass Spectrometry	190
F. X-Ray Crystallographic and Neutron Diffraction Studies	190
G. Ultraviolet Photoelectron Spectroscopy	192
IV. Types of Bonding of Alkynes in Cluster Complexes	194
A. Bonding Modes of Alkynes	194
B. Electron Counting and Bonding Considerations	197
C. The Structures of Alkyne-Substituted Clusters	201
V. Fluxionality in Solution	225
VI. The Reactivity of Alkyne-Substituted Clusters	226
A. Pyrolysis Reactions	227
B. Reactions with Carbon Monoxide and Dihydrogen	228
C. Reactions with Protic Acids	228
D. Reactions with Phosphines and Phosphites	228
E. Reactions with Alkynes	229
F. Reactions with Other Metallic Species	229
G. Other Reactions	231
References	231

I. Introduction

The area of organometallic chemistry concerned with the interactions between transition metal cluster complexes and small molecules has expanded greatly over the last decade. One of the major reasons for this interest has stemmed from the need to understand the role of both homogeneous and heterogeneous catalysts in a variety of important industrial processes (1). Particularly in heterogeneous catalysis, there is an appealing analogy between the interaction of an organic absorbate on a catalytic metal surface and that of an organic ligand bonded to a transition metal cluster, which may itself be viewed as a small fragment of metal. One advantage of the latter situation is that the cluster complex may be probed readily by a number of techniques which give a more detailed view of the chemistry of such species than could be obtained by a study of the surfaces themselves. This use of cluster complexes as structural models for surface chemistry has proved helpful in the understanding of these systems, and the area of the cluster-surface analogy has been the subject of a number of review articles (2-8).

Perhaps another reason for the development of the organometallic chemistry of homonuclear and heteronuclear cluster complexes is the sheer academic fascination at the great synthetic and structural diversity of these molecules. Various aspects of the chemistry of these species, particularly those involving interactions with unsaturated organic molecules, have been discussed in a number of recent publications (9-15).

This article is concerned with one specific aspect of cluster organometallic chemistry, and describes the synthesis, characterization, structure, and reactivity of transition metal clusters containing alkyne, or alkyne-derived ligands. Alkynes display a diverse reactivity in their reactions with carbonyl clusters, and exhibit a wider range of coordination modes than any other simple, unsaturated molecule. It is this compelling diversity that has prompted the authors to undertake this review.

The area of alkyne-cluster chemistry has been the subject of two previous review articles. The first is concerned largely with alkyne-cobalt chemistry (16), while the second provides a comprehensive, systematic review of alkyne-substituted homo- and heterometallic carbonyl clusters of the iron, cobalt, and nickel triads (17). This latter review covers the literature up to the end of 1981. The present work does not set out to be fully comprehensive, but rather reflects the authors' own interests in the subject. A number of key examples are

given in each subsection to illustrate points in the discussion, and, where possible, these examples have been taken from the recent literature, covering the period to the middle of 1984.

Before commencing the discussion, it is advisable to define what is meant by an alkyne or alkyne-derived ligand. The problem arises because the reaction between a cluster and an alkyne or alkene may lead to the same product, and it is difficult to decide whether the ligand is derived from an alkyne or an alkene. It is also possible that an alkyne may fragment upon coordination, or that several alkynes may link together, via C—C bond formation, to give a larger, coordinated organic group. For the purposes of this review molecules are considered which have been formed by the reaction of a cluster complex with an alkyne, or where the bonding and coordination geometry of the coordinated ligand is reminiscent of that of related alkyne-substituted clusters. However, two areas which obey these general conditions are not discussed in great detail. These are the clusters containing capping alkylidyne ligands, derived from alkynes by the rupture of the C—C triple bond, and those in which alkynes have linked together to form complex organic units. These types of complex will only be mentioned where they are relevant to the discussion. Both these areas have been featured in other review articles (11, 15–17).

II. Reactions of Clusters with Unsaturated Ligands

Several factors affect the nature of the products in a reaction between a transition metal cluster and an alkyne or alkene. In this section, the various synthetic routes to alkyne or alkene-substituted clusters will be presented, and these will be used to analyze the changes in reactivity of the cluster systems when one or more of the important reaction parameters is altered. In order to simplify the discussion, tri-, tetra-, and higher nuclearity clusters will be treated separately. Finally, in this section, there is a brief description of the chemistry of alkylidyne-substituted clusters since synthetic routes to alkyne-containing complexes may involve these species.

A. TRINUCLEAR CLUSTERS

1. Thermal Activation

a. Alkynes. The reaction between alkynes or alkenes and binary carbonyl complexes of iron, ruthenium, and osmium has been extensively studied. The quantity of data now available makes it possible to

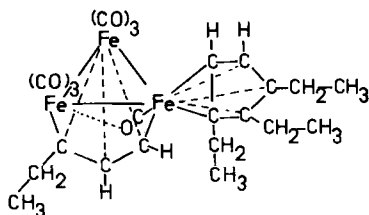
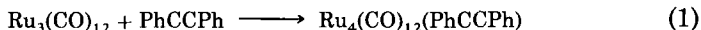


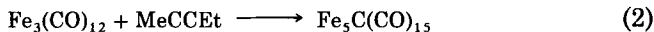
FIG. 1. A triiron cluster containing a larger organic fragment built up from a combination of alkene-based units.

draw some conclusions about the reactivity of the clusters with these unsaturated organic molecules.

The reactions of $M_3(CO)_{12}$ ($M = Fe, Ru, Os$) with disubstituted alkynes ($RC\equiv CR$) produce mononuclear (18, 19), dinuclear (18–25), trinuclear (19–22, 26–36), and tetranuclear species (37–40), as illustrated by Eq. (1). Some of the products involve polymerization of the alkyne (22, 27, 34–36) and interaction with one or more of the carbonyls already bonded to the cluster (20–22). In these reactions, metal–metal bond cleavage occurs more frequently in the case of iron clusters, although the formation of tetranuclear clusters in several of the reactions with $Ru_3(CO)_{12}$ must involve rupture of metal–metal bonds. In the case of osmium, where the metal–metal bonds are stronger, most of the high-yield products are trinuclear. It is also important to mention that some of the reaction products contain larger organic units (Fig. 1), and the formation of these ligands requires the rupture of acetylenic $C\equiv C$ triple bonds (41). There are also examples where the nuclearity of the starting material is retained but the bonds between the metal atoms are broken (42).



In many cases the use of mono-substituted alkynes in reactions with $M_3(CO)_{12}$ ($M = Fe, Ru, Os$) gives products very similar to those obtained with disubstituted alkynes (43–48). Nevertheless, the hydrogen atoms α to the triple bond may undergo a transfer from the ligand to the metal framework (49–52). Another interesting chemical transformation occurs in the reaction of $Fe_3(CO)_{12}$ with 1-pentyne (53). One of the products obtained, in very low yield, is the pentanuclear carbide $Fe_5C(CO)_{15}$ [Eq. (2)].



There are few reports of reactions between alkynes and trinuclear clusters of metals other than iron, ruthenium, or osmium. Some rhodium, platinum, and mixed-metal clusters undergo metal-metal bond rupture in reactions with alkynes (54–56), while in other cases the alkyne coordinates to the trinuclear unit without causing any major changes in framework geometry (56–59), as illustrated in Eq. (3).



b. Alkenes. The thermal reactions between $\text{M}_3(\text{CO})_{12}$ ($\text{M} = \text{Ru}, \text{Os}$) and alkenes have also been extensively studied, and there are some interesting differences in their reactivity when compared to alkynes. In the reaction of $\text{Ru}_3(\text{CO})_{12}$ with mono-substituted alkenes cluster growth is a common feature (60, 61) although trinuclear products are also obtained (62). An example of this type of reaction is shown in Fig. 2. When a high pressure of ethylene is used (60) a carbido cluster is formed in high yield, and ethylene oligomerization is observed in some of the other products. In contrast, the reaction of $\text{Os}_3(\text{CO})_{12}$ with mono-substituted alkenes gives mostly one type of product $\text{Os}_3\text{H}_2(\text{RCCR})(\text{CO})_9$, where hydrogen transfer has occurred (63–66). However, in some cases, under similar conditions, cluster growth does take place.

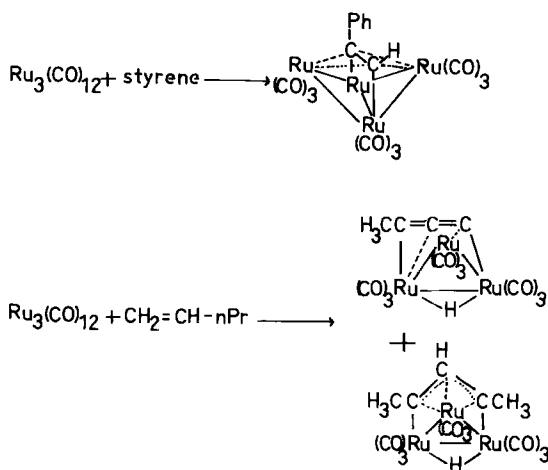


FIG. 2. Reaction of $\text{Ru}_3(\text{CO})_{12}$ with mono-substituted alkenes.

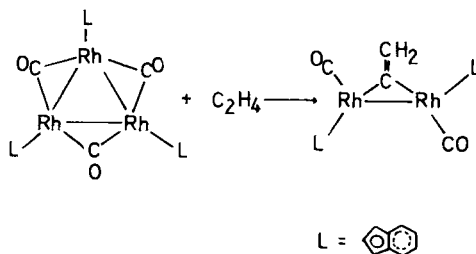


FIG. 3. Cluster breakdown of a trirhodium cluster.

The reaction of $\text{M}_3(\text{CO})_{12}$ with both open-chain and cyclic polyalkenes has attracted some attention, especially in the case of $\text{Ru}_3(\text{CO})_{12}$. In most of the examples reported, the organic fragment bonds to the metal framework in such a way as to interact with more than one of the three metal atoms (68–77). There are some exceptions to this general statement, however. One is the reaction of $\text{Ru}_3(\text{CO})_{12}$ with cyclopentadiene, in which a mononuclear complex is obtained (78). In other cases, tetranuclear and hexanuclear compounds are obtained (79–81). Cluster breakdown has also been observed in the case of a rhodium complex upon reaction with ethylene (55) as shown in Fig. 3.

It is important at this stage to mention that most reactions involving the use of alkynes or alkenes have been carried out in hydrocarbon solvents, such as hexane or octane, or in aromatic ones, such as benzene. When polar solvents are employed there are sometimes variations in the number of products and in the yields obtained (28, 31). For example, in hydrocarbon solvents, the reaction between $\text{Ru}_3(\text{CO})_{12}$ and diphenylacetylene leads to the isolation of $\text{Ru}_3(\text{CO})_9(\text{PhCCPh})$ as the major product. When the same reaction is carried out in basic aqueous methanol, the hydrido complex $\text{Ru}_3\text{H}_2(\text{CO})_9(\text{PhCCPh})$ is obtained in reasonable yield.

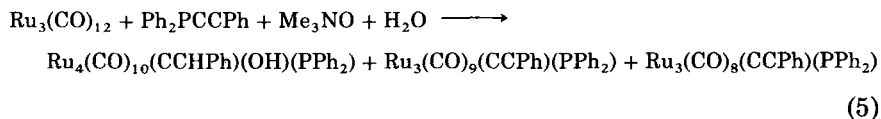
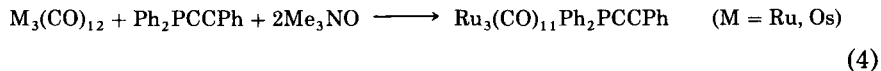
c. Importance of Other Substituents in a Cluster. The nature of the starting cluster also affects the type and characteristics of the products obtained from reactions with alkynes and alkenes. A good example of this is the chemistry of the unsaturated cluster $\text{Os}_3\text{H}_2(\text{CO})_{10}$ as opposed to that of $\text{Os}_3(\text{CO})_{12}$ (Fig. 4). It is known that complexes with the general formula $\text{Os}_3(\text{CO})_{10}(\text{organic ligand})$ may be obtained under much milder conditions when $\text{Os}_3\text{H}_2(\text{CO})_{10}$ is used as the starting material (82–90), although other types of compound can also be obtained (91–97), but in which oligomerization of the ligand does not occur. Other substituted compounds have been made to react with alkynes and alkenes, and the type of product obtained depends, to a

126) have also been treated with cluster compounds. The products obtained from these reactions vary widely, and depend on the donor-acceptor properties of the substituents, and on the availability of groups which can be eliminated from the organic ligand.

2. Photolytic or Chemical Activation

Photolytic and chemical methods of activation have also been employed in the reactions of clusters with unsaturated organic ligands. The photochemical activation of compounds containing metal-metal bonds has not received much attention until relatively recently (127). However, it is now being investigated in some detail. In some cases the photochemical products differ from those obtained by thermal activation alone (127). The reaction of $\text{Ru}_3(\text{CO})_{12}$ with ethylene is an example of such behavior (128).

The best example of chemical activation in cluster chemistry is the use of Me_3NO which results in CO replacement under mild conditions (129). In an interesting example taken from alkyne-cluster chemistry, when Me_3NO is used dry a monosubstituted cluster derivative is obtained, but with damp Me_3NO a tetranuclear vinylidene complex is isolated (130, 131), as illustrated in Eqs. (4) and (5), respectively.



3. Reactions between Different Metallic Species Which Form Trinuclear Clusters

a. With Alkyne Ligands. The reactions between different metallic species when one or both contain coordinated alkyne ligands are particularly useful in the synthesis of mixed-metal clusters. The alkyne can serve as a link which places two kinds of metal atoms at a distance where bond formation can occur. Several nickel-iron and nickel-ruthenium compounds have been prepared by this technique (132-139), although, in some examples, the reaction has resulted in the fusion of ligands (140) or the polymerization of alkynes (141, 142). Reactions between two complexes of the same element have also been

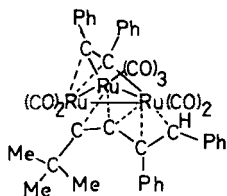
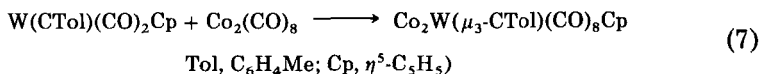
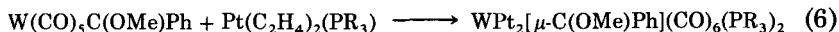


FIG. 6. Polymerization of alkenes on triruthenium clusters.

described (55), and similar reaction processes are observed (Fig. 6). Combinations of complexes of other metals have made it possible to obtain a whole range of mixed-metal clusters containing organic ligands (143–154), although the ligand does not always coordinate through the unsaturated fragment (155), and in some cases no new metal–metal bonds are formed (156).

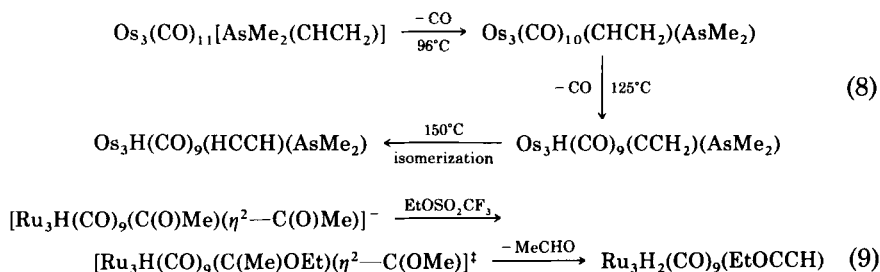
b. With Other Ligands. Another three types of complexes that have been or are being extensively studied are those containing carbyne, carbene, and acetylide ligands. Their reactions with other metallic species have produced a wide range of products (157–166). For example, carbene complexes are formed by reactions of the type shown in Eq. (6), while carbynes may be obtained by the route illustrated in Eq. (7).



4. Other Reactions That Produce Unsaturated Organic Fragments

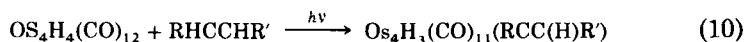
Although the reactions between alkynes or alkenes and metal clusters are the main source of alkyne-substituted complexes, there are other reagents which can produce similar products. Two such reagents are tetraphenylcyclopentadienone, which in the reaction with $\text{Ru}_3(\text{CO})_{12}$ produces $\text{Ru}_3(\text{CO})_{10}(\text{PhCCPh})$ (167), and dimethylvinylarsine, which has been made to react with several carbonyl clusters [Eq. (8)] (168, 169). In the reaction of $\text{M}_3(\text{CO})_{12}$ ($\text{M} = \text{Ru, Os}$) with a number of tertiary phosphines and aromatic alcohols, an oxidative addition takes place and benzyne–triosmium compounds are obtained (170–176). The fact that $\text{Os}_3(\text{CO})_{11}\text{PEt}_3$ can be converted into an alkyne compound (177) suggests that the conversion goes through substituted intermediates. Carbene derivatives of clusters have also

been shown to undergo changes that produce clusters with unsaturated organic ligands (178, 179), as illustrated by Eq. (9).



B. TETRANUCLEAR CLUSTERS

There have been far fewer studies on the reactions between tetranuclear clusters and alkynes or alkenes than have been reported for trinuclear systems. The reactions that have been investigated have largely been with alkenes. Both $\text{Ru}_4\text{H}_4(\text{CO})_{12}$ and $\text{Os}_4\text{H}_4(\text{CO})_{12}$ react with mono- and polyalkenes, and substitution of hydrides and carbon monoxide ligands is observed in most cases (180–187), as shown by Eq. (10). There are a few examples, however, where metal–metal bond cleavage does occur and trinuclear clusters are isolated (181–183, 188). In contrast, when $\text{Rh}_4(\text{CO})_{12}$ and $\text{Ir}_4(\text{CO})_{12}$ are treated with dienes, cluster growth occurs (189–193).



Most of the reported reactions between tetranuclear clusters and alkynes involve mixed-metal cluster species. In these systems hydride and carbon monoxide substitution generally occurs [Eq. (11)] (194–200), although in some cases Me_3NO has been used to activate the starting material (201, 202), and in still others cluster breakdown takes place even under mild reaction conditions (203). $\text{Rh}_4(\text{CO})_{12}$ (204) and $\text{Ir}_4(\text{CO})_{12}$ (205) retain their nuclearity in reactions with alkynes, but in the latter case the metal framework geometry is altered (Fig. 7). The use of $[\text{Ir}_4(\text{CO})_{11}\text{Br}]^-$ instead of $\text{Ir}_4(\text{CO})_{12}$ in reactions with alkenes produces alkene-substituted tetranuclear complexes (189), as shown in Fig. 7. Few other homonuclear clusters have been found to react with alkynes (206–208). In the reaction between the tetranuclear cluster $\text{Cp}_2\text{W}_2\text{Ir}_2(\text{CO})_{10}$ and diphenylacetylene two independent processes

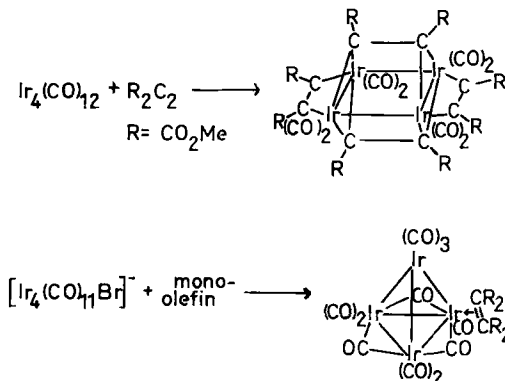
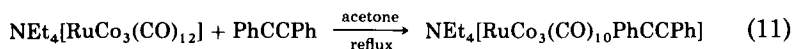
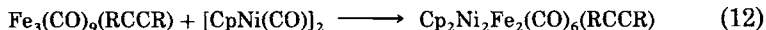


FIG. 7. Reactions of tetrairidium clusters with alkynes and alkenes.

occur. These involve cleavage of either a W—W bond or a W—Ir bond giving rise to two different modes of coordination of the alkyne ligand (209).



The reaction between two metal-containing species, one of which also contains a coordinated alkyne, has produced several tetranuclear species (210–223), such as that shown in Eq. (12).

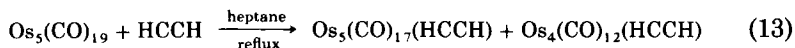


C. HIGHER CLUSTERS

The chemistry of clusters containing more than four metal atoms has only been studied in detail over the last few years, and at the present time there are few reports of reactions of these higher clusters with alkynes or alkenes.

In osmium chemistry, the reaction between $\text{Os}_5\text{H}_2(\text{CO})_{15}$ and some mono- and disubstituted alkynes gives rise to products in which the metal framework geometry differs from that of a trigonal bipyramid, as proposed for the parent hydrido carbonyl. This geometry change requires the rupture of metal–metal bonds (224). In one product of the reaction, $\text{Os}_5(\text{CO})_{13}(\text{PhCCPh})_2$, the two alkyne groups adopt different bonding modes, a characteristic which has been observed in only a few compounds (27, 37, 55, 205, 225). On the other hand, $\text{Os}_5(\text{CO})_{19}$, which is

a cluster with an open "bow-tie" framework (226), undergoes CO substitution when acetylene is added [Eq. (13)] (227).



Three effects are observed in the reactions of $\text{Os}_6(\text{CO})_{18}$ with diphenylacetylene and ethylene. There is modification of the metal framework, rupture of a $\text{C}\equiv\text{C}$ triple bond, and dimerization of ethylene (228–230). When the activated clusters $\text{Os}_6(\text{CO})_{17}(\text{MeCN})$ (230) and $\text{Os}_6(\text{CO})_{20}(\text{MeCN})$ (231) react with mono- and disubstituted alkynes, different penta- and hexanuclear framework geometries are obtained, and the alkyne-derived ligands adopt a range of coordination modes (Fig. 8).

Few other reactions between higher clusters and unsaturated organic ligands have been carried out (231, 232), but there are a number of studies which involve group IB organometallic derivatives (233–236). There are also a few high-nuclearity mixed-metal cluster alkynes which are the products of reactions between two heterometal complexes (237–242).

The main difference between the reactions of high-nuclearity clusters with alkynes and alkenes and those of the smaller clusters is that

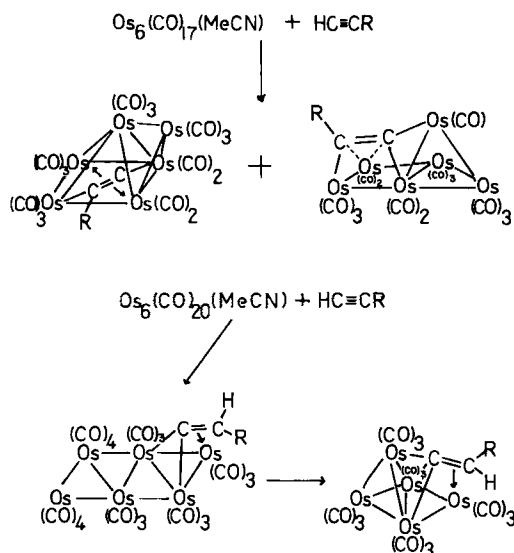
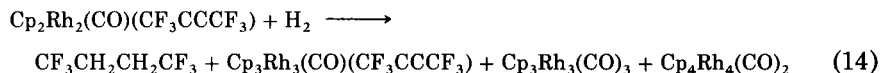


FIG. 8. Reactions of activated hexanuclear osmium clusters with alkynes.

the addition of the organic fragment can produce the rupture of metal-metal bonds without cluster breakdown.

D. REACTIONS THAT INVOLVE CLUSTER BUILD-UP

Several reactions have been reported in which alkyne- or carbyne-substituted clusters have been obtained from mono- or dinuclear complexes, or from the metal in the gas phase. The reagents with which the metallic species are treated range from alkynes, with functionalized substituents in most cases (243-251), to Grignard salts (252, 253) or halogen-substituted cycloalkanes (254). In some cases, the starting metal complex already contains an unsaturated organic fragment which, upon reaction with H_2 [Eq. (14)] (255) or an acid (256), might favor cluster growth.



In some reactions of this type, the increase in nuclearity of the complex does not necessarily involve cluster formation because metal-metal bonds need not be formed if the metals are bridged by ligands (257-260) or if an open structure is adopted (261-263).

E. ALKYLIDYNE CLUSTERS

Although it may be said that alkylidyne clusters do not contain an unsaturated organic fragment, the chemistry of these compounds is related to that of the alkyne and alkene derivatives, and their synthesis will be discussed briefly.

One of the most important links between alkylidyne and alkyne compounds is that one of the first synthetic routes for cobalt alkylidynes involved alkynes as reagents (264-268). In later studies, several other synthetic routes to cobalt (269-280), rhodium (281, 282), iron (283-285), molybdenum (286, 287), ruthenium (288-292), osmium (293, 294), nickel (295, 296), and some mixed-metal (165, 297-302) clusters have been developed. Reagents employed include carbynes (166, 277, 280), alkali metals (269), carbon disulfide (275), dithioesters (276, 282), $RCCl_3$, and acids (281, 282).

The reactivity of alkylidyne compounds has also been widely studied, particularly by Seyferth and co-workers who have carried out a great variety of reactions with cobalt complexes (303-312). Other groups

have shown interest in this area (313–340). It is important to note that reactions of halomethylidene clusters can produce alkyne complexes (341–344).

Alkylidyne clusters may be considered as precursors to carbido species, and a number of studies on iron, ruthenium, and osmium systems have been carried out to investigate this relationship (345–362).

III. Methods of Characterization of Alkyne-Substituted Clusters

A. INTRODUCTION

Alkyne-substituted cluster compounds are amenable to and, indeed, have been subjected to all of the standard techniques for structural characterization. The rather more “sporting techniques” of infrared and NMR spectroscopy have been employed to good effect in solution, while definitive structural data in the solid state is obtained by single-crystal X-ray and neutron diffraction studies. Mass spectroscopic data also give useful information on the molecular weight of the complex. Within the last few years ultraviolet photoelectron spectroscopy has been used successfully in the analysis of bonding in clusters although it is not suited as a direct structural probe. In related work on the adsorption of alkynes on metal surfaces a number of other spectroscopic and diffraction techniques have been used, and this area of research has been the subject of a recent review (2). In this section we will discuss the advantages and disadvantages of each of the standard structural probes, and show to what extent they may be applied to transition metal clusters containing alkyne ligands.

B. INFRARED SPECTROSCOPY

For free acetylene the $\nu(\text{C}—\text{C})$ stretching mode occurs at 2100 cm^{-1} while for ethylene, where the formal bond order is reduced from three to two, the $\nu(\text{C}—\text{C})$ stretch is lowered to 1623 cm^{-1} (363). It might be expected that alkyne molecules coordinated to metal clusters would exhibit stretching frequencies in the range ca. $2100\text{--}1600\text{ cm}^{-1}$, the region where $\nu(\text{C}—\text{O})$ stretching modes for terminal, edge bridging, and face capping carbon monoxide ligands are observed. Unfortunately, in practice, the $\text{C}—\text{C}$ vibrational modes are very difficult to detect because they are very weak, and because a majority of alkyne-substituted clusters also contain carbonyl groups so that any absorptions from the

alkyne may be swamped by or confused with the stronger carbonyl absorptions.

It is possible to overcome this problem partially by investigating the structures of cluster complexes which do not have carbonyl groups bonded to them, or at least those which contain only a small number of terminal carbonyls. These ligands give rise to absorption bands at the higher end of the frequency range, and are less likely to overlap with the weaker alkyne vibrations. An early example of such an investigation is the report of the $\nu(\text{C}\equiv\text{C})$ stretching frequencies in the hexacopper alkyne clusters $\text{Ar}_4\text{Cu}_6\text{R}_2$ [Ar = aryl; R = "PhC \equiv C" (1), "*p*-MeC $_6$ H $_4$ C \equiv C" (2), "2,4,6-Me $_3$ C $_6$ H $_2$ C \equiv C" (3)] (234). The observed $\nu(\text{C}\equiv\text{C})$ vibrations lie in the range 2051–2037 cm^{-1} , and are consistent with the alkynes σ bonding to the two Cu atoms causing little reduction in C \equiv C bond strength. These values may be compared with the $\nu(\text{C}\equiv\text{C})$ stretching frequency of 1933 cm^{-1} in the polymeric copper arylacetylides, (PhC \equiv CCu) $_n$, in which π interactions cause a reduction in C–C bond order (364). In the tetranuclear cluster $\text{Ni}_4(\text{CO})_4(\text{CF}_3\text{CCCF}_3)_3$ (365), where the alkyne ligands adopt the $\mu_3\text{-}\eta^2$ bonding mode (Fig. 9), the $\nu(\text{C}\equiv\text{C})$ stretch, being observed as a weak band at 1564 cm^{-1} , is greatly reduced from the free ligand value, and from the value of 1905 cm^{-1} in the mononuclear complex $\text{Ni}(\text{CO})_2(\text{CF}_3\text{CCCF}_3)$. This reduction in stretching frequency is consistent with significant electron donation from the ligands to the metal framework.

In the last few years the interest in the modes of bonding of unsaturated organic fragments to metal surfaces (4), to aid in the understanding of reactions which occur in catalytic processes, has been a major cause of the redoubling of effort to obtain good quality infrared spectra of discrete, model alkene and alkyne cluster compounds. The vibrational frequencies of the coordinated organic groups in the cluster compounds, where the bonding mode is known, may be related to the infrared spectra of the surface coordinated species. It is assumed that local environments in the two cases are similar, and the mode of coordination on the surface may be established in this way. A number of studies on triosmium alkene and alkyne clusters, involving solution

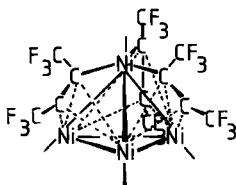


FIG. 9. Structure of $\text{Ni}_4(\text{CO})_4(\text{F}_3\text{CC}_2\text{CF}_3)_3$.

and solid-state infrared and Raman spectra, and using deuterium substitution, have been carried out. For a comparison with the spectra of surface coordinated species an accurate analysis of all the $\nu(\text{CC})$, $\nu(\text{CH})$, $\delta(\text{CH}_2)$, and $\rho(\text{CH}_2)$ modes is required, but since this review is more concerned with the nature of the C—C interaction, and that of the organic fragment within the cluster framework, the $\nu(\text{C—C})$ mode is the most relevant. Table I summarizes the value of this parameter for the clusters studied (366–369). All these complexes show a major reduction in the stretching frequency compared to the free acetylene ligand, and are also lower than for free ethylene, suggesting that there is considerable electron donation to the metal framework. There is a significant reduction in frequency in going from $\text{Os}_3(\text{CO})_9(\mu\text{-H})(\mu_3\text{-}\eta^2\text{-CCH})$, where the ligand retains a greater amount of alkyne character, to any of the next four complexes, in which the stretching frequencies are similar despite the varying modes of coordination of the ligands. These four complexes display greater alkene character. The two final complexes $\text{Os}_3(\text{CO})_{11}(\eta^2\text{-C}_2\text{H}_4)$ and $\text{Os}_3(\text{CO})_9(\mu\text{-H})(\mu\text{-SPr}^n)(\eta^2\text{-C}_2\text{H}_4)$ show the expected reduction in frequency for π -bound alkenes. In general, with a little care, it seems that the values are transferable from one complex to another, and it is possible to draw up a table of expected ranges for the various alkyne and alkene vibrations (366).

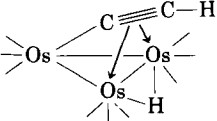
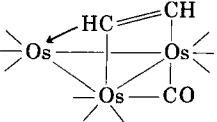
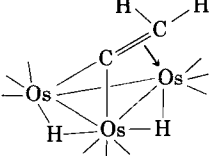
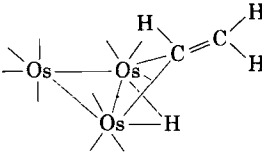
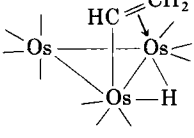
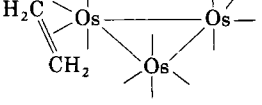
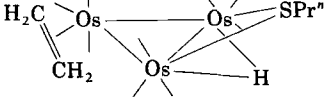
Generally, infrared spectroscopy gives fairly detailed and useful information on the overall symmetry of the molecule under investigation, particularly if the complex contains carbonyl ligands as well as alkyne groups, since the pattern and number of carbonyl stretching bands are related to the molecular symmetry of the complex (370). It is also relatively quick to establish the presence of isomers in solution, if the structure of the complex is known, if more $\nu(\text{C—O})$ stretching bands are observed than would be expected from group theoretical calculations for a molecule of that symmetry. A case in point is that of $(\text{Cp})_2\text{NiRu}_2(\text{CO})_3(\mu_3\text{-CO})(\text{PhCCPh})$, whose solution spectrum shows one more carbonyl absorption in the bridging region than would be expected for the single capping CO group observed in the solid-state structure (136). A second isomer with two bridging CO groups is present in solution.

C. ^1H NMR Spectroscopy

^1H NMR spectroscopy plays an important role in the identification of all organometallic compounds. In cluster complexes this technique has been particularly useful for establishing the presence of hydride ligands

TABLE I

INFRARED $\nu(\text{C}-\text{C})$ STRETCHING FREQUENCIES IN TRIOSMIUM ALKYNE AND ALKENE CLUSTERS

Complex	$\nu(\text{C}-\text{C}) \text{ cm}^{-1}$	Reference
$\text{Os}_3(\mu\text{-H})(\text{CO})_9(\mu_3\text{-}\eta^2\text{-CCH})$ 	1533	366
$\text{Os}_3(\text{CO})_{10}(\mu_3\text{-}\eta^2\text{-HCCH})$ 	1301	367, 368
$\text{Os}_3(\mu\text{-H})_2(\text{CO})_9(\mu_3\text{-}\eta^2\text{-C=CH}_2)$ 	1331	368, 369
$\text{Os}_3(\mu\text{-H})(\text{CO})_{10}(\mu\text{-}\eta^2\text{-CH=CH}_2)$ 	1311	368
$\text{Os}_3(\mu\text{-H})(\text{CO})_{10}(\mu\text{-}\eta^2\text{-CH=CH}_2)$ 	1310	369
$\text{Os}_3(\text{CO})_{11}(\eta^2\text{-C}_2\text{H}_4)$ 	1190	366
$\text{Os}_3(\mu\text{-H})(\text{CO})_9(\mu\text{-SPr}^n)(\eta^2\text{-C}_2\text{H}_4)$ 	1194	366

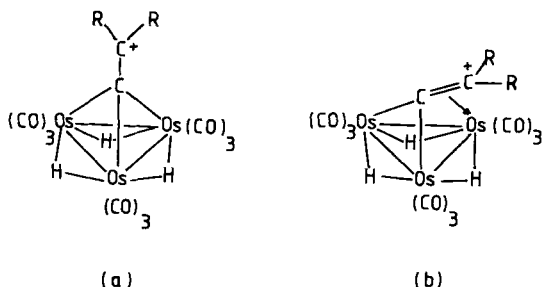


FIG. 10. Possible structures for the $[\text{Os}_3\text{H}_3(\text{CO})_9\text{CCR}_2]^+$ cation.

(371), and by studying the coupling to active metallic elements, such as ^{103}Rh (372) or ^{187}Os (373, 374), it is often possible to find the exact location of the hydride with respect to the cluster framework. The observation of $^{187}\text{Os}-^1\text{H}$ couplings has proved useful in the elucidation of the structures of two clusters containing alkyne-derived ligands. In the mixed-metal cluster $\text{Os}_3\text{M}(\mu\text{-H})(\text{CO})_{14}(\text{PhCCPh})_2$ ($\text{M} = \text{Mn}, \text{Re}$) (375), which contains an organic ligand derived from the coupling of two " $\text{PhC}\equiv\text{C}$ " groups, $^{187}\text{Os}-^1\text{H}$ couplings clearly indicate that the hydride bridges an $\text{Os}-\text{Os}$ edge of the Os_3 triangle. In the cationic cluster $[\text{Os}_3\text{H}_3(\text{CO})_9(\text{CCR}_2)]^+$, the singlet hydride resonance has two sets of satellites of equal intensity caused by $^{187}\text{Os}-^1\text{H}$ spin-spin coupling (376). This rules out the upright carbenium ion structure for the cation (Fig. 10a), and is consistent with the fluxional process involving hydrocarbon ligand rotation about the $\text{C}-\text{CR}_2$ axis in a tilted structure (Fig. 10b), and concomitant rotation of the $\text{Os}_3\text{H}_3(\text{CO})_9$ unit.*

For any cluster complex which incorporates an organic-based ligand, ^1H NMR is one of the most powerful tools for characterizing the organic species, investigating the existence of isomers in solution (216), or determining the nature of any fluxional processes which may occur (294, 377). Aspects of the use of this technique may be found in most research papers on organometallic and cluster chemistry.

Of special relevance to the investigation of alkyne-substituted clusters is the observation of a low-field resonance, generally in the range -1 to $+1.5\tau$, for a proton attached to a carbon atom which is either σ or π bonded to the metals. Values of the chemical shift for this signal for 23 tri- and tetranuclear osmium clusters were presented by

* Recent work by Shapley has led him to propose an alternative explanation for the observed data which does not differentiate between the two possible ligand orientations. See Holmgren *et al.*, *J. Organomet. Chem.* **284**, p. C5, (1985).

Sappa *et al.* in their review (17). This constitutes quite a powerful diagnostic probe for such complexes. The reason for the appearance of this signal at such a low field may be due to the fact that the proton is bonded to a carbon which is partially carbenic in character.

D. ^{13}C NMR Spectroscopy

^{13}C NMR is generally applicable to organometallic and organo cluster compounds, but has the advantage of giving a direct probe on the acetylenic carbon atoms in alkyne-substituted clusters. With the development of more powerful NMR instruments, this technique has been used extensively to characterize organo-substituted cluster complexes in solution. For smaller clusters, the combination of ^{13}C NMR with ^{31}P NMR and resonance studies from metallic nuclei, where appropriate, frequently leads to complete structure elucidation.

However, there are a number of disadvantages in the use of ^{13}C NMR. These include the requirement of a relatively large sample, and the problems of solubility, particularly with larger molecular units. In order to establish the nature of fluxional processes which may occur, it is necessary to run the spectrum at various temperatures. This may again increase experimental complexity. The spectra are not always simple to interpret, which is also true for ^1H NMR results. This problem may sometimes be overcome by means of labeling experiments. For ^1H NMR, specific exchange of some of the hydrogens by deuterium atoms is relatively straightforward, and a comparison of the partially deuterated and nondeuterated spectra frequently leads to the assignment of a majority of the signals. For ^{13}C NMR, treatment of the alkyne-substituted carbonyl cluster with ^{13}C -enriched carbon monoxide will increase the intensity of the signals of the carbonyl carbons compared to those of the alkyne groups, which do not generally exchange, and thus permit assignment of the signals. A number of studies on alkyne-substituted clusters do involve both the fluxionality of the carbonyl ligands and of the alkyne groups and these will be discussed in Section V.

As with the low-field signal for the proton bonded to alkyne carbons coordinated to the metal, the ^{13}C signals often prove a useful diagnostic tool. These ^{13}C signals also tend to be at low field, but the position of the signal may vary by several hundred ppm depending on the environment of the carbon atom. There are a number of important steric and electronic factors which have a major influence on the interaction between the alkyne carbons and the metal framework that prevent the maximum use of this data.

Carty (13) has indicated that for a closely related group of complexes there is a workable correlation between the observed positions of the signals and the reactivity of the carbons with which they are associated. The acetylenic ^{13}C NMR resonances for a number of tri- and tetranuclear clusters have been collected in Table II; the relevant bonding types for the alkyne-derived ligands are also illustrated in this Table (13, 203, 285, 366, 378–380). The shifts for the trinuclear clusters are generally to higher field than the shifts of carbene carbon resonances in carbene complexes, which lie in the range 200–350 ppm. The resonance for the C_α atom in the tetranuclear cluster $\text{FeCo}_3(\text{CO})_9(\text{Cp})(\mu_4\text{-}\eta^3\text{-CCH}_2)$ (285) is within this range, and suggests a more carbenic nature for this carbon. Within a structurally related series of molecules the variations of the C_α and C_β resonances are dependent on the metal atoms to which they are bonded and on the nature of the substituent R groups, and may be indicative of the differences in polarization in the $\text{C}\equiv\text{C}$ triple bond. If it is assumed that a change in $\delta(^{13}\text{C})$ is mainly associated with a change in charge on the carbon atom (381), then $\delta(\text{C}_\alpha) + \delta(\text{C}_\beta)$ gives an idea of the total charge alteration in the $\text{C}\equiv\text{C}$ bond while $\delta(\text{C}_\alpha) - \delta(\text{C}_\beta)$ is a measure of the polarization of that bond (Table II). In the complexes of types A and B the value for the C_β resonance shows a much smaller variation than that for C_α , except in the case of the triosmium cluster $\text{Os}_3\text{H}(\text{CO})_9(\mu_3\text{-}\eta^2 \perp \text{CCH})$ (366), in which the C_β resonance is abnormally low. The data suggest that the overall change in charge is greater for the type A structures than for type B, and that polarization of the C–C bond in type A shows a greater variation than for type B.

The single resonance for the π -bonded alkene ligand in $\text{Os}_3(\text{CO})_{11}(\text{C}_2\text{H}_4)$ (366) lies considerably upfield of the equivalent C_α resonance in the type D complexes, in which σ bonding between the metals and the alkene ligand is important. These C_α resonances are interestingly quite similar to those in the type A and B complexes.

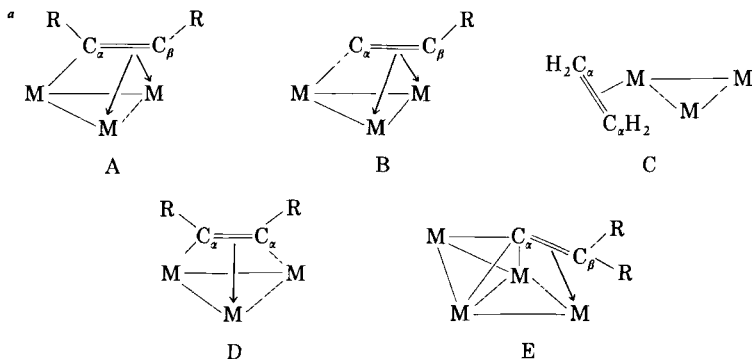
It should be pointed out that the sample considered in this discussion is very small, and a great deal more experimental work is required before any generalization can be made about the relationship between the position of the ^{13}C resonances and the reactivity of the systems.

The observation of ^{13}C – ^{13}C coupling constants in μ_2 - and $\mu_4\text{-}\eta^2$ -alkyne cobalt clusters has also shed some light on the nature of bonding in these complexes (382). There is a drastic decrease in the $^1J(\text{CC})$ coupling constant on going from the free alkyne to complexes where the ligand is bonded to two or four cobalt atoms. In $\text{Co}_4(\text{CO})_{10}(\mu_4\text{-}\eta^2\text{-HCCH})$, the $^1J(\text{CC})$ constant is 21 Hz, compared to that of 171.5 Hz in HCCH, and theoretical calculations indicate that this is consistent with a rehybridization of the formally sp hybridized acetylenic C atoms toward sp^3 hybridization.

TABLE II

¹³CNMR RESONANCES FOR SOME ALKYNE- AND ALKENE-SUBSTITUTED TRI- AND TETRANUCLEAR CLUSTERS

Complex	Type ^a	ppm				Reference
		$\delta(C_\alpha)$	$\delta(C_\beta)$	$\delta(C_\alpha) - \delta(C_\beta)$	$\delta(C_\alpha) + \delta(C_\beta)$	
$\text{Fe}_3(\text{CO})_9(\mu_3\text{-}\eta^2\text{-}\perp\text{-EtC}_2\text{Et})$	A	221.9	106.8	115.1	328.7	378
$\text{Fe}_2\text{Mo}(\text{CO})_8\text{Cp}(\mu_3\text{-}\eta^2\text{-}\perp\text{-CCMe})$	B	181.8	95.9	85.9	277.7	379
$\text{Fe}_2\text{W}(\text{CO})_8\text{Cp}(\mu_3\text{-}\eta^2\text{-}\perp\text{-CCMe})$	B	165.7	108.3	57.4	274.0	379
$\text{Fe}_2\text{W}(\text{CO})_8\text{Cp}(\mu_3\text{-}\eta^2\text{-}\perp\text{-CCTol})$	B	172.9	112.7	60.2	285.6	379
$\text{FeW}_2(\text{CO})_6\text{Cp}_2(\mu_3\text{-}\eta^2\text{-}\perp\text{-C}_2\text{ToI}_2)$	A	168.5	153.8	14.7	322.3	380
$\text{Ru}_3(\text{CO})_9(\mu_3\text{-}\eta^2\text{-}\perp\text{-CCPr}^i)(\text{PPh}_2)$	B	134.4	103.8	30.6	238.2	13
$\text{Ru}_3\text{H}(\text{CO})_8(\mu_3\text{-}\eta^2\text{-}\perp\text{-CCBu}^i)(\text{PPh}_2\text{OEt})$	B	140.5	112.2	28.3	252.7	13
$\text{Ru}_3\text{H}(\text{CO})_9(\mu_3\text{-}\eta^2\text{-}\perp\text{-CCBu}^i)$	B	164.2	110.6	53.6	274.8	13
$\text{RuW}_2(\text{CO})_7\text{Cp}_2(\mu_3\text{-}\eta^2\text{-}\perp\text{-C}_2\text{ToI}_2)$	A	153.1–128.0				380
$\text{Os}_3(\text{CO})_{11}(\mu\text{-C}_2\text{H}_4)$	C	22.4				366
$\text{Os}_3(\text{CO})_{10}(\mu_3\text{-}\eta^2\text{-}\parallel\text{-HCCH})$	D	123.4				366
$\text{Os}_3\text{H}(\text{CO})_9(\mu_3\text{-}\eta^2\text{-}\perp\text{-CCH})$	B	134.4	41.6	92.8	176.0	366
$\text{OsPt}_2(\text{CO})_5(\mu_3\text{-}\eta^2\text{-}\parallel\text{-MeC}_2\text{Me})(\text{PPh}_3)_2$	D	155.5				203
$\text{FeCo}_3(\text{CO})_9\text{Cp}(\mu_4\text{-}\eta^3\text{-CCH}_2)$	E	304.0				285



E. MASS SPECTROMETRY

Mass spectrometry is widely used in organometallic and cluster chemistry as a rapid means of determining the molecular weight, the number of carbonyl and other ligands present, and even the number of metal atoms present. In the case of relatively small molecules it is also possible to detect hydrogen loss.

There are, however, a number of limitations to the technique. First, the complex must be volatile. The presence of ligands such as phosphines or phosphidoalkynes greatly reduces the volatility as does the presence of anionic or large polynuclear cluster frameworks. The results obtained are dependent on the instrument and on the experimental conditions used. In order to increase the volatility it is often necessary to increase the temperature at the probe. This temperature increase may not always be carefully controlled, and can lead to deposition of metal within the instrument, which reduces its sensitivity and produces erroneous molecular weight peaks. At elevated temperatures, cluster breakdown is common, and in the publications on $\text{Ir}_4(\text{CO})_8[\text{C}_2(\text{COOMe})_2]_4$ (205) and $\text{Os}_5(\text{CO})_{17}(\text{HCCH})$ (227), the molecular ion peak obtained from the mass spectrum does not correspond to the molecular formula established by X-ray crystallography. Molecular rearrangements may also occur within the instrument without apparent loss of molecular fragments, and this has been observed in a number of Co-Rh derivatives (383).

A number of developments of the technique are now available but have not been widely used. These include chemical ionization, field ionization or desorption, and negative ionization. The techniques of fast atom bombardment (FAB) and field desorption appear the most promising for detecting the molecular ions in compounds that would otherwise break up in the instrument (9).

Regrettably, alkyne-substituted cluster complexes seem particularly prone to fragmentation and very few accurate mass spectroscopic studies have been reported. A recent exception has been the field-desorption and electron-impact mass spectral investigation of mono- and oligo-nuclear ferracyclic ring systems of the form $\text{Fe}_x(\text{CO})_y(\text{C}_2\text{R}_2)_2$ ($x = 1, 2, 3$; $y = 6, 8$) (384). These species show intense molecular ion peaks, which enable ready recognition of the molecular composition.

F. X-RAY CRYSTALLOGRAPHIC AND NEUTRON DIFFRACTION STUDIES

It is probably fair to say that up to the present time single-crystal X-ray diffraction studies have done more to further the development of cluster chemistry than any other method of structure characterization.

The main reason is that all the systems are relatively complex and, while spectroscopic techniques may give part of the answer as to the nature and stereochemistry of the compound, a full crystallographic study will in a vast majority of cases give a definitive answer. In the reviews on alkyne-substituted clusters and related compounds, a large proportion of the discussion of the chemistry has been based on solid-state structural data, and this review is no exception. The variety of structural cluster types incorporating alkyne ligands will be presented in Section IV.

However, there are a number of limitations and criticisms which may be leveled at the crystallographic technique, and it is worth bearing these in mind when looking at the available structural data. Perhaps, most importantly, the technique deals with the solid state, and a vast majority of reaction chemistry occurs in solution. Also, it is frequently the case that the structural analysis is performed on one crystal, and one crystal only, and this crystal may not be representative of the molecules in the bulk sample. Careful work on a number of ruthenium cluster systems has shown the existence of a number of different solid-state isomers and different crystalline modifications (380, 385). It is probable that in solution there is more than one structural form but that one crystallizes out preferentially.

Another problem involves the accuracy of the data obtained. Particularly with cluster compounds of the second and third row transition metal elements, absorption effects and the like may introduce quite large uncertainties into the positions of the lighter atoms. The estimated standard deviations obtained from most crystallographic programs tend to rather underestimate the errors, and while good, accurate absorption corrections are routinely carried out, the true error on a C-C bond length in, say, a tetranuclear osmium cluster alkyne is probably of the order of ± 0.05 Å. This makes comparisons between bond parameters for the lighter atoms rather less meaningful than some authors would have us believe, and a formal assignment of "bond order" for an acetylenic bond far from certain. The problem is even more severe when the location of hydrogen atoms is being discussed, and in larger clusters these atoms are seldom located directly because the scattering is dominated by the heavy metal atom contribution. A variety of very useful indirect methods (386) have been developed for the location of hydrides, but these have not been applied to the location of acetylenic hydrogen atoms.

The problem of hydrogen atom location may be overcome, and a reduction in the uncertainties in the positions of the lighter atoms obtained, by the use of neutron diffraction. This method is generally similar to X-ray diffraction except that neutrons are diffracted by the

atomic nuclei rather than by the surrounding electron cloud. The scattering power of the nucleus is not dependent on the number of subatomic particles that it contains and it varies almost randomly throughout the periodic table. The difference in neutron scattering power of a hydrogen atom and a third row transition element is far smaller than the difference in X-ray scattering power. Absorption effects for neutrons are also much smaller. So light atoms are located with considerable precision, and it is possible to observe significant variations in bond parameters for these atoms which are consistent with current bonding theories.

Unfortunately, neutron diffraction brings its own problems. These include the requirement of a large single crystal, weighing of the order of 30 mg (which may be larger than the total yield of a typical cluster synthesis), and access to a nuclear reactor for a period of several weeks for a single experimental run. Present day neutron fluxes are an order of magnitude weaker than X-ray sources so that it requires a much longer time to measure the intensity of each reflection.

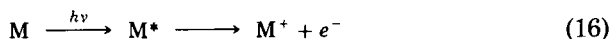
So far only one alkyne-substituted (387) and two vinylic cluster derivatives (186, 388) have been analyzed by neutron diffraction. Hopefully, the development of high-energy neutron sources and two-dimensional detectors over the next few years will see an advance in this area of structural chemistry.

G. ULTRAVIOLET PHOTOELECTRON SPECTROSCOPY

This technique is not a direct structural probe, but has been used as an experimental method to augment theoretical calculations on the bonding in cluster systems, including a number of alkyne-substituted complexes (389–391). The basis of the technique is that photons in the vacuum ultraviolet region of the spectrum, whose energy is about 10 eV, interact with molecules in the gas phase to cause either promotion of electrons from one bound state to another or their ejection as free electrons. Photoelectron spectroscopy is only concerned with processes that liberate electrons, either by direct ionization [Eq. (15)],



or possibly by autoionization [Eq. (16)],



where M^* may be in a stable, metastable, or unstable state (392). The source of radiation for the experiment is obtained from the helium

emission spectrum in which the He(I) line (21.22 eV) predominates, accounting for 98% of the emission, so that for the majority of substances which have ionization potentials of 5 eV or greater, essentially the only ionization caused is due to the He(I) resonance line. The spectra obtained in this way are compared with orbital energy diagrams, and the orbitals from which the electrons are ionized may be identified. This is possible because of close adherence to the precepts of Koopmans' Theorem, which postulates the equality of the negative of an ionization energy to a one-electron orbital energy.

This technique has been used extensively as an experimental comparison for one or other of the types of theoretical molecular orbital calculations for organic and some nonmetallic inorganic compounds. However, for transition metal complexes and cluster compounds, their lower volatility presents some difficulties, and for the photoelectron spectra of the cluster alkyne complexes that have been recorded a heated inlet probe has been used to overcome this problem.

In order to ease the interpretation of the photoelectron spectra, and to obtain the best correlation between experimental data and related theoretical calculations, it is advisable to consider a series of related molecules. In the case of alkyne-substituted clusters He(I)-excited vapor-phase photoelectron spectra have been obtained on the series of molecules $\text{Co}_2(\text{CO})_6(\text{PhCCH})$ (1) (389), $\text{Fe}_3(\text{CO})_9(\text{EtCCEt})$ (2) (390), $\text{M}_3(\text{CO})_9(\mu\text{-H})(\text{CCR})$ ($\text{M} = \text{Ru}, \text{Os}$) (3) (391), and $\text{Co}_4(\text{CO})_{10}(\text{PhCCH})$ (4) (389), which exhibit the range of bonding modes illustrated in Fig. 11.

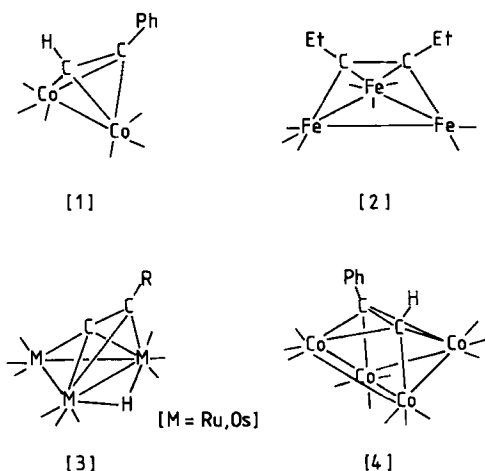


FIG. 11. Alkyne clusters for which photoelectron spectroscopic data are available.

The combined experimental and theoretical results emphasize the carbynic nature of the acetylenic carbon atoms bonded to the cluster, as indicated by NMR experiments (Sections III,C and D), and show that there is an increase in negative charge on the acetylenic carbon as the number of metal atoms to which it is coordinated increases and the C–C bond order decreases. The highest negative charge on these carbons would be obtained by cleaving the C–C bond to form μ_3 -alkylidyne systems. The calculations indicate that the normally accepted model for metal alkyne bonding (Section IV, A) is correct, and that there is a net back donation into ligand π^* orbitals, which increases as the number of metal alkyne bonding (Section IV,A) is correct, and that there is a net describe the alkyne bonding in **2** in terms of two σ bonds and one π bond, and in **3** as one σ bond and two weaker π interactions.

If these results are transferable to other alkyne cluster systems it appears that, in general, the ideas on cluster alkyne bonding developed over the last two decades from the work of Dahl and co-workers (26) are correct.

IV. Types of Bonding of Alkynes in Cluster Complexes

A. BONDING MODES OF ALKYNES

Before considering the bonding of alkynes in cluster complexes it is worth discussing the rather simpler cases of mononuclear alkyne complexes and the free ligand itself.

The molecular orbital energy stacking diagram for free acetylene is shown in Fig. 12. It can be seen that all the available bonding molecular orbitals are filled and that the free ligand has formal triple bond character. Upon coordination to a metal atom, the C–C vector lies perpendicular to the σ -bonding orbital on the metal and donates electron density from a filled π -bonding orbital, as illustrated in Fig. 13.

The bonding in monometal alkyne complexes is usually interpreted in terms of the Dewar–Chatt–Duncanson model (293), since the alkyne molecule has a pair of π and π^* molecular orbitals which lie in the plane of the metal and the two carbon atoms. These two orbitals are denoted π_{\parallel} and π_{\parallel}^* , and are analogous to those in π -bonded alkene complexes (394). There is also a pair of π and π^* molecular orbitals which lie perpendicular to the metal–carbon plane, denoted π_{\perp} and π_{\perp}^* . These orbitals are illustrated in Fig. 14. Both sets of π and π^* orbitals have the correct symmetry to interact with metal d orbitals. The interaction

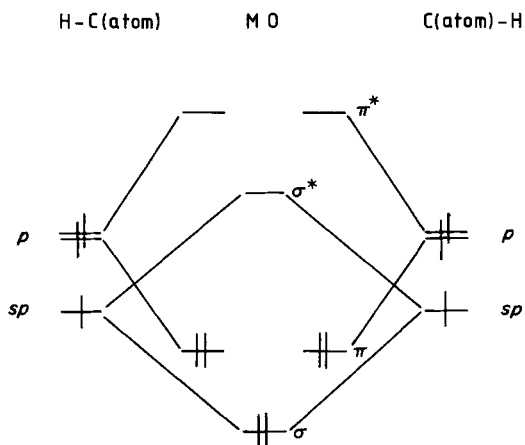


FIG. 12. MO stacking diagram for free acetylene.

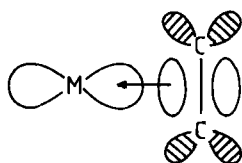


FIG. 13. π -Bonding overlap between acetylene and metal σ bond.

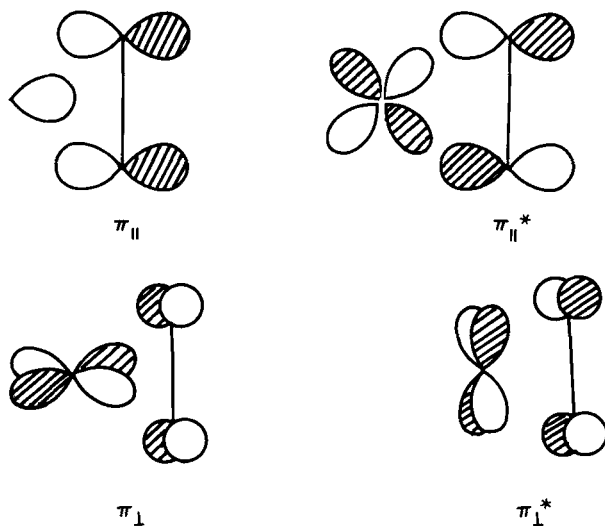


FIG. 14. Interactions between the π and π^* molecular orbitals of an alkyne with metal orbitals of appropriate symmetry.

involving the π_{\perp}^* orbital is not energetically significant because only a δ type overlap is involved. The overlap which involves the filled π_{\perp} molecular orbital is important, and has a magnitude similar to that involving the π_{\parallel}^* orbital. The addition π -donor interaction possible for an alkyne means that it may function simultaneously as a π -acceptor and a π -donor ligand. In terms of electron counting it may formally act as a two- (using π_{\parallel}) or a four-electron (using π_{\parallel} and π_{\perp}) donor. Recent theoretical calculations confirm the importance of the π_{\perp} orbital in bonding to monometal complexes and indicate that the observed orientation of the alkyne is at least partially dependent on the strength of the interaction from this orbital (395).

The bonding scheme described above is consistent with the change in the C-C bond length and the C-C-R bond angle. In free acetylene the C-C bond length is 1.21 Å while upon complexation it is lengthened to a value typically in the range 1.3-1.45 Å. For free alkynes, the C-C-R angle is approximately 180°, but in complexes, a cis bending occurs giving angles in the range 120-150°. Hoffmann and co-workers (396) have made a thorough study of the variation of these parameters in a range of dinuclear alkyne-substituted complexes. For dimetallic systems, the acetylenic C-C bond may lie essentially parallel or perpendicular to the metal-metal vector. The interactions between molecular orbitals which participate in these two stereochemistries are different, and this explains differences in the observed C-C-R angles for the two groups: 120-130° for the parallel bonded alkynes and 130-150° for the perpendicular bonded alkynes. Because of the use of different orbital arrangements there is expected to be a relatively high barrier to rotation between the two orientations which makes fluxionality in these systems less likely at lower temperatures.

For higher cluster complexes containing coordinated alkyne-derived ligands the situation with regard to modes of bonding of the organic fragment is considerably more complicated. A single alkyne may donate between two and six electrons to a cluster depending upon the mode of coordination. Unlike a carbonyl group, an alkyne may fragment upon coordination to a cluster, and in this way, increase the number of electrons which it formally donates. Particularly in the case of acetylene itself, or with mono-substituted alkynes, an acetylenic hydrogen may either transfer to the metal framework to give a hydride, which formally donates one electron to the cluster, or undergo a shift to the other acetylenic carbon, which results in a coordinated organic ligand more reminiscent of an alkene. A "naked C-C" unit, in which all the organic substituents have been lost, would formally donate six electrons. For disubstituted alkynes the nature of the bonded R group

may also have an influence on the mode of bonding, particularly if the group is bulky and exerts a strong steric influence. In all cases fragmentation of the alkyne may result in one of the fragments not appearing in the cluster complex at all, but forming part of another product in the reaction. Alternatively, it is possible that, upon coordination to the cluster, alkynes may link together or with other cluster ligands via C-C bond formation to give extended organic based units bonded to the cluster. A discussion of the variety of bonding modes of such groups is beyond the scope of this review, and only specific examples of direct relevance to the structural chemistry of cluster alkynes will be described. Neither will structures containing capping alkylidyne ligands, obtained by alkyne fragmentation, be discussed in detail since these have been comprehensively reviewed elsewhere (16, 17). The modes of bonding of alkyne ligands, and of ligands derived from alkynes, coordinated to three, four, or five metal atoms in clusters are illustrated in Fig. 15. It is sometimes difficult to decide whether the coordinated ligands in Fig. 15 are derived from alkynes or alkenes, since there are a number of reactions in which the use of either species leads to the same product. However, an examination of these bonding modes suggests that only the ligands in structural types M3, M6, M7, M11, M15, M16, and M17 are truly acetylenic, the remainder may be described as acetylides or ethylenic substituents. Each type of bonding mode will be discussed in Section IV,C.

B. ELECTRON COUNTING AND BONDING CONSIDERATIONS

For alkynes bonded to higher nuclearity clusters no overall molecular orbital treatment encompassing all the variations in geometry has appeared yet.* However, there are a small number of examples of specific alkyne-substituted clusters which have been analyzed by one type of molecular orbital treatment or another, and a number of these have been mentioned in Section III,G because photoelectron spectroscopy has been used as an aid to assignments. CNDO calculations (397) on $\text{Fe}_3(\text{CO})_9(\text{EtCCEt})$ (390) and $\text{M}_3(\text{CO})_9(\mu\text{-H})(\text{CCR})$ ($\text{M} = \text{Ru}, \text{Os}$) (391) and Fenske-Hall calculations (398) on $\text{Co}_4(\text{CO})_{10}(\text{PhCCH})$ (389) indicate that there is net back donation into alkyne π^* orbitals, which increases as the number of metal atoms to which the ligand is bonded increases. The normally accepted view of considering the interaction

* A more comprehensive molecular orbital treatment of the bonding in alkyne-substituted trimetallic clusters has recently appeared. See Halet *et al.*, *Inorg. Chem* **24**, p. 218 (1985).

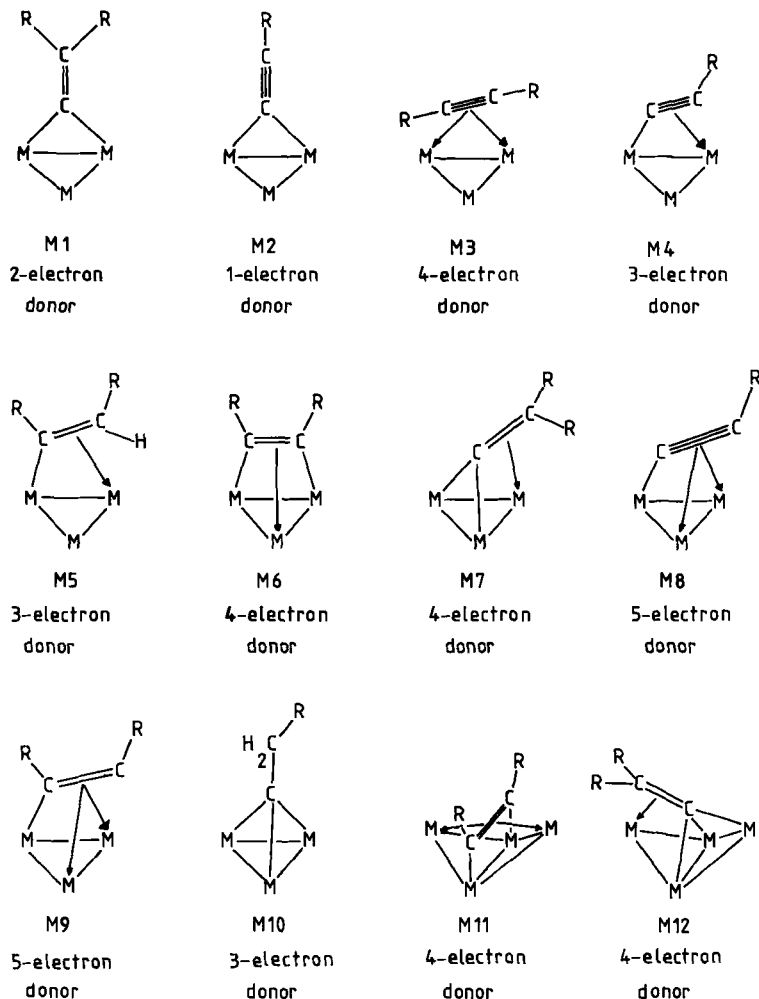


FIG. 15. Observed bonding modes of alkyne and alkyne-derived ligands in cluster complexes.

between the alkyne ligand and the metals in terms of σ and π bonds seems correct, at least for tri- and tetranuclear systems.

More generally, in terms of electron counting, alkyne-substituted clusters may be treated in a manner similar to other cluster systems. In these schemes the ligands are considered primarily as species which donate electrons to the cluster framework and do not have specific donor and acceptor properties of their own. Because of possible

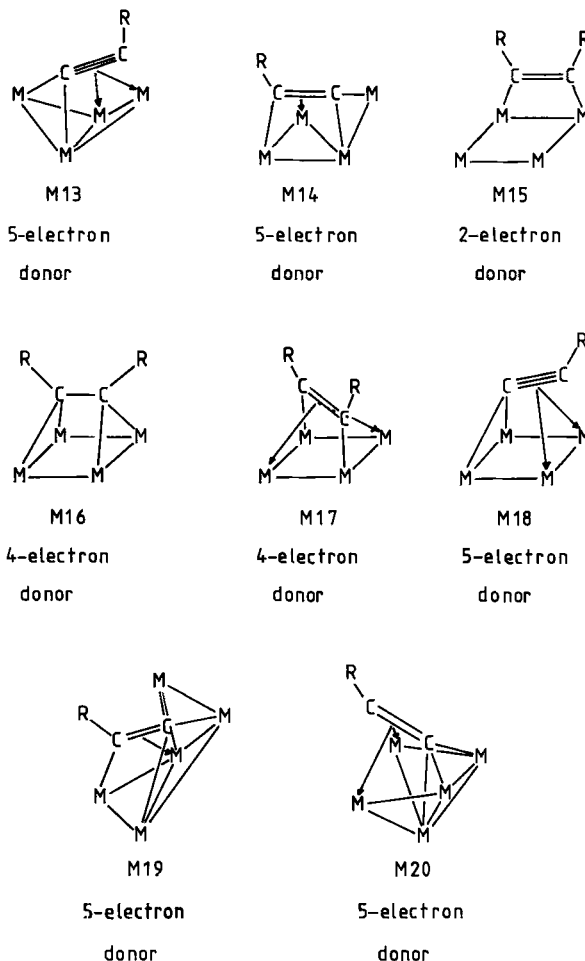


FIG. 15 (Continued)

confusion as to the number of electrons that the alkyne-derived ligand may donate, particularly in the case in which a hydrogen splits off the ligand and bonds to the metal framework independently, it is better to include the electron donated by this hydride in the electron count from the parent, organic free ligand. The simplest of these counting schemes is the "18-Electron Rule" or the "Effective Atomic Number Rule" where the skeletal metal framework is held together by a network of two-centre two-electron bonds (399). This scheme works reasonably well for

relatively small systems such as $\text{Co}_2(\text{CO})_6(\text{RCCR})$, which is a 34-electron system, and indicates the presence of a single metal-metal bond. However, this rule frequently breaks down for larger clusters.

A theory which shows greater applicability to bonding in cluster compounds is the "Polyhedral Skeletal Electron Pair Theory" (PSEPT) which allows the probable structure to be deduced from the total number of skeletal bond pairs (400). Molecular orbital calculations show that a *closed* polyhedron with n vertex atoms is held together by a total of $(n + 1)$ skeletal bond pairs. A *nido* polyhedron, with one vertex vacant, is held together by $(n + 2)$ skeletal bond pairs, and an *arachno* polyhedron, with two vacant vertices, by $(n + 3)$ skeletal bond pairs. Further, more open structures are obtainable by adding additional pairs of electrons. This discussion of these polyhedral shapes is normally confined to metal atoms, but it is possible to consider an alkyne, $\text{RC}\equiv\text{CR}$, either as an external ligand or as a source of two skeletal CR units. So that, for example, the cluster skeleton in the complex $\text{Co}_4(\text{CO})_{10}(\text{RCCR})$, shown in Fig. 16, may be considered as a *nido* trigonal bipyramid (a "butterfly" cluster) with a coordinated alkyne or as a *closo* octahedron with two carbon atoms in the core.

The disadvantages of this approach are twofold. With higher nuclearity clusters the number of geometric possibilities for the same electron count increases, and while the PSEPT may be used to rationalize a number of the observed configurations it is not predictive. Secondly, unlike boranes, for which the theory was originally developed, increasing the nuclearity of the cluster does not always result in a larger *closo* polyhedron, but the observed structure is often best described in terms of a smaller polyhedron where some of the faces are capped. The result of this is that a monocapped polyhedron with n skeletal atoms has n electron pairs available for cluster bonding. This may be thought of as being equivalent to adding a capping group to a *closo* cluster polyhedron without formally adding an electron pair. For a transition metal

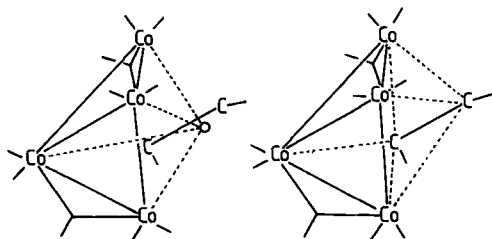


FIG. 16. Two different bonding descriptions of the cluster $\text{Co}_4(\text{CO})_{10}(\text{RCCR})$.

cluster with n skeletal metal atoms the total number of skeletal electron pairs (P) is given by Eq. (17).

$$P = 0.5 (\text{total valence electrons} - 12n). \quad (17)$$

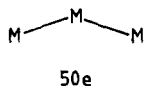
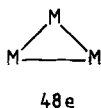
Several groups have performed calculations on the possible geometries adopted by higher nuclearity clusters but these have generally considered the arrangement of the atoms in the metal core only (401). Mingos developed an extension of the PSEPT to include nonconical fragments (402), and has given some general principles for electron counting in condensed polyhedra (403). With these developments it is possible to rationalize all platinum-group metal condensed polyhedral cluster structures.

In practice, specific cluster metal framework geometries are associated with particular electron counts and the number of formal metal-metal bonds present. It is often simplest to analyze structures in terms of these electron counts. Some of the possible metal framework geometries associated with the more common electron counts are illustrated in Fig. 17, and these metal arrays, along with the mode of coordination of the alkyne-substituted ligands, will be used in Section IV,C to order the discussion of the structural types.

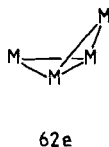
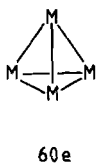
C. THE STRUCTURES OF ALKYNE-SUBSTITUTED CLUSTERS

In alkyne-substituted cluster complexes neither the "side-on" π bond nor the "end-on" acetylide type bond to a single metal center is observed, unlike the situation in mononuclear systems where these are the only modes possible. It is possible to explain the absence of simple π -bound alkynes in a manner similar to that used to rationalize the occurrence of bridging carbonyls in carbonyl clusters. The alkyne is capable of acting as a strong π -acceptor ligand, and with two or three metal atoms available it may be favorable to maximize the back donation by coordinating to all of them. However, it would be interesting to see if an activated cluster, such as $\text{Os}_3(\text{CO})_{11}(\text{MeCN})$, would react with alkynes to give a simple π -bound substitution product. At present, the absence of single-center acetylide interactions in clusters is also generally explained in terms of maximized back donation. This rationalization is supported by the structures of copper acetylides (364), which are polymeric, with the acetylide σ bonded to one metal and π bonded to another (Fig. 18). Similar simultaneous metal-acetylide σ and π bonding occurs in the mixed-metal cluster derivatives $\text{Cu}_4\text{Ir}_2(\text{PPh}_3)_2(\text{CCPh})_8$ (237), $\text{RhAg}_2(\text{CCC}_6\text{F}_5)_5(\text{PPh}_3)$ (164), and

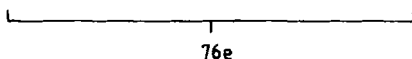
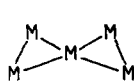
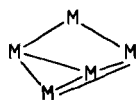
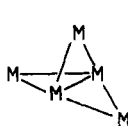
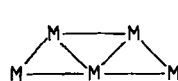
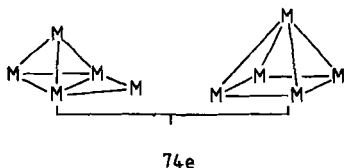
Trinuclear



Tetranuclear



Pentanuclear



78e

FIG. 17. Possible metal cluster framework geometries.

$[\text{CpFe}(\text{CO})_2(\text{CCPh})\text{CuCl}]_2$ (404), and where the acetylenic C-C bond lengths lie in the range 1.18–1.29 Å. In $[\text{CpFe}(\text{CO})_2(\text{CCPh})\text{CuCl}]_2$ (Fig. 19), the C-C-Fe angles both show a marked deviation from linearity, each with a value of $162(2)^\circ$.

In contrast to alkyne ligands, alkenes are observed to bond "side-on" to one metal center in a cluster complex. This may reflect the poorer π -acceptor properties of an alkene compared to an alkyne. In all cases reported for single alkene units the ligand has been coordinated to a metal atom in a trinuclear cluster unit, and in the majority of cases the

Hexanuclear

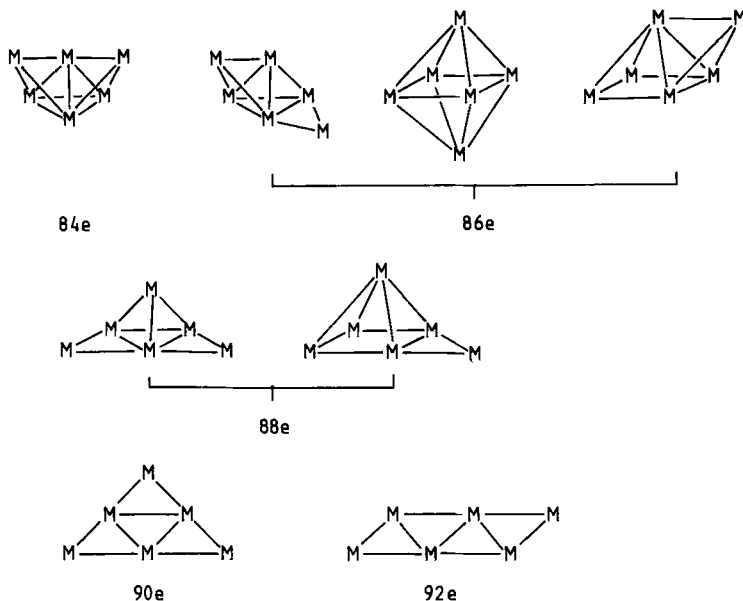


FIG. 17 (Continued)

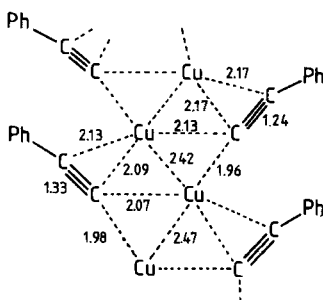
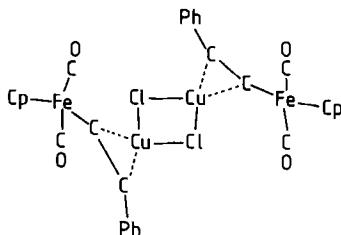


FIG. 18. Structure of phenylethynyl copper. (Bond lengths in Å.)

olefinic C=C bond lies in the plane of the metal triangle (106, 263, 405–408). In these clusters the substituents range from hydrogen to CF_3 groups, and in the case of $\text{Ru}_3(\text{CO})_{10}(\mu\text{-P-}\eta^2\text{-CH}_2=\text{CHC}_6\text{H}_4\text{PPh}_2)$ (106), a substituted phenyl group; the olefinic C–C distances lie in the range 1.36(4)–1.51(4) Å. The plane defined by the olefinic carbons and the atoms of the substituent groups lie approximately perpendicular to the

FIG. 19. Structure of $[\text{CpFe}(\text{CO})_2(\text{C}\equiv\text{CPh})\text{CuCl}]_2$.

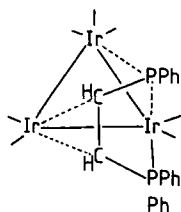
plane of the metal triangle. The C–C–X (substituent) angles show only small deviations from the idealized value of 120° , the largest being in the case of $\text{Ru}_3(\text{CO})_{10}(\mu\text{-P-}\eta^2\text{-CH}_2=\text{CHC}_6\text{H}_4\text{PPh}_2)$ (106), in which the substituent is linked to another coordinating ligand.

A different orientation of the coordinated alkene is observed in the structure of $\text{Ir}_3(\text{CO})_7(\mu\text{-PPhCH=CHPPh}_2)$ (244). The alkene ligand lies above the metal triangle coordinating to one Ir atom while the two substituent P atoms bond to one and two metals, respectively (Fig. 20). The olefinic C–C distance is $1.44(2)$ Å, and the average C–C–P angle is $118(1)^\circ$. The difference in orientation of the alkene presumably results from the interactions of the P substituents with the cluster which are not present in the other alkene-substituted molecules.

Related to the clusters with coordinated alkenes are the diene-substituted complexes $\text{Os}_3(\text{CO})_{10}(\text{cis-C}_4\text{H}_6)$, $\text{Os}_3(\text{CO})_{10}(\text{trans-C}_4\text{H}_6)$ (409), and $\text{Ru}_6\text{C}(\text{CO})_{15}(\text{MeCH=CH-CH=CHMe})$ (60). In these clusters the mode of bonding of the individual olefinic C–C bonds is similar to that of a simple alkene, although in the two latter cases the ligand spans two adjacent metal centers.

1. Interactions of Alkyne Ligands with Two Metal Centers

The simplest type of interaction between an alkyne-derived ligand and two metal centers is mode M1 in Fig. 15. This alkenylidene ligand, which formally donates two electrons to the cluster, has been observed

FIG. 20. Structure of $\text{Ir}_3(\text{CO})_7(\text{PhPCH=CHPPh}_2)$.

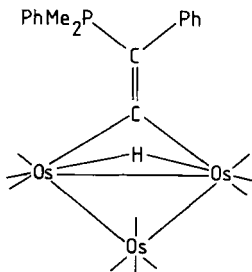


FIG. 21. Structure of $\text{Os}_3(\mu\text{-H})(\text{CO})_{10}(\mu\text{-C}\equiv\text{CPhPMe}_2\text{Ph})$.

in a number of dinuclear complexes (410) but is relatively uncommon in polynuclear species. A recent example appears in the structure of $\text{Os}_3(\mu\text{-H})(\text{CO})_{10}(\mu\text{-C}\equiv\text{CPhPMe}_2\text{Ph})$ (411), which is shown in Fig. 21. The C—C vector lies approximately perpendicular to the metal—metal bond which it spans. The ligand appears to have a strong bond-shortening influence on the bridged metal—metal bond, since this Os—Os bond is ca. 0.07 Å shorter, at 2.802(1) Å, than the two unbridged Os—Os bonds, despite the presence of a bridging hydride along the same Os—Os vector. A hydride bridge normally lengthens a metal—metal bond.

The mode M2, in which an acetylide ligand spans a metal—metal edge and lies perpendicular to the metal—metal vector, has been observed in the trinuclear cluster $\text{Ru}_3(\text{CO})_6(\mu\text{-CCBu}')(\mu\text{-}\eta^2\text{-CCBu}')(\text{PPh}_2)_2$ (113) (Fig. 22). A second $\text{C}\equiv\text{CBu}'$ alkyne ligand adopts bonding mode M4. The Ru—Ru bond bridged by the M2 mode $\text{C}\equiv\text{CBu}'$ group and a PPh_2 ligand is relatively short, at 2.863(1) Å, and the C—C bond length of 1.19(1) Å is indicative of the retention of triple bond character. The same mode of acetylide bonding is observed in the hexanuclear cluster $\text{Cu}_6(\text{C}_6\text{H}_4\text{NMe}_2)_4(\text{CCC}_6\text{H}_4\text{Me})_3$ (263), in which C—C multiple bonding is also retained; C—C 1.18(1) Å.

Bonding mode M3 is truly acetylenic in character, and is common in dinuclear complexes (17). It has been observed in the trinuclear platinum cluster $\text{Pt}_3((\text{PEt}_3)_4(\text{PhCCPh})_2$ (151). The three Pt atoms adopt

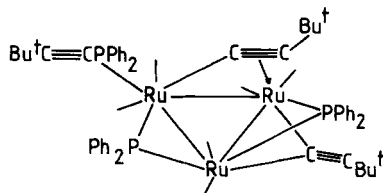


FIG. 22. Structure of $\text{Ru}_3(\text{CO})_6(\text{PPh}_2)_2(\mu\text{-CCBu}')(\mu\text{-}\eta^2\text{-CCBu}')(\text{Ph}_2\text{PCCBu}')$.

an open V-shaped arrangement while the acetylenic units form transverse bridges across the two Pt–Pt vectors on the convex side of the metal V. The C–C bond length is 1.34(3) Å, and the phenyl groups bend away from the metal atoms to give a C–C–Ph angle of 139(1)°.

The bonding mode M4 is again more common for dinuclear species than for polynuclear ones, however, this is the mode of bonding that best describes the coordination of the acetylides in the mixed-metal clusters $\text{Cu}_4\text{Ir}_2(\text{PPh}_3)(\text{CCPh})_8$ (237), $\text{RhAg}_2(\text{CCC}_6\text{F}_5)_5(\text{PPh}_3)_3$ (164), and $[\text{CpFe}(\text{CO})_2(\text{CCPh})\text{CuCl}]_2$ (412), which were discussed previously. Examples are also found in ruthenium chemistry. The cluster $\text{Ru}_3(\text{CO})_6(\mu\text{-CCBu}')(\mu\text{-}\eta^2\text{-CCBu}')(\text{Ph}_2\text{PCCBu}')(\text{PPh}_2)_2$ (113) contains a ligand bonded in this mode, as do the complexes $\text{Ru}_4(\text{CO})_{13}(\mu\text{-}\eta^2\text{-CCBu}')(\mu\text{-PPh}_2)$ and $\text{Ru}_4(\text{CO})_8(\mu\text{-}\eta^2\text{-CCBu}')(\mu_3\text{-}\eta^2\text{-CCBu}')(\text{Ph}_2\text{PC}\equiv\text{CBu}')(\mu\text{-PPh}_2)_2$ (404). The structures of these two compounds are illustrated in Fig. 23. The $\mu\text{-}\eta^2\text{-C}\equiv\text{CBu}'$ ligands act as three-electron donors so that the two complexes are 64-electron systems. This results in an almost planar “butterfly” metal framework with a dihedral angle in the range 167–178°, and contrasts with the 62-electron alkyne-substituted “butterfly” clusters which will be discussed in Section IV,C,2. A 64-electron cluster, by normal electron counting rules, would be expected to have four metal–metal bonds. In this case there appears to be a lengthening of all five metal–metal bonds in the “butterfly” framework.

There are eight cluster complexes that exhibit bonding mode M5. The ligand may be described as an alkenyl group and formally donates three electrons to the cluster via one σ and one π bond. The reported structures include neutron diffraction studies on $\text{Os}_3(\mu\text{-H})(\text{CO})_{10}(\text{HC}=\text{CH}_2)$ (388) and $\text{Os}_4(\mu\text{-H})_3(\text{CO})_{11}[\text{HC}=\text{C}(\text{H})\text{Ph}]$ (186), and relevant bond parameters are displayed in Table III (52, 91, 186, 192, 195, 338, 413, 414).

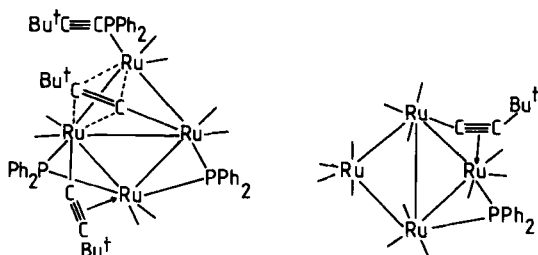
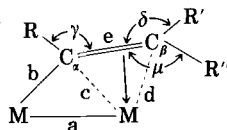


FIG. 23. Structures of $\text{Ru}_4(\text{CO})_{13}(\mu\text{-}\eta^2\text{-C}\equiv\text{CBu}')(\mu\text{-PPh}_2)$ and $\text{Ru}_4(\text{CO})_8(\mu\text{-}\eta^2\text{-C}\equiv\text{CBu}')(\mu_3\text{-}\eta^2\text{-C}\equiv\text{CBu}')(\text{Ph}_2\text{PC}\equiv\text{CBu}')(\mu\text{-PPh}_2)_2$.

TABLE III

PARAMETERS IN CLUSTERS CONTAINING LIGANDS WHICH DISPLAY BONDING MODE M5^a

Compound	a (Å)	b (Å)	c (Å)	d (Å)	e (Å)	γ (degrees)	δ (degrees)	μ (degrees)	Reference
$\text{Os}_3\text{H}(\text{CO})_{10}(\text{HC}=\text{CH}_2)$	2.845(2)	2.107(3)	2.273(3)	2.362(3)	1.396(4)	113.9(3)	121.0(4)	121.6(3)	388
$\text{Os}_4\text{H}_3(\text{CO})_{11}(\text{HC}=\text{CHPh})$	2.830(3)	2.15(1)	2.15(1)	2.30(1)	1.36(2)	113(1)	122(1)	122(1)	186
$\text{Os}_3\text{H}(\text{CO})_{10}(\text{HC}=\text{CHEt})$	2.834(1)	2.15(2)	2.28(2)	2.46(3)	1.40(3)	—	121(4)	—	413
$\text{Os}_3\text{H}(\text{CO})_{10}(\text{HC}=\text{CHBu}')$	2.814(2)	2.10(2)	2.27(2)	2.43(2)	1.38(4)	—	122(2)	—	52
$\text{Os}_3\text{H}(\text{CO})_{10}(\text{PhC}=\text{CHPh})$	2.820(3)	2.11(4)	2.34(4)	2.44(4)	1.40(5)	117(3)	131(3)	—	91
$\text{Os}_3\text{H}(\text{CO})_{11}(\text{PEt}_3)$	2.848(2)	2.16(3)	2.24(3)	2.20(3)	1.41(4)	—	—	—	414
$\text{FeCo}_3(\text{CO})_9(\text{PhC}=\text{CHPh})$ ($\text{F}_3\text{CC}=\text{CCF}_3$)	2.369(4)	1.98(1)	2.00(1)	2.13(1)	1.42(2)	121(1)	126(1)	—	195
$\text{Ir}_7(\text{CO})_{12}(\text{C}_8\text{H}_{12})(\text{C}_8\text{H}_{11})$ (C_8H_{10})	2.665(2)	2.02(3)	2.18(3)	2.29(4)	1.51(5)	—	—	—	192

^a Parameters refer to:

In all the complexes the vinylic C–C distances indicate a formal bond order of less than two, consistent with π donation to the cluster. For the six compounds which also contain a hydrido bridge the complexes may be considered as derived from the interaction of a nonhydrido cluster with an alkene $\text{HRC}=\text{CR}'\text{R}''$, with resultant migration of an alkene hydrogen to the cluster cage. The orientation of the stilbenyl ligand in $\text{Os}_3\text{H}(\text{CO})_{10}(\text{PhC}=\text{CHPh})$ (91) differs from that in the vinyl complexes where the hydrogen atom on the α carbon of the ligand is syn with respect to the σ -bonded Os atom. The phenyl substituent on the α carbon is anti with respect to the same metal atom. Therefore, in the vinyl derivatives with the α carbon bridging one side of the metal triangle, the β carbon points outside the triangle, whereas in the stilbenyl derivative (91), the β carbon points inside the triangle. This is not the case with the "butterfly" cluster $\text{FeCo}_3(\text{CO})_9(\text{PhC}=\text{CHPh})(\text{PhCCPh})$ (195), in which the stilbenyl group adopts the same orientation with respect to the FeCo_2 face as the vinyl.

The molecule $\text{Ru}_3(\text{CO})_7[(\text{CCBu}')(\text{PhC}=\text{CHPh})](\text{PhCCPh})$ (141) contains a stilbenyl ligand related to that just described, except that the group is σ bonded to a C atom of the CCBu' group rather than a metal; this C–C distance is 1.45(2) Å. A *t*-butylacetylene derivative is also known (46).

For alkyne-derived ligands the only other type of coordination involving only two metal centers in a cluster is mode M15. Here the ligand bridges a metal–metal vector by forming a σ bond to each metal, and formally acts as a two-electron donor. This alkyne-derived ligand closely resembles an alkene with two cis substituents replaced by metal atoms. The bonding arrangement has been observed in the planar cluster $\text{Ir}_4(\text{CO})_8[\text{C}_2(\text{COOMe})_2]_4$ (205), whose structure is illustrated in Fig. 24. The acetylenic C atoms of the M15 bonded ligands lie in the Ir_4 plane with the C–C bond parallel to the bridged Ir–Ir bonds. The acetylenic C–C bond lengths of 1.28(1) Å suggests a relatively high bond order, and the bridged Ir–Ir bonds, at 2.715(1) Å, are shorter than the other two Ir–Ir bonds [2.810(1) Å]. The cluster is a 64-electron complex and the planar metal arrangement is consistent with this electron count. The complex also contains two M16 bonded ligands.

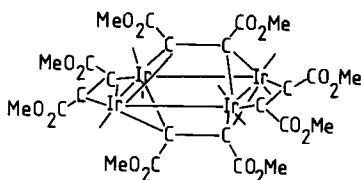


FIG. 24. Structure of $\text{Ir}_4(\text{CO})_8[\text{C}_2(\text{COOMe})_2]_4$.

2. Interactions of Alkyne Ligands with Three Metal Centers

There are more examples of alkyne-derived ligands interacting with a triangle of metal atoms in a cluster than with any other metal arrangement. The triangles may be held together by direct metal-metal interactions or there may be relatively little bonding between them, and the nuclearity of the cluster containing the alkyne-capped unit may range from three to seven.

The first of these bonding modes is denoted M6 and is illustrated in Fig. 15. In this case the alkyne bonds to two different metal atoms via σ bonds, one from each acetylenic carbon, and to the third metal via a π bond. It is generally considered to donate four electrons to the cluster. This mode of bonding causes the acetylenic C-C bond to lie approximately parallel to an edge of the metal triangle, and for this reason it is often given the notation $\mu_3-(\eta^2-||)$ when the ligand arrangement is discussed.

The mode M6 has been reported in a variety of homo- and heteronuclear clusters and is one of the most common modes to have been observed. Both mono- and disubstituted alkynes adopt this geometry and the hydrogen is not transferred to the cluster framework. Not only is this geometry found in simple alkyne-substituted clusters but the coordinated ligand may form part of a cyclodienyl or aromatic ring system, such as in $\text{Ru}_3(\mu\text{-H})_2(\text{CO})_9(\text{C}_8\text{H}_{12})$ (415) or $\text{Os}_3(\mu\text{-H})_2(\text{CO})_9(\text{C}_6\text{H}_4)$ (416). Table IV lists a number of the structurally characterized clusters of this general type together with some relevant bond lengths. The structures of a few examples of complexes exhibiting this bonding mode are illustrated in Fig. 25. A number of trends are evident from these results. The acetylenic C-C bond lengths lie in the range 1.33–1.47 Å, which suggests that the formal bond order is less than two. The two acetylenic carbons and their substituent atoms remain approximately planar in all the complexes despite the asymmetry of the coordination of the alkyne, which may in some cases be attributed to the heterometallic character of the triangle which it caps. As expected, in general, the metal-carbon σ bonds are slightly shorter than the metal-carbon π bonds. It is interesting to note that in a number of the homonuclear clusters, where there are no other groups bridging metal-metal vectors, one of the metal-metal bonds involving the unique metal atom is particularly short. This suggests that the coordination of the alkyne is placing electrons in an orbital which is strongly bonding between this pair of metal atoms.

The bonding mode M7 may be considered as derived from M6 by a shift of one of the substituent groups so that both are coordinated to the

TABLE IV

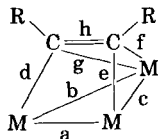
BOND LENGTHS IN $\mu_3\text{-(}\eta^2\text{-)}\text{--ALKYNE SUBSTITUTED CLUSTERS}$

Compound	Bond lengths (Å) ^a				Ref.
	a d	b e	c f	h g	
Cp ₃ Rh ₃ (CO)(PhCCPh)	2.674(1) 2.022(8)	2.655(1) 2.040(7)	2.638(1) 2.110(7)	1.39(1) 2.154(8)	59
Cp ₃ Rh ₃ (CO)[(C ₆ F ₅)CC(C ₆ F ₅)	2.672(1) 2.03(1)	2.599(2) 2.02(1)	2.588(1) 2.09(1)	1.41(2) 2.09(1)	59
Fe ₃ (CO) ₈ (PhCCPh) ₂ ^b	2.469(5) 2.04(2)	2.457(5) 2.06(2)	2.592(5) 1.98(2)	1.39(3) 1.97(2)	27
Ru ₃ (CO) ₇ [(C ₂ Bu')(PhC ₂ HPh) (PhCCPh)]	2.839(5) 2.33(2)	2.682(7) 2.07(2)	2.812(3) 2.10(2)	1.37(2) 2.21(2)	141
Ru ₃ H ₂ (CO) ₈ (HCCC ₆ H ₄ PPh ₂)	3.021(1) 2.098(7)	2.874(1) 2.085(6)	2.731(1) 2.262(7)	— 2.289(7)	106
Ru ₃ H(CO) ₉ (PPh ₂)(PhCCPh)	3.838(1) 2.118(8)	2.813(1) 2.168(7)	2.908(1) 2.274(7)	1.415(11) 2.341(8)	104
Os ₃ (CO) ₁₀ (PhCCPh)	2.888(1) 2.182(8)	2.844(1) 2.070(9)	2.711(1) 2.188(8)	1.44(1) 2.293(9)	417
Os ₃ (CO) ₇ (C ₂ Ph ₂) ₂ (PhC ₂ Ph)	2.680(2) 2.16(2)	2.814(2) 2.08(2)	2.744(2) 2.22(2)	1.33(3) 2.28(2)	34
Os ₃ (CO) ₉ (CH ₂)(PhCCPh)	2.763(1) 2.13(2)	2.765(1) 2.14(2)	2.738(1) 2.27(2)	1.37(3) 2.28(2)	418
Os ₃ H(CO) ₉ (HCCPMe ₂ Ph)	2.980(1) 2.13(1)	2.795(1) 2.06(2)	2.766(1) 2.27(2)	1.41(2) 2.25(2)	411
Os ₃ H(CO) ₉ (MeCCCH ₂ PMe ₂ Ph)	2.987(1) 2.13(2)	2.749(1) 2.13(2)	2.761(1) 2.25(2)	1.42(3) 2.29(2)	411
Ni ₃ (CO) ₃ (C ₈ H ₈)(F ₃ CCCCF ₃)	2.703(2) 1.901(8)	2.458(2) 1.895(9)	2.458(2) —	1.38(1) —	365
MnFe ₂ (CO) ₈ Cp(HCCCCOMe)	2.679(1) 1.973(3)	2.561(1) 1.967(3)	2.577(1) 2.063(3)	1.362(4) 2.094(3)	152
NiFe ₂ (CO) ₆ Cp(PhCCPh) ⁻	2.474(1) 1.918(5)	2.453(1) 1.970(5)	2.506(1) 2.014(5)	1.383(7) 2.104(6)	135
FeCo ₂ (CO) ₉ (EtCCEt)	2.576(1) 1.961(6)	2.479(1) 1.957(6)	2.489(1) 2.047(6)	1.37(1) 2.035(7)	56
NiCoFe(CO) ₅ Cp(PPh ₃)(PhCCPh)	2.486(4) 1.93(2)	2.467(4) 2.03(2)	2.390(4) —	— —	148
NiFeMo(CO) ₅ Cp ₂ (PhCCCCO ₂ C ₃ H ₇) ^c	—	—	—	—	419
NiFeCo(CO) ₆ Cp(PhCCCCO ₂ C ₃ H ₇) ^c	—	—	—	—	419
Ni ₂ Fe(CO) ₃ Cp ₂ (PhCCCCO ₂ C ₃ H ₇) ^c	—	—	—	—	419
Co ₂ Ru(CO) ₉ (HCCMe)	2.699(1) —	2.591(2) —	2.459(2) —	1.34(1) —	57
Co ₂ Ru(CO) ₉ (PhCCPh)	2.688(1) 2.124(2)	2.587(1) 1.976(2)	2.454(1) 2.080(2)	1.370(3) 2.072(2)	199
Ru ₂ Ni(CO) ₄ Cp ₂ (PhCCPh)	2.553(2) 1.926(5)	2.550(3) 2.075(5)	2.712(3) 2.148(6)	1.383(7) 2.091(7)	136
OsW ₂ (CO) ₇ Cp ₂ (TolCCTol) ^d	3.159(2) 2.117(19)	2.863(2) 2.111(24)	2.839(2) 2.320(20)	1.47(3) 2.306(21)	166

TABLE IV (Continued)

Compound	Bond lengths (Å) ^a				Ref.
	a d	b e	c f	h g	
Two isomers	2.981(2)	2.981(2)	3.017(2)	1.43(3)	
OsW ₂ (CO) ₇ Cp ₂ (TolCCTol) ^d	2.198(18)	2.052(20)	2.208(21)	2.304(18)	162
	3.158(1)	2.857(1)	2.836(1)	1.46(3)	
	2.187(18)	2.180(20)	2.229(19)	2.268(19)	
Two isomers	2.987(1)	2.817(1)	3.016(1)	1.42(3)	
(separate determinations ^b)	2.202(18)	2.090(21)	2.284(21)	2.365(19)	
OsPt ₂ (CO) ₅ (PPh ₃) ₂ (MeCCMe)	3.033(2)	2.662(2)	2.662(2)	1.40(1)	203
	2.060(8)	2.055(7)	2.22(1)	2.23(1)	
Os ₃ WH(CO) ₁₀ (TolCCTol)	2.922(3)	2.823(3)	2.775(3)	—	201
	2.21(5)	2.17(4)	2.18(4)	2.13(4)	
Os ₅ (CO) ₁₇ (HCCH)	2.957(3)	2.908(3)	2.715(3)	1.39(4)	227
	2.23(3)	2.09(3)	2.13(3)	2.29(3)	
Os ₅ (CO) ₁₃ (PhCCPh) ₂	2.664(2)	2.768(2)	2.747(2)	1.39(4)	224
	2.09(2)	2.15(2)	2.21(2)	2.24(2)	
Os ₆ (CO) ₁₆ (MeCCEt)	2.817(2)	2.780(2)	2.769(2)	1.35(6)	230
	2.25(4)	2.16(4)	2.25(4)	2.09(5)	

^a Bond lengths refer to the following structure:

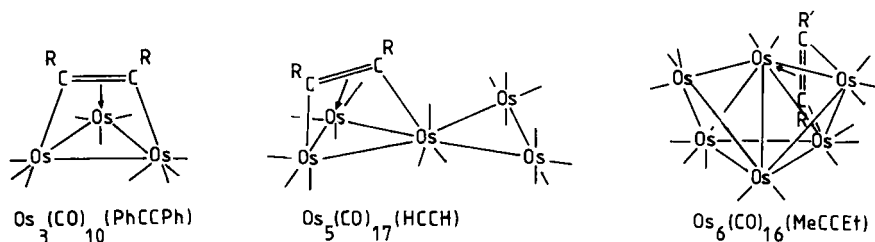
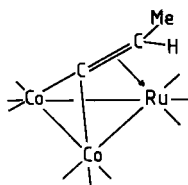
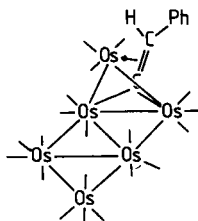


^b Values averaged over two alkynes in the same cluster.

^c Bond parameters not available.

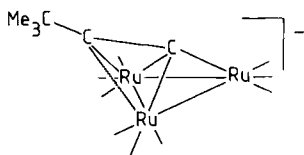
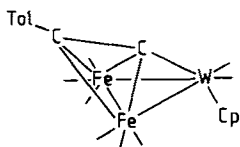
^d Two independent determinations of the same structure.

same acetylenic carbon atom. The α carbon of the alkyne-derived ligand then bonds to two metal atoms via σ interactions, and the unsaturated C–C bond formally donates a pair of electrons to a third metal atom via a π interaction. This type of coordinated ligand has been characterized spectroscopically in a variety of complexes (420) but there have been a relatively small number of crystal structures showing this feature. Four examples are Os₃H₂(CO)₉(C=CH₂) (66), Co₂Ru(CO)₉(C=CHMe) (57)

FIG. 25. Structures of clusters containing $\mu_3-(\eta^2-||)$ -alkyne ligands.FIG. 26. Structure of $\text{Co}_2\text{Ru}(\text{CO})_9(\text{C}=\text{CHMe})$.FIG. 27. Structure of $\text{Os}_6(\text{CO})_{20}(\text{C}=\text{CHPh})$.

(Fig. 26), $\text{Os}_6(\text{CO})_{20}(\text{C}=\text{CHPh})$ (231) (Fig. 27), and $\text{Ru}_3(\text{CO})_9(\text{AuPPh}_3)_2(\text{C}=\text{CHBu}')$ (15). In these structures the acetylenic C-C bond lengths lie in the range 1.32–1.42 Å, and the metal-carbon σ bonds are slightly shorter than the π interactions. The C=CHR plane lies approximately parallel to the capped metal triangle, and the C-C-R angles show only small deviations from the expected angle of 120° for an sp^2 -hybridized carbon atom.

The ligands which adopt bonding mode M8 are best considered as acetylides. They formally donate five electrons to the metal framework via one σ and two π bonds. The orientation of the C-C multiple bond is approximately perpendicular to one side of the capped triangle and is often described by the notation $\mu_3-(\eta^2-\perp)$. Some examples of clusters containing this mode of coordination are listed in Table V together with

FIG. 28. Structure of the anion $[\text{Ru}_3(\text{CO})_9(\text{C}\equiv\text{CBu}')]\text{ }^{-}$.FIG. 29. Structure of $\text{CpWFe}_2(\text{CO})_6(\text{C}\equiv\text{CTol})$.

some relevant bond distances. Two examples of these clusters are illustrated in Figs. 28 and 29. Despite the high formal donation of electrons to the cluster from the unsaturated C–C bond, these bond lengths remain relatively short, lying in the range 1.27–1.32 Å, in comparison with distances in complexes having ligands which adopt bonding modes M6 and M7. As in related clusters the metal–carbon σ bond is significantly shorter than the π distances, and in this case the distances to the β carbon atom are longer than the distances to the α carbon atom. This generally results in the unsaturated C–C bond leaning away from the metal triangle which it caps. The average acetylide C–C–R angle of 140° in these complexes is significantly greater than the equivalent angle in ligands which adopt the related mode M7. This is consistent with a different formal hybridization on the β carbon atom.

There are four clusters which contain the related $\mu_3(\eta^2\text{-}\perp)$ -alkyne ligand in which the alkyne-derived ligand is coordinated to a metal triangle via one σ and two π bonds (bonding mode M9). In the complexes $\text{Fe}_3(\text{CO})_9(\text{PhCCPh})$ (26) (Fig. 30), $\text{Ni}_4(\text{NCBu}')_4(\text{PhCCPh})_3$ (424), $\text{Ni}_4(\text{CO})_4(\text{CF}_3\text{CCCF}_3)_3$ (365), and $\text{Cp}_2\text{W}_2\text{Fe}(\text{CO})_6(\text{MeC}_6\text{H}_4\text{CCC}_6\text{H}_4\text{Me})$ (166), the acetylenic C–C bonds range from 1.27 to 1.41 Å, but, in

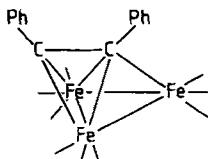
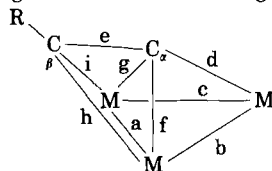
FIG. 30. Structure of $\text{Fe}_3(\text{CO})_9(\text{PhC}\equiv\text{CPh})$.

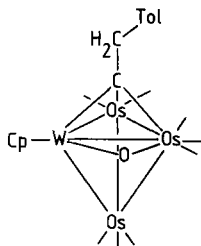
TABLE V
BOND LENGTHS IN $\mu_3\text{-(}\eta^2\text{-}\perp\text{)-ALKYNE}$ SUBSTITUTED CLUSTERS

Compound	Bond lengths (Å) ^a					Reference
	a f	b g	c h	d i	e	
CpFe ₃ (CO) ₇ (C≡CPh)	2.524(1) 2.040(4)	2.632(1) 2.081(5)	2.639(1) 2.006(5)	1.829(6) 2.031(5)	1.299(9)	421
Ru ₃ H(CO) ₉ (C≡CBu')	2.792(3) 2.207(3)	2.795(3) 2.214(3)	2.799(3) 2.268(3)	1.947(3) 2.271(3)	1.315(3)	387
Ru ₃ (CO) ₉ Cl(C≡CPh)	3.277(4) 2.25(2)	2.805(5) 2.30(2)	2.815(5) 2.32(2)	1.95(2) 2.28(2)	1.29(3)	108
[Ru ₃ (CO) ₉ (C≡CBu')] ⁻	2.665(3) 2.18(2)	2.790(3) 2.16(2)	2.800(3) 2.24(2)	1.95(2) 2.24(2)	1.27(3)	422
Ru ₃ H(CO) ₈ (PPh ₂ OEt)(C≡CBu')	2.7988(5) 2.209(4)	2.8212(4) 2.194(4)	2.8407(5) 2.243(4)	1.946(4) 2.252(4)	1.320(6)	114
Ru ₃ (CO) ₉ (PPh ₂)(C≡CPr ⁱ)	3.466(1) —	av. 2.839 —	— —	— —	1.284(8)	130

$\text{Os}_3(\text{CO})_9(\text{PPh}_2)(\text{C}\equiv\text{CPr}^i)$	3.508(1)	av. 2.879	—	—	1.28(1)	130
$\text{Ru}_3(\text{CO})_8(\text{PPh}_2)(\text{C}\equiv\text{CBu}^i)$	2.8257(4)	2.8151(4)	2.7084(4)	—	—	130
$\text{Os}_3\text{H}(\text{CO})_9(\text{C}\equiv\text{CCF}_3)$	2.828(1)	2.872(1)	2.874(1)	2.179(10)	1.331(13)	423
$[\text{Ru}_3(\text{CO})_9(\text{C}\equiv\text{CBu}^i)(\text{HgBr})]_2$	2.262(10)	2.271(10)	2.179(10)	2.181(9)	1.31(3)	146
$\text{Ru}_3\text{H}(\text{CO})_9[\text{CCC}(\text{CH}_2)\text{Ph}]$	2.900(3)	2.813(3)	2.806(2)	1.96(2)	1.27(2)	119
$\text{CpNiFe}_2(\text{CO})_6(\text{C}\equiv\text{CBu}^i)$	2.19(2)	2.20(2)	2.25(2)	2.26(2)	1.28(1)	134
$\text{CpWFe}_2(\text{CO})_8(\text{C}\equiv\text{CTol})$	2.791(2)	2.810(2)	2.812(2)	1.904(14)	1.30(2)	426
	2.18(2)	2.19(2)	2.19(1)	2.28(1)		
	2.378(3)	2.564(3)	2.610(3)	1.813(10)		
	2.010(10)	1.929(10)	2.060(10)	2.034(10)		
	2.503(3)	2.874(3)	2.897(2)	1.999(15)		
	2.025(11)	2.011(11)	2.091(13)	2.086(12)		

^a Bond lengths refer to the following structure:



FIG. 31. Structure of $\text{CpWOs}_3(\text{CO})_8(\mu\text{-O})(\mu_3\text{-CCH}_2\text{Tol})$.

contrast to compounds containing ligands which exhibit bonding mode M8, the metal-carbon π interactions are shorter than or similar in length to the metal-carbon σ bonds.

Clusters which contain ligands that adopt bonding mode M10 are closely related to the capped alkylidyne clusters which have been structurally reviewed elsewhere (16, 17). There are, however, three complexes in which the β carbon atom carries two hydrogen and an organic group, and may be considered as derived from an alkyne without fragmentation of the acetylenic C-C bond. In $\text{Ru}_3(\mu\text{-H})_3(\text{CO})_9(\mu_3\text{-CCH}_2\text{Bu}')$ (425), the $\text{Ru-C}(\alpha)$ distances show slight asymmetry [2.091(5)–2.116(5) Å], and the $\text{C}(\alpha)\text{-C}(\beta)$ bond length of 1.525(9) Å indicates a reduction in the formal bond order to close to unity. Similar trends are observed in $\text{CpWOs}_3(\text{CO})_8(\mu\text{-O})(\mu_3\text{-CCH}_2\text{Tol})$, shown in Fig. 31, where the metal-carbon(α) distances are W-C 2.030(12), Os-C 2.100(10) and 2.291(12) Å (427), and in $\text{Ru}_5(\text{CO})_{12}(\mu_4\text{-PPh})(\mu\text{-PPh}_2)(\mu_3\text{-CH}_2\text{Pr}^i)$ (428).

It is interesting to note the change in angle between the capped metal triangle and the unsaturated C-C bond vector as the mode of coordination of the organic group to the cluster changes. For example, the C-C bond in M7 type clusters is approximately parallel to the plane of the triangle. In M8 type clusters the β carbon is significantly further from the triangle than the α carbon but remains bonded to it. In M10 type clusters the C-C vector is approximately perpendicular to the plane of the triangle. This progressive change of orientation of the organic ligand may perhaps reflect steps in a reaction pathway which could be related to the catalytic adsorption of alkyne ligands on a metal surface.

3. Interactions of Alkyne Ligands with Four-Metal Centers

There are now quite a number of examples of alkyne-derived ligands interacting with four-metal centers. It is sterically difficult for an alkyne to interact with all four metal atoms of a closed tetrahedral

arrangement, but it is possible for an alkyne to interact with an open "butterfly" cluster or with a planar rectangle of metal atoms. In terms of formal electron counting a closed tetrahedron is normally associated with 60 electrons, a "butterfly" arrangement with 62 electrons, and a rectangular arrangement with 64 electrons. As with trinuclear clusters, while the alkyne, in this case, interacts with four metal atoms, the nuclearity of the cluster may be higher, and examples with five or six metals are known.

The bonding mode M11, in which the acetylenic $\text{C}\equiv\text{C}$ bond lies approximately parallel to the "hinge" metal-metal bond of the "butterfly" to give a distorted M_4C_2 octahedron, is one of the most commonly observed modes for tetrametal clusters. This view of the cluster core as an octahedron allows the structures of these complexes to be rationalized in terms of Wade's Rules (400). The alkyne is coordinated to the two "hinge" metal atoms via what may be considered as σ bonds, and to the two "wingtip" metal atoms via π bonds. A number of clusters exhibiting this bonding mode are listed in Table VI together with some relevant structural parameters. It will be noted that the dihedral angle between the "wings" of the "butterfly" remains approximately constant despite the variations in metallic types and nuclearity of the clusters. The acetylenic C-C lengths in this group of compounds show considerable variations, ranging from 1.34(1) to 1.55(4) Å. However, the estimated standard deviations on $\text{Os}_4(\text{CO})_{12}(\text{HCCH})$ (Fig. 32) and $\text{Os}_4(\text{CO})_{12}(\text{HCCEt})$ (67) are rather high and a shorter distance would be more consistent with the other structures.

A related molecule to those listed in Table VI is $\text{Ru}_4(\text{CO})_{11}(\text{C}_8\text{H}_{10})$ (182), in which one unsaturated bond of the octadiene occupies the capping site to make up the octahedron while the other π bonds to one Ru atom (Fig. 33).

The bonding mode M12 may be considered to be related to M7 except that the α carbon of the acetylidyde coordinates to three metal atoms rather than two. In both types the plane defined by the acetylidyde carbons and the two substituent atoms bonded to the β carbon is approximately

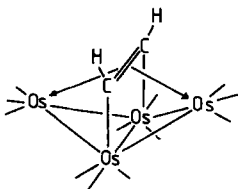


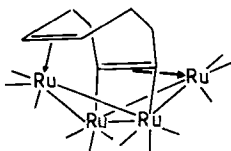
FIG. 32. Structure of $\text{Os}_4(\text{CO})_{12}(\text{HCCH})$.

TABLE VI

STRUCTURAL PARAMETERS IN ALKYNE-SUBSTITUTED "BUTTERFLY" CLUSTERS WHICH ADOPT BONDING MODE M11

Compound	M–M bond lengths (Å)		Acetylenic	Dihedral	Reference
	av. Hinge–wingtip	Hinge–hinge	C–C length (Å)	angle (degrees)	
Co ₄ (CO) ₁₀ (EtCCEt)	2.434	2.522	1.44	118	207
Ru ₄ (CO) ₁₂ (MeCCMe)	2.719	2.880(1)	1.45(1)	116.9	60
Ru ₄ (CO) ₁₂ (PhCCPh)	2.73	2.85(1)	1.46(2)	115.5	40
Os ₄ (CO) ₁₂ (HCCH)	2.793	2.847(2)	1.55(4)	—	67
Os ₄ (CO) ₁₂ (HCCEt)	2.756	2.849(2)	1.54(3)	—	67
Os ₅ (CO) ₁₃ (PhCCPh) ₂	2.734	2.910(2)	1.46(3)	115	224
Os ₆ (CO) ₁₆ C(MeCCMe)	2.826	2.745(4)	1.36(2)	—	229
FeRu ₃ (CO) ₁₂ (PhCCPh)(1st isomer)	2.681 ^a	2.780(1)	1.460(3)	112.7	198
FeRu ₃ (CO) ₁₂ (PhCCPh)(2nd isomer)	2.678 ^a	2.849(1)	1.458(4)	117	198
Ru ₂ Co ₂ (CO) ₁₁ (PhCCPh)	2.595 ^a	2.757(1)	1.432(5)	—	196
RuCo ₃ (CO) ₉ (PPh ₂)(HCCBu')	2.505 ^a	2.776(1)	1.424(5)	115.2	221
[RuCo ₃ (CO) ₁₀ (PhCCPh)] [−]	2.505 ^a	2.725(2)	1.34(1)	115.2	199
FeCo ₃ (CO) ₉ [PhC ₂ (H)Ph](PhCCPh)	2.432 ^a	2.670(4)	1.41(2)	118	195
Ru ₄ (CO) ₁₁ (HCCC ₆ H ₄ PPh ₂)	2.744	2.823(1)	1.455(11)	—	429

^a Averaged M–M bond lengths in mixed-metal clusters.


 FIG. 33. Structure of $\text{Ru}_4(\text{CO})_{11}(\text{C}_8\text{H}_{10})$.

parallel to that of the metal triangle over which it lies and with which there is an interaction. This type of ligand is considered to be a four-electron donor although the interaction with the three metal atoms that are capped by the α carbon must be delocalized. This mode of bonding is observed most frequently in mixed-metal clusters, and a number of examples of homo- and heterometal clusters are presented in Table VII. The acetylide C–C lengths in these clusters indicate a reduction in the formal bond order to less than two, and on average these distances are shorter than those found for ligands which adopt bonding mode M7. This suggests a greater donation to the metal framework in the former case. However, the most interesting feature of these compounds is the increase in dihedral angle of the “butterfly wings” and the lengthening of the two hinge metal atoms on the addition of two more electrons, thus indicating a progression toward a planar metal arrangement. Examples of the 74- and 76-electron complexes are shown in Fig. 34.

Related to bonding mode M12 is mode M13 where a ligand, best described as an acetylide, bonds to a “butterfly” metal framework by forming what may be considered σ bonds to one “hinge” and one “wingtip” metal atom and π bonds to the other two metal atoms. This mode of coordination has been observed in the pentanuclear mixed-metal cluster $\text{NiRu}_4(\text{CO})_9(\mu\text{-PPh}_2)_2(\text{C}\equiv\text{CPr}^i)_2$ (242), in which the dihedral angle between the “wings” of the Ru_4 “butterfly” is only 95.6° ,

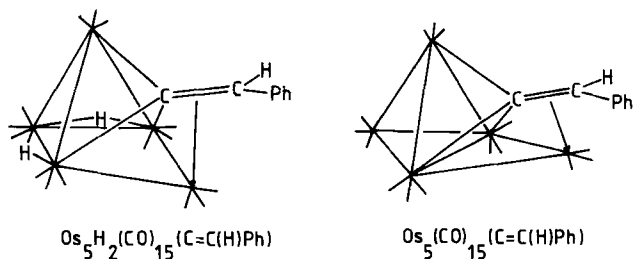
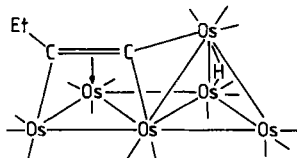

 FIG. 34. Structures of $\text{Os}_5(\text{CO})_{15}[\text{C}=\text{C}(\text{H})\text{Ph}]$ and $\text{Os}_5\text{H}_2(\text{CO})_{15}[\text{C}=\text{C}(\text{H})\text{Ph}]$.

TABLE VII

ALKYNE-SUBSTITUTED CLUSTERS WHICH ADOPT BONDING MODE M12

Compound	Electron count	M-M Bond Lengths (Å)		C-C bond lengths (Å)	"Butterfly" dihedral angle (degrees)	Reference
		av. Wingtip-hinge	Hinge-hinge			
$\text{CpCo}_3\text{Fe}(\text{CO})_9(\text{C}=\text{CH}_2)^a$	62	2.540	2.456(3)	1.431(12)	—	285
$\text{CpRu}_3\text{Ni}(\text{CO})_9[\text{C}=\text{C}(\text{H})\text{Bu}^i]^{a,b}$	61	2.687	2.825(2)	1.436(13)	116.6	215
$\text{CpRu}_3\text{Ni}(\text{CO})_9\text{H}[\text{C}=\text{C}(\text{H})\text{Pr}^i]^a$	62	2.692	2.843(1)	1.417(8)	118.3	217
$\text{CpOs}_3\text{Ni}(\text{CO})_9\text{H}[\text{C}=\text{C}(\text{H})\text{Bu}^i]^a$	62	2.699	2.855(2)	1.44(3)	117.1	211
$\text{Ru}_4(\text{CO})_{10}(\text{OH})(\text{PPh}_2)[\text{C}=\text{C}(\text{H})\text{Pr}^i]$	64	2.766	3.456(1)	1.415(2)	141.5	131
$\text{Ru}_4(\text{CO})_{10}(\text{OEt})(\text{PPh}_2)[\text{C}=\text{C}(\text{H})\text{Pr}^i]$	64	2.758	3.455(1)	—	143.7	131
$\text{Os}_5\text{H}_2(\text{CO})_{15}[\text{C}=\text{C}(\text{H})\text{Ph}]^c$	76	2.872	3.783(2)	1.49(3)	144.1	224
$\text{Os}_5(\text{CO})_{15}[\text{C}=\text{C}(\text{H})\text{Ph}]$	74	2.844	2.830(1)	1.51(3)	115.2	231

^a Averaged mixed-metal bond lengths.^b Reformulated as $\text{CpRu}_3\text{Ni}(\text{CO})_9\text{H}[\text{C}=\text{C}(\text{H})\text{Bu}^i]$ (217).^c Averaged over two independent molecules.

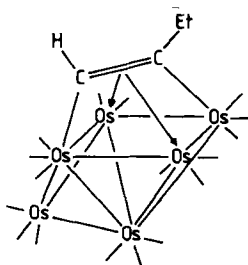
FIG. 35. Structure of $\text{Os}_6(\mu\text{-H})(\text{CO})_{17}(\text{C}\equiv\text{CEt})$.

and the two independent acetylenic C–C distances are 1.34(3) and 1.38(4) Å, respectively.

Another mode of coordination of an alkyne to four-metal centers which may be considered as derived from a “butterfly” geometry is bonding mode M14. In this case it is not the “hinge” bond which has lengthened to form a rectangular arrangement but a “hinge–wingtip” bond which results in a “spiked-triangular” array of metal atoms. This arrangement has been observed in several clusters which contain organic ligands derived from alkynes. These include $\text{Cp}_2\text{Ni}_2\text{Ru}_2(\text{CO})_6[\text{C}_2(\text{H})\text{C}(\equiv\text{CH}_2)\text{CH}_3]$ (218) and $\text{Cp}_2\text{Ni}_2\text{Fe}_2(\text{CO})_6[\text{C}_2(\text{H})\text{C}(\equiv\text{CH}_2)\text{CH}_3]$ (213). There is also one example of an alkyne-substituted cluster with this geometry, $\text{Os}_6(\mu\text{-H})(\text{CO})_{17}(\text{CCEt})$ (230), shown in Fig. 35. The coordination of the alkyne is reminiscent of bonding mode M6, except that one of the R groups has been replaced by a bond to a metal. The relevant C–C–Et and C–C–Os angles do not differ significantly from those in M6-bonded complexes.

In the context of these structures it is interesting to compare the geometries of alkynes bonded to metal clusters and those bound to metal surfaces. While the more common bonding modes such as M6 and M11 may represent models of acetylenes bonded to well-defined metal planes, the less common modes such as M14 and M19 may be representative of the type of bonding that occurs at dislocations on the metal surface.

Turning to modes of alkyne coordination where the metal arrangement is considered to be essentially planar, the structure of $\text{Ir}_4(\text{CO})_8[\text{C}_2(\text{COOMe})_2]_4$ (205) contains two alkyne ligands which exhibit bonding mode M16. The structure was shown in Fig. 24, and it is interesting to note that the acetylenic C–C bond lengths for the two tetracoordinated ligands are significantly longer [1.446(9) Å] than for the two edge-bridging alkynes [1.278(11) Å], which display bonding mode M15. This complex is a rare example of a cluster where the same ligand adopts two different bonding modes in the same molecule.

FIG. 36. Structure of $\text{Os}_6(\text{CO})_{17}(\text{HCCEt})$.

A number of tetra-, penta-, and hexanuclear clusters have been characterized, in which the alkyne-derived ligand adopts bonding mode M17. This mode may be considered a derivative of mode M11 in that addition of further electron pairs has lengthened the "butterfly hinge" bond and increased the dihedral angle to such an extent that the metal framework is approximately planar. In all these complexes there is a small tetrahedral distortion of the rectangle. The acetylenic C–C bond now lies across the diagonal of the rectangle and forms σ bonds to two opposite corners and π bonds with the other two. The structure of one such cluster, $\text{Os}_6(\text{CO})_{17}(\text{HCCEt})$ (230), is shown in Fig. 36. Some structural parameters for this type of complex are listed in Table VIII. The acetylenic C–C bond length lies in the range found for bonding mode M11 ligands (Table VI), and it is unlikely that the strength of electron donation to the cluster is substantially different.

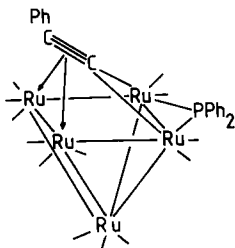
Bonding mode M18 is found in the pentanuclear cluster $\text{Ru}_5(\text{CO})_{13}(\mu\text{-PPh}_2)(\text{C}\equiv\text{CPh})$ (431), shown in Fig. 37. The alkyne-derived ligand which may be considered to be an acetylide is formally σ bonded to two adjacent Ru atoms of the rectangle and involved in a π interaction with the other two; the acetylide C–C bond length is 1.34(1) Å. The acetylide

TABLE VIII

STRUCTURAL PARAMETERS FOR CLUSTERS WHICH CONTAIN ALKYNE-DERIVED
LIGANDS ADOPTING BONDING MODE M17

Compound	Average M–M bond length	Acetylenic C–C length	Reference
$\text{Cp}_2\text{Ni}_2\text{Fe}_2(\text{CO})_6(\text{EtCCEt})^a$	2.420	1.43(2)	210, 419
$\text{Ru}_4(\text{CO})_{11}(\text{MeCCPh})_2$	2.786	1.40(1)	430
$\text{Cp}_2\text{Ni}_2\text{Ru}_3(\text{CO})_8(\text{PhCCPh})^a$	2.570	1.41(1)	431
$\text{Os}_6(\text{CO})_{17}(\text{HCCEt})$	2.862	1.45(2)	230

^a Averaged mixed-metal bond length.

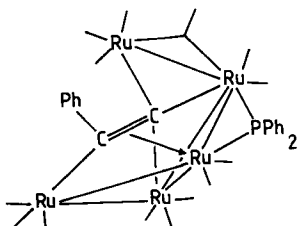
FIG. 37. Structure of $\text{Ru}_5(\text{CO})_{13}(\mu\text{-PPh}_2)(\text{C}\equiv\text{CPh})$.

C-C-C(Ph) angle of $141.4(4)^\circ$ is similar to the average value of 140° found for ligands that adopt the acetylide bonding mode M8.

As has been noted elsewhere (17) the environment of the α carbon atom of the acetylide type ligands such as those observed in bonding modes M8, M13, and M18 resembles, to an extent, that of a carbido carbon. As the nuclearity of the cluster with which the acetylene interacts increases, the similarity between the environments also increases. In the case of $\text{Ru}_5(\text{CO})_{13}(\mu\text{-PPh}_2)(\text{C}\equiv\text{CPh})$ (431), the structure is closely related to the carbido complex $\text{Ru}_5\text{C}(\text{CO})_{15}$ (432).

4. Interactions of Alkyne Ligands with Five-Metal Centers

There are two examples of alkyne-substituted clusters in which there is an interaction between the alkyne and five-metal centers. Both occurrences are found in the related pentanuclear ruthenium complexes $\text{Ru}_5(\text{CO})_{14}(\mu\text{-PPh}_2)(\text{C}\equiv\text{CPh})$ (431) and $\text{Ru}_5(\text{CO})_{12}(\mu\text{-PPh}_2)(\text{PhC}\equiv\text{CC}\equiv\text{CPh})(\text{C}\equiv\text{CPh})$ (104). The ligand in the former complex (Fig. 38) adopts the bonding mode M19 in which the acetylide α carbon caps an Ru_3 triangle, while the β carbons forms a σ bond with a fourth Ru atom, and both acetylide carbons are involved in a π bond to a fifth metal. The acetylide C-C bond length is $1.39(1) \text{ \AA}$, which is longer than the value observed in the cluster $\text{Ru}_5(\text{CO})_{13}(\mu\text{-PPh}_2)(\mu_4\text{-}\eta^2\text{-C}\equiv\text{CPh})$ (431), from which it is prepared. The C-C-C(Ph) angle is $123.6(4)^\circ$, which is similar to that of a coordinated alkyne and ca. 17° less than the

FIG. 38. Structure of $\text{Ru}_5(\text{CO})_{14}(\mu\text{-PPh}_2)(\text{C}\equiv\text{CPh})$.

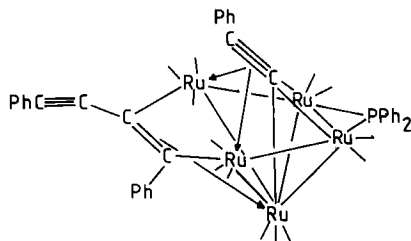


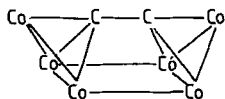
FIG. 39. Structure of $\text{Ru}_5(\text{CO})_{12}(\mu\text{-PPh}_2)(\mu_3\text{-}\eta^2\text{-PhC}\equiv\text{CC}\equiv\text{CPh})(\mu_5\text{-}\eta^2\text{-C}\equiv\text{CPh})$.

acetylide type angle observed in the precursor. The cluster may be considered as a 76-electron species, with the alkyne donating five electrons. The observed "double butterfly" metal framework, with eight formal Ru–Ru bonds, is then consistent with this count.

In the cluster $\text{Ru}_5(\text{CO})_{12}(\mu\text{-PPh}_2)(\text{PhC}\equiv\text{CC}\equiv\text{CPh})(\text{C}\equiv\text{CPh})$ the α carbon atom of the alkyne caps three metal atoms and the acetylenic C–C bond donates π -electron density to the other two metal atoms. This mode of coordination is denoted M20, and the structure of the complex is illustrated in Fig. 39. The $\mu_5\text{-C}\equiv\text{C}$ bond length of 1.340(9) Å is shorter than that in $\text{Ru}_5(\text{CO})_{14}(\mu\text{-PPh}_2)(\mu_5\text{-}\eta^2\text{-C}\equiv\text{CPh})$ but similar to that found in the precursor $\text{Ru}_5(\text{CO})_{13}(\mu\text{-PPh}_2)(\mu_4\text{-}\eta^2\text{-C}\equiv\text{CPh})$. The $\mu_5\text{-C}\equiv\text{C}-\text{C}(\text{Ph})$ angle is 131.6°. The cluster also contains a $\mu_3\text{-}\eta^2\text{-PhC}\equiv\text{CC}\equiv\text{CPh}$ ligand which coordinates through one unsaturated C–C bond in bonding mode M6.

5. Interactions between Clusters and Dicarbide Units

Encapsulated dicarbide clusters of two types have been characterized. Those in which the carbon atoms remain within bonding distance of each other, and those in which the carbon atoms are well separated and occupy separate cavities of a closed metal polyhedron. The former type may be considered to contain an alkyne C–C unit from which all organic substituents have been removed. The closed polyhedral clusters $\text{Rh}_{12}(\text{C}_2)(\text{CO})_{25}$ (433) and $[\text{Co}_{11}(\text{C}_2)(\text{CO})_{22}]^{3-}$ (434), and the open "boat-shaped" cluster $\text{Co}_6(\text{C}_2)(\text{CO})_{14}(\text{S})$ (435), contain this unit. In $\text{Rh}_{12}(\text{C}_2)(\text{CO})_{25}$ (433), the metals adopt a regular polyhedral geometry which may be described in terms of layer packing of atoms. The carbide carbon atoms occupy an irregular cavity with a C–C separation of 1.48(2) Å. There are 14 Rh–C contacts, 9 short and 5 long, with average values of 2.22 and 2.58 Å, respectively. In the anion $[\text{Co}_{11}(\text{C}_2)(\text{CO})_{22}]^{3-}$ (434), the Co polyhedron may be described as a tricapped cube. The C–C separation is 1.62(5) Å, and the Co–C contacts lie in the range 1.86–

FIG. 40. Core geometry of $\text{Co}_6(\mu_6\text{-C}_2)(\mu\text{-CO})_6(\text{CO})_8(\mu_4\text{-S})$.

2.37(3) Å. The peripheral dicarbide cluster $\text{Co}_6(\text{C}_2)(\text{CO})_{14}(\text{S})$ (435) contains a "boat" array of Co atoms, of which the four basal ones form an essentially regular square. The two apical Co atoms are connected through a Co-C-C-Co link; the C-C separation is 1.37(2) Å. These two carbon atoms are also bonded to the four basal Co atoms. The core geometry of the cluster is illustrated in Fig. 40.

V. Fluxionality in Solution

As was mentioned in Section III,C the majority of cluster carbonyls are fluxional molecules. Frequently the nature of the fluxional process is dependent on the temperature, and may involve a varying number of carbonyl groups and hydride ligands, if the latter are present. Examples of alkyne ligands themselves becoming involved in the fluxional processes, however, are comparatively rare. This may stem from the fact that when an alkyne coordinates to two, three, or four metal atoms, there is an extensive formal rehybridization of the carbon atomic orbitals in order to form relatively strong metal-carbon σ bonds. This contrasts with the case of an alkyne bonded to a single metal center. Facile migration would not be expected if terminal and bridging sites differ substantially in energy. Also, if the ligand is a two-electron donor in one coordination mode and a greater-than-two-electron donor in another, facile migration of this ligand is unlikely because of the electronic perturbation at the various metal centers produced in the transition states (4). This argument has been confirmed by the calculations by Hoffman *et al.* (396) on perpendicular and parallel orientations of alkynes in binuclear complexes, which show that interconversions between the modes require a relatively high activation energy.

However, ^1H and ^{13}C NMR studies on a number of alkyne-substituted clusters do show that the alkyne ligand is involved in fluxional processes. ^1H NMR experiments on a range of complexes indicate that a variety of dynamic processes involving hydrogens occur. These include rapid hydride exchange between bridging and terminal positions (41), rotation of the organic fragment bound to the cluster (377), and flipping of the alkyne or alkene (128, 181). A combination of these processes may

take place in a single system (436). The observation of the relative rates of exchange in different dynamic processes taking place within a single molecule may help to discriminate between two possible structures in solution. An example where this has been helpful is in the elucidation of the structure of $\text{Os}_3\text{H}_2(\text{CO})_9(\text{C}=\text{CH}_2)$ (65), in which the rate of exchange of the two vinylidene protons is faster than that of the two hydride ligands, and is consistent with the two latter ligands bridging different Os–Os bonds.

^{13}C NMR has been used to confirm the existence of fluxional processes involving the carbonyl ligands in polynuclear alkyne complexes (40, 330, 339, 437). It is apparent that in the limited number of complexes studied the nature of the dynamic processes is related to the modes of bonding of the organic group (21, 438, 439). It appears that the greater the number of ligands coordinated to a particular metal the higher is the energy barrier that has to be overcome before these ligands become fluxional. For example, in the molecule $\text{Fe}_3(\text{CO})_8(\text{PhCCPh})$, one $\text{Fe}(\text{CO})_2$ unit does not participate in the CO scrambling, and this is believed to be connected with the high formal coordination number for that Fe atom (440).

^{13}C NMR may be used to establish the nature of exchange processes which involve the redistribution of σ and π bonds between the organic group and the metal atoms (441). Flipping (20) and rocking (174) of the coordinated organic group has also been observed, and in some cases enantiomerization of the cluster may be caused by rotation of the ligand about a molecular axis (329).

Combined ^1H and ^{13}C NMR studies indicate that several of the above-mentioned processes may occur simultaneously within a single molecule (442–444). In some instances the solvent appears to have an influence on which dynamic processes predominate under a particular set of conditions (58).

VI. The Reactivity of Alkyne-Substituted Clusters

The reactivity of clusters containing coordinated alkyne or alkyne-derived ligands has not been widely investigated. This review has indicated that quite a significant number of complexes of this type have now been synthesized, but it is important to remember that quite a large proportion of these clusters are obtained in relatively low yield, and it is perhaps this aspect that has hindered further research into their reaction chemistry. However, over the last several years, an increasing number of publications reporting the reactions of alkyne-substituted

clusters have appeared. Common reagents that have been used to investigate the reactivity of these species include carbon monoxide, hydrogen, phosphines, and an excess of the alkynes themselves. These reaction types are discussed below.

A. PYROLYSIS REACTIONS

Thermal activation of alkyne-substituted clusters frequently results in the loss of one or more carbon monoxide ligands (418, 445, 446). Concomitant with this loss is an alteration in the bonding mode of the organic ligand in order to retain the electron balance within the molecule (107). Such a reaction is shown in Fig. 41, where an osmacyclopentadiene ring is transformed into a trisubstituted- η^5 -cyclopentadienyl system. Metal-metal bond formation may take place in some examples (446, 447).

There have also been reports of cluster growth, from trinuclear to tetra- (429) or pentanuclear (448) complexes. However, in these two reactions it is important to note that the clusters involved contain functionalized alkynes. These phosphidoacetylenes show a considerable versatility in their modes of bonding. This is particularly true in the example illustrated in Fig. 42 where different reaction temperatures

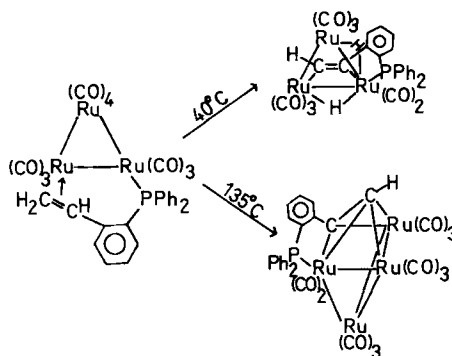


FIG. 41. Reactions of functionalized alkynes.

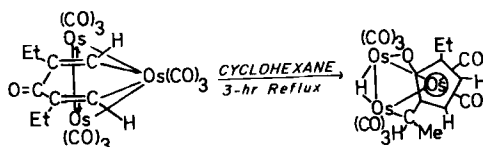


FIG. 42. Thermal activation of alkyne-substituted clusters.

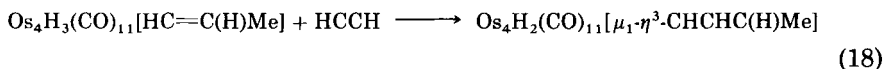
lead to different coordination modes of the ligand and to different nuclearity of the resulting cluster.

Alkyne scission also occurs when a rhodium or iridium trimetallic cluster is heated under vacuum (449).

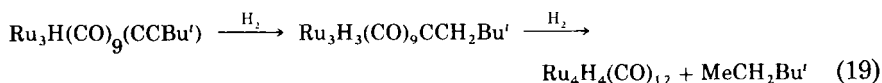
Photochemical activation of an allyl complex results in the loss of carbon monoxide, which leads to the formation of a coordinatively unsaturated species (450).

B. REACTIONS WITH CARBON MONOXIDE AND DIHYDROGEN

Carbonylation reactions may result in the modification of the coordination mode of the organic ligand (407, 451–453). This is sometimes caused by the transfer of hydrides bonded to the metal framework to the unsaturated organic fragment (407, 452, 453), as illustrated by Eq. (18).



Reaction with hydrogen may also result in the hydrogenation of the organic unit (425), but if an excess is used, the acetylenic ligand may be lost [Eq. (19)] (425). A similar process has been observed in the reactions of dinuclear species (454). The nature of the products obtained from the coordinated organic fragment in these reactions seems to depend on the extent of unsaturation in the cluster as a whole or in the organic group itself (455).



C. REACTIONS WITH PROTIC ACIDS

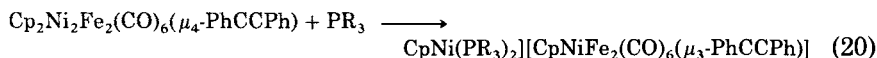
Variable-temperature ^1H NMR studies of the reactions between alkyne-substituted clusters and protic acids indicate that protonation takes place initially at a metal center in the cluster framework with inter- and intramolecular hydride exchange. If a second protonation takes place, as happens in some cases, the site of the reaction is the organic ligand (118, 456, 457).

D. REACTIONS WITH PHOSPHINES AND PHOSPHITES

The reactions of alkyne-substituted clusters with trialkylphosphines or phosphites that have been reported can be divided into two groups. In

one group the phosphine or phosphite forms a bond with one of the metal atoms, and in the second it adds to the ligand.

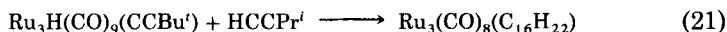
Examples of the first type of these reactions are found in several systems but the reaction mechanisms may follow different pathways. One route is substitution of one of the carbonyl ligands as has been observed in some osmium and ruthenium complexes (458, 459). The other mechanism involves metal-metal bond fission (414, 428), and in some cases this means the formation of cluster compounds with a smaller number of metal atoms [Eq. (20)] (460).



The addition of a phosphine group to the organic fragment has been studied in some detail in compounds with cluster-bound vinyl ligands. The zwitterionic adducts which are formed can then undergo nucleophilic addition reactions (411, 461, 462). A reaction of this type also occurs with amine-substituted alkynes coordinated to osmium and ruthenium complexes (117).

E. REACTIONS WITH ALKYNES

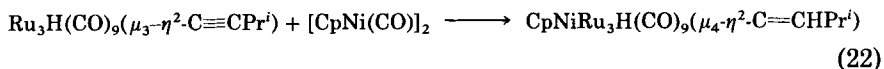
The reaction between clusters containing alkyne ligands and an excess of the same or a different alkyne, in most cases, result in the formation of new C-C bonds by combination of the new organic ligand with the previously coordinated one (141, 147, 430, 463-466). The mechanisms followed by these reactions are not known but the range of products obtained indicates that there are important differences in going from one reaction to another. While in some examples the complexes formed have two distinct, well-separated organic groups bonded to the metal framework (430, 466), in others metal-metal bond rupture occurs [Eq. (21)] (465).



F. REACTIONS WITH OTHER METALLIC SPECIES

Reactions between alkyne-substituted clusters and other metallic species have been used frequently as synthetic routes to mixed-metal clusters, particularly for Ru-Ni (214-217), as exemplified by Eq. (22), and Ru-Fe (220) complexes. In all these reactions the new metallic group forms bonds with the organic unit and with the metallic framework. It is possible that the first step in these reactions is the

coordination of the organic fragment to the incoming metallic unit, and this is followed by the formation of metal-metal bonds to the metals in the cluster cage. In some cases insertion of a metal-hydride bond into a metal acetylide linkage occurs (467).



There are syntheses where the new metallic species enhances a different type of reactivity. This has been observed in the reactions between alkyne-substituted ruthenium clusters and compounds of mercury (145, 146). In most of the characterized products a mercury atom or an HgX_2 (X = halogen) fragment serves as a bridge between two ruthenium cluster frameworks which retain the coordinated alkyne.

Carbon-carbon bond formation has been observed in the reaction of an alkyne-substituted osmium cluster with manganese and rhenium

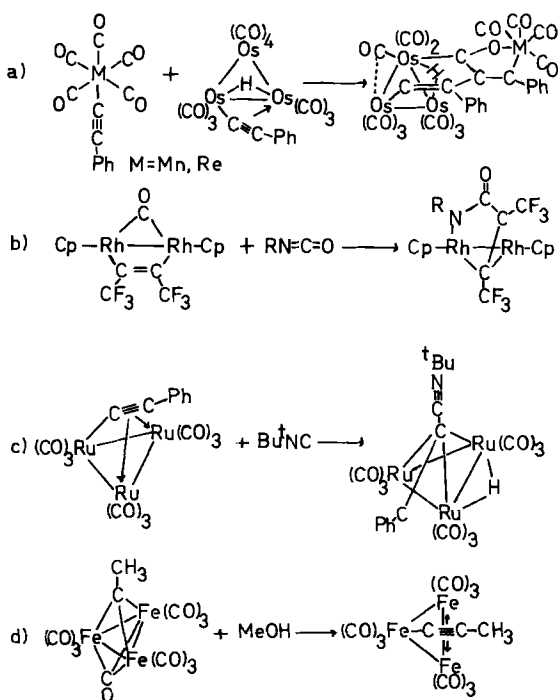


FIG. 43. Reactions of alkyne-substituted clusters with mononuclear complexes and other groups.

acetylides. The C–C bonds are formed by acetylide–alkyne and alkyne–CO couplings, and the manganese or rhenium atom does not form direct metal–metal bonds with the osmium atoms (Fig. 43a) (375).

G. OTHER REACTIONS

Coordinated alkyne and alkylidyne groups can form new C–C bonds by reactions with other compounds such as isocyanates (468), isocyanides (469), or by a reduction mechanism (470) (Fig. 43).

Other reactions of alkyne-substituted clusters include those in which parts of the complex other than the organic ligand itself are modified. However, the bonding mode of the latter may also be altered because of the new electronic requirements of the metallic cage. This occurs in some deprotonation reactions with OH^- (422), $[\text{Me}_3\text{O}]^+$ (423), or by nucleophilic attack of a halide (406, 408). Fragmentation and recombination of the metal framework in $\text{Ru}_3(\text{CO})_{11}(\text{Ph}_2\text{PC}=\text{CPr}^i)$ in the presence of water result in the formation of a tetranuclear complex which contains a face-bridging hydroxo group (131).

Recently, a series of triruthenium clusters containing allenyl or alkynyl ligands have been investigated electrochemically, and two, subsequent one-electron reduction steps have been observed (471). Further studies of this kind should provide a new insight into the electronic processes which take place in alkyne-substituted cluster systems.

ACKNOWLEDGMENTS

The authors would like to express their appreciation to Professor Sir Jack Lewis for his boundless support and encouragement which has kept them going through all the good and bad times of the last five years. Finally, the authors would like to dedicate this article to the memory of Professor Earl Muetterties with whom they had a number of friendly discussions, and whose thoughtful guidance helped develop their interest in cluster–alkyne chemistry.

REFERENCES

1. Masters, C., "Homogeneous Transition-metal Catalysis—A Gentle Art." Chapman & Hall, London, 1981.
2. Muetterties, E. L., *Angew. Chem., Int. Ed. Engl.* **17**, 545 (1978).
3. Muetterties, E. L., *Pure Appl. Chem.* **50**, 941 (1978).
4. Muetterties, E. L., Rodin, T. N., Band, E., Brucker, C. F., and Pretzer, W. R., *Chem. Rev.* **79**, 91 (1979).

5. Mason, R., and Wyn-Roberts, M., *Inorg. Chim. Acta.* **50**, 53 (1981).
6. Muetterties, E. L., *Pure Appl. Chem.* **54**, 83 (1982).
7. Castiglioni, M., Giordano, R., and Sappa, E., *J. Organomet. Chem.* **258**, 217 (1983).
8. Somorjai, G. A., *J. Chem. Soc. Chem. Rev.*, p. 321 (1984).
9. Gladfelter, W. L., and Geoffroy, G. L., *Adv. Organomet. Chem.* **18**, 207 (1980).
10. Johnson, B. F. G., ed., "Transition Metal Clusters." Wiley, New York, 1980.
11. Johnson, B. F. G., and Lewis, J., *Adv. Inorg. Chem. Radiochem.* **24**, 225 (1981).
12. Wilkinson, G., Stone, F. G. A., and Abel, E. W., eds., "Comprehensive Organometallic Chemistry." Pergamon, Oxford, 1982.
13. Carty, A. J., *Pure Appl. Chem.* **54**, 113 (1982).
14. Hahn, J. E., *Prog. Inorg. Chem.* **31**, 205 (1984).
15. Bruce, M. I., and Swincer, A. G., *Adv. Organomet. Chem.* **22**, 59 (1983).
16. Dickson, R. S., and Fraser, P. J., *Adv. Organomet. Chem.* **12**, 323 (1974).
17. Sappa, E., Tiripicchio, A., and Braunstein, P., *Chem. Rev.* **83**, 203 (1983).
18. Hoogzand, C., and Huber, W., in "Organic Synthesis via Metal Carbonyls," (I. Wender and P. Pino, eds.), Vol. I, p. 273. Wiley (Interscience), New York, 1968.
19. Sears, C. T., Jr., and Stone, F. G. A., *J. Organomet. Chem.* **11**, 644 (1968).
20. Aime, S., Milone, L., Sappa, E., Tiripicchio, A., and Tiripicchio Camellini, M., *J. Chem. Soc., Dalton Trans.*, p. 1155 (1979).
21. Aime, S., Milone, L., Sappa, E., Tiripicchio, A., and Manotti Lanfredi, A. M., *J. Chem. Soc., Dalton Trans.*, p. 1669 (1979).
22. Victor, R., Usieli, V., and Sarel, S., *J. Organomet. Chem.* **129**, 387 (1977).
23. Deeming, A. J., in "Transition Metal Clusters" (B. F. G. Johnson, ed.), Wiley, New York, 1980.
24. Nicholas, K., Bray, L. S., Davis, R. E., and Pettit, R., *J. Chem. Soc., Chem. Commun.*, p. 608 (1971).
25. Bruce, M. I., Matisons, J. G., Skelton, B. W., and White, A. H., *J. Organomet. Chem.* **251**, 249 (1983).
26. Blount, J. F., Dahl, L. F., Hoogzand, C., and Hubel, W., *J. Am. Chem. Soc.* **88**, 292 (1966).
27. Dodge, R. P., and Schomaker, V., *J. Organomet. Chem.* **3**, 274 (1965).
28. Cetini, G., Gambino, O., Sappa, E., and Valle, M., *J. Organomet. Chem.* **17**, 437 (1969).
29. Seddon, E. A., and Seddon, K. R., "The Chemistry of Ruthenium," p. 1401. Elsevier, Amsterdam, 1984.
30. Gambino, O., Cetini, G., Sappa, E., and Valle, M., *J. Organomet. Chem.* **20**, 195 (1969).
31. Gambino, O., Sappa, E., and Cetini, G., *J. Organomet. Chem.* **44**, 185 (1972).
32. Ferrari, R. P., and Vaglio, G. A., *Gazz. Chim. Ital.* **105**, 939 (1975).
33. Ferrari, R. P., Vaglio, G. A., Gambino, O., and Cetini, G., *J. Chem. Soc., Dalton Trans.*, p. 1998 (1972).
34. Ferraris, G., and Gervasio, G., *J. Chem. Soc., Dalton Trans.*, p. 1933 (1973).
35. Ferraris, G., and Gervasio, G., *J. Chem. Soc., Dalton Trans.*, p. 1813 (1974).
36. Ferraris, G., and Gervasio, G., *J. Chem. Soc., Dalton Trans.*, p. 1057 (1972).
37. Sappa, E., Tiripicchio, A., and Tiripicchio Camellini, M., *J. Chem. Soc., Dalton Trans.*, p. 419 (1978).
38. Johnson, B. F. G., Lewis, J., and Schorpp, K. T., *J. Organomet. Chem.* **91**, C13 (1975).
39. Rosenberg, E., Aime, S., Milone, L., Sappa, E., Tiripicchio, A., and Manotti Lanfredi, A. M., *J. Chem. Soc., Dalton Trans.*, p. 2023 (1981).
40. Johnson, B. F. G., Lewis, J., Reichert, B. E., Schorpp, K. T., and Sheldrick, G. M., *J. Chem. Soc., Dalton Trans.*, p. 1417 (1977).

41. Sappa, E., Tiripicchio, A., and Manotti Lanfredi, A. M., *J. Chem. Soc., Dalton Trans.*, p. 552 (1978).
42. King, R. B., and Eavenson, C. W., *J. Organomet. Chem.* **42**, C95 (1972).
43. Sappa, E., Milone, L., and Tiripicchio, A., *J. Chem. Soc., Dalton Trans.*, p. 1843 (1976).
44. Gervasio, G., Sappa, E., Manotti Lanfredi, A. M., and Tiripicchio, A., *Inorg. Chim. Acta* **68**, 171 (1983).
45. Aime, S., Milone, L., Sappa, E., and Tiripicchio, A., *J. Chem. Soc., Dalton Trans.*, p. 227 (1977).
46. Cetini, G., Gambino, O., Sappa, E., and Valle, M., *Atti Accad. Sci. Torino, Cl. Sci. Fis. Mat. Nat.* **101**, 813 (1967).
47. Gervasio, G., *J. Chem. Soc., Chem. Commun.*, p. 25 (1976).
48. Gambino, O., Ferrari, R. P., Chinone, M., and Vaglio, G. A., *Inorg. Chim. Acta* **13**, 155 (1975).
49. Aime, S., Milone, L., Osella, D., and Valle, M., *J. Chem. Res.*, p. 77 (1978).
50. Sappa, E., Gambino, O., Milone, L., and Cetini, G., *J. Organomet. Chem.* **39**, 169 (1972).
51. Aime, S., Gervasio, G., Milone, L., Sappa, E., and Franchini Angela, M., *Inorg. Chim. Acta* **26**, 223 (1978).
52. Sappa, E., Tiripicchio, A., and Manotti Lanfredi, A. M., *J. Organomet. Chem.* **249**, 391 (1983).
53. Braye, E. H., Dahl, L. F., Hubel, W., and Wampler, D. L., *J. Am. Chem. Soc.* **84**, 4633 (1962).
54. Al-Obaidi, Y. N., Green, M., White, N. D., and Taylor, G. E., *J. Chem. Soc., Dalton Trans.*, p. 319 (1982).
55. Boag, N. M., Green, M., Howard, J. A. K., Spencer, J. L., Stansfield, R. T. D., Stone, F. G. A., Thomas, M. D. O., Vicente, J., and Woodward, P., *J. Chem. Soc., Chem. Commun.*, p. 930 (1977).
56. Aime, S., Milone, L., Osella, D., Tiripicchio, A., and Manotti Lanfredi, A. M., *Inorg. Chem.* **21**, 501 (1982).
57. Bernhardt, W., and Vahrenkamp, H., *Angew. Chem., Int. Ed. Engl.* **23**, 141 (1984).
58. Dickson, R. S., Mok, C., and Pain, G., *J. Organomet. Chem.* **166**, 385 (1979).
59. Toan, T., Broach, R. W., Gardner, S. A., Rausch, M. D., and Dahl, L. F., *Inorg. Chem.* **16**, 279 (1977).
60. Jackson, P. F., Johnson, B. F. G., Lewis, J., Raithby, P. R., Will, G. M., McPartlin, M., and Nelson, W. H. J., *J. Chem. Soc., Chem. Commun.*, p. 1190 (1980).
61. Johnson, B. F. G., Lewis, J., Aime, S., Milone, L., and Osella, D., *J. Organomet. Chem.* **233**, 247 (1982).
62. Castiglioni, M., Milone, M., Osella, D., Vaglio, G. A., and Valle, M., *Inorg. Chem.* **15**, 394 (1976).
63. Deeming, A. J., Hasso, S., Underhill, M., Canty, A. J., Johnson, B. F. G., Jackson, W. G., Lewis, J., and Matheson, T. W., *J. Chem. Soc., Chem. Commun.*, p. 807 (1974).
64. Deeming, A. J., and Underhill, M., *J. Organomet. Chem.* **42**, C60 (1972).
65. Deeming, A. J., and Underhill, M., *J. Chem. Soc., Chem. Commun.*, p. 277 (1973).
66. Deeming, A. J., and Underhill, M., *J. Chem. Soc., Dalton Trans.*, p. 1415 (1974).
67. Jackson, R., Johnson, B. F. G., Lewis, J., Raithby, P. R., and Sankey, S. W., *J. Organomet. Chem.* **193**, C1 (1980).
68. Churchill, M. R., and Julius, S. A., *Inorg. Chem.* **17**, 1453 (1978).
69. Gambino, O., Valle, M., Aime, S., and Vaglio, G. A., *Inorg. Chim. Acta* **8**, 71 (1974).
70. Bruce, M. I., Cairns, M. A., Cox, A., Green, M., Smith, M. D. H., and Woodward, P., *J. Chem. Soc., Chem. Commun.*, p. 735 (1970).

71. Evans, M., Hursthouse, M., Randall, E. W., Rosenberg, E., Milone, L., and Valle, M., *J. Chem. Soc., Chem. Commun.*, p. 545 (1972).
72. Domingos, A. J. P., Johnson, B. F. G., and Lewis, J., *J. Organomet. Chem.* **36**, C43 (1972).
73. Knox, S. A. R., McKinney, R. J., Riera, V., Stone, F. G. A., and Szary, A. C., *J. Chem. Soc., Dalton Trans.*, p. 1801 (1979).
74. Valle, M., Gambino, O., Milone, L., Vaglio, G. A., and Cetini, G., *J. Organomet. Chem.* **38**, C46 (1972).
75. Gervasio, G., Osella, D., and Valle, M., *Inorg. Chem.* **15**, 1221 (1976).
76. Howard, J. A. K., Stansfield, R. F. D., and Woodward, P., *J. Chem. Soc., Dalton Trans.*, p. 1812 (1979).
77. Cox, A., and Woodward, P., *J. Chem. Soc. A*, p. 3599 (1971).
78. Humphries, A. P., and Knox, S. A. R., *J. Chem. Soc., Dalton Trans.*, p. 1710 (1975).
79. Churchill, M. R., Gold, K., and Bird, P. H., *Inorg. Chem.* **8**, 1956 (1969).
80. Churchill, M. R., and Bird, P. H., *J. Am. Chem. Soc.* **90**, 800 (1968).
81. Aime, S., Milone, L., Osella, D., Vaglio, G. A., Valle, M., Tiripicchio, A., and Tiripicchio Camellini, M., *Inorg. Chim. Acta* **34**, 49 (1979).
82. Deeming, A. J., Hasso, S., and Underhill, M., *J. Organomet. Chem.* **80**, C53 (1974).
83. Bryan, E. G., Johnson, B. F. G., and Lewis, J., *J. Chem. Soc., Dalton Trans.*, p. 1328 (1977).
84. Tachikawa, M., Shapley, J. R., and Pierpont, C. G., *J. Am. Chem. Soc.* **97**, 7172 (1975).
85. Bryan, E. G., Johnson, B. F. G., Kelland, J. W., Lewis, J., and McPartlin, M., *J. Chem. Soc., Chem. Commun.*, p. 254 (1976).
86. Tachikawa, M., Shapley, J. R., Haltwanger, R. C., and Pierpont, C. G., *J. Am. Chem. Soc.* **98**, 4651 (1976).
87. Tachikawa, M., and Shapley, J. R., *J. Organomet. Chem.* **124**, C19 (1977).
88. Deeming, A. J., Hasso, S., and Underhill, M., *J. Chem. Soc., Dalton Trans.*, p. 1614 (1975).
89. Green, M., Orpen, A. G., and Schaerien, C. J., *J. Chem. Soc., Chem. Commun.*, p. 37 (1984).
90. Jackson, W. G., Johnson, B. F. G., Kelland, J. W., Lewis, J., and Schorpp, K. T., *J. Organomet. Chem.* **87**, C27 (1975).
91. Clauss, A. D., Tachikawa, M., Shapley, J. R., and Pierpont, C. G., *Inorg. Chem.* **20**, 1528 (1981).
92. Jackson, W. G., Johnson, B. F. G., Kelland, J. W., Lewis, J., and Schorpp, K. T., *J. Organomet. Chem.* **88**, C17 (1975).
93. Keister, J. B., and Shapley, J. R., *J. Am. Chem. Soc.* **98**, 1056 (1976).
94. Sappa, E., Tiripicchio, A., and Manotti Lanfredi, A. M., *J. Organomet. Chem.* **249**, 391 (1983).
95. Bryan, E. G., Johnson, B. F. G., and Lewis, J., *J. Organomet. Chem.* **122**, 249 (1976).
96. Keister, J. B., and Shapley, J. R., *J. Organomet. Chem.* **85**, C29 (1975).
97. Churchill, M. R., and Lashewycz, R. A., *Inorg. Chem.* **17**, 1291 (1978).
98. Johnson, B. F. G., Lewis, J., Raithby, P. R., and Sankey, S. W., *J. Organomet. Chem.* **231**, C65 (1982).
99. Hanson, B. E., Johnson, B. F. G., Lewis, J., and Raithby, P. R., *J. Chem. Soc., Dalton Trans.*, p. 1852 (1980).
100. Johnson, B. F. G., Lewis, J., Pippard, D., and Raithby, P. R., *J. Chem. Soc., Chem. Commun.*, p. 551 (1978).
101. Brown, S. C., and Evans, J., *J. Chem. Soc., Dalton Trans.*, p. 1049 (1982).
102. Kampe, C. E., Boag, N. M., and Kaesz, H. D., *J. Am. Chem. Soc.* **105**, 2896 (1983).

103. Knox, S. A. R., *Pure Appl. Chem.* **56**, 81 (1984).
104. MacLaughlin, S. A., Taylor, N. J., and Carty, A. J., *Organometallics* **3**, 392 (1984).
105. Regragui, R., Dixneuf, P. H., Taylor, N. J., and Carty, A. J., *Organometallics* **3**, 814 (1984).
106. Bruce, M. I., Nickolson, B. K., and Williams, M. L., *J. Organomet. Chem.* **243**, 69 (1983).
107. Deeming, A. J., Manning, P. L., Rothwell, I. P., Hursthouse, M. B., and Walker, N. P. C., *J. Chem. Soc., Dalton Trans.*, p. 2039 (1984).
108. Aime, S., Osella, D., Deeming, A. J., Manotti Lanfredi, A. M., and Tiripicchio, A., *J. Organomet. Chem.* **244**, C47 (1983).
109. O'Connor, T., Carty, A. J., Mathew, M., and Palenik, G. J., *J. Organomet. Chem.* **38**, C15 (1972).
110. Mathew, M., Palenik, G. J., Carty, A. J., and Paik, H. N., *J. Chem. Soc., Chem. Commun.*, p. 25 (1974).
111. Paik, H. N., Carty, A. J., Mathew, M., and Palenik, G. J., *J. Chem. Soc., Chem. Commun.*, p. 946 (1974).
112. Restivo, R. J., and Ferguson, G., *J. Chem. Soc., Dalton Trans.*, p. 893 (1976).
113. Carty, A. J., Taylor, N. J., and Smith, W. F., *J. Chem. Soc., Chem. Commun.*, p. 750 (1979).
114. Carty, A. J., MacLaughlin, S. A., Taylor, N. J., and Sappa, E., *Inorg. Chem.* **20**, 4437 (1981).
115. King, R. B., and Harmon, C. A., *Inorg. Chem.* **15**, 879 (1976).
116. Daran, J. C., and Jeannin, Y., *Organometallics* **3**, 1150 (1984).
117. Aime, S., Osella, D., Arce, A. J., Deeming, A. J., Hursthouse, M. B., and Galas, A. M. R., *J. Chem. Soc., Dalton Trans.*, p. 1981 (1984).
118. Aime, S., Jannon, G., Osella, D., Arce, A. J., and Deeming, A. J., *J. Chem. Soc., Dalton Trans.*, p. 1987 (1984).
119. Ermer, S., Karpelus, R., Miura, S., Rosenberg, E., Tiripicchio, A., and Manotti Lanfredi, A. M., *J. Organomet. Chem.* **187**, 81 (1980).
120. Aime, S., Milone, L., and Deeming, A. J., *J. Chem. Soc., Chem. Commun.*, p. 1168 (1980).
121. Aime, S., and Deeming, A. J., *J. Chem. Soc., Dalton Trans.*, p. 828 (1981).
122. Aime, S., Tiripicchio, A., Tiripicchio Camellini, M., and Deeming, A. J., *Inorg. Chem.* **20**, 2027 (1981).
123. Aime, S., and Deeming, A. J., *J. Chem. Soc., Dalton Trans.*, p. 1807 (1983).
124. Aime, S., Deeming, A. J., Hursthouse, M. B., and Backer-Dirks, J. D., *J. Chem. Soc., Dalton Trans.*, p. 1625 (1982).
125. Gambino, O., Sappa, E., Manotti Lanfredi, A. M., and Tiripicchio, A., *Inorg. Chim. Acta* **36**, 189 (1979).
126. Laing, M., Sommerville, P., Dawoodi, Z., Mays, M. J., and Wheatley, P. J., *J. Chem. Soc., Chem. Commun.*, p. 1035 (1978).
127. Wrighton, M. S., Graff, J. L., Luong, J. C., Reichel, C. L., and Robbins, J. L., *Am. Chem. Soc. Symp. Ser.* **55**, 85 (1981).
128. Evans, J., and McNulty, G. S., *J. Chem. Soc., Dalton Trans.*, p. 2017 (1981).
129. Johnson, B. F. G., Lewis, J., and Pippard, D., *J. Organomet. Chem.* **160**, 263 (1978).
130. Carty, A. J., MacLaughlin, S. A., and Taylor, N. J., *J. Organomet. Chem.* **204**, C27 (1981).
131. Carty, A. J., MacLaughlin, S. A., and Taylor, N. J., *J. Chem. Soc., Chem. Commun.*, p. 476 (1981).
132. Tinley-Basset, J. F., *J. Chem. Soc.*, p. 4784 (1963).

133. Raverdino, V., Aime, S., Milone, L., and Sappa, E., *Inorg. Chim. Acta* **30**, 9 (1978).
134. Marinetti, A., Sappa, E., Tiripicchio, A., and Tiripicchio Camellini, M., *J. Organomet. Chem.* **197**, 335 (1980).
135. Bruce, M. I., Rodgers, J. R., Snow, M. R., and Wong, F. S., *J. Chem. Soc., Chem. Commun.*, p. 1285 (1980).
136. Sappa, E., Tiripicchio, A., and Tiripicchio Camellini, M., *J. Organomet. Chem.* **213**, 175 (1981).
137. Marinetti, A., Sappa, E., Tiripicchio, A., and Tiripicchio Camellini, M., *Inorg. Chim. Acta* **44**, L183 (1980).
138. Sappa, E., Manotti Lanfredi, A. M., and Tiripicchio, A., *J. Organomet. Chem.* **221**, 93 (1981).
139. Tiripicchio, A., Tiripicchio Camellini, M., and Sappa, E., *J. Chem. Soc., Dalton Trans.*, p. 627 (1984).
140. Yasufuku, K., Aoki, K., and Yamazaki, H., *J. Organomet. Chem.* **84**, C28 (1975).
141. Sappa, E., Manotti, A. M., Predieri, G., and Tiripicchio, A., *Inorg. Chim. Acta* **61**, 217 (1982).
142. Sappa, E., Manotti, A. M., and Tiripicchio, A., *Inorg. Chim. Acta* **42**, 255 (1980).
143. Carty, A. J., Mott, G. N., and Taylor, N. J., *J. Am. Chem. Soc.* **101**, 3131 (1979).
144. Al-Resayes, S. I., Hitchcock, P. B., Meidine, M. F., and Nixon, J. F., *J. Chem. Soc., Chem. Commun.*, p. 1080 (1984).
145. Ermer, S., King, K., Hardcastle, K. I., Rosenberg, E., Manotti Lanfredi, A. M., and Tiripicchio Camellini, M., *Inorg. Chim. Acta* **22**, 1339 (1980).
146. Fahmy, R., King, K., Rosenberg, E., Tiripicchio, A., and Tiripicchio Camellini, M., *J. Am. Chem. Soc.* **102**, 3626 (1980).
147. Buseti, V., Granozzi, G., Aime, S., Gobetto, R., and Osella, D., *Organometallics* **3**, 1510 (1984).
148. Einstein, F. W. B., Freeland, B. H., Tyers, K. G., Sutton, D., and Waterous, J. M., *J. Chem. Soc., Chem. Commun.*, p. 371 (1982).
149. Antonova, A. B., Kovalenko, S. V., Korniyets, E. D., Johansson, A. A., Struchkov, Yu. T., and Yanovsky, A. I., *J. Organomet. Chem.* **267**, 299 (1984).
150. Bruce, M. I., Abu Salah, O. M., Davies, R. E., and Raghavan, N. V., *J. Organomet. Chem.* **64**, C48 (1974).
151. Boag, N. M., Green, M., Howard, J. A. K., Spencer, J. L., Stansfield, R. D. F., Stone, F. G. A., Thomas, M. D. O., Vicente, J., and Woodward, P., *J. Chem. Soc., Chem. Commun.*, p. 930 (1978).
152. Kolobova, N. E., Ivanov, L. L., Zhvanko, O. S., Batsanov, A. S., and Struchkov, Yu. T., *J. Organomet. Chem.* **231**, 37 (1982).
153. Ciriano, M., Howard, J. A. K., Spencer, J. L., Stone, F. G. A., and Wadepohl, H., *J. Chem. Soc., Dalton Trans.*, p. 1749 (1979).
154. Wang, A. H. J., Paul, I. C., and Schrauzer, G. N., *J. Chem. Soc., Chem. Commun.*, p. 736 (1972).
155. Jones, D. F., Dixneuf, P. H., Southern, T. G., Le Marouille, J. Y., Grandjean, D., and Guenot, P., *Inorg. Chem.* **20**, 3247 (1981).
156. Carriedo, G. A., Riera, V., Miguel, D., Manotti Lanfredi, A. M., and Tiripicchio, A., *J. Organomet. Chem.* **272**, C17 (1984).
157. Ashworth, T. V., Berry, M., Howard, J. A. K., Laguna, M., and Stone, F. G. A., *J. Chem. Soc., Dalton Trans.*, p. 1615 (1980).
158. Shapley, J. R., Park, J. T., Churchill, M. R., Bueno, C., and Wasserman, H., *J. Am. Chem. Soc.* **103**, 7385 (1981).
159. Chetuti, M. J., Chetuti, P. A. M., Jeffery, J. C., Mills, R. M., Mitprachachon, P.,

- Pickering, S. J., Stone, F. G. A., and Woodward, P., *J. Chem. Soc., Dalton Trans.*, p. 699 (1982).
160. Busetto, L., Green, M., Hessner, B., Howard, J. A. K., Jeffery, J. C., and Stone, F. G. A., *J. Chem. Soc., Dalton Trans.*, p. 519 (1983).
161. Chetcuti, M., Green, M., Howard, J. A. K., Jeffery, J. C., Mills, R. M., Pain, G. N., Porter, S. J., Stone, F. G. A., Wilson, A. A., and Woodward, P., *J. Chem. Soc., Chem. Commun.*, p. 1057 (1980).
162. Churchill, M. R., Bueno, C., and Wasserman, H. J., *Inorg. Chem.* **21**, 640 (1982).
163. Abu Salah, O. M., and Bruce, M. I., *J. Chem. Soc., Dalton Trans.*, p. 2311 (1975).
164. Abu Salah, O. M., Bruce, M. I., Churchill, M. R., and DeBoer, B. G., *J. Chem. Soc., Chem. Commun.*, p. 688 (1974).
165. Churchill, M. R., and DeBoer, B. G., *Inorg. Chem.* **14**, 2630 (1975).
166. Busetto, L., Green, M., Howard, J. A. K., Hessner, B., Jeffrey, J. C., Mills, R. M., Stone, F. G. A., and Woodward, P., *J. Chem. Soc., Chem. Commun.*, p. 1101 (1981).
167. Sappa, E., Cetini, G., Gambino, O., and Valle, M., *J. Organomet. Chem.* **20**, 201 (1969).
168. Bird, P. H., and Fraser, A. R., *J. Chem. Soc., Chem. Commun.*, p. 681 (1970).
169. Cooksey, C. J., Deeming, A. J., and Rothwell, I. P., *J. Chem. Soc., Dalton Trans.*, p. 1718 (1981).
170. Gainsford, G. J., Guss, J. M., Ireland, P. R., Mason, R., Bradford, C. W., and Nyholm, R. S., *J. Organomet. Chem.* **40**, C70 (1972).
171. Bradford, C. W., Nyholm, R. S., Gainsford, G. J., Guss, J. M., Ireland, P. R., and Mason, R., *J. Chem. Soc., Chem. Commun.*, p. 87 (1972).
172. Bruce, M. I., Shaw, G., and Stone, F. G. A., *J. Chem. Soc., Dalton Trans.*, p. 2094 (1972).
173. Deeming, A. J., Kimber, R. E., and Underhill, M., *J. Chem. Soc., Dalton Trans.*, p. 2589 (1973).
174. Brown, S. C., Evans, J., and Smart, L. E., *J. Chem. Soc., Chem. Commun.*, p. 1021 (1980).
175. Azam, K. A., and Deeming, A. J., *J. Chem. Soc., Chem. Commun.*, p. 852 (1976).
176. Azam, K. A., Deeming, A. J., Rothwell, I. P., Hursthouse, M. B., and New, L., *J. Chem. Soc., Chem. Commun.*, p. 1086 (1978).
177. Deeming, A. J., *J. Organomet. Chem.* **128**, 63 (1977).
178. Parkin, A. W., Fischer, E. O., Huttner, G., and Regler, D., *Angew. Chem., Int. Ed. Engl.* **9**, 663 (1970).
179. Jensen, C. M., and Kaesz, H. D., *J. Am. Chem. Soc.* **105**, 6969 (1983).
180. Doi, Y., Koshizuka, K., and Keu, T., *Inorg. Chem.* **21**, 2732 (1982).
181. Carty, A. J., Johnson, B. F. G., and Lewis, J., *J. Organomet. Chem.* **43**, C35 (1972).
182. Mason, R., and Thomas, K. M., *J. Organomet. Chem.* **43**, C39 (1972).
183. Carty, A. J., Domingos, A. J. P., Johnson, B. F. G., and Lewis, J., *J. Chem. Soc., Dalton Trans.*, p. 2056 (1973).
184. Belford, R., Taylor, H. P., and Woodward, P., *J. Chem. Soc., Dalton Trans.*, p. 2425 (1972).
185. Johnson, B. F. G., Kelland, J. W., Lewis, J., and Rehani, S. K., *J. Organomet. Chem.* **113**, C42 (1976).
186. Johnson, B. F. G., Lewis, J., Orpen, A. G., Raithby, P. R., and Rouse, K. D., *J. Chem. Soc., Dalton Trans.*, p. 788 (1981).
187. Bhaduri, S., Johnson, B. F. G., Kelland, J. W., Lewis, J., Raithby, P. R., Rehani, S., Sheldrick, G. M., Wong, K., and McPartlin, M., *J. Chem. Soc., Dalton Trans.*, p. 562 (1979).
188. Carty, A. J., Johnson, B. F. G., Lewis, J., and Norton, J. R., *J. Chem. Soc., Chem. Commun.*, p. 1331 (1972).

189. Kitamura, T., and Joh, T., *J. Organomet. Chem.* **65**, 235 (1974).
190. Ros, R., Canziani, F., and Roulet, R., *J. Organomet. Chem.* **267**, C9 (1984).
191. Stuntz, G. F., Shapley, J. R., and Pierpont, C. G., *Inorg. Chem.* **17**, 2596 (1978).
192. Pierpont, C. G., Stuntz, G. F., and Shapley, J. R., *J. Am. Chem. Soc.* **100**, 618 (1978).
193. Pierpont, C. G., *Inorg. Chem.* **18**, 2972 (1979).
194. Cooke, C. G., and Mays, M. J., *J. Organomet. Chem.* **74**, 449 (1974).
195. Aime, S., Osella, D., Milone, L., Manotti Lanfredi, A. M., and Tiripicchio, A., *Inorg. Chim. Acta* **71**, 141 (1983).
196. Roland, E., and Vahrenkamp, H., *Organometallics* **2**, 183 (1983).
197. Castiglioni, M., Sappa, E., Valle, M., Lanfranchi, M., and Tiripicchio, A., *J. Organomet. Chem.* **241**, 99 (1983).
198. Fox, J. R., Gladfelter, W. L., Geoffroy, G. L., Tavanaiepour, I., Abdul-Mequid, S., and Day, V. W., *Inorg. Chem.* **20**, 3230 (1981).
199. Braunstein, P., Rose, J., and Bars, O., *J. Organomet. Chem.* **252**, C101 (1983).
200. Burgess, K., Ph. D. Thesis, University of Cambridge, Cambridge, England (1982).
201. Park, J. T., Shapley, J. R., Churchill, M. R., and Bueno, C., *J. Am. Chem. Soc.* **105**, 6182 (1983).
202. Churchill, M. R., Bueno, C., Park, J. T., and Shapley, J. R., *Inorg. Chem.* **23**, 1017 (1983).
203. Farrugia, L. Y., Howard, J. A. K., Mitrprachachon, P., Stone, F. G. A., and Woodward, P., *J. Chem. Soc., Dalton Trans.*, p. 162 (1981).
204. Booth, B. L., Else, M. J., Fields, R., and Haszeldine, R. N., *J. Organomet. Chem.* **27**, 119 (1971).
205. Heveldt, P. F., Johnson, B. F. G., Lewis, J., Raithby, P. R., and Sheldrick, G. M., *J. Chem. Soc., Chem. Commun.*, p. 340 (1978).
206. Kruerke, U., and Hubel, W., *Chem. Ber.* **94**, 2829 (1961).
207. Dahl, L. F., and Smith, D. L., *J. Am. Chem. Soc.* **84**, 2450 (1962).
208. Kelland, J. W., Ph. D. Thesis, University of Cambridge, Cambridge, England (1976).
209. Shapley, J. R., McAteer, C. H., Churchill, M. R., and Vollaro Biondi, L., *Organometallics* **3**, 1595 (1984).
210. Sappa, E., Tiripicchio, A., and Tiripicchio Camellini, M., *J. Organomet. Chem.* **199**, 243 (1980).
211. Sappa, E., Tiripicchio, A., and Tiripicchio Camellini, M., *J. Organomet. Chem.* **246**, 287 (1983).
212. Sappa, E., Tiripicchio, A., and Tiripicchio Camellini, M., *J. Chem. Soc., Chem. Commun.*, p. 254 (1979).
213. Nanni Marchino, M. L., Sappa, E., Manotti Lanfredi, A. M., and Tiripicchio, A., *J. Chem. Soc., Dalton Trans.*, p. 154 (1984).
214. Osella, D., Sappa, E., Tiripicchio, A., and Tiripicchio Camellini, M., *Inorg. Chim. Acta* **34**, L289 (1979).
215. Sappa, E., Tiripicchio, A., and Tiripicchio Camellini, M., *Inorg. Chim. Acta* **41**, 11 (1980).
216. Osella, D., Sappa, E., Tiripicchio, A., and Tiripicchio Camellini, M., *Inorg. Chim. Acta* **42**, 183 (1980).
217. Carty, A. J., Taylor, N. J., Sappa, E., and Tiripicchio, A., *Inorg. Chem.* **22**, 1871 (1983).
218. Lanfranchi, M., Tiripicchio, A., Tiripicchio, M., Gambino, O., and Sappa, E., *Inorg. Chim. Acta* **64**, L269 (1982).
219. Belford, R., Bruce, M. I., Cairns, M. A., Green, M., Taylor, H. P., and Woodward, P., *J. Chem. Soc., Chem. Commun.*, p. 1159 (1970).
220. Aime, S., and Osella, D., *Inorg. Chim. Acta* **57**, 207 (1982).

221. Jones, D. F., Dixneuf, P. H., Benoit, A., and Le Marouille, J. Y., *J. Chem. Soc., Chem. Commun.*, p. 1217 (1982).
222. Abu Salah, O. M., and Bruce, M. I., *J. Chem. Soc., Dalton Trans.*, p. 2302 (1974).
223. Nesmeyanov, A. N., Struchkov, Yu. T., Sedova, N. N., Andrianov, V. G., Volgin, Y. V., and Sazonova, V. A., *J. Organomet. Chem.* **137**, 217 (1977).
224. Farrar, D. H., John, G. R., Johnson, B. F. G., Lewis, J., Raithby, P. R., and Rosales, M. J., *J. Chem. Soc., Chem. Commun.*, p. 886 (1981).
225. Drage, J. S., Tilset, M., Vollhardt, P. C., and Weidman, T. W., *Organometallics* **3**, 812 (1984).
226. Farrar, D. H., Johnson, B. F. G., Lewis, J., Raithby, P. R., and Rosales, M. J., *J. Chem. Soc., Dalton Trans.*, p. 2051 (1982).
227. Johnson, B. F. G., Lewis, J., Raithby, P. R., and Rosales, M. J., *J. Chem. Soc., Dalton Trans.*, p. 2645 (1983).
228. Fernandez, J. M., Johnson, B. F. G., Lewis, J., and Raithby, P. R., *Acta Crystallogr., Sect. B*, p. 3086 (1978).
229. Eady, C. R., Fernandez, J. M., Johnson, B. F. G., Lewis, J., Raithby, P. R., and Sheldrick, G. M., *J. Chem. Soc., Chem. Commun.*, p. 421 (1978).
230. Gomez-Sal, M. P., Johnson, B. F. G., Kamarudin, R. A., Lewis, J., and Raithby, P. R., unpublished results.
231. Jeffrey, J. G., Johnson, B. F. G., Lewis, J., Raithby, P. R., and Welch, D. A., unpublished results.
232. Ciani, G., Sironi, A., Chini, P., Ceriotti, A., and Martinengo, S., *J. Organomet. Chem.* **192**, C39 (1980).
233. ten Hoedt, R. W. M., Noltes, J. G., van Koten, G., and Spek, A. L., *J. Chem. Soc., Dalton Trans.*, p. 1800 (1978).
234. van Koten, G., and Noltes, J. G., *J. Chem. Soc., Chem. Commun.*, p. 575 (1974).
235. ten Hoedt, R. W. M., van Koten, G., and Noltes, J. G., *J. Organomet. Chem.* **133**, 113 (1977).
236. van Koten, G., ten Hoedt, R. W. M., and Noltes, J. G., *J. Org. Chem.* **42**, 2705 (1977).
237. Abu Salah, O. M., Bruce, M. I., Churchill, M. R., and Bezman, S. A., *J. Chem. Soc., Chem. Commun.*, p. 858 (1972).
238. Bartsch, R., Hitchcock, P. B., Meidine, M. F., and Nixon, J. F., *J. Organomet. Chem.* **266**, C41 (1984).
239. Churchill, M. R., and Bezman, S. A., *Inorg. Chem.* **13**, 1418 (1974).
240. Abu Salah, O. M., and Bruce, M. I., *Aust. J. Chem.* **29**, 531 (1976).
241. Abu Salah, O. M., and Bruce, M. I., *Aust. J. Chem.* **30**, 2639 (1977).
242. Lanfranchi, M., Tiripicchio, A., Sappa, E., MacLaughlin, S. A., and Carty, A. J., *J. Chem. Soc., Chem. Commun.*, p. 538 (1982).
243. Klabunde, K., Groshens, T., Brezinski, M., and Kennelly, W., *J. Am. Chem. Soc.* **100**, 4437 (1978).
244. Rafalko, J. J., Watson, P. M., Malueg, D. H., Davis, R. E., and Gates, B. C., *Inorg. Chem.* **20**, 3540 (1981).
245. Davidson, J. L., Green, M., Stone, F. G. A., and Welch, A. J., *J. Chem. Soc., Dalton Trans.*, p. 506 (1979).
246. Freeman, M. B., Hall, L. W., and Sneddon, L. G., *Inorg. Chem.* **19**, 1132 (1980).
247. Fritch, D. R., Vollhardt, K. P. C., Thompson, M. R., and Day, V. W., *J. Am. Chem. Soc.* **101**, 2768 (1979).
248. Fritch, J. R., and Vollhardt, K. P. C., *Angew. Chem., Int. Ed. Engl.* **19**, 559 (1980).
249. King, R. B., and Efraty, A., *J. Am. Chem. Soc.* **94**, 3021 (1972).
250. Gardner, S. A., Andrews, P. S., and Rausch, M. D., *Inorg. Chem.* **12**, 2396 (1973).

251. Varadi, G., Galamb, V., Palagyi, J., and Palyi, G., *Inorg. Chim. Acta*, **53**, L29 (1981).
252. Roe, D., and Massey, A. G., *J. Organomet. Chem.* **23**, 547 (1970).
253. Muller, J., Menig, H., and Pickardt, J., *Angew. Chem., Int. Ed. Engl.* **20**, 401 (1981).
254. Seyferth, D., Spoku, R. J., Churchill, M. R., Gold, R., and Scholer, F. R., *J. Organomet. Chem.* **23**, 237 (1970).
255. Dickson, R. S., and Pain, G. N., *J. Chem. Soc., Chem. Commun.*, p. 277 (1979).
256. Markby, R., Wender, I., Friedel, R. A., Cotton, F. A., and Steinberg, H. W., *J. Am. Chem. Soc.* **80**, 6529 (1958).
257. Carty, A. J., and Ng, T. W., *J. Chem. Soc., Chem. Commun.*, p. 149 (1970).
258. Hota, N. K., Patel, H. A., Carty, A. J., Mathew, M., and Palenik, G. J., *J. Organomet. Chem.* **32**, C55 (1971).
259. Frisch, P. D., Posey, R. G., and Khare, G. P., *Inorg. Chem.* **17**, 402 (1978).
260. Jonas, K., Kruger, C., and Sekutowski, J. C., *Angew. Chem., Int. Ed. Engl.* **18**, 487 (1979).
261. Wilson, D. R., Liu, J. Z., and Ernst, R. D., *J. Am. Chem. Soc.* **104**, 1120 (1982).
262. Boag, N. M., Green, M., Howard, J. A. K., Spencer, J. L., Stansfield, R. F. D., Thomas, M. D. O., Stone, F. G. A., and Woodward, P., *J. Chem. Soc., Dalton Trans.*, p. 2182 (1980).
263. Boag, N. M., Howard, J. A. K., Spencer, J. L., and Stone, F. G. A., *J. Chem. Soc., Dalton Trans.*, p. 1051 (1981).
264. Seyferth, D., *Adv. Organomet. Chem.* **14**, 97 (1976), and references therein.
265. Clauss, A. D., Shapley, J. R., Wilker, C. N., and Hoffmann, R., private communication.
266. Sutton, P. W., and Dahl, L. F., *J. Am. Chem. Soc.* **89**, 261 (1967).
267. Fachinetti, G., Pucci, S., Zanazzi, P. F., and Methong, U., *Angew. Chem., Int. Ed. Engl.* **18**, 619 (1979).
268. Seidler, P. F., Bryndza, H. E., Frommer, J. E., Stuhl, L. S., and Bergman, R. G., *Organometallics*, **2**, 1701 (1983).
269. Fieldhouse, S. A., Freeland, B. H., Mann, C. D. M., and O'Brien, R. J., *J. Chem. Soc., Chem. Commun.*, p. 181 (1970).
270. Parry, R. B. A., Smith, G. W., and Vickers, M. E., *J. Organomet. Chem.* **252**, 341 (1983).
271. Fachinetti, G., *J. Chem. Soc., Chem. Commun.*, p. 397 (1979).
272. Booth, B. L., Haszeldine, R. N., and Anglis, T., *J. Chem. Soc., Dalton Trans.*, p. 1449 (1975).
273. Schmid, G., *Angew. Chem., Int. Ed. Engl.* **17**, 392 (1978).
274. Bailey, W. I., Cotton, F. A., and Jamerson, J. D., *J. Organomet. Chem.* **173**, 317 (1979).
275. Bor, G., Dietler, U. K., Stanghellini, P. L., Gervasio, G., Rosetti, R., Sbrignadelli, G., and Battison, G. A., *J. Organomet. Chem.* **213**, 277 (1981).
276. Patin, H., Mignani, G., and van Aulle, M. T., *Tetrahedron Lett.*, p. 2441 (1979).
277. Mignani, G., Patin, H., and Dabard, R., *J. Organomet. Chem.* **169**, C19 (1979).
278. Seyferth, D., Scott Eschbach, C., Williams, G. H., and Hung, P. L., *J. Organomet. Chem.* **134**, 67 (1977).
279. Fischer, E. O., and Daviertiz, A., *Chem. Ber.* **111**, 3525 (1978).
280. Fischer, E. O., and Daviertiz, A., *Angew. Chem., Int. Ed. Engl.* **14**, 346 (1975).
281. Herrmann, W. A., Plank, J., Riedel, D., Ziegler, M. L., Weidenhammer, K., Guggolz, E., and Balbach, B., *J. Am. Chem. Soc.* **103**, 63 (1981).
282. Dimas, P. A., Duesler, E. N., Lawson, R. J., and Shapley, J. R., *J. Am. Chem. Soc.* **102**, 7787 (1980).
283. Rybin, L. V., Petrovskaya, E. A., Struchkov, Yu. T., Batsanov, A. S., and Rybinskaya, M. I., *J. Organomet. Chem.* **226**, 63 (1982).

284. Wong, K. S., and Fehlner, T. P., *J. Am. Chem. Soc.* **103**, 966 (1981).
285. Brun, P., Dawkins, G. M., Green, M., Mills, R. M., Salaun, J. Y., Stone, F. G. A., and Woodward, P., *J. Chem. Soc., Dalton Trans.*, p. 1357 (1983).
286. Bino, A., Cotton, F. A., and Dori, Z., *J. Am. Chem. Soc.* **103**, 243 (1981).
287. Ardon, M., Bino, A., Cotton, F. A., Dori, Z., Kaftory, M., Kolthammer, B. W. S., Kapon, M., and Reisner, G., *Inorg. Chem.* **20**, 4083 (1981).
288. Keister, J. B., *J. Chem. Soc., Chem. Commun.*, p. 214 (1979).
289. Eady, C. R., Johnson, B. F. G., and Lewis, J., *J. Chem. Soc., Dalton Trans.*, p. 477 (1977).
290. Sheldrick, G. M., and Yesinowski, J. P., *J. Chem. Soc., Dalton Trans.*, p. 873 (1975).
291. Johnson, B. F. G., Lewis, J., Orpen, A. G., Raithby, P. R., and Suss, G., *J. Organomet. Chem.* **173**, 187 (1979).
292. Shore, S. G., Yang Jan, D., Hsu, W. L., Kennedy, S., Huffmann, J. C., Wang, T. L., and Marshall, A. G., *J. Chem. Soc., Chem. Commun.*, p. 392 (1984).
293. Shapley, J. R., Sievert, A. C., Churchill, M. R., and Wasserman, H. J., *J. Am. Chem. Soc.* **103**, 6975 (1981).
294. Yesinowski, J. P., and Bailey, D., *J. Organomet. Chem.* **65**, C27 (1974).
295. Voevodskaya, T. I., Pribtkova, I. M., and Ustynyuk, Y. A., *J. Organomet. Chem.* **37**, 187 (1972).
296. Booth, B. L., and Casey, G. C., *J. Organomet. Chem.* **178**, 371 (1979).
297. Kruppa, W., and Schmid, G., *J. Organomet. Chem.* **20**, 2379 (1980).
298. Mlekuz, M., Bougeard, P., McGlinchy, M. J., and Jaouen, G., *J. Organomet. Chem.* **253**, 117 (1983).
299. Beurich, H., and Vahrenkamp, H., *Angew. Chem., Int. Ed. Engl.* **17**, 863 (1978).
300. Ros, J., and Mathieu, R., *Organometallics* **2**, 771 (1983).
301. Beurich, H., and Vahrenkamp, H., *Angew. Chem., Int. Ed. Engl.* **20**, 98 (1981).
302. Epstein, R. A., Withers, H. W., and Geoffroy, G. L., *Inorg. Chem.* **18**, 942 (1979).
303. Seyferth, D., Hung, P. L. K., and Hallgren, J. E., *J. Organomet. Chem.* **44**, C55 (1972).
304. Seyferth, D., Williams, G. H., and Hallgren, J. E., *J. Am. Chem. Soc.* **95**, 266 (1973).
305. Seyferth, D., Williams, G. H., Hung, P. L. K., and Hallgren, J. E., *J. Organomet. Chem.* **71**, 97 (1974).
306. Seyferth, D., Ozolins Nestle, M., and Scott Eschbach, C., *J. Am. Chem. Soc.* **98**, 6724 (1976).
307. Seyferth, D., Williams, G. H., and Nivert, C. L., *Inorg. Chem.* **16**, 758 (1977).
308. Seyferth, D., and Ozolins Nestle, M., *J. Am. Chem. Soc.* **103**, 3320 (1981).
309. Seyferth, D., Nivert Rudie, C., and Merola, J. S., *J. Organomet. Chem.* **162**, 89 (1978).
310. Seyferth, D., Nivert Rudie, C., and Ozolins Nestle, M., *J. Organomet. Chem.* **178**, 227 (1979).
311. Seyferth, D., and Williams, G. H., *J. Organomet. Chem.* **38**, C11 (1972).
312. Hallgren, J., Scott Eschbach, C., and Seyferth, D., *J. Am. Chem. Soc.* **94**, 2547 (1972).
313. Dawson, P. A., Robinson, B. H., and Simpson, J., *J. Chem. Soc., Dalton Trans.*, p. 1762 (1979).
314. Rahman, Z. A., Beanan, L. R., Bavaro, L. M., Modi, S. P., Keister, J. B., and Churchill, M. R., *J. Organomet. Chem.* **263**, 75 (1984).
315. Dellaca, R. J., and Penfold, B. R., *Inorg. Chem.* **11**, 1855 (1972).
316. Holingren, J. S., and Shapley, J. R., *Organometallics* **3**, 1322 (1984).
317. Brice, M. D., Dellaca, R. J., Penfold, B. R., and Spencer, J. L., *J. Chem. Soc., Chem. Commun.*, p. 72 (1971).
318. Dolby, R., and Robinson, B. H., *J. Chem. Soc., Chem. Commun.*, p. 1058 (1970).
319. Sutton, P. W., and Dahl, L. F., *J. Am. Chem. Soc.* **89**, 261 (1967).

320. Elder, P. A., Robinson, B. H., and Simpson, J., *J. Chem. Soc., Dalton Trans.*, p. 1771 (1975).
321. Dolby, R., and Robinson, B. H., *J. Chem. Soc., Dalton Trans.*, p. 2046 (1972).
322. Robinson, B. H., and Spencer, J. L., *J. Chem. Soc. A*, p. 2045 (1971).
323. Geoffroy, G. L., and Epstein, R. A., *Inorg. Chem.* **16**, 2795 (1977).
324. Brice, M. D., Penfold, B. R., Robinson, W. T., and Taylor, S. R., *Inorg. Chem.* **9**, 362 (1970).
325. Vahrenkamp, H., *Angew. Chem., Int. Ed. Engl.* **17**, 379 (1978).
326. Einstein, F. W. B., and Jones, R. D. G., *Inorg. Chem.* **11**, 395 (1972).
327. Keister, J. B., and Horling, T. L., *Inorg. Chem.* **19**, 2304 (1980).
328. Brice, M. D., and Penfold, B. R., *Inorg. Chem.* **11**, 1381 (1972).
329. Edidin, R. T., Norton, J. R., and Mislou, K., *Organometallics* **1**, 561 (1982).
330. Aime, S., Milone, L., and Valle, M., *Inorg. Chim. Acta* **18**, 9 (1976).
331. Miller, D. C., and Brill, T. B., *Inorg. Chem.* **17**, 240 (1978).
332. Khand, I. V., Knox, G. R., Pauson, P. L., and Watts, W. E., *J. Organomet. Chem.* **73**, 383 (1974).
333. Xiang, S. F., Bakke, A. A., Chem, H. W., and Jolly, W. L., *Organometallics* **1**, 699 (1982).
334. King, R. B., *J. Am. Chem. Soc.* **88**, 2075 (1966).
335. Seyferth, D., Williams, G. H., and Traficante, D. D., *J. Am. Chem. Soc.* **96**, 604 (1974).
336. Ryan, R. C., Pittman, C. V., Jr., and O'Connor, J. P., *J. Am. Chem. Soc.* **99**, 1986 (1976).
337. Schilling, B. E. R., and Hoffmann, R., *J. Am. Chem. Soc.* **100**, 6274 (1978).
338. Buckingham, A. D., Yesinowski, J. P., Carty, A. J., and Rest, A. J., *J. Am. Chem. Soc.* **95**, 2732 (1973).
339. Forster, A., Johnson, B. F. G., Lewis, J., and Matherson, T. W., *J. Organomet. Chem.* **104**, 225 (1976).
340. Sherwood, D. E., Jr., and Hall, M. B., *Organometallics* **1**, 1519 (1982).
341. Dellaca, R. J., Penfold, B. R., Robinson, B. H., Robinson, W. T., and Spencer, J. L., *Inorg. Chem.* **9**, 2204 (1970).
342. Robinson, B. H., and Spencer, J. L., *J. Organomet. Chem.* **30**, 267 (1971).
343. Dellaca, R. J., Penfold, B. R., Robinson, B. H., Robinson, W. T., and Spencer, J. L., *Inorg. Chem.* **9**, 2196 (1970).
344. Dellaca, R. J., and Penfold, B. R., *Inorg. Chem.* **10**, 1269 (1971).
345. Vites, J., and Fehlner, T. P., *Organometallics* **3**, 491 (1984).
346. Kolis, J. W., Holt, E. M., Hriljac, J. A., and Shriver, D. F., *Organometallics* **3**, 496 (1984).
347. Dahan, F., and Mathieu, R., *J. Chem. Soc., Chem. Commun.*, p. 432 (1984).
348. Dawson, P. A., Johnson, B. F. G., Lewis, J., and Raithby, P. R., *J. Chem. Soc., Chem. Commun.*, p. 781 (1980).
349. Whitmire, K. H., Shriver, D. F., and Holt, E. M., *J. Chem. Soc., Chem. Commun.*, p. 780 (1980).
350. Holt, E. M., Whitmore, K. H., and Shriver, D. F., *J. Chem. Soc., Chem. Commun.*, p. 778 (1980).
351. Brun, P., Dawkins, G. M., Green, M., Mills, R. M., Salaun, J. Y., Stone, F. G. A., and Woodward, P., *J. Chem. Soc., Chem. Commun.*, p. 966 (1981).
352. Kolis, J. W., Holt, E. M., and Shriver, D. F., *J. Am. Chem. Soc.* **105**, 7307 (1983).
353. Manassero, M., Sansoni, M., and Longoni, G., *J. Chem. Soc., Chem. Commun.*, p. 919 (1976).
354. Beno, M. A., Williams, J. M., Tachikawa, M., and Muetterties, E. L., *J. Am. Chem. Soc.* **103**, 1485 (1981).

355. Tachikawa, M., and Muetterties, E. L., *J. Am. Chem. Soc.* **102**, 4541 (1980).
356. Hodali, H. A., Shriver, D. F., and Ammlung, C. A., *J. Am. Chem. Soc.* **100**, 5239 (1978).
357. Wong, W. K., Chiu, K. W., Wilkinson, G., Galas, A. M. R., Thornton Pett, M., and Hursthouse, M. B., *J. Chem. Soc., Dalton Trans.*, p. 1557 (1983).
358. Churchill, M. R., and Wasserman, H. J., *Inorg. Chem.* **21**, 825 (1982).
359. Arce, A. J., and Deeming, A. J., *J. Chem. Soc., Chem. Commun.*, p. 364 (1982).
360. Churchill, M. R., and Lashewycz, R. A., *Inorg. Chem.* **18**, 848 (1979).
361. Sievert, A. C., Strickland, D. S., Shapley, J. R., Steinmetz, G. R., and Geoffroy, G. L., *Organometallics* **1**, 214 (1982).
362. Bogdan, P. L., Whitmire, K. H., Kolis, J. W., Shriver, D. F., and Holt, E. M., *J. Organomet. Chem.* **272**, 169 (1984).
363. Coates, G. E., Green, M. L. H., Powell, P., and Wade, K., "Principles of Organometallic Chemistry." Methuen, London, 1971.
364. Corfield, P. W. R., and Shearer, H. M. M., in "Organometallic Compounds" (G. E., Coates, M. L. H., Green, and K. Wade, eds.), Vol 2, p. 274, 278. Methuen, London, 1968; Coates, G. E., and Parkin, C., *Adv. Chem. Co-ord. Compounds*, p. 173 (1961).
365. Davidson, J. L., Green, M., Stone, F. G. A., and Welch, A. J., *J. Am. Chem. Soc.* **97**, 7490 (1975).
366. Evans, J., and McNulty, G. S., *J. Chem. Soc., Dalton Trans.*, p. 79 (1984).
367. Anson, C. E., Keiller, B. T., Oxtan, I. A., Powell, D. B., and Sheppard, N., *J. Chem. Soc., Chem. Commun.*, p. 470 (1983).
368. Evans, J., and McNulty, G. S., *J. Chem. Soc., Dalton Trans.*, p. 639 (1983).
369. Andrews, J. R., Kettle, S. F. A., Powell, D. B., and Sheppard, N., *Inorg. Chem.* **21**, 2874 (1982).
370. Cotton, F. A., and Wilkinson, G., "Advanced Inorganic Chemistry," 4th Ed. Wiley, New York, 1980.
371. Muetterties, E. L., *J. Organomet. Chem.* **200**, 177 (1980); Humphries, A. P., and Kaesz, H. D., *Progr. Inorg. Chem.* **25**, 146 (1979).
372. Heaton, B. T., Strona, L., Martinengo, S., Strumolo, D., Goodfellow, R. J., and Sadler, I. H., *J. Chem. Soc., Dalton Trans.*, p. 1499 (1982); Heaton, B. T., Strona, L., Pergola, R. D., Vidal, L. J., and Schoening, R. C., *J. Chem. Soc., Dalton Trans.*, p. 1941 (1983).
373. Constable, E. C., Johnson, B. F. G., Lewis, J., Pain, G. N., and Taylor, M. J., *J. Chem. Soc., Chem. Commun.*, p. 754 (1982).
374. Aime, S., Gobetto, R., Osella, D., Hawkes, G. E., and Randall, E. W., *J. Chem. Soc., Dalton Trans.*, p. 1863 (1984).
375. Koridze, A. A., Kizas, O. A., Kolobova, N. E., Vinogradova, V. N., Ustynyuk, N. A., Petrovskii, P. V., Yanovsky, A. I., and Struchkov, Yu. T., *J. Chem. Soc., Chem. Commun.*, p. 1158 (1984).
376. Koridze, A. A., Kizas, O. A., Kolobova, N. E., Petrovskii, P. V., and Fedin, E. I., *J. Organomet. Chem.* **265**, C33 (1984).
377. Deeming, A. J., *J. Organomet. Chem.* **150**, 123 (1978).
378. Granozzi, G., Tondello, E., Casarin, M., Aime, S., and Osella, D., *Organometallics* **2**, 430 (1983).
379. Green, M., Marsden, K., Salter, I. D., Stone, F. G. A., and Woodward, P., *J. Chem. Soc., Chem. Commun.*, p. 446 (1983).
380. Busetto, L., Green, M., Howard, J. A. K., Hessner, B., Jeffery, J. C., Mills, R. M., Stone, F. G. A., and Woodward, P., *J. Chem. Soc., Chem. Commun.*, p. 1101 (1981).
381. Hagens, W., Bos, H. J. T., and Arens, J. F., *Recl. Trav. Chim. Pays-Bas* **92**, 762 (1973).

382. Aime, S., Osella, D., Giamello, E., and Granozzi, G., *J. Organomet. Chem.* **262**, C1 (1984).
383. Chini, P., *Inorg. Chim. Acta Rev.* **2**, 31 (1968); Chini, P., and Heaton, B. T., *Top. Curr. Chem.* **71**, 1 (1977); Gladfelter, W. L., and Geoffroy, G. L., *Adv. Organomet. Chem.* **18**, 207 (1980).
384. Bild, N., Gesing, E. R. F., Quiquerez, C., and Wehrli, A., *J. Organomet. Chem.* **248**, 85 (1983).
385. Jackson, P. F., Johnson, B. F. G., Lewis, J., McPartlin, M., and Nelson, W. J. H., *J. Chem. Soc., Chem. Commun.*, p. 920 (1978).
386. Churchill, M. R., DeBoer, B. G., and Rotella, F. J., *Inorg. Chem.* **15**, 1843 (1976); Orpen, A. G., *J. Chem. Soc., Dalton Trans.*, p. 2509 (1980).
387. Catti, M., Gervasio, G., and Mason, S. A., *J. Chem. Soc., Dalton Trans.*, p. 2260 (1977).
388. Orpen, A. G., Pippard, D., Sheldrick, G. M., and Rouse, K. D., *Acta Crystallogr., Sect. B* **34**, 2466 (1978).
389. Deshmukh, P., Dutta, T. K., Hwang, J. L.-S., Housecraft, C. E., and Fehlner, T. P., *J. Am. Chem. Soc.* **104**, 1740 (1982); DeKock, R. L., Deshmukh, P., Dutta, T. K., Fehlner, T. P., Housecraft, C. E., and Hwang, J. L.-S., *Organometallics* **2**, 1108 (1983).
390. Granozzi, G., Tondello, E., Casarin, M., Aime, S., and Osella, D., *Organometallics* **2**, 430 (1983).
391. Granozzi, G., Tondello, E., Bertocello, R., Aime, S., and Osella, D., *Inorg. Chem.* **22**, 744 (1983).
392. Turner, D. W., Baker, C., Baker, A. D., and Brundle, C. R., "Molecular Photoelectron Spectroscopy." Wiley (Interscience), New York, 1970.
393. Dewar, M. J. S., *Bull. Soc. Chim. Fr.* **18**, C71 (1951); Chatt, J., and Duncanson, L. A., *J. Chem. Soc.*, p. 2939 (1953).
394. Greaves, E. O., Lock, C. J. L., and Maitlis, P. M., *Can. J. Chem.* **46**, 3879 (1968).
395. Tatsumi, K., Hoffmann, R., and Templeton, J. L., *Inorg. Chem.* **21**, 466 (1982).
396. Hoffmann, D. M., Hoffmann, R., and Fisel, C. R., *J. Am. Chem. Soc.* **104**, 3858 (1982); Hoffman, D. M., and Hoffman, R., *J. Chem. Soc., Dalton Trans.*, p. 1471 (1982).
397. Tondello, E., *Inorg. Chim. Acta* **11**, L5 (1974).
398. Hall, M. B., and Fenske, R. F., *Inorg. Chem.* **11**, 768 (1972).
399. Tolman, C. A., *Chem. Soc. Rev.* **1**, 337 (1972).
400. Wade, K., *Adv. Inorg. Chem. Radiochem.* **18**, 1 (1976).
401. Ciani, G., and Sironi, A., *J. Organomet. Chem.* **197**, 233 (1980); Stone, A. J., *Inorg. Chem.* **20**, 563 (1981); Lauher, J. W., *J. Am. Chem. Soc.* **100**, 5305 (1978); **101**, 2604 (1979); Teo, B. K., *Inorg. Chem.* **23**, 1251 (1984); Teo, B. K., Longoni, G., and Chung, F. R. K., *ibid* **23**, 1257 (1984).
402. Evans, D. G., and Mingos, D. M. P., *Organometallics* **2**, 435 (1983).
403. Mingos, D. M. P., *J. Chem. Soc., Chem. Commun.*, p. 706 (1983).
404. Bruce, M. I., Clark, R., Howard, J., and Woodward, P., *J. Organomet. Chem.* **42**, C107 (1972).
405. Johnson, B. F. G., Lewis, J., Pippard, D., and Raithby, P. R., *Acta Crystallogr., Sect. B* **36**, 703 (1980).
406. Dawoodi, Z., Mays, M. J., Raithby, P. R., and Henrick, K., *J. Chem. Soc., Chem. Commun.*, p. 641 (1980).
407. Dawoodi, Z., Mays, M. J., and Henrick, K., *J. Chem. Soc., Chem. Commun.*, p. 696 (1982).
408. Dawoodi, Z., Mays, M. J., Raithby, P. R., Henrick, K., Clegg, W., and Weber, G., *J. Organomet. Chem.* **249**, 149 (1983).
409. Pierpont, C. G., *Inorg. Chem.* **17**, 1976 (1978).

410. Mills, O. S., and Redhouse, A. D., *J. Chem. Soc., Chem. Commun.*, p. 444 (1966).
411. Henrick, K., McPartlin, M., Deeming, A. J., Hasso, S., and Manning, P., *J. Chem. Soc., Dalton Trans.*, p. 899 (1982).
412. Carty, A. J., MacLaughlin, S. A., van Wagner, J., and Taylor, N. J., *Organometallics* **1**, 1013 (1982).
413. Guy, J. J., Reichert, B. E., and Sheldrick G. M., *Acta Crystallogr., Sect. B* **32**, 3319 (1976).
414. Dawoodi, Z., Mays, M. J., and Raithby, P. R., *J. Chem. Soc., Chem. Commun.*, p. 721 (1979).
415. Lewis, J., and Johnson, B. F. G., *Pure Appl. Chem.* **44**, 43 (1975).
416. Goudsmit, R. J., Johnson, B. F. G., Lewis, J., Raithby, P. R., and Rosales, M. J., *J. Chem. Soc., Dalton Trans.*, p. 2257 (1983).
417. Pierpont, C. G., *Inorg. Chem.* **16**, 636 (1977).
418. Clauss, A. D., Shapley, J. R., and Wilson, S. R., *J. Am. Chem. Soc.* **103**, 7387 (1981).
419. Jaouen, G., Marinetti, A., Mentzen, B., Mutin, R., Saillard, J.-Y., Sayer, B. G., and McGlinchey, M. J., *Organometallics* **1**, 753 (1982).
420. Castiglioni, M., Giordano, R., and Sappa, E., *J. Organomet. Chem.* **275**, 119 (1984).
421. Yasufuku, K., Aoki, K., and Yamazaki, H., *Bull. Chem. Soc. Jpn.* **48**, 1616 (1975).
422. Barner-Thorsen, C., Hardcastle, K. I., Rosenberg, E., Siegel, J., Manotti Lanfredi, A. M., Tiripicchio, A., and Tiripicchio Camellini, M., *Inorg. Chem.* **20**, 4306 (1981).
423. Dawoodi, Z., Mays, M. J., and Henrick, K., *J. Chem. Soc., Dalton Trans.*, p. 1769 (1984).
424. Thomas, M. G., Muetterties, E. L., Day, R. O., and Day, V. W., *J. Am. Chem. Soc.* **98**, 4645 (1976).
425. Castiglioni, M., Gervasio, G., and Sappa, E., *Inorg. Chim. Acta* **49**, 217 (1981).
426. Green, M., Marsden, K., Salter, I. D., Stone, F. G. A., and Woodward, P., *J. Chem. Soc., Chem. Commun.*, p. 446 (1983).
427. Shapley, J. R., Park, J. T., Churchill, M. R., Ziller, J. W., and Beanan, L. R., *J. Am. Chem. Soc.* **106**, 1144 (1984).
428. Kwek, K., Taylor, N. J., and Carty, A. J., *J. Am. Chem. Soc.* **106**, 4636 (1984).
429. Bruce, M. I., Horn, E., Snow, M. R., and Williams, M. L., *J. Organomet. Chem.* **255**, 255 (1983).
430. Aime, S., Nicola, G., Osella, D., Manotti Lanfredi, A. M., and Tiripicchio, A., *Inorg. Chim. Acta* **85**, 161 (1984).
431. MacLaughlin, S. A., Taylor, N. J., and Carty, A. J., *Organometallics* **2**, 1194 (1983).
432. Johnson, B. F. G., Lewis, J., Nicholls, J. N., Puga, J., Raithby, P. R., Rosales, M. J., McPartlin, M., and Clegg, W., *J. Chem. Soc., Dalton Trans.*, p. 277 (1982).
433. Albano, V. G., Chini, P., Martinengo, S., Sansoni, M., and Strumolo, D., *J. Chem. Soc., Dalton Trans.*, p. 459 (1978).
434. Albano, V. G., Braga, D., Ciani, G., and Martinengo, S., *J. Organomet. Chem.* **213**, 293 (1981).
435. Gervasio, G., Rossetti, R., and Stanghellini, P. L., *Inorg. Chem.* **23**, 2073 (1984).
436. Jackson, W. G., Johnson, B. F. G., and Lewis, J., *J. Organomet. Chem.* **139**, 125 (1977).
437. Evans, J., Johnson, B. F. G., Lewis, J., Matherson, T. W., and Norton, J. R., *J. Chem. Soc., Dalton Trans.*, p. 626 (1978).
438. Hickey, J. P., Wilkinson, J. R., and Todd, L. J., *J. Organomet. Chem.* **99**, 281 (1975).
439. Aime, S., Milone, L., Osella, D., Valle, M., and Randall, E. W., *Inorg. Chim. Acta* **20**, 217 (1976).
440. Aime, S., Milone, L., and Sappa, E., *Inorg. Chim. Acta* **16**, L7 (1976).

441. Shapley, J. R., Richter, S. I., Tachikawa, M., and Keister, J. B., *J. Organomet. Chem.* **94**, C43 (1975).
442. Evans, J., Johnson, B. F. G., Lewis, J., and Matheson, T. W., *J. Organomet. Chem.* **97**, C16 (1975).
443. Deeming, A. J., Rothwell, I. P., Hursthouse, M. B., and Backer-Dirks, J. D. J., *J. Chem. Soc., Dalton Trans.*, p. 1879 (1981).
444. Aime, S., Gobetto, R., Osella, D., Milone, L., and Rosenberg, E., *Organometallics* **1**, 640 (1982).
445. Churchill, M. R., Lashewycz, R. A., Tachikawa, M., and Shapley, J. R., *J. Chem. Soc., Chem. Commun.*, p. 699 (1977).
446. Carty, A. J., Ferguson, G., Paik, H. N., and Restivo, R., *J. Organomet. Chem.* **74**, C14 (1974).
447. Nucciarone, D., Taylor, N. J., and Carty, A. J., *Organometallics* **3**, 177 (1984).
448. Carty, A. J., MacLaughlin, S. A., and Taylor, N. J., *J. Am. Chem. Soc.* **103**, 2456 (1981).
449. Clauss, A. D., Shapley, J. R., Wilker, C. N., and Hoffmann, R., *Organometallics* **3**, 619 (1984).
450. Amadelli, R., Carassiti, V., Maldotti, A., Aime, S., Osella, D., and Milone, L., *Inorg. Chim. Acta* **81**, L11 (1984).
451. Gambino, O., Vaglio, G. A., Ferrari, R. P., and Cetini, G., *J. Organomet. Chem.* **30**, 381 (1971).
452. Dawoodi, Z., and Mays, M. J., *J. Chem. Soc., Dalton Trans.*, p. 1931 (1984).
453. Johnson, B. F. G., Kelland, J. W., Lewis, J., Mann, A. L., and Raithby, P. R., *J. Chem. Soc., Chem. Commun.*, p. 547 (1980).
454. Aime, S., Castiglioni, M., Gobetto, R., and Osella, D., *Polyhedron* **3**, 175 (1984).
455. Castiglioni, M., Giordano, R., and Sappa, E., *J. Organomet. Chem.* **258**, 217 (1983).
456. Bryan, E. G., Jackson, W. G., Johnson, B. F. G., Kelland, J. W., Lewis, J., and Schorpp, K. T., *J. Organomet. Chem.* **108**, 385 (1976).
457. Barner-Thorsen, C., Rosenberg, E., Saatjian, G., Aime, S., Milone, L., and Osella, D., *Inorg. Chem.* **20**, 1592 (1981).
458. Jangala, C., Rosenberg, E., Skinner, D., Aime, S., Milone, L., and Sappa, E., *Inorg. Chem.* **19**, 1571 (1980).
459. Bracker, J., Rosenberg, E., and Gelbert, R. W., *Coord. Chem.: Abstr. Int. Conf. Coord. Chem. 1984*, p. 599 (1984).
460. Bruce, M. I., Rodgers, J. R., Snow, M. R., and Wong, F. S., *J. Organomet. Chem.* **240**, 299 (1982).
461. Deeming, A. J., and Hasso, S., *J. Organomet. Chem.* **112**, C39 (1976).
462. Churchill, M. R., DeBoer, B. G., Shapley, J. R., and Keister, J. B., *J. Am. Chem. Soc.* **98**, 2357 (1976).
463. Jeffery, J. C., Mead, K. A., Razay, H., Stone, F. G. A., Went, M. J., and Woodward, P., *J. Chem. Soc., Chem. Commun.*, p. 867 (1981).
464. Nuel, D., Lourdich, M., Dahan, F., and Mathieu, R., *Coord. Chem.: Abstr. Int. Conf. Coord. Chem. 1984*, p. 651 (1984).
465. Sappa, E., Manotti Lanfredi, A. M., and Tiripicchio, A., *Inorg. Chim. Acta* **36**, 197 (1979).
466. Aime, S., Milone, L., Sappa, E., Tiripicchio, A., and Tiripicchio Camellini, M., *Inorg. Chim. Acta* **32**, 163 (1979).
467. Afzal, D., Lenhert, P. G., and Lukehart, C. M., *J. Am. Chem. Soc.* **106**, 3050 (1984).
468. Dickson, R. S., Nesbit, R. J., Pateras, H., Patrick, J. M., and White, A. H., *J. Organomet. Chem.* **265**, C25 (1984).

- 469. MacLaughlin, S. A., Johnson, J. P., Taylor, N. J., Carty, A. J., and Sappa, E., *Organometallics* **2**, 352 (1983).
- 470. DeMontauzon, D., Dahan, F., and Mathieu, R., *Coord. Chem.: Abstr. Int. Conf. Coord. Chem. 1984*, p. 650 (1984); DeMontauzon, D., and Mathieu, R., *J. Organomet. Chem.* **252**, C83 (1983).
- 471. Zanello, P., Aime, S., and Osella, D., *Abstr. Int. Conf. Chem. Platinum Group Met., 2nd, 1984*, No. A22 (1984).

This Page Intentionally Left Blank

ORGANIC SUPERCONDUCTORS: SYNTHESIS, STRUCTURE, CONDUCTIVITY, AND MAGNETIC PROPERTIES

JACK M. WILLIAMS* AND KIM CARNEIRO**

*Chemistry and Materials Science and Technology Divisions,
Argonne National Laboratory Argonne, Illinois, and

**Physics Laboratory I, University of Copenhagen,
H. C. Ørsted Institute, Copenhagen, Denmark

I. Introduction	249
II. The Synthesis of TMTSF and BEDT-TTF (ET), and Crystal Growth of Conducting Salts	253
A. The Synthesis of TMTSF and Chalcogenide Derivatives	254
B. The Synthesis of BEDT-TTF (ET) and Chalcogenide Derivatives	254
C. Electrocrystallization of 2:1 Derivatives of TMTSF	256
III. Crystal Structures of (TMTSF) ₂ X and (ET) ₂ X Conductors	258
A. (TMTSF) ₂ X	258
B. (ET) ₂ X	269
C. X-Ray Diffuse Scattering Studies of Anion Ordering	274
IV. Electrical Conduction	278
A. Resistivity along the Chains	279
B. Conduction Anisotropy	283
C. Pressure Studies	284
V. Magnetic Properties	286
A. Magnetic Susceptibility	286
B. ESR Linewidths.	290
VI. Concluding Remarks	291
References	292
Note Added in Proof	296

I. Introduction

It is now well established that synthetic materials may be prepared with mechanical properties closely resembling those of elemental metals and alloys. As a result, we have come a long way from the ebonite handles and fragile plastic toys of 30 years ago to the overwhelming occurrence of plastics in modern mechanical structures. Similarly, it is now possible to mimic the electrical properties of elemental metals

using synthetic materials although the applications of these systems are still at their infancy. Hence, by a synthetic metal we define a compound with electrical properties resembling those of ordinary metals, despite the fact that it contains no metallic elements. And, from a basic scientific point of view, the success in reproducing electrical properties in synthetic metals, including superconductivity, by *designing* appropriate molecular materials is as pronounced as it has been for the mechanical properties.

The first indication that molecular compounds could exhibit interesting electrical properties apart from those of an insulator was given in 1954, when Akamatu *et al.* (1) reported a resistivity of $\rho = 10 \Omega \text{ cm}$ for a bromine salt of perylene. Normally perylene crystals themselves are insulating with $\rho = 10^{14}\text{--}10^{16} \Omega \text{ cm}$; therefore, a dramatic change in electronic structure had occurred. The perylene molecule is shown in Fig. 1.

It was not until 1960 when the molecule TCNQ (tetracyanoquinodimethane, also shown in Fig. 1) was shown to form highly conducting crystals that molecular conductors became the subject of large-scale solid-state investigations (2). In particular, $M(\text{TCNQ})_2$ salts, where M is a monovalent cation (alkali metal or organic), have been extensively studied. As is the case for the original bromine-perylene compound, they are semiconductors (i.e., having thermally activated electrical conduction) with activation energies of 50–200 meV, but possibly exhibiting metallic behavior (non thermally activated conduction) at high temperatures. Figure 2, which shows the development of the temperature-dependent resistivity in molecular conductors in a historical perspective, includes $\text{TEA}(\text{TCNQ})_2$ (TEA = triethyl ammonium).

During the same period, the understanding of superconductivity in elemental metals underwent dramatic improvements with the development of the now well-known theory of Bardeen, Cooper, and Schrieffer (BCS) (3). According to this theory, electrons form bound pairs (the Cooper pairs) as a result of their interactions with the lattice vibrations (the phonons). The upper limit for the superconducting transition temperature is determined by the maximum phonon frequency, the Debye frequency. This understanding led Little (4) to propose that high transition temperatures could be achieved in *molecular* metals (if these could be made) since the high frequencies of their internal vibrations might serve to play the same role phonons play in ordinary superconductors. Little's proposal sparked considerable interest and marked the onset of the search for superconductivity in molecular materials. The promise of possible high-temperature superconductivity has remained a goal since that time.

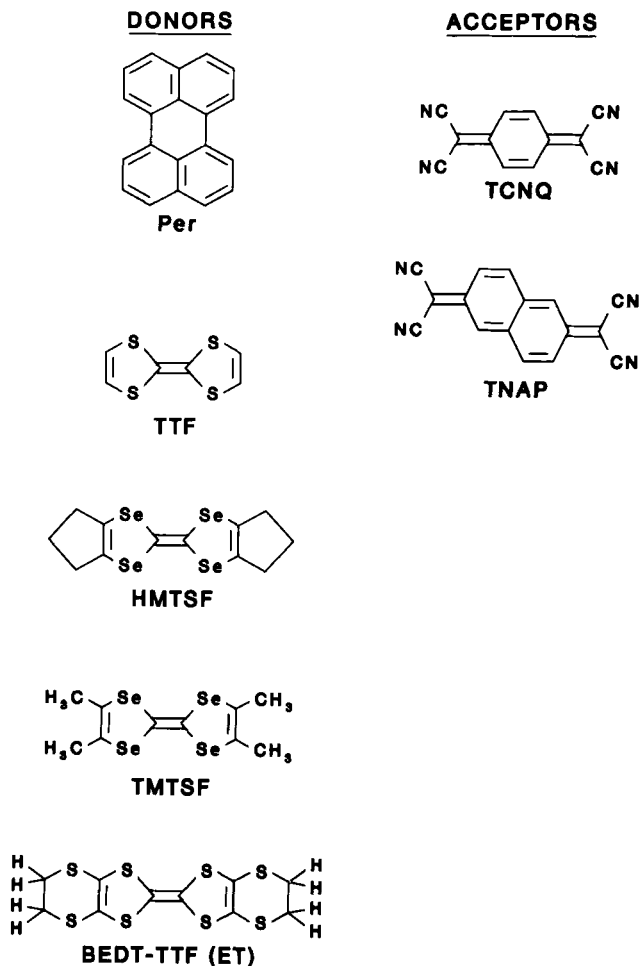


FIG. 1. Molecules that form conducting crystals described in this article. The left column contains the donors: perylene (Per), tetrathiafulvalene (TTF), hexamethyltetraselenafulvalene (HMTSF), tetramethyltetraselenafulvalene (TMTSF), and bis(ethylenedithio)-TTF (BEDT-TTF or "ET"). To the right are the acceptor molecules tetracyanoquinodimethane (TCNQ) and tetracyanonaphthalene (TNAP).

The first molecular crystal exhibiting genuine metallic behavior was TTF-TCNQ (TTF = tetrathiafulvalene) (5). Between 54 K and room temperature, TTF-TCNQ behaves like a metal (decreasing electrical resistance with decreasing temperature), although the concept of a metal must of course be modified to take into account the complicated

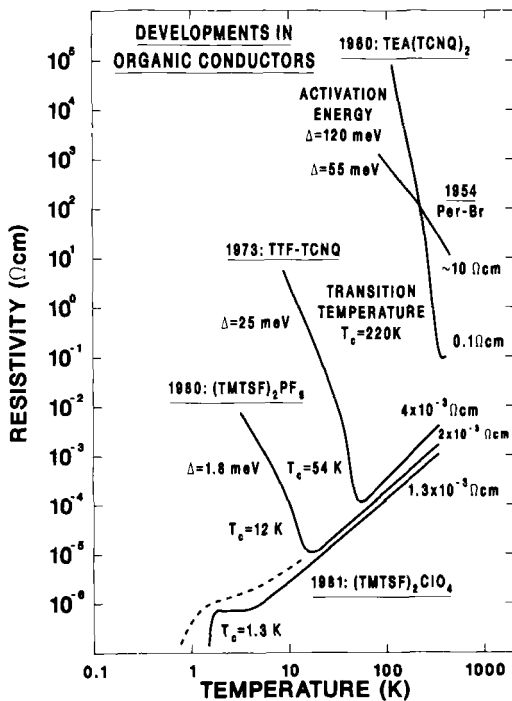


FIG. 2. Temperature dependence of the electrical resistivity of some organic conductors: historical development. The dashed line shows $(\text{TMTSF})_2\text{PF}_6$ at high pressure.

electronic structure of a two-component molecular compound. Below 54 K, TTF-TCNQ exists in a semiconducting state similar to the compounds mentioned earlier. This state, often referred to as the Peierls insulator, was predicted to exist in one-dimensional conductors by Peierls in 1954 and arises from an electron-phonon instability of a one-dimensional metal (6). The Peierls instability is a clear competitor to superconductivity in molecular conductors since these materials are generally formed by (one-dimensional) stacks of planar, or nearly planar, molecules and these systems tend to undergo lattice distortions, dimerization, etc. at the Peierls transition temperature. Hence, the Peierls instability (and other one-dimensional instabilities to which we shall return) must be prevented by some means if superconductivity is to occur in molecular systems. We now turn to a discussion of the means whereby such transitions, which often result in electron localization, can be suppressed.

One way to induce superconductivity in a molecular metal has proven to be the application of pressure which often prevents or removes the

tendency toward a Peierls transition. Two chemical modifications of the TTF molecule, TMTSF (7) (tetramethyltetraselenafulvalene) and BEDT-TTF [bis(ethylenedithio)tetrathiafulvalene] (8, 9) form superconductors under pressure and, in a very few cases, at ambient pressure. Several (TMTSF)₂X salts, known as Bechgaard salts ($X = \text{PF}_6^-$, AsF_6^- , TaF_6^- , FSO_3^- , and ReO_4^-), show this behavior, and in one instance ($X = \text{ClO}_4^-$) superconductivity is observed without the application of pressure (10, 11). The superconducting transition temperatures (T_c) for (TMTSF)₂X and (BEDT-TTF)₂X materials ($X =$ monovalent anion) range from ~ 0.9 – 1.2 K for the former and 1.5 – 2.7 K for the latter synthetic metals. A number of salts of the BEDT-TTF, or "ET",¹ family exhibit ambient-pressure superconductivity, viz. β -(ET)₂I₃ (9, 105, 106, 114) and β -(ET)₂IBr₂ (107, 108), while (ET)₂ReO₄ requires pressures above 4–6 kbar to suppress a metal–insulator transition that occurs at ~ 81 K (8).

An attempt to explain the physical properties of molecular metals by using the concepts commonly invoked for ordinary metals may seem a very ambitious and highly risky task, and we do not pretend to present here, in any way, the final answers. Nevertheless, we find that penetrating and useful insight is gained by analyzing the crystallographic structures of synthetic metals and correlating them with their solid-state properties as exemplified by their electrical conductivities and magnetic susceptibilities. We shall focus only on TMTSF and ET salts, since they form the basis for all known organic superconductors, and because they display, more or less, all of the structural features and properties of earlier synthetic conductors. And as we will demonstrate, despite the complexity of the problem, it is possible to give several ingredients that contribute to the recipe for the synthesis of an improved synthetic metal or superconductor.

II. The Synthesis of TMTSF and BEDT-TTF (ET), and Crystal Growth of Conducting Salts

Synthesizing a molecular conductor generally falls into two separate parts. First, the starting material, the organic donor "conducting molecule" has to be prepared, and secondly, single crystals of the desired conducting salts must be grown. Both procedures must be

¹ As it appears from Fig. 1, the short names for "conducting molecules" are descriptive but in no way unambiguous. As even descriptive short names become longer and longer, there may be a need for shortening them. Hence, BEDT-TTF is often abbreviated ET, not entirely independent of the fact that the Spielberg movie "ET" (Extra Terrestrial)[®] occurred within a few months of the discovery of superconductivity in (ET)₂ReO₄ (in a California laboratory).

independently optimized, and, in particular, care must be taken to design the crystal growth procedure in order to maximize the yield of crystals of desired stoichiometry and crystal structure. The latter problem has recently proven to be a severe one for $(\text{ET})_2\text{X}$ conductors, which often form a multiplicity of phases, sometimes even of the *same stoichiometry* but with different crystal structures and electrical properties, all during a single growth cycle.

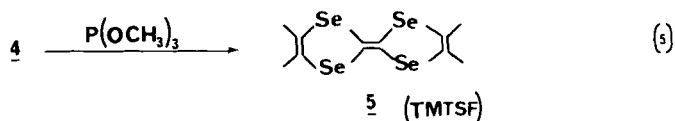
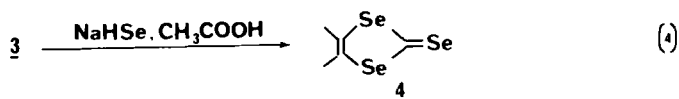
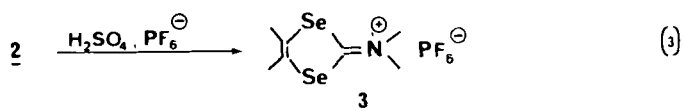
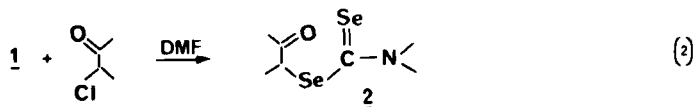
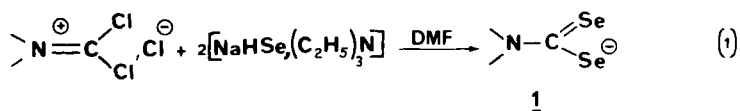
A. THE SYNTHESIS OF TMTSF AND CHALCOGENIDE DERIVATIVES

The original synthesis of TMTSF required CSe_2 as a starting material (13–15) and that route has been patented (16). Since CSe_2 is difficult to handle and extremely malodorous (rotten radishes!), syntheses in which gaseous H_2Se replaced CSe_2 in the syntheses of TMTSF were subsequently reported using selenoureas (17) or *N,N*-dimethylphosgeneiminium chloride (18, 19). A synthesis based on the use of H_2Se , and which can easily be accomplished by students, has become available (20). However, gaseous H_2Se is extremely toxic, with an approximate LC_{50} (30 min) in guinea pigs of 6 ppm, and must be handled with great care (21). Therefore, it is not surprising that a TMTSF synthesis has been developed that does not require either CSe_2 or H_2Se , but rather uses elemental Se as shown in Scheme 1 (22).

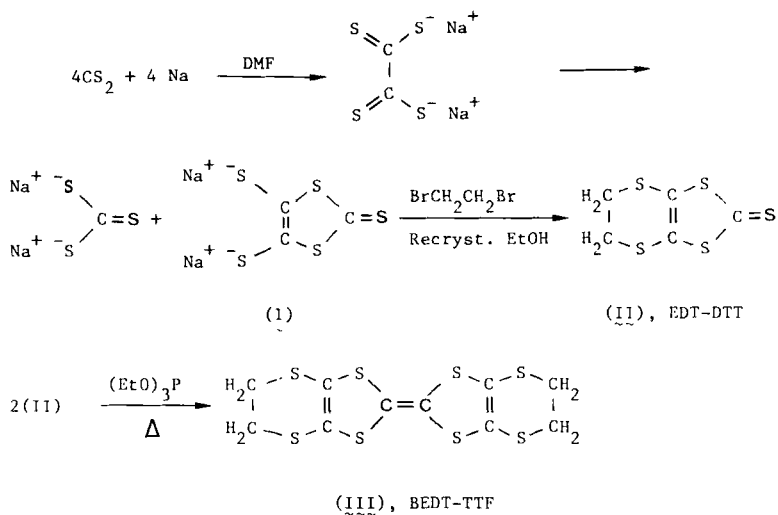
Although these improvements in the synthesis of TMTSF were welcome, it appears that the presence of a minor sulfur (<1–2%) impurity is observed in any of the procedures, other than that using CSe_2 , in which *N,N*-dimethylphosgeneiminium chloride is used as an intermediate. This sulfur impurity apparently suppresses the superconducting transition temperatures of $(\text{TMTSF})_2\text{X}$ derivatives; when $\text{X} = \text{ClO}_4^-$, T_c is reduced by $\sim 0.1\text{--}0.3$ K from 1.3 K. Careful vacuum gradient sublimation of the *N,N*-dimethylphosgeneiminium chloride apparently results in the removal of the sulfur contaminant (23). In passing, it should be noted that the preparation of perdeuterio-TMTSF (19), tetraselenafulvalene-TCNQ (24), and dibenzotetraselenafulvalene charge-transfer salts have also been reported (25, 26).

B. THE SYNTHESIS OF BEDT-TTF (ET) AND CHALCOGENIDE DERIVATIVES

Sulfur-based ET and alkyl derivatives were prepared (27, 29) in the late 1970s using CS_2 as starting material. A preparative procedure suitable for student use which involves the reduction of CS_2 with metallic sodium has also been developed (28), as indicated in Scheme 2.



SCHEME 1. Synthesis of TMTSF using elemental selenium (22).

SCHEME 2. Synthesis of BEDT-TTF by reduction of CS₂ with metallic sodium (28).

Preparative schemes for the systematic modification of the ET framework through the insertion of Se, and S-Se combinations, have been advanced and some derivatives have been prepared (30). At this time the only derivatives of ET that form superconductors are for $X = I_3^-$ (9, 105, 106, 114), IBr_2^- (107, 108), and ReO_4^- (8).

C. ELECTROCRYSTALLIZATION OF 2:1 DERIVATIVES OF TMTSF

As mentioned, only 2:1 (radical-cation: monovalent anion) derivatives of organic synmetals appear to form salts that exhibit superconductivity. Crystals of these conductors are produced using simple electrochemical oxidation techniques in an H-shaped cell, or a variation of this type cell, as shown in Fig. 3. Solutions of the organic donor (TMTSF or ET), and a salt of the desired anion as a tetraalkylammonium derivative to increase solubility in the organic medium, are prepared using redistilled, dried, and deoxygenated organic solvents such as tetrahydrofuran or 1,2,2-trichloroethane. Tetrabutylammonium($n\text{-Bu}_4\text{N}^+$) salts are the most commonly used because

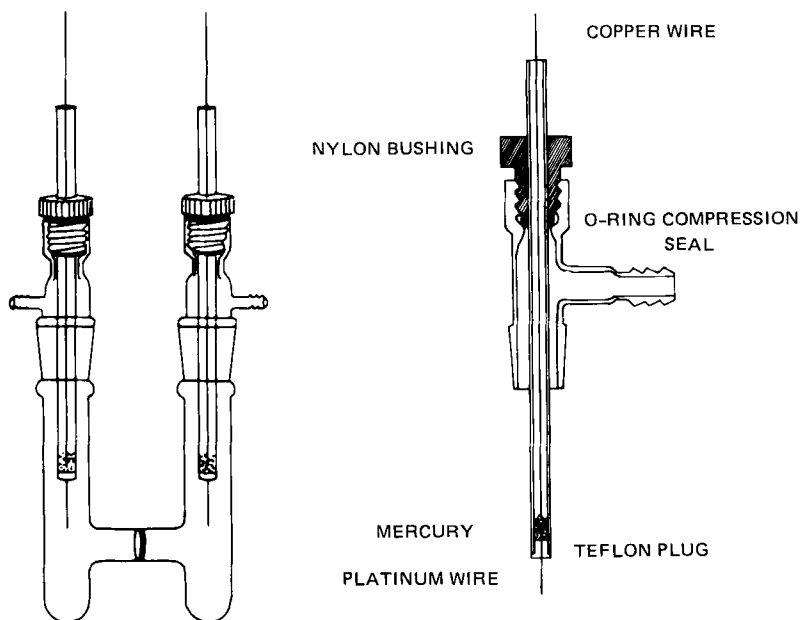
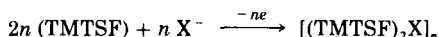


Fig. 3. Cell and electrodes used in the electrocrystallization of organic conductors (29).

high-quality crystals ($\sim 0.5 \times 0.5 \times 10$ mm) of TMTSF derivatives are frequently grown. Some typical crystals are shown in Fig. 4.

Before electrocrystallization is initiated the solvent and anionic derivative are placed in the cathode compartment of the cell while the solvent, anionic derivative, and organic donor are loaded in the anode (oxidizing) compartment. Platinum electrodes are then inserted in both compartments and oxidation, with concomitant crystal growth at the anode, is accomplished using either constant voltage or constant current techniques. In the case of $(\text{TMTSF})_2\text{X}$, crystals grow on the anode according to the reaction:



Generally speaking, only one crystalline phase grows when employing TMTSF and an octahedral or tetrahedral anion. However, in the case of ET, as many as four or more different crystallographic phases may form in one growth cycle. As might be expected, sorting out the different ET:X phases is a very complicated task. Using the constant-current technique (current = $1\text{--}5 \mu\text{A}$), long shiny black needle-shaped crystals form when TMTSF is used while metallic black crystals of differing morphologies are found when using ET (8, 31, 106). In all cases the

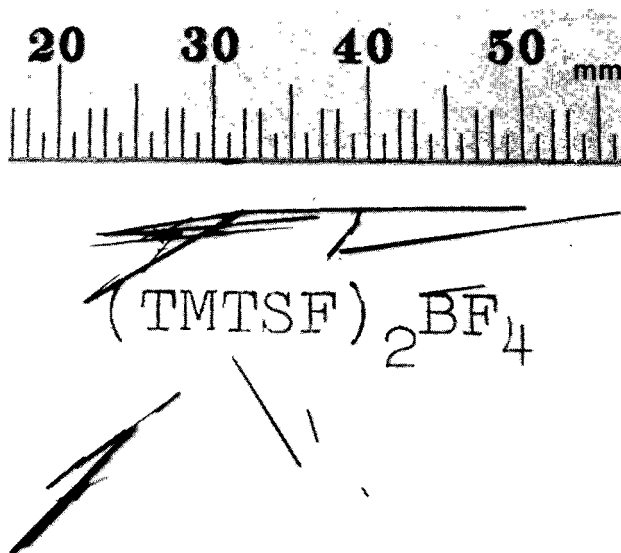


FIG. 4. Photograph of freshly harvested $(\text{TMTSF})_2\text{BF}_4$ crystals which were grown using the cell shown in Fig. 3.

crystals formed have a metallic luster but may have electrical properties that vary from insulating to semiconducting to metallic in nature. A detailed description of electrocrystallization, including donor concentration, solvents used, current densities, etc., has been given for $(\text{TMTSF})_2\text{ClO}_4$, (11) as well as for other TMTSF salts (20). A brief review of the preparation and electrical properties of TMTSF derivatives, some with stoichiometries other than the common 2:1 phases, has been published (10). The detailed electrocrystallization procedures for $(\text{ET})_2\text{X}$ ($\text{X} = \text{ReO}_4^-$ and FSO_3^-) derivatives have also been described (28).

III. Crystal Structures of $(\text{TMTSF})_2\text{X}$ and $(\text{ET})_2\text{X}$ Conductors

A. $(\text{TMTSF})_2\text{X}$

Understanding the crystal structures of the known organic superconductors is essential because they provide some of the vital insight needed to unravel the variety of physical properties exhibited by these materials. Their understanding also provides a means for varying the electrical properties and for engineering new organic metals. For example, although *all* $(\text{TMTSF})_2\text{X}$ compounds possess the same triclinic (space group $P\bar{1}$) crystal structure at room temperature, which is an unusual characteristic of these materials, they may have vastly different properties at low temperature or high pressures. This is demonstrated by the facts that (1) a pressure of 6.5 kbar must be applied to $(\text{TMTSF})_2\text{PF}_6$ before it will become superconducting at 0.9 K, (2) $(\text{TMTSF})_2\text{ReO}_4$ has an anion-assisted disorder/order transition at 180 K where it loses its metallic properties (unless pressure is applied which suppresses the transition), and (3) $(\text{TMTSF})_2\text{ClO}_4$ is the only known *ambient pressure* Se-based superconductor with $T_c = 1.3$ K (10). The differences in physical behavior are associated with very minute differences in the crystallographic structure. Thus, although the anion plays no obvious role in the actual conduction process, which occurs through a network of Se-Se interactions (*vide infra*), it does cause pronounced changes in electrical properties which we shall discuss in Section IV.

The crystal structure of $(\text{TMTSF})_2\text{BrO}_4$ is shown in Fig. 5 as representative of the series (32). The basic architectural feature of the isostructural $(\text{TMTSF})_2\text{X}$ salts is the zig-zag columnar stacking of nearly planar TMTSF molecules parallel to the high-conductivity a axis (10, 11, 32-40). The structures of the salts are different from that of

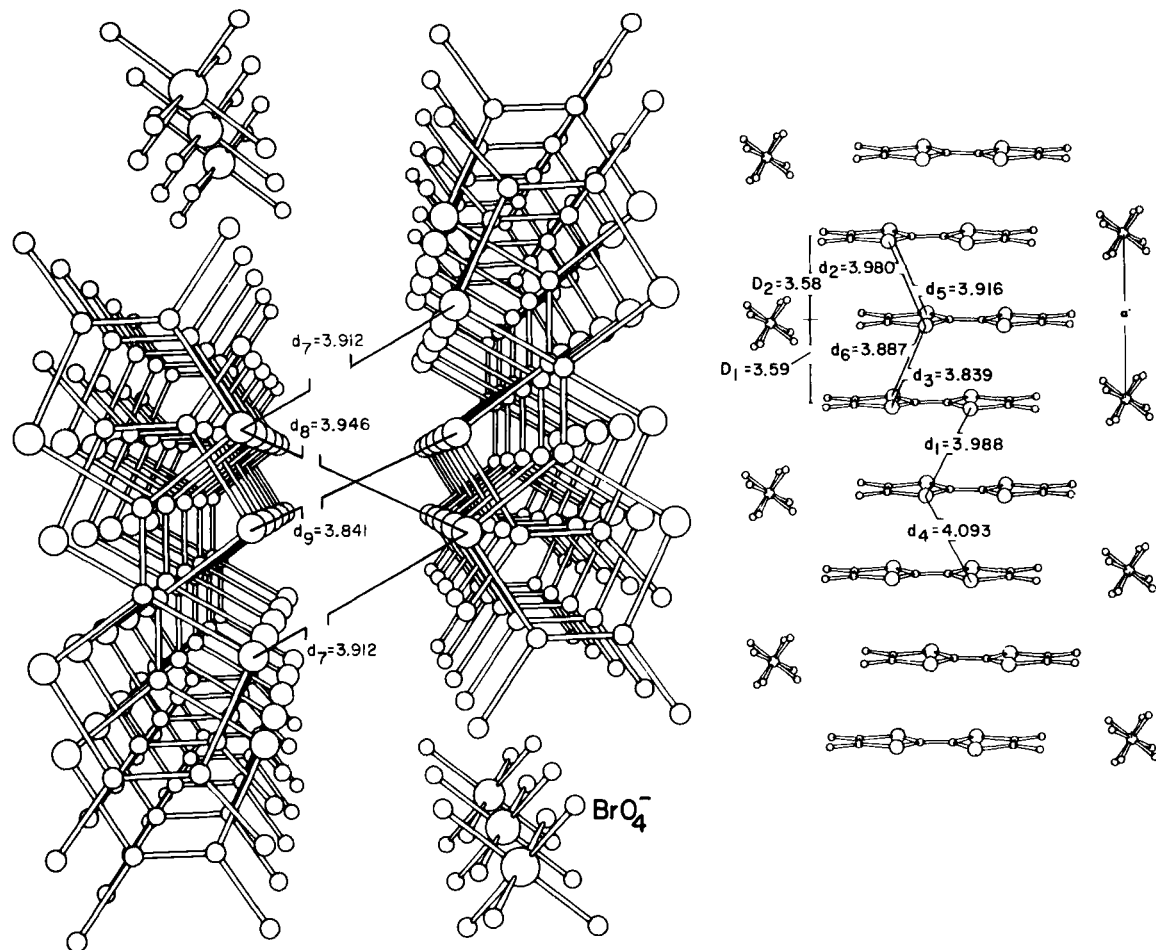


FIG. 5. Perspective views of the crystal structure of $(\text{TMTSF})_2\text{BrO}_4$, looking down the stacks along the a axis (left) and perpendicular to them, approximately along the b axis (right). Not all of the oxygen atom positions of the anion, which result from crystallographic disorder, are shown. The Se...Se contact distances (d 's) are indicated.

neutral TMTSF itself (41). The TMTSF molecules in $(\text{TMTSF})_2\text{X}$ salts form stacks along the a crystallographic axis, which turns out to be the direction of highest electrical conductivity. These stacks also result in the formation of infinite two-dimensional molecular sheets, which extend in the a - b plane, with the TMTSF molecules connected through *interstack* $\text{Se} \cdots \text{Se}$ interactions, thereby providing added "dimensionality" to the system beyond that provided solely by the one-dimensional stacks of TMTSF molecules. However, the TMTSF molecules themselves do not form a three-dimensional network because the sheets are separated along c by the anions (X).

Possibly the most important structural feature that has been revealed from crystallographic studies performed at two temperatures (298 and 125 K) is the existence of an "infinite sheet network" (32) of Se-Se interactions as shown in Fig. 6. At room temperature the intermolecular *intra*- and *interstack* Se-Se distances are all similar and have values of 3.9–4.9 Å, compared to the van der Waals radius sum for the selenium atom (52) of 4.0 Å. However, as the temperature is lowered (298 \rightarrow 125 K) rather unusual changes occur, viz. the ratio of the decrease in the *interstack*:*intrastack* Se-Se distances is not unity but is approximately 2:1 (32, 40). Thus, the distances between the "chains" shown in Fig. 6 decrease, on the average, by twice as much as the distances between TMTSF molecules in each stack. This most certainly leads to increased *interchain* bonding and electronic delocalization through the selenium atom network as the temperature is decreased (42).

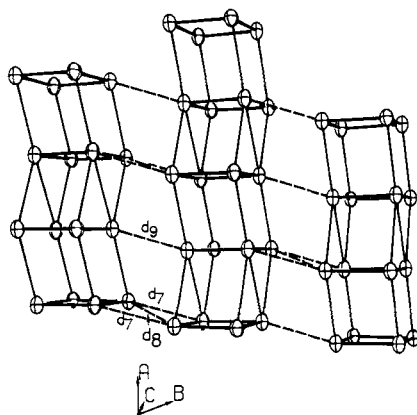


FIG. 6. Representation of the selenium atom "infinite sheet network" in $(\text{TMTSF})_2\text{X}$ salts. This network is the main pathway for electrical conduction. Lines connect selenium atoms that are closer than the van der Waals' radius sum ($\text{Se} \cdots \text{Se}$) of 4.0 Å. Full lines show *intrastack*, broken lines, *interstack* distances: d_7 , d_8 , and d_9 .

Given the importance of the specific anions for the physical behavior of the $(\text{TMTSF})_2\text{X}$ salts it seems worthwhile to dwell upon the influence of their sizes and shapes on the crystallographic properties. Contrary to previous reports, even the centrosymmetric anions AsF_6^- and PF_6^- are in crystallographic disorder with their central atom most likely always residing at the inversion center (1 site) in the triclinic unit cell (39). When X^- is highly symmetric (octahedral or tetrahedral), the network of interstack Se-Se distances expands and contracts in a surprisingly predictable fashion as the size of the anion is varied. This network expansion, not surprisingly, is accompanied by systematic changes in the crystallographic unit cell volume. These features are demonstrated in Figs. 7 and 8. We define the anion volume V_A by using effective ionic radii (43). Adopting the method of Shannon and Prewitt (44) for deriving effective multiautomic radii we define V_A by the volume of the sphere that has the correct multiautomic radius. Hence, $V_A = \frac{4}{3}\pi(r_i + 2r_o)^3$, where r_i is the radius of the inner ion (e.g., Cl in ClO_4^-) and r_o is that associated with the outer ion.

By plotting known V_c values for six TMTSF salts ($\text{X} = \text{PF}_6^-$, ReO_4^- , BrO_4^- , ClO_4^- , BF_4^- , and FSO_3^-) versus V_A , a linear relation between

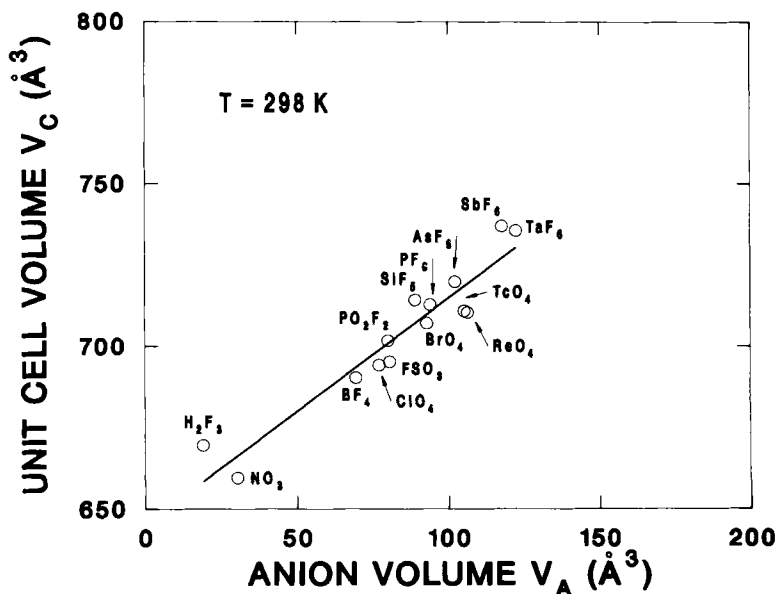


FIG. 7. Plot of unit cell volume V_c of $(\text{TMTSF})_2\text{X}$ salts at room temperature vs. anion volume V_A .

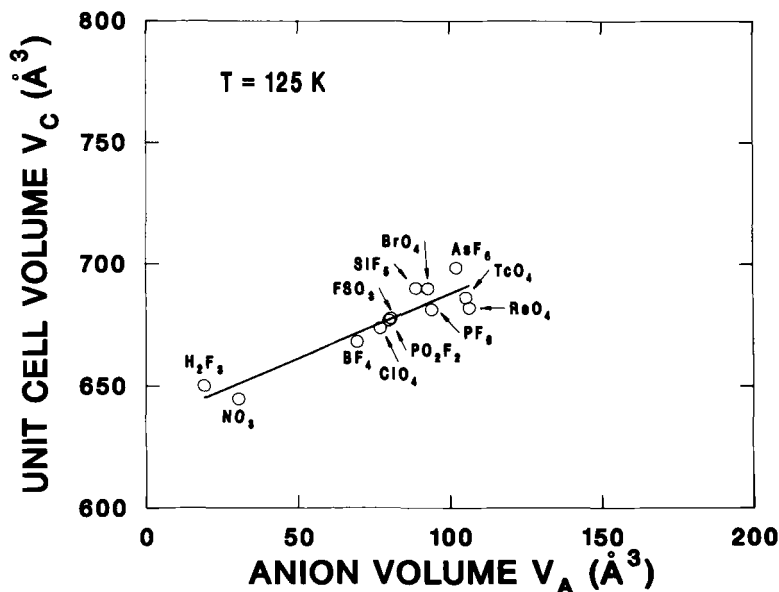


FIG. 8. Plot of unit cell volume V_c of $(\text{TMTSF})_2\text{X}$ salts at 120–125 K vs. anion volume V_A .

V_c and V_A is observed, both at $T = 295 \text{ K}$ (Fig. 7) and at $T = 125 \text{ K}$ (Fig. 8). This suggests that V_c may be accurately estimated by using a linear least-square fit, to yield a calculated volume (40)

$$V_{cp} = 0.65 V_A + 645 \quad (T = 298 \text{ K})$$

or

$$V_{cp} = 0.42 V_A + 642 \quad (T = 125 \text{ K}).$$

For example, for ClO_4^- ($r_{\text{Cl}}^{7+} = 0.22 \text{ \AA}$ and $r_{\text{O}}^{2-} = 1.21 \text{ \AA}$), the calculated V_c is 675 \AA^3 and the observed V_c is 673.7 \AA^3 ($T = 125 \text{ K}$). Concerning bond lengths within an anion, our use of effective radii is justified because the results are identical to those obtained from molecular orbital calculations (45, 46). But the empirical effective anion volume, i.e., its contribution to V_c , is only about 50% of the calculated V_A [65% (298 K) and 42% (125 K)] of calculated V_A . Values of these volumes are given in Table I and we conclude that our approach provides a very good measure of the anion volumes, in particular their relative sizes.

TABLE I

INTERNUCLEAR DISTANCES (r) AND ANIONIC VOLUMES (V_A) CALCULATED FROM MOLECULAR ORBITAL CALCULATIONS (MO), EFFECTIVE IONIC RADII (EIR), AND COMPARED TO EXPERIMENTAL VALUES (EXP)

Anion		Internuclear Distance (Å)			$V_A(\text{\AA}^3)$	
		MO ^a	EIR	EXP ^a	EIR	EXP ^b
H ₂ F ₃					19	25
NO ₃	$r_{\text{N-O}}$	1.277	1.28	1.22–1.27	30	20
BF ₄	$r_{\text{B-F}}$	1.380	1.42	1.40–1.43	70	45
ClO ₄	$r_{\text{Cl-O}}$	1.542	1.44	1.41–1.43	77	49
FSO ₃	$r_{\text{S-F}}$	1.601	1.42	1.55–1.555	81	50
	$r_{\text{S-O}}$	1.459	1.48	1.424–1.455		
BrO ₄					93	62
PF ₆	$r_{\text{P-F}}$	1.612	1.68	1.60–1.63	94	59
AsF ₆	$r_{\text{As-F}}$	1.744	1.76	1.59–1.96	102	74
TcO ₄					105	66
ReO ₄					106	65
SbF ₆	$r_{\text{Sb-F}}$	1.895	1.90	1.53–1.99	118	72
TaF ₆					122	91
CF ₃ SO ₃					153	95

^a Data from refs. 45, 46.

^b Room temperature value = $V_c - 645 \text{ \AA}^3$.

It appears that the search for new superconducting (TMTSF)₂X derivatives should center around those for which the unit cell volume is close to that of (TMTSF)₂ClO₄ [$V_c = 694.3 \text{ \AA}^3$ (298 K) and 673.7 \AA^3 (125 K)]. Thus, the equations and methodology given here are of practical use because, for any imaginable anion, the unit cell volume can be predicted before the salt is prepared. For example, based on the equations above, candidates for superconductivity might be (TMTSF)₂PO₂F₂ [$V_{cp} = 675.6 \text{ \AA}^3$ (125 K)], (TMTSF)₂CrO₃F [$V_{cp} = 679.1 \text{ \AA}^3$ (125 K)], and (TMTSF)₂WF₆ [$V_{cp} = 692.4 \text{ \AA}^3$ (125 K)]. While (TMTSF)₂PO₂F₂ has been prepared (47, 48), it undergoes a metal-insulator transition at 137 K (47) and pressures up to 15 kbar do not induce superconductivity; the CrO₃F[−] anion oxidizes TMTSF and a derivative cannot be prepared (68); and (TMTSF)₂WF₆ has not yet been prepared but it is expected that pressure would be required to induce superconductivity because of the larger (predicted) unit cell volume compared to that of (TMTSF)₂ClO₄.

Important further illuminations of the relationships between the structural and transport properties is provided by crystallographic studies under pressure. As yet, very limited information is available. However, from studies of $(\text{TMTSF})_2\text{PF}_6$, the volume compressibility is estimated to be $0.5\% \text{ kbar}^{-1}$ (49). It, therefore, requires $\sim 6 \text{ kbar}$ to compress $(\text{TMTSF})_2\text{PF}_6$ into the same volume as $(\text{TMTSF})_2\text{ClO}_4$, which is in rough agreement with the critical pressure for superconductivity in the PF_6^- compound.

As indicated above, the major structural changes upon cooling involve the interstack Se-Se distances (d_7 , d_8 , and d_9 in Fig. 6), which are given in Table II. Inspection of the interstack Se-Se contact distances in Table II reveals that upon cooling large decreases in Se-Se distances occur which are as much as 0.30 \AA less than the van der Waals radius sum for Se, thus suggesting considerable bonding interaction (42). It has also been observed (40) that the Se-Se distances are anion dependent, and vary systematically depending on the anion size, suggesting that *correlations* between crystallographic unit cell volumes, which reflect anion size, and interstack Se-Se distances might

TABLE II
INTERSTACK Se-Se CONTACT DISTANCES (\AA) AND UNIT CELL
VOLUMES (\AA^3) FOR $(\text{TMTSF})_2\text{X}^a$

Anion (X^-)	d_7 (\AA)	d_8 (\AA)	d_9 (\AA)	V_c (\AA^3)
AsF_6^- : 298 K	3.9449(9)	3.9627(11)	3.9053(13)	719.9
	125 K	3.8159(5)	3.8861(7)	695.9
PF_6^- 298 K	3.9342(20)	3.9586(27)	3.8786(28)	714.3
	125 K	3.7847(14)	3.8706(22)	681.3
ReO_4^- 298 K	3.902(2)	3.933(2)	3.827(2)	710.5
	125 K	3.794(4)	3.845(5)	681.9
BrO_4^- 298 K	3.9118(9)	3.9457(14)	3.8411(13)	707.2
	125 K	3.8149(8)	3.8618(12)	689.8
FSO_3^- 298 K	3.8676(7)	3.9516(11)	3.7815(9)	695.3
	125 K	3.7565(5)	3.8382(8)	677.7
ClO_4^- 298 K	3.8653(14)	3.9553(24)	3.7783(20)	694.3
	125 K	3.7596(5)	3.8485(9)	673.7
BF_4^{-b} 298 K	3.850	3.978	3.743	690.4
	125 K	3.7526(11)	3.8792(17)	668.1

^a Estimated standard deviations are in parentheses.

^b Values at 298 K were given without estimated standard deviations (109).

exist. As shown in Fig. 9 there is a very striking correlation between the anion volume V_A (and hence, unit cell volume V_c) and the average interstack Se-Se distance [$d_{\text{avg}} = (2d_7 + d_9)/3$] in $(\text{TMTSF})_2\text{X}$ metals and these structural features also correlate well with the observation of pressure-induced superconductivity in the majority of these systems.

Within the series of octahedral and tetrahedral anions the ClO_4^- anion has a small volume V_A , and also a very small d_{avg} and V_c . It is, therefore, tempting to make $(\text{TMTSF})_2\text{X}$ salts with even smaller anions than ClO_4^- , and examples of such ions are the triangular (pancake-shaped) NO_3^- and (banana-shaped) H_2F_3^- . It is now interesting to compare the unit cell volumes V_c and the interstack distances d_{avg} of these compounds to what is expected from the larger and more symmetric anions treated above. From Figs. 7 and 8 it appears that V_c behaves regularly, i.e., it follows the usual linear behavior versus V_A . However, the d_{avg} value when $\text{X} = \text{H}_2\text{F}_3^-$ departs appreciably from the expected dependence as is shown in Fig. 9. This deviation is related to the fact that although the very small anions NO_3^- and H_2F_3^- do make the unit cell volume smaller than that for $\text{X} = \text{ClO}_4^-$, the interstack selenium atom network does not contract accordingly. It is tempting to

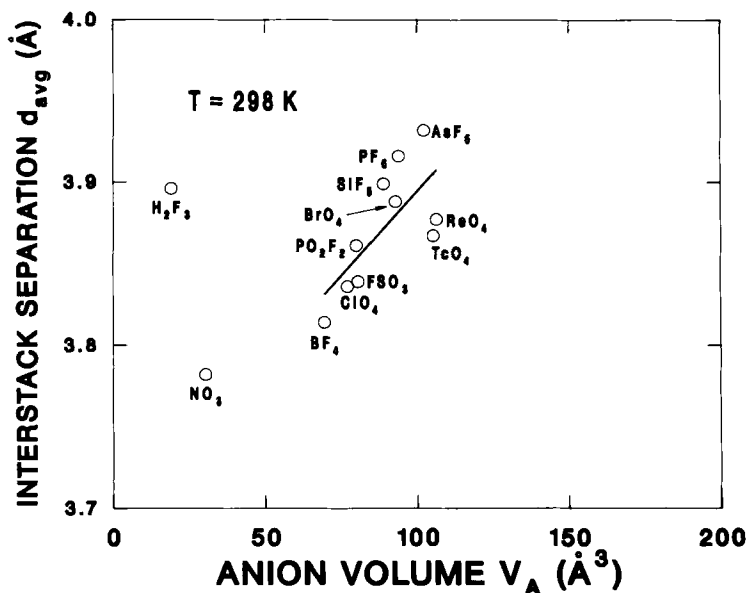


FIG. 9. Average interstack distance, d_{avg} (see text), in $(\text{TMTSF})_2\text{X}$ salts at room temperature vs. anion volume V_A .

relate this structural observation with the fact that superconductivity is not observed in $(\text{TMTSF})_2\text{NO}_3$ and $(\text{TMTSF})_2\text{H}_2\text{F}_3$ (50).

Another possibly important correlation between crystal structure and the occurrence of superconductivity in $(\text{TMTSF})_2\text{X}$ materials may be related to short cation-anion contact distances which occur through Se---F or Se---O interactions (51). In the $(\text{TMTSF})_2\text{X}$ series superconductivity has definitely been observed for $\text{X} = \text{PF}_6^-$, AsF_6^- , TaF_6^- , SbF_6^- , ReO_4^- , and ClO_4^- ; in the latter case only is superconductivity observed at ambient pressure. The van der Waals contact distances for Se-Se, Se-F, and Se-O are 4.00, 3.35, and 3.40 Å, respectively (52). The cation-anion contacts through Se-(F,O) are given in Table III and they reveal very short contact distances except for $(\text{TMTSF})_2\text{NO}_3$, which does not undergo a superconducting transition. Since the short contacts lie approximately in the *c* direction, Parkin *et al.* used these observations to suggest that it is the length of the *c* axis that determines the critical pressure for superconductivity (104). However, compressibility studies show that it would require a much higher pressure to compress the *c* axis of $(\text{TMTSF})_2\text{PF}_6$ into that of $(\text{TMTSF})_2\text{ClO}_4$ than the pressure needed for superconductivity (49). Hence, the *c* axis criterion is unlikely to play a determining role for the occurrence of superconductivity in $(\text{TMTSF})_2\text{X}$ salts.

A third interesting aspect concerning the detailed structures of $(\text{TMTSF})_2\text{X}$ materials and the role the anions play, in addition to the correlations previously described and the finding of short Se-(F,O) anion distances discussed above, is the observation that the peripheral atoms of the anions, viz. AsF_6^- , PF_6^- , and ClO_4^- , are involved in weak van der Waals interactions with the hydrogen atoms of the methyl groups in $(\text{TMTSF})_2\text{X}$, indicating interactions resembling weak hydrogen bonds (39, 53). For example, the immediate nearest neighbor

TABLE III
SHORT CATION-ANION Se-(O,F) DISTANCES IN $(\text{TMTSF})_2\text{X}$
MATERIALS AT ROOM TEMPERATURE

	X					
	NO_3^-	ClO_4^-	ReO_4^-	PF_6^-	TaF_6^-	PO_2F_2^-
Se-(O,F) Å	3.94	3.34	3.16	3.23	3.09	2.91 ^a

^a This short contact, which is the shortest Se-O distance observed in any $(\text{TMTSF})_2\text{X}$ salt, arises because below the metal-insulator transition at 137 K (47) the anion is shifted off the center of symmetry resulting in a crystallographic disorder (48).

environment about the disordered (39) octahedral AsF_6^- anion in $(\text{TMTSF})_2\text{AsF}_6$ reveals a nearly isotropic (symmetric) sea of nearby ($d < 2.6$ Å) hydrogen atoms (see Fig. 10) arising from the fact that in these materials the anion resides in a "methyl-group H-atom cavity" (53).

In contrast, the tetrahedral ClO_4^- anion in $(\text{TMTSF})_2\text{ClO}_4$ possesses a very asymmetric methyl-group hydrogen atom environment as shown in Fig. 11. This asymmetric distribution of oxygen atom to methyl-group hydrogen atom $[\text{H}_2\text{C}-\text{H} \cdots \text{O}-\text{ClO}_3^-]$ bonding interactions results in a "pinning" of the anion, which may be associated with the critical anion-ordering phase transition, a necessary prerequisite to superconductivity in $(\text{TMTSF})_2\text{ClO}_4$, observed at 24 K using X-ray diffraction techniques (54). As illustrated in Fig. 11, the lower relative thermal motion, as observed in their thermal vibration ellipsoids, of O(1) and O(2) compared to O(3) and O(4) undoubtedly results from the greater involvement of O(1) and O(2) in what could be termed "weak H-bond formation." It has also been proposed that the anion-ordering phenomena observed in many $(\text{TMTSF})_2\text{X}$ compounds may be associated with methyl-group ordering which occurs at low temperature in these materials (53). If this is the case, then the synthesis of new superconducting materials requires anions that interact with the methyl groups in such a fashion that they produce anion-ordered derivatives. It is, perhaps, pertinent to point out that controlling the formation of $\text{C}-\text{H} \cdots \text{X}$ interactions in a crystal is an extremely difficult task.

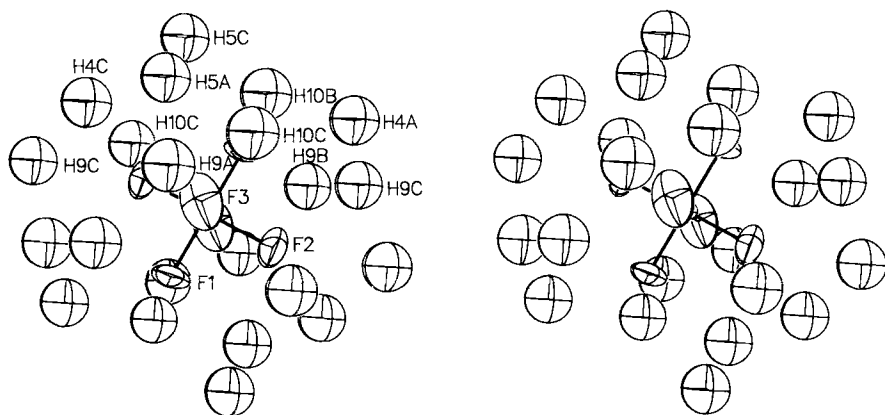


FIG. 10. The H-bonding environment (stereoview) about the AsF_6^- anion, derived from the low-temperature (125 K) X-ray crystal structure of $(\text{TMTSF})_2\text{AsF}_6$, is far more symmetrical than that of the ClO_4^- anion (39). For clarity the AsF_6^- anion has been drawn in an ordered configuration with the fluorine atoms occupying six positions. A disordered model with 12 partially occupied fluorine positions gives similar results.

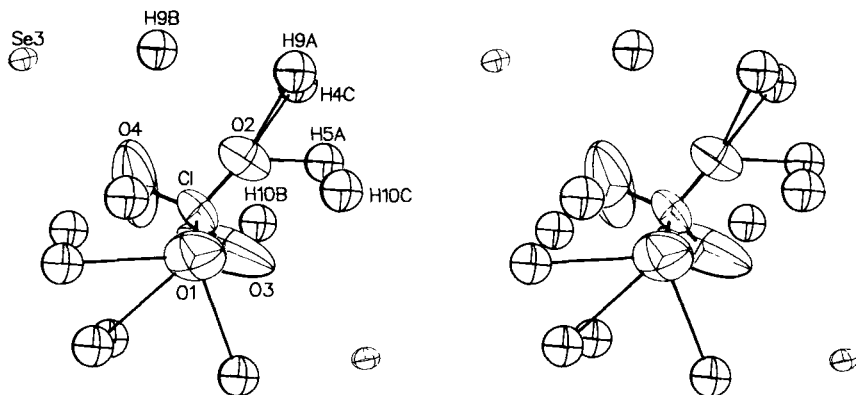


FIG. 11. A stereoview of the ordered ClO_4^- anion environment in the low-temperature (125 K) X-ray-determined crystal structure of $(\text{TMTSF})_2\text{ClO}_4$. Short $\text{H}_2\text{C}-\text{H}\cdots\text{O}-\text{ClO}_3^-$ hydrogen bonding interactions (drawn as faint lines for $\text{O}\cdots\text{H} < 3.0 \text{ \AA}$) exist for O(1) and O(2), which limit the thermal motion of these atoms and may be responsible for "pinning" the ClO_4^- anion in the lattice (53).

As a final point regarding the structure of $(\text{TMTSF})_2\text{X}$ conductors, it seems worth mentioning that, contrary to a previous report (55), there is no significant dimerization in the (TMTSF) stacks, as indicated by the interplanar distances D_1 and D_2 given in Table IV (50). Such a dimerization could influence the electronic properties, since it would create a gap in the electronic spectrum at the wave-vector $2\mathbf{k}_F (= \pi/a)$,

TABLE IV

INTERPLANAR DISTANCES FOR $(\text{TMTSF})_2\text{X}$ SALTS^a

Anion (X^-) ^b	D_1^c	D_2^c	$\Delta (D_1 - D_2)$
AsF_6^-	3.65; 3.57	3.62; 3.57	0.03; 0.0
PF_6^-	3.66; 3.59	3.63; 3.59	0.03; 0.0
ReO_4^-	3.64; 3.59	3.64; 3.56	0.0; 0.03
BrO_4^-	3.63; 3.59	3.65; 3.58	-0.02; 0.01
FSO_3^-	3.62; 3.58	3.63; 3.57	-0.01; 0.01
ClO_4^-	3.63; 3.58	3.63; 3.57	0.0; 0.01
BF_4^-	3.63; 3.57	3.63; 3.55	0.0; 0.02

^a The first value is for $T = 298 \text{ K}$; the second value for $T = 125 \text{ K}$.

^b Data from the author's laboratory, except for $\text{X}^- = \text{ReO}_4^-$, from ref. 110.

^c The interplanar distances D_1 and D_2 are the distances between the best plane for the four Se atoms of a TMTSF molecule.

where \mathbf{k}_F is the Fermi vector. Usually only a gap at \mathbf{k}_F will affect transport properties of a metal, but if Coulomb repulsion between electrons is of importance, the "dimerization gap" is effective and decreases conductivity. With this in mind, it should be noted that both the dimerization (observed from crystallographic studies) and Coulomb repulsion effects (derived from transport measurements) are small in $(\text{TMTSF})_2\text{X}$ salts but appear appreciable in the sulfur family of $(\text{TMTTF})_2\text{X}$ (TMTTF = tetramethyltetrafulvalene).

B. $(\text{ET})_2\text{X}$

Turning now to a discussion of the crystal structures of $(\text{ET})_2\text{X}$ conductors, we start by noting that these do not always crystallize with one single type of structure. Therefore, at this time, it is not feasible to carry the analysis of their structure-property relationships to nearly the same degree of detail as was done for the $(\text{TMTSF})_2\text{X}$ series.

As an illustration of the structures adopted by the tetrahedral anion materials, the crystal structure of $(\text{ET})_2\text{BrO}_4$ is shown in Fig. 12 (56). At room temperature it crystallizes with a triclinic unit cell (space group $P\bar{1}$) and this compound is isostructural (56) with the pressure-induced superconductor $(\text{ET})_2\text{ReO}_4$ (8, 57). At first sight, this structure somewhat resembles that of the $(\text{TMTSF})_2\text{X}$ materials for the following reason: loosely packed molecular stacks are formed along a with the molecular planes placed approximately perpendicular to the stacking axis. The stacks are in close contact along b and are separated along c by the anions, so that the ab planes contain sheets of interacting sulfur atoms.

However, significant differences occur between the $(\text{TMTSF})_2\text{X}$ and $(\text{ET})_2\text{X}$ structures which are important to point out. Compared to the TMTSF salts the ET donor molecules are far from planar and do not stack in the same zig-zag array as shown in Fig. 5, but clearly in a more complicated array. And a striking difference is observed between the sulfur atom "corrugated sheet network" (56) of $(\text{ET})_2\text{X}$ ($\text{X} = \text{ReO}_4^-$ or BrO_4^-) (Fig. 13) and the selenium atom sheet network in $(\text{TMTSF})_2\text{X}$ (Fig. 6).

It appears that there are no *intrastack* $\text{S} \cdots \text{S}$ contact distances (along the stacks) shorter than the $\text{S} \cdots \text{S}$ van der Waals radius sum of 3.6 Å, either at room temperature or at 120 K. Only between chains are short *interstack* contacts formed in $(\text{ET})_2\text{X}$ ($\text{X} = \text{BrO}_4^-$, ReO_4^-). Hence, from a structural point of view, these two salts are not quasi-one-dimensional, a fact, however, which does not preclude that the

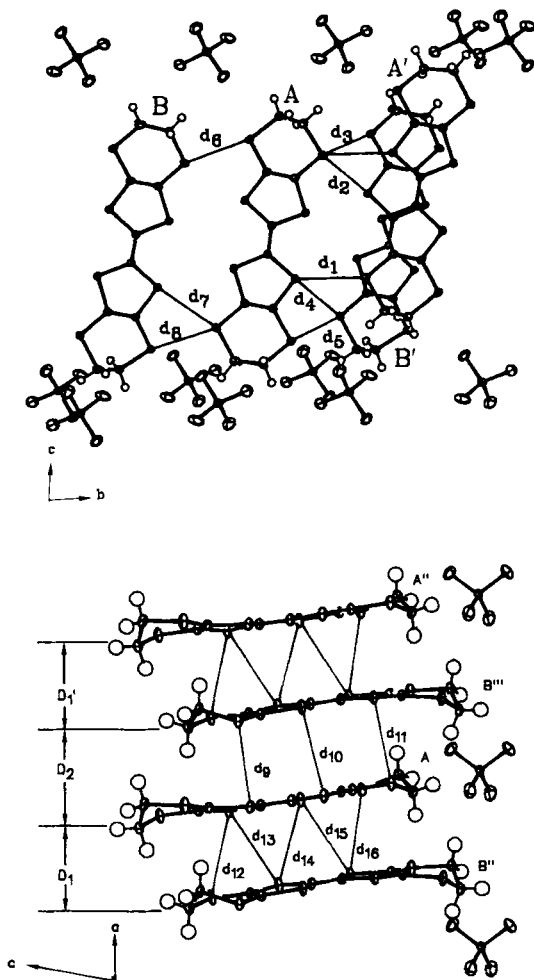


FIG. 12. View of the intermolecular S...S interactions in (ET)₂BrO₄. The top figure indicates the *interstack* S...S contact distances less than the van der Waals sum of 3.60 Å (298/125 K); $d_1 = 3.581(2)/3.505(2)$, $d_2 = 3.499(2)/3.448(2)$, $d_3 = 3.583(2)/3.483(2)$, $d_4 = 3.628(2)/3.550(2)$, $d_5 = 3.466(2)/3.402(2)$, $d_6 = 3.497(2)/3.450(2)$, $d_7 = 3.516(2)/3.434(2)$, and $d_8 = 3.475(2)/3.427(2)$ Å. The S...S contact distances, d_9 – d_{16} (bottom), are, by contrast, all longer than 3.60 Å even at 125 K. In addition the loose zig-zag molecular packing of ET molecules is such that they are not equally spaced, $D_1 = 4.01/3.95$ Å and $D_2 = 3.69/3.60$ Å. As a result of the (apparently) weak intrastack and strong interstack interactions, (ET)₂X molecular metals are *structurally* different from the previously discovered (TMTSF)₂X based organic superconductors. Almost identical S...S distances and interplanar spacings are observed in (ET)₂ReO₄ at both 298 and 125 K. Only theoretical calculations will reveal the extent, if any, of chemical bonding associated with the various S...S distances observed in (ET): X systems.

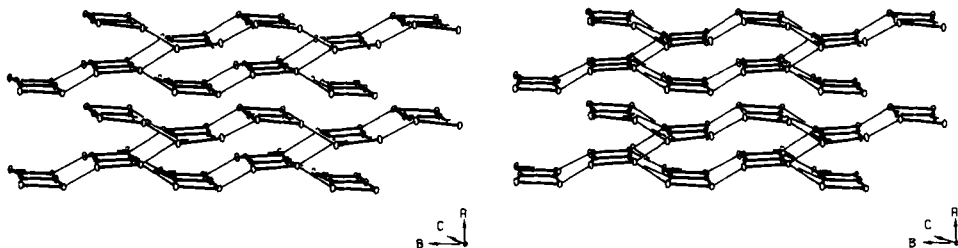


FIG. 13. A stereoview of the short ($< 3.60 \text{ \AA}$) intermolecular interstack S-S interactions in $(\text{ET})_2\text{ReO}_4$ and $(\text{ET})_2\text{BrO}_4$ which form a two-dimensional "corrugated sheet" network (56). This network, which is the principal pathway for electrical conduction, is much different from that observed in $(\text{TMTSF})_2\text{X}$ salts, but similar to the network of interstack S-S interactions observed in $\text{ET}_2(\text{ClO}_4)(\text{TCE})_{0.5}$ (59).

electronic structure may well be so. The ambient-pressure superconductor $\beta\text{-(ET)}_2\text{I}_3$ has a crystal structure which is markedly similar to the above mentioned $(\text{ET})_2\text{X}$ conductors (58, 102, 106), in terms of the long *intrastack* and short *interstack* $\text{S} \cdots \text{S}$ contacts. It is also noteworthy that compared to the $(\text{ET})_2\text{X}$ ($\text{X} = \text{BrO}_4^-$ and ReO_4^-) conductors, the molecular stacks in $\beta\text{-(ET)}_2\text{I}_3$ are not perpendicular to any specific crystallographic axis, but rather the $[110]$ direction (see Fig. 14).

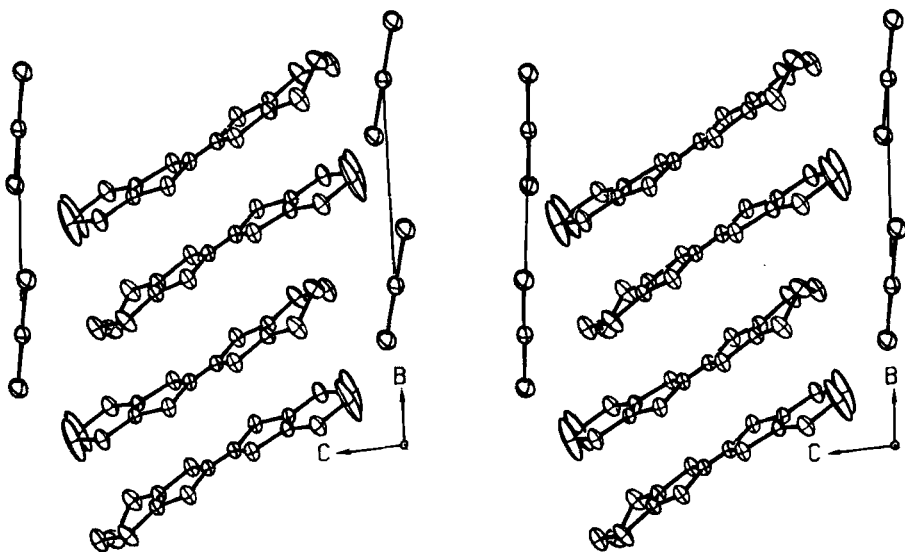


FIG. 14. Molecular packing (stereoview) of ET molecules and linear (centrosymmetric) I_3^- anions in $\beta\text{-(ET)}_2\text{I}_3$. Note that the loose molecular stacks occur in the $[110]$ direction rather than a crystallographic axis as found in $(\text{TMTSF})_2\text{X}$ salts.

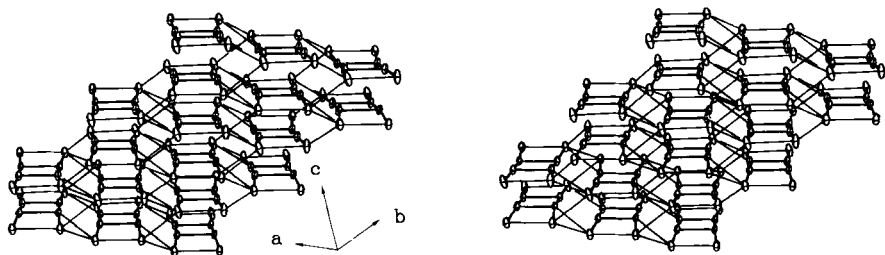


FIG. 15. Stereoview of the "corrugated sheet network" of short *interstack* S \cdots S interactions (faint lines) between nonplanar and nonparallel ET molecules in β -(ET) $_2$ I $_3$ at 125 K (90% ellipsoids). For clarity, only the sulfur atoms of ET are shown.

At first sight, β -(ET) $_2$ I $_3$ bears remarkable resemblance to the 1:2 M(TCNQ) $_2$ salts, where the conducting molecules form stacks of dimers and where the molecules are tilted with respect to the conducting axis. But as pointed out above, one observes mainly short *interstack* distances compared to the *intrastack* S \cdots S separations, and this superconductor appears to be rather two-dimensional in structure (see Fig. 15).

Finally, it should be noted that exactly the same 2:1 ET:I $_3^-$ stoichiometry results, during electrocrystallization, in the simultaneous formation of two different forms of (ET) $_2$ I $_3$, i.e., the α and β forms, respectively. The crystal structure of α -(ET) $_2$ I $_3$ (102, 111) differs markedly from that of β -(ET) $_2$ I $_3$ (58, 102, 106). Not surprisingly, the electrical properties are also very different with the α form undergoing a metal insulator transition at 135 K (111) while the β form is the first sulfur-based ambient-pressure organic superconductor (9, 105, 106, 114). A most surprising structural feature of β -(ET) $_2$ I $_3$ is the development, at 200 K and down to at least 11 K, of a novel incommensurate "modulated" structure (112, 113) observed for the first time in an organic superconductor. The main features of the modulated structure involve displacements from the "average" crystal structure positions of the I $_3^-$ anion and ET molecules, which have *different* direction and magnitude, viz. 0.281(1) Å for I $_3^-$ and 0.124(3) Å for the ET molecules, respectively (112, 113). The modulated structure is shown in Fig. 16 and it must be noted that the resulting local fluctuations of the interatomic S \cdots S distances due to the displacive modulation are very significant and will have to be taken into account in any future theoretical studies of this material.

The same type of corrugated sheet network (see Fig. 17) of short ($d < 3.6$ Å) S \cdots S contacts found in β -(ET) $_2$ I $_3$ is also observed in

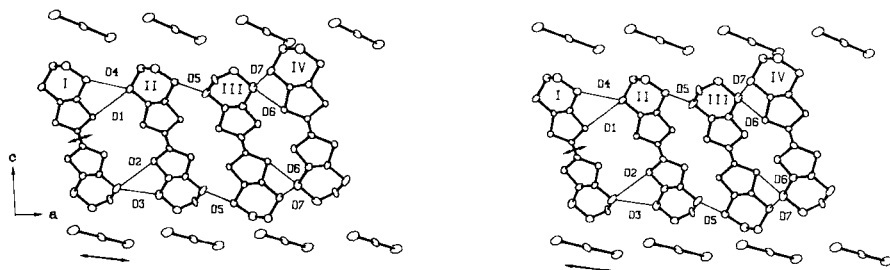


FIG. 16. Stereoview of the molecular packing in β -(ET) $_2$ I $_3$ on the ac plane showing the observed structural modulations of the ET molecules and the I $_3^-$ anions. The allowed displacement vectors of an ET molecule (0.124 Å) and an I $_3^-$ anion (0.281 Å) are indicated by a pair of arrows whose length is approximately five times the magnitude of the observed displacements.

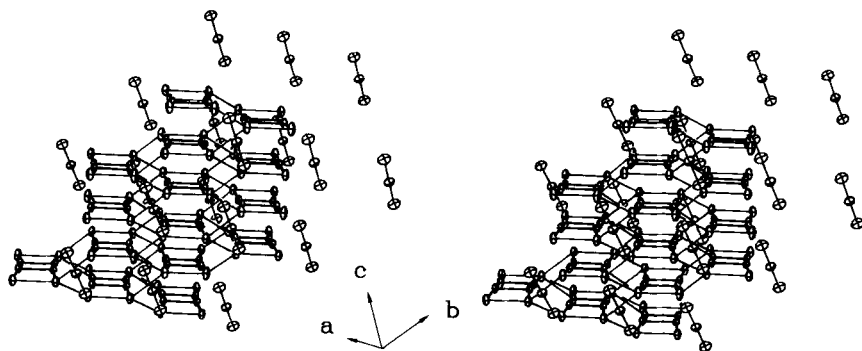


FIG. 17. Stereoview of the novel sandwich or *layered* structure of β -(ET) $_2$ IBr $_2$ composed of alternating two-dimensional sheets of linear (Br-I-Br) $^-$ anions, between which a "corrugated sheet" network of short *interstack* S...S interactions is inserted. Only the S atoms of the ET molecules are shown in the network and light lines indicate the *interstack* ($d_{s \cdots s} < 3.60$ Å) interactions. The —CH $_2$ groups at ET protrude from both ends of the molecule (directly out of the plane of the page) and grasp the X $_3^-$ anions in a pincer hold. Therefore, by varying the length of the X $_3^-$ anion the *interstack* S...S distances can be directly altered (108).

β -(ET) $_2$ IBr $_2$, with the latter having a much higher superconducting transition temperature of ~ 2.4 – 2.7 K (107, 108). More important, because the IBr $_2^-$ anion is $\sim 5\%$ shorter than the I $_3^-$ anion, the unit cell volume of the former is less (828.7 vs. 855.9 Å 3), with the result that the average *interstack* S...S contact distance in β -(ET) $_2$ IBr $_2$ is markedly shorter (0.02 Å) than in β -(ET) $_2$ I $_3$. Thus, for the first time in any organic system, ambient-pressure superconductivity has been maintained in

two materials having the same donor molecule. The synthesis of β -(ET)₂IBr₂ resulted from a rational and systematic approach involving polyhalide anion displacement with the aim of modifying only slightly the corrugated sheet network in (ET)₂X materials (108). This design strategy resulted in direct reduction of the interstack S ··· S distances with anion replacement (see Fig. 17 caption). This occurs because the trihalide anion resides in a cavity formed by —CH₂ group hydrogen atoms (108) similar to the methyl-group hydrogen atom cavity in (TMTSF)₂X systems. Additional ET:I₃[−] salts of presently unknown composition have been reported to be ambient-pressure superconductors with T_c values of 2.5 K (115, 116).

For (ET)₂ClO₄(TCE)_{0.5} (TCE = trichloroethane), solvent is incorporated into the structure at positions similar to those occupied by the anions, i.e., separating the sheets of ET molecules (59). For this structure definite stacks cannot be identified at all, and, as a consequence, the electronic structure is also very two-dimensional. It is not unlikely that this structure (triclinic with space group $P\bar{1}$) is also adopted by (ET)₂ReO₄(THF)_{0.5} with the only difference being that the solvent here is THF (tetrahydrofuran) (57).

As examples of an (ET) conductor with clearly separated stacks, we mention β -(ET)₂PF₆ (60) and (ET)₂AsF₆ (103). They have structures which clearly resemble those typical of the earlier mentioned M(TCNQ)₂ conductors and while β -(ET)₂PF₆ undergoes a metal-insulator transition at 297 K (60), the same type of transition occurs above 125 K in (ET)₂AsF₆ (103).

It is noteworthy that the β -(ET)₂PF₆ structure was indeed what one might have predicted for both the (TMTSF)₂X and (ET)₂X salts, based on the analogy between the 2:1 conductors and the previously studied 1:2 TCNQ conductors. Organic superconductivity would probably not have existed if this structural prediction had come true!

We now turn to a discussion of "anion ordering" phenomena in organic conductors in order to better understand the structural transitions often associated with them.

C. X-RAY DIFFUSE SCATTERING STUDIES OF ANION ORDERING

Almost two decades ago theoreticians predicted that in a quasi-one-dimensional metal, characterized as having a one-dimensional gas of weakly interacting electrons, instabilities could arise leading to transitions to various ground states, such as charge density wave (CDW), spin density wave (SDW), or superconducting (61). Previously, it had been predicted that electron-phonon coupling in a one-dimensional

metal would lead to a CDW state (the Peierls instability) (6), and in this case a structural distortion accompanies the formation of an insulating state. In a simple case such as that which occurs in one-dimensional platinum chain systems (62), the lattice instability is produced by the softening of a phonon branch at wave vectors of component $2\mathbf{k}_F$ (\mathbf{k}_F is the Fermi wave vector) in the direction of the chains, thereby forming a Kohn (63) anomaly in the phonon spectrum.

Because the amplitude of the lattice distortion in the Peierls insulator is very small, the X-ray scattering associated with it is weak. Furthermore the one-dimensional nature of this distortion gives rise to diffuse Bragg planes instead of the usual well-defined Bragg reflections. These two facts have led to the development of a special diffuse X-ray photographic technique often referred to as the "monochromatic Laue technique" or XDS (for X-ray diffuse scattering) (64).

For $(\text{TMTSF})_2\text{X}$ salts the one-dimensional lattice distortion seems to play a less important role than in other quasi-one-dimensional conductors although faint diffuse $2\mathbf{k}_F$ scattering has been observed (64-66). Therefore, the usual Peierls instability is not (or only weakly) active. This is easy to understand in the case of centrosymmetric anions in $(\text{TMTSF})_2\text{X}$ ($\text{X} = \text{PF}_6^-$, AsF_6^- , SbF_6^- , TaF_6^-) since they undergo phase transitions to an antiferromagnetic SDW ground state (66, 67), a transition which according to theory does not involve electron-phonon coupling. Under applied pressure the SDW state is suppressed resulting in a superconducting ground state (see Section IV). Hence, for centrosymmetric anions, no new structural features appear at low temperatures.

However, the $(\text{TMTSF})_2\text{X}$ derivatives containing noncentrosymmetric anions ($\text{X} = \text{ClO}_4^-$, ReO_4^- , FSO_3^- , H_2F_3^- , BrO_4^- , and NO_3^-) show structural phase transitions at relatively high temperatures compared to the temperatures associated with magnetic (SDW) or superconducting transitions (69). These phase transitions are generally associated with anion-ordering phenomena. In this regard it should be remembered that for the noncentrosymmetric anion cases the anion is located at an inversion center (space group $P\bar{1}$), resulting in orientational disorder of the anion at ambient temperature, and XDS studies show that as the temperature is reduced, anion-ordering phase transitions occur (69). The transition temperatures, associated wave vectors, and superstructure unit cells are given in Table V (58, 65, 70-78).

With the exception of $\text{X} = \text{NO}_3^-$ and ClO_4^- , these compounds exhibit a doubling of their crystallographic axes at the phase transition corresponding to a superstructure with wavevector $(1/2, 1/2, 1/2)$ or $(2\mathbf{k}_F, 1/2, 1/2)$. This has the usual symmetry of the

TABLE V
 SUPERSTRUCTURES IN (TMTSF)₂X AND (ET)₂X SALTS

Salt	Anion symmetry	Transition temperature T_0 (K)	Wave vector ^a	Unit cell ^a	References
(TMTSF) ₂ H ₂ F ₃		63	1/2, 1/2, 1/2	2a, 2b, 2c	65
(TMTSF) ₂ NO ₃	Triangular	41	1/2, 0, 0	2a, b, c	74, 78
(TMTSF) ₂ ClO ₄	Tetrahedral	24	0, 1/2, 0	a, 2b, c	70-72
(TMTSF) ₂ BrO ₄	Tetrahedral	~250	1/2, ?, ?	2a, ?, ?	73
(TMTSF) ₂ ReO ₄	Tetrahedral	177	1/2, 1/2, 1/2	2a, 2b, 2c	74-76
(TMTSF) ₂ FSO ₃		88	1/2, 1/2, 1/2	2a, 2b, 2c	76, 77
(ET) ₂ ReO ₄	Tetrahedral	>300	0, 1/2, 0	a, 2b, c	8
(ET) ₂ ClO ₄ ·(TCE) _{0.5}	Tetrahedral	≈200	1/2, 1/2, 1/2	2a, 2b, 2c	80

^a Referred to the room-temperature (TMTSF)₂X unit cell. [Also for (ET)₂ClO₄ and (ET)₂ReO₄].

Peierls distortion. A metal-insulator transition occurs simultaneously with the lattice ordering and, as such, the ground state is indistinguishable from a CDW. But the lack of one-dimensional XDS above the transition suggests that the anions play a direct role in establishing the ground state. The two salts with anomalous superstructures also have peculiar electronic properties. Thus, (TMTSF)₂NO₃ with its (1/2, 0, 0) superstructure has an SDW ground state and (TMTSF)₂ClO₄ with its (0, 1/2, 0) superstructure becomes superconducting only when *slowly cooled* through the anion-ordering transition at 24 K (70-72).

Except in the case of (TMTSF)₂ClO₄, the only ambient-pressure organic superconductor based on TMTSF, the period of the *a* axis (organic molecule chain axis), doubles at the structural transition. For (TMTSF)₂ClO₄ this is an important observation considering the band structure of these materials since $0.5a^*$ (a^* is the reciprocal lattice vector) corresponds to $2\mathbf{k}_F$ for the one-dimensional electron system, i.e., one electron is shared by two molecules in the TMTSF molecular chain. This could lead to the possible opening of a gap at the Fermi level thereby leading to an insulating state. Again, \mathbf{k}_F is the in-chain Fermi wave vector for independent (or weakly interacting) electrons. However, (TMTSF)₂ClO₄ undergoes a transition which may be characterized as being of the $4\mathbf{k}_F$ wave vector type which could result from another type of instability of the electron gas arising from Coulomb interaction between electrons. This $4\mathbf{k}_F$ instability can be coupled to the lattice and induce the softening of the $4\mathbf{k}_F$ phonon. However, the lack of

other evidence of strong Coulomb interactions (not the least that superconductivity occurs) suggests a nonelectronic origin of the superstructure. As discussed earlier, in *slowly cooled* ($R = \text{"relaxed state"}$) samples only, anion-ordering is a precursor to superconductivity and if samples are cooled suddenly ($Q = \text{"quenched state"}$) superconductivity does not develop (78). Thus, fast cooling of the sample suppresses superconductivity and stabilizes the SDW ground-state and associated antiferromagnetism. The situation is not yet well understood in terms of the detailed structural changes in $(\text{TMTSF})_2\text{ClO}_4$ and this is a topic of intense investigation. In the only other detailed XDS study, of $(\text{TMTSF})_2\text{ReO}_4$, the situation is complicated because the ReO_4^- tetrahedra are both ordered below the 176 K phase transition and displaced from their centrosymmetric high-temperature position, and this is accompanied by a " $2k_F$ " distortion of the TMTSF stack (76, 79). It should be noted that from a crystallographic point of view, it is often technically difficult to arrive at a refined crystal structure based on both the usual strong reflections and the very weak superstructure reflections.

The similarity between the $(\text{TMTSF})_2X$ salts and $(\text{ET})_2\text{ReO}_4$ makes it interesting to look into its structure using as a reference point the room-temperature structure of a $(\text{TMTSF})_2X$ salt. As shown in Table V the room-temperature structure of $(\text{ET})_2\text{ReO}_4$ resembles the $(0, 1/2, 0)$ superstructure i.e., that of $(\text{TMTSF})_2\text{ClO}_4$ below 24 K. However, transport measurements suggest a new ordering in $(\text{ET})_2\text{ReO}_4$ at 81 K, so the analogy is not entirely clear between the structural characteristics of the two superconductors.

Diffuse X-ray scattering experiments reveal a superstructure in $(\text{ET})_2\text{ClO}_4(\text{TCE})_{0.5}$ below 200 K of wavevector $(1/2, 0, 1/2)$ which is associated with anion ordering (80). When compared to the $(\text{TMTSF})_2X$ structure, it corresponds to a transition from $(0, 1/2, 0)$ at high temperatures to $(1/2, 1/2, 1/2)$ at low temperature but without any noticeable signatures in conductivity or susceptibility. Hence, in this case, where the two basic structures of $(\text{ET})_2\text{ClO}_4(\text{TCE})_{0.5}$ and of $(\text{TMTSF})_2X$ are very different, there is no analogy between the effects of their superstructures.

In conclusion, XDS studies of numerous TMTSF systems have provided a great deal of information on the nature of the anion-ordering transitions that occur at various temperatures. However, detailed single-crystal structural analyses are still required in order to determine the precise structural changes associated with these transitions.

IV. Electrical Conduction

Despite the great similarity in crystallographic structures of $(\text{TMTSF})_2\text{X}$ compounds, their electronic properties vary considerably. This is clear from Fig. 18, where the electrical resistivities of some salts are shown as functions of temperature. By comparison to Fig. 2, one finds that the TMTSF molecule is able to reproduce almost all previously studied molecules in giving highly conducting salts with a great variation in metal-insulator transition temperatures (T_{MI}) and even superconductivity (at T_s). This conclusion contradicts former suggestions that mostly molecular features are responsible for the variation of solid-state properties, because in $(\text{TMTSF})_2\text{X}$ compounds identical molecules in very similar crystallographic environments behave quite differently.

The situation in $(\text{ET})\text{:X}$ salts is different, since they form very different crystallographic structures. Even the same anion may give rise to a multiplicity of crystallographic phases as demonstrated by

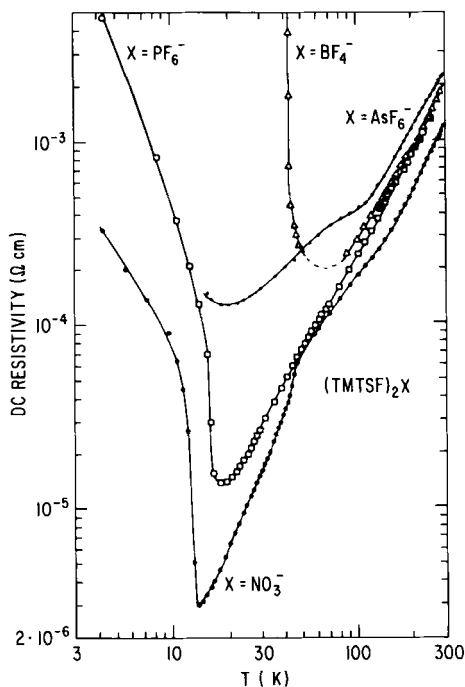


FIG. 18. The electrical resistivities of selected $(\text{TMTSF})_2\text{X}$ salts, having anions of various geometries, at ambient pressure (redrawn from ref. 81).

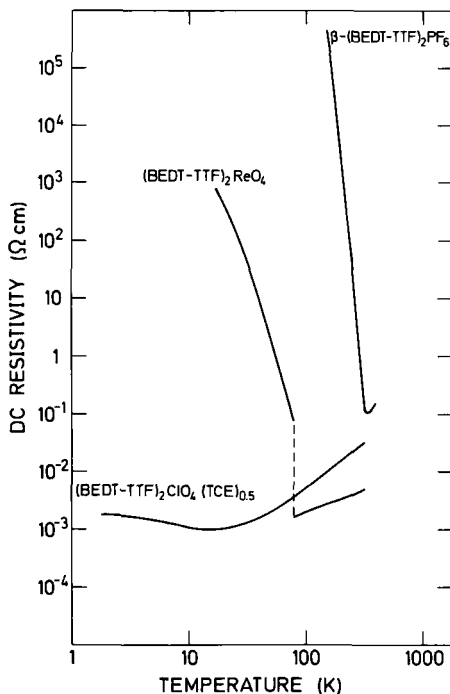


FIG. 19. The electrical resistivities of selected $(\text{ET})_2\text{X}$ salts at ambient pressure. Both $\beta\text{-(ET)}_2\text{I}_3$ and $\beta\text{-(ET)}_2\text{IBr}_2$ (not shown) are ambient pressure superconductors with $T_c = 1.5$ and 2.7 K, respectively.

$\text{X} = \text{ReO}_4^-$, for which four phases have been found. It is, therefore, not astonishing that $(\text{ET})_2\text{X}$ salts have different conduction properties as shown in Fig. 19. The fact that $\beta\text{-(ET)}_2\text{I}_3$ and $\beta\text{-(ET)}_2\text{IBr}_2$ are the second and third ambient-pressure organic superconductors, respectively, and that one phase of $(\text{ET})_2\text{ReO}_4$ becomes superconducting under pressure, make the other phases extremely interesting from the point of view of addressing the following question: Which features of the crystallographic environment provide the grounds for superconductivity in an organic conductor? We now turn to this question.

A. RESISTIVITY ALONG THE CHAINS

1. $(\text{TMTSF})_2\text{X}$ Salts

The usual features of the electrical resistivities of $(\text{TMTSF})_2\text{X}$ compounds shown in Fig. 18 are as follows. The room-temperature value

along the needle axis is typically $\rho_a = 1.5 \times 10^{-3} \Omega \text{ cm}$ (75, 81). This is very similar to the value for TTF-TCNQ and somewhat higher than the best conducting organic salt HMTSF-TNAP (TNAP = tetracyanonaphthalene) ($0.5 \times 10^{-3} \Omega \text{ cm}$) (82). The temperature dependence of the resistivity follows an approximate T^2 behavior typical of organic conductors when the temperature is above the electronic transition temperatures, T_{MI} or T_s . In the cases where the anion-ordering transition at T_o described above does not coalesce with the electronic transition, it results in a small deviation from the T^2 dependence of the resistivity.

Below the electronic-transition temperature T_{MI} or T_s the properties change from metallic to either semiconducting ($X = \text{PF}_6^-$, SbF_6^- , BF_4^- , FSO_3^- , ReO_4^- , H_2F_3^-) (65, 75, 77, 81, 84, 85) or superconducting ($X = \text{ClO}_4^-$) (85), where the electronic density of states in both cases is characterized by an energy gap 2Δ . Although it cannot be concluded from the electrical conductivity, we note that the semiconducting salts fall into two classes. One contains the usual dielectric semiconductors [$X = \text{ReO}_4^-$ (81), FSO_3^- (77), BF_4^- (65), and H_2F_3^- (85)] and they may be characterized as anion-assisted Peierls insulators, since their properties in many respects are like those of the Peierls CDW insulator; but some aspects of their behavior can only be understood as stemming from a direct influence of the anions. The other class of semiconductors has an antiferromagnetic ground state often referred to as the SDW; it contains salts of anions ($X = \text{SbF}_6^-$, AsF_6^- , PF_6^- , and possibly also NO_3^-) (10). Published values of the activation energy Δ are given in Table VI.

The classification given above is documented to varying degrees for the different compounds. Compelling evidence exists for $(\text{TMTSF})_2\text{ClO}_4$ (superconductor), $(\text{TMTSF})_2\text{ReO}_4$ (dielectric semiconductor), and $(\text{TMTSF})_2\text{PF}_6$ (magnetic semiconductor), so that these salts may be considered as prototypes for the three kinds of low-temperature behavior of the regularly behaving $(\text{TMTSF})_2X$ salts.

Some salts show behaviors which are different from that described above; but most of these have not been well characterized. For example, for $X = \text{BrO}_4^-$, which has only recently been well studied, anion disorder seems to lead to localized electronic states (85).

2. $(\text{ET})_2X$

The electrical resistivities in the molecular stacking direction of some $(\text{ET}):X$ salts are shown in Fig. 19. The first material studied, $(\text{ET})_2\text{ClO}_4(\text{TCE})_{0.5}$, has a room-temperature value of $4 \times 10^{-2} \Omega \text{ cm}$

TABLE VI

CONDUCTION CHARACTERISTICS OF (TMTSF)₂X AND (ET)₂X SALTS

X	V _A (Å ³)	V _c (Å ³)	T _o (K)	T _{MI} (K)	Δ (meV)	P _c (kbar)	T _s (K)
(TMTSF) ₂ X							
H ₂ F ₃	10	669.6	63	63 ^b	—	—	—
NO ₃	30	659.5	41	12 ^c	—	—	—
BF ₄	70	690.4	40	40 ^b	—	—	—
ClO ₄	77	694.3	24	—	—	0	1.4
FSO ₃	81	695.8	87.5	86 ^b	47	~7	1.4
BrO ₄	93	707.2	≈ 250	≈ 220 ^c	—	—	—
PF ₆	94	712.9	—	12 ^c	2.0	6.5	0.9
AsF ₆	102	719.9	—	12 ^c	2.0	12	0.9
TcO ₄	105	711.0	—	—	—	—	—
ReO ₄	106	710.5	177	182 ^b	83	9.5	1.0
SbF ₆	118	737.0	—	17 ^c	—	11	0.8
TaF ₆	122	735.6	—	11 ^c	1.8	12	0.8
CF ₃ SO ₃	153	739.5	≈ 280	280 ^b	—	—	—
(ET) ₂ X							
ClO ₄ (TCE) _{0.5}	—	1684 (Z = 2)	—	—	—	—	—
PF ₆ (α)	94	794.3	—	—	54	—	—
PF ₆ (β)	94	3256.4 (Z = 4)	—	297	276	—	—
ReO ₄	106	1565 (Z = 2)	—	81	45	4–6	1.3
I ₃ (β)	—	855.9	—	—	—	0	1.4
IBr ₂ (β)	—	828.7	—	—	—	0	2.7
AsF ₆	102	3274	—	125	—	—	—

^a V_A and V_c are the calculated anion volume and measured unit cell volume, T_o is the anion-ordering temperature, T_{MI} is the metal-insulator transition temperature, Δ is the activation energy, P_c is the critical pressure, and T_s is the superconducting transition temperature.

^b Ground State: anion-assisted charge density wave.

^c Ground State: spin density wave.

decreasing to about $1 \times 10^{-3} \Omega \text{ cm}$ at $T = 16 \text{ K}$ (31). At this temperature the resistivity goes through a broad minimum rising to $1.5 \times 10^{-3} \Omega \text{ cm}$ at the lowest temperatures. This situation is similar to what has been observed in HMTSF-TCNQ under pressure (86) and in HMTSF-TNAP (82) (HMTSF = hexamethylenetetraselenafulvene).

In the (ET):ReO₄ salts the conductivity varies (8, 57). The 2:1 salt, which becomes superconducting under pressure, has a sharp metal-insulator transition at 81 K whereas the 3:2 salt has a broader transition at a similar temperature. In the 2:1:½ salt (where "½" indicates incorporation of ½ solvent molecule of THF per formula unit) there is no indication of a transition from the conductivity data.

A third 2:1 salt, β -(ET)₂PF₆, shows a usual Peierls instability, as judged from the resistance data of Fig. 19, with an activation energy of 230 meV (60). In fact, it looks much like the classical platinum chain conductor K₂[Pt(CN)₄]Br_{0.3}·3.2H₂O (KCP) (62) as do some of the structurally similar M(TNCQ)₂ conductors (2). It appears that α -(ET)₂PF₆ has an activated conductivity over the entire temperature region with a low activation energy of 50 meV (87). In terms of the optical conductivity derived from polarized specular reflectance data, β -(ET)₂I₃ exhibits, for the first time in an organic conductor, a "cross-over" from one-dimensional behavior at 298 K to three-dimensional behavior at 40 K (12).

Finally, the resistivity characteristics of the ambient-pressure superconductor β -(ET)₂I₃ resemble those of (TMTSF)₂ClO₄ a great deal except for the much higher T_c of the triiodide salt [its room temperature value is 0.03 Ω cm (9, 105, 106, 114)].

3. Discussion

The ratio $k_B T_{MI}/\Delta$ can be used to illuminate the anisotropy of the electronic structure in a quasi-one-dimensional material. The ratio is 0.567 in the mean field (or molecular field) approximation which holds fairly well for three-dimensional instabilities (e.g., BCS superconductivity); but it approaches zero as the dimensionality goes to unity. With $k_B = 0.086$ meV/K the values of Table VI yield results for $k_B T_{MI}/\Delta$ close to 0.567 for (TMTSF)₂X, suggesting that these salts are not very one dimensional. However, the lack of a transition in (ET)₂ClO₄(TCE)_{0.5} should not be confused with extreme one dimensionality. Rather, this compound would appear to be so slightly anisotropic that the one-dimensional instabilities which give rise to the transitions are not active. The extraordinary variation of conductivity behavior of (TMTSF)₂X and (ET):X salts at ambient pressure makes the two donor molecules involved unique. In the metallic phase at high temperature they behave much like previously studied organic conductors apart from the possible features at the anion-ordering temperature T_o . But their low-temperature behavior has provided novel superconductivity, spin density waves, and anion-assisted Peierls insulators to condensed-matter physics. Measurements of the resistivity itself contributes to the characterization of these phases by giving information about the electronic and ionic transition temperatures T_{MI} , T_s , and T_o , respectively, and the semiconducting gap parameter Δ below T_{MI} . Values for the different salts are given in Table VI.

B. CONDUCTION ANISOTROPY

1. (TMTSF)₂X and (ET)₂X

The electrical resistivity in directions other than the molecular stacking axis has been measured in a few cases. In (TMTSF)₂PF₆ one finds $\rho_a:\rho_{b'}:\rho_{c^*} \simeq 1:200(3000):3 \times 10^4(10^6)$, where numbers in parentheses refer to $T = 20$ K, i.e., just above the transition (88). Here b' is a vector in the ab plane perpendicular to a , and c^* is the reciprocal lattice vector orthogonal to the same plane. The situation in (TMTSF)₂PF₆ is probably typical for the series, whereas in (ET)₂ClO₄(TCE)_{0.5} one finds $\rho_{\perp}/\rho_{\parallel} \simeq 1-2$ (86), which suggests a very two-dimensional electronic structure in agreement with other experimental results, as well as band structure calculations (89).

2. Discussion

The anisotropy of a quasi-one-dimensional conductor provides considerable insight into the directional dependence of the electronic structure of the compound. It is, however, difficult to measure in (TMTSF)₂X salts and in some of the (ET):X salts. Because of the low crystallographic symmetry, crystal faces are not perpendicular to high-symmetry directions. Nevertheless, adopting a simple tight-binding form for the electronic energy band:

$$\varepsilon(k) = 2t_a \cos(k_a a) + 2t_{b'} \cos(k_{b'} b') + 2t_{c^*} \cos[k_{c^*}(2\pi/c^*)],$$

with

$$k = k_a \hat{a} + k_{b'} \hat{b}' + k_{c^*} \hat{c}^*,$$

(where carets denote a unit vector) one may estimate the ratios between the transfer integrals $t_a, t_{b'}, t_{c^*}$ from the conductivity results. For a quasi-one-dimensional conductor, a rough estimate (90) for $\rho_{\parallel}/\rho_{\perp} \simeq (t_{\perp}/t_{\parallel})^2$, the anisotropy given above for (TMTSF)₂PF₆, yields $t_a:t_{b'}:t_{c^*} \simeq 1:\frac{1}{10}:\frac{1}{200}$, which is in rough agreement with more accurate determinations. In (ET)₂ClO₄(TCE)_{0.5} the low anisotropy of the conductivity suggests a rather two-dimensional electronic structure in accordance with the crystallographic structure and the associated "corrugated sheet network" of *interstack* S...S interactions (56).

C. PRESSURE STUDIES

Because of the "softness" of organic metals one expects them to show interesting behavior under applied pressures. This had been demonstrated earlier by Jerome and co-workers on several compounds and in the case of TMTSF-DMTCNQ (DMTCNQ = dimethyltetracyanoquinodimethane) a pressure of 10 kbar transforms it abruptly from a Peierls semiconductor with $T_{MI} = 50$ K to a metal at all temperatures (91). When the temperature-dependent resistance of the $(\text{TMTSF})_2\text{X}$ family became known, the very low transition temperatures in some of the compounds suggested that these salts would easily become metallic, and maybe even superconducting, under pressure.

1. $(\text{TMTSF})_2\text{X}$

Indeed the pressure dependence of the resistivity of $(\text{TMTSF})_2\text{X}$ salts shows a very rich behavior. $(\text{TMTSF})_2\text{PF}_6$ was the first organic metal to show superconductivity at a pressure of 6.5 kbar at 0.9 K (7). Up to this pressure the metal-insulator transition temperature gradually decreases, possibly with a strong dependence close to P_c . The superconducting transition temperature also decreases, but slowly, with increasing pressure. Several of the octahedral anion salts show the same behavior with somewhat different P_c values, as one would expect from the anion volumes discussed above (P_c values are listed in Table VI). The octahedral anion salts ($\text{X} = \text{ReO}_4^-$, ClO_4^-) show a greater variation in behavior than their tetrahedral counterparts, viz. $(\text{TMTSF})_2\text{ReO}_4$ with $T_{MI} = 182$ K at ambient pressure and which becomes superconducting at 1.0 K above $P_c \simeq 12$ kbar, whereas $(\text{TMTSF})_2\text{ClO}_4$ becomes superconducting at 1.2 K at ambient pressure (70). Both of these results are exciting and astonishing. First, the success with the ClO_4^- salt may be considered the victory of more than two decades of struggle to find an organic superconductor; but, secondly, the ReO_4^- salt demonstrated that superconductivity can be achieved with modest pressures even if the metal-insulator transition temperature is quite high.

The common pressure dependence of the $(\text{TMTSF})_2\text{X}$ salts is illustrated in Fig. 20. Below the critical pressure P_c the electronic ground state is an insulator of either the spin density wave type or the anion-assisted Peierls type. Above P_c the ground state is superconducting. The critical pressure P_c varies monotonically with the anion volume discussed above; but the transition temperature at ambient pressure and the type of low-pressure ground state depend specifically on the

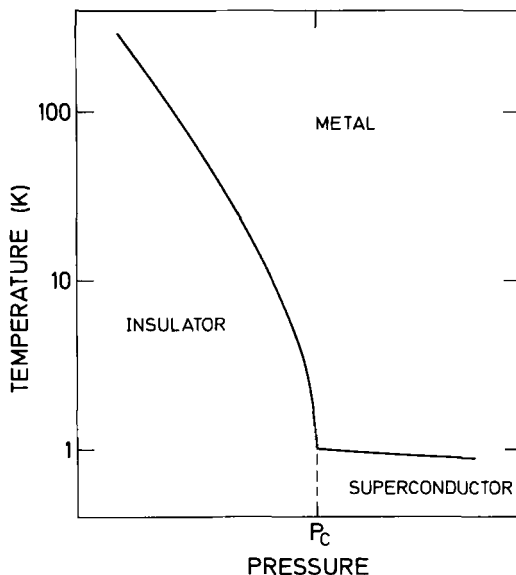


FIG. 20. Illustration of the temperature-pressure phase diagram for $(\text{TMTSF})_2\text{X}$ salts. The critical pressure P_c varies between ambient pressure and 12 kbar for different compounds.

symmetry of the anion. The latter observation demonstrates a correspondence between the lattice superstructure and the nature of the ground state, and this is substantiated by studies in $(\text{TMTSF})_2\text{ClO}_4$ where the anion order can be obstructed by rapid cooling through $T_o = 24$ K (78, 92). In this “quenched” state the salt has a spin density wave ground state associated with the “freezing in” of a ClO_4^- anion disorder.

Since the ambient-pressure superconductor $(\text{TMTSF})_2\text{ClO}_4$ has a very small anion volume, it is tempting to go to even smaller anions in order to increase the superconducting transition temperature. The cases $\text{X} = \text{NO}_3^-$, BF_4^- , and H_2F_3^- are examples of such conductors but the existence of superconductivity has not been established in $(\text{TMTSF})_2\text{X}$ salts for these anions. Lack of superconductivity suggests a different Se network in compounds with very small anions, and low-temperature structural results provide some evidence for this.

An unusual pressure-dependent resistivity has been reported for $(\text{TMTSF})_2\text{PO}_2\text{F}_2$ (47). This compound has a metal-insulator transition at 135 K at ambient pressure, which is quite high considering that the anion volume of PO_2F_2^- is very close to that of ClO_4^- . Furthermore, pressure has a relatively small effect, and even at pressures of 14.5 kbar

there is some indication of the transition. However, a crystallographic study performed at a temperature below T_{MI} revealed a frozen-in $PO_2F_2^-$ anion disorder which is likely the cause of the transition (48).

2. $(ET)_2X$

Only in the case of the 2:1 ReO_4^- salt, and of course $X = I_3^-$ and IBr_2^- , do the *properties* of the $(ET)_2X$ salts resemble the $(TMTSF)_2X$ series (8). With a critical pressure of 4–6 kbar, the ReO_4^- salt fits the phase diagram in Fig. 20. The great similarity in properties of salts based on different molecules suggests that the solid-state environment is as crucial to the physical behavior as are the molecular characteristics.

V. Magnetic Properties

The magnetic susceptibility $\chi(T)$ of organic conductors is of interest because it, in several ways, reflects properties other than the conductivity. In particular, it provides a clear means of discriminating between the CDW and the SDW states which conductivity measurements cannot distinguish. The value of χ may be measured by either static or resonance techniques. Static measurements contain in general contributions from (i) molecular core diamagnetism, (ii) Curie-like susceptibility stemming from localized spin-carrying defects, and (iii) spin susceptibility from the conduction electrons. Electron spin resonance (ESR) measures only the two latter contributions which contain the interesting information about the electronic properties of the conductor. In order to compare results of static and ESR measurements the temperature-independent contribution (i) must, therefore, be subtracted from the former. Furthermore, the ESR signal has a width which measures the interactions of the spins.

A. MAGNETIC SUSCEPTIBILITY

1. $(TMTSF)_2X$

The room-temperature electronic susceptibility is typically 3×10^{-4} emu cm³ mol⁻¹ for $(TMTSF)_2X$ compounds and decreases approximately linearly with decreasing temperature until the transition occurs (93–95). Below the transition there is a clear distinction between the three possible ground states discussed above (61, 94). This

is illustrated in Fig. 21. In the case of an anion-assisted charge density wave system with $X = \text{ReO}_4^-$, χ becomes activated with an activation energy similar to Δ from conductivity, both when measured statically and by ESR (95). For spin density wave systems, e.g., $X = \text{PF}_6^-$, the situation is much more complicated (94, 96). Whereas the ESR signal vanishes both from decreasing χ as well as from line broadening, the static susceptibility vanishes only when the magnetic field is in the direction of the spins. Consequently χ has a strong directional dependence and in a powder, which is most often used in static measurements, only a very small anomaly is seen at T_{MI} . For superconducting

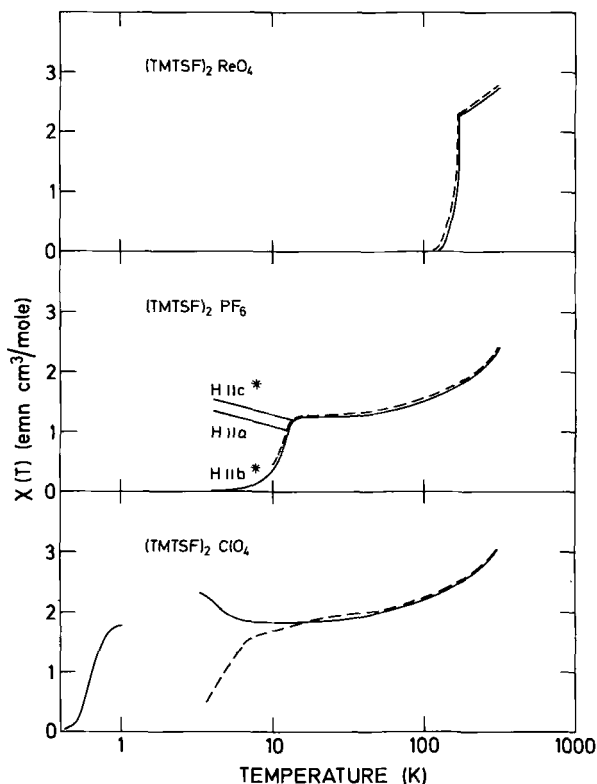


FIG. 21. Magnetic susceptibility of $(\text{TMTSF})_2\text{X}$ salts with $\text{X} = \text{ReO}_4^-$, PF_6^- , and ClO_4^- . Full lines indicate static measurements on powders (ReO_4^- and ClO_4^-) and on single crystals (PF_6^-). Dashed lines show ESR single-crystal results. The three cases illustrate anion-assisted charge density wave (ReO_4^-), spin density wave (PF_6^-), and spin density wave precursors of superconductivity (ClO_4^-). A separate result showing the superconducting transition is also shown for $\text{X} = \text{ClO}_4^-$.

(TMTSF)₂ClO₄ the two susceptibilities give evidence for an incomplete spin density wave transition at $T \simeq 5$ K at intermediate cooling rates reminiscent of the features in some conductivity measurements (93). At the superconducting transition the susceptibility vanishes, but the transition temperature is lower than that deduced from conductivity (97).

2. (ET):ReO₄

ESR measurements have been performed on three (ET):ReO₄ phases (97), but $\chi(T)$ is not known on an absolute scale. The results are shown in Fig. 22. The 2:1 salt has features similar to (TMTSF)₂ReO₄; it has a constant susceptibility in the metallic regime and an abrupt transition to a very low value below T_{MI} . The 3:2 salt has a $\chi(T)$ similar to what one expects from a Peierls transition without influence of anion ordering, i.e., somewhat similar to TTF-TCNQ if scaled to the present T_{MI} . Finally, the 2:1:½ salt has a rather featureless susceptibility with a

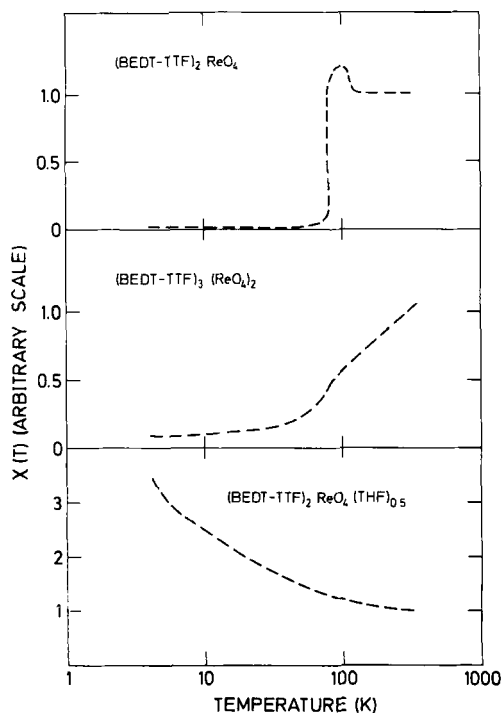


FIG. 22. The magnetic susceptibility of various ET:ReO₄⁻ phases on an arbitrary scale.

Curie-like ($1/T$) tail at low temperatures, signifying a high concentration of defects.

3. Discussion

The high-temperature susceptibility may be understood as originating from two contributions. First, the so-called Pauli susceptibility stems from the band nature of the electronic states. It may be calculated from the transfer integral $t_{||}$, which from optical measurements and calculations is 260 meV for (TMTSF)₂X salts and corresponds to a bandwidth of 1.1 eV. The contribution to $\chi(T)$ is a temperature-independent susceptibility of 0.6×10^{-4} emu cm³ mol⁻¹, approximately half the measured χ at temperatures just above T_{MI} . This excess susceptibility is attributed to a "correlation enhancement" owing to the Coulombic repulsion between electrons. This effect is often parameterized into an on-site Coulombic energy, the "Hubbard U ." An enhancement factor of 2 as observed for (TMTSF)₂X gives $U = 4t_{||}$ according to the zero-temperature theory of Takahashi (98), but later analysis with the temperature dependence of χ taken into account yields $U/4t_{||} = 0.4$ (99). These values for $U/4t_{||}$ are typical of good organic conductors but the importance of correlations is difficult to assess from such estimates of $U/4t_{||}$. However, it should be noted that there is no evidence for strong effects on the conductivity originating from the dimerization gap in the electronic band structure, so in this respect U is not large in (TMTSF)₂X salts.

The low value of U in (TMTSF)₂X salts in view of their $\frac{3}{4}$ filled electron band (or the $\frac{1}{4}$ hole band) is in striking contrast to the high U s in $\frac{1}{4}$ -filled M(TCNQ)₂ conductors, which often have a susceptibility enhancement over the Pauli susceptibility of factors of 10–30, suggesting that $U/4t_{||} \gg 1$. As pointed out by Mazumdar and Bloch (100), U is an effective parameter which is "magnified" at the band filling of $\frac{1}{4}$. This makes it much easier to understand why M(TCNQ)₂ and (TMTTF)₂X salts show strong correlation effects and why in (TMTSF)₂X salts U is so low.

With respect to the (ET):ReO₄ salts, a similar analysis cannot be carried out since the absolute value of χ is not known. However, the fact that $\chi(T)$ is constant above T_{MI} in the 2:1 salts suggests a low value of $U/4t_{||}$.

The low-temperature behavior of $\chi(T)$ can be understood from the usual concepts of a charge density wave, where the abruptness of the phase transition seems to be the major signature of the effects of anion ordering on the magnetic properties. In the case of the spin density wave, Overhauser's theory for itinerant antiferromagnetism gives a

satisfactory description of the observed phenomena (101). Regarding the superconducting transition temperature in $(\text{TMTSF})_2\text{ClO}_4$, which is lower when measured by susceptibility than by conductivity, a possible explanation is as follows. At some temperature superconducting lamellae develop, presumably parallel to ab planes, giving a zero resistance; but in between the lamellae, the normal metal still contributes to $\chi(T)$. Only when the entire crystal at some lower temperature is in its zero-resistance state does one observe the magnetic transition.

B. ESR LINEWIDTHS

In Fig. 23 we show the ESR linewidths ΔH_{pp} for the six compounds discussed above. The larger widths of $(\text{TMTSF})_2\text{X}$ salts, compared to the $(\text{ET})\text{:ReO}_4$ derivatives, is due to the larger spin-orbit coupling in Se than in S. Apart from this, the linewidths show the following features.

1. In the case of an anion-assisted Peierls transition, the linewidth changes abruptly, e.g., $(\text{TMTSF})_2\text{ReO}_4$ and $(\text{ET})_2\text{ReO}_4$, whereas the usual Peierls transition in $(\text{ET})_3(\text{ReO}_4)_2$ is more gradual.
2. The linewidth increases below a spin density wave transition.

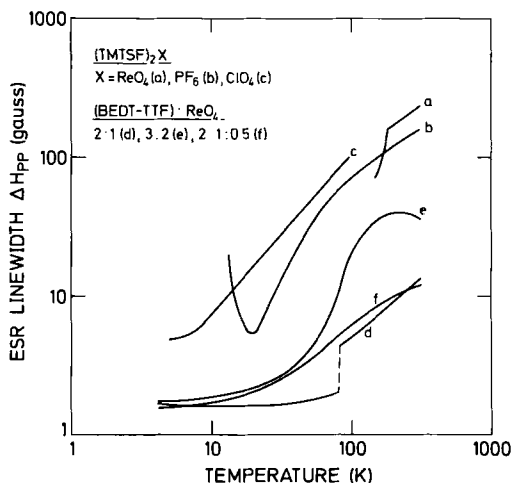


FIG. 23. A comparison of the ESR linewidths of various $(\text{TMTSF})_2\text{X}$, X = monovalent anion, and $\text{ET}:\text{ReO}_4^-$ salts.

3. Even in the absence of a transition, the linewidth does change appreciably with temperature. Hence, the ESR lineshape ΔH_{pp} provides a good means of discriminating between the different phases of the salt (83, 97). For example, ΔH_{pp} (298 K) is ~ 20 gauss in β -(ET) $_2$ I $_3$ and 95 gauss in α -(ET) $_2$ I $_3$ (83).

VI. Concluding Remarks

From structural and transport studies of the organic conductors based on (TMTSF) $_2$ X and (ET) $_2$ X, their varied properties appear both rich and complex. Although charmed by their unique richness, but often frustrated by their complexity, we are, nevertheless, able to point out several cases of correspondence between their crystallographic and physical properties, which may be summarized as follows.

1. As synthetic metals they are by no means unique in terms of high metallic conductivity since several salts of other systems have higher conductivity. This is in agreement with both experimental and theoretical results based on their intrachain electronic bandwidth $4t_{||}$, which is not particularly high, and certainly very small compared to ordinary metals.

2. A unique feature is, however, the very small role that Coulomb interactions play, in particular when considering their stoichiometry. Their low values of U are, at least in part, a molecular property, but studies of different phases of ET:ReO $_4$ indicate that U depends specifically upon the crystallographic environment. That the electrons are not strongly influenced by Coulomb repulsions appears to be necessary for superconductivity.

3. As one-dimensional conductors, they are often not very one-dimensional. Both from a crystallographic as well as from an electronic point of view these compounds have a rather strong coupling between the stacks. There is variation in this coupling within both the (TMTSF) $_2$ X and the (ET):X series, although the variation is much greater in the latter case. It is likely that the richness in behavior is related to a crossover in effective dimensionability, from compound to compound, or as a function of pressure in one compound, so that both one-dimensional instabilities (spin density and charge density waves) as well as three-dimensional superconductivity may occur.

For the isostructural series (TMTSF) $_2$ X the differences in physical behavior for different anions X are associated with very minute changes in the crystallographic structure. The anion volume

determines uniquely the unit cell volume, but in particular, the average interstack $\text{Se}\cdots\text{Se}$ distance, which is directly related to the dimensionality, and this seems to correlate with the occurrence of superconductivity. The symmetry of the anion also plays a determining role as it is responsible for structural order-disorder transitions of varying symmetries. In the case of the Peierls transition there is a direct relation between the symmetry (or periodicity) of this superlattice and the symmetry of the Peierls instability, but the role of symmetry is not understood in detail. The same is true for the role of disorder since superconductivity is not destroyed by disorder in ordinary superconductors, whereas in $(\text{TMTSF})_2\text{X}$ organic superconductors it appears to be. A possible explanation for this could be that ordering influences the interchain distances enough to change the effective dimensionality.

It is clear that the field of organic conductors is continually providing new and unusual materials for study by chemists, physicists, materials scientists, and theorists. There is no doubt that the potential for future surprises in this area of research is bright.

ACKNOWLEDGMENTS

J.M.W. wishes to acknowledge the invaluable collaboration of the colleagues and students whose names appear in many of the articles cited, and he expresses his special thanks to Drs. M. A. Beno, P. C. W. Leung, T. J. Emge, H. H. Wang, A. J. Schultz, and Mrs. V. Bowman for her excellent editorial assistance on this manuscript. Similarly, K.C. would like to thank K. Bechgaard, C. S. Jacobsen, and J. C. Scott.

This study was supported in part by NATO (Grant No. 016.81). We also want to thank our laboratories for the mutual hospitality and support extended to us during visits abroad. Work at Argonne National Laboratory is sponsored by the United States Department of Energy, Office of Basic Energy Sciences, Division of Materials Science, under Contract W-31-109-ENG-38.

REFERENCES

1. Akamatsu, H., Inokuchi, H., and Matsunaga, Y., *Nature (London)* **173**, 168 (1954).
2. Acker, D. S., Harder, R. J., Hertler, W. R., Mahler, W., Melby, L. R., Benson, R. E., and Mochel, W. E., *J. Am. Chem. Soc.* **82**, 6408 (1960).
3. Bardeen, J., Cooper, L. N., and Schrieffer, J. R., *Phys. Rev.* **108**, 1175 (1957).
4. Little, W. A., *Phys. Rev. A* **134**, 1416 (1964).
5. Coleman, L. B., Cohen, M. J., Sandman, D. J., Yamagishi, F. G., Garito, A. F., and Heeger, A. J., *Solid State Commun.* **12**, 1125 (1973).
6. Peierls, R. E., "Quantum Theory of Solids," p. 107. Oxford Univ. Press, London and New York, 1954.
7. Jerome, D., Mazaud, A., Ribault, M., and Bechgaard, K., *J. Phys. Lett.* **41**, 95 (1980).
8. Parkin, S. S. P., Engler, E. M., Schumaker, R. R., Lagier, R., Lee, V. Y., Scott, J. C., and Greene, R. L., *Phys. Rev. Lett.* **50**, 270 (1983).
9. Yagubskii, E. B., Shchegolev I. F., Laukhin, V. N., Kononovich, P. A., Karatsovnik, M. W., Zvarykina A. V., and Buravov, L. I., *JETP Lett. (Engl. Trans.)* **39**, 12 (1984).
10. Bechgaard, K., *Mol. Cryst. Liq. Cryst.* **79**, 1 (1981).
11. Bechgaard, K., Carneiro, K., Rasmussen, F. B., Olsen, M., Rindorf, G., Jacobsen, C. S., Pedersen, H., and Scott, J. C., *J. Am. Chem. Soc.* **103**, 2440 (1981). [There is an

- error in footnote 10; $(\text{TMTSF})_2\text{ClO}_4$ was prepared by anodic oxidation of $10^{-3} M$ (not $10^{-5} M$) (TMTSF)].
12. Jacobsen, C. S., Williams, J. M., and Wang, H. H., *Solid State Commun.* **54**, 937 (1985).
 13. Bechgaard, K., Cowan, D. O., and Bloch, A. N., *J. Chem. Soc., Chem. Commun.*, p. 937 (1974).
 14. Andersen, J. R., and Bechgaard, K., *J. Org. Chem.* **40**, 2016 (1975).
 15. Bechgaard, K., Cowan, D. O., Bloch, A. N., and Henriksen, L., *J. Org. Chem.* **40**, 746 (1975).
 16. Cowan, D. O., Bloch, A. N., and Bechgaard, K., U. S. Pat. 4,246,173 (1981).
 17. Shu, P., Bloch, A. N., Carruthers, T. F., and Cowan, D. O., *J. Chem. Soc., Chem. Commun.*, p. 505 (1977).
 18. Wudl, F., and Nalewajek, D., *J. Chem. Soc., Chem. Commun.*, p. 866 (1980).
 19. Wudl, F., Aharon-Shalom, E., and Bertz, S. H., *J. Org. Chem.* **46**, 4612 (1981).
 20. Braam, J. M., Carlson, C. D., Stephens, D. A., Rehan, A. E., Compton, S. J., and Williams, J. M., *Inorg. Synth.* **24** (1985).
 21. Spector, W. S., ed., "Handbook of Toxicology," Vol. I, p. 340. Saunders, Philadelphia, 1956.
 22. Moradpour, A., Peyrussan, V., Johansen, I., and Bechgaard, K., *J. Org. Chem.* **48**, 388 (1982).
 23. Moradpour, A., Bechgaard, K., Barrie, M., Lenoir, C., Murata, K., Lacoe, R. C., Ribault, M., and Jerome, D., *Mol. Cryst. Liq. Cryst.* **119**, 69 (1985).
 24. Engler, E. M., and Patel, V. V., *J. Am. Chem. Soc.* **96**, 7376 (1974).
 25. Lerstrup, K., Lee, M., Wiygul, F. M., Kistenmacher, T. J., and Cowan, D. O., *J. Chem. Soc., Chem. Commun.*, p. 294 (1983).
 26. Johannsen, I., Bechgaard, K., Mortensen, K., and Jacobsen, C. S., *J. Chem. Soc., Chem. Commun.*, p. 295 (1983).
 27. Mizuno, M., Garito, A. F., and Cava, M. P., *J. Chem. Soc., Chem. Commun.*, p. 18 (1978).
 28. Reed, P. E., Braam, J. M., Sowa, L. M., Barkhau, R. A., Blackman, G. S., Cox, D. D., Ball, G. A., Wang, H. H., and Williams, J. M., submitted for publication.
 29. Krug, W. P., Ph.D. Dissertation, Johns Hopkins University, Baltimore, Maryland (1977).
 30. Schumaker, R. R., Lee, V. Y., and Engler, E. M., *J. Phys., Colloq.* **44**, C3-1139 (1983).
 31. Saito, G., Enoki, T., Toriumi, T., and Inokuchi, H., *Solid State Commun.* **42**, 557 (1982).
 32. Williams, J. M., Beno, M. A., Appelman, E. H., Capriotti, J. M., Wudl, F., Aharon-Shalom, E., and Nalewajek, D., *Mol. Cryst. Liq. Cryst.* **79**, 319 (1982).
 33. Thorup, N., Rindorf, G., Soling, H., and Bechgaard, K., *Acta Crystallogr., Sect. B* **37**, 1236 (1981).
 34. Soling, H., Rindorf, G., and Thorup, N., *Cryst. Struct. Commun.* **11**, 1980 (1982).
 35. Tanaka, C., Tanaka, J., Dietz, K., Katayama, C., and Tanaka, M., *Bull. Chem. Soc. Jpn.* **56**, 405 (1983).
 36. Soling, H., Rindorf, G., and Thorup, N., *Acta Crystallogr. Sect. C: Cryst. Struct. Commun.* **39**, 490 (1983).
 37. Rindorf, G., Soling, H., and Thorup, N., *Acta Crystallogr., Sect. B* **38**, 2805 (1982).
 38. Guy, D. R. P., Boebinger, G. S., Marseglia, E. A., and Friend, R. H., *J. Phys. C* **16**, 691 (1983).
 39. Williams, J. M., Beno, M. A., Banovetz, L. M., Braam, J. M., Blackman, G. S., Carlson, C. D., Greer, D. L., Loesing, D. M., and Carneiro, K., *J. Phys. Colloq.* **44**, C3-941 (1983).
 40. Williams, J. M., Beno, M. A., Sullivan, J. C., Banovetz, L. M., Braam, J. M., Blackman, G. S., Carlson, C. D., Greer, D. L., and Loesing, D. M., *J. Am. Chem. Soc.* **105**, 643 (1983).

41. Kistenmacher, T. J., Emge, T. J., Shu, P., and Cowan, D. O., *Acta Crystallogr., Sect. B* **35**, 772 (1979).
42. Whangbo, M. H., Williams, J. M., Beno, M. A., and Dorfman, J. R., *J. Am. Chem. Soc.* **105**, 645 (1983).
43. Huheey J. E., "Inorganic Chemistry—Principles of Structure and Reactivity," 2nd Ed., p. 71. Harper, New York, 1978.
44. Shannon R. D., and Prewitt, C. T., *Acta Crystallogr., Sect. B* **25**, 925 (1969); Shannon, R. D., *Acta Crystallogr., Sect. A* **32**, 751 (1976).
45. Teramae, H., Tanaka, K., Shiotani, K., and Yamabe, T., *Solid State Commun.* **46**, 633 (1983).
46. Teramae, H., Tanaka, K., and Yamabe, T., *Solid State Commun.* **44**, 431 (1982).
47. Cox, S., Boysel, R. M., Moses, D., Wudl, F., Chen, J., Ochsenein, S., Heeger, A. J., Walsh, W. M., Jr., and Rupp, L. W., *Solid State Commun.* **49**, 259 (1984).
48. Eriks, W., Wang, H. H., Reed, P. E., Beno, M. A., Appelman, E. H., and Williams, J. M., *Acta Crystallogr., Sect. C: Cryst. Struct. Commun.* **41**, 257 (1985).
49. Morosin, B., Schirber, J. E., Greene, R. L., and Engler, E. M., *Phys. Rev. B: Condens. Matter* **26**, 2660 (1982).
50. Williams, J. M., Beno, M. A., Sullivan, J. C., Banovetz, L. M., Braam, J. M., Blackman, G. S., Carlson, C. D., Greer, D. L., Loesing, D. M., and Carneiro, K., *Phys. Rev. B: Condens. Matter* **28**, 2873 (1983).
51. Thorup, N., Rindorf, G., Soling, H., Johannsen, I., Mortensen, K., and Bechgaard, K., *J. Phys. Colloq.* **44**, C3-1017 (1983).
52. Pauling, L., "The Nature of the Chemical Bond," 3rd ed., pp. 537–540. Cornell Univ. Press, Ithaca, New York, 1960.
53. Beno, M. A., Blackman, G. S., Leung, P. C. W., and Williams, J. M., *Solid State Commun.* **48**, 99 (1983).
54. Pouget, J. P., Shirane, G., Bechgaard, K., and Fabre, J. M., *Phys. Rev. B: Condens. Matter* **27**, 5203 (1983).
55. Emery, V. J., Bruinsma, R., and Barisic, S., *Phys. Rev. Lett.* **48**, 1039 (1982).
56. Williams, J. M., Beno, M. A., Wang, H. H., Reed, P. E., Azevedo, L. J., and Schirber, J. E., *Inorg. Chem.* **23**, 1790 (1984).
57. Parkin, S. S. P., Engler, E. M., Schumaker, R. R., Lagier, R., Lee, V. Y., Voiron, J., Carneiro, K., Scott, J. C., and Greene, R. L., *J. Phys. Colloq.* **44**, C3-791 (1983).
58. Kaminskii, V. F., Prokhorova, T. G., Shibaeva, R. P., and Yagubskii, E. B., *JETP Lett. (Engl. Transl.)* **39**, 17 (1984).
59. Kobayashi, H., Kobayashi, A., Sasaki, Y., Saito, G., Enoki T., and Inokuchi, H., *J. Am. Chem. Soc.* **105**, 297 (1983).
60. Kobayashi, H., Mori, T., Kato, R., Kobayashi, A., Sasaki, Y., Saito, G., and Inokuchi, H., *Chem. Lett.*, p. 681 (1983).
61. Bychkov, Y. A., Gor'kov, L. P., and Dzyaloshinskii, I. E., *Sov. Phys. JETP (Engl. Transl.)* **23**, 489 (1966); for reviews see Emery, V. J., in "Highly Conducting One-Dimensional Solids" (J. T. Devreese, R. P. Evrard, and V. E. Van Doren, eds.), p. 247. Plenum, New York, 1979; Solyom, J., *Adv. Phys.* **28**, 201 (1979).
62. Williams, J. M., Schultz, A. J., Underhill, A. E., and Carneiro, K., in "Extended Linear Chain Compounds" (J. S. Miller, ed.), Vol. I, p. 73. Plenum, New York, 1982; also see Williams, J. M., *Adv. Inorg. Chem. Radiochem.* **26**, 235 (1983).
63. Kohn, W., *Phys. Rev. Lett.* **2**, 393 (1959).
64. For reviews and background on X-ray diffuse and inelastic neutron scattering studies see Comès, R., in "One Dimensional Conductors" (H. G. Schuster, ed.), p. 32. Springer-Verlag, Berlin and New York, 1975; Renker, B., Pintschovius, P. Glaeser, W. Rietschel, H., and Comès, R., *ibid*, p. 53; Renker, B., and Comès, R., in "Low Dimensional Cooperative Phenomena" (J. H. Keller, ed.), p. 235. Plenum, New York,

- 1975; Megtert, S., Pouget, J. P., and Comès, R., *Ann. N. Y. Acad. Sci.* **313**, 234 (1973).
65. Mortensen, K., Jacobsen, C. S., Lindegaard-Andersen, A., and Bechgaard, K., *J. Phys. Colloq.* **44**, C3-963 (1983).
66. Pouget, J. P., Moret, R., Comès, R., Bechgaard, K., Fabre, J. M., and Giral, L., *Mol. Cryst. Liq. Cryst.* **79**, 129 (1982).
67. Torrance, J. B., Pedersen, H. J., and Bechgaard, K., *Phys. Rev. Lett.* **49**, 881 (1982), and references therein.
68. Williams, J. M., in preparation.
69. Moret, R., Pouget, J. P., Comès, R., and Bechgaard, K., *J. Phys. Colloq.* **44**, C3-957 (1983), and references therein.
70. Gubser, D. U., Fuller, W. W., Poehler, T. O., Stokes, J., Cowan, D. O., Lee, M., and Bloch, A. N., *Mol. Cryst. Liq. Cryst.* **79**, 225 (1982).
71. Pouget, J. P., Shirane, G., Bechgaard, K., and Fabre, J. M., *Phys. Rev. B: Condens. Matter* **27**, 5203 (1983).
72. Pouget, J. P., Moret, R., Comès, R., Shirane, G., Bechgaard, K., and Fabre, J. M., *J. Phys. Colloq.* **44**, C3-969 (1983).
73. Tomić, S., Pouget, J. P., Jerome, D., Bechgaard, K., and Williams J. M., *J. Phys. (Paris)* **44**, 375 (1983).
74. Pouget, J. P., Moret, R., Comès, R., and Bechgaard, K., *J. Phys. Lett.* **42**, 543 (1981).
75. Jacobsen, C. S., Pedersen, H. J., Mortensen, K., Rindorf, G., Thorup, N., Torrance, J. B., and Bechgaard, K., *J. Phys. C* **15**, 2651 (1982).
76. Moret, R., Pouget, J. P., Comès, R., and Bechgaard, K., *Phys. Rev. Lett.* **49**, 1008 (1982).
77. Wudl, F., Aharon-Shalom, E., Nalewajek, D., Waszczak, J. V., Walsh, W. M., Jr., L. W., Rupp, Jr., Chaikin, P., Lacoe, R., Burns, M., Poehler, T. O., Beno, M. A., and Williams, J. M., *J. Chem. Phys.* **76**, 5497 (1982).
78. Takahashi, T., Jérôme, D. D., and Bechgaard, K., *J. Phys. Lett.* **43**, 565 (1982).
79. Fournel, A., More, C., Roger, G., Sorbier, J. P., Delrieu, J. M., Jerome, D., Ribault, M., and Bechgaard, K., *J. Phys. Lett.* **42**, 445 (1981).
80. Kagoshima, S., Pouget, J. P., Saito, G., and Inokuchi, H., *Solid State Commun.* **45**, 1001 (1983).
81. Bechgaard, K., Jacobsen, C. S., Mortensen, K., Pedersen, H. J., and Thorup, N., *Solid State Commun.* **33**, 1119 (1980).
82. Bechgaard, K., Jacobsen, C. S., and Hessel Andersen, N., *Solid State Commun.* **25**, 875 (1978).
83. Leung, P. C. W., Beno, M. A., Emge, T. J., Wang, H. H., Bowman, M. K., Firestone, M. A., Sowa, L. M., and Williams, J. M., *Mol. Cryst. Liq. Cryst.* **125**, 113 (1985).
84. Maaroufi, A., Coulon, C., Flandrois, S., Delhaes, P., Mortensen, K., and Bechgaard, K., *Solid State Commun.* **48**, 555 (1983).
85. Mortensen, K., Jacobsen, C. S., Bechgaard, K., and Williams, J. M., *Synth. Met.* **9**, 63 (1984).
86. Friend, R. H., Jérôme, D., Fabre, J. M., Giral, L., and Bechgaard, K., *J. Phys. C* **11**, 263 (1978).
87. Kobayashi, H., Kato, R., Mori, T., Kobayashi, A., Sasaki, Y., Saito, G., and Inokuchi, H., *Chem. Lett.*, p. 759 (1983).
88. Jacobsen, C. S., Mortensen, K., Thorup, N., Tanner, D. B., Weger, M., and Bechgaard, K., *Chem. Scr.* **17**, 103 (1981).
89. Mori, T., Kobayashi, A., Sasaki, Y., Kobayashi, H., Saito, G., and Inokuchi, H., *Chem. Lett.*, p. 1963 (1982).
90. Soda, G., Jérôme, D., Weger, M., Alizon, J., Gallice, J., Robert, H., Fabre, J. M., and Giral, L., *J. Phys. (Paris)* **38**, 931 (1977).
91. Andrieux, A., Duroure, C., Jerome D., and Bechgaard, K., *J. Phys. Lett.* **40**, 381 (1979).
92. Garoche, P., Brusetti, R., and Bechgaard, K., *Phys. Rev. Lett.* **49**, 1346 (1982).

93. Scott, J. C., *Mol. Cryst. Liq. Cryst.* **79**, 49 (1982).
94. Scott, J. C., Pedersen, H. J., and Bechgaard, K., *Phys. Rev. B: Condens. Matter* **24**, 475 and 5014 (1981).
95. Pedersen, H. J., Scott, J. C., and Bechgaard, K., *Phys. Scr.* **25**, 849 (1982).
96. Mortensen, K., Tomkiewicz, Y., and Bechgaard, K., *Phys. Rev. B: Condens. Matter* **25**, 3319 (1982).
97. Carneiro, K., Scott, J. C., and Engler, E. M., *Solid State Commun.* **50**, 477 (1984).
98. Takahashi, M., *Prog. Theor. Phys.* **40**, 348 (1970).
99. Tanaka, J., and Tanaka, C., *J. Phys. Colloq.* **44**, C3-997 (1983).
100. Mazumdar, S., and Bloch, A. N., *Phys. Rev. Lett.* **50**, 207 (1983).
101. Overhauser, A. W., *Phys. Rev.* **128**, 1437 (1962).
102. Mori, T., Kobayashi, A., Sasaki, Y., Kobayashi, H., Saito, G., and Inokuchi, H., *Chem. Lett.*, p. 957 (1984).
103. Leung, P. C. W., Beno, M. A., Blackman, G. S., Coughlin, B. R., Miderski, C. A., Joss, W., Crabtree, G. W., and Williams, J. M., *Acta Crystallogr. Sect. C: Cryst. Struct. Commun.* **40**, 1331 (1984).
104. Parkin, S. S. P., Creuzet, F., Ribault, M., Jerome, D., Bechgaard, K., and Fabre, J. M., *Mol. Cryst. Liq. Cryst.* **79**, 249 (1981).
105. Crabtree, G. W., Carlson, K. D., Hall, L. N., Copps, P. T., Wang, H. H., Emge, T. J., Beno, M. A., and Williams, J. M., *Phys. Rev. B: Condens. Matter* **30**, 2958 (1984).
106. Williams, J. M., Emge, T. J., Wang, H. H., Beno, M. A., Copps, P. T., Hall, L. N., Carlson, K. D., and Crabtree, G. W., *Inorg. Chem.* **23**, 2558 (1984).
107. Carlson, K. D., Crabtree, G. W., Hall, L. N., Behroozi, F., Copps, P. T., Sowa, L. M., Nuñez, L., Firestone, M. A., Wang, H. H., Beno, M. A., Emge, T. J., and Williams, J. M., *Mol. Cryst. Liq. Cryst.* **125**, 159 (1985).
108. Williams, J. M., Wang, H. H., Beno, M. A., Emge, T. J., Sowa, L. M., Copps, P. T., Behroozi, F., Hall, L. N., Carlson, K. D., and Crabtree, G. W., *Inorg. Chem.* **23**, 3839 (1984).
109. Kobayashi, H., Kobayashi, A., Saito, G., Inokuchi, H., *Chem. Lett.*, p. 245 (1982).
110. Rindorf, G., Soling, H., and Thorup, N., *Acta Crystallogr. Sect. C: Cryst. Struct. Commun.* **40**, 1137 (1984).
111. Bender, K., Dietz, K., Endres, H., Helberg, H. W., Hennig, I., Keller, H. J., Schafer, H. W., and Schweitzer, D., *Mol. Cryst. Liq. Cryst.* **107**, 45 (1984).
112. Emge, T. J., Leung, P. C. W., Beno, M. A., Schultz, A. J., Wang, H. H., Sowa, L. M., and Williams, J. M., *Phys. Rev. B: Condens. Matter* **30**, 6780 (1984).
113. Leung, P. C. W., Emge, T. J., Beno, M. A., Wang, H. H., Williams, J. M., Petricek, V., and Coppens, P., *J. Am. Chem. Soc.* **106**, 7644 (1984); *Mol. Cryst. Liq. Cryst.* **119**, 347 (1985).
114. Carlson, K. D., Crabtree, G. W., Hall, L. N., Copps, P. T., Wang, H. H., Emge, T. J., Beno, M. A., and Williams, J. M., *Mol. Cryst. Liq. Cryst.* **119**, 357 (1985).
115. Yagubskii, E. B., Shchegolev, I. F., Pesotskii, S. I., Laukhin, V. N., Kononovich, P. A., Karatsovnik, M. V., and Zvarykina, A. V., *JETP Lett. (Engl. Transl.)* **39**, 328 (1984).
116. Shibaeva, R. P., Kaminskii, V. F., Yagubskii, E. B., *Mol. Cryst. Liq. Cryst.* **119**, 361 (1985).
117. Wang, H. H., Beno, M. A., Geiser, U., Firestone, M. A., Webb, K. S., Nuñez, L., Crabtree, G. W., Carlson, K. D., Williams, J. M., Azevedo, L. J., Kwah, J. F., and Schirber, J. E., *Inorg. Chem.* **24**, 2465 (1985).

NOTE ADDED IN PROOF. Since the preparation of the original manuscript, *ambient pressure* superconductivity has been reported in β -(ET)₂AuI₂ (117). The transition temperature ($T_c = 5$ K) is the highest reported to date.

WHERE ARE THE LONE-PAIR ELECTRONS IN SUBVALENT FOURTH-GROUP COMPOUNDS?

S.-W. NG¹ and J. J. ZUCKERMAN

Department of Chemistry, University of Oklahoma, Norman, Oklahoma

I. Introduction	297
II. Divalent Fourth-Group Structures	299
III. History	302
IV. Symmetrical Subvalent Systems	304
A. Molecular	304
B. Extended Lattices	307
V. Conclusions	319
References	321

I. Introduction

In July 1983 we began to collect the literature describing the structures of subvalent compounds of the main fourth-group elements, hereafter designated generically as E. Our goal at that time was to provide in one place a complete and up-to-date source of structural information from methods capable of yielding internuclear distances and angles for these systems, from carbon to lead. This file has now grown to over 1500 references ranging from material on carbenes and transition metal carbene complexes to crystallographic studies on the heavier fourth group congeners found in the mineralogical literature.

A subsidiary goal from the outset was to identify those systems in which the lone-pair electrons present in these subvalent species show no stereochemical activity; that is, in which the fourth-group atoms occupy sites of perfect symmetry in the solid state. Our search brought forth various scattered examples of such structural systems, and reading of their unusual properties heightened our interest. However, with the fortuitous synthesis by C. Janiak in our own laboratory

¹ Present address: Institute of Advanced Studies, University of Malaya, Pantai Valley, Kuala Lumpur, Malaysia.

of a molecular example in decaphenylstannocene (77), $[\eta^5\text{-(C}_6\text{H}_5)_5\text{C}_5]_2\text{Sn(II)}$ (see Section IV,A,3), we decided that it would be useful to draw attention to these systems by preparing a shorter review devoted entirely to this subject.

The enumeration and description of the symmetrical subvalent species before you are restricted to those in which the lone-pair electrons are totally inert stereochemically; that is, in which the geometry at the fourth-group atom reflects the situation expected for one fewer electron pair than is in fact present. The evidence we regard as acceptable for authenticating this situation is limited to that deriving from methods yielding precise internuclear distances and angles, primarily single-crystal X-ray diffraction with some neutron, gas-phase, and solid state electron diffraction. The structural formula serves to specify the subvalent nature of the fourth-group species.

Caution must be exercised in using much of the earlier gas-phase electron diffraction data in view of limitations on instrumentation and experimental and computational methods which often required that implicit assumptions about portions of the molecular geometry be made. Unfortunately as well, many of the early X-ray studies lack the accuracy required to draw definite conclusions about the geometry of the E(II) coordination sphere because of the inability to locate precisely lighter atoms in the presence of the heavy E atom. The caveat of Jones (89) regarding even modern results has been extremely useful in guiding our efforts to interpret the literature. The difficulties in interpreting vibrational spectra in terms of structure are well known and rule out their use for our purposes. Likewise, the absence of resolvable quadrupole splitting (QS) in tin-119m Mössbauer spectra may not be used to specify perfect cubic symmetry since small splittings may not be detected in the relatively broad resonance lines. Some quite low symmetry structures give sharp spectral singlets (177, 178). The same is true of single nuclear quadrupole resonance (NQR) signals suggesting high symmetry sites; the other (weaker) lines may just not have been detected. The converse is not true, however. Spectroscopic evidence of lowered symmetry, if reliable, must be regarded seriously since these techniques may operate on a more rapid timescale and not be subject to the averaging involved in recording crystallographic data (see below).

If in a complex the direct neighbor nuclei have the same atomic number and are located at identical distances from the central atom, then the coordination number of this atom can be specified exactly. Complexes with identical ligands are called homoleptic. However, when the nearest neighbor nuclei are not identical, the distances from the central atom will be different, although those nuclei may still be located on the Cartesian coordinates. In these heteroleptic complexes, specify-

ing the complete absence of stereochemical activity on the part of a lone pair of electrons on the central atom becomes less certain, even when the distances to the nearest neighbor nuclei are similar. When the various distances differ by larger amounts, the value of the coordination number of the central atom is itself thrown into doubt as well. Generally, internuclear distances at most 10% longer than the shortest tend to be taken into account in determining the coordination number. Since our goal is to enumerate the cases in which a lone pair of electrons on a central atom is totally inert stereochemically, we will confine our attention to the homoleptic complexes only, and further to those cases in which the E(II) atom is located at the exact center of a perfect polyhedron. For two and three coordination we seek linear and trigonal-planar arrangements, for four coordination the tetrahedron or the unknown square plane, for five coordination the familiar trigonal bipyramid, and for six coordination the octahedron. While for 8 and 12 coordination the cube or square antiprism and cube octahedron or dodecahedron, respectively, are available, for 7, 9, 10, and 11, coordination it is more difficult to specify the regular shapes sought. Moreover, since the energy differences between the coordination numbers 7-12 are generally small, solid-state data reveal many examples of situations in which the coordination number appears to be intermediate. This is especially true the larger the central atom. Transformations among the choices of idealized geometries are often comparable with the distortions imposed by vibrationally excited states. Thus, for experimental results from techniques involving long-term observation or averaging ($>10^{-2}$ sec), the structures should be considered as stereochemically nonrigid species. Thus solid-state optical activity having its origin the central atom may be short-lived in solution, and geometrical isomerization may be also a low-energy barrier process, with smaller differences than packing forces in the solid state, solvation energies in the solution state, or association energies in the liquid state (122).

It should be recalled that the solution of crystal structures by diffraction techniques involves at least two kinds of averaging, the time average and the average content of the unit cell. Other techniques which observe on a shorter time scale may legitimately suggest a lower local symmetry in the same phase than that obtained by crystallography.

II. Divalent Fourth-Group Structures

The divalent state does not usually enter into carbon or silicon chemistry except at high temperatures or where transient reaction

intermediates are involved. However, a number of Ge(II) derivatives are stable at ambient temperature, and the prevalence of the subvalent state increases with Sn(II) (38, 67) and Pb(II).

The elements in their lower oxidation states are less electronegative, and comparable bonds are longer. While all the heavier main-group elements form compounds in an oxidation state two units lower than their group number, no compelling and comprehensive explanation is available for this behavior. Bond lengths involving the same atoms increase with the coordination number of E, whether in ionic or extended covalent lattices or molecular compounds. This correlation is sufficiently consistent to use in establishing the coordination number in doubtful cases. Increasing the tin coordination number by one unit, for example, increases tin-ligand distances by ca. 0.1 Å. However, a change from two to three coordination can be much greater (ca. 0.20 for Sn-F, 0.15 for Sn-O, and 0.13 Å for Sn-N).

In descending the fourth group, at germanium and lead is seen the effect of the introduction of an inner shell of, respectively, 10 and 14 electrons residing in rather diffuse orbitals, to produce ${}_{32}\text{Ge}[\text{Ar}]-3d^{10}4s^24p^2$ and ${}_{82}\text{Pb}[\text{Xe}]4f^{14}5d^{10}6s^26p^2$. There is as a consequence a rise in ionization potential and a shrinkage in size of these elements in comparison with their immediate congeners.

As the electronegativity of the E atom increases, the electron pair shared by the E(II) atom will be more contracted. Thus, the space occupied will be less. Bonds adjacent to lone pairs should experience the largest repulsions and become longer than those farther away. While long bonds are usually trans to each other, short bonds are usually trans to a vacancy in the coordination sphere. We infer the position of the lone pair from the nature of these geometric distortions.

Neither the force law governing the repulsions of lone and bonding electron pairs between themselves and each other, nor the precise nature of the force, is known. The ratio of the lone pair-lone pair/bonding pair-bonding pair repulsions is also unknown. The details of this potential, especially the hardness of the pair repulsion law, which might be expressed as the magnitude of n in $\sum r_{ij}^{-n}$ where r is a distance parameter, varies with the individual system.

In analyzing the available data we have adopted an *inclusive* position with respect to coordination number; that is, if the distance to a neighboring atom is within van der Waals radii sums, or the atom is in a suggestive stereochemical position, then it will be regarded by us to be within the coordination sphere. Thus, although we take note of the arguments presented by the original authors, we may raise many of their assigned coordination numbers.

Distortions in molecular solids seem to reflect a compromise between optimal packing or lattice energy, on the one hand, and optimal shape for the molecule, on the other. Deformations follow paths of least resistance which can be discerned theoretically from molecular orbital (MO) studies, semitheoretically from electrostatic or nonbonding models, or empirically from force constants associated with internal vibrations.

When ligand—ligand distances lessen to the sum of their normal van der Waals radii, repulsive forces may begin to override the stereochemical influence of the lone pair. In addition, the stronger (shorter) are the same as bonds holding the ligands, the larger are the angles between them. Ligand–ligand repulsions are greater when the ligands are either tightly bound or sterically demanding. Thus, high-symmetry environments in E(II) compounds should tend to be found in their heavier halide and chalcogenide derivatives and where these anions are in close contact. Repulsions between the bonding electrons may also be important.

The geometric arrangements resulting from five and seven or more electron pairs are not immediately obvious, and in these cases the actual result depends upon the precise details of the potential invoked between the charges. Such systems with large numbers of electrons are usually flexible, with several arrangements close in energy.

The Lewis acidity of E(II) derivatives is characteristic; the Lewis basicity (42, 43, 69), on the other hand, has proved difficult to demonstrate conclusively.² Basicity involving the lone-pair electrons should increase with $R_2E(II)$ angles since the lone-pair orbital will acquire more p character as the bonding orbitals become more s .

No examples of the bare E^{2+} cation exist in any of the structures studied thus far. Neither does the RE^+ cation appear, except in $\eta^5-(CH_3)_5C_5Sn^+BF_4^-$ (91, 92), $\eta^5-(CH_3)_5C_5Sn \cdot bipy^+SO_3CF_3^-$ ($bipy =$ bipyridyl) (99), $\eta^5-(CH_3)_5C_5SnC_5H_5N^+SO_3CF_3^-$ (93), $\{[BF_4]^-[\mu-\eta^5-(C_5H_5)_2Sn]-\mu-\eta^5-C_5H_5Sn^+ \cdot THF\}_n$ (43), and perhaps in $[(\eta^5-C_5H_5)_2Pb]_n$,¹ whose solid-state structure (133) can be regarded as being composed of $[\eta^5-C_5H_5Pb]^+[\mu-C_5H_5]^-$ units. A recent claim for a bare Sn^{2+} ion in $Sn^{2+}(AsF_3)_2(SbF_6^-)_2$ is based on a very high-velocity tin-119m Mössbauer isomer shift (IS), but in the solid state structure the tin(II) atom appears to be coordinated by nine fluorine atoms in a distorted arrangement, thus revealing the presence of the lone pair (46).

² The structure of $[(CH_3)_3CNSn(II)]_4 \cdot 2AlCl_3$ in which Sn(II) functions as a Lewis base has been crystallographically authenticated [Veith, M., and Frank, W., *Angew. Chem., Int. Ed. Engl.* 24, 223 (1985)].

III. History

The idea of lone pairs was originated by W. J. Pope of Cambridge in 1900 who extended the concept of the three-dimensionality of carbon and nitrogen compounds to those of sulfur. His resolution of sulfonium cations $RR'R''S^+$ with three different substituents into optically active enantiomers suggested that these species were tetrahedral with an invisible substituent. The influence of these lone pairs can hardly be detected in transition metal compounds, but the situation is different for post-transition group central atoms such as Ge(II) As(III), Se(IV), and Br(V) with 30 electrons, In(I), Sn(II), Sb(III), Te(IV), I(V), and Xe(VI) with 48 electrons, and Au(-I), Tl(I), Pb(II), and Bi(III) with 80 electrons (90).

Although W. H. Zachariasen of the University of Chicago correctly pointed out in 1932 that central atoms with certain numbers of valence electrons seem to be displaced away from the centers of their respective coordination polyhedra (173), it remained for N. V. Sidgwick and H. M. Powell of Oxford in their 1940 Bakerian Lecture to specify the unshared (inert) pair of electrons as lying at the root of the geometrical distortion (155). This point was further elaborated by R. J. Gillespie and R. Nyholm of University College, London, in a widely read review of inorganic stereochemistry in 1957 (55). It was here that the simple electrostatic model linking geometry with the number of electron pairs in the valence shell was further refined by the recognition that electron pair repulsions in the valence shell decrease in the sequence lone pair-lone pair > lone pair-bonding pair > bonding pair-bonding pair. L. E. Orgel of Cambridge used mixing of *s* and *p* orbitals to account for the influence of lone pairs on the stereochemistry of subvalent lead ions in 1959 (131). R. J. Gillespie of McMaster expounded on the idea of the stereochemical influence of the lone pair in a series of articles beginning in 1960 (52-54), but D. S. Urch of Queen Mary College, London, pointed out in 1964 that exceptions to this influence could be found among octahedral hexahalo anions of groups V-VII, in which the lone pair is accommodated in an A_{1g} antibonding molecular orbital (165).

Examples of authenticated structures which exhibit stereochemically inert lone-pair electrons (21) lying beyond the scope of this review include the linear Li_2O ; the trigonal-planar Si_3N systems in trisilylamine, $(H_3Si)_3N$, and $\beta-Si_3N_4$, and the carbon atoms in the carbanions $C(CN)_3^-$ and $C(NO_3)_3^-$; the square-planar P(III) porphyrin; the octahedral $SbCl_6^{3-}$, $SbBr_6^{3-}$, SbI_6^{3-} , $BiCl_6^{3-}$, $[BiBr_4]_n^{n-}$, $[BiBr_5]_n^{n-}$, $SeCl_6^{2-}$, $SeBr_6^{2-}$, $SeCl_4py_2$, $TeCl_6^{2-}$, $[TeCl_5]_n^{n-}$, $TeBr_6^{2-}$, TeI_6^{2-} ,

$\text{TeCl}_4 \cdot 2\text{SC}(\text{NMe}_2)_2$, $\text{TeBr}_4 \cdot 2\text{SC}(\text{NMe}_2)_2$; and the square-antiprismatic Cs_2XeF_8 , which adopts a geometry characteristic of a species with one fewer electron pair at the xenon atom (eight rather than nine). Another area of exceptions involves the gauche conformations adopted by molecules with adjacent atoms each holding a lone pair. Hydrazine, for example, in its lowest energy conformation places its lone-pair electrons gauche rather than in the expected anti conformation. However, at least for the hexachloro- and bromotellurate(IV)s, the lone-pair electrons are not spectroscopically inert, because relatively low energy transitions are observed in the electronic spectra involving them, implying delocalization to the halide ligands (32). In addition, TeCl_6^{2-} provides a considerably larger cubic unit cell parameter than SnCl_6^{2-} .

More recent models treat the lone pairs as a ligand (54, 147) or as a dibasic anion (19), or even as possibly residing at a site remote in the lattice (65)! The valence-shell electron-pair repulsion (VSEPR) model developed by Gillespie (52–54) has come under criticism as a teaching device (44) because nonbonded atoms often exert a governing influence on geometry (12); because in simple, small, approximately tetrahedral molecules the bond angles do not decrease as the number of lone-pair electrons on the central atom increases (147); because the magnitudes of the total angular space requirements of the bond and lone pairs of electrons, which vary from situation to situation, must be known before molecular geometries can be predicted (147); because lone-pair electrons are seldom purely derived from single atoms alone, but instead usually contain considerable bonding and hybrid character (154); because more examples of stereochemically inactive lone pairs (Y) are known for AX_6Y systems than examples in which they are active (171); because the so-called “Pauli force” which is supposed to keep electrons of like spin separated in space, and lies at the basis of the VSEPR model, is a fiction (17); and because of the ambiguity concerning whether the basis for the VSEPR rules is electrostatic at all (18). The VSEPR model cannot be applied to transition-metal derivations.

For systems which possess stereochemically active lone-pair electrons in the crystalline state, a definitive experimental answer to the title question is at least in principle available from difference density analysis of X-ray results where the potential for deriving electron distributions from elastic diffraction data is now being realized (13, 31, 104). In one application to subvalent molecules (164), $(\text{CH}_3)_2\text{TeCl}_2$ was shown to possess a peak of $0.27 \text{ e}/\text{\AA}^3$ centered at 0.9 \AA from the Te(IV) atom in the position expected for a lone pair of electrons (175).

IV. Symmetrical Subvalent Systems

A. MOLECULAR

1. *The Divalent Hydrides and Halides*

The simplest divalent main group-four molecule is methylene, $:\text{CH}_2$. Methylene is a three-atom system with six valence electrons that can be bent or linear. In accordance with both the Aufbau and Pauli Principles, four valence electrons are in the C—H bonds, leaving two nonbonded electrons. If these go into separate p orbitals on the carbon atom with their spins parallel, a triplet state is the result. An energy advantage in this arrangement derives from the larger average separation of the two electrons relative to the spin-paired arrangement in the singlet state.

For methylene the ground state has been found experimentally to be the triplet with the singlet state a low-lying neighbor. The triplet and singlet energies and the gap between them vary as the groups attached to the carbon atom are changed (47). However, in both the singlet and triplet states, the CH_2 system is bent ($\angle \text{H—C—H} = 103$ and 133.84° , respectively) (56).

On the other hand, the cyanomethylene $\text{H—}\ddot{\text{C}}\text{—C}\equiv\text{N}$ triplet as well as a number of odd alternant methylene compounds, propargylene and its homologues, $\text{H—}\ddot{\text{C}}\text{—C}\equiv\text{CR}$ ($\text{R} = \text{H}, \text{CH}_3, \text{C}_6\text{H}_5$), and $\text{H—}\ddot{\text{C}}\text{—C}\equiv\text{CC}\equiv\text{CR}$ [$\text{R} = \text{CH}_3, \text{C}(\text{CH}_3)_3, \text{C}_6\text{H}_5$] have been predicted to be linear on the basis of the zero-field splitting parameters from electron spin resonance (ESR) experiments (15). The linear nature of the first named $\text{H—}\ddot{\text{C}}\text{—C}\equiv\text{N}$ triplet carbene has been confirmed by a microwave study in the gas phase. However, if the potential well in which the linear configuration lies is shallow, the ground state may not show the effects of nonlinearity (142).

All techniques employed agree that the divalent hydrides and halides of silicon to lead are nonlinear in all phases (22, 74, 84, 105, 125, 153).

2. $[\eta^5\text{-C}_5\text{H}_5\text{Mn}(\text{CO})_2]_2\text{Ge}$

Acetic acid treatment of the transition metal Ge(IV) hydride salt $\text{K}[\eta^5\text{-C}_5\text{H}_5\text{Mn}(\text{CO})_2\text{GeH}_3]$ yields a red product, $[\eta^5\text{-C}_5\text{H}_5\text{Mn}(\text{CO})_2]_2\text{Ge}$, which contains a linear Mn—Ge—Mn system in which the germanium atom occupies a special position with equal Ge—Mn distances of 2.204 Å. Solution infrared spectra show four $\nu(\text{CO})$ stretching absorptions instead of the two expected from the centrosymmetric structure in the solid state, implying free rotation about the Ge—Mn bonds. Simple application of the rare-gas rule would favor a double-bonded formulation containing Ge(IV), but a molecular-orbital

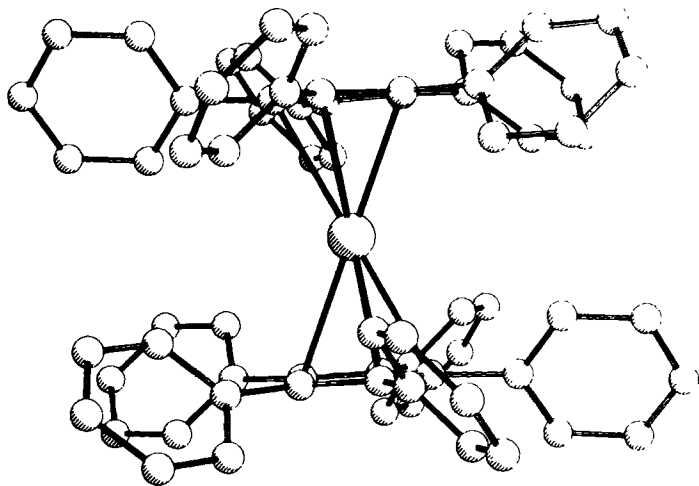


FIG. 1. Decaphenylstannocene, $[\eta^5\text{-(C}_6\text{H}_5)_5\text{C}_5\text{]}_2\text{Sn}$, viewed parallel to the plane of the cyclopentadiene rings (from ref. 77).

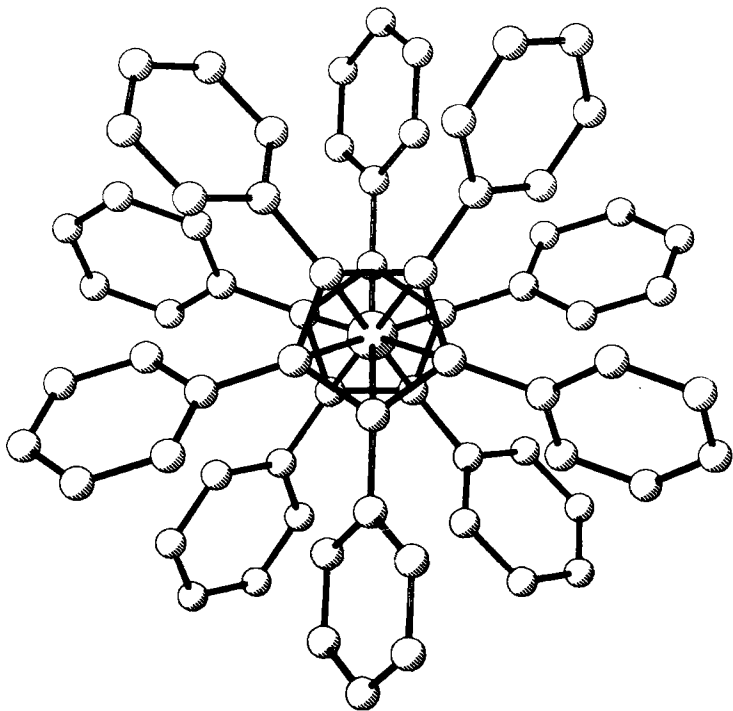


FIG. 2. Decaphenylstannocene, $[\eta^5\text{-(C}_6\text{H}_5)_5\text{C}_5\text{]}_2\text{Sn}$, viewed perpendicular to the plane of the cyclopentadienyl rings (from ref. 77).

calculation suggests partial three-center bonding in agreement with the rather free rotation found. The short Ge–Mn bonds favor the multiple-bond description (110).

3. $[\eta^5\text{-(C}_6\text{H}_5)_5\text{C}_5]_2\text{Sn}$

Decaphenylstannocene is the only molecule to occupy the S_{10} symmetry class. The tin atom sits on an inversion center between symmetry-related, equidistant [2.401 Å to the ring centers; $d(\text{Sn}-\text{C}_{\text{ring}}) = 2.692$ Å (av.)] cyclopentadienes that are perfectly planar, perfectly staggered, and exactly parallel (see Figs. 1 and 2). The attached phenyl groups are canted to each cyclopentadienyl ring oppositely in an opposed paddle wheel fashion. There are no short intermolecular contacts in the solid (see Fig. 3) (7, 8, 77).

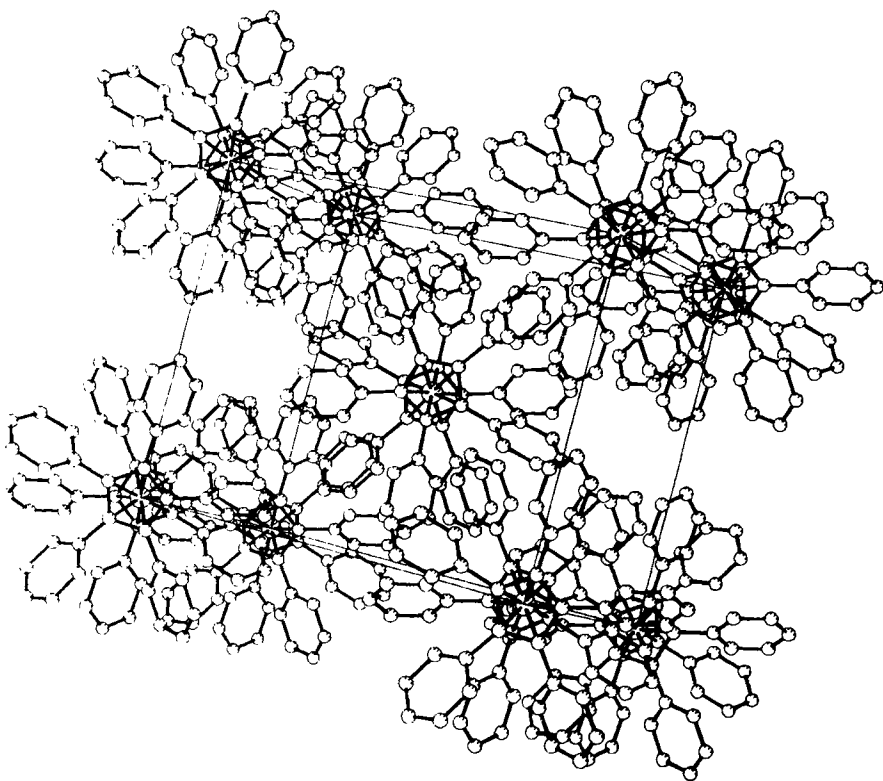


FIG. 3. Packing diagram of decaphenylstannocene, $[\eta^5\text{-(C}_6\text{H}_5)_5\text{C}_5]_2\text{Sn}$ (from ref. 77).

The fortuitous formation of η^5 -pentaphenylcyclopentadienyl derivatives of the transition metals under mild reaction conditions is evidence for the stabilizing power of that ligand. Aside from imparting high kinetic stability through its large volume, electron withdrawal by the phenyl groups makes low oxidation states of the transition metals more accessible. Since the tin(II) $5s^2$ electrons are not occupying their usual nonbonding orbital, and all the bonding orbitals are filled, then these electrons must occupy an orbital with antibonding character. The phenyl rings, which are not antiparallel to the cyclopentadiene rings, can help to delocalize these electrons. The germanium and lead derivatives are also available (88). The tin-119m Mössbauer spectrum of decaphenylstannocene is unremarkable (38, 88, 140, 177, 178) for a structurally authenticated (38, 157, 176) stannocene or its derivatives (42, 68, 69).

Pentaphenylstannocene, $\eta^5\text{-(C}_6\text{H}_5)_5\text{C}_5\text{Sn(II)C}_5\text{H}_5\text{-}\eta^5$, is bent, although some charge delocalization is possible because the five attached phenyl groups are not perpendicular to their cyclopentadiene ring (27). The decabenzylmetallocenes, $[\eta^5\text{-(C}_6\text{H}_5\text{CH}_2)_5\text{C}_5]_2\text{E(II)}$ (E = Ge, Sn, Pb), are also bent (27, 151a, 151b).

B. EXTENDED LATTICES

1. Germanium

a. GeCl_3^- Salts. In the salts of GeCl_3^- with Rb^+ (111), Cs^+ (28), $[\text{N}(\text{CH}_3)_4]^+$ (35), and $[\text{NH}(\text{CH}_3)_3]^+$ (114), as well as the pilocarpine ($\text{C}_{11}\text{H}_{17}\text{N}_2\text{O}_2$) hemihydrate (49), the germanium atom occupies a site with three short and three long Ge-Cl distances to give a distorted octahedron with two very different opposite triangular faces showing the structure-distorting effect of the lone-pair electrons. However, CsGeCl_3 undergoes a transition at 155°C as shown by differential thermal analysis (DTA) from its rhombohedrally distorted perovskite lattice to a cubic high-temperature phase (space group $Pm\bar{3}m$), and this transition is accompanied by a discontinuity in specific electrical conductance. The dielectric constant (1500 at 25°C) rises to 5800 at 155°C and then falls (28). The $[\text{N}(\text{CH}_3)_4]^+$ salt also undergoes a phase transition from space group $Pna2$ to an anionic, conducting cubic phase at 151°C (space group $Pm\bar{3}m$) (35). The room-temperature electrical conductivity of 10^{-8} increases to $10^{-2} \Omega^{-1} \text{ cm}^{-1}$, and the lattice constants expand by ca. 20%. The heat of transformation (115) is 3.1 kJ mol^{-1} , but the thermal stability range of the cubic phase is quite narrow since decomposition occurs at 22°C above the transition point (35).

b. Germanium Monochalcogenides. The orthorhombic GeS (157a, 170, 173) and GeSe (45, 87, 95, 130, 149, 157a, 173) compounds display anomalies of thermal expansion in the range 230–500 and 400–500°C, respectively; GeSe transforms in one step at 651°C to the rock-salt structure, and GeS melts at 658°C before a potential transition to the NaCl structure can take place. For GeTe, the rhombohedral, face-centered lattice (57, 150, 174) is converted in a first-order phase transition to the NaCl structure (16) at 300°C, accompanied by a shrinkage in volume of 1.4% (174).

c. GeBi₂Te₄. Electron diffraction (at the $R = 23\%$ level) of a hexagonal film of GeBi₂Te₄ (space group $R\bar{3}m$) on NaCl reveals the germanium atoms lying on octahedral sites symmetrically surrounded by six tellurium atoms (3).

d. Ge₃Bi₂Te₆. Electron diffraction (at the $R = 19.6\%$ level) of a hexagonal film of Ge₃Bi₂Te₆ (space group $R3m$) on NaCl gives a closest packed cubic arrangement of germanium atoms in octahedral sites symmetrically surrounded by six tellurium atoms (134).

e. K₂Ge₂O₃. The oxogermanate(II), K₂Ge₂O₃, has a body-centered cubic structure from X-ray powder data. Annealing at 380°C for 1 week produces no changes (81).

2. Tin

a. CsSnCl₃. Monoclinic (136) [or triclinic (20)] white CsSnCl₃ (space group $P2_1/n$, m.p. 383°C) undergoes an irreversible phase transition at 117°C to a bright yellow, ideal cubic perovskite (11, 138, 146). While the low-temperature form exhibits a tin-119m Mössbauer QS of 0.90 mm sec⁻¹, the cubic form has a single, sharp line with no resolvable QS, consistent with the tin atoms being located at a cubic site (11). In addition, the low-temperature form exhibits three chlorine-35 NQR resonances of equal intensity, consistent with three inequivalent chlorine atom sites in the pyramidal SnCl₃⁻ anion. Unfortunately, the resonance in the cubic form could not be observed (146). Both the high- and low-temperature forms are electrical insulators (146). The cell length reported previously (136) has been determined to be erroneously too small (11).

b. CsSnBr₃. Black CsSnBr₃ exhibits metallic luster and is cubic (11) (space group $Pm\bar{3}m$) at room temperature ($R = 11\%$) (41). The conductivity is 0.05 Ω⁻¹ cm⁻¹ at ambient temperature and shows metallic-type behavior between 100 and 350°C with no major change in conductance observed. The material turns dark red between 350 and 400°C and melts to a clear, dark-red liquid at 450°C. The color changes

reverse upon cooling (146). The conductivity and color behavior reported (11) are said to correspond to the material treated in air (146). There is no resolvable QS in the tin-119m Mössbauer spectrum, consistent with the tin atoms occupying sites of cubic symmetry at the center of a regular octahedron of bromine atoms (11, 39–41). At 12°C, some weak extra X-ray powder lines appear, and a transformation to a lower symmetry form is corroborated by bromine-81 NQR and DTA data. However, a single NQR resonance is observed in the range 19.6–100°C (146).

c. $[\text{CH}_3\text{NH}_3]^+\text{SnBr}_3^-$. This compound crystallizes in a perovskite structure with the tin(II) atom in octahedral coordination (108).

d. CsSnI_3 . Yellow, orthorhombic CsSnI_3 (m.p. 452°C) crystallizes in needle form (space group $Pnam$) with the tin(II) atoms at the center of a distorted octahedron of iodine atoms (107). The yellow material begins to darken above 100°C, and at 152°C transforms to a shiny black, cubic perovskite form which is an electrical conductor (conductivity at room temperature is $0.04 \Omega^{-1} \text{ cm}^{-1}$). Between 350 and 400°C it turns slightly dark red. The melt is black and opaque, and the vapor yellow. Upon solidification, CsSnI_3 remains black when cooled to room temperature. Unfortunately, no iodine-127 NQR signals could be found for the black, cubic form, but the yellow monoclinic form gives a single line whose frequency decreases approximately linearly with increasing temperature from 35 to 105°C (146).

e. $[\text{CH}_3\text{NH}_3]^+\text{SnBr}_x\text{I}^{3-x}_3$ ($x = 0-3$). These intensely colored, electrically conducting compounds exhibit cubic perovskite structures on the basis of X-ray powder data, with the tin(II) atoms at the center of octahedra formed by the halogen atoms. The data can be indexed in terms of a primitive cubic lattice. For the anthracite-colored $[\text{CH}_3\text{NH}_3]^+\text{SnI}_3$, the $Pm3m$ space group can be assigned. For this compound there are no resolvable tin-119m Mössbauer QS at 85 or 298 K, and none at 298 K for the wine-red SnBr_3^- analogue. Both the latter and the black SnBr_2I^- derivative show small QS values at 85 K. At 290–300°C, the SnBr_3^- and SnI_3^- salts melt to light yellow and blue-black liquids, respectively, with decomposition to a vapor, presumably containing $\text{CH}_3\text{NH}_3\text{Br}$ and $\text{CH}_3\text{NH}_3\text{I}$. The electrical conductivity maximizes with the SnI_3^- derivative (169).

f. $[(\text{C}_2\text{H}_5)_4\text{N}]^+\text{SnI}_3^-$. The tin(II) atom here occupies an octahedral site surrounded by six iodine atoms. Linear, one-dimensional chains of tin atoms parallel to the c -axis are bridged by iodine atoms (108).

g. Cs_4SnBr_6 . The white, ambient-temperature form turns black on heating or when prepared from the molten CsBr-SnBr_2 system. X-Ray powder data for the black form suggest a hexagonal structure (41) similar to that of Cs_4PbBr_6 , which contains discrete $[\text{PbBr}_6]^{4-}$ anions (118). The tin-119m Mössbauer resonance is a narrow singlet at 4.2 K, consistent with a high-symmetry $[\text{SnBr}_6]^{4-}$ environment (41). This regular octahedral geometry has been confirmed by an unpublished single-crystal X-ray study (6).

h. SnTe . Both the ambient α (170) and high-temperature (β) forms (168) of SnS and SnSe (157a) are orthorhombic, with space groups $Pbnm$ for the former and $Cmcm$ for the latter. Earlier reports of cubic phases (132, 141) or films (112, 113) are in error (9).

Cubic SnTe has an NaCl structure at room temperature with two interpenetrating face-centered cubic sublattices formed by tin(II) and tellurium atoms (1, 2, 72, 73, 126, 128). The cubic form undergoes a transition to a rhombohedral structure at temperatures below 5 K (16, 123) and to an orthorhombic one (space group $Pnma$) at 18 kbar (94).

i. SnI_2 . Brilliant red tin(II) iodide crystallizes in the monoclinic space group $C2/m$ as needles which contains two distinct tin sites, one of seven coordination occupied by two-thirds of the tin atoms, and one of six coordination occupied by the rest (121). The former is of distorted geometry with tin-iodine distances suggestive of a primary trigonal pyramid in a trigonal prism with an additional nearest neighbor. In the latter the tin atom lies on a center of symmetry and is surrounded octahedrally by iodine atoms (82). The monoclinic crystals have also been described as transparent bright yellow from growth in silica gel (36). The tin-119m Mössbauer spectrum fails to reveal the true complexity of the structure. The two tin sites apparently have quite similar IS, and the seven-coordinated site exhibits only a weak QS (82).

j. $[\text{Rh}(\text{NH}_3)_6]_3^{3+}[\text{Rh}(\text{SnCl}_3)_4\text{SnCl}_4]^{5-}[\text{SnCl}_6]^{4-} \cdot 4\text{H}_2\text{O}$. This violet, extremely polychroic salt consisting of three $[\text{Rh}(\text{NH}_3)_6]^{3+}$ cations, two kinds of anions, $[\text{Rh}(\text{SnCl}_3)_4\text{SnCl}_4]^{5-}$ and $[\text{SnCl}_6]^{4-}$, and four waters of crystallization forms in the monoclinic space group $P2/n$. The tin(II) atom in the hexachlorostannate(II) dianion lies on a twofold axis with Sn-Cl distances ranging from 2.7631 to 2.8942 Å, and Cl-Sn-Cl angles of 84.29, 95.96, and 175.83° (97). Tin-119m Mössbauer data show the presence of this tin(II) atom (96, 144). While the unique tin(II) atom is at the center of a slightly less-than-perfect octahedron of chlorine atoms, the extremely long Sn-Cl bonds (97) signal the stereochemical inertness of the lone-pair electrons, and hence this compound is included here.

3. Lead

a. PbF_2 . Orthorhombic $\alpha\text{-PbF}_2$ (145) (space group $Pmnb$) undergoes a phase transition at 315°C to a cubic β form (154) (space group $Fm3m$) (172), accompanied by a lattice expansion. The anions and cations coordinate one another in the form of regular cubes and regular tetrahedra, respectively. Thus the Pb(II) atoms are eight coordinated with the fluorine atoms located at the corners of a regular cube, and each fluorine atom is surrounded by four metal atoms at the corners of a regular tetrahedron. This fluorite-structure material exhibits high ionic conductivity ($1\ \Omega^{-1}\text{ cm}^{-1}$) at high temperatures (ca. 425°C) (152). At lower temperatures the ionic conduction is carried mainly by extrinsic defects which can be generated by doping $\beta\text{-PbF}_2$ with either divalent anions (e.g., O^{2-}) or mono- or trivalent cations (e.g., Ag^+ , La^{3+}). At higher temperatures the ionic conduction is carried by intrinsic defects (10, 37, 86, 101).

b. PbI_2 . Yellow PbI_2 (m.p. 400°C) has the CdI_2 hexagonal layer lattice structure (163, 166). The material is a photoconductor and decomposes on exposure to green light ($\lambda = 494.9\text{ nm}$). The lead atoms are in alternate layers of octahedral sites sandwiched between layers of iodine atoms. Organic donor molecules can intercalate into the layer lattice, which retains its hexagonal symmetry (100).

c. CsPbF_3 . At 615°C CsPbF_3 transforms into a primitive cubic perovskite lattice. The lower-temperature β form also has a perovskite lattice, but with a tetragonal distortion (148). The melting point is 725°C .

d. CsPbCl_3 . The pale-yellow rectangular crystals (109) of CsPbCl_3 undergo three successive phase transformations: at 37°C , from monoclinic to orthorhombic; at 42°C , from orthorhombic to tetragonal; and at 46.9°C , from tetragonal to cubic (50, 117, 119, 129). The structure of the high-temperature form is not entirely straightforward since single-crystal neutron diffraction data (at the $R = 9\%$ level) at 55°C can be interpreted in terms of a cubic perovskite structure with anisotropic thermal vibration, or a disordered structure with several potential minima for the cesium and chlorine atoms (66). X-Ray powder data can be interpreted in terms of distortions from the ideal cubic structure arising from various tilts of the PbCl_6 octahedra about one or more of the cubic faces (4). The anharmonicity in cubic CsPbCl_3 is quite marked (50), and the cubic to tetragonal transition is discontinuous (83), with the PbCl_6 octahedra oscillating in phase along a particular direction (50). In addition, there may be competing instabilities in the cubic phase

(83). Disordered models for the chlorine atoms are not currently favored (66, 83), but the origin of the lead atom anharmonicity cannot be said to be settled yet (83, 124a). The lower temperature phases may be better understood (25, 80).

e. $[\text{CH}_3\text{NH}_3]^+\text{PbX}_3^-$ ($\text{X} = \text{Cl}, \text{Br}, \text{I}$). These three compounds have the cubic perovskite structure. With the exception of the colorless chloride, they show intense color (red-orange for the bromide and black for the iodide). However, there is no significant conductivity under normal conditions. The mixed halides have intermediate colors. Decomposition occurs at ca. 300°C without melting, but they are far more stable to oxidation than the corresponding tin(II) analogues (see Sections IV, B, 2, c and IV, B, 2, e, above). Apparently, the nonspherically symmetrical methylammonium cation does not encroach upon the octahedral symmetry of the lead halide system (169).

f. CsPbBr_3 . The white, low-temperature form of CsPbBr_3 is orthorhombic (space group $Pmnb$) (106) and contains distorted PbBr_6 octahedra. Above 130°C , however, a cubic perovskite structure forms (119, 120). This material behaves like the analogous chloride, whose structure is discussed in Section IV, B, 3, d, in that there are anisotropic thermal vibrations and anomalously large thermal parameters for the cesium and bromine atoms (143).

g. MPbI_3 ($\text{M} = \text{Rb}, \text{Cs}, \text{R}_4\text{N}^+$). Yellow, orthorhombic CsPbI_3 (space group $Pmnb$) contains distorted PbI_6 octahedra. On heating these crystals to $305\text{--}308^\circ\text{C}$, they undergo a phase change to an unstable, black, monoclinically distorted perovskite structure (116). The material is photoconductive, having its maximum spectral sensitivity in the red region, the one complementary to the color of the crystal (120).

The isomorphous rubidium analogue crystallizes in the orthorhombic space group $Pnam$. Again, the PbI_6 octahedra are not precisely ideal. The lead-iodine internuclear distances are in the range $3.037\text{--}3.382 \text{ \AA}$ (76).

Tetramethylammonium triiodolead(II), $[(\text{CH}_3)_4\text{N}]^+\text{PbI}_3^-$, is hexagonal (space group $P6_3/m$) with octahedrally coordinated Pb(II) atoms. The $(\text{CH}_3)_4\text{N}^+$ cations are disordered. Two unique angles, 86.25 and 93.75° , characterize the lead atom site which has crystallographic $\bar{3}$ point symmetry. The octahedron is stretched along one axis. The lead-iodine internuclear distance is 3.223 \AA (30).

The hydrates $\text{KPbI}_3 \cdot 2\text{H}_2\text{O}$, $\text{NH}_4\text{PbI}_3 \cdot 2\text{H}_2\text{O}$, and $\text{RbPbI}_3 \cdot 2\text{H}_2\text{O}$ are isostructural, crystallizing in the space group $Pnma$. The PbI_6 octahedra are distorted. The lead-iodine internuclear distances range from 3.03 to 3.46 \AA (14).

Thus, while all the PbI_6 octahedra in these structures are distorted, the materials are included here for completeness.

h. PbS. Lead(II) sulfide (m.p. 1112°C), which crystallizes with the NaCl structure (23), is opaque and possesses a brilliant metallic luster as the black mineral galena. This is the principal ore of lead and its only sulfide. The pure material is an intrinsic semiconductor, which, in the presence of impurities or in stoichiometric imbalance, can develop either n- or p-type semiconductor properties. It is also a photoconductor, and is one of the most sensitive detectors of infrared radiation. The photovoltaic effect in this material is the basis for its use in photographic exposure meters.

The charge distribution in the cubic PbS rock-salt structure (6:6 coordination; space group $Fm\bar{3}m$) has been studied at ambient temperature by X-ray diffraction at the $R = 1.5\%$ level. The direct integration of charge density, the observed atomic scattering factors, and the population analysis of the valence electrons all indicate that the lead atom is negatively charged, i.e., electrons are transferred from sulfur to lead. No overlap density was observed in the deformation density map. Thus the bonding electrons in this crystal may be delocalized like free electrons in metals. The thermal parameters of the lead atoms are larger than those of the chalcogens. Anharmonic thermal vibration of the lead atom is detected in the difference electron density map (127).

i. PbSe. The three lead(II) chalcogenides (137), PbS, PbSe, and PbTe, are unusual in that their color diminishes with increasing mass of the chalcogen. Lead(II) sulfide (see Section IV, B, 3, *h*) is black, the selenide is grey, and PbTe (see Section IV, B, 3, *j*) is white. All three materials possess the cubic rock-salt structure (space group $Fm\bar{3}m$); all three are photoconductors.

Lead(II) selenide, (m.p. 1075°C), found as the mineral Clausthalite, has been studied by X-ray diffraction at the $R = 1.1\%$ level. The results of this study are the same as those described in Section IV, B, 3, *h* for PbS, except that the ratio of thermal parameters for lead vs. the chalcogen is even larger in PbSe (127).

j. PbTe. Lead(II) telluride (m.p. 917°C) occurs naturally as the mineral Altaite, but can be made directly by heating stoichiometric amounts of the elements. The product is a white material which crystallizes in the cubic rock-salt structure (space group $Fm\bar{3}m$). Study by X-ray diffraction at the $R = 1.5\%$ level yields results similar to those discussed for PbS in Section IV, B, 3, *h*, except that here the ratio of the thermal parameters for lead vs. the chalcogen is even greater than for PbS or PbSe. A valence electron population analysis gives effective

charges at the lead atom of -1.2 , -0.9 , and -2.7 for PbS, PbSe, and PbTe, respectively (see Sections IV, B, 3, h and IV, B, 3, i) (127, 157a).

k. Lead(II) Thiourea Complexes. Thio- and selenoureas can serve as precursors in the synthesis of the Pb(II) chalcogenides described above. The thiourea complexes of Pb(II) show many different compositions and structural types (58–64, 78, 79), which include six- and eightfold coordination of the lead(II) atoms by sulfur. While in no case reported thus far has the lead(II) atom been found at a site of perfect symmetry, the following two compounds are included here because in each one there is a lead(II) atom at the center of a polyhedron which is only slightly distorted.

(1) $\frac{3}{4}\text{Pb}(\text{HCO}_2)_2 \cdot 4\text{SC}(\text{NH}_2)_2$. The title compound, unlike several analogues, is fully ordered and has one lead(II) atom in a symmetrical, eight-coordinated site. The structure consists of infinite polymeric chains, but with every fourth lead position along the chain vacant. These ordered vacancies account for the unusual stoichiometry. The material precipitates from saturated greenish-yellow aqueous formic acid solutions of Pb(II) formate and thiourea as white needles (space group *I422*). The structural motif consists of three lead atoms in twisted trigonal prisms (twist angle $\sim 28^\circ$) formed by the sulfur atoms of the thiourea molecules. One lead atom is at the center of gravity (not a center of symmetry) of the central prism. Successive motifs along a lead–thiourea chain are separated by empty prisms. The distances between successive squares of sulfur atoms (these four sulfur atoms are related by a fourfold axis and hence lie in one plane) are equal whether the prism is occupied by a lead atom or not. The central Pb(II) atom is symmetrically situated at long but equal distances from the surrounding sulfur atoms (see Figs. 4–6) (59).

(2) $\text{Pb}[\text{SC}(\text{NH}_2)_2]_6^+ [\text{ClO}_4]_2^-$. White, triclinic needles (space group *P1*) precipitate from saturated aqueous thiourea to which stoichiometric $\text{Pb}(\text{ClO}_4)_2$ has been added (1:6). The lead(II) atom lies at the origin of the unit cell, equidistant from six sulfur atoms at the center of a slightly distorted octahedron characterized by three independent angles ($\bar{1}$ symmetry) ranging from 79 to 100° (see Fig. 7) (58).

l. $\text{M}_2\text{PbCo}(\text{NO}_2)_6$ ($\text{M} = \text{Rb}, \text{Cs}$). The $\text{M} = \text{Rb}$ and Cs materials crystallize in cubic phases (24, 48) (space group *Fm3*) containing both $\text{Co}(\text{NO}_2)_6$ and Pb(II) groups with *m3* symmetry (103). A wide range of hexanitrito complexes of the first-row transition metal ions are known (74a), and many have been shown to take face-centered cubic structures. The presence of the lead(II) ion may contribute to the stabilization of

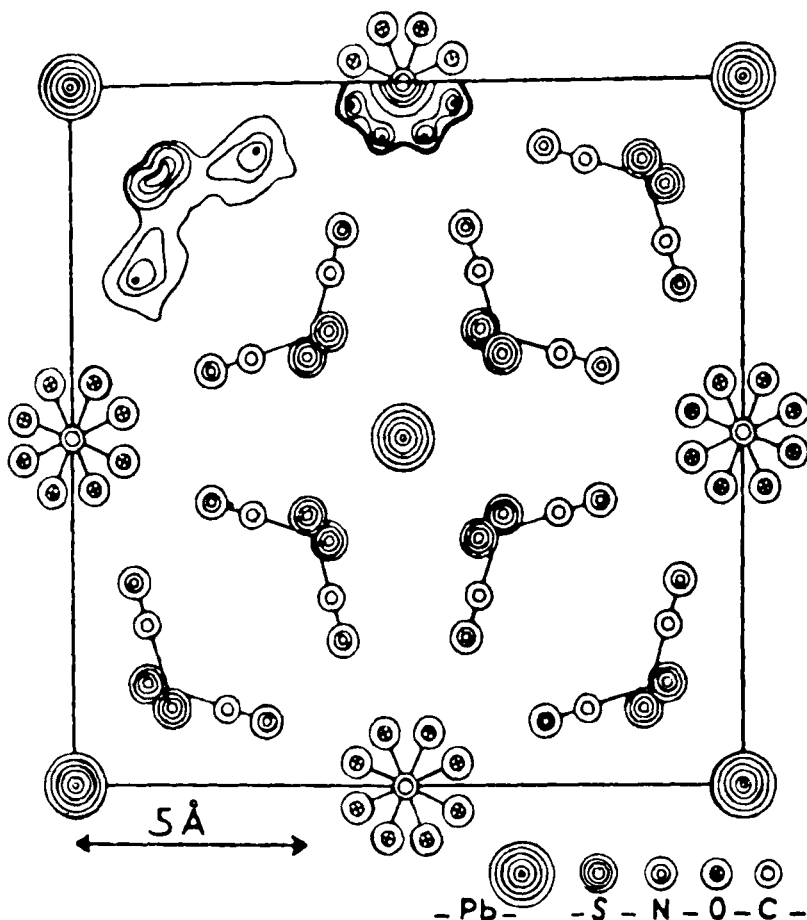


FIG. 4. The structure of $\frac{3}{4}\text{Pb}(\text{HCO}_2)_2 \cdot 4\text{SC}(\text{NH}_2)_2$ in projection down $[001]$ (from ref. 59).

these cubic phrases (48). Powder electron spin resonance (ESR) spectra at 296 K are isotropic as expected. The lead(II) atom is found at the center of 12 nitrite oxygen atoms in a cubic geometry (103).

m. $\text{K}_2\text{PbNi}(\text{NO}_2)_6$. The lead(II) atom is found at the center of a cube formed by the 12 nitrite oxygen atoms in this cubic (space group $Fm\bar{3}$) crystal in which the $\text{Ni}(\text{NO}_2)_6$ groups also have $m\bar{3}$ symmetry. The cubic symmetry is retained down to 130 K unlike the copper homologue (see Section IV,B,3,n), which transforms to an orthorhombic form at 233 K (158, 160). Among the hexanitritonickelates, the lead(II) derivative exhibits different electronic and electron spin resonance (ESR) behavior than, for example, the alkaline-earth analogues (75).

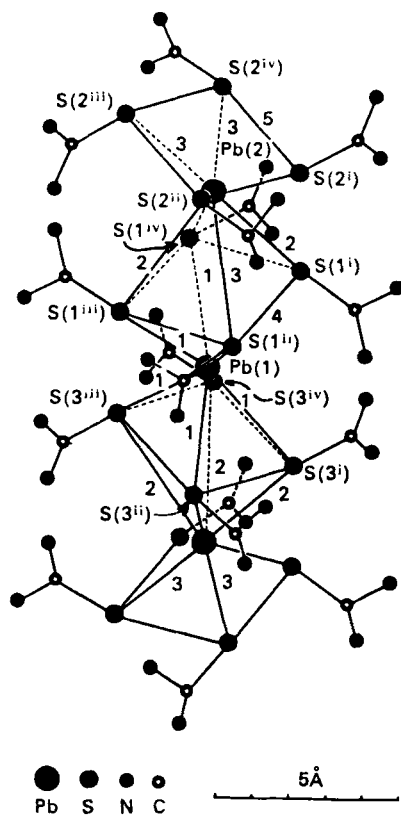


FIG. 5. The structural motif in $\frac{3}{4}\text{Pb}(\text{HCO}_2)_2 \cdot 4\text{SC}(\text{NH}_2)_2$ (from ref. 59).

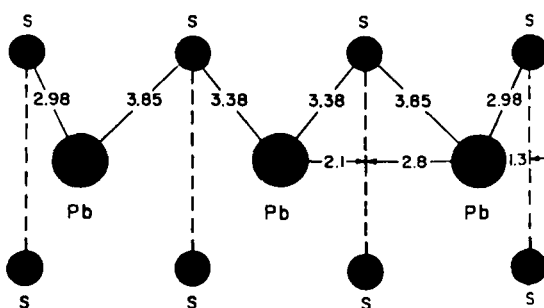


FIG. 6. Internuclear distances in the cation motif in $\frac{3}{4}\text{Pb}(\text{HCO}_2)_2 \cdot 4\text{SC}(\text{NH}_2)_2$ (from ref. 59).

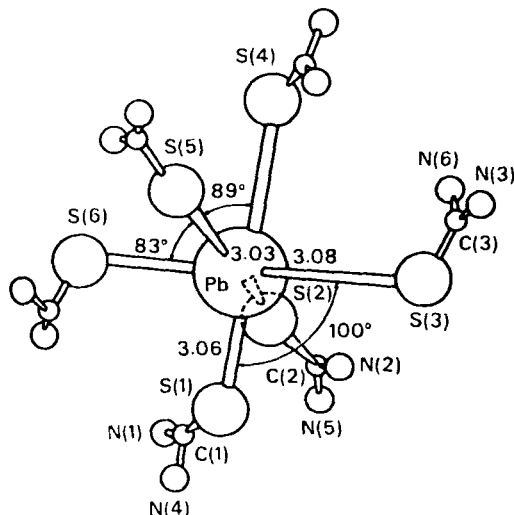


Fig. 7. Geometry of the $\text{Pb}[\text{SC}(\text{NH}_2)_2]_6^{2+}$ cation in the perchlorate salt (from ref. 58).

n. $\text{M}_2\text{PbCu}(\text{NO}_2)_6$ ($\text{M} = \text{K}, \text{Rb}, \text{Cs}, \text{Tl}$). The $\text{M} = \text{K}$ derivative is face-centered cubic (space group $Fm\bar{3}$) with the copper atoms at the centers of regular octahedra and the lead(II) atoms at the centers of perfect cubes (25, 33, 167) (see Fig. 8) (85). Reversible transformations to less symmetrical tetragonal phases occur at 281 and 273 K (48). In the $\text{Cu}(\text{NO}_2)_6^{4-}$ anion the NO_2 groups trans to each other are coplanar and parallel to the axial plane to give T_h symmetry. The electron spin resonance (ESR) spectrum is a single isotropic line at 300 K, but the spectrum at 77 K is anisotropic (71). The cubic $\text{M} = \text{Tl}$ derivative is isomorphous (space group $Fm\bar{3}$) at 295 K and undergoes phase changes at 245 and 241 K, which give rise to changes in the ESR spectra and lattice dimensions (70, 159). The $\text{M} = \text{Rb}$ derivative is orthorhombic (space group $Fmmm$), but transforms to a cubic structure (139) (space group $Fm\bar{3}$) above 317 K (161, 162). The phase transitions in $\text{Cs}_2\text{PbCu}(\text{NO}_2)_6$ take place at 275 and 289 K and at 381 and 391 K (on cooling and heating, respectively). A third transition occurs at 294 and 310 K. The first of these transitions gives an orthorhombic material (space group $Fmmm$). The lead-oxygen distances are in the range 2.849–2.858 Å (124). A second material is monoclinic (space group $B2/b$) (98).

o. Miscellaneous Lead(II) Oxides. The question of the stereochemical activity of the lone-pair electrons in divalent tin and lead oxides has been carefully treated recently (138). No examples of sites of perfect symmetry are available, but the following systems deserve mention.

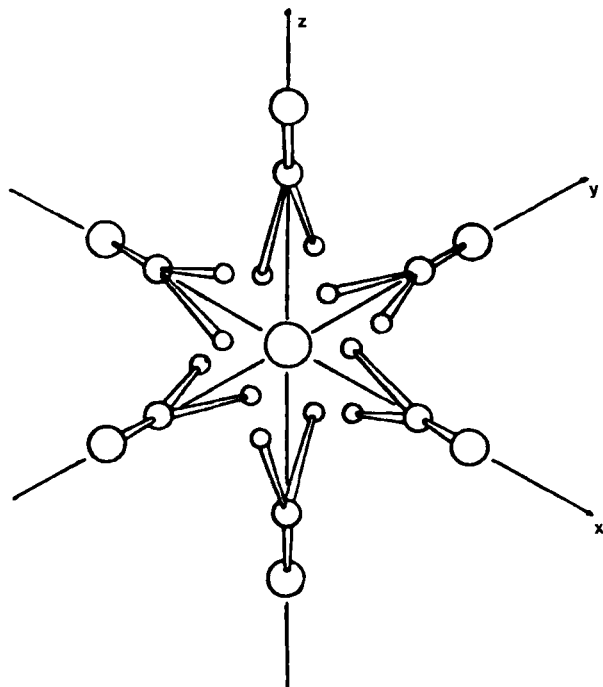


FIG. 8. The arrangement of the nitrito groups about the lead(II) atom in $\text{K}_2\text{PbCu}(\text{NO}_2)_6$ (from ref. 85).

(1) PbWO_4 . Lead(II) tungstate is isostructural with Scheelite, CaWO_4 , whose structure is built up from isolated WO_4 tetrahedra which are connected through PbO_8 polyhedra. The lead(II)–oxygen internuclear distances fall into two groups of four at near 2.645 and 2.670 Å (mean 2.66 Å). These values are comparable with those observed in the strontium (2.49 and 2.59 Å) and barium (2.68 and 2.688 Å) homologues. Thus it appears that the lone-pair electrons at Pb(II) play little role here (135, 156).

(2) PbCrO_4 . The orthorhombic form of lead(II) chromate is also built up from CrO_4 tetrahedra linked through PbO_{12} polyhedra characterized by lead(II)–oxygen distances in the range 2.64–3.57 Å (29).

(3) PbNb_2O_6 . The rhombohedral form of PbNb_2O_6 is only stable at low temperatures, transforming to the tetragonal tungsten-bronze structure at above 100°C. The former is built up from edge- and corner-sharing NbO_6 octahedra forming two kinds of tunnels—large triangular ones, and others which are very distorted hexagonal. Pyramidal

PbO_3^{4-} anions are located in these tunnels. In the ferroelectric tetragonal phase, on the other hand, there are pentagonal and perovskite tunnels. The Nb atoms are displaced inside their octahedra and the Pb atoms likewise inside their polyhedra in the pentagonal tunnels. However, there are other lead(II) atoms in the pentagonal tunnels which, along with all of those in the perovskite tunnels, are characterized by rather long lead-oxygen distances (2.65–2.89 Å) and relatively small displacements inside their polyhedra (102).

(4) *Cubic pyrochlores*, $\text{Pb}_2\text{M}_2\text{O}_7$. All known exactly stoichiometric cubic pyrochlores of tin and lead (possibly excepting the $\text{M} = \text{U}$ material of lead) are rhombohedrally distorted from the ideal $Fd3m$ space group. Nonstoichiometric, usually oxygen-deficient, pyrochlores of the precious metals, M, can be cubic with the cations in a face-centered array. These materials exhibit metallic conductivity and paramagnetism, but some Pb(IV) atoms often occupy the M sites. In the ideal case the lead(II) cation would be eight-coordinated by oxygen atoms in a hexagonal-bipyramidal geometry. However, the value of x in the oxygen-deficient pyrochlores $\text{Pb}_2\text{M}_2\text{O}_{7-x}$ is nearly one ($\text{M} = \text{Ru}, \text{Ir}, \text{Re}, \text{etc.}$). The M cations are found in perfect octahedra (138).

V. Conclusions

We present in Table I a listing of compounds in which subvalent group-four atoms occupy perfectly symmetrical sites. Only two discrete molecular forms are represented, the rest being extended lattices. The inclusion of compounds with highly, but not perfectly, symmetrical sites would have greatly expanded this list (Table I). Some of these materials are mentioned in the text as an encouragement to further research seeking perfect symmetry phases.

Generalization for these materials is difficult because at the present time not all the desired information has been developed for each system. However, a pattern involving the following phenomena begins to emerge from our survey.

1. Certain subvalent, fourth-group compounds undergo single or a series of first-order phase transformations at increasing temperatures from their expected distorted phases to give successively more symmetrical structures;

2. If the material does not melt first, this may include a phase in which the subvalent group-four atom occupies a site of perfect cubic symmetry;

TABLE I

SYMMETRICAL E(II) STRUCTURES

Molecular	
Ge:	$[\eta^5\text{-C}_5\text{H}_5\text{Mn(CO)}_2]_2\text{Ge}$
Sn:	$[\eta^5\text{-(C}_6\text{H}_5)_5\text{C}_5]_2\text{Sn}$
Extended Lattices	
Ge:	MGeCl ₃ (M = Cs ⁺ , Me ₄ N ⁺)
	GeSe at >651°C
	GeTe at >300°C
	GeBi ₂ Te ₄ film on NaCl
	Ge ₃ Bi ₂ Te ₆ film on NaCl
	K ₂ Ge ₂ O ₃
Sn:	CsSnCl ₃ at >117°C
	MSnBr ₃ (M = Cs ⁺ , MeNH ₃ ⁺)
	MSnI ₃ (M = Cs ⁺ at >152°C, MeNH ₃ ⁺ , Et ₄ N ⁺)
	Cs ₄ SnBr ₆
	SnTe
	SnI ₂
	$[\text{Rh(NH}_3)_6]_3^{3+}[\text{Rh(SnCl}_3)_4\text{SnCl}_4]^{5-}[\text{SnCl}_6]^{4-} \cdot 4\text{H}_2\text{O}$
Pb:	PbF ₂ at >315°C
	PbI ₂
	CsPbF ₃ at >615°C
	MPbCl ₃ (M = Cs ⁺ at >46.9°C, MeNH ₃ ⁺)
	MPbBr ₃ (M = Cs ⁺ at >130°C, MeNH ₃ ⁺)
	MPbI ₃ (M = Cs ⁺ at >305°C, MeNH ₃ ⁺)
	PbS
	PbSe
	PbTe
	M ₂ PbCo(NO ₂) ₆ (M = Rb ⁺ , Cs ⁺)
	K ₂ PbNi(NO ₂) ₆
	M ₂ PbCu(NO ₂) ₆ (M = K ⁺ , Rb ⁺ , Cs ⁺ , Tl ⁺)

3. The materials which contain perfectly symmetrical sites for the subvalent fourth-group atom have regular octahedral (six) or cubic (eight-) or dodecahedral (12-coordinated) environments consisting of equidistant halogen (F, Cl, Br, or I) or chalcogen (O, S, Se, or Te) nearest neighbors. In the regular cubic examples only oxygen has been found thus far to be present; all the regular cubic geometries discovered have lead(II) atoms surrounded by 12 oxygen atoms. Examples with asymmetric gegen ions exist, as do examples arising from epitaxial effects on materials deposited on rock-salt surfaces;

4. Evidence for the cubic symmetry can come from the observation of single lines in Mössbauer (Fortin), pure nuclear quadrupole resonance (NQR), or electron-spin resonance (ESR) spectra, or from X-ray or neutron diffraction studies;

5. The transformations to the cubic phase are accompanied by isotropic expansion of the lattices and large thermal parameters for the fourth-group atom;

6. The resulting cubic phases are often intensely colored and electrically conducting.

There seems at the present time no general theory available that would allow one to predict which compositions would exhibit these unusual behaviors (cf. ref. 33).

REFERENCES

1. Abrikosov, N. Kh., Novikova, S. I., Shelimova, L. E., and Zhdanova, V. V., *Izv. Akad. Nauk SSSR, Neorg. Mater.* **5**, 1895 (1969).
2. Abrikosov, N., Vasserman, A. N., and Porestskaya, I. V., *Dokl. Akad. Nauk SSSR* **123**, 279 (1958).
3. Agaev, K. A., and Semiletov, S. A., *Sov. Phys., Crystallogr. (Engl. Transl.)* **10**, 86 (1965).
4. Alexandrov, K. S., Besnosikov, B. V., and Posdnjakova, L. A., *Ferroelectrics* **12**, 197 (1976); *Chem. Abstr.* **86**, 36578j (1977).
5. Andersson, S., and Astrom, A., *NBS Spec. Publ.* **364**, *Solid State Chem. Proc. 5th Mater. Res. Symp.* (July, 1974).
6. Andrews, R. H., Ph. D. Thesis, University of London, (1977), quoted in refs. 34, 38.
7. Anon., *Chem. Eng. News*, 6 Aug., 1984, p. 20.
8. Anon., *Chem. Unser. Zeit* **18**(5), 179 (1984).
9. Avilov, A. S., Imamov, R. M., and Navasardyan, S. N., *Sov. Phys., Crystallogr. (Engl. Transl.)* **24**, 504 (1979).
10. Bachmann, R., and Schulz, H., *Solid State Ionics* **9**, **10**, 521 (1983).
11. Barrett, J., Bird, S. R. A., Donaldson, J. D., and Silver, J., *J. Chem. Soc. A*, p. 3105 (1971).
12. Bartell, L. S., *J. Chem. Educ.* **45**, 754 (1968).
13. Becker, P., ed., "Electron and Magnetization Densities in Molecules and Crystals," Plenum, New York, 1980.
14. Bedlivy, D., and Mereiter, K., *Acta Crystallogr., Sect. B* **B36**, 782 (1980).
15. Bernheim, R. A., Kempf, R. J., Gramas, J. V., and Skell, P. S., *J. Chem. Phys.* **43**, 196 (1965).
16. Bierly, J. N., Muldower, L., and Beckman, O., *Acta Metall.* **11**, 447 (1963).
17. Bills, J. L., and Snow, R. L., *J. Am. Chem. Soc.* **97**, 6340 (1975).
18. Bills, J. L., and Steed, S. P., *Inorg. Chem.* **22**, 2401 (1983).
19. Brown, I. D., in "Structure and Bonding in Crystals," M. O'Keefe and A. Navrotsky, eds., p. 1. Academic Press, New York, 1981.
20. Bulanova, G. G., Podlesskaya, A. V., Soboleva, L. V., and Soklakov, A. I., *Inorg. Mater. (Engl. Transl.)* **8**, 1698 (1972).
21. Burdett, J. K., "Molecular Shapes." Wiley, New York, 1980.
22. Burger, H., and Eujen, R., *Top. Curr. Chem.* **50**, 1 (1974).
23. Bystrom, A., *Arkiv Kemi, Mineral., Geol.* **25A**, No. 13 (1947).
24. Cambi, L., Ferrari, A., Coriselli, C., Solenghi, P., and Colla, C., *Gazz. Chim. Ital.* **65**, 1162 (1935).
25. Cavalca, L., Nardelli, M., and Grazioli, D., *Gazz. Chim. Ital.* **86**, 1041 (1956).

26. Chabin, M., and Gilletta, F., *J. Appl. Crystallogr.* **13**, 533 (1980).
27. Chambers, J. W., Heeg, M.-J., Janiak, C., Rausch, M. D., Schumann, H., and Zuckerman, J. J., *Abstr. 189th Am. Chem. Soc. Meet. Miami Beach, FL, Apr. 1985*.
28. Christensen, A. N., and Rasmussen, S. E., *Acta Chem. Scand.* **19**, 421 (1965).
29. Collotti, G., Conti, L., and Zocchi, R., *Acta Crystallogr.* **12**, 416 (1959).
30. Contreras, J. G., Seguel, G. V., Ungerer, B., Maier, W. F., and Hollander, F. J., *J. Mol. Struct.* **102**, 295 (1983).
31. Coppens, P., and Hall, M. B., eds., "Electron Distributions and the Chemical Bond." Plenum, New York, 1982.
32. Couch, D. A., Wilkins, C. J., Rossman, G. R., and Gray, H. B., *J. Am. Chem. Soc.* **92**, 307 (1970).
33. Cullen, D. L., and Lingafelter, E. C., *Inorg. Chem.* **10**, 1264 (1971).
34. Cusack, P. A., Smith, P. J., Donaldson, J. D., and Grimes, S. M., *Int. Tin Res. Inst. Publ.* **588** (1981).
35. Depmeier, W., Moller, A., and Klaska, K.-H., *Acta Crystallogr., Sect. B* **B36**, 803 (1980).
36. Desai, C. C., and Rai, J. L., *J. Cryst. Growth* **50**, 562 (1980).
37. Dickens, M. H., Hayes, W., Hutchings, M. T., and Smith, C., *J. Phys. C* **15**, 4043 (1982).
38. Donaldson, J. D., and Grimes, S. M., *Rev. Silicon, Germanium, Tin, Lead Compd.* **8**, 1 (1984).
39. Donaldson, J. D., Laughlin, D. H., Ross, S. D., and Silver, J., *J. Chem. Soc., Dalton Trans.*, p. 1985 (1973).
40. Donaldson, J. D., and Silver, J., *J. Chem. Soc., Dalton Trans.*, p. 666 (1973).
41. Donaldson, J. D., Silver, J., Hadjiminolis, S., and Ross, S. D., *J. Chem. Soc., Dalton Trans.*, p. 1500 (1975).
42. Dory, T. S., and Zuckerman, J. J., *J. Organomet. Chem.* **264**, 295 (1984).
43. Dory, T. S., Zuckerman, J. J., and Barnes, C. L., *J. Organomet. Chem.* **281**, C1 (1985).
44. Drago, R. S., *J. Chem. Educ.* **50**, 244 (1973).
45. Dutta, S. N., and Jeffrey, G. A., *Inorg. Chem.* **4**, 1363 (1965).
46. Edwards, A. J., and Khallo, K. I., *J. Chem. Soc., Chem. Commun.*, p. 50 (1984).
47. Eiseenthal, K. B., Moss, R. A., and Turro, N. J., *Science* **225**, 1439 (1984).
48. Elliot, H., Hathaway, B. J., and Slade, B. C., *Inorg. Chem.* **5**, 669 (1966).
49. Fregerlev, S., and Rasmussen, S. E., *Acta Chem. Scand.* **22**, 2541 (1968).
50. Fujii, Y., Hoshino, S., Yamada, Y., and Shirane, G., *Phys. Rev. B* **9**, 4549 (1974).
51. Galy, J., Meunier, G., Andersson, S., and Astom, A., *J. Solid State Chem.* **13**, 142 (1975).
52. Gillespie, R. J., *Can. J. Chem.* **38**, 818 (1960).
53. Gillespie, R. J., *J. Chem. Educ.* **47**, 18 (1970).
54. Gillespie, R. J., "Molecular Geometry." Van Nostrand-Rheinhold, New York, 1972.
55. Gillespie, R. J., and Nyholm, R. S., *Q. Rev. Chem. Soc.* **11**, 339 (1957).
56. Goddard, W. A. III, *Science* **227**, 917 (1985).
57. Goldak, J., Barrett, C. S., Innes, D., and Yudelis, W., *J. Chem. Phys.* **44**, 3323 (1966).
58. Goldberg, I., and Herbstein, F. H., *Acta Crystallogr., Sect. B* **B28**, 400 (1972).
59. Goldberg, I., and Herbstein, F. H., *Acta Crystallogr., Sect. B* **B28**, 410 (1972).
60. Goldberg, I., and Herbstein, F. H., *Acta Crystallogr., Sect. B* **B29**, 246 (1973).
61. Goldberg, I., and Herbstein, F. H., *Isr. J. Chem.* **7**, VIP (1969).
62. Goldberg, I., Herbstein, F. H., and Kaftory, M., *Progr. Coord. Chem.* p. 238 (1968).
63. Goldberg, I., Herbstein, F. H., Kaftory, M., and Kapon, M., *Acta Crystallogr., Sect. A* **A28**, S 85 (1972).
64. Goldberg, I., Herbstein, F. H., and Reisner, M., *Isr. J. Chem.* **5**, 24p (1967).

65. Goodenough, J. B., cited in ref. 5, p. 14.
66. Harada, J., Sakata, M., Hoshino, S., and Hirotsu, S., *J. Phys. Soc. Jpn.* **40**, 212 (1976).
67. Harrison, P. G., *Coord. Chem. Rev.* **20**, 1 (1976).
68. Harrison, P. G., and Healy, M. A., *J. Organomet. Chem.* **51**, 153 (1973).
69. Harrison, P. G., and Zuckerman, J. J., *J. Am. Chem. Soc.* **92**, 2577 (1970).
70. Harrowfield, B. V., Dempster, A. J., Freeman, T. E., and Pilbrow, J. R., *J. Phys. C: Solid State Phys.* **6**, 2058 (1973).
71. Harrowfield, B. V., and Pilbrow, J. R., *J. Phys. C* **6**, 755 (1973).
72. Hashimoto, K., *J. Phys. Soc. Jpn.* **12**, 1423 (1957).
73. Hashimoto, K., and Hirakawa, K., *J. Phys. Soc. Jpn.* **11**, 716 (1956).
74. Hastie, J. W., Hauge, R. H., and Margrave, J. L., *Annu. Rev. Phys. Chem.* **21**, 475 (1970).
- 74a. Hathaway, B. J., *Struct. Bonding (Berlin)* **57**, 55 (1984).
75. Hathaway, B. J., and Slade, R. C., *J. Chem. Soc. A*, p. 85 (1968).
76. Haupt, H. J., Huber, F., and Preut, J., *Z. Anorg. Allg. Chem.* **408**, 209 (1974).
77. Heeg, M. J., Janiak, C., and Zuckerman, J. J., *J. Am. Chem. Soc.* **106**, 4295 (1984).
78. Herstein, F. H., *Z. Kristallogr* **157**, 39 (1981).
79. Herstein, F. H., and Kaftory, M., *Acta Crystallogr., Sect. B* **B28**, 405 (1972).
80. Hidaka, M., Okamoto, Y., and Zikumar, Y., *Phys. Status Solidi A* **79**, 263 (1983).
81. Hoppe, R., and Nowitzki, B., *Z. Anorg. Allg. Chem.* **509**, 145 (1984).
82. Howie, R. A., Moser, W., and Trevena, I. C., *Acta Crystallogr., Sect. B* **B28**, 2965 (1972).
83. Hutton, J., Nelmes, R. J., Meyer, G. M., and Eiriksson, V. R., *J. Phys. C* **12**, 5393 (1979).
84. Ioffe, A. I., and Nefefov, O. M., *Mendeleev Chem. J. (Engl. Transl.)* **24**, 58 (1979).
85. Isaacs, N. W., and Kennard, C. H. L., *J. Chem. Soc. A*, p. 386 (1969).
86. Ito, Y., and Koto, K., *Solid State Ionics* **9**, **10**, 527 (1983).
87. Ivanov-Emin, B. N., *Zh. Obshch. Khim.* **10**, 1813 (1940).
88. Janiak, C., Schumann, H., and Zuckerman, J. J., unpublished results.
89. Jones, P. G., *Chem. Soc. Rev.* **113**, 157 (1984).
90. Jørgensen, C. K., *Top. Curr. Chem.* **124**, 1 (1984).
91. Jutzi, P., Kohl, F., Hofmann, P., Krüger, C., and Tsay, Y.-H., *Chem. Ber.* **113**, 757 (1980).
92. Jutzi, P., Kohl, F., and Krüger, C., *Angew. Chem., Int. Ed. Engl.* **18**, 59 (1979).
93. Jutzi, P., Kohl, F., Krüger, C., Wolmershauser, G., Hofmann, P., and Stauffert, P., *Angew. Chem., Int. Ed. Engl.* **21**, 70 (1982).
94. Kafalas, J. A., and Mariano, A. N., *Science* **143**, 952 (1965).
95. Kannewurf, C. R., Kelly, A., and Cashman, R. J., *Acta Crystallogr.* **13**, 449 (1960).
96. Kimura, T., *Sci. Pap. Inst. Phys. Chem. Res. Jpn.* **73**, 31 (1979).
97. Kimura, T., and Sakurai, T., *J. Solid State Chem.* **34**, 369 (1980).
98. Klein, S., and Reinen, D., *J. Solid State Chem.* **32**, 311 (1980).
99. Kohl, F. X., Schluter, E., Jutzi, P., Krüger, C., Wolmershauser, G., Hoffman, P., and Stauffert, P., *Chem. Ber.* **117**, 1178 (1984).
100. Koshkin, V. M., Kukol', V. V., Mil'ner, A. P., Sabrodsii, Yu. R., and Katrunov, K. A., *Sov. Phys. Solid State (Engl. Transl.)* **19**, 939 (1977).
101. Koto, K., Schulz, H., and Huggins, R. A., *Solid State Ionics* **1**, 355 (1980).
102. Labbe, Ph., Frey, M., and Allais, G., *Acta Crystallogr., Sect. B* **B29**, 2204 (1973).
103. Lenhart, P. G., and Joesten, M. D., *Acta Crystallogr., Sect. B* **B36**, 1181 (1980).
104. Malen, E. N., in "Methods and Applications in Crystallographic Computing," (S. K. Hall and T. Ashida, eds.), p. 333. Oxford Univ. Press, London and New York, 1984.

105. Margrave, J. L., *Top. Curr. Chem.* **26**, 1 (1972).
106. Marstrander, A., and Møller, C. Kn., *Mat. Fys. Medd. K. Dan. Vidensk. Selsk.* **35**, No. 5 (1966).
107. Mauersberger, P., and Huber, F., *Acta Crystallogr., Sect. B*, **B36**, 683 (1980).
108. Mauersberger, P., and Huber, F., *Abstr. 3rd. Int. Conf. Organomet. Coord. Chem., Ge, Sn, Pb*, Univ. Dortmund (1980).
109. Mehl, M., and Nespal, W., *Z. Kristallogr. Kristallgeom. Kristallphys. Kristallchem.* **88**, 345 (1934).
110. Meizer, D., and Weiss, E., *J. Organomet. Chem.* **263**, 67 (1984).
111. Messer, D., *Z. Naturforsch., B Anorg. Chem. Org. Chem.* **33**, 366 (1978).
112. Mikolaichuk, A. G., Dutchak, Ya. I., and Freik, D. M., *Sov. Phys. Crystallogr. (Engl. Transl.)* **13**, 490 (1968).
113. Mikolaichuk, A. G., and Freik, D. M., *Sov. Phys. Crystallogr. (Engl. Transl.)* **11**, 2033 (1970).
114. Möller, A., and Felsche, J., *J. Appl. Crystallogr.* **15**, 247 (1982).
115. Möller, A., Wildermuth, G., and Felsche, J.,
116. Møller, C. Kn., *Mat.-Fys. Medd. K. Dan. Vidensk. Selsk.* **32**, No. 1 (1959).
117. Møller, C. Kn., *Mat.-Fys. Medd. K. Dan. Vidensk. Selsk.* **32**, No. 2 (1959).
118. Møller, C. Kn., *Mat.-Fys. Medd. K. Dan. Vidensk. Selsk.* **32**, No. 3 (1960).
119. Møller, C. Kn., *Nature (London)* **180**, 981 (1957).
120. Møller, C. Kn., *Nature (London)* **182**, 1436 (1957).
121. Moser, W., and Tevena, I. C., *J. Chem. Soc., Chem. Commun.*, p. 25 (1969).
122. Muetterties, E. L., and Wright, C. M., *Q. Rev. Chem. Soc.* **21**, 109 (1967).
123. Muldrew, L., *J. Nonmet.* **1**, 177 (1973).
124. Mullen, D., Heger, G., and Reinen, D., *Solid State Commun.* **17**, 1249 (1975).
- 124a. Muradyn, L. A., Sirota, M. L., Makarova, I. P., and Simonov, V. I., *Krystallografiya* **30**, 258 (1985).
125. Nefedov, O. M., Kolesnikov, S. P., Ioffe, A. I., *J. Organomet. Chem. Libr.* **5**, 181 (1977).
126. Nesterova, Y. M., Pashinkin, A. S., and Novoselova, A. V., *Russ. J. Inorg. Chem. (Engl. Transl.)* **6**, 1031 (1961).
127. Noda, Y., Ohba, S., Sato, S., and Saito, Y., *Acta Crystallogr., Sect. B* **B39**, 312 (1983).
128. Novikova, S. I., and Shelimova, L. E., *Sov. Phys., Solid State (Engl. Transl.)* **7**, 2052 (1966).
129. Ohta, H., Harada, J., and Hirotsu, S., *Solid State Commun.* **13**, 1969 (1973).
130. Okazaki, A., *J. Phys. Soc. Jpn.* **13**, 1151 (1958).
131. Orgel, L. E., *J. Chem. Soc.*, p. 3815 (1959).
132. Palatnik, L. S., and Levitin, V. V., *Dokl. Akad. Nauk SSSR* **96**, 975 (1954).
133. Panattoni, C., Bombieri, G., and Croatto, U., *Acta Crystallogr.* **21**, 823 (1966).
134. Petrov, I. I., and Imamov, R. M., *Sov. Phys., Crystallogr. (Engl. Transl.)* **15**, 134 (1970).
135. Platkhev, G. F., Pobedinskaya, E. A., Simonov, M. A., and Belov, N. V., *Sov. Phys., Crystallogr. (Engl. Transl.)* **15**, 928 (1971).
136. Poulsen, F.R., and Rasmussen, S. E., *Acta Chem. Scand.* **24**, 150 (1970).
137. Ramsdell, L. S., *Am. Mineral.* **10**, 281 (1925).
138. Raveau, B., *Rev. Silicon, Germanium, Tin, Lead, Compd.* **6**, 287 (1982).
139. Reinen, D., Freibell, C., and Reetz, K. P., *J. Solid State Chem.* **4**, 103 (1972).
140. Ruddick, J. N. R., *Rev. Silicon, Germanium, Tin, Lead, Compd.* **2**, 115 (1976).
141. Rundle, R. E., and Olson, D. H., *Inorg. Chem.* **3**, 596 (1964).
142. Saito, S., Endo, Y., and Hirota, E., *J. Chem. Phys.* **80**, 1327 (1984).
143. Sakata, M., Nishiwaki, T., and Harada, J., *J. Phys. Soc. Jpn.*, 232 (1979).
144. Sakurai, T., and Kobayashi, K., *Rikagaku Kenkyusho Hokoku* **55**, 69 (1979).
145. Sauka, Ya., *Zh. Fiz. Khim.* **25**, 41 (1951).

146. Scaife, D. E., Weller, P. F., and Fisher, W. G., *J. Solid State Chem.* **9**, 308 (1974).
147. Schmiedekamp, A., Cruickshank, D. W. J., Skaarup, S., Pulay, P., Hargittai, I., and Boggs, J. E., *J. Am. Chem. Soc.* **101**, 2002 (1979).
148. Schmitz-Dumont, O., and Bergerhoff, G., *Z. Anorg. Allg. Chem.* **283**, 314 (1956).
149. Schubert, K., and Fricke, H., *Z. Metallkd.* **44**, 457 (1953).
150. Schubert, K., and Fricke, H., *Z. Naturforsch.*, **A 6**, 781 (1951).
151. Schumann, H., *Zentralbl. Mineral. Geol. Palaeontol.* **33**, 122 (1933); *Chem. Abstr.*, **27**, 3127 (1933).
- 151a. Schumann, H., Janiak, C., Hahn, E., Loebel, J., and Zuckerman, J. J., *Angew. Chem.*, in press.
- 151b. Schumann, H., Janiak, C., Hahn, E., Loebel, J., Kolax, C., Heag, M.-J., Pickardt, J., Rauseh, M. D., and Zuckerman, J. J., unpublished results.
152. Shaplygin, I. S., and Lazarev, V. B., *Russ. J. Inorg. Chem. (Engl. Transl.)* **23**, 403 (1978).
153. Shiryayev, V. I., and Mironov, Y. F., *Russ. Chem. Rev. (Engl. Transl.)* **52**, 184, (1983).
154. Shustorovich, E., and Dobosh, P. A., *J. Am. Chem. Soc.* **101**, 4090 (1979).
155. Sidgwick, N. V., and Powell, H. M., *Proc. R. Soc., London Ser. A* **176**, 153 (1940).
156. Sillen, L. G., and Nylander, A.-L., *Ark. Kemi., Mineral. Geol.* **17A**, No. 4 (1943).
157. Smith, P. J., *J. Organomet. Chem. Libr.* **12**, 97 (1981).
- 157a. Smorodina, T. A., and Tsuranov, A. P., *Izv. Akad. Nauk SSSR, Neorg. Mater.* **20**, 1358 (1984).
158. Takagi, S., Joesten, M. D., and Lenhert, P. G., *Acta Crystallogr., Sect. B* **B31**, 1968 (1975).
159. Takagi, S., Joesten, M. D., and Lenhert, P. G., *Acta Crystallogr., Sect. B* **B32**, 326 (1976).
160. Takagi, S., Joesten, M. D., and Lenhert, P. G., *Acta Crystallogr., Sect. B* **B32**, 668 (1976).
161. Takagi, S., Joesten, M. D., and Lenhert, P. G., *Acta Crystallogr., Sect. B* **B32**, 1278 (1976).
162. Takagi, S., Joesten, M. D., and Lenhert, P. G., *J. Am. Chem. Soc.* **97**, 444 (1975).
163. Terpstra, P., and Westenbrink, H. K., *Verhs. K. Ned. Akad. Wet. Amsterdam* **35**, 75 (1926); *Chem. Abstr.* **20**, 1735 (1926).
164. Troup, J. M., Estine, M. W., and Ziolo, R. F., in ref. 31, p. 285.
165. Urch, D. S., *J. Chem. Soc.*, p. 5775 (1964).
166. van Arkel, A. E., *Rec. Trav. Chim. Pays-Bas* **45**, 437 (1926).
167. van Driel, M., and Verweel, H. J., *Z. Kristallogr.* **95**, 308 (1936).
168. von Schnering, H. G., and Weidemeier, H., *Z. Kristallogr.* **156**, 143 (1981).
169. Weber, D., *Z. Naturforsch.*, **B 33**, 862 (1978).
170. Weidemeier, H., and von Schnering, H. G., *Z. Kristallogr.*, **148**, 295 (1978).
171. Wynne, K. J., *J. Chem. Educ.* **50**, 328 (1973).
172. Yamzin, I. I., Nozik, Yu. Z., and Belov, N. V., *Sov. Phys. Dokl. (Engl. Transl.)* **6**, 370 (1961).
173. Zachariasen, W. H., *Phys. Rev.* **40**, 917 (1932).
174. Zhukova, T. B., and Zaslavskii, A. I., *Sov. Phys. Crystallogr., (Engl. Transl.)* **12**, 28 (1967).
175. Ziolo, R. F., and Troup, J. M., *J. Am. Chem. Soc.* **105**, 229 (1983).
176. Zubieta, J. A., and Zuckerman, J. J., *Prog. Inorg. Chem.* **24**, 251 (1978).
177. Zuckerman, J. J., *Adv. Organomet. Chem.* **9**, 21 (1970).
178. Zuckerman, J. J., in "Chemical Mössbauer Spectroscopy" (R. H. Herber, ed.), p. 267. Plenum, New York, 1984.

This Page Intentionally Left Blank

INDEX

A

Actinides, solvent extraction of carboxylates, 152–153, 156–157

Alkynes, bonding, 194–195

- in mononuclear complexes, 194–196
- in clusters, 196–197
- in dinuclear complexes, 196

Alkyne-substituted transition metal clusters, *see also* individual metals, 169–247

- bonding, 196–201
- diffraction studies, 190–192
 - limitations, 191–192
- electron counting, 197–199
 - fluxionality, 225–226
- hexanuclear species, 180–181
- infrared spectra, 182–185
 - C–C stretching frequencies, 185
- mass spectra, 190
- MO calculations, 197–198
- ¹³C NMR spectra, 187–189, 225–226
 - chemical shifts vs reactivity, 188
- ¹H NMR spectra, 184, 186–187, 225–226
- pentanuclear species, 179–180
- photoelectron spectra, 192–194, 197
- polyhedral skeletal electron pair theory, 200–201
- reactions, 226–231
 - with alkynes, 229
 - with carbon monoxide, 228
 - with hydrogen, 228
 - with metal complexes, 229–231
 - with phosphines and phosphites, 228–229
 - with protic acids, 228
 - pyrolysis, 227–228
- structures, 201–225
 - bond lengths and angles, 207, 210–211, 214–215, 218, 220, 222
 - with dicarbide linkages, 224–225
 - with five metal centers, 223–224
 - with four metal centers, 216–223

- with three metal centers, 209–216
- with two metal centers, 204–208

tetranuclear species, 178–179

trinuclear species, 171–178

- via alkenes, 173–174
- via alkynes, 171–173
- via chemical activation, 176
- via coupling of two metallic species, 176–177
- from demethyvinyl arsine, 177–178
- via photochemical activation, 176
- from tetraphenylcyclopentadienone, 177
- via thermal activation, 171–176

Aluminum

- solvent extraction of carboxylates, 152
- trifluorophosphine complex, 42

Antimony, compounds with stereochemically inert lone pairs, 302

B

Barium, solvent extraction of carboxylates, 152

Beryllium, solvent extraction of carboxylates, 151, 160

BEDT-TTF salts, as molecular conductors, 251, 253

- electrical conduction, 278–279
 - along chains, 280–282
 - anisotropy, 283
 - characteristics, 281
 - pressure effects, 286
 - temperature and anion dependence, 279
- magnetic properties of perbromate, 288–289
 - and ESR linewidths, 290–291
- structures, 269–274
 - anion disordering, 274–277
 - comparison with TCNQ salts, 272
 - comparison with TMTSF salts, 269–271

- dibromiodide, 273–274
- perbromate, 269–271
- perchlorate, 274
- perrhenate, 269, 271
- α - and β -triiodides, 271–273
- synthesis by electrocrystallization, 256–258
- crystallographic phases, 257, 269
- X-ray diffuse scattering, 277
- Bis(ethylenedithio)tetrathiofulvalene (BEDT-TTF), synthesis, 254–256
- Bismuth, compounds with stereochemically inert lone pairs, 302
- Borane, trifluorophosphine adduct, 42

C

- Cadmium, solvent extraction of carboxylates, 154, 159–160
- Calcium, solvent extraction of carboxylates, 151
- Carboxylate complexes, solvent extraction, 143–168
- Carboxylic acids, solvent partition, 145–147
- and dimerization, 145–147
- Chromium, solvent extraction of carboxylates, 160
- Chromium, trifluorophosphine complexes
 - alkenes, 77, 80–81, 83
 - allyls, 93–94
 - arenes, 89
 - structures, 90–93
 - carbonyls, 105–107
 - dienyls, 100, 102
 - hexakis complex, 44–46, 53
 - photoelectron spectra, 62–65
- Cluster complexes
 - alkylidynes, 181–182
 - alkyne derivatives, 169–247
 - analogy with surfaces, 170
- Cobalt, alkyne-substituted clusters, 188
- photoelectron spectra, 193
- polyhedral skeleton electron pair theory, 200
- structures, 218, 224–225
- with iron, 188–189
- ^{13}C NMR spectra, 188–189
- structures, 207–208, 218

- with ruthenium, 173, 179
- with tungsten, 177
- Cobalt, solvent extraction of carboxylates, 153, 158–162
- Cobalt, trifluorophosphine complexes
 - alkyls, 122–124
 - allyls, 94–96
 - carbonyls, 105–108
 - clusters, 71–73
 - cyclopentadienyls, 98, 102
 - halide, 74, 78
 - hydrides, 45, 49–50, 62, 64
 - fluxionality, 57
 - structure, 55–57
 - nitrosyls, 109–111
 - tetrakis anion, 49, 52
 - with difluorophosphide bridges, 68–70
 - with group IV donor ligands, 127–128
 - with group V donor ligands, 112, 118
- Copper
 - alkyne-substituted clusters, 183
 - infrared spectra, 183
 - with iridium, 201, 206
 - with iron, 202, 204, 206
 - structures, 201, 203, 205
 - solvent extraction of carboxylates, 153–154, 158–163
 - trifluorophosphine complex, 129–130

D

- Dichlorosilylene, 6–15
- action reactions, 12–15
 - with alkynes, 12–13
 - with conjugated dienes, 13
 - with cyclopentadiene, 14
 - with ethylene, 12
 - with furan, 14–15
 - with propene, 12
 - with silacyclohexadiene, 14
- insertion reactions, 6–12
 - and chlorine elimination, 9–12
 - and cyclization, 7–8
 - into carbon–halogen bonds, 8–11
 - into carbon–hydrogen bonds, 6–8
 - into silicon–hydrogen bonds, 6–7
 - mechanisms, 8–10
 - with boron trichloride, 6
 - with halogens, 6
 - with hydrogen, 6–7

- with hydrogen chloride, 6-7
- with phenol, 8-9
- Difluorosilylene, 15-36
 - alternate layer reactions, 26-27
 - in nuclear recoil systems, 22
 - polymerization, 15
 - reactions
 - addition vs insertion, 16, 19-21
 - effects of reaction conditions, 24-27
 - with acetylene, 16
 - with benzene, 16
 - with boron trifluoride, 16
 - with butadiene, 23-24, 27
 - with cycloheptatriene, 25, 34-35
 - with cyclohexadiene, 32-33
 - with cyclopentadiene, 25, 32-33
 - with cyclopentene, 32
 - with 1,2-dichloroethylene, 21-22
 - with 1,2-difluoroethylene, 19-20, 23-24, 26-28
 - with ethylene, 16
 - with fluoroalkenes, 16
 - with fluorobenzene, 16
 - with isonitriles, 34-36
 - with propene, 23-24, 30-31
 - with vinyl chloride, 21, 23-24, 27
 - with vinyl fluoride, 23-24, 26-30
 - reaction mechanisms
 - in gas phase, 28, 32-34
 - under co-condensation conditions 28-32, 34-35
 - with alkenes and alkynes, 17-19
 - with isonitriles, 35-36
- Disilacyclohexadienes, 12-13
- Disilacyclohexanes, 12

E

- Electrical conduction, in organic superconductors, 278-286
- Electron spin resonance (ESR) spectra
 - of organic conductors, 286-291
 - of subvalent lead compounds, 314, 317

F

- Fluxionality
 - of alkyne-substituted clusters, 225-226
 - of trifluorophosphine complexes, 53, 55, 57-59, 81-82, 88

G

- Gallium, solvent extraction of carboxylates, 152
- Germanium
 - solvent extraction of carboxylates, 156
 - subvalent compounds, structures, 299-301
 - bis(dicarbonocyclopentadienylmanganese) complex, 304, 320
 - bismuth tellurides, 308, 320
 - decabenzylgermanocene, 307
 - monochalcogenides, 307, 320
 - oxogermanate, 308, 320
 - trichloride anion, 307
- Gold, alkyne-substituted ruthenium cluster, 212
- Group IV elements, subvalent compounds, *see also* individual elements, 297-325
 - and cubic symmetry, 320-321
 - and electronegativity, 300
 - Lewis acidity, 301
 - phase transitions, 307-321
 - and increased symmetry, 319-321
 - lattice expansion, 321
 - to cubic phases, 319-321
 - stereochemically inactive lone pairs, 297-299
 - diffraction studies, 298-299
 - spectral determination, 298
 - symmetrical systems, 301-321
 - with extended lattices, 307-319
 - with molecular structures, 303-307

H

- Hafnium
 - solvent extraction of carboxylates, 160
 - trifluorophosphine cyclopentadienyl complexes, 103

I

- Indium, solvent extraction of carboxylates, 152, 155
- Inorganic silylenes, *see* individual compounds, 1-40
- Iridium
 - alkyne-substituted clusters, 179
 - mass spectra, 190

- pyrolysis, 228
 - structures, 204, 207–208, 221
 - with copper, 201, 206
 - trifluorophosphine complexes
 - alkenes, 85
 - binuclear chloride, 75–76, 78
 - binuclear octakis derivative, 45, 47, 58–59
 - halide, 74, 78–79
 - hydride, 45, 51, 57, 62, 64
 - of gold, 129–130
 - pentamethylcyclopentadienyl, 103
 - tetrakis anion, 52
 - trinuclear clusters, 71–73
 - with group IV donor ligands, 127–128
 - with phosphines, 116, 122
 - Iron, alkyne-substituted clusters, 172–173, 189, 230
 - fluxionality, 226
 - mass spectra, 190
 - MO calculations, 197
 - photoelectron spectra, 193
 - structures, 210, 213–214
 - with cobalt, 188
 - ¹³C NMR spectra, 188–189
 - structures, 207–208, 218
 - with copper, 202, 204, 206
 - with manganese, 210
 - with molybdenum, 189
 - with nickel, 176, 179
 - reaction with phosphines, 229
 - structures, 210, 215, 221–222
 - with ruthenium
 - structure, 218
 - synthesis, 229–230
 - with tungsten, 189
 - structures, 213, 215
 - Iron, solvent extraction of carboxylates, 153, 157, 160–161
 - Iron, trifluorophosphine complexes
 - alkenes, 77, 81, 83–84
 - allyls, 94, 96–97
 - arenes, 91–92
 - carbonyls, 105–107
 - clusters, 71–72
 - cyclopentadienyls, 100, 102, 104
 - dihydride, 49–50, 62
 - halides, 74, 78
 - hydride anion, 57
 - nitrosyls, 109–111
 - pentakis derivatives, 44–46, 53
 - photoelectron spectra, 62–65
 - with difluorophosphide bridges, 68–70
 - with group IV donor ligands, 127
 - with phosphines, 112, 118, 120–121
- L**
- Lanthanides, solvent extraction of carboxylates, 152, 156, 160, 162
 - Lead, solvent extraction of carboxylates, 152, 156
 - Lead, structures of subvalent compounds, 300–301
 - decabenzylplumbocene, 307
 - difluoride, 310–311, 320
 - diiodide, 311, 320
 - hexabromo tetraanion, 309
 - hexanitrito metal complexes, 314–317, 320
 - cobaltate, 314, 320
 - cuprate, 315, 317–318, 320
 - ESR spectra, 314, 317
 - nickelate, 315, 320
 - oxides, 318–319
 - chromate, 318
 - niobate, 318–319
 - pyrochlores, 319
 - tungstate, 318
 - selenide, 313, 320
 - sulfide, 312–313, 320
 - telluride, 313, 320
 - thiourea complexes, 313–317
 - with eight-coordinate lead, 314–316
 - trihalide anions, 311–312, 320
- M**
- Magnesium, solvent extraction of carboxylates, 151
 - Magnetic susceptibility, of organic superconductors, 286–290
 - Manganese
 - alkyne-substituted clusters
 - with iron, 210
 - with osmium, 230
 - solvent extraction of carboxylates, 153, 157

- trifluorophosphine complexes
 carbonyls, 106–107
 cyclopentadienyls, 98, 102
 fluoroalkyls, 123–124
 hydride, 49–50, 62
 nitrosyls, 109–111
 of borane, 129–130
 with group IV donor ligands, 127–128
- Mercury**
 solvent extraction of carboxylates, 154, 159
 trifluorophosphine complexes, 129
- Methylene**, 303–304
- Molecular orbital (MO) calculations**, trifluorophosphine complexes, 60–62, 65, 67
- Molybdenum**
 alkyne-substituted iron clusters, 189
 trifluorophosphine complexes
 alkyls, 123, 125
 arenes, 92
 carbonyls, 105–109
 cyclopentadienyl, 103
 hexakis species, 44–46, 53, 62–65
 photoelectron spectra, 62–65
 stannyl, 127
 with N-donor ligands, 115
- Mössbauer spectra**, of subvalent tin compounds, 298, 306–307, 309
- N**
- Nickel**, alkyne-substituted clusters
 infrared spectra, 183
 structures, 210, 213
 with iron, 176, 179
 reactions with phosphanes, 229
 structures, 210, 215, 221–222
 with osmium, 220
 with ruthenium, 176, 184
 structures, 210, 219–222
 synthesis, 229–230
- Nickel**, solvent extraction of carboxylates, 153, 158, 160–162
- Nickel**, trifluorophosphine complexes
 alkenes, 77, 81, 84–85
 allyl, 95
 carbonyls, 42, 105–107
 tetrakis species, 42–46, 108, 123
 photoelectron spectra, 62–65
 structure, 52–53
 with group V donor ligands, 112–115, 120–121
- Niobium**
 solvent extraction of carboxylates, 160
 trifluorophosphine complexes
 cyclopentadienyl, 103
 hexakis anion, 53–54
- Nuclear Magnetic Resonance (NMR) spectra**
 of alkyne-substituted clusters
 ¹³C spectra, 187–189, 225–226
 ¹H spectra, 184, 186–187, 225–226
 of trifluorophosphine complexes
 ⁵⁹Co spectrum, 52
 ¹⁹F spectra, 53, 55, 57–58, 88–89, 105
 ¹H spectra, 57, 104
 ⁹⁵Mo spectrum, 53
 ⁹³Nb spectrum, 53–54
 ⁶¹Ni spectrum, 52–53
 ³¹P spectra, 53, 81–82, 105
- Nuclear Quadrupole Resonance spectra**, of subvalent compounds, 298, 308–309
- O**
- Organic superconductors**, *see* individual compounds, 249–296
- Osmium**
 alkyne-substituted clusters, 172–181, 204
 fluxionality, 226
 infrared spectra, 184–185
 mass spectra, 190
 MO calculations, 197
 ¹³C NMR spectra, 188–189
 ¹H NMR spectra, 186–187
 photoelectron spectra, 193
 pyrolysis, 227–228
 reaction with carbon monoxide, 229
 structures, 204–205, 207–212, 215, 217–219, 220–222
 with nickel, 220
 with tungsten, 210–211, 216
- trifluorophosphane complexes**
 clusters, 72, 87–88
 dihydride, 45, 47, 51
 halides, 73–74, 78
 hydride anion, 57

with group V donor liquids, 115–116, 118

P

Palladium, trifluorophosphine complexes
halides, 79

tetrakis species, 43–44, 47, 52
with phosphines, 116

Peierls instability, 252–253, 275, 282

Platinum, alkyne-substituted clusters
structures, 205–206

with osmium, 211

with tungsten, 177

Platinum, trifluorophosphine complexes
halides, 42, 73, 75–76, 79

tetrakis species, 41–44, 48
photoelectron spectra, 62–65
structure, 52

with phosphines, 116, 121

R

Rhenium

alkyne-substituted osmium complex, 230
trifluorophosphine complexes
carbonyls, 108–109
decakis dimer, 43, 47
halide, 74, 78
hydride, 45, 49, 51

Rhodium, alkyne-substituted clusters, 181
pyrolysis, 228
structures, 210, 224
with silver, 201, 206

Rhodium, trifluorophosphine complexes

alkenes, 82, 85
alkyls, 122–126
allyls, 95–96
binuclear with alkyne bridge, 59, 86–87
fluxionality, 88–89
carbonyls, 108–109
clusters, 71–73
cyclopentadienyls, 98, 100, 103
dimeric carboxylates, 129–131
structures, 130–131

halides, 74–76, 78

hydride, 45, 49–50, 62, 64
structure, 55–57

nitrosyls, 110–111

octakis dimer, 43, 45, 47

structure, 58–59

of gold, 129–130

tetrakis anion, 49, 52

with group IV donor ligands, 127–129

with group V donor ligands, 116–118, 121

Ruthenium, alkyne-bridged clusters, 172–177, 189

MO calculations, 197

photoelectron spectra, 193

pyrolysis, 227–228

reactions

with alkynes, 229

with carbon monoxide, 228

with water, 231

structures, 203–206, 208–210, 212–219, 222–224

with cobalt, 173, 179

structures, 210–211, 218

with gold, 212

with iron

structure, 218

synthesis, 229–230

with nickel, 176, 184

with tungsten, 189

Ruthenium, solvent extraction of carboxylates, 160

Ruthenium, trifluorophosphine complexes

alkenes, 77, 85

fluxionality, 81–82

allyls, 95–97

carbonyls, 108–109

trinuclear species, 69, 72

dihydride, 45

halides, 73, 78

hydride anion, 57

pentakis species, 43, 45, 47

fluxionality, 53, 55

photoelectron spectra, 62–65

with group IV donor ligands, 127–128

with group V donor ligands, 115, 118–121

S

Scandium, solvent extraction of carboxylates, 152, 156, 160

Selenium, compounds with stereochemically inert lone pairs, 302

- Silacyclohexadienes, 14
Silacyclopentenes, 13
 conversion to disilacycles, 13–14
 decomposition mechanism, 13
Siliranes, from silylenes and alkenes, 12, 23
Silirenes
 dimerization, 13
 from silylenes and alkynes, 12
Silver
 alkyne-substituted rhodium clusters, 201, 206
 trifluorophosphine complex, 129–130
Silylene, 2–6
 addition reactions, 4–6
 mechanism, 4
 nitric oxide scavenging, 4
 to butadiene, 4
 to ethylene, 4
 to hexadienes, 5
 insertion into element–hydrogen bonds, 3–4
 relative reaction rates, 3–4
 with silanes, 3
 in silane pyrolyses, 2–3
 singlet vs triplet state, 4–6
 via fast-neutron bombardment, 2–3
 mechanism, 3
Sodium, solvent extraction of carboxylates, 151, 160
Solvent extraction of metal carboxylates, *see also* individual metals, 143–168
 actinides, 152–153, 156–157
 alkali metals, 151
 alkaline earth metals, 151, 155
 coextraction, 160
 equilibrium treatment, 147–150
 group III elements, 152, 155
 group IV elements, 152, 156
 lanthanides, 152, 156
 scandium and yttrium, 152, 156
 solvent effects, 162–163
 synergistic extraction, 160–162
 transition metals, 153–154, 157–159
 zinc group, 154, 159
Strontium, solvent extraction of carboxylates, 151, 159–160
Superconductivity
 in metals, 250
 in organic salts, 249–296
- T**
- Tantalum, allyl trifluorophosphine complexes, 93, 95
Tellurium, compounds with stereochemically inert lone pairs, 302–303
Tetracyanoquinodimethane (TCNQ) metal salts, 250
 as semiconductors, 250–251
Tetramethyltetraselenafulvalene (TMTSF), synthesis, 254–255
Thallium, solvent extraction of carboxylates, 152, 155, 162
Thorium, solvent extraction of carboxylates, 152, 157, 160
Tin, solvent extraction of carboxylates, 156, 161
Tin, structures of subvalent compounds, 300–301
 decabenzylstannocene, 307
 decaphenylstannocene, 298, 304–306, 320
 Mössbauer spectrum, 306
 diiodide, 310, 320
 divalent cations, 301
 hexahlaotetraanions, 309–310, 320
 rhodium complex, 310, 320
 pentaphenylstannocene, 307
 telluride, 310, 320
 trihalide anions, 308–309, 320
Titanium, trifluorophosphine complexes
 carbonylphosphine, 112
 structure, 118–119
 cyclopentadienyls, 98
 structures, 98–99, 102
 pentadienyl, 100–102
TMTSF salts, as molecular conductors
 effect of sulfur impurity, 254
 electrical conduction
 along chains, 279–280, 282
 anisotropy, 283
 characteristics, 281
 effect of pressure, 284–286
 temperature and anion dependence, 278, 280
 magnetic properties
 and ESR linewidths, 290–291
 susceptibility, 286–289
 structures, 258–269
 and selenium sheets, 258

- anion ordering in perchlorate, 267–268
 - cation–anion distances, 266
 - cation stacking, 260
 - comparison with BEDT-TTF salts, 269–271
 - hydrogen bonding, 266–267
 - influence of anion, 261–263
 - interplanar distances, 268
 - of perbromate, 258–260
 - pressure effects, 264
 - selenium–selenium distances, 265
 - space group, 258
 - temperature affects, 264
 - unit cell and anion volumes, 261–262
 - van der Waal's interactions, 266
 - synthesis by electrocrystallization, 256–258
 - tetrafluoroborate, 257
 - X-ray diffuse scattering, 275–277
 - anion ordering, 275–277
 - and phase transitions, 275–277
 - with noncentrosymmetric anions, 275–277
 - with symmetric anions, 275
 - Trifluorophosphine
 - adsorption on metal surfaces, 65–67
 - comparison with carbon monoxide, 53, 67–68, 105
 - cone angle, 68
 - frontier orbitals, 61
 - gas-phase basicity, 59
 - ionization potentials, 60
 - MO calculations, 61
 - π -acceptor orbitals, 61–62
 - Trifluorophosphine metal complexes, *see also* individual metals, 41–141
 - alkenes, 77, 80–85
 - alkenyls, 122–123, 125–126
 - alkyls, 122–126
 - alkynes, 86–89
 - allyls, 93–97
 - arenes, 89–93
 - binary compounds, 43–48
 - physical properties, 46–48
 - synthesis, 43–45
 - bonding, 42, 62–65, 90–91
 - borane, 129–130
 - carbonyls, 104–109
 - carboxylates, 129–131
 - cyclopentadienyls, 97–104
 - dienyls, 100–102
 - halides, 73–79
 - hydrides, 45, 49–52
 - acidity, 45
 - physical properties, 50–51
 - indenyl, 100, 103
 - MO calculations, 62
 - nitrosyls, 109–111
 - photoelectron spectra, 62–65
 - polynuclear compounds, 69, 71–73
 - structures, 52–59
 - binuclear compounds, 58–59
 - mononuclear compounds, 52–58
 - with difluorophosphide bridges, 68–70
 - with group IV donor ligands, 126–128
 - with group V donor ligands, 111–122
 - Tungsten, alkyne-substituted mixed-metal clusters
 - with cobalt, 177
 - with iron, 189
 - structures, 213, 215
 - with osmium
 - structures, 210–211, 216
 - with platinum, 177
 - with ruthenium, 189
 - Tungsten, trifluorophosphine complexes
 - alkyls, 125–126
 - carbonyls, 105, 108–109
 - hexakis species, 43–44, 47, 53
 - photoelectron spectra, 62–65
- U**
- Uranium
 - solvent extraction of carboxylates, 152–153, 157, 160–161
 - trifluorophosphine complexes, 44, 48, 69–70
- V**
- Vanadium
 - solvent extraction of carboxylates, 149, 153, 157, 161
 - trifluorophosphine complexes
 - cyclopentadienyl, 102
 - hydride, 49–50, 53
 - pentadienyl, 100–102

X

X-ray diffuse scattering, and molecular
conductors, 275–277

Y

Yttrium, solvent extraction of carboxyl-
ates, 152, 160

Z

Zinc, solvent extraction of carboxylates,
154, 159–162

Zirconium

solvent extraction of carboxylates, 157,
160

trifluorophosphine cyclopentadienyl
complexes, 98, 102, 104

with dinitrogen bridges, 99–100, 102

This Page Intentionally Left Blank